

2009

Proxy records of paleohurricanes for the western and southern caribbean

Terrence Allen McCloskey

Louisiana State University and Agricultural and Mechanical College

Follow this and additional works at: https://digitalcommons.lsu.edu/gradschool_dissertations



Part of the [Oceanography and Atmospheric Sciences and Meteorology Commons](#)

Recommended Citation

McCloskey, Terrence Allen, "Proxy records of paleohurricanes for the western and southern caribbean" (2009). *LSU Doctoral Dissertations*. 399.

https://digitalcommons.lsu.edu/gradschool_dissertations/399

This Dissertation is brought to you for free and open access by the Graduate School at LSU Digital Commons. It has been accepted for inclusion in LSU Doctoral Dissertations by an authorized graduate school editor of LSU Digital Commons. For more information, please contact gradetd@lsu.edu.

PROXY RECORDS OF PALEOHURRICANES FOR THE
WESTERN AND SOUTHERN CARIBBEAN

A Dissertation

Submitted to the Graduate Faculty of the
Louisiana State University and
Agricultural and Mechanical College
in partial fulfillment of the
requirements for the degree of
Doctor of Philosophy

in

The Department of Oceanography and Coastal Sciences

by
Terrence Allen McCloskey
B.A., Princeton University, 2003
December, 2009

ACKNOWLEDGMENTS

I would like to thank Dr. Kam-biu Liu, my major professor, for opening the world of paleoenvironmental reconstruction to me, and for mentoring me throughout my graduate career. Dr. Liu has been very patient in explaining both the concepts and details of this complex field and has been extremely accessible and generous with his time; all of which has been tremendously helpful to me, both personally and professionally. I would also like to thank the members of my committee, namely Dr. Nina Lam, Dr. Jaye Cable, Dr. Robert Rohli, and Dr. Quang Cao, for the effort they have expended in supervising this work. As my dissertation committee was originally based in the Department of Geography and Anthropology I would also like to thank Dr. Michael Leitner, my former committee member from that department.

Tremendous thanks go to all the people who helped me on my numerous coring trips. In Belize this includes Andre Cho, Craig Moore and Ms. Evadne Waight (deceased) from the Belizean Department of Geology and Petroleum, Rennick Jackson from Fisheries, Cliff Vernon of the Lands Department, Dr. Leandra Cho Ricketts of the University of Belize, formerly with the Coastal Zone Management Authority Institute, as were Gina Young and Kirk Rodriguez; and Brian Holland of Belize Dolomite. On Turneffe Atoll, Faustino Chi provided all the logistical support and brought two undergraduate assistants, Adria Hussain and Emily Mitchell, for field help. In Barbados, Fatima Patel provided invaluable logistical and geological advice, while Dr. Leo Brewster of the Coastal Zone Management Authority facilitated the paperwork. I was introduced to the Caribbean coast of Nicaragua by Dr. Gerald Urquhart of Michigan State University, and was aided in the field by Clifford Hebert and Claudia Taleno of CIRA-UNAN, while her boss, Dr. Salvadore Montenegro Guillen, arranged all the necessary permits and

government contacts. My undergraduate advisor, Dr. Gerta Keller of Princeton got me started on the paleotempestology path, and is the co-author of what became Chapter 6 in this dissertation. My lab partners were a large part of the effort, particularly Dr. Jason Knowles, who provided field assistance in Belize and Barbados and is the co-author of Chapter 4. Tom Bianchette helped me fight my way through a number of different computer programs.

I would also like to thank my wife, Gabina, who provided tremendous financial, logistical, and moral support during the entire academic process, as well as my two sons, Oaky and Jeffery, who put up with my long absences and excessive grumpiness throughout this seemingly endless ordeal.

Financial support was provided by LSU in the form of a Board of Regents Scholarship and a Dissertation Fellowship; the Inter-American Institute for Global Change Research provided a research fellowship, and the NSF provided both a Graduate Research Fellowship and a Doctoral Dissertation Research Improvement (DDRI) grant. Research grants were also received from the American Association of Geographers, Sigma Xi (from both the national and local chapters), the Geological Society of America, and the Department of Geography and Anthropology at LSU. Travel grants were awarded by International Research Institute for Climate and Society (Columbia University), Aegean Conferences and the NCAR Junior Faculty Forum programs. Funds for radiocarbon dating were supplied in part by the Inter-American Institute for Global Change Research.

I would also like to thank Springer Verlag and Quaternary International for the permission to include Chapters 3 and 6 respectively, previously published by them.

TABLE OF CONTENTS

ACKNOWLEDGMENTS	ii
LIST OF TABLES	ix
LIST OF FIGURES	x
ABSTRACT	xix
CHAPTER 1 INTRODUCTION	1
1.1 Introduction	1
1.2 Paleotempestology	3
1.3 Hypotheses	10
1.4 Hypotheses Testing	11
1.5 References	11
CHAPTER 2 LITERATURE REVIEW	19
2.1 Physical Parameters	19
2.1.1 Selected Proxy	19
2.1.2 Site Selection	25
2.2 External Factors	26
2.2.1 Relative Sea-level Rise	26
2.2.2 Geologic Setting	44
2.2.3 Tsunami	49
2.2.4 Vegetation	57
2.3 Modern Analog	84
2.4 Methods	84
2.5 References	85
CHAPTER 3 TC AND THE ATMOSPHERE: SHORT TERM RELATIONSHIP	100
3.1 Introduction	100
3.2 North Atlantic Circulation System	100
3.3 Geographical/Physical Relationships between Circulation Features	104
3.3.1 BH-NAO	104
3.3.2 BH-TC	105
3.3.3 ITCZ-BH	107
3.3.4 Oceanic-atmospheric	108
3.4 General NA Circulation System	110
3.5 Theoretical Model	111
3.5.1 Structure	111
3.5.2 QBO and ENSO	113
3.5.3 Phase Changes	114
3.5.4 Empirical Correlation	116
3.5.5 Feedback System	120

3.6 Conclusions	124
3.7 References	124
CHAPTER 4 TC AND THE ATMOSPHERE: LONG TERM RELATIONSHIP	131
4.1 Introduction	131
4.2 Data	132
4.3 Current Seasonal Variations in the NA Circulation System	133
4.4 Geographical Relationships	134
4.4.1 Short Term	134
4.4.2 Long Term	140
4.5 Paleo Conditions	146
4.5.1 ITCZ	146
4.5.2 BH	146
4.5.3 TC	147
4.6 Hindcast	149
4.7 Hypothesis Testing	149
4.8 Summary	151
4.9 References	152
CHAPTER 5 PHYSICAL BACKGROUND, BELIZE	160
5.1 Background	160
5.2 Geologic Setting	160
5.2.1 Geologic History	162
5.2.2 Continental Margin	164
5.2.3 Continental Slope and Isolated Carbonate Platforms	166
5.2.4 Tectonic Regime	170
5.3 Sea Level	174
5.4 Discussion	180
5.5 References	182
CHAPTER 6 GALES POINT-MULLINS RIVER, BELIZE	188
6.1 Introduction	188
6.2 Regional Setting	191
6.2.1 Geological	191
6.2.2 Gales Point	193
6.2.3 Mullins River	193
6.3 Methods	194
6.4 Results	197
6.4.1 Hurricane Events	197
6.4.2 Geomorphic Stability	204
6.5 Discussion	206
6.5.1 Hurricanes and the Historical Record	206
6.5.2 An Extreme Event	208
6.5.3 Clustered Hurricane Events	210
6.5.4 Activity Regimes	210

6.5.5 Sea Level Rise.....	211
6.5.6 Tsunami	212
6.5.7 Annual Hurricane Strike Probability	214
6.5.8 Cyclicity in Hurricane Frequency	217
6.5.9 Hurricanes and the Ancient Maya	219
6.6 Conclusions	221
6.7 References	222
CHAPTER 7 COMMERCE BIGHT-HOPKINS MARSH, BELIZE.....	229
7.1 Regional Setting	229
7.2 Study Sites.....	231
7.2.1 Commerce Bight Lagoon.....	232
7.2.2 Hopkins Village	235
7.3 Hurricane History	235
7.3.1 Major Hurricanes.....	238
7.3.2 Minor Hurricanes	240
7.4 Methods.....	241
7.5 HPN Transect	241
7.5.1 Results	241
7.5.2 Discussion.....	260
7.6 CBL Transect	292
7.6.1 Results	292
7.6.2 Discussion.....	317
7.7 Overall Summary.....	338
7.7.1 CB-HPN-GP/MR Hurricane Activity Correspondence	338
7.8 Conclusions	340
7.9 References	341
CHAPTER 8 TURNEFFE ATOLL, BELIZE.....	345
8.1 Introduction	345
8.2 Setting	345
8.3 Study Sites.....	349
8.3.1 GC	349
8.3.2 Blackbird Cay	349
8.3.3 HJ Cay	349
8.3.4 Main Calabash Cay	351
8.3.5 DC	351
8.3.6 Cross Cay.....	351
8.4 Hurricane History	351
8.4.1 Unnamed Hurricane of 1941.....	353
8.4.2 Hurricane Hattie (1961).....	353
8.4.3 Hurricane Keith (2000).....	353
8.5 Methods.....	355
8.6 Results.....	355
8.6.1 HJ Cay	355

8.6.2 GC	366
8.6.3 BB.....	373
8.6.4 Main Calabash Cay	377
8.6.5 DC	377
8.6.6 Cross Cay.....	379
8.7 Discussion	383
8.7.1 Hurricane Hattie	383
8.7.2 Regional Paleoenvironmental History.....	386
8.7.3 Inferred Local Paleoenvironmental History	389
8.7.4 Carbonate Layers.....	396
8.7.5 Forest Taxa	410
8.7.6 Carbonate-Organic Relationship	412
8.8 Conclusions	414
8.9 References	417
 CHAPTER 9 SOUTHERN CARIBBEAN COAST, NICARAGUA	 424
9.1 Geographic Setting	424
9.2 Geologic Setting	424
9.2.1 Chortis Block	424
9.3 Environmental Setting	427
9.4 Study Sites.....	428
9.4.1 Bluefields Bay.....	429
9.4.2 Laguna de las Perlas	433
9.5 Sea Level.....	434
9.6 Hurricane History	438
9.6.1 Hurricane Joan	438
9.6.2 Hurricane Beta	441
9.7 Methods.....	441
9.8 FBM Transect.....	441
9.8.1 Results	441
9.9 IV Transect.....	461
9.9.1 Results	461
9.10 TASN Transect.....	467
9.10.1 Results	467
9.11 Discussion	477
9.11.1 FBM Transect	477
9.11.2 IV Transect.....	485
9.11.3 TASN Transect.....	490
9.11.4 Integrated Site Correlation.....	495
9.11.5 Regional Constraints	497
9.12 Conclusions	500
9.13 References	501
 CHAPTER 10 ST. LAWRENCE GAP, BARBADOS	 506
10.1 Geographic Setting	506

10.2 Geologic Setting	506
10.3 Environmental Setting.....	508
10.4 Study Sites.....	510
10. 5 Sea Level.....	511
10.6 Hurricane History	511
10.7 Methods.....	515
10.8 Results.....	515
10.8.1 SL Transect	515
10.9 Discussion	525
10.9.1 SL transect	525
10.9.2 Carbonate-Organic Ratio	527
10.9.3 Graeme Hall	530
10.9.4 Sedimentation Rates	531
10.9.5 Hurricane Activity.....	533
10.9.6 Clastic Layers.....	533
10.9.7 Paleoclimatic Record.....	536
10.10 Summary	538
10.11 References	541
CHAPTER 11 SUMMARY	543
11.1 General.....	543
11.2 Temporal Correlation.....	543
11.2.1 Southern Locations.....	543
11.2.2 Northern Locations.....	547
11.2.3 Combined Locations.....	550
11.3 Landfall vs. Track.....	552
11.4 Regional Integration.....	563
11.5 Climatic Controls.....	565
11.6 References	567
APPENDIX A: LOSS ON IGNITION GRAPHS	569
A.1 BELIZE	570
A.2 NICARAGUA	644
A.3 BARBADOS	665
APPENDIX B NOTES ON THE SPATIAL VARIABILITY OF SAND DEPOSITION RESULTING FROM HURRICANE FELIX ON THE CARIBBEAN COAST OF NICARAGUA IN REFERENCE TO PALEOTEMPESTOLOGICAL STUDIES.....	676
APPENDIX C RELEASE LETTERS.....	697
VITA	702

LIST OF TABLES

5.1 Characteristics of the three Belizean Atolls.....	168
6:1 Gales Point chronology.....	196
7.1 HPN5 chronology.....	250
7.2 HPN1 chronology.....	258
7.3 CB7 chronology.....	299
7.4 CB1 chronology.....	305
8.1 HJ3 chronology.....	362
9.1 List of tropical cyclones for Bluefields Bay since 1851.....	439
9.2 LOI data as used to identify sedimentological features	445
9.3 FBM1 chronology.....	454
9.4 FBM4 and FBM5 chronologies.....	458
9.5 IV1 chronology.....	465
9.6 TASN7 chronology.....	472
10.1 SL1 chronology.....	520

LIST OF FIGURES

1.1 Study sites	9
2.1 Hurricane generated overwash sand lobes.....	21
2.2 An example from Navarre Beach, Florida of the overwash process.....	22
2.3 A diagram displaying the effects of distance, location, and intensity.....	24
2.4 Major factors influencing eustatic sea level rise.....	28
2.5 4,272 radiocarbon dated sea level indicators.....	30
2.6 Diagram showing calculated current rates of siphoning.....	32
2.7 Regional sea level curves.....	34
2.8 Two early eustatic sea level curves.....	37
2.9 Western Atlantic sea level curves.....	39
2.10 Combined peat and coral based sea level curve for the western Atlantic.....	41
2.11 Geoidal deformation.....	42
2.12 Belize specific sea level curve.....	45
2.13 Four western Atlantic sea level curves.....	46
2.14 Regional sea level curves.....	47
2.15 Tectonic setting of the Caribbean region.....	50
2.16 An estimation of Caribbean earthquake-generated tsunami hazard.....	53
2.17 The Pleistocene-Holocene boundary at Lake Valencia, Venezuela.....	63
2.18 Composite paleoenvironmental history of Lake Valencia, Venezuela.....	66
2.19 Map of Yucatan, showing sites mentioned in the text.....	70
2.20 Pollen record from Lake Coban, Yucatan. From Leyden et al., 1997.....	72
2.21 Environmental history for Cenote San Jose Chulchaca, Yucatan.....	73

2.22 Isotopic record from Lake Punta Laguna, Yucatan.....	75
2.23 Pollen percentage diagram from Lake Salpeten, Guatemala.....	77
2.24 Pollen by vegetation types for Lake Peten-Itza, Guatemala.....	78
2.25 Multi-proxy evidence of anthropogenic impact for Lake Salpeten, Guatemala.....	79
2.26 Insolation control.....	83
3.1 Diagram displaying the postulated relationships between important features	115
3.2 NA TC regimes.....	117
3.3 Correlation of NA oceanic and atmospheric features.....	118
3.4 Frequency of formation for all NA TC north/south of 23.5° N.....	121
4.1 Interannual variability in TC track location.....	136
4.2 Plot of kernel density values of TC tracks.....	138
4.3 Three dimensional surface representation.....	139
4.4 Kernel density surface interpolation.....	142
4.5 Latitude of subtropical high pressure ridge.....	143
5.1 Google Earth image of Belize.....	161
5.2 Geologic setting of Belize.....	163
5.3 The continental margin of Belize.....	165
5.4 Tilt of the Pleistocene basement of the continental margin.....	171
5.5 Wave and wind regime for coastal Belize.....	173
5.6 Large historical Caribbean earthquakes.....	175
5.7 Submerged archeological sites in southern Belize.....	178
5.8 Map of Wild Cane Cay.....	179
5.9 Belize specific sea level curves.....	181

6.1 Map of Belize.....	189
6.2 Site map.....	192
6.3 Photo of Mullins River Line 2 site.....	195
6.4 Litholog and loss on ignition data for Core GP-12.....	199
6.5 Identification of hurricane events along Gales Point Line 1.....	200
6. 6 Identification of hurricane events along Mullins River Line 1.....	203
6.7 Identification of hurricane events along Mullins River Line 2.....	205
6.8 Inferred hurricane activity regimes for GP/MR area.....	213
6.9 Sea level curve for northern Belize.....	215
7.1 Site map, Commerce Bight Lagoon-Hopkins Marsh.....	230
7.2 Hopkins topography and beach bathymetry.....	233
7.3 Commerce Bight Lagoon photos.....	234
7.4 Hurricane history, Hopkins area.....	236
7.5 Hopkins topography and core sites.....	243
7.6 Loss on ignition (LOI) curves and litholog for core HPN5.....	245
7.7 Photos of clastic layers occurring in core HPN5.....	246
7.8 The relationship between carbonate and organic values for core HPN5.....	247
7.9 Depth-date graphs for HPN5, including the root zone.....	251
7.10 Depth-date graphs for HPN5, excluding the root zone.....	253
7.11 HPN5 zonation based on LOI and lithologic data.....	254
7.12 Combined LOI curve and photos of clastic layers for core HPN1.....	257
7.13 The HPN transect as depicted by combined LOI curves.....	259
7.14 Grain size for sand samples from cores HPN2, 3 and Hopkins beach	261

7.15 Conceptual model temporal transect correlation	264
7.16 Potential chronological matches between cores HPN1 and HPN5.....	265
7.17 Stretched stratigraphic matching of the HPN transect.....	267
7.18 Google Earth imagery depicting HPN topography.....	269
7.19 Alternative HPN5 chronologies.....	271
7.20 Chrono-stratigraphic correlation between cores HPN1 and HPN 5.....	276
7.21 Alternative stratigraphic correlation between HPN5 and HPN1.....	277
7.22 Chrono-stratigraphic correlation/zonation for the HPN transect.....	278
7.23 HPN transect correlation/zonation, with clastic layers added.....	279
7.24 Identification by probable origin of transect clastic layers.....	285
7.25 Paleostrike record for the HPN transect.....	291
7.26 CBL topography and core placement.....	294
7.27 LOI curves and litholog for core CB7.....	295
7.28 Photos of core CB7 clastic layers.....	297
7.29 Depth-date graphs for core CB7.....	300
7.30 Zonation for core CB7, based on LOI and lithologic data.....	302
7.31 Photos of core CB1 clastic layers.....	306
7.32 Depth-date graphs for core CB1.....	307
7.33 LOI curves and litholog for core CB2.....	310
7.34 Core CB2 (disturbed section).....	311
7.35 LOI and gamma density curves for cores CB3, 4, 5, and 6.....	312
7.36 Photos of cores CB3, 4, 5, and 6.....	313
7.37 Grain size distribution of samples of CB barrier and offshore sand.....	315

7.38 Grain size distribution of sand samples from core intervals.....	316
7.39 Conceptual model of the isolating effects of the subsurface topography.....	318
7.40 Photos of Zone1 across the CB transect.....	321
7.41 Chrono-stratigraphic correlation between cores CB1 and CB7.....	324
7.42 CB transect zonation, excluding core CB2.....	326
7.43 Three alternative zonations for the CB transect.....	327
7.44 Grain size distribution and photos of CBL barrier and offshore sediment samples.....	329
7.45 Paleostrike record for the CB transects.....	335
7.46 Core depth/ages and sea level rise for the CB transect.....	337
7.47 Hurricane activity regimes for mainland Belize sites.....	339
8.1 Map of Turneffe Atoll.....	347
8.2 Physical characteristics of Turneffe Atoll.....	350
8.3 Study site map.....	352
8.4 Hurricane history for Turneffe Atoll.....	354
8.5 LOI curves and litholog for core HPN5.....	357
8.6 HJ3 sedimentological units and zonation.....	359
8.7 HJ3 depth-age graphs.....	363
8.8 Pollen grains photos.....	364
8.9 Litholog of core HJ3 showing stratigraphy.....	365
8:10 HJ transect.....	367
8.11 LOI curves and litholog for core GC1.....	369
8.12 GC1 sedimentological units and zonation.....	372
8.13 GC1 transect.....	374

8.14 LOI curves and litholog for core BB1.....	375
8.15 BB1 sedimentological units and zonation.....	378
8.16 BB transect.....	380
8.17 MC transect.....	381
8.18 DC1 and CC1 sedimentological units and zonation.....	382
8.19 BB transect top clastic layer.....	385
8.20 All Turneffe transects.....	392
8.21 Duration of ecological periods.....	393
8.22 Conceptual model of hurricane-controlled HJ3 sedimentology.....	400
8.23 Organic-carbonate relationship.....	415
9.1 Geologic setting I, Nicaragua.....	426
9.2 Geologic setting II, Nicaragua.....	430
9.3 Bluefields Bay, physical properties.....	432
9.4 Falso Bluff coring site.....	435
9.5 Coastal sediment supply.....	437
9.6 Hurricane history for the Caribbean coast of Nicaragua.....	440
9.7 LOI curves and litholog for core FBM1.....	443
9.8 Core photo for FBM1.....	444
9.9 Matching of LOI curve and sedimentological data for the top of core FBM1.....	447
9.10 Matching of LOI curve and sedimentological data for the bottom of core FBM1.....	449
9.11 FBM1 zonation based on LOI and lithologic data.....	450
9.12 Depth-age graphs for FBM1 and FBM5.....	455
9.13 FBM transect zonation based on LOI data.....	456

9.14 FBM transect clastic layers.....	457
9.15 Photos of FBM transect clastic layer	459
9.16 LOI curves and litholog for core IV1.....	462
9.17 IV1 clastic layers.....	464
9.18 IV transect clastic layers.....	466
9.19 LOI curves and litholog for core TASN1.....	470
9.20 TASN1 zonation based on LOI and lithologic data.....	471
9.21 TASN transect zonation.....	473
9.22 Photos of the TASN transect clastic layers	475
9.23 Photos of the top FBM clastic layer.....	479
9.24 Non-event clastic layers for the FBM transect.....	481
9.25 Paleostrike and activity regime record for the FBM transect.....	483
9.26 Strike record correlation between the FBM and IV transects.....	487
9.27 Activity regime record for the TASN transect.....	492
9.28 Combined activity regime record for the IV, FBM, and TASN transects.....	496
10.1 Geological and geographical setting, Barbados.....	507
10.2 SL site map.....	512
10.3 Coring transect.....	513
10.4 Hurricane history, Barbados.....	514
10.5 LOI curves and litholog for core SL1.....	517
10.6 SL1 zonation based on LOI and lithologic data	518
10.7 Depth-age graphs for SL1	521
10.8 Probable disturbance at the top of core SL1.....	523

10.9 SL transect zonation based on LOI data.....	526
10.10 Carbonate-organic relationship.....	529
10.11 Comparison of Graeme Hall and SL LOI curves.....	532
10.12 Potential hurricane generated clastic layers.....	537
10.13 Correlation with the paleoclimate record.....	539
11.1 Paleoactivity/climatic/depositional regime correlations for southern sites.....	545
11.2 Paleoactivity regime correlations for the Belizean mainland sites.....	549
11.3 Combined paleoactivity/climate regimes.....	551
11.4 Hurricane histories for the southern Caribbean.....	553
11.5 Hurricane histories for selected locations in the Gulf of Mexico.....	555
11.6 Hurricane histories for selected locations along the US Atlantic coast	556
11.7 Hurricane histories for the Caribbean and Gulf of Mexico.....	557
11.8 Hurricane histories for selected Caribbean locations.....	559
11.9 Tropical cyclone histories for Puerto Rico and Barbuda.....	560
11.10 Hurricane track zones.....	561
11.11 Tropical cyclone history for Barbados.....	562
11.12 Comparison of activity regime chronologies.....	564
11.13 Comparison of regional activity patterns.....	566
B.1 GoogleEarth image of Cabo Gracias a Dios region.....	680
B.2 Beach at Dakura, showing shallow gradient.....	682
B.3 Wind damage in Dakura village from Hurricane Felix.....	684
B.4 Spatial variability in sand transport.....	686
B.5 Close-up of the sand sheet showing hummocky nature.....	687

B.6 Effect of vegetation on thickness of sand deposition.....	689
B.7 Effect of topography on thickness of sand deposition.....	690
B.8 Wind ripples indicating post event sand movement.....	691

ABSTRACT

This dissertation evaluates the hypothesis that hurricane activity levels in the North Atlantic during the late Holocene have been driven by latitudinal movements of the North Atlantic circulation system. Multi-millennial sedimentary proxy records, based on the occurrence of overwash clastic layers, provide clear evidence of abruptly alternating periods of hurricane landfall frequency for Nicaragua and Belize. Three Belizean transects exhibit an Active period (hyperactivity) occurring from ~2000-6000 cal yr BP, although dating is inconsistent across the transects. An Active period covering the last 500 years is found at one location. The Nicaraguan record, derived from three transects covering >90 km of coastline, consistently displays an Active period covering the last 800 years, preceded by a Quiet period that lasts until at least ~2800 years BP, before which time environmental factors render the sites insensitive. For both coastlines the calculated strike frequency increased by a factor of 3-12 during Active periods. The Barbados depositional record is characterized by sudden shifts from organic to clay, attributed to increased aridity, with the arid periods being roughly contemporaneous with the Active periods occurring in Belize and Nicaragua, as well as periods of southern residency of the Intertropical Convergence Zone. Latitudinal movements of a unified North Atlantic circulation system were probably the driver of these changes, with southern migration increasing both landfall frequency and aridity regionally.

When correlated with published records, the timing of activity regime changes identified from our sites indicates that periods of increased hurricane activity proceed across the North Atlantic in a time-transgressive manner, with the Caribbean hyperactive period preceding that of the Gulf of Mexico. The Active period for Nicaragua beginning ~850 years BP is anti-phase with a recently published model, predicated upon basin-wide synchronicity in activity patterns. This

discrepancy possibly results from differences in spatial coverage, as correlations between hurricane landfall and track patterns indicate three distinct groupings resulting from atmospheric conditions. The basin-wide pattern is derived from locations contained within a single (Atlantic coast) track set, while our time-transgressive model is derived from sites within both the Caribbean and Gulf of Mexico track sets.

CHAPTER 1 INTRODUCTION

1.1 Introduction

Tropical cyclones are extremely powerful events that can cover tens of thousands of square kilometers, produce battering waves, high storm surges, heavy rainfall and winds > 300 kph. Globally, they cause more death and property damage than any other class of natural disasters (Murnane, 2004). In the North Atlantic (NA) these storms, called hurricanes, have killed between 300,000-500,000 people over the last 500 years (Rappaport and Fernandez-Partagas, 1997) and have caused damages averaging ~ \$10 billion/year (in 2005 dollars) since 1900 in the United States alone (Pielke et al., 2008). Even in the highly industrialized United States individual storms can cause vast destruction producing long lasting politico-economic effects at the national scale, as evidenced by such recent storms as Ivan (2004), Katrina and Rita (2005), and Ike in 2008. The human suffering resulting from tropical cyclones, though unquantifiable, is tremendous, especially in less developed countries. Examples are the unnamed 1970 cyclone that killed more than 300,000 people in Bangladesh (Murnane, 2004); and Cyclone Nargis that killed >100,000 in Myanmar in 2008 (United Nations, 2008). The damages caused by Mitch in 1998 in both Nicaragua and Honduras approached their respective gross domestic products (Murnane, 2004), while Haiti was devastated by a series of storms in 2008 that damaged or destroyed > 50,000 homes and left >100,000 people homeless (International Federation of Red Cross and Red Crescent Societies, 2008).

Hurricane can also cause tremendous ecological damage, with Katrina, Rita and Ike all demonstrating that hurricanes can lead to the collapse of barrier islands, drive shoreline retreat and devastate forests along the northern coast of the Gulf of Mexico (Chambers et al., 2007;

Culver et al., 2007; FEMA, 2008). This, of course, increases the potential damage of future hurricanes.

The effect of climate change on the frequency and intensity of tropical cyclones has recently become a focus of intense debate. Several studies, both empirical (Emanuel, 1987, 2005; Walsh and Ryan, 2000; Webster et al., 2005; Elsner et al., 2008; Saunders and Lea, 2008) and modeling-based (Knutson et al., 1998; Knutson and Tuleya, 1999, 2004) indicate that the current global warming regime does/should result in an increasing percentage of intense hurricanes and/or an overall general intensification of storms. Many researchers have disagreed strenuously with this view, based primarily on the inability of reliably distinguishing trends from the current data set, given its various instrumental inadequacies (Landsea, 2005, 2007; Pielke et al., 2005; Kossin et al., 2007), but also due to objections raised by theoretical and atmospheric constraints (Wang and Lee, 2008). As ~85% of the damage in the United States is inflicted by major storms (category 3 or above on the Saffir-Simpson scale) (Pielke et al., 2008) increases in either average or maximum hurricane intensity could result in very significant increases in overall damages.

Clearly, a better understanding of tropical cyclone mechanics is of great societal importance. Of particular importance are controls over track locations. From a societal viewpoint even large, intense hurricanes that stay far enough offshore to not affect coastal areas are of little concern. Therefore, in addition to understanding frequency and intensity changes, attention must be paid to the geo-spatial distribution of landfall locations. The determination of accurate long-term return intervals and average annual probability of landfall for hurricanes for any (or all) coastal locations throughout the North Atlantic would be extremely useful for governmental agencies, coastal managers and other policy making entities. However, currently this is not possible, especially for major hurricanes, as the instrumental record extends, with decreasing

accuracy, only back to the mid nineteenth century (Neumann et al., 1993; <http://www.nhc.noaa.gov/pastall.shtml>.) Return intervals have been calculated for coastal communities along the entire coast from Mexico to Canada (Keim et al., 2007); however, even based on a 120 km wide storm swath, calculations for 22 of the 45 localities are based on a single major hurricane strike for the entire 105 year period investigated; eight others have been hit only twice. Clearly, this data set is too small to generate useful statistics. Calculating return intervals for the most damaging storms is statistically impossible, as there have been only three category 5 landfalling US hurricanes during the length of the NOAA database (Blake et al., 2005), for all localities the number of cases is either zero or one. Additionally, these return intervals are calculated by dividing the number of years examined by the total number of strikes, ignoring well recognized changes in activity levels, such as the Atlantic Multidecadal Oscillation (AMO), under which North Atlantic hurricane activity fluctuates between “Active” and “Quiet” periods on a multidecadal time scale (Enfield et al., 2001). Naturally, lower frequency oscillations (centennial length and longer) will be completely missed in the historical record, although shifts in hazard regimes need to be incorporated into risk and vulnerability calculations (Nott, 2003).

1.2 Paleotempestology

This inability to identify longer term changes in hurricane activity is being met by paleotempestology, which is the examination of the hurricane record by historical and geological investigative methods. The driving force behind this relatively new field is the desire to extend the database chronologically in order to determine temporal-spatial changes in hurricane activity. Hurricanes in the North Atlantic Basin (which includes the Gulf of Mexico and the Caribbean) have been recorded sporadically for centuries, with the earliest known records dating from the

time of the Maya civilization (Konrad, 1985; Rappaport and Fernandez-Partagas, 1997; Dunning, personal communication), with an enigmatic glyph from Naranjo Alter I possibly recording an event dated June 3, 544 AD (Houston, 2006). More accessible and systematic records began in the earliest post-Colombian period with the town of Isabella on Hispaniola, founded by Columbus, being recorded as destroyed by a hurricane in 1495 (Rappaport and Fernandez-Partagas, 1997). These early records are far from complete, however, as storms were at best recorded only in populated land areas and when encountered at sea. Many of these records were subsequently lost through happenstance over the intervening centuries, particularly from the sinking of ships. Land based records are naturally skewed by the lack of literate populations in many areas. The most complete and accurate North Atlantic record is NOAA's HURDAT, or "best track" data, based principally on U.S. Weather Bureau information and currently extending to 1851 (Neumann et al., 1993; HURDAT database <http://www.nhc.noaa.gov/pastall.shtml>), but complete and reliable information for the North Atlantic as a whole only began with aircraft reconnaissance in the 1940's. Satellite data has since improved this record. Lack of instrumental/procedural homogeneity, however, limits the ability of the even the best track record to identify long-term trends (Landsea, 2005, 2007; Pielke et al., 2005; Kossin et al., 2007).

Due at least partially to the brevity of this historical record, no clear understanding of hurricane activity changes has emerged. Various researchers have proposed frequency cycles of varying lengths, resulting from a variety of causative agents, but no consensus has emerged. For example, Reading (1990) detects an obvious decadal variation in frequency, while Caviedes (1991) views the variation as "surges", subdecadal in period, caused by a connection with the El Nino-Southern Oscillation (ENSO) system; Liu and Fearn (2000a,b) see a negative correlation

between activity in the Gulf of Mexico and the Atlantic coast of the United States on a millennial timescale, whereas Boose et al. (1997) views New England hurricanes as temporally clustered.

In order to resolve these issues, paleotempestology attempts to extend the hurricane record by a variety of means. One method recreates historical storms by combining historical data with computer models in order to improve track paths (Boose et al., 1997, 2001). This model, of course, depends upon the availability of sufficient historical records and can, at best, only extend the record through colonial times. Other researchers correct the historical records by a variety of archival means (Sandrik and Jarvinen, 1999; Mock, 2004, 2009; Chenoweth, 2006, 2007; Garcia-Herrera et al., 2007). An example of this method is Rappaport's (1999) reconstruction of the 1775 hurricane(s), which researched colonial newspapers, dairies, Lloyd's List, company reports and logs from more than 20 vessels, including a canoe. Several studies compiled primary sources to establish regional records; important early ones being Poey (1856); Redfield (1831); Stormy Jack (1848); Tannehill (1956); Ludlum (1963); Millas (1968); and Salivia (1972). Particularly complete is the six volume work by Partagas and Diaz (1995a, 1995b, 1996a, 1996b, 1997 and 1999), covering the period 1851-1910. The longest known historical storm records (>1000 years in length), though of varying accuracy and completeness, are preserved in county gazettes from southern China (Liu et al., 2001).

The investigation of pre-historic storms, however, requires the examination of the geologic record, and most importantly, the selection of an appropriate proxy. To be useful, the chosen proxy must be:

1. Instrumentally measurable and individually resolvable
2. Preservable
3. Datable

4. Verifiable by modern analog

5. Attributable solely (or at least principally) to storms (i.e., preclusion of other causes).

A variety of proxy records have been attempted, including the dating of beach ridges (Hayne and Chappell, 2001; Nott and Hayne, 2001), speleothems (Malmquist, 1997; Frappier et al., 2007), tree rings (Stonebrunner, 1978; Johnson and Young, 1992; Doyle and Gorham, 1996; Donnelly, 2006; Miller et al., 2006; Rodgers et al., 2006) and corals (Nyberg et al., 2007).

However, to date the most effective and oft-utilized method is the identification of overwash sand layers within the sediments of coastal wetlands, a technique pioneered by Liu and Fearn, (1993). The underlying assumption is that intense storms generate such large storm surges that the barrier dunes are crested and sand is deposited in fans landward of the dunes. Commonly, major storms (Category 3 or greater on the Saffir-Simpson hurricane scale; storms with wind speeds greater than 50 meters/second [110 mph]) are required to deposit these proxy layers. The layers can be quite distinct, usually consisting of light colored clastic material (quartz) interbedded with the typically dark, normally occurring back barrier organic deposition.

These candidate layers are then subjected to a variety of more intense analyses to confirm their marine/beach origin, generally through the identification of environment-specific microfossils, such as diatoms, dinoflagellates, phytoliths and foraminifera (Collins et al., 1999; Scott et al, 2003; Donnelly and Webb, 2004; Liu, 2004). Sedimentary evidence, such as clastic layers thinning and fining landward also support marine origin, while internal structure, particularly fining upward sequences can identify the layers as event-generated. Dating is usually accomplished through radiometric and/or stratigraphic methods (Donnelly and Webb, 2004; Liu, 2004). ^{14}C is commonly used to date events older than 200 years BP, while ^{137}Cs and ^{210}Pb

methods are used for more recent events. Loss-on-ignition analyses record the organic content of the material; abrupt drops in organic content commonly reflect a transported clastic layer.

Working along the northern section of the Atlantic coast of the United States, investigators (Bravo et al., 1997; Donnelly et al., 2001a, 2001b, 2004; Scileppi and Donnelly, 2007) have successfully identified sand layers that represent historically documented storms using a variety of stratigraphical methods. On the Gulf Coast Liu and Fearn (1993, 1997, 2000a,b) have similarly identified coastal sand layers as representing historical storms and have established a strike record extending up to 7000 years (Liu and Fearn, 2000a, b, 2002; Liu, 2004). Similar studies conducted on the Carolina coast (Collins et al., 1999; Scott et al., 2003) have obtained a 5000-year hurricane record. Recently research has been extended to the Caribbean, with hurricane strike records being produced for Puerto Rico (Donnelly, 2005; Donnelly and Woodruff, 2007), Belize (McCloskey and Keller, 2009), St. Martin (Bertran et al., 2004), Nicaragua (Urquhart, 2009) and the Bahamas, Barbuda and Anguilla (Knowles, 2008).

Significantly, the majority of the long records show long-term fluctuations in landfall (Liu and Fearn, 1993, 2000; Donnelly et al., 2001a, b; Scott et al., 2003; Liu 2004; Donnelly and Woodruff, 2007; Scileppi and Donnelly, 2007; Knowles, 2008; McCloskey and Keller, 2009). Typically, cores preserving a long enough record display alternating “Active” (characterized by a high frequency of events), and “Quiet” (much less frequent landfalls) periods, with these oscillations usually occurring on multi-centennial to millennial time scales. The changes in landfall frequency between the differing activity regime are too large to be explained (Donnelly, 2008) as random. The existence of these activity regimes changes is tremendously important for both practical and scientific reasons. From a societal perspective, investigators (Liu, 2004; McCloskey and Liu, 2009) have shown that a return from the current “Quiet” to the previous

“Active” period for the northern Gulf of Mexico results in a three to five fold increase in regional hurricane landfall. Similar increases have been found for the Caribbean coast of Nicaragua (McCloskey et al., 2009). Scientifically, being able to correlate changes in hurricane behavior with paleoclimatic conditions offers the potential of better understanding the atmospheric forcing mechanisms behind such changes. If short- and long-term drivers are similar, documenting paleo changes may significantly improve our short-term predictive abilities.

Two main hypotheses have been presented attempting to explain these observed low frequency changes. One correlates NA hurricane activity with general climatic conditions, especially the state of ENSO, NA sea surface temperature (SST) and the West African monsoon, as the proximate cause of basin-wide activity increase (Donnelly and Woodruff, 2007; Mann et al., 2009). This is based on the synchrony of active periods found in cores from a number of sites, mainly Puerto Rico and the Atlantic coast of the United States, particularly New England. The competing model, the Bermuda High hypothesis, regards increased landfall as a time transgressive feature with temporally staggered periods of increased activity migrating latitudinally across the NA (Liu and Fearn, 1993, 2004; McCloskey and Keller, 2009; McCloskey and Knowles, 2009).

The Bermuda High hypothesis, advanced by Liu and Fearn (1997, 2000a,b; Liu, 2004), is based on their identification of a hyperactive period along the northern coast of the Gulf of Mexico for the period 3400-1000 ^{14}C yr BP, which they attribute to changes in location/intensity of the Bermuda High (BH). Tropical cyclones (counterclockwise rotating low pressure systems) generally form off the coast of Africa and drift westward across the Atlantic, where they are forced to curve around the blocking BH, a clockwise rotating high pressure



1.1 Study sites

system, thereby producing their typical parabolic track pattern. This steering control over NA hurricane tracks exerted by the BH apparently operates on a variety of time scale, from short- (Elsner et al., 2000) to long-term (Liu and Fearn, 1997, 2000; Liu, 2004). The BH hypothesis argues that a long-term southwestward shift in the mean annual position occurred ~ 3400 ^{14}C yr BP, thereby funneling storms into the Gulf of Mexico, accounting for increased landfall along the northern Gulf coast until ~ 1000 ^{14}C yr BP, when a movement back to the northeast allowed earlier recurvature of the BH and subsequent increased landfall along the Atlantic coast (Liu and Fearn, 1993, 2000; Liu 2004). This model implies an anti-phase relationship between landfall frequency for northern and southern locations (specifically the US Atlantic and Gulf coasts), which has been supported by findings from New England (Liu and Lu, 2005) and South Carolina (1999; Scott et al., 2003). Timing of the movement of the long-term mean position is also supported by paleoenvironmental data (Hodell et al., 1991).

1.3 Hypotheses

Accepting long-term geographical movement in the mean position of the BH as the primary control over millennial scale variability in hurricane landfall, the purpose of this dissertation is to move the question one level higher and examine the causes of this movement. The guiding hypotheses are:

1. That tropical cyclones are an integrated feature of the NA circulation system
2. That large scale movement of this system has occurred throughout the Holocene, resulting in quantifiable latitudinal migration of the hurricane zone.
3. That this movement is driven by variations in the pole-equator temperature differences, with stronger pole-equator temperature gradients (colder NA) driving the hurricane zone south ward and weaker gradients (warmer NA) driving the zone northward.

1.4 Hypotheses Testing

The dissertation tests these hypotheses by establishing hurricane strike records from the southern and western Caribbean, based on the geologic proxy of overwash sand lobes. To this end a total of ~150 meters of sediment cores were extracted from coastal wetlands in Barbados, the southern Caribbean coast of Nicaragua, along the mainland coast of Belize and from a number of mangrove cays in Turneffe Atoll, offshore of Belize (**Figure 1:1**).

1.5 References

- Bertran, P., Bonnissent, D., Imbert, D., Lozouet, P., Serrand, N., Stouvenot, C., 2004. Paleoclimat des Petites Antilles depuis 4000 BP: l'enregistrement de la lagune de Grand-Case a Saint-Martin. *Comptes Rendus Geoscience* 336, 1501–1510.
- Blake, E. S., Jarrell, J. D., Mayfield, M., and Rappaport, E.N., 2005. The deadliest, costliest, and most intense United States tropical cyclones from 1851-2004 (and other most frequently requested hurricane facts). NOAA Technical Memorandum NWS TPC-1. <http://www.nhc.noaa.gov/pastint.shtml>.
- Boose, E.R., Chamberlin, K.E., and Foster, D. R., 1997. Reconstructing historical hurricanes in New England. 22nd Conference on Hurricanes and Tropical Meteorology. Fort Collins, CO. American Meteorological Society.
- Boose, E.R., Chamberlin, K.E., and D.R. Foster, 200. Landscape and regional impacts of hurricanes in New England. *Ecological Monographs* 71, 27-48.
- Bravo, J., Donnelly, J. P., Dowling, J., and Webb, T. 1997. Sedimentary evidence for the 1938 hurricane in southern New England. 22nd Conference on Hurricanes and Tropical Meteorology. Fort Collins, CO. American Meteorological Society.
- Caviedes, C.N., 1991. Five hundred years of hurricanes in the Caribbean: their relationship with global climatic variabilities. *GeoJournal* 23, 301-310.
- Chambers, J.Q., Fisher, J. I., Zeng, H., Chapman, E. L., Baker, D. B., and Hurtt, G. C., 2007. Hurricane Katrina's Carbon Footprint on U.S. Gulf Coast Forests. *Science* 318, 1107. DOI: 10.1126/science.1148913.

- Chenoweth, M., 2006. A reassessment of historical Atlantic basin tropical activity, 1700–1855. *Climatic Change* 76, 169–240.
- Chenoweth, M., 2007. Objective classification of historical tropical cyclone intensity. *Journal of Geophysical Research-Atmospheres* 112 (D5) Article No. D05101.
- Collins, E.S., Scott, D.B., Gayes, P.T., 1999. Hurricane records on the South Carolina Coast: Can they be detected in the sediment record? *Quaternary International* 56, 15-26.
- Culver, S. J., Grand Pre', C. A., Mallinson, D. J., Riggs, S. R., Corbett, D.R., Foley, J., Hale, M., Metger, L., Ricardo, J., Rosenberger, J., Smith, C. G., Smith, C. W., Synder, S. W., Twamley, D., 2007. Late Holocene barrier island collapse; Outer Banks, North Carolina, USA. *The Sedimentary Record* 5, 4-8.
- Donnelly, J.P. 2005: Evidence of past intense tropical cyclones from backbarrier salt pond sediments: A case study from Isla de Culebrita, Puerto Rico, USA. *Journal of Coastal Research*. SI 41, 201-210.
- Donnelly, J. P., 2006. Tropical cyclones in the geologic record: understanding variability on centennial to millennial time scales. *Tropical Cyclone and Climate Change Workshop*. International Research Institute for Climate and Society. Lamont-Doherty Earth Observatory, Columbia University, March 28, 2006.
- Donnelly, J. P., 2008. Late Holocene coastal archives of intense tropical cyclone activity: patterns and climatic forcing. *Association of American Geographers Annual Meeting*. Boston, MA.
- Donnelly, J.P. and Webb, T. III, 2004. Back-barrier sedimentary records of intense hurricane landfalls in the northeastern United States. . In Murnane, R.J., and Liu, K-b. (eds), *Hurricanes and Typhoons: Past, Present and Future*. Columbia University Press, New York, 58-95.
- Donnelly, J.P. and Woodruff, J.D., 2007, Intense hurricane activity over the past 5,000 years controlled by El Nino and the West African monsoon. *Nature* 447, 465-468.
- Donnelly, J.P., Bryant, S.S., Butler, J., Dowling, J., Fan, L., Hausmann, N., Newby, P., Shuman, B., Stern, J., Westover, K. and Webb, T. 2001a. 700 yr sedimentary record of intense hurricane landfalls in southern New England. *Geological Society of America Bulletin* 113, 714-727.
- Donnelly, J.P., Roll, S., Wengren, M., Butler, J., Lederer, R. and Webb, T. 2001b. Sedimentary evidence of intense hurricane strikes from New Jersey. *Geology* 29, 615-618.
- Donnelly, J.P., Butler, J., Roll, S., Wengren, M. and Webb, T. 2004: A backbarrier overwash record of intense storms from Brigantine, New Jersey. *Marine Geology* 210, 107-121.

Doyle, T. W., and Gorham, L.E., 1996. Detecting hurricane impact and recovery from tree rings. In *Tree Rings, Environment and Humanity*, Dean, J.S., and Swetnam, T. W. (eds), Radiocarbon 1996, 405-412

Elsner J.B., Liu K-b, Kocher B., 2000. Spatial variations in major U.S. hurricane activity: Statistics and a physical mechanism. *Journal of Climate* 13, 2293-2305.

Elsner, J. B., J. P. Kossin, and T. H. Jagger, 2008. The increasing intensity of the strongest tropical cyclones. *Nature* 455, 92-95.

Emanuel, K.A., 1987. The dependency of hurricane intensity on climate. *Nature* 326, 483-485.

Emanuel K. A., 2005. Increasing destructiveness of tropical cyclones over the past 30 years. *Nature* 436, 686-688.

Enfield, D. B., Mestez-Nunez, A., and Trimble, P.J., 2001: The Atlantic multidecadal oscillation and its relation to rainfall and river flows in the continental U.S. *Geophysical Research Letters* 28, 2077-2080.

FEMA, 2008. Hurricane Ike impact report.
http://www.fema.gov/pdf/hazard/hurricane/2008/ike/impact_report.pdf. Accessed Feb 6, 2009.

Frappier, A.B., Sahagian, D., Carpenter, S.J., González, L.A., and Frappier, B.R., 2007. A stalagmite proxy record of recent tropical cyclone events. *Geology* 7, 111-114 . DOI: 10.1130/G23145A.

Garcia-Herrera, R., Gimeno, L., Ribera, P., Hernandez, E., Gonzalez, E., Fernandez, G., 2007. Identification of Caribbean hurricanes from Spanish documentary sources. *Climatic Change* 83, 55–85.

Hayne, M. and Chappell, J., 2001. Cyclone frequency during the last 5000 years at Curacao Island North Queensland Australia. *Palaeogeography, Palaeoclimatology, Palaeoecology* 168, 207-219.

Hodell, D. A., Curtis, J. H., Jones, G.A., Higuera-Gundy, A., Brenner, M., Binford, M.W., and Dorsey, K. T., 1991. Reconstruction of Caribbean climate change over the past 10,500. *Nature* 352, 790-793.

Houston, S., 2006. Hurricane! Mesoweb Publication,
www.mesoweb.com/articles/houston/hurricane.pdf. Accessed Feb.6, 2009.

International Federation of Red Cross and Red Crescent Societies, 2008. Emergency Appeal no. MDHT005. Glide no. TC-2008-00147.

Johnson, S. R., and Young, D. R., 1992. Variation in tree ring width in relation to storm activity for mid-Atlantic barrier island populations of *Pinus taeda*. *Journal of Coastal Research* 8, 99-104.

Keim, B.D, Muller, R.A., and Stone, G.W., 2007. Spatiotemporal patterns and return intervals of tropical storm and hurricane strikes from Texas to Maine. *Journal of Climate* 20, 3498-3509.

Knowles, J.T., 2008. A 5000 year history of Caribbean environmental change and hurricane activity reconstructed from coastal lake sediments of the West Indies. Unpublished dissertation, Louisiana State University, Baton Rouge, Louisiana.

Knutson T. R., Tuleya R E., and Kurihara,Y. , 1998. Simulated increase of hurricane intensities in a CO₂-warmed climate. *Science* 279, 1018-1021. DOI: 10.1126/science.279.5353.1018.

Knutson, T. R., and Tuleya, R. E., 1999. Increased hurricane intensities with CO₂-induced warming as simulated using the GFDL hurricane prediction system. *Climate Dynamics* 15, 503–519.

Knutson T. R., Tuleya R. E., 2004. Impact of CO₂-induced warming on simulated hurricane intensity and precipitation: sensitivity to the choice of climatic model and convective parameterization. *Journal of Climate* 17, 3477-3495.

Konrad, H. W., 1985. Fallout of the war of the Chacs; the impact of hurricanes and implications for prehispanic Quintana Roo Maya processes. In Thompson, M., Garcia, M. T., and Kense, F. J., (eds), *Status, Structure and Stratification Current Archaeological Reconstruction*. Proceedings of the sixteenth Annual Conference, University of Calgary, 1985.

Kossin, J. P., K. R. Knapp, D. J. Vimont, R. J. Murnane, and Harper, B. A. , 2007. A globally consistent reanalysis of hurricane variability and trends. *Geophysical Research Letters* 34, L04815. DOI:10.1029/2006GL028836.

Landsea, C.W., 2005. Hurricanes and global warming. *Nature* 438, E11-E13.

Landsea, C.W., 2007. Counting Atlantic tropical cyclones back to 1900. *EOS*, 88, 197-2008.

Liu, K-b., 2004. Paleotemstology: principles, methods and examples from Gulf coast lake sediments. In Murnane, R.J., and Liu, K-b. (eds), *Hurricanes and Typhoons: Past, Present and Future*. Columbia University Press, New York, 13-57.

Liu, K-b. and Fearn, M.L., 1993. Lake-sediment record of late Holocene hurricane activities from coastal Alabama. *Geology* 21, 793-796.

Liu, K-b., and Fearn M.L., 1997. Lake sediment records of Hurricane Opal and prehistoric hurricanes from the Florida Panhandle. In; 22nd Conference on Hurricanes and Tropical Meteorology. Fort Collins, CO. American Meteorological Society.

Liu, K-b., and Fearn, M.L., 2000a. Reconstruction of prehistoric landfall frequencies of catastrophic hurricanes in northwestern Florida from lake sediment records. *Quaternary Research* 54, 238-245. DOI:10.1006/qres.2000.2166.

Liu, K-b., and Fearn, M.L., 2000b. Holocene history of catastrophic hurricane landfalls along the Gulf of Mexico coast reconstructed from coastal lake and marsh sediments. In Ning ,Z.H., and Abdollahi, K.. K., (eds), *Vulnerabilities: Implications of Global Change for the Gulf Coast Region of the United States*. GCRCC and Franklin Press.

Liu, K-b., and Fearn, M.L. 2002: Lake sediment evidence of coastal geologic evolution and hurricane history from Western Lake, Florida: Reply to Otvos. *Quaternary Research* 57, 429-431.

Liu, K-b., and Lu, H.Y., 2005. A paleotempestological record from Nobska pond, Cape Cod: testing the Bermuda High hypothesis. Association of American Geographers Annual Meeting. Denver, CO.

Liu, K-b., Shen, C.M. and Louie, K.S. 2001. A 1,000-year history of typhoon landfalls in Guangdong, southern China, reconstructed from Chinese historical documentary records. *Annals of the Association of American Geographers* 91, 453-464.

Ludlum, D.M., 1963 Early American hurricanes, 1492-1870. American Meteorological Society, Boston.

Malmquist, D. L., 1997. Oxygen isotopes in cave stalagmites as a proxy record of past tropical cyclone activity. In Preprints of the 22nd Conference on Hurricanes and Tropical Meteorology, 393-394. Boston. American Meteorological Society.

Mann, M. E., Woodruff, J. D., Donnelly, J. P., and Zhang, Z., 2009. Atlantic hurricanes and climate over the past 1,500 years. *Nature*, 460, 880-883. DOI:10.1038/nature08219.

McCloskey, T. A., and Liu, K-b., 2009. Paleotempestology: geological records of prehistoric hurricane activity. Mineral Management Service Annual Meeting, New Orleans, LA

McCloskey, T. A., and Keller, G., 2009. 5000 year sedimentary record of hurricane strikes on the central coast of Belize. *Quaternary International* 195, 53-68. DOI:10.1016/j.quaint.2008.03.003.

McCloskey, T. A., and Knowles, J. T., 2009. Migration of the tropical cyclone zone through the Holocene. In Elsner, J. B., and Jagger, T. H (eds) *Hurricanes and climate change*. Springer Verlag, Berlin. 169-180.

McCloskey, T. A., Liu, K-b, Urquhart, G. R., Taleno, C., 2009. Hurricane history for the southern Caribbean coast of Nicaragua. Association of American Geographers Annual Meeting. Las Vegas, NV.

- Millas, J.C., 1968. Hurricanes of the Caribbean and adjacent regions, 1492-1800. Academy of Arts and Sciences of the Americas, Miami, Florida.
- Miller, D. L., Mora, C. I., Grissino-Mayer, H. D., Mock, C. J., Uhle, M. E., and Sharp, Z., 2006. Tree-ring isotope records of tropical cyclone activity. *Proceedings of the National Academy of Science*, 10.1073/pnas.0606549103.
- Mock, C.J., 2004. Tropical cyclone reconstructions from documentary records; examples from South Carolina. In Murnane, R.J., Liu, K-b (eds), *Hurricanes and Typhoons: Past, Present, and Future*. Columbia University Press, New York, 121–148.
- Mock, C.J., 2009. Urban U.S. hurricanes and history. Association of American Geographers Annual Meeting. Las Vegas, NV.
- Murnane, R.J., 2004. Introduction. In Murnane, R.J., and Liu, K-b. (eds), *Hurricanes and Typhoons: Past, Present and Future*. Columbia University Press, New York. 1-10.
- Neumann, C.J., Jarvinen, B.R., McAdie, C.J., and Elms, J.D. 1993. Tropical cyclones of the North Atlantic, 1871-1992. NOAA Historical Climatology Series 6-2, Asheville, North Carolina
- Nott, J. 2003. The Importance of prehistoric data and variability of hazard regimes in natural hazard risk assessment – examples from Australia. *Natural Hazards* 30, 43-58.
- Nott, J, and Hayne, M., 2001. High frequency of “SuperCyclones” along the Great Barrier Reef over the past 5000 years. *Nature* 413, 508-512.
- Nyberg, J., Malmgren, B.A. Winter, A., Jury, M.R., Kilbourne, K.H. and Quinn. T.M. 2007. Low Atlantic hurricane activity in the 1970s and 1980s compared to the past 270 years. *Nature* 447, 698-702.
- Partagas, J.F. and Diaz, H.F., 1995a. A Reconstruction of Historical Tropical Cyclone Frequency in the Atlantic from Documentary and other Historical Sources: 1851-1880 Part I: 1851-1870. Climate Diagnostics Center, NOAA, Boulder, CO.
- Partagas, J.F. and Diaz, H.F. 1995b. A Reconstruction of Historical Tropical Cyclone Frequency in the Atlantic from Documentary and other Historical Sources: 1851-1880 Part II: 1871-1880. Climate Diagnostics Center, NOAA, Boulder, CO.
- Partagas, J.F. and Diaz, H.F., 1996a. A Reconstruction of Historical Tropical Cyclone Frequency in the Atlantic from Documentary and other Historical Sources Part III: 1881-1890. Climate Diagnostics Center, NOAA, Boulder, CO.
- Partagas, J.F. and Diaz, H.F., 1996b. A Reconstruction of Historical Tropical Cyclone Frequency in the Atlantic from Documentary and other Historical Sources Part IV: 1891-1900. Climate Diagnostics Center, NOAA, Boulder, CO.

Partagas, J.F. and Diaz, H.F., 1997. A Reconstruction of Historical Tropical Cyclone Frequency in the Atlantic from Documentary and other Historical Sources Part V: 1901-1908. Climate Diagnostics Center, NOAA, Boulder, CO.

Partagas, J.F. and Diaz, H.F., 1999. A Reconstruction of Historical Tropical Cyclone Frequency in the Atlantic from Documentary and other Historical Sources Part VI: 1909-1910. Climate Diagnostics Center, NOAA, Boulder, CO.

Pielke, R. A., Jr., Landsea, C. W., Mayfield, M., Laver, J., and Pasch. R., 2005. Hurricanes and global warming. Bulletin of the American Meteorological Society 86, 1571-1575. DOI: 10.1175/BAMS-86-11-1571.

Pielke, R. A., Jr., Gratz, J., Landsea, C. W., Collins, D., Saunders, M. A., and Musulin, R., 2008. Normalized hurricane damages in the United States: 1900-2005. Natural Hazards Review 2, 29-42.

Poey, A., 1856. Chronological table of cyclonic hurricanes. J ournal of the Royal Geographical Society, 25, 291-328.

Rappaport, E.N., 1999 The catastrophic 1775 hurricane(s): the search for data and understanding In: 23rd Conference on Hurricanes and Tropical Meteorology. Dallas, TX. American Meteorological Society, Boston, MA, 787-790.

Rappaport, E.N. and Fernandez-Partagas, J., 1997. History of the deadliest Atlantic tropical cyclones since the discovery of the New World. In . Diaz. H. F., and Pulwarty, R.S. (eds), Hurricanes, Climate and Socioeconomic Impacts. Springer-Verlag, Berlin, 93-108.

Reading, A. J., 1990 Caribbean tropical storm activity over the past four centuries International Journal of Climatology 10, 365-376.

Redfield, W.C., 1831. On the several hurricanes of the American seas and their relations to the Northers, so called, of the Gulf of Mexico and the Bay of Honduras, with charts illustrating the same. The American Journal of Science, 52, 162-187, 311-334.

Rodgers, J.C., Gamble, D. W., McCay, D. H., and Phipps, S., 2006. Tropical cyclone signals within the tree-ring chronologies from Weeks Bay National Estuary and Research Reserve, Alabama. Journal of Coastal Research 22, 1320-1329.

Salivia, L.A., 1972. Historia de los Temporales de Puerto Rico y las Antillas, editorial Edil, Inc., San Juan, Puerto Rico.

Sandrik, A. and Jarvinen, B., 1999. A reevaluation of the Georgia and northeast Florida tropical cyclone of 2 October 1898. Preprints, 23rd Conferences on Hurricanes and Tropical Meteorology, Dallas, TX, American Meteorological Society. Boston, MA. 475-478.

- Saunders, M. A. and Lea, A.S., 2008. Large contribution of sea surface warming to recent increase in Atlantic hurricane activity. *Nature* 45, 557-560. DOI:10.1038/nature06422.
- Scileppi, E. and Donnelly, J.P., 2007. Sedimentary evidence of hurricane strikes in western Long Island, New York. *Geochemistry Geophysics Geosystems* 8.
- Scott, D.B. , Collins, E.S., Gayes, P.T. and Wright, E., 2003. Records of prehistoric hurricanes on the South Carolina coast based on micropaleontological and sedimentological evidence, with comparison to other Atlantic Coast records .*Geological Society of America Bulletin* 115, 1027-1039.
- Stoneburner, D. L., 1978. Evidence of hurricane influence on barrier island slash pine forests in the northern Gulf of Mexico. *The American Midland Naturalist* 99,234-237.
- Stormy Jack (alias Lieut. Evans, R. N.) 1848. A chronological list of the hurricanes which have occurred in the West Indies since the Year 1493 with interesting descriptions. *Nautical* 397, 453, 524.
- Tannehill, I.R., 1956. *Hurricanes: their Nature and History*. Princeton University Press, Princeton, New Jersey.
- United Nations, Office for the Coordination of Humanitarian Affairs, 2008. Myanmar Cyclone Nargis OCHA Situation Report No. 33.
- Urquhart, G. R., 2009. Paleoecological record of hurricane disturbance and forest regeneration in Nicaragua. *Quaternary International* 195, 88-97. DOI:10.1016/j.quaint.2008.05.012.
- Walsh, K. J. E., and Ryan, B. F., 2000. Tropical cyclone intensity increase near Australia as a result of climate change. *Journal of Climate* 13, 3029–3036.
- Wang, C., and Lee, S-k., 2008. Global warming and United States landfalling hurricanes, *Geophysical Research Letters* 35, L02708, DOI:10.1029/2007GL032396.
- Webster, P. J., Holland, G. J., Curry, J. A., and Chang, H-R., 2005. Changes in tropical cyclone number, duration and intensity in a warming environment. *Science* 309, 1844-1846.

CHAPTER 2 LITERATURE REVIEW

2.1 Physical Parameters

Testing of the hypotheses requires both a rigorous approach to field and lab work and a thorough understanding of background conditions and influencing factors. Presented below is a discussion of the key environmental and methodological factors forming the foundation upon which the field and lab work stands.

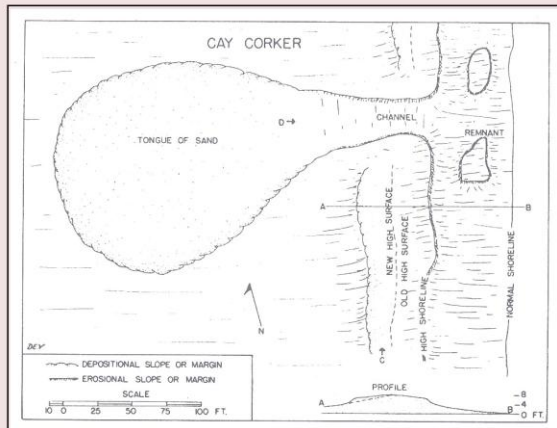
2.1.1 Selected Proxy

2.1.1.1 Overwash Sand Lobes

One of the most visually obvious features of landfalling hurricanes is the vast amount of coastal material moved at the point of impact. Depending upon topography and the intensity of the storm, the storm surge and accompanying waves will move material from the near shore, intertidal area and beach/dune area inland. If the energy involved is large enough this material will be transported beyond the barrier dunes and deposited in the back barrier area. Typically storm cut passages through a barrier's lower elevations, channeling the transported material through narrow cuts (which can occur at intervals all along the beach), and then depositing the material in a fan shape sheet in the back areas. This process results in a very typical geomorphic feature, commonly referred to as overwash sand lobes. Overwashes were described as early as 1919 (Johnson, 1919), characterized by a narrow neck through the barrier and a fan shaped deposition beyond the barrier. These fans are usually well sorted, thinning and fining landward with standard foreset bedding at the edges (Kraft, 1971) (**Figure 2:1**). The edges of these fans can be quite abrupt, especially when encountering water. Overwash commonly occurs during storms, and is particularly well documented for barrier islands, where it is recognized as the main

driver of island rollover (Kraft, 1971; Leatherman, 1979a, b, 1981, 1983; Rampino and Sanders, 1981), whereby material is moved from the front to the back of the island. During times of sea level rise this leads to landward migration of the barrier island (Roy et al., 1994), often preceded by a narrowing of the island width sufficient to permit overwash material to be transported from the beach to back barrier locations (Leatherman, 1979 b, 1983 (**Figure 2:2**). Insufficient sediment supply relative to sea-level rise may result in a drowning of the islands (Masselink and Hughes, 2003; Carter, 1988). The deposition and preservation of storm generated overwash fans can be extremely idiosyncratic. Deposition in the back barrier area depends on the relative heights of storm waves and barrier crests. Total wave height is the additive sum of storm surge, tidal stage, and significant wave height, and thus varies with storm intensity and size, offshore bathymetry, track location, and distance from site, fetch, duration of maximum wind speed, tide stage, and direction and speed of storm movement. Barrier crest heights are controlled by an equally large number of factors. Geographically, therefore, overwash fans may vary dramatically over relatively short area (from meters to kilometers, see Reese et al., 2009; Appendix B this dissertation). Temporal variations are also potentially significant, as geomorphological changes may change a site's sensitivity over time. Common examples include the opening/closing of inlets and the reduction of barriers by storms (Donnelly and Webb, 2004). Preservation may also present a problem, as thin layers may be disturbed by bioturbation, leaving no visual record of the storm. Investigators working in coastal ponds and salt marshes near the Apalachicola Bay Florida, suggest that an original deposition depth of > 1 cm is needed for the event to be preserved in the geological record (Mertz et al., 2003).

Many of these difficulties can be overcome, however. Paleotempestology seeks to establish a minimum record of storm strikes, and, given the random nature of the factors

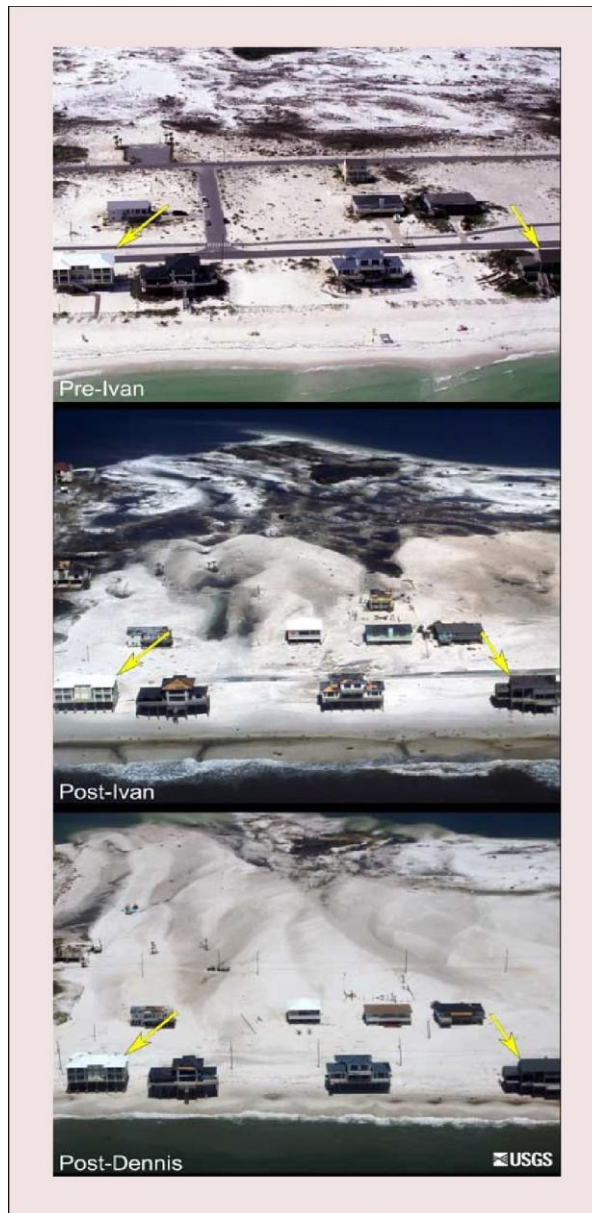


a.



b.

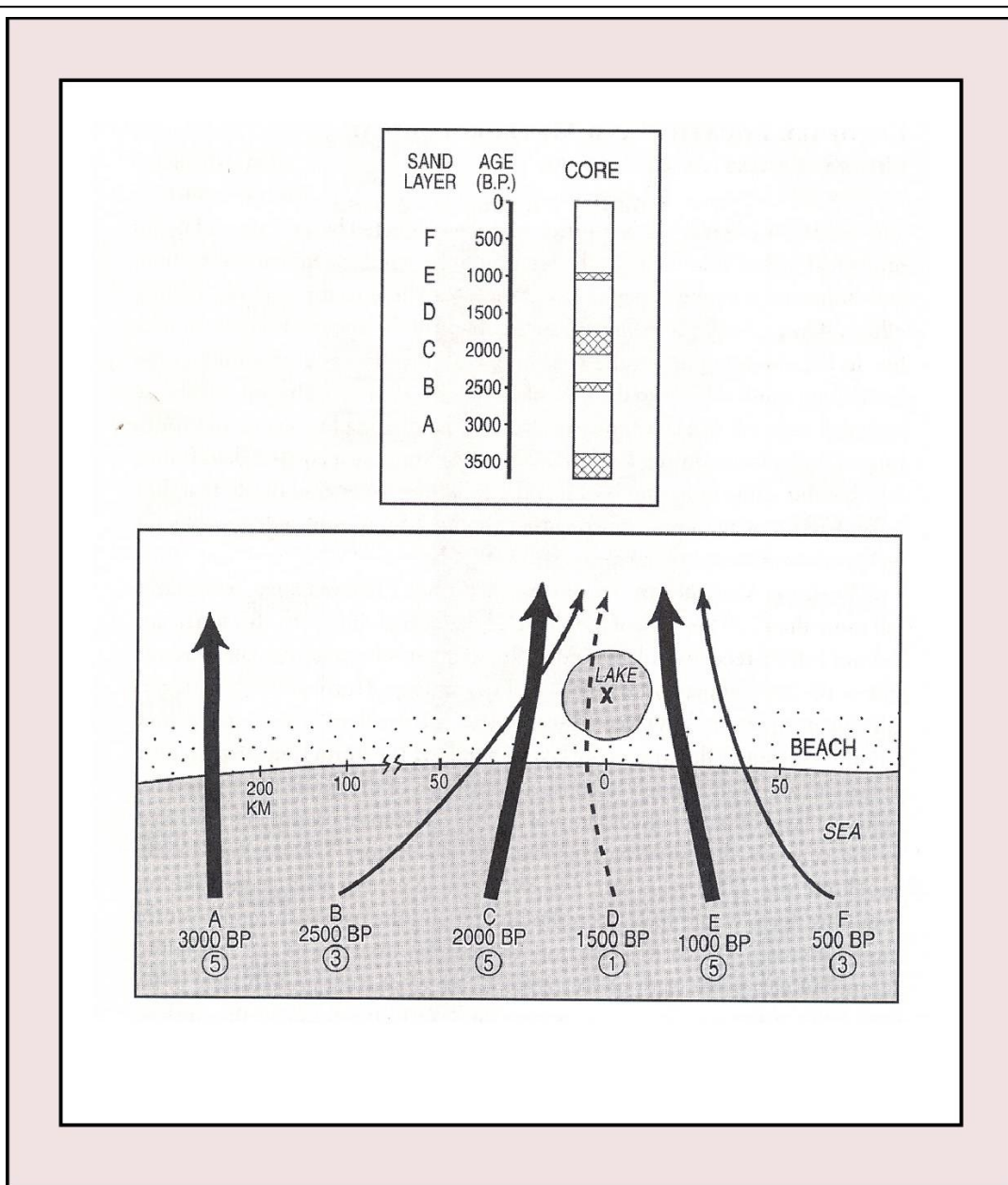
2.1 Hurricane-generated overwash sand lobes; (a) diagram of an overwash lobe on Caye Caulker, Belize deposited by Hurricane Hattie, 1961, from Vermeer, 1963; (b) overwash fan in Homer Pond, Massachusetts, following Hurricane Bob, 1991, photo courtesy of Kam-biu Liu.



2.2 An example from Navarre Beach, Florida of the overwash process whereby hurricanes transport sediments (predominately sand) from the front to rear of a barrier island. The picture is from <http://coastal.er.us.gov/hurricanes/dennis2005/photosets/images/Navarre-Overwash-05>, accessed 02-12-09.

controlling wave height, spatial distribution and preservation, the rate of underestimation should remain fairly constant over time, thus preserving the ability to distinguish between activity regimes. The microtidal nature of the Gulf coast and the Caribbean makes tidal stage basically irrelevant for those areas. Deposition resulting from inlet openings and/or fluvial influence should be readily discernable, and site specific geomorphic change can be controlled for by correlating a number of regional locations. Bioturbation, resulting in mixing and subsequent lack of visual clastic layers, can be overcome by several laboratory methods capable of identifying subvisual clastic content.

Perhaps of greater importance is the consideration that overwash fans occur only over restricted distances near the point of eyewall impact. Because of this constraint, the identification of overwash clastic layers records storms over a limited area, and is almost entirely a storm surge proxy; conveying only inferred information about wind speed at landfall and nothing about previous track pattern or location. It also only informs as to relative intensity between storms for each site, and is unable to separate the conflicting effects of storm strength and distance (i.e. a more intense storm crossing the coast farther away and a less intense storm making landfall closer to the site may leave equivalent sedimentary signatures (**Figure 2:3**) (Liu, 2004). Appropriately spaced coring sites along a kilometers-scale transect would clarify these relationships if individual storms could be identified consistently. However, although specific events can often be identified visually by distinguishing geologic markers (grain size, color, stratigraphic position, intensity) across a single site, current methods do not permit definitive identification across larger distances. Dating can suggest probable matches, but given the numerous possible date ranges typically associated with radiocarbon dating methods,



2.3 A diagram displaying the effects of distance, location, and intensity on the sedimentary signature of storms within a single study location. The magnitude of the signature (as represented by the thickness of the hatched layers in the upper diagram) will depend on all three factors, with increased distance and unfavorable geographical positioning reducing the signal. In this case a small storm passing close to the site (“B”) leaves a signal, while a larger storm, passing farther away (“A”) does not. Diagram from Liu (2004).

identification of specific storms remains uncertain.

A further consideration is that the dependency upon a supply of unconsolidated material renders this proxy less effective on rocky coasts. Combining the overwash information with precipitation proxies, such as tree rings (Miller et al., 2006), speleothems (Malmquist, 1997; Frappier et al., 2007a), coral (Nyberg et al., 2007) and slope wash (Bianchette, 2009; Dunning, personal communication), which record events over much larger areas, is one way of minimizing this spatial limitation (Frappier et al., 2007b).

2.1.2 Site Selection

Due to the idiosyncratic nature of overwash deposition and preservation, site selection is crucial in determining the maximum age and usefulness of cores, with minimal temporal geomorphic change being the goal. Changes in barrier height and distance to the sea affect the recording sensitivity of the site, as does uplift and subsidence, by changing the elevation of the recording environment relative to sea level. The opening/closing of inlets changes the amount of sand in the system as well as the water chemistry and microfossil composition. Changing ecological conditions (marsh to swamp to forest, for example) can alter the distance that clastic material can be transported, while changing water depth will be reflected in differing depositional characteristics. Fluvial influences and meandering river beds can mimic overwash effects.

The ideal site would be an anoxic coastal wetland, without a water course, at or near sea level situated behind a rock sill covered by a sandy barrier of appropriate height, all at appropriate distances from the sea. The accompanying geologic conditions would be surrounding bedrock, tectonic stability, and a steep, micro-tidal coast, as steeper bathymetry results in smaller shore movement with sea level changes. Naturally, all these conditions can rarely (if ever) be

met, but form selection criteria. The characteristics of each site will be discussed in the relevant chapters.

2.2 External Factors

The accuracy of any proxy record can be compromised by changes in a large number of external factors, each of which must be carefully controlled for in order to correctly interpret the data. This is especially true in highly dynamic coastal settings which are usually characterized by rapid changes and a host of high energy processes. This section will describe the major external factors capable of invalidating/confusing results.

2.2.1 Relative Sea-level Rise

One of the most important external factors is change in relative sea-level (RSL), which can potentially alter a site's recording sensitivity, especially along low gradient coasts. As sea level rises, the ocean transgresses landward, in effect moving the beach closer to all inland locations. Because sea level has been rising in the NA throughout the Holocene, the energy required to record storm occurrences potentially varies with depth for each core. Therefore, a thorough understanding of sea level changes is a necessary foundation for all long paleostrike records. For this reason, I will here present a fairly detailed synopsis of Holocene sea level changes from the global to regional perspective. Country specific details will be included in the relevant chapters.

2.2.1.1 Global

The accepted model of post Wisconsin sea level change has become increasingly complex over the past few decades. The original assumption of a globally applicable eustatic rise since the Last Glacial Maximum (LGM) has fragmented to the point that now "no sea level changes can be strictly global" (Moerner, 1987, p. 338). The causes of such variability range

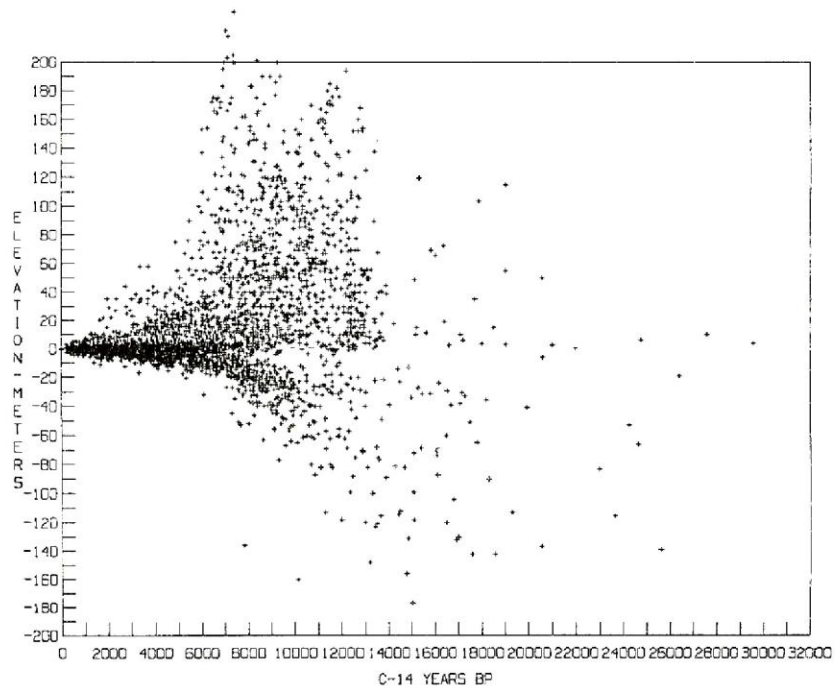
from local to global in scale and are not yet fully resolved. **Figure 2:4** (from Moerner, 1987) lists the major factors involved. Although I will not discuss each factor individually, it is obvious that their impacts are important over vastly differing temporal scales. Clearly, factors such as “Orogeny” and “Mid- Oceanic Ridge Growth” operate at much longer scales than do meteorological and hydrological features. For the purpose of this discussion, the important factors are those categorized as “Isostasy”, “Ocean Water Volume” and, to a lesser degree, “Geodial Eustasy”. Although the overall direction of sea level change since the LGM is generally accepted, the local details are usually difficult to ascertain, particularly at fine scales, either temporally or spatially (Masselink and Hughes, 2003).

Nearly all short term (< millions of years) absolute sea level change results from changes in total ocean water volume (i.e. the eustatic change, consisting of both the changing number of water molecules due to glacial melt/growth and the increased volume of water, due to thermal expansion). However, the primary measurable indicator of such change is relative sea level, which is strongly dependent upon local vertical land movement, and (to a lesser extent), local deformation of the geoid. Therefore, although nearly all post Wisconsin eustatic change is driven by global climatic changes resulting from the transition from glacial to interglacial conditions, the observable relative effects have varied substantially both locally and regionally. As **Figure 2:5** (from Newman et al., 1989) shows, there is immense scatter in both the amount and direction of observable sea level change across the Holocene and beyond. The major cause of the large spread in this data is the inability to separate eustatic and isostatic effects. Uncertainty over the relationship between these factors goes back as far as the 18th century when the general theory of sea level changes was divided between the “plutonists” (holding crustal movement as the major control) and the “neptunists”, who emphasized oceanic control (water volume) (Moerner, 1987).

This is not surprising, considering that absolute sea level is difficult to determine even for present conditions, as a globally uniform level does not exist, due to geoidal (oceanic surface level) deformations caused by the uneven distribution of water masses over the ocean surface. These deformations, which can vary as much as 100 meters, are due to a number of temporally variable internal and external stresses, such as lithospheric loading and regionally variability in water balances (Hallam, 1992). For example Hallam (1992) calculated that of the observed 127 meter rise in the central Pacific, 27 meters results for the deformation of the geoid. The effects of tides and waves further complicate the issue. However, even after determining a calculated Mean Sea Level (MSL), the lack of paleo records for absolute sea levels only permits the measurement of relative change, which, of course, depends upon the vertical movement at each specific site. Most importantly, it can be seen that neither the absolute or relative sea level rises uniformly across the planet as oceanic water volume increases.

Since the continental deglaciation of ice sheets was predominantly a northern hemispheric phenomenon, the eustatic response to their melting has varied regionally. This is because changes in the location and amount of the glacial ice masses caused changes in the spatial distribution of the internal mass of the planet itself, thus altering the gravitational field, which, in turn affects the geoid. One such effect is Mitrovica and Peltier's (1991) proposed "equatorial ocean syphoning", whereby water from the equatorial regions is drawn to the higher latitudes in response to the isostatic uplift of the periglacial regions following deglaciation (discussed below). The net result is that eustatic changes can be grouped regionally, based principally on distance from the former centers of continental glaciations (**Figure 2:6**)

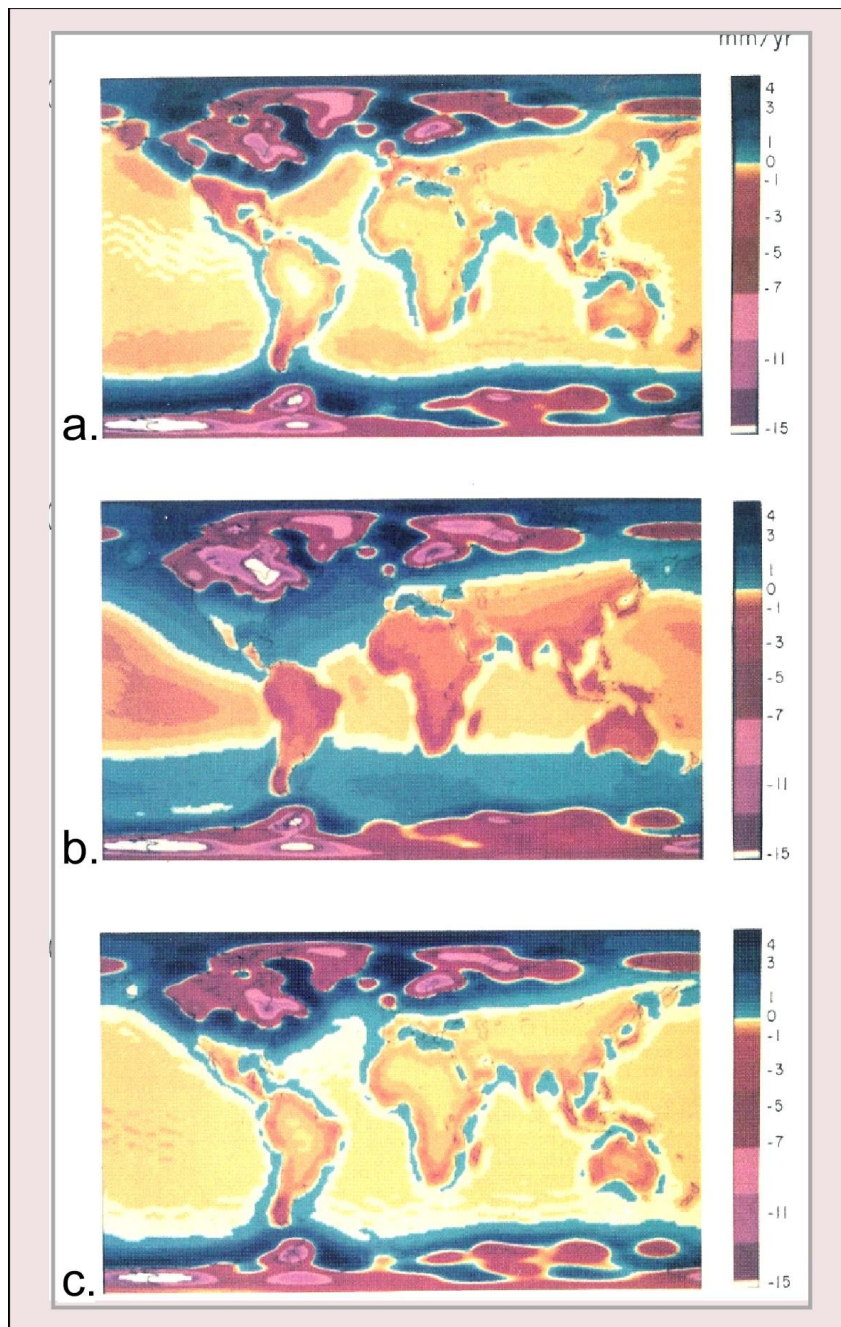
However, the regional geoidal differences are generally overshadowed by regional relative differences. Since the outer skin of the Earth is basically a thick fluid upon which the



2.5 4,272 radiocarbon dated sea level indicators. From Newman et al. (1989).

crust and continents float, changes in mass of the suspended entities result in changes in buoyancy. Thus the removal of the significant mass of kilometers thick ice sheets will result in increased buoyancy (uplift) for the affected area. This concept of glacial isostasy was developed in the mid 19th century, with De Greer providing a clear demonstration by 1889 (Moerner, 1987). Surrounding areas are also affected, and depending upon their specific geologic nature and distance, peripheral areas will either be depressed or uplifted. Specifically, areas immediately beyond the area depressed by the glacial mass generally form an elevated “forebulge”, which then collapses with the retreat/melting of the ice sheet. Thus generalized regional sea level curves can be created for any specific eustatic change, with strong regional gradients of vertical movements occurring in the area of forebulges. As a first approximation, for the Holocene transgression, the world can be regionalized into Near, Intermediate, and Far-fields, each with their respective generalized curve (Moerner, 1987; Bloom, 1977; Komar, 1998), as shown in **Figure 2:7**.

Naturally, these regional curves are somewhat of an abstraction, as individual local records can exhibit considerable variation. One of the most important local controls is hydroisostasy, the principal impact of which is the structural response of shelves and sea floors to changing water depths. In the context of Holocene eustatic sea level increase this generally means a downward deformation, or increased relative sea level rise. Bloom (1967) advanced this theory after examining five submergence curves for the Atlantic coast of the United States. The acceptance of this theory was the death knoll for the idea of a universal (or even regional) sea level curve(s), as it became obvious that under such conditions, each locality, controlled by local geologic conditions, could exhibit a unique response to eustatic change. Eventually it was realized that both the “flexurality” of the crust and lithosphere, as well as the viscosity of the

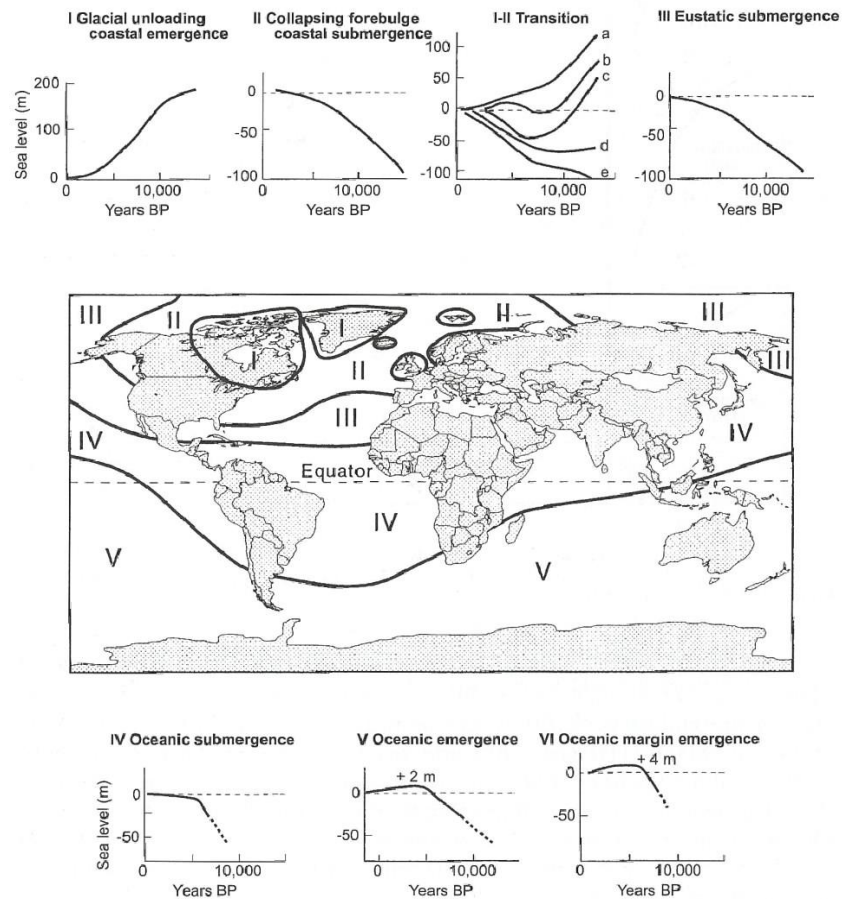


2.6 Diagram showing Mitrovica and Peltier's (1991) calculated current rates of siphoning of water from low to high latitudes as a result of changes in the geoid, These changes are calculated from changes in the earth's internal masses resulting from continental deglaciation. Three scenarios are presented based on lower mantle viscosities of (a) 1021 Pa/s; (b) 1022 Pa/s; (c) 1025 Pa/s.

mantle exhibited important control over the amount of deformation. Moerner (1987) even argues that such lithospheric loading can have significant bathymetric effects through the medium of altered rates of mid-ocean ridge growth and sea floor spreading. Severe loading can result in faulting, which results in stepped discontinuities in local sea level curves (Scott et al., 1989). Unrelated tectonic activity can also, naturally, have important local impact (either negative or positive) on relative sea level change, as can subsidence by sediment loading. Subsidence is particularly important near areas of heavy sediment deposition, such as the mouths of large or sediment-laden rivers. The subsidence, which generally occurs at a fairly constant rate, results from both the mass of the material and the dewatering that occurs in the finer grained materials therein.

2.2.1.2 Empirically Determined Sea Level Curves

Sea levels curves have a long history and have been produced for various time spans from many different types of data sets and proxy records, with the resolution increasing both over time and for more recent periods. Early curves were forced to rely on relative dating, generally based on biostratigraphy. Relatively crude geological proxies have been utilized for many years as a way of comparing long scale changes over geologic time spans. These include such indicators as wave cut platforms, terraces, notches and caves, relict beach deposits (including encrusting organisms), and stratigraphic correlations. More recently, deep ocean cores have been used to yield records of such indirect proxies as relative global oceanic water volume or relative depth of deposition through micropaleontological and isotopic analyses (Hallam, 1992). Ice cores have yielded high-resolution records of total oceanic water volume through the last four glacial/interglacial periods (Alley, 2000; Dansgaard et al., 1993; Petit et al., 1999; Steig et al., 1998).



2.7 Regional sea level curves; generalized regional hydro-isostatic response to post glacial deglaciation. From Masselink and Hughes (2003), based on Komar (1998), modified from Clarke et al. (1978).

For the Holocene, however, the emphasis has been on radiocarbon dated marine proxies. The most commonly used proxies are mollusks, corals, emergent micro-atolls, mangrove peats, and basal clays and salt marsh peats. For Australia, where oceanic transgression has been less severe due to the global geoidal effects discussed above, storm shingle ridges, coastal dunes, and eustarine sediments have served as sea level markers (Hallam, 1992).

The ideal proxy occupies a narrow, clearly understood and recognized depth zone, and consists of material that can be dated easily and accurately. Under such conditions, a time series of depths and ages can be compiled and an accurate sea level curve determined. Naturally, however, there are no perfect markers and each proxy has their particular advantages/disadvantages. Living organisms may occupy a broader depth range than desired, or the preferred depth may vary over time or conditions. Peat and other soils can be compacted, and both organisms and inorganic markers, such as dune ridges or beach lag, may be transported either landward or seaward, which can result in false depth/age correlations (Lighty et al., 1982), as can the inability to distinguish between similar species with different elevational ranges.

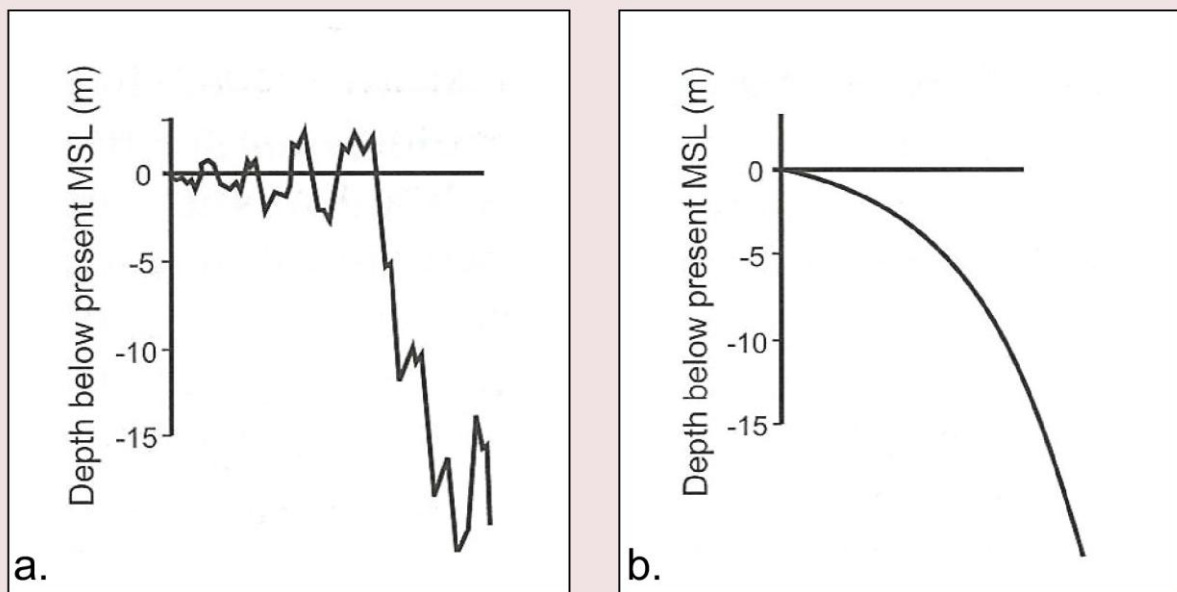
Accurate dating control can also be difficult to achieve. Although ^{14}C dating, which can be used for the entire Holocene, is generally regarded as less problematic than the $^{230}\text{Th}/^{234}\text{U}$ geochronological method used for dating Pleistocene material, (which accuracy can be compromised by geochemical alteration), contamination by either younger material (principally roots) or reworked older material often occurs. Likewise, the effect of tides, storm events, and rapidly changeable riverine and eustarine environmental gradients can confuse the determination of paleo sea levels (Moerner, 1987).

Two of the earliest and most influential radiocarbon dated curves were those compiled by Fairbridge (1961) and Shepard (1963), whose basic differences generated a long running debate

(**Figure 2:8.** The Fairbridge curve shows episodic movement over the past 5000 years, including several highstands above present mean sea level, while Shepard's shows a smooth, continuous curve with an incrementally decreasing rate of rise as it approaches the present (Hallam, 1992). Due to the early date, both of these curves were based on the idea of a global eustatic sea level curve and incorporate data from various regions (Scott et al., 1989; Moerner, 1987; Cronin, 1987). Although this approach is no longer regarded as valid, the general argument over form has endured, with consensus generally supporting Shepard's smooth curve (Cronin, 1987).

2.2.1.3 Western Atlantic Sea Level Curves

After the realization of the chimerical nature of a global curve, workers began producing regional curves. An important experimental approach was the idea that oceanic “pinnacle” islands would provide ideal locations for determining sea level curves, since they would act like “a dipstick thrust into the ocean floor” (Bloom, 1967, p. 1490) recording the eustatic change, due to the lack of isostatic deformation. Fairbank's (1989) study of the massive coral *Acopora palmata* in southern Barbados was an especially influential paper based on this concept. This species has several properties that qualify it as a near ideal candidate for sea level studies. It is extremely common, often dominating West Indies reefs, and has a fairly restricted depth range, usually occurring at less than 5 meters, often accompanied by coralline algae with an even more restricted depth range (Lighty et al., 1982; Fairbanks, 1989). Due to its large size, transport is reduced, while its aragonite structure facilitates both ^{14}C and $^{230}\text{Th}/^{234}\text{U}$ dating. The orientation and shape of the coral permits easy identification of disturbed/transported specimens. Similarly, geological conditions make southern Barbados an excellent location for such studies. The area has experienced a fairly uniform uplift of ~ 34 cm/1000 years over recent geologic time, with the result that not only have the paleo coral records been preserved, their preuplift elevation can be

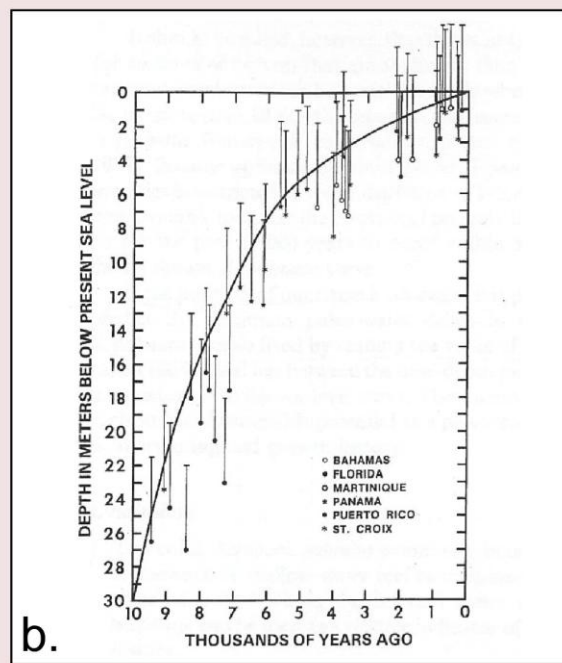
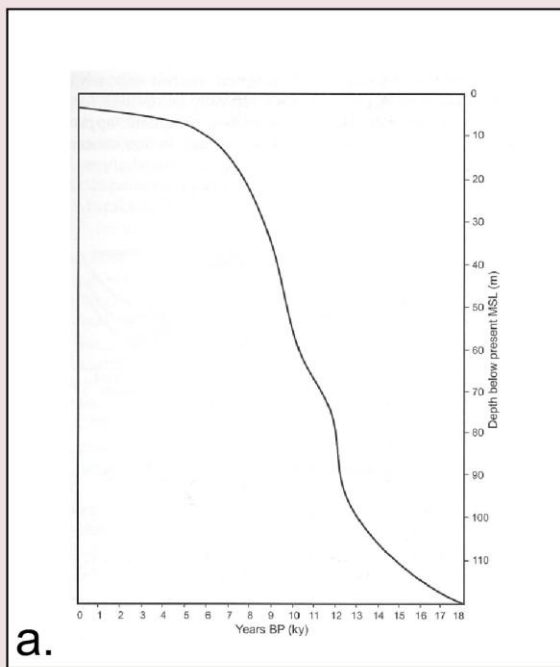


2.8 Two early eustatic sea level curves based on conflicting conceptual models. Figure is from Masselink and Hughes, 2003; (a) is the curve by Fairbridge (1961); (b) is by Shepard (1963).

calculated. Additionally, Barbados happens to be located in an area where eustatic and local sea level history are very similar (Peltier, 2002; Fairbanks, 1989; Lambeck et al., 2002). This study produced a curve resembling Shepard's, marked by two periods of rapid rise (**Figure 2:9a**). However, Moerner (1987) argues that such islands are “unsuitable for eustatic analyses” because they can create local geoid rises of 4 meters.

It should be pointed out that analysis based on *Acropora palmata* results in a minimum sea level curve, as the coral itself is subaqueous. An exact sea level curve cannot be determined as the organisms occur over a depth of ~ 5 meters, with occasional individuals occurring at depths of 17 meters (Lighty et al., 1982). Lighty et al. (1982) produced a general sea level curve for the western Atlantic based on their examination of 42 radiocarbon dated *Acropora palmata* samples from the literature (**Figure 2:9b**). This curve resembles the Shepard curve, with a decreased rate of rise through the late Holocene. The length of the error bars should be noted.

A more recent regional sea level curve is that by Toscano and Macintyre (2003). This is an attempt to place a more specific curve by means of combining maximum and minimum sea level curves. The curve is based on 145 samples (both new and culled from the literature) of coral (*Acopora palmata*) and mangrove peat (mainly *Rhizophora mangle*) from the western Atlantic/ Caribbean. Since intertidal mangroves grow at or slightly above MSL, while corals grow slightly below, the time/depth plot of each establishes maximum (mangrove) and minimum (coral) curves, which can be expected to bracket actual MSL. However, the correlation of these two curves requires the use of a common dating framework (calendar years), as does any correlation between the resulting curve and paleoclimatic events. Previously the dates for each group were generally reported in ^{14}C years, which differed between the terrestrial and marine records. The conversion of these dates to universally usable calendar years required the



2.9 Western Atlantic sea level curves. Shown are (a) Fairbanks' (1989), based on Barbadian coral; (b) is from Lighty et al. (1982), derived from coral from several western Atlantic locations.

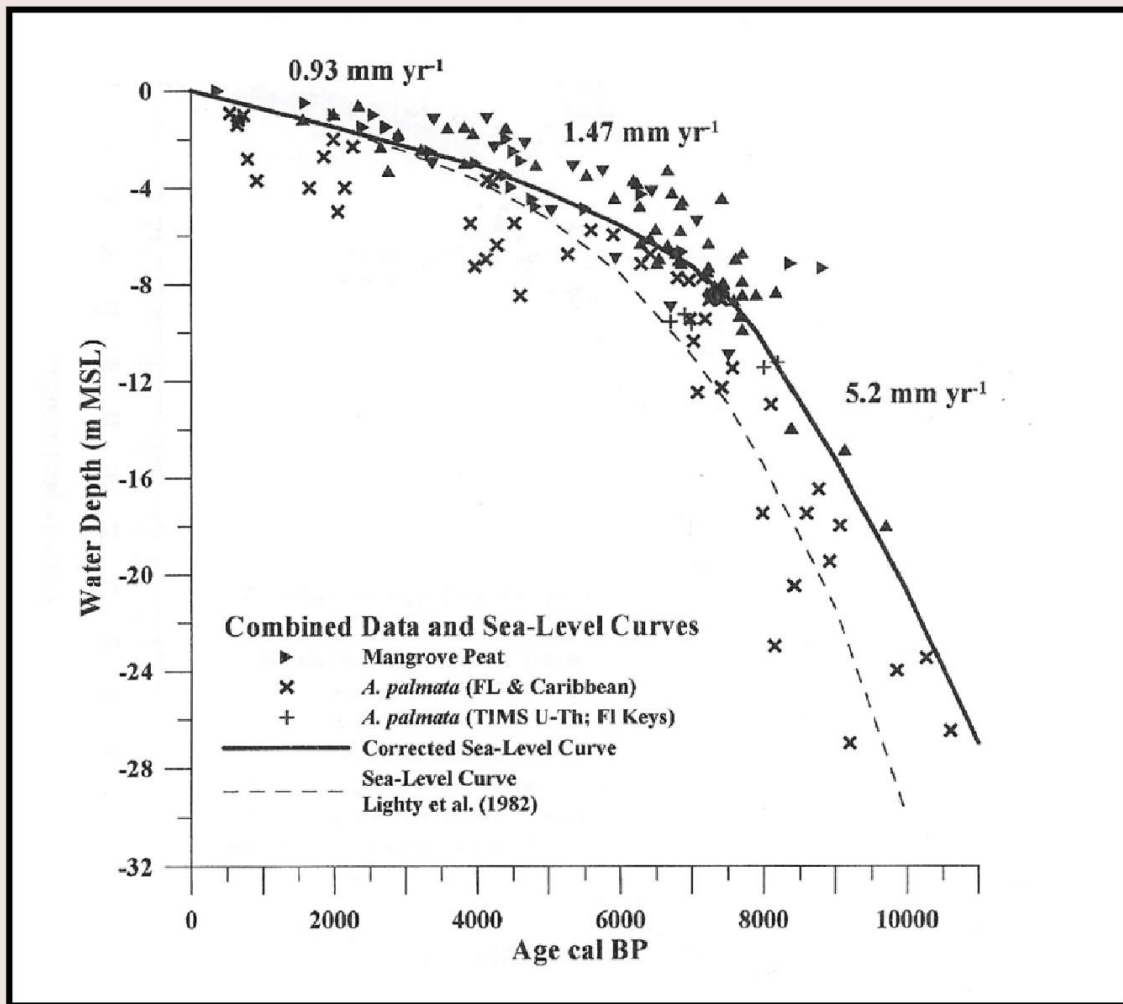
recalibration and correction of all of the previously published samples. Three major modifications were required in order to achieve accurate calendar dates; namely:

1. The calibration to calendar years based on the more accurate ^{14}C half life of 5,730 years, as opposed to the generally used “Libbey” half life of 5,568 years
2. Correction for $\delta^{13}\text{C}$ effects
3. Correction for the oceanic reservoir effect

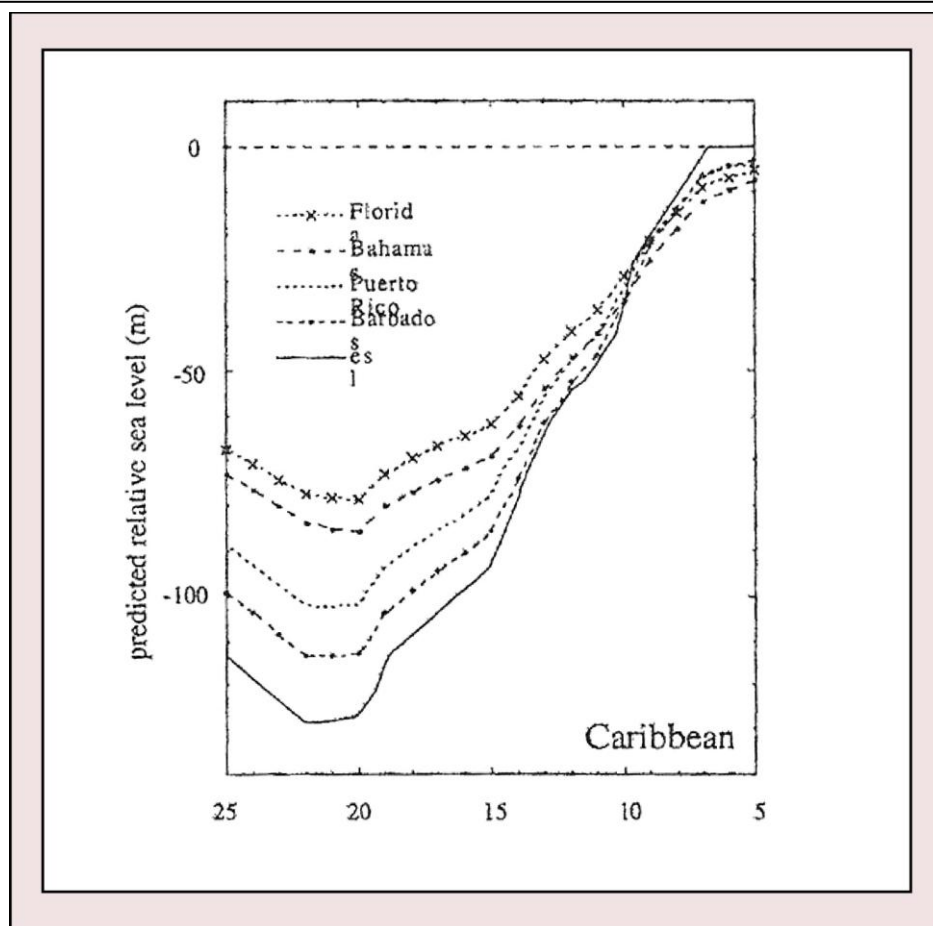
Making these adjustments resulted in increasingly older dates as sample age increased, resulting in a progressively higher curve for the early Holocene. These upward shifts in elevation for the older dates are particularly noticeable when compared to the Lighty et al. (1982) curve (dashed line, **Figure 2:10**).

The placement of the curve was based on the best fit between the peat and coral samples, attempting a complete separation of the two groups, although this was not entirely successful. There are several possible explanations for these discrepancies, mainly the inaccurate dating of peat samples, due to such factors as differing elevational environments for similar species, the compaction of peat either *in situ* or during coring, and the contamination by younger roots. Although Woodroffe (1995) argues that mangroves only occur over a 15 cm elevational range in Belize, this is not necessarily true for all sample sites. Toscano and Macintyre (2003) included non-basal peats in this study, after demonstrating that such samples achieved a good fit with the basal peat curves. By including the non-basal peats, gaps in the curve were filled. A major objection to this curve is that it does not control for geoidal deformation, which, according to Lambeck et al. (2002), can be as much as 3 meters for the northernmost sites (Florida) (**Figure 2:11**).

Gischler (2006) has objected to the manner in which Toscano and Macintyre (2003) used



2.10 Combined peat and coral based sea level curve for the western Atlantic. From Toscano and Macintyre (2003). The curve from Lighty et al. (1982) is shown as a dashed line.



2.11 Geoidal deformation. Calculated differences in relative sea level between various sites in the western Atlantic due to geoidal deformation. The solid line represents the eustatic sea level curve. From Lambeck et al. (2002). The units for the X axis are cal yr BP.

the data in determining this curve, particularly the inclusion of non-basal peat and the interpretation of published coral data (from Gischler and Hudson, 2004) as being supratidal storm rubble. The Gischler and Hudson (2004) data delineates a curve that parallels that of Toscano and McIntyre (2003), but sits considerably higher (**Figure 2:12**). This curve will be discussed more fully in Chapters 5 and 7. Despite the precise nature of the data collection, the general shape and placement of these more recent curves do not differ significantly from previously published curves for the area, especially for the late Holocene, although they do plot higher (**Figure 2:13**). In fact, due to the equatorial position of the Caribbean and the lack of either dramatic hydro-isostatic response, or active seismicity, these curves are simply a more precise placement of a generally accepted curve. A recent sea level curve for the northern Gulf of Mexico, based on basal peat and swash zone deposits (Milliken et al., 2008) displays very similar trends, further supporting the accepted pattern. Further examples of older, similar curves are offered in **Figure 2:14**. All have very similar profiles, with **14c** (Panama) showing lower and more episodic sea level rise, while **14b** (Guyana and Central America) shows an earlier approach to, and in some cases rise above, present MSL. Sea level curve specifics will be discussed more fully for each site in the relevant chapters.

2.2.1.4 Minimizing Procedures

Regardless of the specific curve chosen, the general shape of the post glacial sea level rise in the western Atlantic is clear; with early rapid rise changing to a more gradual increase over the last few millennia. Although the exact date given to this slowing of the rate of sea level rise varies by location (and investigator), throughout the region the wetland development that began ~5-6000 yr BP is commonly attributed to this decrease (Masselink and Hughes, 2003). Because few of the sediment cores discussed in this dissertation extend much beyond this date,

extensive shoreline translation is generally not a problem. Internal evidence can be extremely useful in resolving core-beach distance problems. A standard sequence of ecological environments occurs moving inland from a beach, each of which results in distinctive sedimentary facies, with both transgressive and regressive barrier movement marked by recognizable sedimentary sequences (Roy et al., 1994; Mitch and Gosselink, 2007). Any significant transgression should be detectable in individual cores; i.e. a core in a location transitioning from back barrier wetland to shore front will display a change in deposition environment from dark, anoxic, fibrous organic material to laminated sands and shells. Unlike an event layer, such a change resulting from transgression will not be replaced farther upcore by a resumption of the wetland depositional environment.

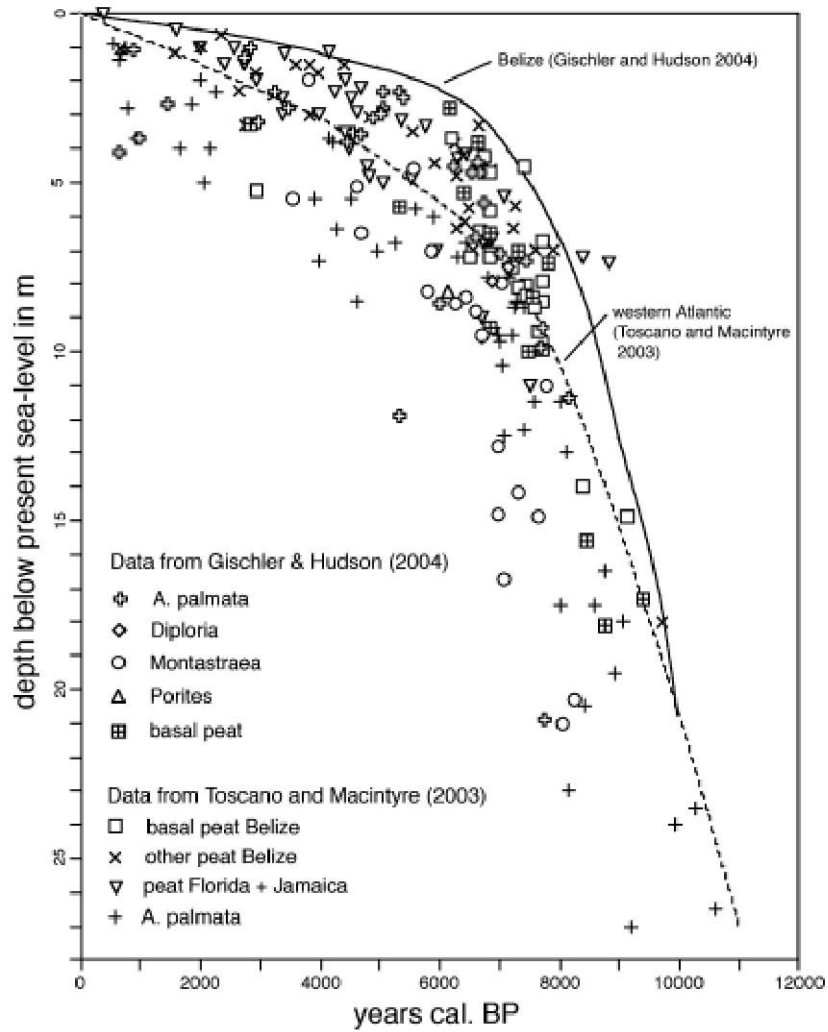
It is important to note that regional sea level changes may not always be expressed at all sites, as local factors, such as sediment supply, erosion, uplift, and subsidence can dominate, thereby negating or reversing regional effects. Coastal regression/progradation can occur locally regardless of direction of sea level regime (Masselink and Hughes, 2003; Psuty, 1992).

2.2.2 Geologic Setting

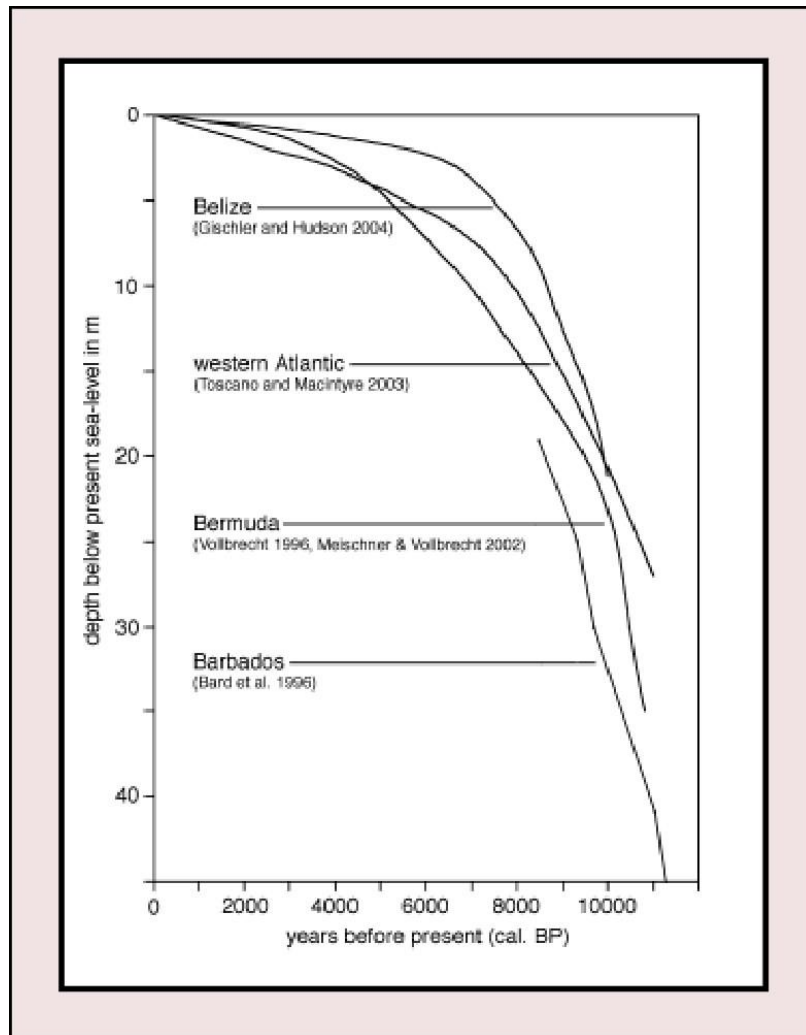
The geologic setting can be extremely important in selecting sites for paleotempestological studies. Geologic influences vary from such large scale effects as plate movement to such local factors as geomorphic stability and beach bathymetry. What follows is a short description of the important geologic influences at the regional level; country and site specific details will be included in the relevant chapters.

2.2.2.1 Global

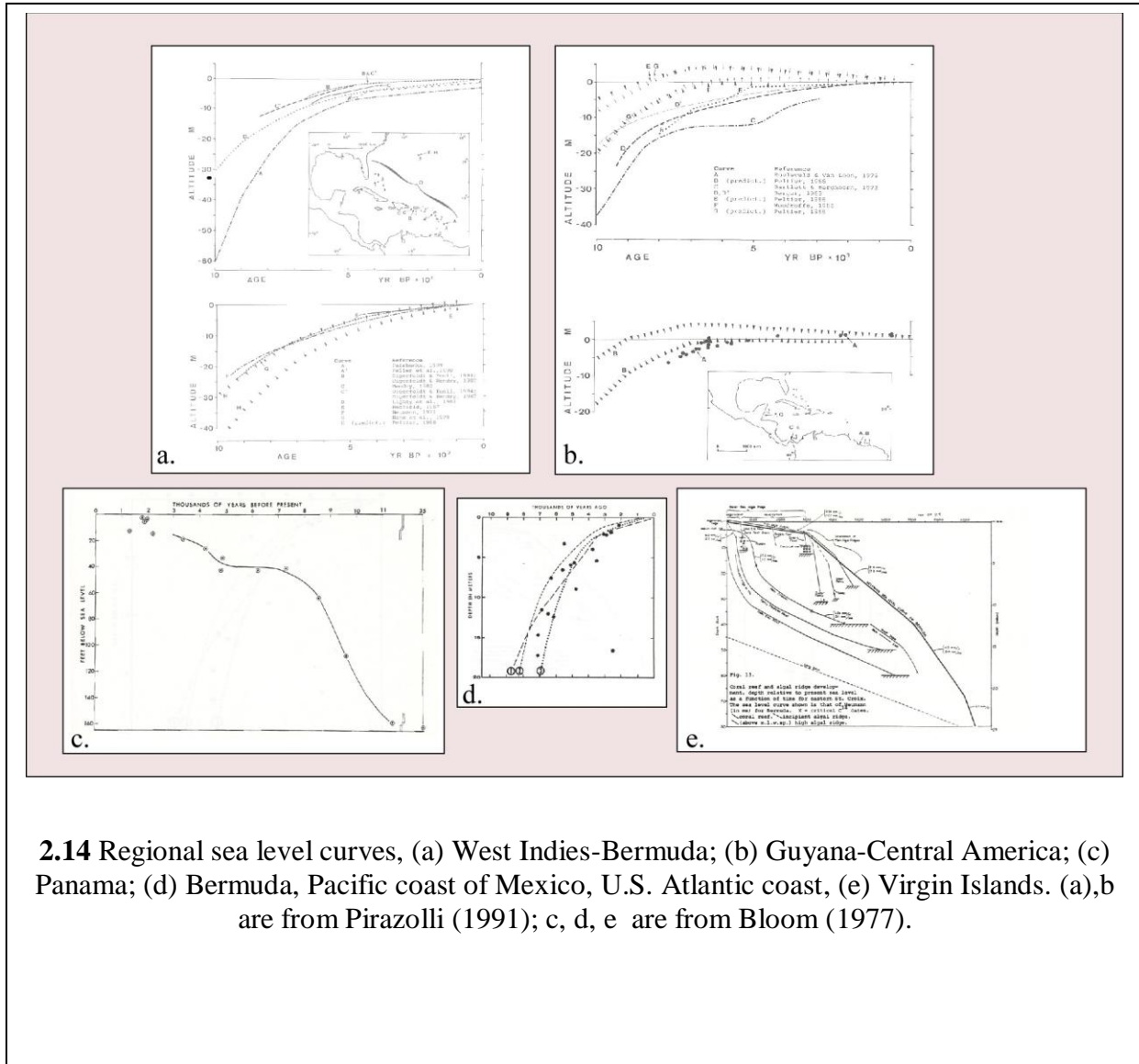
As is well known, the lithosphere of the Earth, consisting of the crust and uppermost mantle, floats on top of the more plastic asthenosphere. The lithosphere is divided into a number



2.12 Belize specific sea level curve derived from a combination of basal peat and coral. From Gischler (2006).



2.13 Four western Atlantic sea level curves showing increasingly higher plotting by date of publication. From Gischler (2006).



2.14 Regional sea level curves, (a) West Indies-Bermuda; (b) Guyana-Central America; (c) Panama; (d) Bermuda, Pacific coast of Mexico, U.S. Atlantic coast, (e) Virgin Islands. (a),b are from Pirazolli (1991); c, d, e are from Bloom (1977).

of rigid plates which are in constant, slow movement, driven by mantle convection. Like saucers moving on the surface of a basketball, these rigid plates converge and diverge in a variety of ways, resulting in large scale movements of continents and oceanic crusts. The tremendous forces involved ensure that the first order control over any region is its geographical position on the plate it occupies, and the relationship between this plate and its neighbors.

2.2.2.2 Regional

Five of these rigid plates come together in the Caribbean region (**Figure 2:15**). The Caribbean Plate (CAR) is sandwiched between the North American Plate (NAP) to the north and east, and South American Plate (SAP) to the south and east, with the Cocos and Nazca Plates (formed from the breakup of the Farallon Plate ~ 23 mya) subducting beneath it along the Middle America Trench off the western edge of Central America (Duncan and Hargraves, 1984; Mann et al., 2007). The boundary between the NAP and SAP is somewhat indistinct, with relative movement being only a few mm/year (McCann, 2006). Although all three plates are moving westward relative to the global hotspot reference frame (Meschede and Frish, 2002), the CAP is moving slowest, (by ~ 1.5 cm/year (Meschede and Frish, 2002) to 2 cm/year (Mann et al., 2002, Dixon and Mao, 1997), resulting in relative westward movement of the NAP and SAP, which are therefore subducting under the eastern edge of the CAR along a 1000 km face (McCann, 2006). Along the southeastern boundary of the CAR the subduction is covered by a large sediment wedge; moving northward it becomes increasingly well-marked by the Lesser Antilles Trench (McCann, 2006). Rounding the corner, the east-west trending boundary is more complicated, confused by a number of microplates and changing from transpressional to collisional to strike-slip moving from Puerto Rico west past Jamaica (McCann, 2006) where the lateral displacement of the NAP and the northern boundary of the and CAR is estimated at

between 120 and 1000 km over the Cenozoic (Lara, 1993; Coates, 1997; Meschede and Frish, 2002). Transitions along the southern CAR-SAP boundary are similar, changing from convergent offshore to strike-slip on the continent.

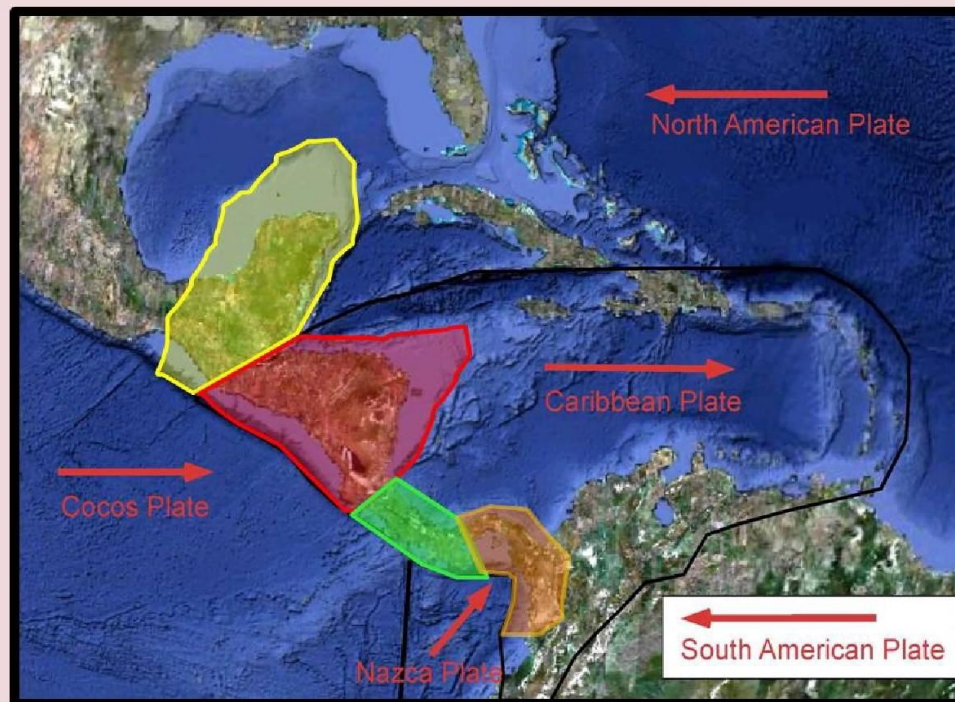
The Central American land mass is split between the NAP and CAR, with the plate division occurring in the Motagua valley in southern Guatemala. Each plate consists of a number of blocks. The northern section of Central America, consisting of Guatemala north of the Motagua, Belize, the Yucatan peninsula, and all of Mexico west to the Isthmus of Tehuantepec, is on the Maya block of the NAP. Southern Guatemala, El Salvador, Honduras, and Nicaragua are on the Chortis block, which is part of the CAR (Donnelly et al., 1990). These two blocks, although located on separate plates, form the nucleus of Central America (Donnelly et al., 1990) and differ significantly, both structurally and stratigraphically, from the southern section of Central America (Weyl, 1980; Escalante, 1990). The southern section, referred to variously as the Isthmian Link (Schuchert, 1935) and the South Central Orogen (Dengo, 1962, Lloyd, 1963) is composed of the Chorotega and Choco blocks (Dengo, 1985), both which are more closely related to western Columbia (**Figure 2:15**). Due to plate position, the entire Caribbean coast of Central America is considered a passive margin (Cortes, 2007).

2.2. 3 Tsunami

Tsunami of varying sizes occur fairly commonly in the Caribbean (Lander et al., 2002; O'Loughlin and Lander, 2003). Because their geomorphic effects can resemble those of hurricanes, a discussion of their frequency, location of occurrence, and the physical properties of their sedimentary signature is necessary here.

2.2.3.1 Calculated Caribbean Tsunami Risk

There are several sources of tsunami; they can form as a direct result of earthquakes



2.15 Tectonic setting of the Caribbean region, showing the five plates and the four blocks relevant to our study.

(usually submarine) or volcanic explosions (and subsequent slumping) or from volcanic flank failure or submarine slides (usually earthquake-generated). All forms occur in the Caribbean region. Shallow earthquakes have been recorded historically along the entire edge of the plate. Due to the configuration of the plates and the composition of the subducting NAP, the northeast section of the CAR is particularly prone to large earthquakes, capable of producing tsunamis. This is also the area of increased potential for “slow” earthquakes, capable of generating large tsunamis, which are believed to result from ruptures of the softer sediments within accretionary prisms (McCann, 2006). Submarine slide activity is a serious tsunami risk in the northeastern Caribbean, as demonstrated by large paleo slope failures along the Puerto Rico trench (ten Brink et al., 2006). Elsewhere submarine slides are made possible by a large accretionary prism and several areas of steep submarine slopes ($>10^0$) within transtensional belts characterized by high angle faulting (McCann, 2006). An estimation of the regional earthquake-generated tsunami hazard, including earthquake generated submarine slides, is shown in **Figure 2:16**.

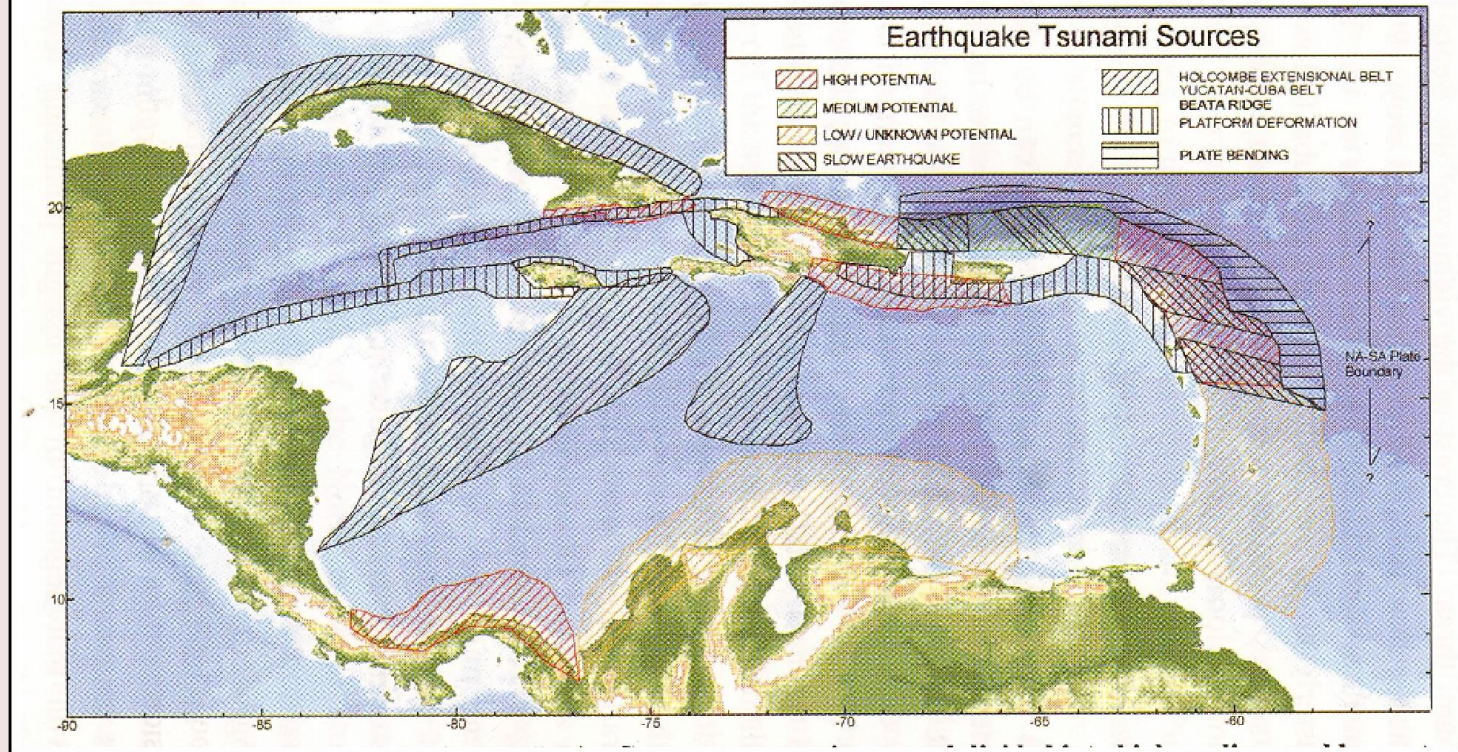
Volcanic generated Caribbean tsunamis are restricted to the southeastern Caribbean, where the Lesser Antilles, an island arc, features more than a dozen volcanoes, both submarine and terrestrial, eruptive and effusive (Pararas-Carayannis, 2006; Sigurdsson et al., 2006). Several of the eruptive volcanoes have exploded violently during the historic period, at times generating tsunamis, while flank failure is a common occurrence on the effusive shield volcanoes. Submarine dome collapse is another potential source of tsunamis.

Paleodata indicates that at least three tsunamis, probably generated by large submarine slides on the western flanks of the Lesser Antillean islands have impacted the islands of Aruba, Curacao, and Bonaire in the far southern Caribbean during the late Holocene (Scheffers et al., 2002). More generally, evidence of Holocene as well as Pleistocene tsunamis have been found

throughout the Lesser Antilles, including the islands of St. Lucia, Barbados, Guadeloupe, St. Martin, and Anguilla (Kelletat et al., 2004; Scheffers et al., 2002). Evidence from the Bahamas indicates an extremely large Pleistocene age tsunami that transported boulders weighing > 2000 tons, as well as two Late Pleistocene age tsunami that transported boulders weighing > 2000 tons, as well as two Holocene events. Significantly, these events, as well as those responsible for paleo tsunami deposits found on Barbados, St. Martin, and Anguilla indicate that the waves approached from the east, indicating teletsunami, originating in the open Atlantic (Kelletat et al., 2004; Scheffers and Kelletat, 2006).

2.2.3.2 Sedimentary Signatures of Tsunami

Tsunami, like hurricanes, can exhibit great variability during their interface with the coast, resulting in a wide range of depositional features (Dawson and Shi, 2000; Peters et al., 2007). However, a fairly large literature describing the sedimentary signature of tsunami has developed over the last two decades, from which certain general characteristics can be identified. After generation, tsunami move across the ocean at great speeds (up to 800 kph), until nearing the coast, where due to their long wave lengths (typically in the 100s of km) they begin interacting with the bottom at much greater depths than storm waves. As a result, while still out on the continental shelf tsunami begin suspending and transporting benthic material as they slow and steepen, resulting in potentially tremendous wave heights when approaching the coast (Masselink and Hughes, 2003; Morton et al., 2007). On land the waves are bi-directional, moving inland until reaching zero forward velocity and then rolling back to the sea, a movement (called backwash (Dawson and Shi, 2000). Often marine material is transported inland and terrestrial material transported seaward. Tsunami can occur as wave sets, with each wave capable of leaving two distinctive sedimentary layers (one for each direction of flow) and/or eroding the



2.16 An estimation of Caribbean earthquake-generated tsunami hazard, including earthquake generated submarine slides. From McCann (2006).

material deposited/transported by the previous wave (Nanayama et al., 2000). Perhaps the most distinctive feature of tsunami is their enormous energy, as they are capable of moving, overturning, transporting and emplacing extremely large boulders at very great heights above sea level. The famous Huloepoe Gravel, which, at 375 m above sea level contains basalt boulders and coral fragments, has been identified as a tsunami deposit (Dawson and Shi, 2000).

Although the investigation of tsunami has occurred worldwide, the most studied area has been Cascadia, along the northwest Pacific coast of the United States, where a great number of sites have been studied in detail (Atwater, 1987, 1992, 1996; Atwater and Yamagucci, 1991; Peterson et al., 1993; Darienzo et al., 1994; Atwater and Hemphill-Haley, 1996; Clague et al, 2000; Kelsey et al., 2002; Peters et al, 2007). One of the most famous findings has been a giant (estimated Richter scale 9) prehistoric earthquake that has been so precisely identified and dated by the correlation of Yurok oral history and historical record of the tsunami arrival time in Japan that researchers have been able to resolve the time of occurrence to the hour (21:00 local time, January 26, 1700 AD) (Satake et al., 1996).

In general, tsunami deposits include a continuous, moderately well sorted, massive sand sheet, often mixed with terrestrial material, containing a mix of marine organisms from various depths. Boulders are often mixed in, and a series of subunits and fining upward sequences related to different waves may be encountered. Occasionally the entire interval is capped by a mud layer, resulting from the final settling of fine clay particles. Typically these deposits erode the underlying material, severing the covering vegetation and entraining clasts (Dawson and Shi, 2000; Nanayama et al., 2000; Goff et al., 2004; Tuttle et al., 2004; Kortekaas and Dawson, 2007; Peters et al., 2007). These deposits usually thin and fine landward, with the sand sheets becoming discontinuous before terminating. Most remarkable are the distances inland that the deposits can be found, extending up river valleys as far as 10 km (Peters et al., 2007).

Deposition usually terminates below/seaward of the farthest/highest inundation, as evidenced by microfossil evidence (Hemphill-Haley, 1995a, 1995b, 1996) Eyewitness accounts of tsunami waves can be chilling, as is that by a Lieutenant Billing, who was aboard a US postal steamer that was carried two miles inland at “unbelievable speed” by a “half-liquid, half-solid mass of water and sand” in 1868 near Arica, Chile (Myles, 1985).

2.2.3.3 Distinguishing Tsunami and Storm Deposits

Several recent articles have examined the differences between tsunami and storm generated clastic deposits (Nanayama et al., 2000; Goff et al., 2004; Tuttle et al., 2004; Kortekaas and Dawson, 2007); with “storms” including nor’easters (Tuttle et al., 2004), and winter storms (Kortekaas and Dawson, 2007), as well as tropical cyclones (typhoons and hurricanes). Some investigations have examined historically identifiable examples of each type in the same location, thereby minimizing the differences resulting from different geomorphic parameters (Goff et al., 2004; Kortekaas and Dawson, 2007). The ability to differentiate the two events in the sedimentary record is, of course, crucial for determining accurate long-term hazard regimes for either. Kortekaas and Dawson (2007) call this ability the “main problem”. General consensus exists that sufficient fundamental differences exist between the sedimentary signatures to distinguish the two types of events. Not surprisingly, the differences relate to the differing energy processes involved, particularly the tsunami’s early contact with the sea floor, the bidirectional nature of the tsunami onland flow, and the short duration of inundation. As with tropical cyclones, post- event preservation needs to be considered (Dominey-Howes et al., 2006; Kortekaas and Dawson, 2007).

The most important differences are:

1. Tsunami deposits are generally more massive and less well-sorted (Dawson and Shi, 2000;

Goff et al., 2004; Tuttle et al., 2004; Morton et al., 2007). This applies to both the grain size of the sand within the sand sheets and the common bimodal deposition of boulders and finer material (Goff et al., 2004). Also, delta foreset bedding is more common in storm layers, particularly when encountering water barriers (Nanayama et al., 2000; Tuttle et al., 2004).

2. Bidirectional flow is almost universally lacking for storm deposits, meaning that, unlike tsunami deposits, terrestrial material is rarely transported seaward by storms. Also tsunami deposits are likely to contain a greater percentage of sea floor material, including a mix of benthic organisms from greater depths (Dawson and Shi, 2000; Dawson and Stewart, 2007; Morton et al., 2007).

3. Tsunami more commonly erode the underlying material and/or sever the vegetation. They also are more likely to incorporate rip up clasts in their bottom layers. In co-seismic tsunami accompanied by subsidence, entire ecological communities (marshes, forests) can be buried (Atwater and Yamagucci, 1991; Dawson and Shi, 2000), which, of course, does not occur with hurricanes.

4. Tsunami can be tremendously large. A rockslide-generated tsunami in Alaska in 1958 produced a tsunami cresting at >1700 feet (Miller, 1960), while the tsunami associated with the Chicxulub bolide impact ~ 65 mya has been calculated as reaching 5 km in height (Smit et al., 1996). Because of this extreme magnitude, larger material can be transported much farther/higher inland (Dawson and Shi, 2000; Goff et al., 2004; Tuttle et al., 2004).

Although these studies indicate that tsunami and storm deposits can be distinguished under ideal conditions, it does not mean that this is always possible. Many of these studies were conducted on well recorded surface deposits, or with the aid of trenching. Bi-directional flow can be much harder to recognize 3 meters down in a 2" diameter core. In Portugal, Kortekaas and

Dawson, (2007) found it “impossible” to distinguish tsunami and other sand layers within cores. Additionally, smaller tsunami may be harder to identify as many of the distinguishing marks will generally be more recognizable for large tsunami (i.e. size/distance/height of material transported, erosion of basal material, presence of rip up clasts, backwash of terrestrial sediments/biotics), while degree of sorting can be masked by bioturbation, especially in thin layers. The ability to clearly distinguish the sedimentary signatures of equivalent size storms/tsunami is uncertain, especially if the energy generated by the tsunami is below the level required to transport boulders, erode the existent sediment surface, rip up plants and clasts or reach to the beginning of back barrier vegetation (and so does not transport terrestrial material in the backwash). Microfossil identification and grain size analysis might be necessary to correctly classify some of these smaller, less distinctive events (Kortekaas and Dawson, 2007).

There is even some debate over the unequivocal identification of agent of transport of large blocks, with Robinson et al. (2006) presenting anecdotal eyewitness accounts of coral boulders up to 33 tons in weight being moved by hurricanes in Jamaica. Hernandez-Avila et al. (1977) provide calculations demonstrating that hurricane waves are sufficiently powerful to breakup and transport large *Acropora palmata* blocks from 8-10 m depth 300 meters offshore to build boulder ramparts 4.5 m above mean sea level.

It appears that large tsunami can be distinguished reliably from storm deposits, with potential confusion/misidentification mainly restricted to large storm and smaller tsunami deposits in areas where trenching is not possible.

2.2.4 Vegetation

Vegetative cover is another important consideration in paleotempestology. Amount and type of vegetation can affect the transportation and deposition of materials during/following a

storm, thereby influencing not only the amount and size of material deposited at any location but also the maximum distance that materials will be moved. Calibration of relative storm intensity by sedimentary evidence in a single core or transect therefore requires recognition of vegetation changes, as does recognition of facies change in order to control for shoreline movement. Because climatic factors are the major constraints on an area's vegetation, a general knowledge of low frequency regional climate changes is necessary in order to interpret sedimentary evidence accurately in regard to hurricane history. Large scale changes that significantly change a location's depositional environment (fluctuations in water level, for example) can mask changes in hurricane activity.

A brief synopsis of general earth history is presented, followed by a more detailed Holocene climate history of the Caribbean.

2.2.4.1 General

The earth was formed ~4.6 billion years ago, over which time the atmospheric composition and the climate have changed dramatically. Earth history has been divided into named intervals by geologists. The most important divisions are the two eons; the Precambrian, which cover >88% of the planet's history, and was characterized by extremely simple life forms, and the Phanerozoic, which begins with the first fish and shellfish (Christopherson, 2003). The Phanerozoic, beginning 540 million years ago (mya), is divided into three eras, the Paleozoic, Mesozoic, and Cenozoic. The Cenozoic, beginning at the end of the Cretaceous ~ 64.7 mya, encompasses two periods, the Tertiary and the Quaternary. The Quaternary, covering the last ~1.8 million years, consists of two epochs, the Pleistocene and the Holocene. The Pleistocene had the lowest temperatures since the Paleozoic, and the first ice ages since the Permo-Carboniferous, ~250 mya. This cooling has been attributed to the positioning of the continents,

which has led to increased polar circulation (Mikolajewicz et al, 1993), and a 15-20⁰C drop in polar sea surface temperatures from the beginning of the Tertiary (Shackleton and Kennett, 1975). A contributing factor has been the increase in albedo related to both the polarward drift of the major landmasses and a tectonic driven increase in high altitude grasslands and deserts and subsequent increased scrubbing of atmospheric CO₂ (Kennett, 1982; Liu, 1988; Liu et al., 1986; Shi et al., 1986; Kuhle, 1988, 2004, 2007; Ruddiman and Kutzbach, 1991; Raymo et al., 1988). Massive polar ice sheets, continental in size, have repeatedly occurred during the Pleistocene, as evidenced by ice cores from Greenland and Antarctica (Imbrie and Imbrie, 1979; Fullerton and Richmond, 1986; Alley and Bender, 1998; Alley, 2000; Bender et al., 1994; Dansgaard et al., 1993; Petit et al., 1999) and deep sea sediments (Bond et al., 1993; Bond and Lotti, 1995). The last four glacial periods are particularly well studied, having left abundant terrestrial evidence (Richmond and Fullerton, 1986). The longer glacial periods (~100,000 years in length) have been separated by shorter interglacial periods (~10,000 years in length). The latest glacial, the Wisconsin, reached its nadir, referred to as the Last Glacial Maximum (LGM) ~18,000 BP, after which warmer temperatures resulted in melting of the ice sheets. Due to both astronomical forcings and complex feedback systems the warming has been neither linear or even unidirectional. ~12,000 cal yr BP, following the warmer Bölling and Allerød periods, a thousand year cold interval, named the Younger Dryas after a common European alpine/tundra wildflower *Dryas octopetala* established itself. The Younger Dryas was at least hemispheric in extent, affecting all of the NA, and perhaps larger, as evidenced by sediment (Hughen et al., 1996; Haug et al., 2001) and ice cores (Thompson et al., 1995) from tropical areas. This 1000 year return to cold temperatures is commonly attributed to the shutdown of the Meridional Overturning Current (MOC) in the NA as the result of massive freshwater flooding of the surface

NA. This flooding was usually been attributed to the rapid draining of large proglacial lakes down the St. Lawrence valley following melting of the blocking glaciers (Teller, 1995; Flower and Kennett, 1990; Broecker et al., 1989; Marchitto and Wei, 1995; Brown and Kennett, 1998). Recently, however, researchers have suggested that this melting might have been triggered by the explosion of an extraterrestrial object over Canada (Firestone et al., 2007; Kennett et al., 2009). The warm Holocene began 10,000 years ago at the end of the Younger Dryas.

2.2.4.2 Circum- Caribbean Climate History

2.2.4.2.1 History of Regional Paleoclimatic Studies

The climatic history of the region can, of course, be examined by a great variety of means. Pollen studies reveal changing plant assemblages, which can be related to climatic changes, especially through the use of transfer functions and response surfaces, although the magnitude of the vegetative response time and the appropriate application of the palynological record as a proxy of climatic conditions is debated (Davis, 1981, 1984). Similarly, investigations of the relative abundance and fossil assemblages of diatoms, phytoliths, and foraminifera can also yield much useful climatic information. More direct proxies of specific climatic parameters such as precipitation and temperature are supplied by isotopic examinations, particularly the $\delta^{18}\text{O}$ ratio of marine cores and ostracod/gastropod shells obtained from closed basin lakes. Stratigraphic geochemical and lake level analyses can be utilized to understand gross climatic change, a method that, again, is particularly effective in closed basin lakes. Since all of these proxy records display different responses to changing climatic conditions, multi-proxy approaches are generally more successful in identifying changes accurately. The effect of rising sea level is particularly important in the area, given the prevalence of data supplied by lakebed sediments taken from locations where the phreatic aquifer is strongly affected by sea level

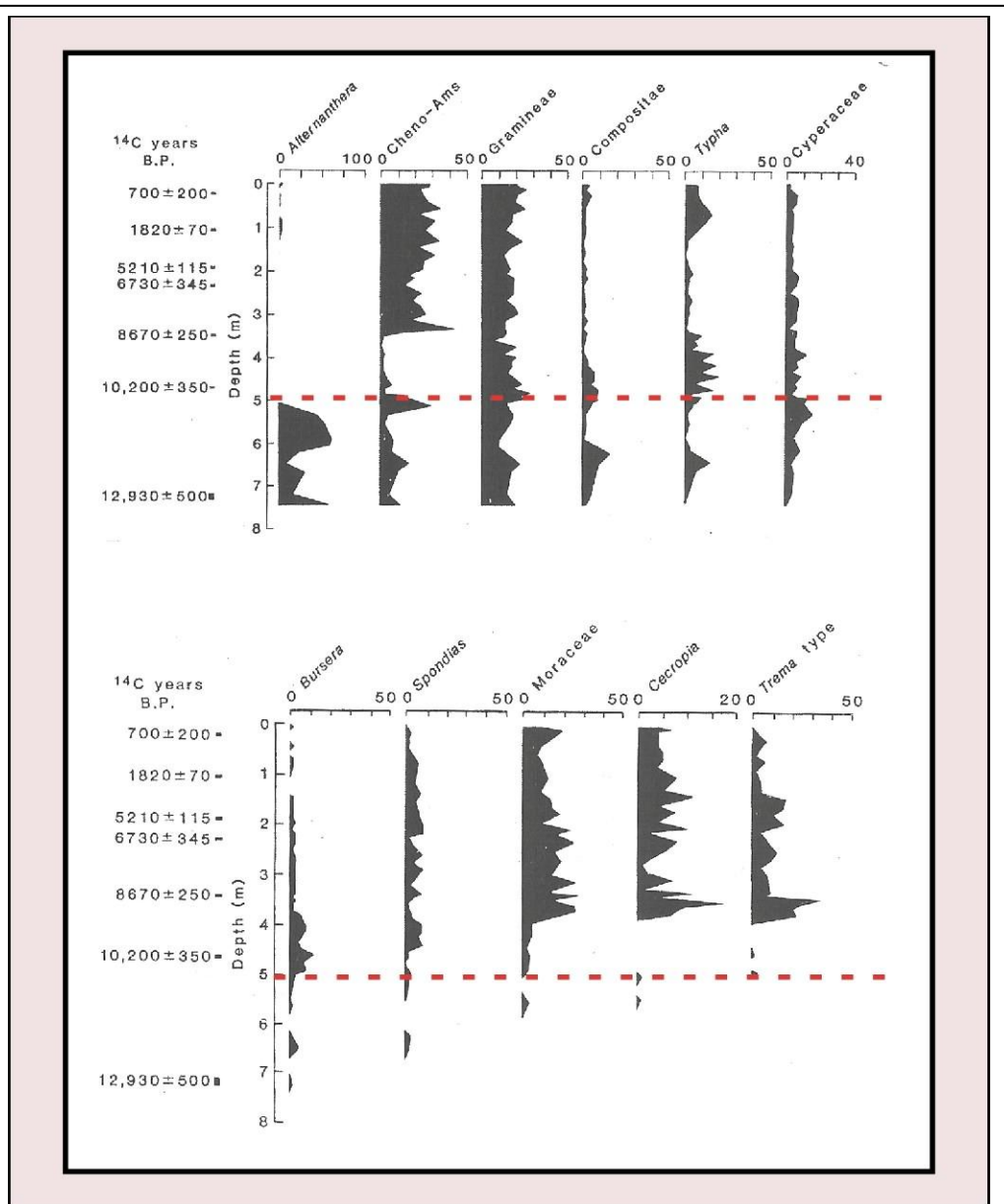
changes. Naturally, accurate and correlatable dating control is necessary in order to reconstruct the regional picture accurately.

Although this discussion primarily focuses on the region's Holocene history, mention should be briefly made of the conditions that existed during the late Pleistocene, which was much colder even at tropical latitudes, as evidenced by the formation of mountain glaciers at high elevations in central Mexico, Guatemala, Costa Rica, and the Dominican Republic (Horn, 2007). Several studies have obtained significant Pleistocene records, such as the 120,000 year record from the Wallywash Great Pond in Jamaica (Street-Perrot et al., 1993), and especially the Funza-2 core from Colombia, which reaches ages of 450,000 years (Marchant et al., 2002). Evidence from this core demonstrates that temperature and precipitation are not the only important atmospheric controls on vegetative response, but that over longer periods atmospheric CO₂ levels have played an important role in community composition, with the biotic community demonstrating a degree of secular evolution. Unique combinations of these three components significantly different from Holocene conditions occurred during the Pleistocene, resulting in no-analog biotic assemblages. Throughout Central America, mean temperature was probably 5°-6° C lower at LGM than at present, indicated by a regional descent of montane taxa of ~ 800 m, approximately matching a 1000m pantropical descent of alpine glacier (Colinvaux, 1997). Changed circulation patterns reduced rainfall over some of the Caribbean lowlands (Peten and Belize were probably arid shrub/savanna), but forests seem to have persisted throughout the Pleistocene, though with several non analog assemblages resulting from the periodic invasion of the lowlands by montane plants (Colinvaux, 1997).

Although early studies generally lacked close dating control, general regional climatic trends were clearly recognized. One of the earliest important paleoenvironmental reconstructions

was based on a study of a 7.5 m core from Lake Valencia, Venezuela, that utilized chemical, paleontological, and mineralogical analyses to identify the basic late Pleistocene/Holocene changes (Bradbury et al., 1981). Based on seven ^{14}C dates (presumably of bulk sediments, since this seems to predate AMS testing methods), the authors divided the core into three major zones. Zone 1 covers the period from 13 ^{14}C kyr BP to 10 ^{14}C k BP, during which period the area was an intermittent saline marsh, surrounded by dry savanna. Zone 2 occurred from ~ 10 ^{14}C kyr BP to 8.7 ^{14}C kyr BP, during which a permanent lake with fluctuating water and salinity levels was established, along with a gradual increase in arboreal taxa, particularly of early successional species. Zone 3 covers the period from ~ 8.5 ^{14}C kyr BP to the present, during which the lake became less saline and began discharging on a regular basis, while the surrounding environment achieved a basically modern vegetative assemblage (Bradbury et al., 1981).

These changes, of course, can be interpreted as the change from a cold and dry Pleistocene to a warmer and wetter Holocene, marked by a dramatic lithologic change at around 10.5 ^{14}C kyr BP. The authors found evidence for maximum lake freshness, implying maximum precipitation, ~ 3 ^{14}C kyr BP, with two periods of non-discharge since 8.5 ^{14}C kyr BP, with the second endorheic period including the Pleistocene-Holocene boundary. This boundary is clearly discernible in the pollen diagram (**Figure 2:17**), especially in the disappearance of the marsh taxa (*Alternanthera*), ~ 10.2 ^{14}C kyr BP. *Typha* can be seen as a proxy for the increase in littoral communities resulting from the expanding lake, while the increase in species such as *Bursera*, *Spondias*, *Moraceae*, *Cecropia*, and *Trema* indicate the increase in forest species (Bradbury et al., 1981). The appearance of the Chenopodiaceae types (Cheno-Ams), mark the establishment of the modern pollen assemblages. Diatom and arthropod analyses are in rough agreement especially in the disappearance of the marsh taxa (*Alternanthera*), ~ 10.2 ^{14}C kyr BP. *Typha* can



2.17 The Pleistocene-Holocene boundary as identified in the palynological record from Lake Valencia, Venezuela, displaying (a) nonarboreal species; (b) arboreal species. The red dashed line marks the Pleistocene-Holocene boundary. From Bradbury et al. (1981).

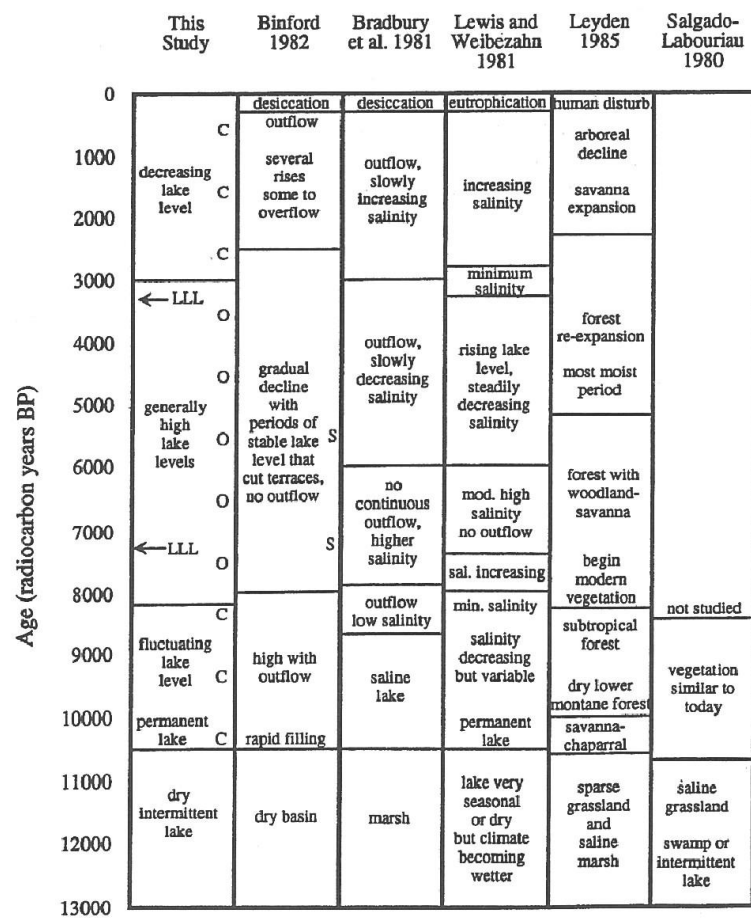
be seen as a proxy for the increase in littoral communities resulting from the expanding lake, while the increase in species such as *Bursera*, *Spondias*, *Moraceae*, *Cecropia*, and *Trema* indicate the increase in forest species. The appearance of the Chenopodiaceae types (Cheno-Ams), mark the establishment of the modern pollen assemblages. Diatom and arthropod analyses are in rough agreement with these changes (Bradbury et al., 1981).

Other studies of Lake Valencia have generally confirmed the validity of these findings. Leyden (1985) suggests a wetter early Holocene, based primarily on pollen data, arguing that the early Holocene taxa are the most mesic in the record, with the mid Holocene forest being more open as the mesic taxa moved upslope. Overall, however, she proposes the same general pattern as the earlier study, as the pollen record shows a transition from a saline marsh, to a halophytic littoral environment with an increasing shrub component, to a dry lower montane forest, to a *Brosimum* dominated semi-evergreen and deciduous subtropical forest, and eventually, by ~ 8.3 ^{14}C k yr BP a forest similar to the present.

A much more recent study of the lake (Curtis et al., 1999), reached very similar conclusions by means of $\delta^{18}\text{O}$ analysis. The principle of such analysis is that in closed basin lakes the $^{18}\text{O}/^{16}\text{O}$ ratio of the lake water is principally determined by the evaporation/precipitation (E/P) ratio. Since this ratio is reproduced in the shells of crustaceans living in the lake, these shells can be used as a proxy for the E/P ratio, and, by extrapolation, increasing/decreasing aridity. Normally several shells of the short lived ostracods are combined in a single sample since, due to repeated moultings, their shells only record the short term, seasonally varying $^{18}\text{O}/^{16}\text{O}$ ratio. Since the longer lived, macroscopic gastropods accrete only single shells, which reflect the average E/P condition during their lifetimes, a test sample can consist of a single shell. This study tends to support the earlier conclusions of Bradbury et al.

(1981) in that the $\delta^{18}\text{O}$ record indicates that the period of maximum precipitation occurred from the mid to early Holocene ($\sim 8.2 - 3 \text{ }^{14}\text{C}$ kyr BP) (Curtis et al., 1999). This study was able to improve the dating chronology due to the use of 13 ^{14}C dates, including nine AMS terrestrial wood samples, and thereby avoiding the Hard Water Lake Error problem (HWLE) inherent in the use of lake sediments in limestone areas. Four additional dates obtained from ostracod shells were used to calibrate the HWLE, which in this case proved to be non-existent. The general inter-study agreement as to the vegetative/hydrological/climatic history of the Lake Valencia area can be seen in **Figure 2:18** (Curtis et al., 1999).

Another well-studied location is Lake Miragoane, Haiti. An important early study was a 10.5 kyr reconstruction of climatic change in the Caribbean based on a $\delta^{18}\text{O}$ analysis of ostracod shells (Hodell et al., 1991). Approximately the same general changes were observed there as in Lake Valencia; namely a dry period correlating to the late Pleistocene, followed by increased precipitation and temperature levels, with the period of maximum precipitation occurring from the early to mid Holocene, followed by a return to significantly dryer conditions after 3.2 k BP, with the level of aridity increasing again at 2.4 k BP; with a short period of increased precipitation from 1.5 – 0.9 k BP. The palynological record shows changes in the abundance of mesic taxa correlating with the lake level and isotopic records. A pollen based study of the lake (Higuera-Gundy et al., 1999) yielded very similar results. The dates of the major climatic changes occurring in Lake Miragoane do not match perfectly with those from Lake Valencia, generally being somewhat younger. However, the accuracy of the Lake Miragoane dates are perhaps debatable, since the dating control consists of 13 samples from the 7.7 m core, mostly AMS tested ostracod shells. All of the ostracod dates were reduced by 1,025 years, which was the amount of HWLE, based on the comparison of a single terrestrial wood sample with an



2.18 Paleoenvironmental history of Lake Valencia summarized from six separate studies. From Curtis et al. (1999).

adjacent ostracod sample.

Generally though, the two lakes display very similar paleoenvironmental patterns, which are supported by other regional records. Studies conducted in Floridian sinkholes support the general trend, although the dating differs somewhat (Watts and Hansen, 1994). In fact, pollen records of the Pleistocene-Holocene boundary from the Peten (northeast Guatemala) display such similar trends that Leyden (1984), concludes that the shift from cold/dry to warm/wet was pantropical in the lowlands. The Pleistocene-Holocene transition is also an important and obvious marker in the longer cores, such as the 120,000 year Jamaican record (Street-Perrot et al., 1993). A pollen and phytolith study from Lake La Yeguada in Panama (Piperno et al., 1989) further supports the extent and timing of the transition. Again, a dramatic change occurred around 11,000 ^{14}C yr BP, in this case estimated as a 5°C increase in temperature accompanied by increased precipitation. These calculations are based on an 800 meter depression in montane taxa during the late Pleistocene. Other studies (Bartlett and Baghoorn, 1973; Liu and Colinvaux, 1985) suggest similar tree line depression in Panama and the Amazon.

A common concern in several of the early studies was the question of the location/existence of Pleistocene refugia for the mesic taxa. The idea had been advanced (Haffer, 1969) that the tropic response to glaciation had been expressed mainly as a reduction in precipitation, with average temperatures remaining fairly constant. This implies that the reemergence/colonization of mesic taxa required geographically specific refugia for these species during the periods of intense glaciations. Based on the modern distribution of such diverse organisms as plants, anoline lizards and butterflies, certain areas were identified as the potential sites of refugia, including both Lake Valencia and the Peten (Vanzolini and Williams, 1970; Prance, 1973; Brown et al., 1974; Toledo, 1982). However, the severe aridity of these sites

during the late Pleistocene, as evidenced in the previously discussed studies, clearly show that these areas could not, in fact, have served as refugia. In order to account for the persistence of these mesic taxa, several hypotheses, such as specific, geographically limited micro-habitats (riparian forests) and adaptive mechanisms (low but persistent species abundance) have been suggested.

2.2.4.2.1.1 The Maya Lowlands

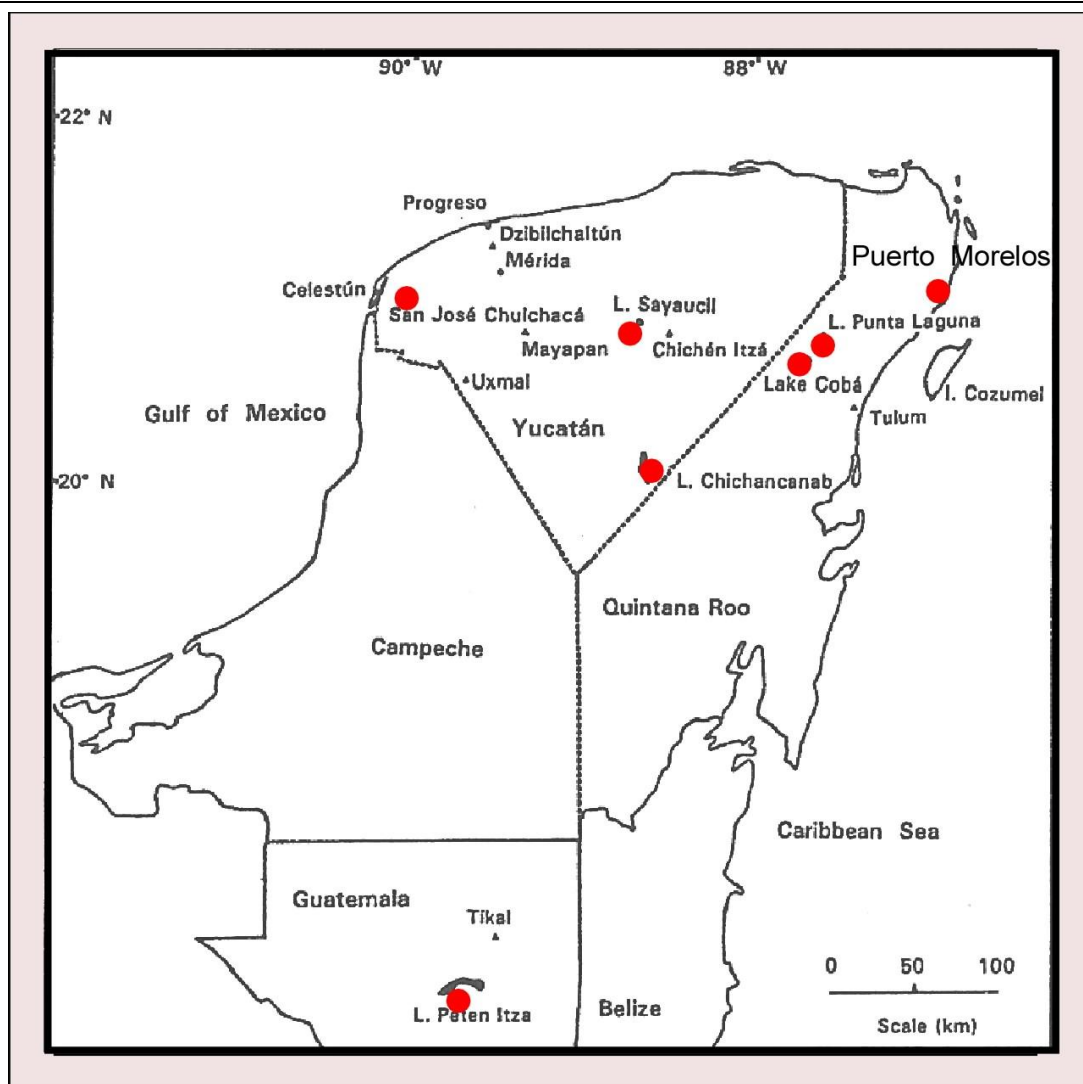
The most intensely studied area in the region is probably the Yucatan Peninsula, the northern half of which is presently within the borders of Mexico, while the southern half lies within Belize and Guatemala. The abundance of paleoenvironmental investigations in the area is attributable to the fact that this was the heartland of the ancient Maya civilization, whose sudden cultural collapse ~ AD 900 during the Terminal Classic period may possibly have been related to climatically driven environmental stress, particularly changes in the precipitation regime (Hodell et al., 1995, 2001; Gill, 2001, Haug et al., 2003). Paleoenvironmental reconstruction for the area has been particularly difficult due to the possible confusion, existent across a wide range of proxy records, between anthropogenic and climate driven environmental changes (Horn, 2007). For example, reduction in forest taxa may have resulted from either increased aridity or clearing for agricultural/cultural purposes; increased sedimentation rates may have resulted from agriculturally induced erosion or climatic change; lake level changes may result from hydrologic engineering or altered precipitation regimes, just as lowered water tables may result from either improved drainage, or reduced precipitation. The effort to distinguish between cultural and climatic effects has led to a general sharpening of the investigative tools, and particularly, an increasingly multi-proxy approach. The quality of the area's archeological record permits a more accurate estimate of anthropogenic input than in many other parts of the world, thus facilitating

the development of methods for separating the two factors. For example, the existent knowledge is of sufficient resolution to permit estimates of average population density for large areas and total population of many major population centers for over 1000 years (Culbert and Rice, 1990). Naturally, the comingling of anthropogenic and climatic effects is not unique to the area, but the quality of the archeological record, combined with the rapidity of the large scale alteration of the environment, followed by an even more abnormally rapid return to near natural conditions, aids in establishing environmental baselines, which, in turn, makes this area a superior laboratory for the untangling of these mixed webs.

As in most Holocene records, the main focus of paleoenvironmental research has been lakebeds, originally mainly palynologically driven, but rapidly expanded to include the entire spectrum of investigative tools. Although the general outline of the area's Holocene climatic history is similar to that of the region as a whole, the intensity of the investigation has resulted in the discovery of significant local variations. The cultural history of the area can itself be used as a proxy of climatic conditions, with some startling high resolution correlations with proxy climatic records (Haug et al., 2003), although, naturally, these correlations must be regarded with great caution in order to avoid attributing unproved causality.

2.2.4.2.1.1 Yucatan

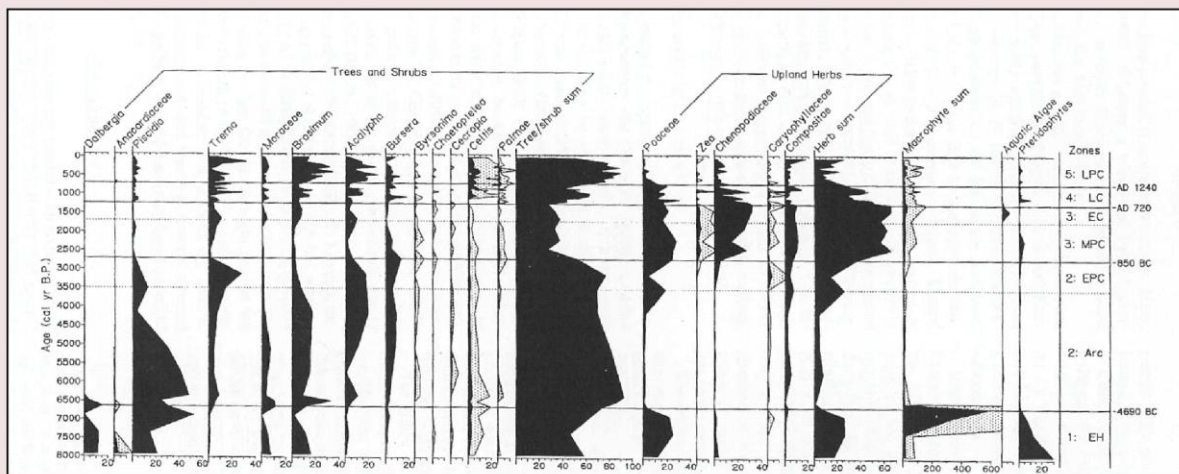
A representative study for the northern Maya lowlands is the multi-disciplinary investigation of Lake Coba, in Quintana Roo, Mexico (Leyden et al., 1998), where an 8.8 m core, covering ~ the last 8.5 k years, was obtained. Coba was an important Late Classic (AD 550-850) city, with an estimated population of ~ 60,000 people. (See map, **Figure 2:19**). Palynological, sedimentological, geochemical, diatomical, and loss on ignition (LOI) analyses were conducted; dating control was by radiometric dating of bulk sediments, ostracod shells, and



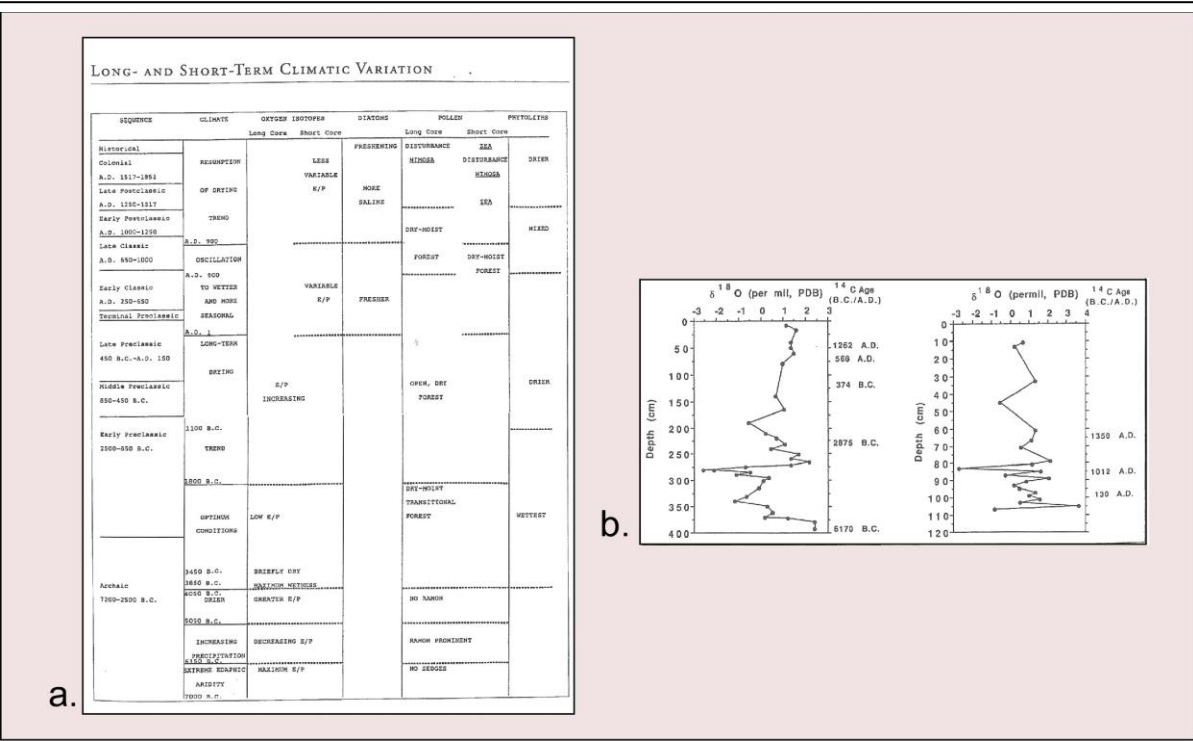
2.19 Map of Yucatan, showing sites mentioned in the text, modified from Leyden et al. (1997).

a single terrestrial wood sample (thermoluminescence and optically stimulated luminescence methods proved unsatisfactory). The dating remained somewhat tentative as a HWLE of 1320 years was subtracted from all dates, based on the age difference between a paired ostracod sample and an adjacent wood sample. Nevertheless, a detailed pollen record was produced, divided into five periods, assigned absolute dates, and correlated to cultural events (**Figure 2: 20**). This diagram presents examples of both anthropogenic and climatic control of the pollen record. The changes at the bottom of the core clearly reflect climatic effects; first the creation of a wooded swamp resulting from a raising phreatic aquifer accompanying sea level rise (Zone 1), and then the expansion of the dry forest (Zone 2). The appearance of *Zea mays* pollen at the beginning of Zone 3 marks the inception of significant anthropogenic influence, with an accompanying decrease in forest and an increase in disturbance taxa continuing through Zone 4, while Zone 5 marks a return to more “natural” (climatically controlled) pollen assemblages. That the disequilibrium between the diatom and pollen records was interpreted as evidence of hydrological engineering (the dyking of the lake), is an example of both the benefit of multi-proxy investigations and the complex relationship between natural and anthropogenic influences.

A study based on cores from the cenote San Jose Chulchaca provides a useful comparison to Coba, as this cenote, located farther to the west (see map-**Figure 2:19**) along the negative axis of a steep precipitation gradient, occupies an area of maximum aridity and minimum human disturbance (Leyden et al., 1996). Again, a multidisciplinary approach was taken, expanded to include the analyses of stable isotopes, charcoal and phytoliths, the results of which are shown in **Figure 2:21a**. Of particular interest is the strong variability in the $\delta^{18}\text{O}$ record (**Figure 2:21b**), presumably due to the small size of the lake (130 m in diameter), and seasonal variations (ostracods being the organisms tested). By comparing the paleoenvironmental records of these



2.20 Pollen record from Lake Coban, Yucatan. From Leyden et al. (1997).



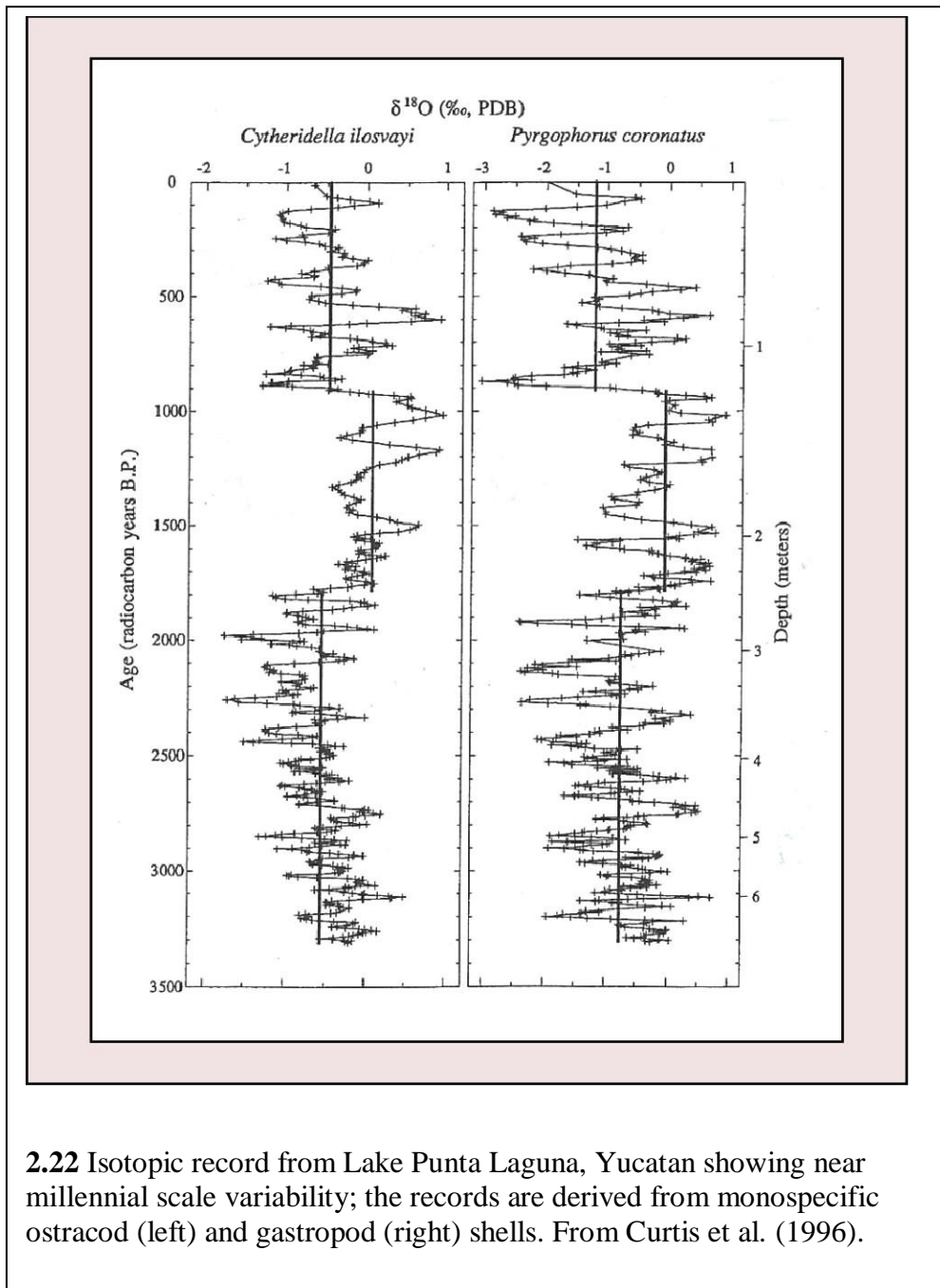
2.21 Environmental history for Cenote San Jose Chulchaca, Yucatan. Summary of multi-proxy results correlated with ancient Maya cultural epochs (a); oxygen isotopes from ostracods shells in a long core (right), and gastropod shells from a short core (left) (b). From Leyden et al. (1996).

two lakes, along with Lake Sayaucil which occupies an intermediate position along the precipitation gradient, Whitmore et al. (1996) found evidence of low frequency climatic change; namely that the east-to-west precipitation gradient may have been more intense in the past.

A $\delta^{18}\text{O}$ based investigation of monospecific ostracods and gastropods conducted at Lake Punta Laguna (Figure 3) also shows significant low frequency climatic oscillation over the last 3.5 kyr, namely in the form of near-millennial scale changes in the E/P ratio (**Figure 2:22**) (Curtis et al., 1996). Significantly, the aridity peaks correspond to periods of intense cultural stress for the Maya civilization, as they do in a similar study from Lake Chichcanab (Hodell et al., 1995), as well as a study based on metal concentration from a marine core obtained off the coast of Venezuela (Haug et al., 2003). A pollen-based chronology covering the last 2.5 k yr, which also correlates increased aridity with the period of cultural collapse, followed by a wetter period, was obtained from mangrove marshes on the Caribbean coast of the Yucatan (Islebe and Sanchez, 2002).

2.2.4.2.1.1.2 Peten

The general pattern of environmental changes in the Peten follows the regional pattern, as shown by an early pollen chart from Lake Salpeten (**Figure 2:23**) (Leyden, 1987). Although somewhat lacking in dating control, the movement from *Juniperus* scrub, through halophytic *Alternanthera* marsh, through a *Brosimum* and *Chlorophora* dominated semi-evergreen forest, with increasingly larger percentages of disturbance taxa (*Cecropia*) replacing the forest taxa (period of maximum anthropogenic disturbance), followed by return to mesic forest, closely replicates the Mexican Yucatan records. The correlation of the 6.85 m of erosion-driven “Maya clay” with the period of maximum disturbance should be noted. This period also corresponds to

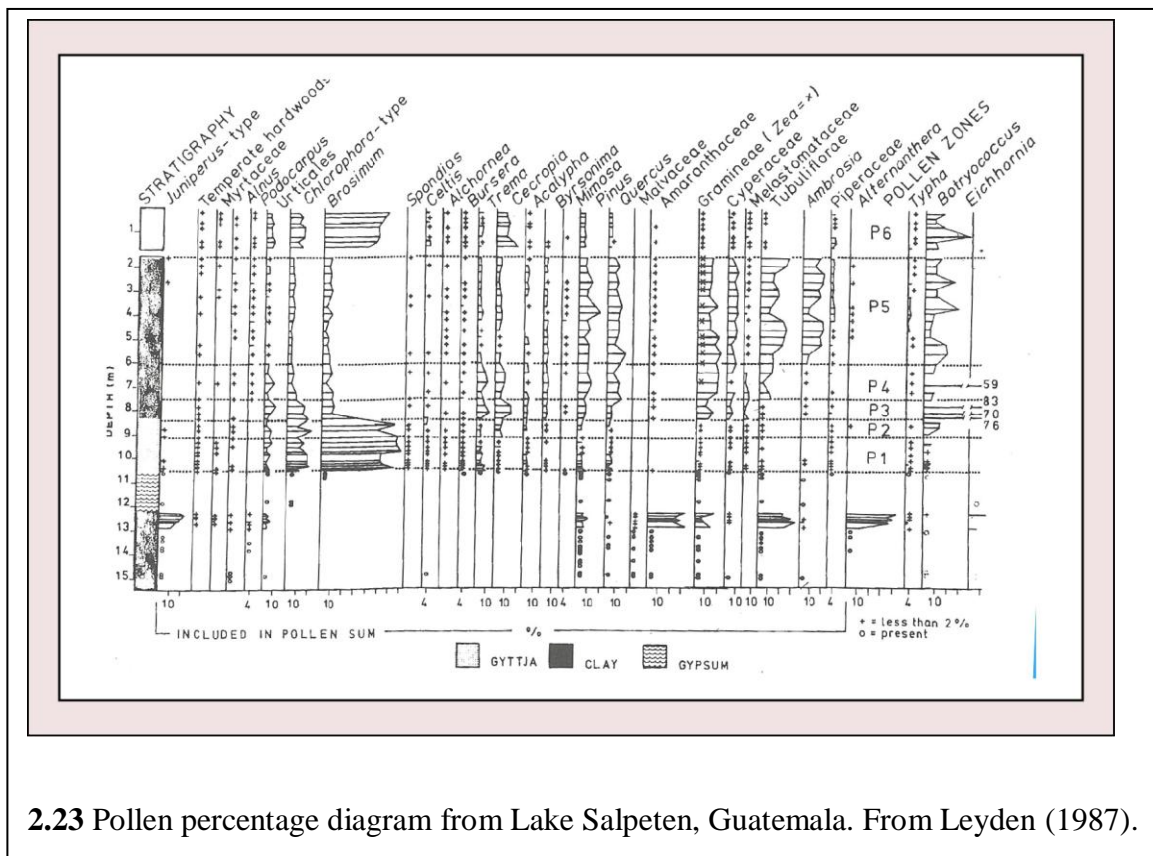


2.22 Isotopic record from Lake Punta Laguna, Yucatan showing near millennial scale variability; the records are derived from monospecific ostracod (left) and gastropod (right) shells. From Curtis et al. (1996).

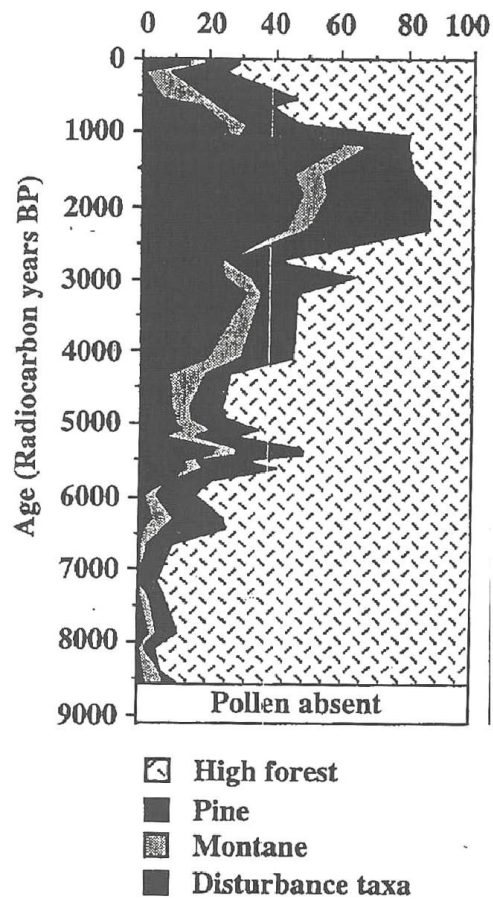
low pollen concentrations, attributed to both increased sedimentation rates and decreased pollen production.

Very similar results were obtained from two separate studies from Lake Peten-Itza. A 8.6 kyr reconconstruction (Islebe et al., 1996) based on palynological and sedimentological data agrees in all major points with the regional pattern, as a very wide spectrum multi-proxy examination (Curtis et al., 1998); as evidenced by their simplified pollen diagram (**Figure 2:24**). Once again, initial flooding occurs due to increased precipitation and a raising phreatic water table (here beginning ~ 9 ^{14}C kyr BP), followed by a moist mid Holocene, featuring anthropogenically generated deforestation and erosion, followed by reforestation subsequent to the cultural collapse. Significantly, this study produced no clear evidence of a Terminal Classic drought, nor excessive thicknesses of the erosional “Maya clay”, perhaps relating to the low temporal sensitivity of this large, deep lake. Another probable result of the lake bathymetry is disequilibrium between the pollen and the $\delta^{18}\text{O}$ record around 8.5 ^{14}C kyr BP, with the pollen record indicating wetter conditions than the $\delta^{18}\text{O}$ calculated E/P ratio. The authors argue that the $\delta^{18}\text{O}$ record does not record the E/P ratio accurately for this period due to the high surface area/volume ratio resulting from the initial filling of the basin. The reconstruction of the last 4 kyr derived from a core obtained from Lake Salpeten, matches the familiar pattern, again clearly displaying the anthropogenic impact as recorded by the pollen assemblages (**Figure 2:25**) (Rosenmeier, 2002).

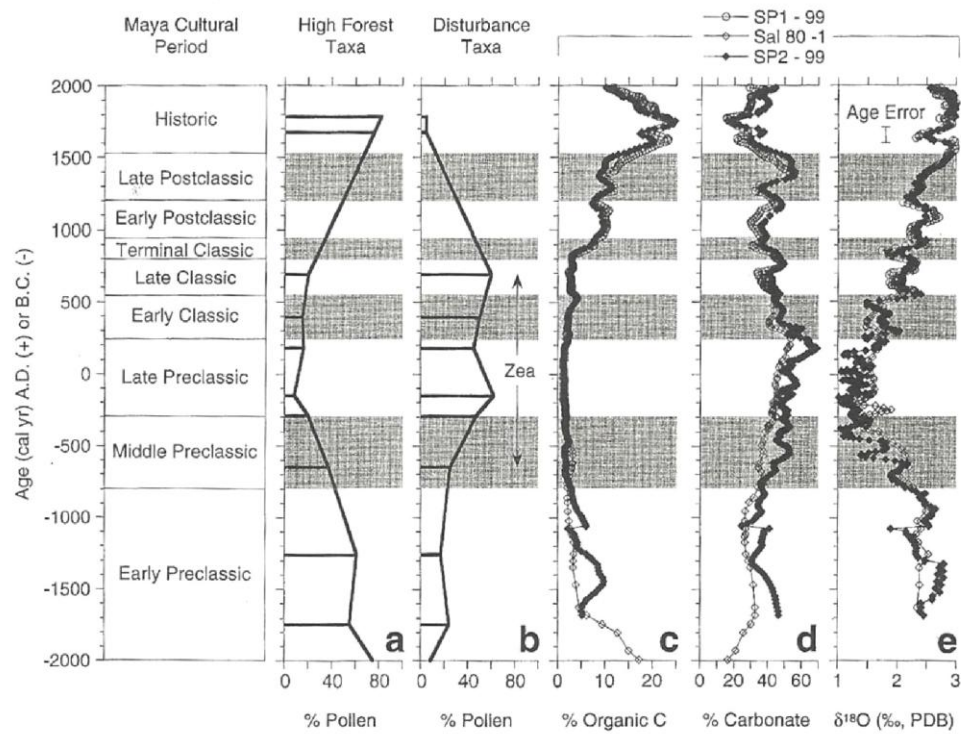
Cores from four lakes farther to the south (highland Guatemala and El Salvador), generally covering only the last 3 kyr, show similar (though moderated) palynological evidence of anthropogenic disturbance, preceding the reestablishment of forest taxa following the Classic collapse (Tsukada and Deevey, 1967). In fact, the pollen zones show such close similarities with



2.23 Pollen percentage diagram from Lake Salpeten, Guatemala. From Leyden (1987).



2.24 Pollen by vegetation types for Lake Peten-Itza, Guatemala. From Curtis et al. (1998).



2.25 Multi-proxy evidence of anthropogenic impact for Lake Salpeten, Guatemala. From Rosenmeier et al. (2002).

those obtained from the Peten lakes, that the dates were estimated by means of stratigraphic correlation with the Peten cores, the dating control for the study itself being extremely rudimentary, consisting of only two radiocarbon dates.

A general pattern emerges for the post glacial environmental history of the region; a cold, dry Pleistocene (often characterized by temperate scrub or intermittent swamp), being replaced by a wet and humid Holocene (deepening lakes and increasingly diverse and mesic forests), with a period of maximum precipitation and/or warmth occurring sometime during either the early or mid Holocene, followed by a slightly dryer, cooler period lasting until the present. In the Maya area the later part of this pattern usually exhibits severe anthropogenic impacts, with the typical lake bed sediment core displaying a transition from gyttja (pre-Maya) through a section of erosional “Maya clay”, consisting of a low pollen abundance dominated by disturbance taxa, before returning to gyttja and forest taxa following the cultural collapse (Rice, 1996). Clearly, mechanisms operating on at least the regional scale must be responsible for such coordinated climatic responses over such a large area.

2.2.4.3 Controls

Since paleoenvironmental reconstruction is most useful when utilized to shed light upon the underlying mechanisms in order to improve our understanding of the interrelated workings of the earth systems, it is important to consider the nature of these large-scale controls. In the case of the circum-Caribbean, there appears to be one primary control (amount of solar insolation reaching the earth) whose effect is felt through a variety of related secondary mechanisms (such as sea level raise and the position of the ITCZ), and possibly an indirectly related higher frequency control, namely the ~ 200 year solar cycle.

2.2.4.3.1 Milankovitch Cycles

There is widespread consensus among the reviewed studies that the most important control over regional climate has been the change in solar radiation as explained by the Milankovitch cycles (Hodell et al., 1991; Leyden et al., 1994; Watts and Hansen, 1994; Curtis et al., 1999). A clear depiction of the temporal changes in insolation occurring over the period at ~ 20° N is shown in **Figure 2:26a**, while **2:26b** displays the correlation between insolation received at 10° N (at the top of the atmosphere) and a specific proxy record. Insolation curves vary by latitude, as does the relative importance of the three main orbital parameters. At high latitudes the effect of obliquity is of greater relative importance, while at low latitudes the effects of the precessional aspects dominate (Berger, 1978; Berger and Louté, 1991). Although no single proxy record will exactly parallel the local insolation curve due to the barrage of intervening factors and processes, clear approximations are generally evident. Two of the most important of these intervening factors are sea level raise and position of the ITCZ. Holocene sea level rise results, of course, from global deglaciation, a direct result of increased solar insolation. In the area under discussion, sea level is particularly important due to the control it exerts over the phreatic water level, which is an important determinate to the time of initial basin filling, particularly in the Yucatan, which sits on top of a thin freshwater lens, resting on sea level saline water. The position of the ITCZ is also largely determined by solar insolation factors, particularly the precessional aspects. Over the period under discussion, a general southward migration of the mean annual position of the ITCZ has occurred, largely due to the increased seasonality of the southern hemisphere and decreased seasonality of the northern (Haug et al., 2001). The position of the ITCZ is of great importance meteorologically for the tropical Americas, as it controls the area of maximum rainfall, with a northward position

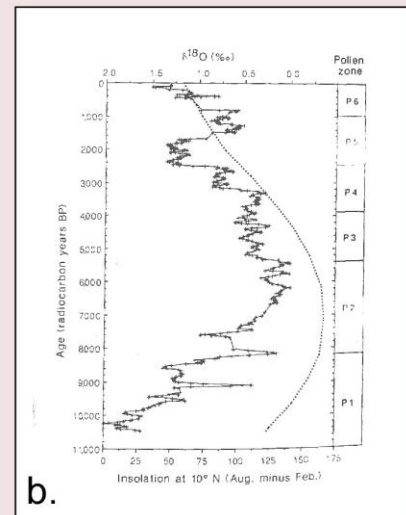
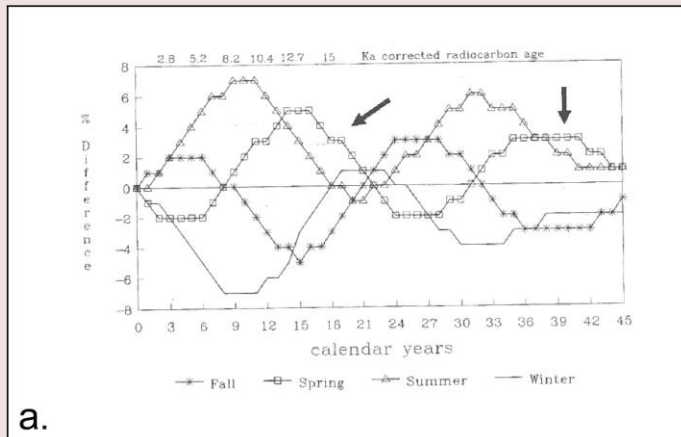
resulting in increased rainfall for areas to the north (northern South America, the Caribbean, and Central America), and reduced precipitation for areas to the south (the Amazon, and the Altiplano). A southern position produces the opposite effects.

2.2.4.3.2 Solar Cycle

Another mechanism thought to contribute to the control of regional climatic conditions is the solar cycle. Support for this hypothesis mainly consists of a correlation between the ~200 year cosmogenic carbon 14 production cycle and climatic conditions, particularly drought in the Yucatan (Hodell et al., 2001), upwelling in the Cariaco basin off the coast of Venezuela (Peterson et al., 1991), and mineral magnetic parameters near Puerto Rico (Nyberg et al., 2001). To date, no satisfactory explanation/description of an enabling mechanism capable of amplifying the relatively minor change in sunspot activity into dramatic climatic changes has been proposed.

2.2.4.4 Paleoclimate/Vegetation Summary

Climatic conditions in the tropical Americas have generally exhibited a common pattern since the late Pleistocene. Initial cold and dry conditions gave way to warmer, wetter conditions, with a thermal maximum occurring some time before the late Holocene. In most areas the vegetation became increasingly mesic and decreasingly seasonal, with the general trend being a change towards increasing amounts of semi-evergreen and evergreen species, with at least some montane species retreating upslope. These changes have been slightly reversed over the late Holocene. Throughout the new world tropics anthropogenic impacts have been observed, with the impacts being so large in the area of the ancient Maya civilization that they mimic the effects of climate change, thereby confusing the interpretation of the proxy records. The ultimate driver of the changes appears to be changes in the amount of solar insolation, resulting from orbital parameters. A higher frequency oscillation of ~ 200 years, correlating to the sunspot cycle has



2.26 Insolation control. Seasonal insolation for the Yucatan Peninsula over the past 45,000 years, from (a) Berger (1978); and (b), the difference in insolation (Langleys) received at the top of the atmosphere at 10°N latitude between August and February for the last 11,000 14 C years. This measure of the intensity of the annual cycle displays a fairly close correlation with the oxygen isotope record from monospecific ostracods shell from Lake Miragoane, Haiti, which functions as an aridity proxy. From Hodell et al. (1991).

been observed in a number of proxy records, although a mechanism by which the sunspot cycle affects regional climate has not been identified.

2.3 Modern Analog

The use of a modern analog is a common practice in paleo studies. In this technique the physical parameters of a known historical event/process are analyzed and quantified in order to create a baseline from which to calibrate prehistorical events. Because overwash lobes in coastal wetlands are the main proxy employed in sedimentary paleotempestology, the most important modern analog data is the intensity of storm required to deposit sand in the back barrier locations. The most common method of gathering this data is to core a wetlands after a storm of known intensity has made landfall in the area and check for the presence/size/extent of sand layers. An alternative method is to identify a slightly older event (particularly one that can be definitively pinpointed chronologically through cesium dating) and perform the same analyses. This operation should be performed in each locality as recording sensitivity is site-specific, and, additionally, can change over time. An entire range of analyses, including microfossil, grain size, isotopic, and geochemical, can be performed on the modern analog as a means of calibrating prehistoric events. An example is the use of grain size characteristics to parameterize an advection settling model that can be used to estimate the wave heights for prehistoric storms (Woodruff et al., 2008).

2.4 Methods

Three field methods were used for obtaining cores. A 2" diameter modified Livingstone corer, capable of obtaining up to 130 cm of sediments per core, was used in soft sediments. In less penetrable material a Russian Peat Borer was used, which removes a 50 cm long 2" hemispherical section of sediments. A gas powered vibracorer was used in a few sites. Under

both piston and peat borer methods, coring proceeded through a sequence of cores in slightly offset holes until refusal. Coring sites were registered on a hand held GPS unit. Sand/sediment samples were collected from the beaches and at various distances offshore and across the barriers, and diagrams were created in order to capture all the salient topographical and vegetation features.

Cores were transported to the Global Change and Coastal Paleoecology Laboratory in the Department of Oceanography and Coastal Sciences at Louisiana State University, where they were stored in a cold room. When opened the cores were photographed, visually inspected and logged. Loss on ignition (LOI) was performed on all cores, following the standard procedures outlined by Dean (1974) to determine water, carbonate, and residual content; macrofossils were collected. Precise overlap between core sections in composite cores were determined by visual examination and matching of LOI data. Selected cores were run through a GeoThek MultiSensor Core Logger to determine bulk density. Several core tops were sent to Memorial University of Newfoundland for ^{137}Cs and ^{210}Pb analyses. Samples of terrestrial material (almost exclusively plant material) were sent to NOSAMS lab at Woods Hole Oceanographic Institute and Beta Analytic in Miami, FL for radiocarbon dating. Selected sand intervals were shaken through a set of nine stacked sieves at 0.5 Φ intervals ranging from -0.5 to 4.5 Φ to determine grain size characteristics.

2.5 References

- Alley, R. B., 2000. Ice-core evidence of abrupt climate change. *Proceedings of the National Academy of Science* 97, 1331-1334.
- Alley, R. B. and Bender, M., 1998. Greenland ice cores: frozen in time. *Scientific American* 278, 80-88

- Atwater, B.F., 1987. Evidence of great Holocene earthquakes along the outer coast of Washington state, *Science* 236, 942–944.
- Atwater, B.F., 1992. Geologic evidence for earthquakes during the past 2000 years along the Copalis River, southern coastal Washington. *Journal of Geophysical Research* 97, 1901–1919.
- Atwater, B. F., 1996. Coastal evidence for great earthquakes in western Washington. In assessing earthquake hazards and reducing risk in the Pacific Northwest. In: Rogers, A.M. , Walsh, T. J. , Kockelman W .J., and Priest, G.R., (eds), U. S. Geological Survey Professional Paper 1560, 77–90.
- Atwater ,B.F. and Yamagucci, D. K., 1991. Sudden, probably coseismic submergence of Holocene trees and grass in coastal Washington State. *Geology* 19, 706–709.
- Atwater, B.F. and. Hemphill-Haley, E., 1996. Preliminary estimates of tsunami recurrence intervals for great earthquakes of the past 3500 years at Northeastern Willapa Bay, Washington. U.S., Geological Survey Open-File Report 96-001.
- Bartlett, A. S., and Baghoorn, E. S., 1973. Phytogeographic history of the Isthmus of Panama during the past 12,000 years (a history of vegetation, climate and sea-level change). In Graham, A. (ed), *Vegetation and Vegetational History of northern Latin America*. Elsevier, New York. 203-299.
- Bender, M., Sowers, T., Dickson, M-l., Orchado, J., Grootes, P., Mayewski, P., and Meese, D., 1994. Climate correlations between Greenland and Antarctica during the past 100,000 years. *Nature* 372, 663-666.
- Berger, A., 1978. Numerical values of caloric insolation from 1,000,000 YBP to 100,000 YBP (astronomical solution of Berger, 1978). Contributing Institution of the Geophysics. Universidad Catholique, Loivain-la-Neuve, Belgium. 37.
- Berger, A., and Loute, M. F., 1991. Insolation values for the climate for the last 10 million years. *Quaternary Science Reviews* 10, 297-317.
- Bianchette, T., Liu, K-b., 2009. Eastern North Pacific hurricane trajectories and rainfall climatology: implications and possibilities for Mexican paleotempestology. Association of American Geographers Annual Meeting. Las Vegas, NV.
- Bloom, A., 1967. Pleistocene shorelines: a new test of isostasy *Geological Society of America Bulletin* 78, 1477-1494.
- Bloom, A., (ed), 1977. *Atlas of Sea-level Curves*. International Geological Coorelation Programme Project 61 Sea-level Project. IUGS UNESCO.

Bond, G., and Lotti, R., 1995. Iceberg discharges into the North Atlantic on millennial timescales during the last glaciations. *Science* 267, 1005-1010.

Bond, G., Broecker, W., Johnsen, S., McManus, J., Labeyrie, L., Jouzel, J., and Bonani, G., 1993. Correlations between climate records from North Atlantic sediments and Greenland ice. *Nature* 365, 143-147.

Bradbury, J. P., Leyden, B. W., Salgado-Labouriau, M., Lewis, W. M., Schubert, C., Binford, M. W., Frey, D. G., Whitehead, D. R., and Weibezahn, F. H., 1981. Late Quaternary environmental history of Lake Valencia, Venezuela. *Science* 214, 1299-1305.

Broecker, W.S., Kennett, J.P., Flower, B.P., Teller, J.T., Trumbore, S., Bonani, G., and Wolfli, W., 1989. Routing of meltwater from the Laurentide ice sheet during the Younger Dryas cold episode. *Nature* 314, 318-321.

Brown, K. S., Sheppard, P. M., and Turner, J. R. G., 1974. Quaternary refugia in tropical America: evidence from race formation in *Heliconius* butterflies. *Proceedings of the Royal Society of London, B* 187, 369-378.

Brown, P. A., and Kennett, J. P., 1998. Megaflood erosion and meltwater plumbing changes during last North American deglaciation recorded in Gulf of Mexico sediments. *Geology* 26, 599-602.

Carter, R.W.G., 1988. *Coastal Environments*. Academic Press, London

Christopherson, R. W., 2003. *Geosystems: An Introduction to Physical Geography* (5th Edition), 2003. Prentice Hall, Upper Saddle River New Jersey.

Clague, J.J., 1997. Evidence for large earthquakes at the Cascadia subduction zone. *Reviews of Geophysics* 35. 439-460.

Clague, J.J., Bobrowsky, P.T., and Hutchison, I. 2000. A review of geological records of large tsunamis at Vancouver Island, British Columbia, and implications for hazards. *Quaternary Science Review* 19, 849-863.

Clarke, J.A., Farrell, W.E., and Peltier, W. R., 1978. Global changes in postglacial sea level: a numerical calculation. *Quaternary Research* 9, 265-287

Coates, A.G., 1997. The forging of Central America. In Coates, A. G., (ed) *Central America: a natural and cultural history*. Yale University Press, New Haven. 1-37.

Colinvaux, P., 1997. The history of forests on the Isthmus from the Ice Age to the present. In Coates, A. G., (ed) *Central America: a natural and cultural history*. Yale University Press, New Haven. 123-136.

Cortes, J., 2007. Coastal morphology and coral reefs. In Bundschuh, J., and Alvarado, G. E., (eds), *Central America Geology Resource Hazards*. Taylor and Francis, London. Vol. 1, 185-200.

Cronin, T. M., 1987. Quaternary sea-level studies in the Eastern United States of America: a methodological perspective. In Tooley, M. J. and Shennan, I., (eds), *Sea-level Changes*. The Institute of British Geographers Special Publication Series 20, Basil Blackwell Ltd, New York. 225-248.

Culbert, T. P., and Rice, D. S., (eds), 1990. *Precolumbian Population History in the Maya Lowlands*. University of New Mexico Press, Albuquerque.

Curtis, J., H., and Hodell, D. A., 1996. Climate variability on the Yucatan peninsula (Mexico) during the past 3500 years, and the implications for Maya cultural evolution. *Quaternary Research* 46, 37-47.

Curtis, J., H., Brenner, M., Hodell, D. A., Balser, R. A., Islebe, G. A., and Hooghiemstra, H., 1998. A multi-proxy study of Holocene environmental change in the Maya lowlands of Peten, Guatemala. *Journal of Paleolimnology* 19, 139-159.

Curtis, J., H., Brenner, M., and Hodell, D. A., 1999. Climate change in the Lake Valencia basin, Venezuela, ~12 600 yr BP to present. *The Holocene* 9, 609-619.

Dansgaard, W., Johnson, S., Clausen, H., Dahl-Jensen, D., Hammer, C., Hvidberg, C., Steffensen, J., Sveinbjornsdotter, A., Jouzel, J., and Bond, G., 1993. Evidence of general instability of past climate from a 250-kyr ice core record. *Nature* 364, 218-220.

Darlenzo, M.E., Peterson, C.D., and Clough, C., 1994. Stratigraphic evidence for great subduction-zone earthquakes at four estuaries in northern Oregon. *Journal of Coastal Research* 10, 850-876.

Davis, M. B., 1981. Quaternary history and the stability of forest communities. In West, D.C., Shurgart, H. H. and Botkin, D.B., (eds), *Forest Succession Concepts and Applications*. Springer-Verlag, New York, 132-153.

Davis, M. B., 1984. Climatic instability, time lags, and community disequilibrium. In Diamond, J. and Case, T. J. (eds), *Community Ecology*. Harper and Row, New York, 269-284.

Dawson, A.G. and Shi, S., 2000. Tsunami deposits. *Pure and Applied Geophysics* 157. 875-897.

Dawson, A. G., and Stewart, I. 2007. Tsunami deposits in the geological record. *Sedimentary Geology* 200, 166-183.

Dean, W. E., 1974. Determination of carbonate and organic matter in calcareous sediments and sedimentary rocks by loss on ignition: comparison with other methods. *Journal of Sedimentary Petrology* 44, 242-248.

Dengo, G., 1962. Tectonic-igneous sequence in Costa Rica. In Engel, A. E. J., James, H. L., and Leonard, B. F., (eds), *Petrologic Studies: Geological Society of America Buddington Volume*, 133-161.

Dengo, G., 1985. Mid America: tectonic setting for the Pacific margin from southern Mexico to northwestern Colombia. In Nairn, A. E. M, and Stehli, F. G., (eds), *The Ocean s and Margins*. Plenum Press, New York, vol. 7, 123-180.

Dixon, T. H. and Mao, A., 1997. A GPS estimate of relative motion between North and South America. *Geophysical Research Letters* 24, 535-538.

Dominey-Howes, D. T. M., Humphreys, G. S., and Hesse, P. P., 2006. Tsunami and paleotsunami depositional signatures and their potential in understanding the late-Holocene tsunami record. *The Holocene* 16, 1095-1107. Doi:10.1177/09596835606069400.

Donnelly, J.P., and Webb, T III, 2004. Back-barrier sedimentary records of intense hurricane landfalls in the northeastern United States. In Murnane, R.J., and Liu, K-b. (eds), *Hurricanes and Typhoons: Past, Present and Future*. Columbia University Press, New York, 58-95.

Donnelly, T.W., Horne, G. S., Finch, R. C, Lopez-Ramos, E., 1990. Northern Central America; the Maya and Chortis blocks. In Dengo, G., and Case, J.E., (eds), *The Geology of North America, Vol. H, The Caribbean region*. The Geologic Society of America, Boulder, Colorado. 37-76.

Duncan, R. A., and Hargraves, R. B., 1984. Plate tectonic evolution of the Caribbean region in the mantle reference frame. In Bonini, W. E., Hargarves, R. B., and Shagam, R. (eds), *The Caribbean-South American Plate Boundary and Regional Tectonics*. Geological Society of America Memoirs 162, 81-93.

Escalante, G., 1990. The geology of southern Central America and western Colombia. In Dengo, G., and Case, J.E., (eds), *The Geology of North America, Vol. H, The Caribbean region*. The Geologic Society of America, Boulder, CO. 201-230.

Fairbanks, R. G., 1989. A 17,000-year glacio-eustatic sea level record: influence of glacial melting rates on the Younger Dryas event and deep-ocean circulation. *Nature* 342, 637-642.

Fairbridge, R.W, 1961. Eustatic changes in sea level. *Physics and Chemistry of the Earth*. 4, 99-185.

Firestone, R. B., West, A., Kennett, J. P., Becker, L., Bunch, T. E., Revay, Z. S., Schultz, P. H., Belgia, T., Kennett, D. J., Erlandson, J. M., Dickerson, O.J., Goodyear, A. C., Harris, R. S., Howard, G. A., Kloosterman, J. B., Lechler, P., Mayewski, P. A., Montgomery, J., Poreda, R., Darrah, T, Hee, S. S. Q., Smitha, A. R., Stich, A., Topping, W., Wittke, J. H., Wolbach, W. S., 2007. Evidence for an extraterrestrial impact 12,900 years ago that contributed to the megafaunal extinctions and the Younger Dryas cooling. *Proceedings of the National Academy of Sciences*. 104, 16016-16021.

- Flower, B.P., and Kennett, J. P., 1990. The Younger Dryas cool period in the Gulf of Mexico. *Paleoceanography* 5, 949-961.
- Frappier, A.B., Sahagian, D., Carpenter, S.J., González, L.A., and Frappier, B.R., 2007a. A stalagmite proxy record of recent tropical cyclone events. *Geology* 7, 111-114. DOI: 10.1130/G23145A.
- Frappier, A. B., Knutson, T., Liu, K.-b., Emanuel, K., 2007b. Coordinating paleoclimate research on hurricanes with hurricane-climate theory and modeling. *Tellus A*.
- Fullerton, D.S. and Richmond, G.M., 1986. Comparison of the marine oxygen isotope record, the eustatic sea level record, and the chronology of glaciation in the United States of America. *Quaternary Science Reviews* 5, 197-200.
- Gill, R. B., 2001. *The Great Maya Droughts*. University of New Mexico Press, Albuquerque.
- Gischler, E, 2006. Comment on “Corrected western Atlantic sea-level curve for the last 11,000 years based on calibrated ^{14}C dates from *Acropora palmate* framework and intertidal mangrove peat” by Toscano and Macintyre. *Coral Reefs* 22:257-270 (2003), and their response in *Coral Reefs* 24:187-190 (2005). *Coral Reefs* 25, 273-279.
- Gischler, E. and Hudson, J. H., 2004. Holocene development of the Belize Barrier reef. *Sedimentary Geology* 164, 223-236.
- Goff, J., McFadgen, B.G., and Chague-Goff, C., 2004. Sedimentary differences between the 2002 Easter storm and the 15th-century Okoropunga tsunami, southeastern North Island, New Zealand. *Marine Geology* 204, 235–250.
- Haffer, J., 1969. Speciation in Amazonian forest birds. *Science* 165, 131-137.
- Hallam, A., 1992. *Phanerozoic Sea-level Changes*. Columbia University Press, New York.
- Haug, G. H., Hughen, K. A., Sigman, D. M., Peterson, L. C., and Rohl, U., 2001. Southward migration of the Intertropical Convergence Zone through the Holocene. *Science* 292, 1304-1314.
- Haug, G. H., Gunther, D., Peterson, L. C., Sigman, D. M., Hughen, K. A., and Aeschlimann, B., 2003. Climate and the collapse of Maya civilization. *Science* 299, 1731-1735.
- Hemphill-Haley, E. 1995a. Diatom evidence for earthquake-induced subsidence and tsunami 300 years ago in southern coastal Washington. *Geological Society of America Bulletin*. 107, 367-378.
- Hemphill-Haley, E. 1995b. Intertidal diatoms from Willapa Bay, Washington: application to studies of small-scale sea-level changes. *Northwest Science*. 69, 29-45.

Hemphill-Haley, E. 1996. Diatoms as an aid in identifying late-Holocene tsunami deposits. *The Holocene* 6, 439-448.

Hernandez-Avila, M. L., Roberts, H. H., and Rouse, L. E., 1977. Hurricane -generated waves and coastal rampart formation. *Proceedings, Third International Coral Reef Symposium*. Miami, Florida, May, 1977.

Higuera-Gundy, A., Brenner, M., Hodell, D.A., Curtis, J. H., Leyden, B. W., and Binford, M. W., 1999. A 10 300 ^{14}C yr record of climate and vegetation change from Haiti. *Quaternary Research* 52, 159-170.

Hodell, D. A., Curtis, J. H., Jones, G. A., Higuera-Gundy, A., Brenner, M., Binford, M. W., and Dorsey, K. T., 1991. Reconstruction of Caribbean climate change over the past 10,500. *Nature* 352, 790-793.

Hodell, D. A., Curtis, J. H., and Brenner, M., 1995. Possible role of climate in the collapse of Classic Maya civilization. *Nature* 375, 391-394.

Hodell, D. A., Brenner, M., Curtis, J. H., and Guilderson, T., 2001. Solar forcing of drought frequency in the Maya lowlands. *Science* 292, 1367-1370.

Horn, S. P., 2007. Late Quaternary lake and swamp sediments: recorders of climate and environment. In Bundschuh, J., and Alvarado, G. E., (eds), *Central America Geology Resource Hazards*. Taylor and Francis, London. Vol. 1, 423-441.

Hughen, K. A., Overpeck, J. T., Peterson, L. C., Trumbore, S., 1996. Rapid climate changes in the tropical Atlantic region during the last deglaciation. *Nature* 380, 51-54.

Imbrie, J., and Imbrie, K.T., 1979. *Ice ages: Solving the Mystery*. Harvard University Press, Cambridge, Massachusetts.

Islebe, G. A., and Sanchez, O., 2002. History of Late Holocene vegetation at Quintana Roo, Caribbean coast of Mexico. *Plant Ecology* 160, 187-192.

Islebe, G. A., Hooghiemstra, H., Brenner, M., Curtis, J. H., and Hodell, D. A., 1996. A Holocene vegetation history from lowland Guatemala. *The Holocene* 6, 265-271.

Johnson, D. W., 1919. *Shore Processes and Shoreline Development*. New York, Wiley.

Kelletat, D., Scheffers, A., Scheffers, E and Scheffers, S., 2004. Holocene tsunami deposits on the Bahaman islands of Long Island and Eleuthera. *Zeitschrift fur Geomorphologie* 48, 519-540.

Kelsey, H.M., Witter R.C., and Hemphill-Haley, E., 2002. Plate-boundary earthquakes and tsunamis of the past 5500 yr, Sixes River estuary, southern Oregon. *Geological Society of America Bulletin* 114, 298-314.

- Kennett, J.P. 1982. *Marine Geology*. Prentice-Hall, New Jersey.
- Kennett, D.J., Kennett, J.P. , West, A., Mercer, C., Hee, S. S. Q., Bement, L., Bunch, T. E., Sellers, M., and Wolbach, W. S., 2009. Nanodiamonds in the Younger Dryas boundary sediment layer. *Science* 323, 94-94.
- Komar, P. D., 1998. *Beach Processes and Sedimentation* (2nd edition) . Prentice Hall, New Jersey.
- Kortekaas, S., and Dawson, A.G., 2007. Distinguishing tsunami and storm deposits: an example from Martinhal SW Portugal. *Sedimentary Geology* 200, 208-211.
- Kraft, J.C., 1971. Sediment facies patterns and geologic history of a Holocene marine transgression . *Geological Society of America Bulletin* 82, 2131-2158.
- Kuhle, M., 1988. The Pleistocene glaciation of Tibet and the onset of ice ages- an autocycle hypothesis. *GeoJournal* 17, Tibet and High-Asia. Results of the Sino-German Joint Expeditions (I), 581-596.
- Kuhle, M., 2004. The High Glacial (last ice age and LGM) ice cover in high and central Asia. In Ehlers, J., Gibbard, P. L., (eds), *Development in Quaternary Science 2c (Quaternary Glaciation - Extent and Chronology, Part III: South America, Asia, Africa, Australia, Antarctica)*. Elsevier B.V., Amsterdam. 175-199.
- Kuhle, M., 2007. The past ice stream network in the Himalayas and the Tibetan ice sheet during the last glacial period and its glacial-isostatic, eustatic and climatic consequences. *Tectonophysics* 445, 116-144.
- Lambeck, K., Yokoyama, Y., Purcell, T., 2002. Into and out of the last glacial maximum: sea level change during oxygen isotope stages 3 and 2. *Quaternary Science Reviews* 21, 343-360.
- Lander, J.F., Whiteside, L. S., and Lockridge P. A., 2002. A brief history of tsunamis in the Caribbean. *Science of Tsunami Hazards* 20, 57-94.
- Lara, M. E., 1993. Divergent wrench faulting in the Belize southern lagoon: implications for Tertiary Caribbean plate movements and Quaternary reef distribution. *American Association of Petroleum Geologists Bulletin* 77, 1041-1063.
- Leatherman, S.P., 1979a. *Barrier Island Handbook*. National Park Service, Boston, MA.
- Leatherman, S.P., 1979b. Migration of Assateague Island, Maryland, by inlet and over-wash processes. *Geology* 7, 104-107.
- Leatherman, S.P. 1981. *Benchmark papers in geology Vol 58: Overwash processes*. Hutchinson Ross Publishing, Stroudsburg, PA.

Leatherman, S.P. 1983. Barrier dynamics and landward migration with Holocene sea-level rise. *Nature* 301, 415-417.

Leyden, B. W., 1984. Guatemalan forest synthesis after Pleistocene aridity. *Proceedings of the National Academy of Sciences* 81, 4856-4859.

Leyden, B. W., 1985. Late Quaternary aridity and Holocene moisture fluctuations in the Lake Valencia basin, Venezuela. *Ecology* 66, 1279-1295.

Leyden, B. W., 1987. Man and climate in the Maya lowlands. *Quaternary Research* 28, 407-417.

Leyden, B. W., Brenner, M., Hodell, D. A., and Curtis, J. H., 1994. Orbital and internal forcing of climate on the Yucatan Peninsula for the past ca. 36 ka. *Paleogeography, Paleoclimatology, Paleoecology* 109, 193-210.

Leyden, B. W., Brenner, M., Whitmore, T., Curtis, J. H., Piperno, D. R., and Dahlin, B., 1996. A record of long- and short-term climatic variation from northwest Yucatan: cenote San Jose Chulchaca. In Fedick, S. L., (ed), *The Managed Mosaic; ancient Maya Agriculture and Resource Use*. University of Utah Press, Salt Lake City. 30-52.

Leyden, B. W., Brenner, M., and Dahlin, B., 1998. Cultural and climatic history of Cuba', a lowland Maya city in Quintana Roo, Mexico. *Quaternary Research* 49, 111-122.

Lighty, R. C., Macintyre, I. G., and Stuckenrath, R., 1982. *Acropora palmata* reef frameworks: a reliable indicator of sea level in the western Atlantic for the past 10,000 years. *Coral Reefs* 1, 125-130.

Liu, K-b., 1988. Quaternary history of the temperate forests of China. *Quaternary Science Reviews* 7, 1-20.

Liu, K-b., 2004. Paleotempestology: principles, methods and examples from Gulf coast lake sediments. In Murnane, R.J., and Liu, K-b., (eds), *Hurricanes and Typhoons: Past, Present and Future*. Columbia University Press, New York. 13-57.

Liu, K-b, and Colinvaux, P., 1985. Forest changes in the Amazon basin during the last glacial maximum. *Nature* 318, 556-557.

Liu, T., Zhang, S., and Han, J., 1986. Stratigraphy and paleoenvironmental changes in the loess of central China. *Quaternary Science Reviews* 5, 489-495.

Lloyd, J.J., 1963. Tectonic history of the south Central America Orogen. *American Association of Petroleum Geologists Memoirs* 2, 88-100.

Malmquist, D. L., 1997. Oxygen isotopes in cave stalagmites as a proxy record of past tropical cyclone activity. In *Preprints of the 22nd Conference on Hurricanes and Tropical Meteorology*, 393-394. Boston, American Meteorological Society.

Mann, P., Calais, E., Ruegg, J-C., DeMets, C., Jansma, P. E., and Mattioli, G. S., 2002. Oblique collision in the northeastern Caribbean from GPS measurements and geological observations. *Tectonics* 21, 1057. DOI:10.1029/2001TC00134, 2002.

Mann, P., Rogers, R. D., and Gahagan, L., 2007. Overview of plate tectonic history and its unresolved tectonic problems. In Bundschuh, J., and Alvarado, G. E., (eds), *Central America Geology Resource Hazards*. Taylor and Francis, London. Vol. 1, 201-237.

Marchant, R., Boom, A., and Hooghiemstra, H., 2002. Pollen-based biome reconstruction for the past 450 000 yr from the Funza-2 core, Colombia: comparisons with model-based vegetation reconstructions. *Palaeogeography, Palaeoclimatology, Palaeoecology* 177, 29-45.

Marchitto, T. M., and Wei, K., 1995. History of Laurentide meltwater flow to the Gulf of Mexico during the last deglaciation, as revealed by reworked calcareous nannofossils. *Geology* 23, 779-782.

Masselink, G., and Hughes, M.G., 2003. *Introduction to Coastal Processes and Geomorphology*. Arnold Publishing, London.

McCann, W. R., 2006. Estimating the threat of tsunamigenic earthquakes and earthquake induced-landslide tsunamis in the Caribbean. In Mercado-Irizarry and Liu, P. (eds), *Caribbean Tsunami Hazard*. World Scientific Publishing Company, New Jersey. 43-65.

Mertz, L. M., Hart, M., and Jaeger, J., 2003. Preservation of Paleocyclone deposits in Gulf of Mexico coastal sediments. *GCAGS/GCSSEPM Transactions* 53, 537-547.

Meschede, M. and Frish, W., 2002. The evolution of the Caribbean Plate and its relation to global plate motion vectors: geometric constraints for an inter-American origin. In Jackson, T. A., (ed), *Caribbean Geology into the Third Millennium: Transactions of the Fifteen Caribbean Geological Conference* University of the West Indies Press, Barbados. 1-14.

Mikolajewicz, U., Maier-Reimer, E., Crowley, T. J., and Kim, K-Y., 1993. Effects of Drake and Panamanian gateways on the circulation of an ocean model. *Paleoceanography* 8, 409-426.

Miller, D. J., 1960. The Alaska earthquake of July 10, 1958: giant wave in Lituya Bay. *Bulletin of the Seismological Society of America* 50, 253-266.

Miller, D. L., Mora, C. I., Grissino-Mayer, H. D., Mock, C. J., Uhle, M. E., and Sharp, Z., 2006. Tree-ring isotope records of tropical cyclone activity. *Proceedings of the National Academy of Science*, 10.1073/pnas.0606549103.

Milliken, K. T., Anderson, J. B., Rodriguez, A. B., 2008. A new composite Holocene sea-level curve for the northern Gulf of Mexico. *The Geological Society of America Special Paper* 443, 1–11, DOI: 10.1130/2008.2443(01).

Mitch, W.J. and Gosselink, J.G., 2007. *Wetlands* (4th Ed.), New York: John Wiley and Sons, Inc.

Mitrovica, J. X. and Peltier, W. R. 1991. On post-glacial geoid subsidence over the equatorial oceans. *Journal of Geophysical Research* 96, 20,053-20,071.

Moerner, N.A., 1987. Models of global sea-level change. In Tooley, M. J. and Shennan, I., (eds) *Sea-level Changes*. The Institute of British Geographers Special Publication Series 20, Basil Blackwell Ltd, New York. 332-355.

Morton, R. A., Gelfenbaum, G., and Jaffe, B. E., 2007. Physical criteria for distinguishing sandy tsunami and storm deposits using modern examples. *Sedimentary Geology* 200, 184-207. DOI:10.1016/j.sedgeo.2007.01.003.

Myles, D., 1985. *The Great Waves*. Robert Hale Ltd., London.

Nanayama, F., Shigeno, K., Satake, K. Shimokawa, K., Koitabashi, S., Miyasaka, S. and Ishii, M., 2000. Sedimentary differences between the 1993 Hokkaido–Nansei–Oki tsunami and the 1959 Miyakojima typhoon at Taisei, southwestern Hokkaido, northern Japan, *Sedimentary Geology* 135. 255–264.

Newman, W. S., Pardi, R. R., and Fairbridge, R. W., 1989. Some considerations of the compilation of Late Quaternary sea level curves: a North American perspective. In Scott, D.B., Pirazolli, P. A., and Honig, C. A., (eds), *Late Quaternary Sea-level Correlation and Applications* NATO ASU Series, Kluwer Academic Publishers, Dordrecht.

Nyberg, J., Kuijpers, A., Malmgren, B. A., and Kunzendorf, H., 2001. Late Holocene changes in precipitation and hydrology recorded in marine sediments from the northeastern Caribbean Sea. *Quaternary Research* 56, 87-102.

Nyberg, J., Malmgren, B.A. Winter, A., Jury, M.R., Kilbourne, K.H. and Quinn. T.M. 2007. Low Atlantic hurricane activity in the 1970s and 1980s compared to the past 270 years. *Nature* 447, 698-702.

O’Loughlin, K. F., and Lander, J. F., 2003. *Caribbean tsunamis: a 500 year History, 1498-1998*. Kluwer Academic Publishers, Norwell, MA.

Pararas-Carayannis, G., 2006. Risk assessment of tsunami generation from active volcanic sources in the eastern Caribbean region. In Mercado-Irizarry and Liu, P., (eds), *Caribbean Tsunami Hazard*. World Scientific Publishing Company, New Jersey. 91-137.

Peltier, W. R., 2002. On eustatic sea level history; Last Glacial Maximum to Holocene. *Quaternary Science Reviews* 21, 377-396.

Peters, R., Jaffe, B. E., and Gelfenbaum, G., 2007. Distribution and sedimentary characteristics of tsunami deposits along the Cascadia margin of western North America. *Sedimentary Geology* 200, 372-386.

Peterson, C. D., Darienzo, M. E., Burns, S. F. and Burris, W.K.. 1993. Field trip guide to Cascadia paleoseismic evidence along the northern Oregon coast: evidence of subduction zone seismicity in the central Cascadia margin. *Oregon Geology* 55, 99-114.

Peterson, L.C., Overpeck, J. T., Kipp, N. G., and Imbrie, J., 1991. A high-resolution Late Quaternary upwelling record from the Caricaco Basin, Venezuela. *Paleoceanography* 60, 99-119.

Petit, J., Jouzel, J., Raynaud, D., Barkov, N., Barnola, J-M., Basile, I., Bender, M., Chappellaz, J., Davis, M., Delaygue, G., Delmotte, M., Kotlyakov, V., Legrand, M., Lipenkov, V., Lorius, C., Pepin, L., Ritz, C., Saltzman, E., and Stievenard, M., 1999. Climate and atmospheric history of the past 420,000 years from the Vostock ice core, Antarctica. *Nature* 399, 429-436.

Piperno, D. R., Bush, M. B., and Colinvaux, P. A., 1989. Paleoenvironments and human occupation in late-glacial Panama. *Quaternary Research* 33, 108-116.

Pirazolli, P. A. 1991. *World Atlas of Holocene Sea Level Changes* Elsevier, Amsterdam.

Prance, G. T., 1973. Phytogeographic support for the theory of Pleistocene forest refuges in the Amazon basin based on evidence from the distribution pattern in *Caryocaraceae*, *Chrysobalanaceae*, *Dichapetalaceae*, and *Lecthidaceae*. *Acta Amazonica* 3, 5-28. Biology, Caracas, Venezuela. Columbia University Press, New York.

Psuty, N. 1992. Spatial variation in coastal foredune development. In Carter, R. W. G., Curtis, T. G. F., and Sheehy-Skeffington, M.J. (eds), *Coastal Dunes, Proceedings, Third European Dune Congress*, Rotterdam. 3-13.

Rampino, M. R., and Sanders, J.E., 1981. Evolution of the barrier islands of southern Long-Island, New-York. *Sedimentology* 28, 37-47.

Raymo, M. E., Ruddiman, W. F., and Froelich, P.N., 1988. Influence of late Cenozoic mountain building on ocean geochemical cycles. *Geology* 16, 649-653.

Reese, C. A., Strange, T. P., Lynch, W. D, and Liu, K-b. 2009. Geologic evidence of Hurricane Katrina recovered from the Pearl River Marsh, MS/LA. *Journal of Coastal Research* 24, 1601-1607.

Rice, D. S., 1996. Paleolimnological analysis in the central Peten, Guatemala. In Culbert, T. P., and Rice, D. S., (eds), *Precolumbian Population History in the Maya Lowlands*. University of New Mexico Press, Albuquerque. 193-206.

Richmond, G. M., and Fullerton, D.S., 1986. Summation of Quaternary glaciations in the United States of America. *Quaternary Science Reviews* 5, 183-196.

- Robinson, E., Rowe, D-A., C., and Khan, S. A., 2006. Wave-emplaced boulders on Jamaica's rocky shores. *Zeitschrift fur Geomorphologie Supplementary Volume* 146, 39-57.
- Rosenmeier, M. F., Hodell, D. A., Brenner, M., and Curtis, J. H., 2002. A 4000-year lacustrine record of environmental change in the southern Maya lowlands, Peten, Guatemala. *Quaternary Research* 57, 183-190.
- Roy, P.S., Cowell, P.J., Ferland, M. A., and Thom, B. G., 1994. Wave-dominated coasts. In Carter, R. W. G., and Woodroffe, C. D., (eds), *Coastal Evolution: Late Quaternary Shoreline Dynamics*. Cambridge University Press, Cambridge.
- Ruddiman, W.F. and Kutzbach, J.E., 1991. Plateau uplift and climate change. *Scientific American* 264, 66-74.
- Satake, K., Shimazaki, K., Tsuji, Y., and Ueda, K., 1996. Time and size of a giant earthquake in Cascadia inferred from Japanese tsunami records of January 1700. *Nature* 379, 246-249.
- Scheffers, A., and Kelletat, D., 2006. New evidence and dating of Holocene paleo-tsunami events in the Caribbean (Barbados, St. Martin and Anguilla). In Mercado-Irizarry, A., and Liu, P., (eds), *Caribbean Tsunami Hazards*. World Scientific Press, New Jersey. 178-202.
- Scheffers, A., Scheffers, S., and Kelletat, D., 2002. Paleo-tsunamis on the southern and central Antillean island arc. *Journal of Coastal Research* 21, 263-273.
- Schuchert, C., 1935. *Historical Geology of the Antillean-Caribbean Region*. John Wiley and Sons, New York.
- Scott, D.B., Pirazolli, P. A., and Honig, C. A., (eds), 1989. *Late Quaternary Sea-level Correlation and Applications*. NATO ASU Series, Kluwer Academic Publishers, Dordrecht.
- Shackleton, N. J., and Kennett, J.P., 1975. Paleotemperature history of the Cenozoic and the initiation of Antarctic glaciations: oxygen and carbon analyses of DSDP sites 277, 279, 281. *Initial Reports of Deep Sea Drilling Project* 29. US Government Printing Office., Washington, DC.
- Shepard, F. P., 1963. *Submarine Geology* (2nd edition). Harper and Row, New York.
- Shi, Y., Ren, B., Wang, J., and Derbyshire, E., 1986. Quaternary glaciations in China. *Quaternary Science Reviews* 5, 503-507.
- Sigurdsson H., Carey, S., and Wilson, D., 2006. Debris avalanche formation at Kick'em Jenny submarine volcano (Abstract). In Mercado-Irizarry and Liu, P., (eds), *Caribbean Tsunami Hazard*. World Scientific Publishing Company, New Jersey, 66.

- Smit, J., Roep, T.B., Alvarez, W., Montanari, A., Claeys, P., Grajales-Nishimura, J.M., and Bermudez, J., 1996. Coarse-grained, clastic sandstone complex at the K/T boundary around the Gulf of Mexico: deposition by tsunami waves induced by the Chicxulub impact. In Ryder, G., Fastovsky, D., and Gartner, S., (eds), *The Cretaceous -Tertiary Event and other Catastrophes in Earth History: Geological Society of America Special Paper 307*, 151-182.
- Steig, E., Brook, E., White, J., Sucher, C., Bender, M., Lehman, S., Morse, E., Waddington, E., and Clow, G., 1998. Synchronous climate change in Antarctica and the north Atlantic. *Science* 282, 92-95.
- Street-Perrott, F. A., Hales, P. E., Perrott, R.A., Fontes, J. Ch., Switsur, V. R., and Pearson, A., 1993. Late Quaternary palaeolimnology of a tropical marl lake: Wallywash Great Pond, Jamaica. *Journal of Paleolimnology* 9, 3-22.
- Teller, J. T., 1995. History and drainage of large ice-dammed lakes along the Laurentide ice sheet. *Quaternary Science Reviews* 13, 795-799.
- ten Brink U. S., Geist, E. L., Lynett, P. J., and Andrews, B. D., 2006. Submarine slides north of Puerto Rico and their tsunami potential. In Mercado-Irizarry, A., and Liu, P., (eds), *Caribbean Tsunami Hazards*. World Scientific Press, New Jersey. 67-90.
- Thompson, L.G., MosleyThompson, E., Davis, M.E., Henderson, K. A., Coledai, J., Bolzan, J. F., Liu, K-b., 1995. Late-glacial stage and Holocene tropical ice core records from Huescaran, Peru. *Science* 269, 46-50.
- Toledo, V. M., 1982. Pleistocene changes in vegetation in tropical Mexico. In Prance, G. T. (ed), *Biological Diversification in the Tropics. Proceedings of the Fifth International Symposium of the Association for Tropical Biology*. 93-111.
- Toscano, M. A., and Macintyre, I. G., 2003. Corrected western Atlantic sea-level curve for the last 11,000 years based on calibrated C-14 dates from *Acropora palmate* framework and intertidal mangrove peat. *Coral Reefs* 22, 257-270.
- Tsukada, M., and Deevey, E. S., 1967. Pollen analyses from four lakes in the southern Maya area of Guatemala and El Salvador. In Cushing, E. J. and Wright, E., (eds), *Quaternary Paleoecology*. Yale University Press, New Haven.
- Tuttle, M.P., Ruffman, A., Anderson, T., and Hewitt, J., 2004. Distinguishing tsunami from storm deposits in eastern North America. The 1929 Grand Banks tsunami versus the 1991 Halloween storm. *Seismological Research Letters* 75, 117-131.
- Vanzolini, P. E., and Williams, E. E., 1970. South American anoles: the geographic differentiation and evolution of the *Anolis chrysolepis* species group (*Sauria, Iguanidae*). *Archivos de Zoologia* 19, 1-124.

Watts, W. A., and Hansen, B. C. S., 1994. Pre-Holocene and Holocene pollen records of vegetation history from the Florida peninsula and their climate implications. *Palaeogeography, Palaeoclimatology, Palaeoecology* 109, 163-176.

Weyl, R., 1980. *Geology of Central America*. Gebrueder Borntraeger, Berlin.

Whitmore, T. J., Brenner, M., Curtis, J. H., Dahlin, B. H., and Leyden, B. W., 1996. Holocene climate and human influences on lakes of the Yucatan Peninsula, paleolimnological approach. *The Holocene* 6, 273-287.

Woodroffe, C. D., 1995. Mangrove vegetation of Tobacco Range and nearby mangrove ranges, central Belize barrier reef. *Atoll Research Bulletin* 427.

Woodruff, J.D., Donnelly, J.P., Mohrig, D. and Geyer, W.R., 2008. Reconstructing relative flooding intensities responsible for hurricane-induced deposits from Laguna Playa Grande, Vieques, Puerto Rico. *Geology* 36, 391-394.

CHAPTER 3 TC AND THE ATMOSPHERE: SHORT TERM RELATIONSHIP

3.1 Introduction

Many recent studies (both empirical and modeling-based) have focused on the relationship between climatic change and tropical cyclone (TC) behavior. Although the inexactitude of the instrumental data (Landsea, 2005, 2007) prevents a clear resolution at this point, the studies have chiefly viewed climate as the driver and TCs as a responding feature, postulating changes in TC intensity and/or frequency as resulting from global warming (Knutson et al., 1998; Knutson and Tuleya, 1999, 2004; Walsh and Ryan, 2000; Emanuel, 2005; Webster et al., 2005; Wang and Lee, 2008, Saunders and Lea, 2008). However, the relationship is not unilinear, as TCs, particularly in their role as important poleward transporters of heat, can also affect climate (Elsner, 2007). The aim of this paper is to show that TCs are an integral feature of a coherent North Atlantic (NA) atmospheric/oceanic circulation system, which, integrated through a system of feedback loops, tend to drive the behavior of the various features in coordinated patterns. From this perspective, TCs are not viewed as responding to chance changes to specific features, such as sea surface temperature (SST), or trade wind strength, but rather as both driver and responder in a coordinated, interactive system.

3.2 North Atlantic Circulation System

The atmosphere above the NA is dominated by a set of distinct structures, lying in roughly parallel sequential latitudinal belts. The Intertropical Convergence Zone (ITCZ), characterized by high temperature, high precipitation and rising air, is situated at the lowest latitudes. Poleward of the ITCZ is the subtropical high pressure ridge. The point of highest pressure within this belt is referred to as either the Bermuda (BH) or the Azores High (AH).

Although BH and AH display some differences in the winter, they are basically interchangeable during the summer months (Davis et al., 1997). (In this paper we use the term BH, except when referring specifically to winter values). Farther north is a low pressure zone, the central node of which is the Icelandic Low (IL). The BH and IC are often referred to as the “action centers” of the NA (Sahsamanoglou, 1990; Kapala et al., 1998; Machel et al., 1998). The Polar High is found at the highest latitudes. Although this spatial ordering remains constant throughout the year, the relationships between the various components are not static. Because these relationships exert important controls over the basin’s weather patterns, the interaction between the different features are an important source of weather/climate variability on a number of scales.

On an annual basis, the system moves as a unit, with the components drifting north and south in rough parallel, following the apparent movement of the sun. During the northern winter this moves the BH equatorward, resulting in the December to May dry season in the Caribbean and Central America, as the accompanying zone of subsiding air leads to frequent atmospheric inversions, increased trade wind strength and generally dry conditions in the region (Hastenrath, 1966; Trewartha, 1981). In June the region’s wet season begins as the BH moves north out of the area and the ITCZ approaches from the south, and conditions become dominated by uplift, condensation, and precipitation (Hastenrath, 1966; Trewartha, 1981; Sahsamanoglou, 1990; Davis et al., 1997; Black et al., 1999; Nyberg et al., 2001, 2002; Portis et al., 2001).

Of special importance are the pressure gradients between the features. The clockwise rotating BH generates the northeasterly trade winds off the south flank and the mid latitude westerlies off the north, with the strength of these zonal winds controlled to a great extent the by the pressure gradient between the BH and the adjacent low pressure system (Sahsamanoglou, 1990; Kapala et al., 1998; Machel et al., 1998). Strengthening of the BH can therefore result in

an intensification of the entire NA circulation and abrupt basin-wide changes in weather patterns, particularly when correlated with decreased pressure in the adjacent low pressure systems (Hurrell 1995; Kapala et al., 1998; Machel et al., 1998; Marshall et al., 2001; Nyberg et al., 2001, 2002; Visbeck et al., 2001).

The NA Ocean is dominated by the basin-scale clockwise rotating North Atlantic central gyre on the surface, and the thermohaline circulation system at depth (Broecker, 1991; Broecker et al., 1985). The warm Gulf Stream flows north on the western edge and the cooler North Equatorial current flows south on the eastern edge. In the Caribbean the two main upper water masses are the Caribbean Surface Water, and below 200 m, the high-salinity Subtropical Underwater (Etter et al., 1987). Surface salinity (SSS), temperature, and pressure (SLP) are controlled by a variety of factors, including precipitation, general climatic conditions, and inter-basin water movement, such as the cross-equatorial current from the South Atlantic and water vapor transport from the eastern Pacific. In general, however, oceanic heat storage for the Caribbean Sea is controlled by the movement of water masses, the upper 200 m of which are primarily driven by the trade winds (Etter et al., 1987). Because evaporation exceeds the combined effect of precipitation and river influx, water leaving the Caribbean is more saline than water entering (Etter et al., 1987).

On decadal scales NA SST exhibits an alternating pattern of gradual increase and decrease, termed the Atlantic Multi-decadal Oscillation (AMO) (Enfield et al., 2001). Over longer periods the meridional overturning circulation (MOC), the NA section of the thermohaline circulation system, is important, as the rate of movement impacts regional heat transfer. NA deep water (NADW) formation, the sinking of cold, salty water in the NA, drives this section of the oceanic conveyor belt. The rate of the poleward transport of warm water (the

Gulf Stream being a prime example) is related to the rate of sinking, which varies on a number of time scales (Broecker, 1991; Schlosser et al., 1991, Ruhlemann et al., 1999, Nyberg, et al., 2001, 2002; Sarmiento and Gruber, 2006).

TCs are episodic circulation features that result from/interact with both atmospheric and oceanic conditions, as evidenced by the requirements of cyclogenesis. TCs require specific atmospheric conditions, such as low vertical shear, high relative humidity in the middle troposphere, and a pre-existing disturbance. The main oceanic requirement is a threshold SST of $\sim 26.5^{\circ}\text{C}$ extending 50 meters in depth (Goldenberg et al., 2001; Nyberg et al., 2007), as it is this heat that powers the system. TCs are large Carnot engines that, driven by the latent heat of evaporation (Emanuel, 1987), move energy from the ocean to the atmosphere, and transport heat poleward. Geographically, the formation area of TCs occupies a fairly narrow band between the ITCZ and the BH, as 60% of all TC and 85% of major hurricanes (category 3 or greater) form in the Atlantic between 10 and 20°N latitude, a region named the Main Development Region (MDR) (Goldenberg and Shapiro, 1996; Goldenberg et al., 2001). The southern limit of cyclogenesis is around 8° (Elsner and Kara, 1999), south of which of the vorticity generated by the Coriolis force falls below the necessary threshold level. Once formed, TCs typically move westward and northward, their latitudinal range expanding rapidly as track position and shape are influenced by a large number of short-term meteorological controls. A spatially separate set of TCs forms in the western Caribbean and the Gulf of Mexico, often tracking in a mainly northward direction. Temporally, the annual NA TC season lasts from May through November, matching the circum-Caribbean wet season.

Activity is not distributed evenly along the western edge of the NA, as evidenced by counts of tropical cyclones passing within 75 nautical miles of 57 sites spaced ~ 50 miles apart

along the coastline of the United States from the Mexican border through Maine for the period 1886-1998 (Neumann et al., 1999). This record shows a generally constant and gradual increase in activity from southern Texas through Cape Hatteras, NC, with subpeaks at Grand Isle, LA and Miami, FL. North of Cape Hatteras, which records the highest level of activity (>80 events/100 years), storm frequency decreases rapidly, with a small subpeak at Nantucket, MA. Hurricanes and major hurricane frequencies display a very similar pattern. Data from three Caribbean sites (in Puerto Rico and the Virgin Islands) show an intermediate amount of activity (Neumann et al., 1999).

3.3 Geographical/Physical Relationships between Circulation Features

3.3.1 BH-NAO

The BH is the central node of the subtropical high pressure ridge, its exact definition varying with the investigator (Sahsamanoglou, 1990; Davis et al, 1997; Portis et al., 2001). The BH exhibits both latitudinal and longitudinal movement on a variety of time scales. Annually, the BH moves southwest in the winter and northeast in the summer, on decadal timescales there is both latitudinal and longitudinal displacement (Sahsamanoglou, 1990; Portis et al., 2001). Generally, a higher (stronger) central pressure correlates to a northeastern, and a lower (weaker) central pressure to a southwestern position (Sahsamanoglou, 1990; Machel et al., 1998), and a more northeasterly-southwesterly tilt (Nyberg et al., 2001).

Of great importance to NA circulation is the pressure gradient between the BH and the adjacent low pressure systems. The gradient between the BH and the IL to the north is referred to as the North Atlantic Oscillation (NAO) and quantified by the NAO Index, which is the normalized difference, measured at a number of different locations, between the SLP below the BH and the IL (Hurrell, 1995; Jones et al., 1997; Portis et al., 2001). As indicated by the name,

this relationship tends to behave in a “see-saw” fashion (Elsner et al., 2000b), alternating between a “strong” (high BH/low IC central pressures, large/positive index values) and “weak” (low BH/high IL central pressure, small/negative index values) conditions. The inverse pressure relationship between the BH and IL means that high BH values correlate closely with high NAO values. It also means that NAO values are a good proxy of the intensity of the NA circulation that correlates well with a number of circulation and climatic features, such as NA SST, and SLP, as well as precipitation and temperature patterns for areas as distant as Asia and the Middle East. A strong NAO strengthens and shifts the both the trade winds and the mid latitude westerlies southward, resulting in milder, wetter winters for northern Europe and drier conditions farther south, including the Caribbean (Hurrell, 1995; Black et al., 1999; Marshall et al., 2001; Nyberg et al., 2001; Visbeck et al., 2001).

3.3.2 BH-TC

During the TC season, TC track location movement parallels that of the BH, moving to the northeast out of the Caribbean in June, and then returning southwestward in the fall, with TC formation staying somewhat to the south of the BH (Neumann et al., 1999). This probably indicates the inhibitory control the BH exerts on cyclogenesis, with formation only possible in areas not directly under the influence of the subsiding air associated with the BH (i.e., formation occurs in areas that the BH has vacated). Because TCs must curve around the BH rather than plow through it, the position of the BH exerts an important control over TC track pattern and location, and consequently, location of landfall. Due to the fact that NAO intensity is such a key feature of the NA circulation system, studies often use the NAO index rather than the central intensity record of the BH to help understand the relationship between different components. Because the NAO Index captures the relative intensities of the two NA action centers, NAO

values are valid proxies for both overall circulation and BH intensity; because stronger central pressure of the BH correlates to a northeast position the NAO values can also be used as a rough proxy for BH location.

Using bootstrap analysis to examine the location of major hurricane landfalls along the US coast since 1865, Elsner et al. (2000b) demonstrate statistically significant differences between NAO values and latitude of landfall, with higher July NAO values correlating to a more northern location of landfall. McCloskey and Knowles (2009) (Chapter 3) use a GIS-based approach to extend this work. Using data for the period 1948-2003, they show visually that extreme eastern (western) track years and extreme high (low) NAO Index value years display remarkably similar patterns. Surface interpolations of TC track locations for the period's nine extreme western years show a southwest concentration curving around a long, narrow central trough in activity, presumably corresponding to the location of the BH. Similar visualization of the nine extreme eastern track years show a northeast displacement in track location, and a smaller, more hemispherical shape to the central trough. For the eastern (western) years the annual values are positive (negative) for both of two NAO indices. They then used the reverse approach and plotted all six-hour tropical cyclone segments that occurred during months with extreme ($\pm 2.5 \delta$) NAO values. The surface interpolation patterns derived from this process were extremely similar to those derived from the extreme location data, with the pattern for extreme positive (negative) values correlating to the extreme eastern (western) years. The surface interpolation that resulted when the extreme negative pattern was subtracted from the extreme positive pattern suggested that high NAO values correlate to northwest track position and increased recurvature of the storm track, while low NAO value correlate to southwestern track displacement and more horizontal track.

Surface interpolations were performed on three separate data sets;

- 1) All TCs for the period
- 2) All hurricanes for the period
- 3) All major hurricanes for the period

All three surface interpolations showed a similar pattern, namely a common pathway from the Cape Verde islands westward, until reaching a point northeast of the Greater Antilles, where the track pattern split into two distinct track sets, both recurving to the northeast, but with one displaying tighter recurvature and an eastern displacement. Changes in NAO intensity are suggested as responsible for this bimodal track pattern. A spatially distinct set of storm tracks were noted in the western Caribbean and Gulf of Mexico.

These studies support the idea the BH has an important physical relationship with TC tracks, with a weak, southwestern BH (as proxied by NAO values), corresponding to less recurved, southern tracks, and a strong, northeastern BH corresponding to increased recurvature and more northern tracks.

3.3.3 ITCZ-BH

A statistical examination of the variability of the entire summer NA surface circulation system, including location and intensity of the ITCZ, showed that the first principal component, (which explained 19.5% of the variance) was characterized primarily by the location of the BH (Machel et al., 1998), indicating that the BH has an important mechanical relationship with the other main atmospheric features, in this case, the ITCZ, IL, and the South Atlantic subtropical high.

Over the instrumental record, latitudinal movement of the ITCZ has been shown to have a positive correlation with rainfall anomalies in the tropical Atlantic (Hastenrath, 1976, 1985,

2000a, b; Lamb, 1978, Kapala et al., 1998; Curtis and Hastenrath, 1999). This has been demonstrated for both the Caribbean-Central American region and the Sahel to the north and northeast Brazil to the south of the ITCZ. On both sides of the ITCZ movement of the ITCZ toward (away from) the location tend to result in positive (negative) rainfall anomalies rainfall on an inter-annual basis. Assuming the negative rainfall anomalies result from the approach of the following subtropical highs, this indicates coordinated movement between them and the ITCZ. This parallel movement is only approximate, however, as the relationship between the ITCZ and the BH is complex, controlled by a positive relationship between pressure gradient and distance. Increased pressure difference between the ITCZ and the BH increases trade wind strength and drives the two features apart. Indeed, for the period 1881-1989 during “strong” NAO (≥ 1 standard deviation above the long-term mean) years the ITCZ was “forced” 1.3 degrees south compared to “normal” years (Kapala et al., 1998). Both empirical data (Curtis and Hastenrath, 1999) and modeling studies (Broccoli et al., 2006) demonstrate that intensified trade winds correlate with a southward shift in the ITCZ, while Nyberg et al. (2001, 2002) advance the corollary argument, namely that northern movement of the ITCZ weakens the trade winds. Since strengthened trade winds increase heat transfer from the ocean to the atmosphere, lowering SST in the affected area (Giannini et al., 2000; Hasanean, 2004; Chiang and Bitz, 2005; Chiang, 2006), a stronger BH can be expected to generally reduce NA SST and force a southern movement in the zone of maximum SST (SST-max), as indeed was found by Kapala et al. (1998).

3.3.4 Oceanic-atmospheric

The NA ocean plays an important, though, due to thermal inertia, slower role in the circulation, principally through the control it exerts over SST, which, though controlled on the short term by trade wind speed, is subject to much longer scale control by water mass

movements (Etter et al., 1987). This is particularly true in the Caribbean, where the entrance of Atlantic water masses into the area can be blocked by a northern movement of the ITCZ (Nyberg et al., 2001, 2002). On a long temporal scale, a reduction in the rate of North Atlantic Deep Water (NADW) formation slows the thermohaline circulation, with less sinking of water in the NA resulting in reduced northern transport of warm tropical waters. This leads to higher SST at low latitudes, lower SST at high latitude and a steeper meridional temperature gradient (Ruhlemann et al., 1999). On century to millennial scales, colder NA SSTs are associated with slower MOC rate (Nyberg et al., 2001, 2002). Over both short and long temporal scales, a colder NA means increased SLP for the NA, strengthened trade winds and a southern movement of the ITCZ, thus permitting increased water movement into the Caribbean. Black et al. (1999) has shown that lowered SST in the northern Atlantic have had a significant correlation with increased wind speed and upwelling in the tropical Atlantic for at least the last 800 years. Naturally, solar radiation is also of great importance, varying on a number of temporal scales (Peterson et al., 1991; Black et al., 1999, 2004; Poore et al., 2003, 2004).

NA SST is an important oceanic parameter as it affects SSS due to changes in water vapor transport to/from the Pacific Ocean and the cross-equatorial heat transport from the SA (Nyberg et al., 2001). Although ENSO is episodically an important influence on SSS, warmer SST at low latitudes are generally associated with increased precipitation and reduced surface salinity for the area. NA SST has well documented relationships with several atmospheric components. Warmer SSTs have a negative correlation with both atmospheric stability and vertical shear, especially in the MDR (Goldenberg et al., 2001; Nyberg et al., 2007). Thus, increased SST correlates to increased instability and reduced wind shear, both of which are of crucial importance for TC formation. Goldenberg et al. (2001) also state that higher SST

increases the resistance of a TC to vertical shear. Wang and Lee (2008), however, argue that the reduction of vertical shear resulting from heightened SST in the MDR actually becomes a net overall increase when the effect of global SST increase is considered. Using a statistical model, Saunders and Lea (2008) show that a relatively small ($\sim 0.5^{\circ}\text{C}$) increase in SST correlates to a large ($\sim 40\%$) increase in hurricane frequency and activity in the NA for storms forming south of 20°N .

By definition, a strong NAO means increased SLP under the BH; it also correlates to reduced NA SST, probably mainly through the energy lost due to increased zonal winds speeds. Because a strong NAO correlates to decrease precipitation in the Caribbean, this tends to increase regional SSS.

3.4 General NA Circulation System

Theoretically, combining the various relationships should result in positive relationships between BH intensity, trade wind strength, vertical shear, separation between the BH and ITCZ, SLP, SSS in the lower latitudes and latitude of TC track position and strength of recurvature; and a negative relationship with SST south of the BH, and the latitude of the ITCZ. Therefore strengthened BH intensity/strong NAO should correspond to:

- a. Northeastern shift in TC track location, with increased recurvature
- b. Increased separation between the BH and ITCZ
- c. Southern migration of the ITCZ
- d. Increased SSS for the tropical NA
- e. Increased SLP for the subtropical and tropical NA

- f. Increased trade wind strength
- g. Decreased NA SST
- h. Increased vertical shear
- i. Increased atmospheric stability

The last four conditions should contribute to reduced TC activity. Vertical shear, which is commonly recognized as a primary inhibitor of TC formation (Goldenberg and Shapiro, 1996; Shapiro and Goldenberg, 1998), is increased due to both the increased strength of the trade winds and the inverse relationship with lowered SST. Tropical SST is reduced in a number of ways, including the cooling effect of the trade winds, and the southern movement of the ITCZ and SST-max. Increased atmospheric stability and increases in the percentage/area of ocean with SST below the threshold necessary for formation and vertical shear tend to inhibit cyclogenesis, while lower SST reduces the energy available for developed TC, perhaps reducing a storm's longevity and total power (Emanuel, 2005). Strong NAO conditions should also lead to increased salinity for tropical NA waters due to reduced precipitation in the circum-Caribbean region.

3.5 Theoretical Model

3.5.1 Structure

Based on the above analysis we are presenting a preliminary model of TC activity under current conditions in which:

1. TCs occur in a zone between 8° N and the BH
2. TCs follow three basic paths
3. Strong NAO moves
 - TC formation/tracks/landfall to the northeast
 - Decreases TC frequency

- Increases separation between BH and ITCZ
- Increases trade wind intensity
- Increases vertical wind shear
- Decreases NA SST
- Increases tropical SSS

4. Weak NAO moves

- TC formation/tracks/landfall to the southwest
- Increases TC activity
- Decreases separation between BH and ITCZ
- Decreases trade wind intensity
- Decreases vertical wind shear
- Increases NA SST
- Decreases tropical SSS

We further suggest that disparate climatic phenomena, interrelated through a system of mutually connected feedback, form a coherent system responsible for the oscillation in NA TC activity/frequency. Specifically, we suggest that the intensity of the BH, the separation between it and the ITCZ, trade wind strength, and SST, SSS, SLP, precipitation, MOC rate, and water mass movement are all interconnected features, whose relationships tend to drive NA TC activity into either of two alternating modes;

1. An “Active/Warm” phase with more southern storms, characterized by a weaker BH, situated closer to the ITCZ, lower SLP, higher SSTs, lower tropical SSS and weaker trade winds

2. A “Cold/Inactive” phase characterized by a stronger BH, less TC activity, with more northern storms, displaying increased recurvature, higher SLP, lower SST, higher tropical SSS and stronger trade winds.

The expected correlations and the two end members of such relationships are displayed in **Figure 3:1**. These two phases are postulated as corresponding to the multi-decadal oscillation observed in TC activity and NA SST (AMO).

3.5.2 QBO and ENSO

Both the quasi-biennial oscillation (QBO) and the El Niño-Southern Oscillation (ENSO) have significant influences on NA TC activity. For the QBO, the westerly phase corresponds to increases in both number of TC and major hurricanes (Gray and Shaeffer, 1991; Elsner et al., 1999; Elsner and Kara, 1999; Landsea et al., 1999; Goldenberg et al., 2001). For Enso, El Niño (La Niña) periods reduce (increase) overall activity, with some regional variation (Gray, 1984; Richards and O’Brien, 1996; Bove et al., 1998; Elsner and Kara, 1999; Pielke and Landsea, 1998; Bengtsson, 2001; Tartaglione et al., 2003). ENSO phase also affects the transport of water vapor and heat between the eastern equatorial Pacific and western equatorial Atlantic (Nyberg et al., 2002), with the export of freshwater increasing during El Niño years (Schmittner et al., 2000). The ENSO cycle, therefore, directly influences circulation conditions in the NA. However, because the duration of the extreme modes (La Niña or El Niño) needs to be on the order of decades to have significant effect on thermohaline circulation (Schmittner et al., 2000), the influences of these events are not sufficient to force phase change in the Warm/Active and Cold/Inactive system, and therefore remains outside the system. The same argument applies to the QBO.

It has been suggested, however, that increases in ENSO frequency dramatic enough to

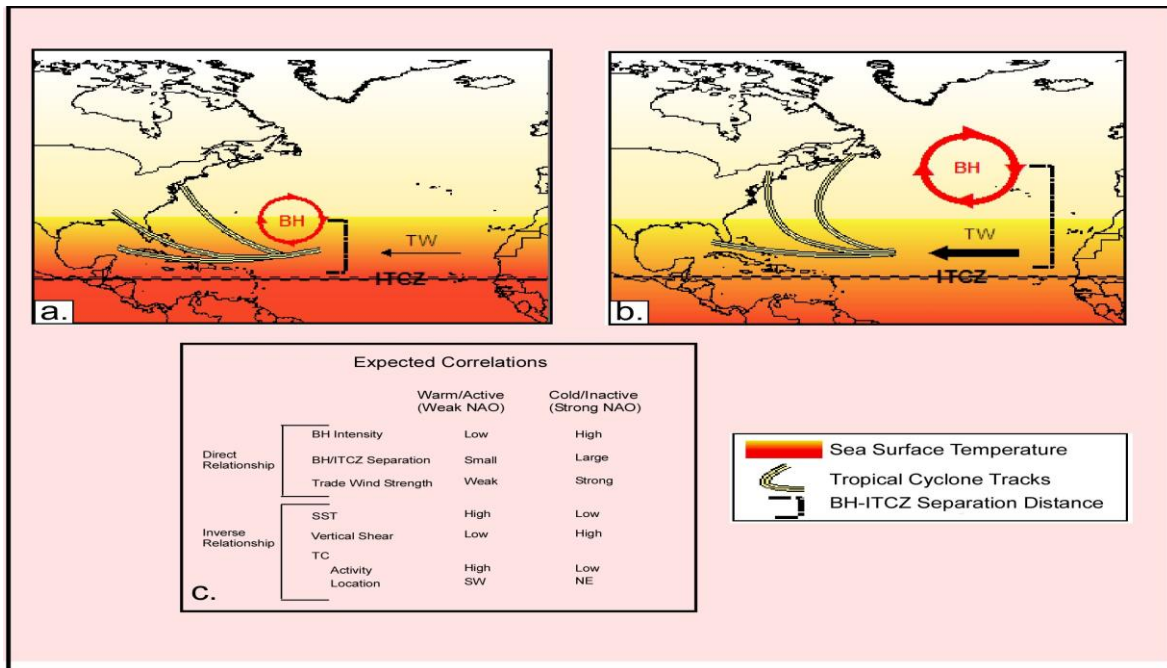
result in ENSO control over NA phase changes may have occurred in the past, both on a centennial scale associated with the Medieval Warm Period (Nyberg et al., 2002) and on a millennial scale during the mid Holocene (Haug et al., 2001; Koutavas and Olive, 2006). For the multi-decadal time scale of our proposed system, however, both the QBO and ENSO can be considered as noise; basically high frequency oscillations superimposed on the underlying system, and therefore not incorporated into this paper.

3.5.3 Phase Changes

Based on this model we used a combination of the various factors (BH and ITCZ location and intensity, trade wind strength, TC activity, vertical wind shear, and SST) to visually set a “best fit” for NA circulation regimes since 1881, which is incorporated in Figures 2-4. In these figures red (blue) background shading indicates periods we classify as Warm/Active (Cold/Inactive). The first year of each period is listed.

3.5.3.1 TC Regimes

To support these theoretical relationships with empirical observation requires an index of NA TC regimes, for which no commonly accepted version exists. Therefore we present one here based on a simple averaging of the annual number of a) tropical storms and b) hurricanes, divided into periods displaying obvious numerical differences. The data is taken from Neumann et al. (1999), starting with the differentiation of tropical storms and hurricanes in 1886, through 1998 (**Figure 3:2a**). Active (inactive) periods are shaded red (blue). Although this method is somewhat subjective, it agrees well with other published indices, including the calculations of change points of 20th century major hurricane frequency, (Elsner et al, 2000a), and the Atlantic Multi-decadal Oscillation (AMO) curve (Enfield et al., 2001) (**Figure 3:2b, c**). The AMO records NA SST, and is often used as a proxy for TC activity, with warm (cold) intervals corresponding to

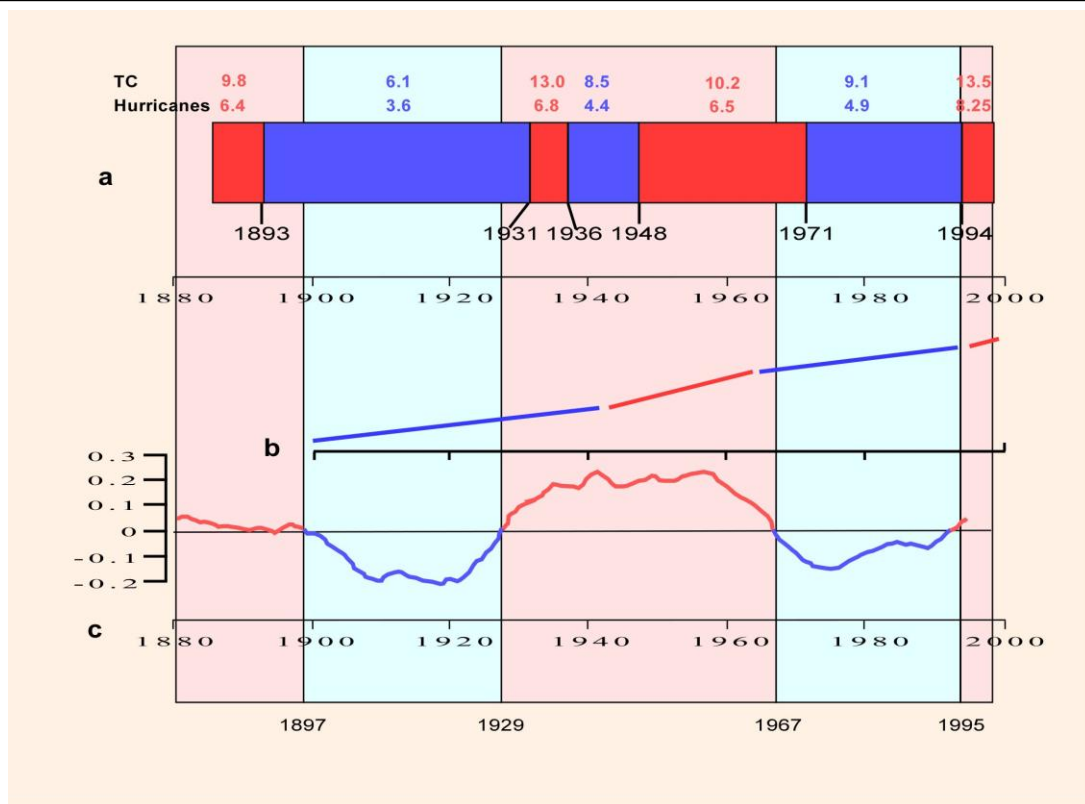


3.1 Diagram displaying the postulated relationships between important features of our theoretical model. The two end members of the NA circulation system are (a) a warm/active period, and (b) a cold/inactive period. The atmospheric/oceanic characteristics associated with each are listed in (c).

active (inactive) TC periods (Goldenberg et al., 2001; Keim et al., 2007; Virmani and Weisberg, 2006).

3.5.4 Empirical Correlation

A rough correlation can be seen between the latitudinal positions of the ITCZ and BH (**Figure 3:3a, b**) and BH intensity (**Figure 3:3c**) since 1881. From 1881-1896 (red) generally, low BH intensities correspond to generally southern (northern) average position of the BH (ITCZ). The period from 1897 – 1928 (blue) shows an intensification of the BH corresponding to a southern movement in the ITCZ average latitude, while the following period (1929-1966) (red) shows the reverse—a weakening of BH intensity and a northern movement of the ITCZ. From 1968 until the end of the record (1995) (blue) the separation between the two features increases, with the ITCZ (BH) showing southern (northern) movement, indicating increasing spatial separation. However, during this period neither the summer (JJAS) BH nor trade winds intensify as expected; rather both continue to weaken (not shown). Substituting winter (DJFM) values for BH intensity and trade wind strength (Figs. 3 c, d) improves the match significantly, especially for the period after 1970, when both intensity and strength increase as expected given the increasing spatial separation of the ITCZ and the BH (**Figure 3a, b, c, d**). This suggests that the much sharper winter temperature gradients exert important control over summer conditions, presumably through the lag resulting from the thermal inertia of the ocean. Since the NAO is basically a winter condition, its summer effect is mainly felt through residual changes in SST. The behavior of NA TC activity, AMO cycle, and vertical wind shear roughly approximate that predicted by the model, with periods of increased BH strength, trade wind intensity, and vertical wind shear (blue) corresponding to reduced TC activity and cold AMO intervals, with the opposite TC and AMO conditions predominating during reversed circulatory conditions (red)



3.2 NA TC regimes; (a) numerical scheme devised by author based on a visual analysis of NOAA data from Neumann et al. (1999), average annual frequency of TC and Hurricanes are listed for each period, the active (inactive) periods are shaded red (blue), first year of each regime listed below the curve; (b) the regression line for change points based on analysis of the cumulative frequency of NA major hurricanes for the period 1900-1999, active (inactive) periods are shaded red (blue), modified from Elsner et al. (2000a); (c) ten year running mean of detrended NA SST for the period 1856-1999 (units are $^{\circ}\text{C}$), periods above (below) the long-term average periods are shaded red (blue), modified from Enfield et al. (2001). Background shading represents a “best fit” regime system based on a visual correlation of the various schemes, in which red shading indicates “Warm/Active” periods, while blue shading indicates “Cold/Inactive” periods. This is consistent for Figures 3.2-4, with the first year of each regime listed below the curve.

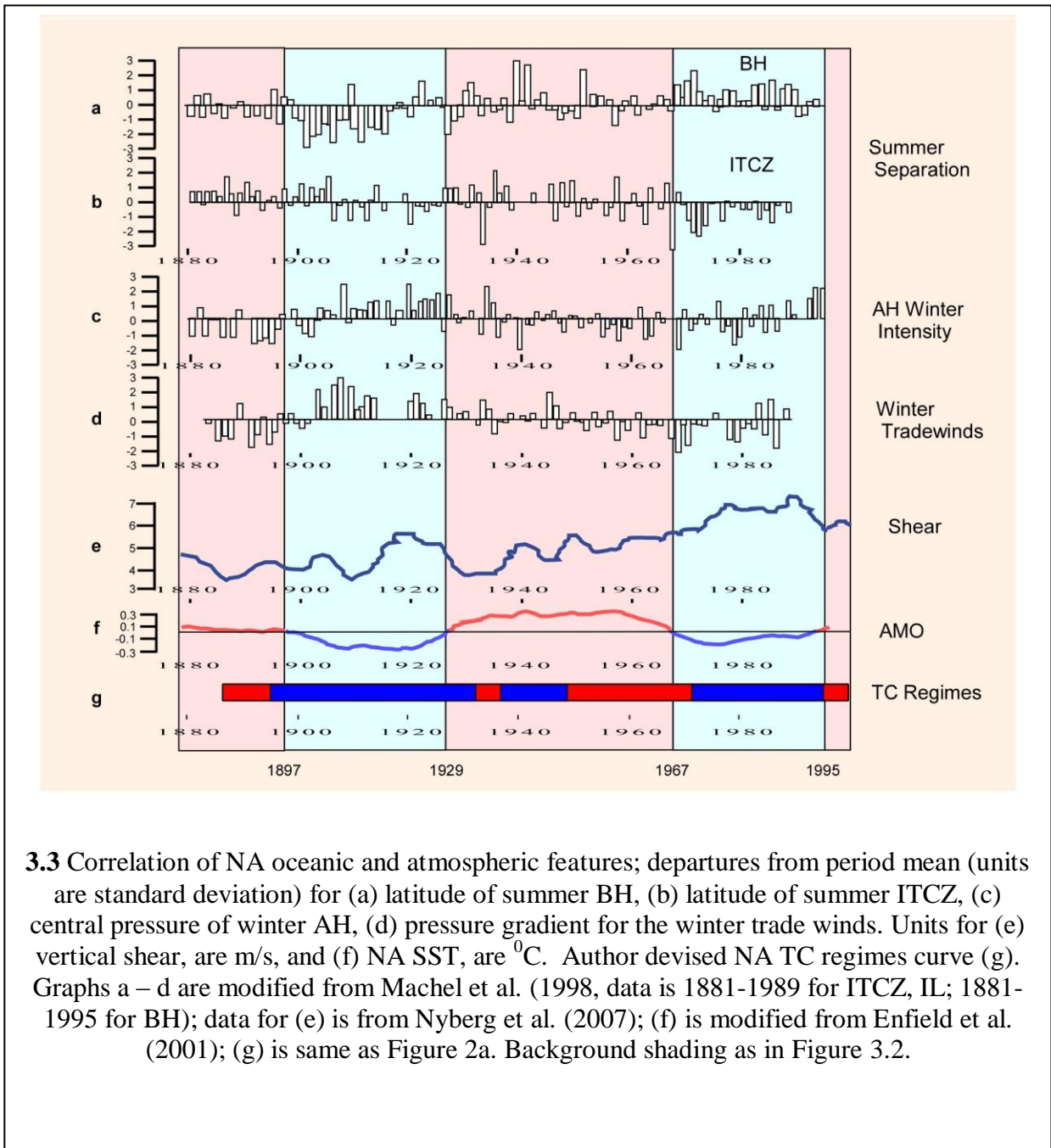


(**Figure 3e, f, g**). The fit with separation of the ITCZ and BH is not as close.

Support for a northeast shift in track location related to BH intensification and the general circulation conditions during Cold/Inactive phases is provided by Bell and Chelliah (2006) who show that the Accumulated Cyclone Energy (ACE, not shown) index for extra-tropical (northern) regions peaked during the relatively inactive period from the early 1970s through the mid 1990s. An examination of the latitude of formation for all NA TC from 1944 to 1996 demonstrates the predicted relationship between TC frequency, the AMO cycle and track location. During this interval, the peak period of TC forming north of 23.5°N (**Figure 3:4a**) (blue) roughly correlates to both cold AMO and inactive TC intervals, Fig. 4a, c, d) while the period of peak TC formation to the south (**Figure 3:4b**) (red) occurs during warm AMO and active TC intervals (data from Landsea et al., 1999). Trend lines for each region demonstrate both the distinct shift in area of formation corresponding to phase change (**Figure 3:4a, b**), as well as correlated incremental change between the regions. As the Warm/Active phase (red) draws to a close with decreasing SST, TC formation decreases in the south, while increasing in the north. Concurrent with the phase change, TC formation abruptly increases in the north and drops in the south; when SST again begin to rise TC activity gradually decreases in the north and increases to the south. The phase change in 1995 corresponds to an abrupt increase (decrease) in southern (northern) formation.

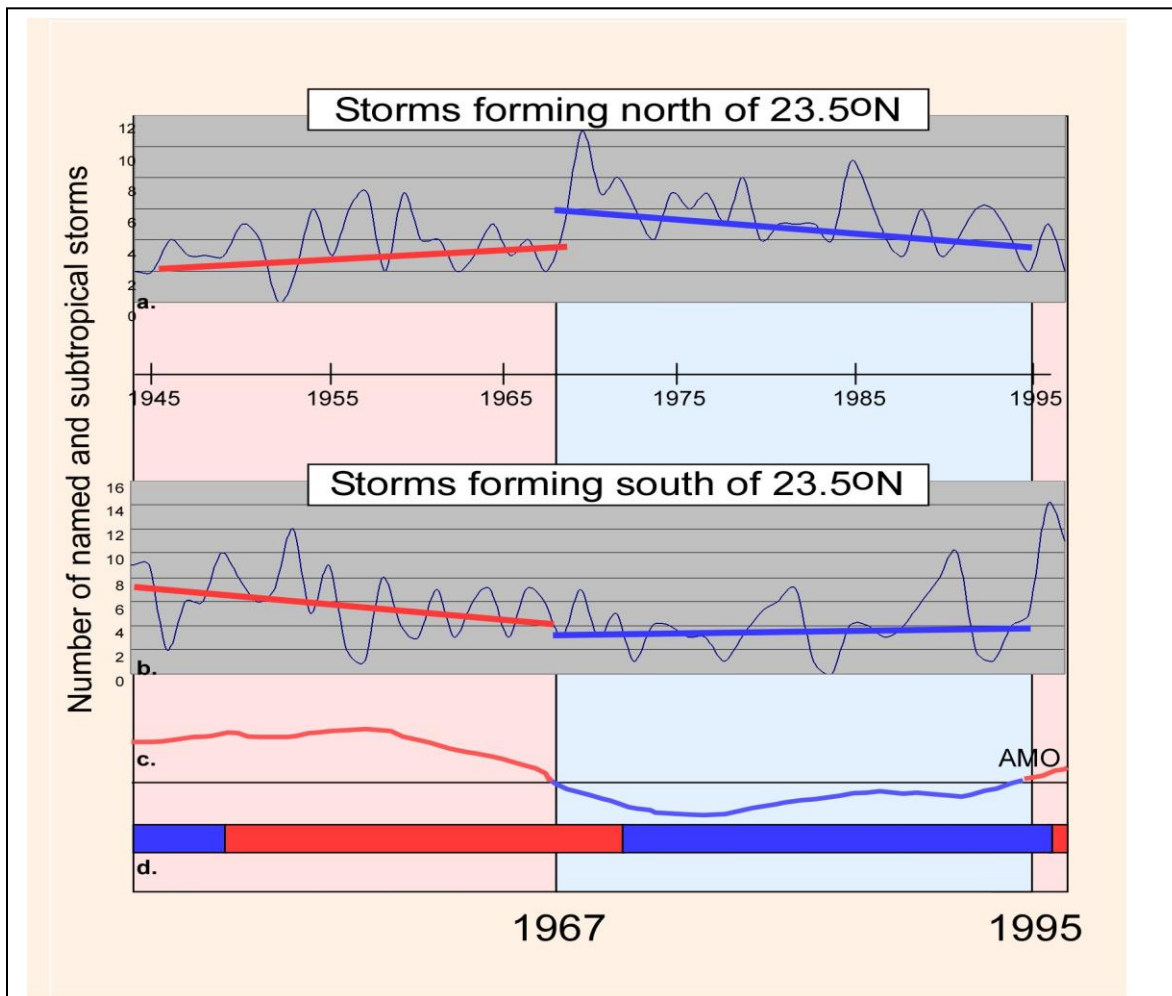
The anti-phase relationship between northern and southern areas for both ACE values (Bell and Chelliah, 2006) and area of TC formation (**Figure 3:4**) supports the view of feedback between the forcing mechanisms working to push conditions to either of two end members, thereby accounting for the abrupt multi-decadal shifts in NA TC activity. The sudden shift to an active period in 1995 (Goldenberg et al., 2001), characterized by a dramatic increase in NA TC

activity immediately following the largest annual decrease in winter NAO values in the record that extends to 1823 (Jones et al., 1997) and an accompanying reduction in vertical wind shear (Goldenberg et al., 2001) further supports this view.

3.5.5 Feedback System

While the precise physical mechanisms by which the various circulation components modulate each other are not fully understood, it seems reasonable that the atmospheric components exert greater influence on the short term, with the oceanic components maintaining the long term equilibrium. The covariance between NAO strength, zonal wind intensity, SLP, SST, and precipitation are well recognized (Marshall et al., 2001; Nyberg et al., 2001, 2002), and the feedbacks between these features relatively straightforward; namely that increased circulation (strong NAO) increases zonal wind strength, which cools off the surface waters due to evaporation. This in turn drives the SST-max and ITCZ southward, resulting in lower tropical precipitation, and increased tropical salinity. By leading to a reduced cross equatorial heat transport and increasing SLP in the tropical NA, these conditions form a positive feedback loop, thereby explaining the coordinated movement of the circulation features toward the Cold/Inactive end member phase. A similar positive feedback system can be envisioned for the Warm/Active phase, whereby high tropical NA SST pulls the ITCZ northward, thereby weakening the trade winds and further increasing SST. Meridional SST gradients reduce during warm phases, as the heat spreads northward, leading to relaxed pressure gradients and a less intense circulation. The opposite occurs during cold phases.

Thus, although we can postulate scenarios explaining movement towards the end members, what mechanism can be invoked to explain the phase changes? One possibility, suggested by Nyberg et al. (2001, 2002) involves SSS and the MOC. Warm/Active periods result in lowered



3.4 Frequency of formation for all NA TC from 1944 to 1996; (a) annual number of storms forming north of the Tropic of Cancer; (b) annual number of storms forming south of the Tropic of Cancer, data from Landsea et al. (1999); (c) NA SST; (d) NA TC regime. Background shading as in Figure 3.2. Both (a) and (b) display trend lines displaying changes in regional TC activity corresponding to regime changes. Note that northern activity is higher during period of low SST while southern activity is higher during periods of high SST. The trendlines indicate that regional TC activity and SST have correlated incremental responses, (i.e. activity slowly increases (decreases) in the north (south) as SST decreases from 1944 –1966, after which the trend reverses, suggesting an intimate coupled response.

SSS in the tropical NA, due, firstly, to increased regional precipitation and, secondly, to the blocking of the movement of the high-salinity Subtropical Underwater into the Caribbean through shallow passages in the eastern Caribbean (Nyberg et al., 2002). Because warm conditions generally increase the thermohaline circulation (Schmittner et al., 2000), this warm, low-salinity water propagates northward fairly quickly. When it reaches the area of NADW formation, its buoyancy slows down the conveyor belt, thereby “throwing the switch”. This initiates a period of reduced MOC rates and decreased meridional circulation, reducing the heat transport northward, and steepening the NA meridional temperature gradient. This leads to an intensification of the circulation pattern (i.e. Cold/Inactive phase). This phase continues, strengthening through the previously mentioned positive feedback loop, and thereby further slowing the MOC rate. Salinity increases in the lower latitude due to both decreased precipitation and the increased influence of the high-salinity waters entering from the east, driven by stronger trade winds and the opening of the shallow passages by the southern movement of the ITCZ. The slowed northern transport leads to increasing heat storage in the tropical NA (note the gradual increase in SST during the Cold/Inactive phase, **Figure 3:4c**), which eventually spreads northward, at which point the system again switches directions, the meridional heat gradient reduces, the circulation begins to relax and the MOC begins speeding up.

Support for this type of SSS/MOC interdependence comes from the Great Salinity Anomaly, when during the 1970-80s an estimated 80% rate decrease for NADW correlated to anomalously low NA SSS values (Schlosser et al., 1991). Opposite conditions prevailed in the 1950s (Greatbatch et al., 1991). The association between reduction in MOC rates and SSS appears to operate on much longer time scales as well (Nyberg et al., 2002; Ruhlemann et al., 1999).

3.5.5.1 TC as Possible Feedback Component

TCs are possibly a significant contributing feature of this feedback system. During Warm/Active phases the increasing frequency/intensity/accumulated power of TCs aids in the northern transport of warm, low salinity water, and the subsequent slowdown of NADW. Conversely, during Cold/Inactive phases the reduced frequency and more northern location of TC reduce the amount of heat they transport poleward. This supports the view that TCs are a participatory, integrated feature of a coherent oscillatory circulation system, and not a passive artifact of climatic conditions.

Earlier studies have suggested either temporal correlations or coherent relationships between several of these same atmospheric/oceanic features. Examples include Hasanean's (2004) interrelated view of BH intensity, trade wind strength and SST anomalies, while Giannini et al. (2000) note correlations between NA SLP, trade wind strength, SST, and Caribbean rainfall. Goldenberg et al. (2001) suggest a correspondence between vertical shear, SST, lower tropospheric moisture, SLP, QBO, and TC activity; Gray et al. (1997) discuss the relationship between SST, SLP, temperature and atmospheric circulation, and the thermohaline circulation, while Gray (1990) correlates Sahelian rainfall and major hurricanes. Bell and Chelliah (2006) suggest a set of atmospheric and oceanic conditions somewhat similar to ours as being responsible for interannual to multi-decadal oscillations in TC activity since 1950. Gill (2000) identifies southern movement of the BH as the proximate cause of drought in the Yucatan, and Virmani and Weisberg (2006) associate SST, SLP, zonal winds with hurricane activity. The theorized relationships between the various circulation features are, naturally, obscured by a number of other atmospheric conditions that exert independent control over TC location/frequency, the most important being ENSO and the QBO. Natural variability inherent to

each individual atmospheric/oceanic feature also masks the larger trends. Significantly, spectral analysis of both overall NA circulation (Machet et al., 1998) and the central pressure of the subtropical high (Hasanean, 2004) show peaks above the 95% confidence interval only for the lowest frequency (total length of the time series; 1881-1995 for Machet et al.; 1950-2002 for Hasanean). This seems to indicate high frequency masking of lower frequency trends. Chapter 4 argues that this coherent NA circulation system has been in place throughout the Holocene.

3.6 Conclusions

1. BH intensity (proxied by NAO values) controls steering of TC tracks by means of exerting control over intensity/location of recurvature which affects subsequent track location
2. BH (proxied by NAO values) controls trade wind strength/SLP/SST/latitude of SST-max
3. These conditions control TC frequency/location
4. Feedback makes this a coherent system
5. This system oscillates between the two end members
 - a. Warm/Active
 - b. Cold /Inactive,

thereby accounting for the observed multi-decadal oscillation in SST and TC activity.

3.7 References

- Bell, G. D., and Chelliah, M., 2006. Leading tropical modes associated with interannual and multidecadal fluctuations in North Atlantic hurricane activity. *Journal of Climate* 19, 590-612.
- Bengtsson, L., 2001. Enhanced hurricane threats. *Science* 293, 440-442.
- Black, D. E., Peterson, L. C., Overpeck J. T., Kaplan, A., Evans, M. N., and Kashgarian, M. 1999. Eight centuries of North Atlantic Ocean atmosphere variability. *Science* 286, 1709-1713.

Black, D. E., Thunell, R. C., Kaplan, A., Peterson, L. C., and Tappa, E. J., 2004. A 2000-year record of Caribbean and tropical North Atlantic hydrographic variability. *Paleoceanography* 19, PA2022. DOI:10.1029/2003PA000982,2004.

Bove, M. C., Elsner, J. B., Landsea, C. W., Niu, X-F., and O'Brien, J. J., 1998. Effects of El Nino on U.S. landfalling hurricanes, revisited. *Bulletin of the American Meteorological Society* 76, 2477-2482.

Broccoli, A. J., Dahl, K. A., and Stouffer, R. J., 2006. Response of the ITCZ to northern hemisphere cooling. *Geophysical Research Letters*. 33, L01702.

Broecker, W.S., 1991. The great ocean conveyor. *Oceanography* 4, 79-90.

Broecker, W.S., Takahashi, T., and Takahashi, T., 1985. Source and flow pattern of deep-ocean waters as deduced from potential temperature, salinity and initial phosphate concentration. *Journal of Geophysical Research* 90, 6925-6939.

Chiang, J. C. H., 2006. Tropical Atlantic climate variability as a model for marine ITCZ displacements. Unpublished paper presented at the Joint Assembly of the American Geophysical Union; Baltimore, Maryland.

Chiang, J. C. H. and Bitz, C. M., 2005. Influence of high latitude ice cover on the marine Intertropical Convergence Zone. *Climate Dynamics* 25, 477-496. DOI:10.1007/s00382-005-0040-5.

Curtis, S. and Hastenrath, S., 1999. Trends of upper-air circulation and water vapour over equatorial South America and adjacent oceans. *International Journal of Climate* 19, 863-876.

Davis, R. E., Hayden, B. P., Gay, D. A., Phillips, W. L., and Jones, G. V., 1997. The North Atlantic subtropical anticyclone. *Journal of Climate* 10, 728-744.

Elsner, J. B., 2007. Tempests in time. *Nature* 447, 647-649.

Elsner, J. B. and Kara, A. B., 1999. *Hurricanes of the North Atlantic: Climate and Society*. Oxford University Press, Oxford.

Elsner J.B., Kara, A. B., and Owen, M. A., 1999. Fluctuations in North Atlantic hurricane frequency. *Journal of Climate* 12, 427-437.

Elsner J.B., Jagger, T., and Niu, X-F., 2000a. Changes in the rate of North Atlantic major hurricane activity during the 20th century. *Geophysical Research Letters* 27, 1743-1746.

Elsner J.B., Liu, K-B., and Kocher B., 2000b. Spatial variations in major U.S. hurricane activity: statistics and a physical mechanism. *Journal of Climate* 13, 2293-2305.

Emanuel, K. A., 1987. The dependence of hurricane intensity on climate. *Nature* 326, 483-485.

- Emanuel, K. A., 2005. Increasing destructiveness of tropical cyclones over the past 30 years. *Nature* 436, 686-688.
- Enfield, D. B., Mestez-Nunez, A., and Trimble, P. J., 2001. The Atlantic multidecadal oscillation and its relation to rainfall and river flows in the continental U.S. *Geophysical Research Letters* 28, 2077-2080.
- Etter, P. C., Lamb, P. J., and Portis, D. H., 1987. Heat and freshwater budgets of the Caribbean Sea with revised estimates for the Central American Seas. *Journal of Physical Oceanography* 17, 1232-1248.
- Giannini, A., Kushnir, Y., and Crane, M. A., 2000. Interannual variability of Caribbean rainfall, ENSO, and the Atlantic Ocean. *Journal of Climate* 13, 297-311.
- Gill, R. B., 2000. *The Great Maya Droughts*. University of New Mexico Press, Albuquerque.
- Goldenberg, S. B., Landsea, C. W., Mestas-Nunez, M. A., and Gray, W. M., 2001. The recent increase in Atlantic hurricane activity: causes and implications. *Science* 293, 474-479.
- Goldenberg, S. B., and Shapiro, L.J., 1996. Physical mechanisms for the association of El Nino and West African rainfall. *Journal of Climate* 9, 1169-1187.
- Gray, W. M., 1984. Atlantic seasonal hurricane frequency Part I-El Nino and 30 mb quasi-biennial oscillation influences. *Monthly Weather Review* 112, 1649-1668.
- Gray, W. M., 1990. Strong association between West African rainfall and U.S. landfall of intense hurricanes. *Science* 249, 1251-1256.
- Gray, W. M., and Shaeffer, J. D., 1991. El Nino and QBO influences on tropical cyclone activity. In Glantz, M. H. , Katz, R. W., and Nichols, N., (eds), *Teleconnections Linking Worldwide Climate Anomalies*. Cambridge University Press, Cambridge. 257-284.
- Gray, W. M., Shaeffer, J. D., and Landsea, C. W., 1997. Climate trends associated with multidecadal variability of Atlantic hurricane activity. In Diaz, H. F. and Pulwarty, R.S., (eds), *Hurricanes, Climate and Socioeconomic Impacts*. Springer-Verlag, Berlin. 15-53.
- Greatbatch, R. J., Fanning, A. F., Goulding, A. D., and Levitus, S., 1991. A diagnosis of interpentadal circulation changes in the North Atlantic. *Journal of Geophysical Research* 96, 22009-22023.
- Hasanean, H. M., 2004. Variability of the North Atlantic subtropical high and associations with tropical sea-surface temperature. *International Journal of Climatology* 24, 945-957.
- Hastenrath, S., 1966. On general circulation and energy budget in the area of the Central American seas. *Journal of Atmospheric Science* 23, 694-711.

Hastenrath, S., 1976. Variations in low-latitude circulation and extreme climatic events in the tropical Americas. *Journal of Atmospheric Science* 33, 202-215.

Hastenrath, S., 1985. *Climate and Circulation in the Tropics*. D. Reidel Publishing Company, Dordrecht.

Hastenrath, S., 2000a. Interannual and longer-term variability of upper air circulation in the Northeast Brazil-tropical Atlantic sector. *Journal of Geophysical Research* 105, 7327-7335.

Hastenrath, S., 2000b. Interannual and longer term variability of upper-air circulation over the tropical Atlantic and West Africa in boreal summer. *International Journal of Climatology* 20, 1415-1430.

Haug, G. H., Hughen, K. A., Sigman, D. M., Peterson, L. C., and Rohl, U., 2001. Southward migration of the Intertropical Convergence Zone through the Holocene. *Science* 292, 1304-1314.

Hurrell, J. W., 1995. Decadal trends in the North Atlantic Oscillation and relationships to regional temperature and precipitation. *Science* 269, 676-679.

Jones, P. D., Jonsson, T., and Wheeler, D., 1997. Extension to the North Atlantic Oscillation using early instrumental pressure observations from Gibraltar and south-west Iceland. *International Journal of Climatology* 17, 433-450.

Kapala, A., Machel, H., and Flohn, H., 1998. Behaviour of the centres of action above the Atlantic since 1881. Part II: associations with the regional climate anomalies. *International Journal of Climatology* 18, 23-36.

Keim, B.D, Muller, R.A., and Stone, G. W., 2007. Spatiotemporal patterns and return intervals of tropical storm and hurricane strikes from Texas to Maine. *Journal of Climate* 20, 3498-3509.

Knutson, T. R. and Tuleya, R. E, 1999. Increased hurricane intensities with CO₂-induced warming as simulated using the GFDL hurricane prediction system. *Climate Dynamics* 15, 503–519.

Knutson T. R. and Tuleya R. E., 2004. Impact of CO₂-induced warming on simulated hurricane intensity and precipitation: sensitivity to the choice of climatic model and convective parameterization. *Journal of Climate* 17, 3477-3495.

Knutson T. R., Tuleya R. E., and Kurihara Y., 1998. Simulated increase of hurricane intensities in a CO₂-warmed climate. *Science* 279, 1018-1021 DOI: 10.1126/science.279.5353.1018.

Koutavas, A. and Olive, G. C., 2006. Holocene modulation of ENSO by the Intertropical Convergence Zone. Unpublished paper presented at the Joint Assembly of the American Geophysical Union; Baltimore, Maryland.

Lamb, P.J., 1978. Case studies of tropical Atlantic surface circulation patterns during recent sub-Saharan weather anomalies: 1967 and 1968. *Monthly Weather Review* 106, 482-491.

Landsea, C.W., 2005. Hurricanes and global warming. *Nature* 438, E11-E13.

Landsea, C.W., 2007. Counting Atlantic tropical cyclones back to 1900. *EOS* 88, 197-202.

Landsea, C.W., Pielke R. A. Jr., Mestas-Nunez, A., and Knaff, J. A., 1999. Atlantic Basin hurricanes: indices of climate change. *Climate Change* 42, 89-129.

Machel, H., Kapala, A., and Flohn, H., 1998. Behaviour of the centres of action above the Atlantic since 1881. Part I: characteristics of seasonal and interannual variability. *International Journal of Climatology* 18, 1-22.

Marshall, J., Kushnir, Y., Battisti, D., Chang, P., Czaja, A., Dickson, R., Hurrell, J., McCartney, M., Saravanan, R., and Visbeck, M., 2001. North Atlantic climate variability: phenomena, impacts and mechanisms. *International Journal of Climatology* 21, 1863-1898.

McCloskey, T.A. and Knowles, J. T., 2009. Migration of the Tropical Cyclone Zone throughout the Holocene. In Elsner, J. B., Jagger, T. H., (eds), *Hurricanes and Climate Change*. Springer, New York. 169-188.

Neumann, C. J., Jarvinen, B. R., McAdie, C. J., and Hammer, G. R., 1999. *Tropical Cyclones of the North Atlantic Ocean, 1871-1998*.: NOAA Press, Asheville, North Carolina.

Nyberg, J. B., Kuijpers, A., Malmgren, B. A., and Kunzendorf, H., 2001. Late Holocene changes in precipitation and hydrology recorded in marine sediments from the northeastern Caribbean Sea. *Quaternary Research* 56, 87-102.

Nyberg, J. B., Malmgren, B. A., Kuijpers, A., and Winter, A., 2002. A centennial-scale variability of tropical North Atlantic surface hydrography during the late Holocene. *Palaeogeography, Palaeoclimatology, Palaeoecology* 183, 25-41.

Nyberg, J., Malmgren, B.A., Winter, A., Jury, M.R., Kilbourne, K.H., and Quinn, T.M., 2007. Low Atlantic hurricane activity in the 1970s and 1980s compared to the past 270 years. *Nature* 447, 698-702. DOI:10.1038/nature05895.

Peterson, L.C., Overpeck, J. T., Kipp, N. G., and Imbrie, J., 1991. A high-resolution Late Quaternary upwelling record from the Caricaco Basin, Venezuela. *Paleoceanography* 6, 99-119.

Pielke, R.A., Jr., and Landsea, C.W., 1998. Normalized U.S. hurricane damages, 1925-1995. *Weather Forecastin* 13, 621-631.

Poore, R.Z., Dowsett, H. J., Verardo, S., and Quinn, T.M., 2003. Millennial- to century-scale variability in the Gulf of Mexico Holocene climate records. *Paleoceanography* 18, 1048. DOI: 10.1029/2002PA000868, 2003.

- Poore, R.Z., Quinn, T.M., and Verardo, S., 2004. Century-scale movement of the Atlantic Intertropical Convergence Zone linked to solar variability. *Geophysical Research Letter* 31, L12214. DOI: 10.1029/2004GL019940,2004.
- Portis, D. H., Walsh, J.E., Hanley, M. E., and Lamb, P.J., 2001. Seasonality of the North Atlantic Oscillation. *Journal of Climate* 14, 2069-2078.
- Richards, T. S. and O'Brien, J.J., 1996. The effect of El Nino on U.S. landfalling hurricanes. *Bulletin of the American Meteorological Society* 77, 773-774.
- Ruhlemann, C., Mulitza, S., Muller, P. J. Wefer, G., and Zahn, R., 1999. Warming of the tropical Atlantic Ocean and slowdown of thermohaline circulation during the last deglaciation. *Nature* 402, 511-514.
- Sahsamanoglou, H. S., 1990. A contribution to the study of action centers in the North Atlantic. *International Journal of Climatology* 10, 247-261.
- Sarmiento, J. L. and Gruber, N., 2006. *Ocean Biogeochemical Dynamics*. Princeton University Press, Princeton, NJ.
- Saunders, M. A. and Lea, A.S., 2008. Large contribution of sea surface warming to recent increase in Atlantic hurricane activity. *Nature* 45, 557-560. DOI:10.1038/nature06422.
- Schlosser, P., Bonisch, G., Rhein, M., and Bayer, R., 1991. Reduction of deepwater formation in the Greenland Sea during the 1980s: evidence from tracer data. *Science* 251, 1054-1056.
- Schmittner, A., Appenzeller, C, and Stocker, T.F., 2000. Enhanced Atlantic freshwater export during El Nino. *Geophysical Research Letters* 27, 1163-1166.
- Shapiro, L. J., and Goldenberg, S. B., 1998. Atlantic sea surface temperatures and tropical cyclone formation. *Journal of Climate* 11, 578-590.
- Tartaglione, C. A., Smith, S. R., and O'Brien, J.J., 2003. ENSO impacts on hurricane landfall probabilities for the Caribbean. *Journal of Climate* 16, 2925-2931.
- Trewartha, G. T., 1981. *The Earth's Problem Climates*, Second Edition. The University of Wisconsin Press, Madison, Wisconsin.
- Virmani, J.I., and Weisberg, R. H., 2006. The 2005 hurricane season: an echo of the past or a harbinger of the future? *Geophysical Research Letters* 33, L05707. DOI:10.1029/2005GL025517.
- Visbeck, M. H., Hurrell, J. W., Polvani, L., and Cullen, H. M., 2001. The North Atlantic Oscillation: past, present and future. *Proceedings of the National Academy of Science* 98, 12876-12877.

Walsh, K. J. E., and Ryan, B. F., 2000. Tropical cyclone intensity increase near Australia as a result of climate change. *Journal of Climate* 13, 3029–3036.

Wang, C., and Lee, S-k., 2008. Global warming and United States landfalling hurricanes, *Geophysical Research Letters* 35, L02708. DOI:10.1029/2007GL032396.

Webster, P. J., Holland, G. J., Curry, J. A., and Chang, H-r., 2005. Changes in tropical cyclone number, duration and intensity in a warming environment. *Science* 309, 1844-1846.

CHAPTER 4 TC AND THE ATMOSPHERE: LONG TERM RELATIONSHIP*

4.1 Introduction

The damage hurricanes inflicted upon the Caribbean and the United States during the 2004 and 2005 seasons dramatically demonstrate the societal importance of changes in hurricane tracks and frequencies. The increase in coastal development that occurred during the relatively inactive Tropical Cyclone (TC) regime that existed during the 1970s, 80s and early 90s, has contributed to the mounting property losses and death toll that ensued following the return to a more active TC regime, beginning in 1995 (Pielke and Landsea, 1998). Clearly, an increased understanding of the causes of these spatial/temporal oscillations is critical to achieving an effective response to this natural hazard. The proximate causes of these shifts, which occur across a variety of scales, from interannual to millennial (Reading, 1990; Walsh and Reading, 1991; Liu and Fearn, 2000; Elsner et al., 2000), are not well understood. This paper attempts to identify the average latitudinal position of the Intertropical Convergence Zone (ITCZ) as an important primary control over the location of the hurricane zone.

It should be noted that the correlation between the ITCZ and the hurricane zone is expected to manifest itself more clearly over longer (millennial) time scales, with the shorter term correspondence masked by “noisy” higher frequency atmospheric oscillations. Connecting the frequency/track pattern shifts to larger, better understood, and more easily tracked features of the general circulation system may lead not only to an improved understanding of the relationship between hurricanes and climate, but also to improved coastal management.

*Reprinted by permission of Springer

4.2 Data

Storm track data was downloaded from the National Oceanic and Atmospheric and Administration (NOAA) Hurricane Data set (HURRRDAT) (<http://hurricane.csc.noaa.gov/hurricanes/index.html>) and imported into a geographic information system (GIS). In order to minimize the use of less reliable (pre aircraft reconnaissance) data, our investigation covers the period 1948 –2003. Two North Atlantic Oscillation (NAO) indices were used, the standard index (<http://www.cru.uea.ac.uk/cru/data/nao.htm>) which we refer to as NAOj and a mobile NAO index which calculates the NAO index data as the difference in the normalized sea level pressures (SLP) anomalies at the locations of maximum negative correlation between the subtropical and sub polar North Atlantic SLP (Portis et al., 2001), referred to here as NAOm. Monthly and annual values from both NAO indices were added to the storm vectors database.

Three data sets were then created, 1. “Tropical Cyclones”, including all vectors of all storms; 2. “Hurricanes”, which included all vectors of all storms whose wind speed exceeded 74 mph at any point during the storm’s lifetime, and 3. “Major Hurricanes”, which included all vectors of all storms whose wind speed exceeded 111 mph at any point, corresponding to category 3 storms or greater on the Saffir-Simpson scale. Using geoprocessing techniques the center of each 6 hr storm vector was converted to a point coverage in order to apply kernel density surface interpolation, which is a technique that generalizes individual point locations or events, si , to an entire area and provides density estimates, $\hat{e}(s)$, at any location within the study region (Bailey and Gatrell, 1995). For a more detailed description of the methodology and different visualization results see Knowles and Leitner (2007).

4.3 Current Seasonal Variations in the NA Circulation System

As is well known, the NA circulation system basically consists of a series of stacked belts, starting near the Equator with the ITCZ, and proceeding poleward through the trade wind belt, the Subtropical High Pressure Ridge, characterized by the Bermuda High (BH), the zone of mid latitude westerlies, the high latitude low pressure belt, characterized by the Icelandic Low (IL), and the Polar High. These components exhibit an annual latitudinal migration, following the apparent annual solar movement. In the boreal winter these components drift south, moving the BH and its zone of subsiding air equatorward (Hastenrath, 1966; Sahsamanoglou, 1990; Davis et al., 1997; Machel et al., 1998; Portis et al., 2001). In the Caribbean and Central America this results in frequent atmospheric inversions, increased trade wind strength and generally dry conditions, (i.e. the annual December to May dry season) (Hastenrath 1966; Trewartha 1981). Around June when the ITCZ approaches from the south, the BH and the associated zone of subsiding air moves north out of the Caribbean, resulting in uplift, condensation, precipitation, and the region's annual wet season (Hastenrath, 1966; Trewartha, 1981; Sahsamanoglou, 1990; Davis et al., 1997; Portis et al., 2001). From May to November TCs form between the ITCZ and the BH, with cyclogenesis being dependent upon the same general conditions as regular rainfall, in addition to certain additional requirements, such as a threshold sea surface temperatures (SST), low vertical shear, an existing disturbance and high relative humidity in middle troposphere. TCs typically form in a narrow band off the west coast of Africa, with the Main Development Region (MDR), between 10 and 20⁰ N, accounting for 60% of all TC and 85% of major hurricanes (Goldenberg and Shapiro, 1996, Goldenberg et al., 2001). TCs then drift westward, spreading latitudinally, their track and eventual location of landfall (if any) controlled by a variety of transient meteorological factors. Since the southern limit of TC activity is

determined by a threshold level of vorticity generated by the Coriolis force, generally agreed to be around 8° N (Elsner and Kara, 1999), the zone of TC formation consists of the area lying between 8° N and the subtropical high pressure zone, although the latitude of track movement and landfall covers a much larger latitudinal range.

4.4 Geographical Relationships

4.4.1 Short Term

The subtropical high pressure zone in the NA is referred to as either the BH or the Azores High (AZ), which, though displaying some differences in the winter are basically interchangeable during the summer months (Davis et al., 1997). Here, except when referring specifically to winter values we use the term BH. Being a northern hemisphere high pressure system the BH rotates clockwise, spinning the northeasterly trade winds off its southern flank and the midlatitude westerlies to the north. Although the BH is a well-recognized atmospheric phenomenon, it remains a rather nebulous entity, defined in a number of ways (Sahsamangolou, 1990; Davis et al., 1997; Portis et al., 2001). Because of this, the BH is most readily quantified by the NAO Index, which is the normalized difference, measured at a number of different locations, between the SLP below the BH and the IL (Hurrell, 1995; Jones et al., 1997; Portis et al., 2001). These two components generally behave in a “see-saw” manner, with high BH pressure intensity values correlating with low IL values, during which phase large/positive NAO Index values occur. This phase is referred to as a “strong” NAO. Low BH values generally correlate with high IL pressure intensity values, resulting in a “weak” NAO, with small/negative NAO Index values (Elsner et al. 2000). Since a more intense BH generally correlates to a northeastern position and a weaker BH to a southwestern position (Sahsmangolou, 1990; Machel et al., 1998), a “strong” NAO generally means a northeastern position of the BH, and a “weak”

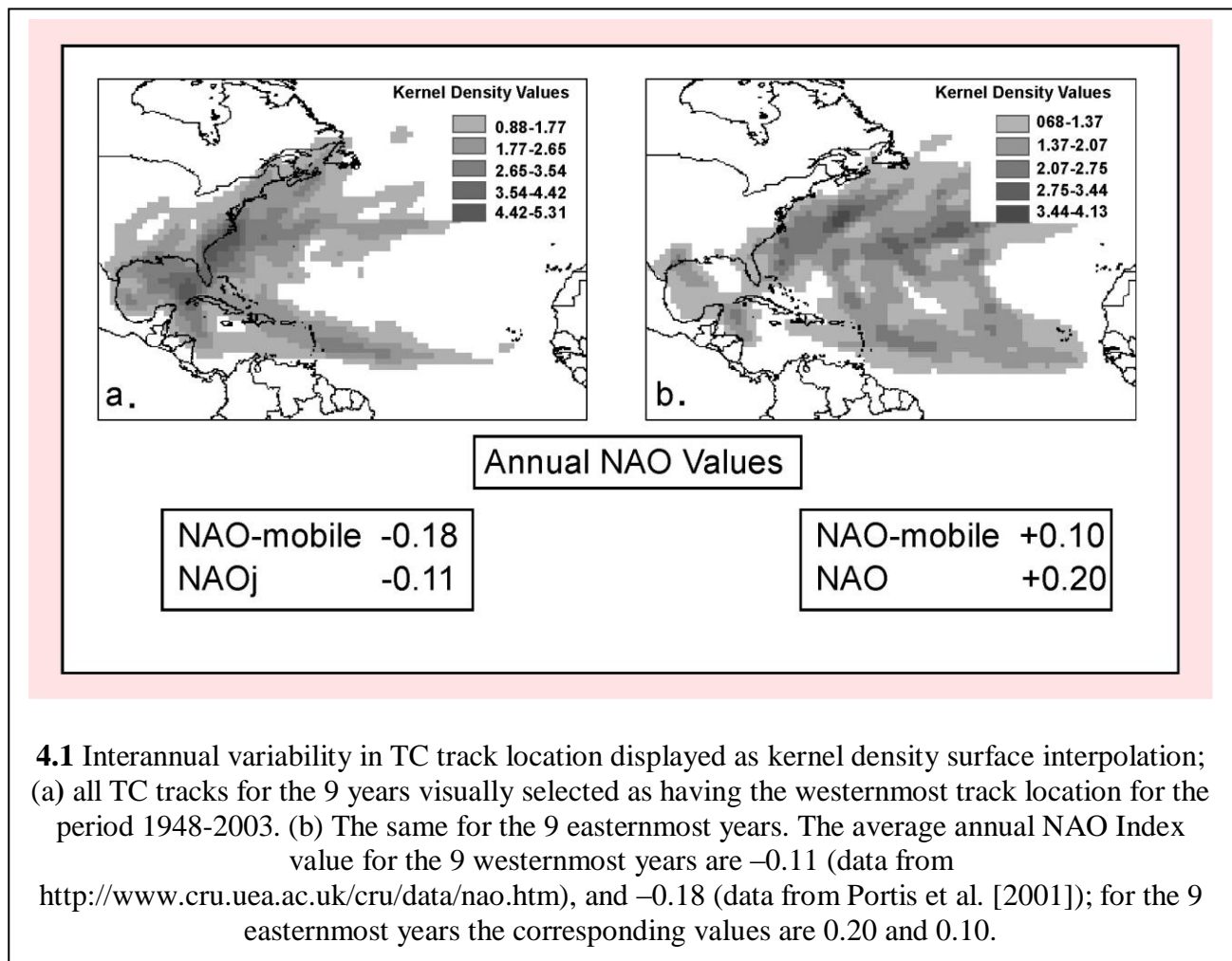
NAO a southwestern one. Stronger NAO values, driven by the intensification of the BH, generally increase the intensity of the trade winds to the south and the mid latitude westerlies to the north, significantly impacting weather in the circum-NA region (Hurrell, 1995; Machel et al., 1998; Kapala et al., 1998; Visbeck et al., 2001).

The close positive geographical relationship between the BH and TCs is demonstrated by a roughly tandem movement of TC and the BH throughout the hurricane season, as they move first northeastward, before returning to the southwest in the fall. The BH also operates as an important control over the steering of TC tracks, and consequently, for location of landfall. Elsner et al. (2000) show a direct relationship between NAO values and latitudinal position of landfalls for major hurricanes making landfall along the US coast since 1865. Using bootstrap analysis, they show statistically significant differences between the July NAO values for years with at least one major hurricane strike along the Gulf coast (south) and Atlantic coast (north), with lower NAO values for the Gulf coast strike years.

Using the NOAA dataset (Neumann et al., 1999) for the period 1948-2003, we visually selected the 9 extreme years each for the most eastern and western group of TC tracks, and applied a kernel density surface interpolation to display their geographical distribution (**Figure 4:1**). A calculation of the average annual NAO index values shows, for both the NAOj and NAOm indices, negative values for the extreme western track years and positive values for the extreme eastern years.

Using a data set consisting of all 6 hour segments for all TC for the period, we queried out all TC segments by monthly NAO value, forming two groups

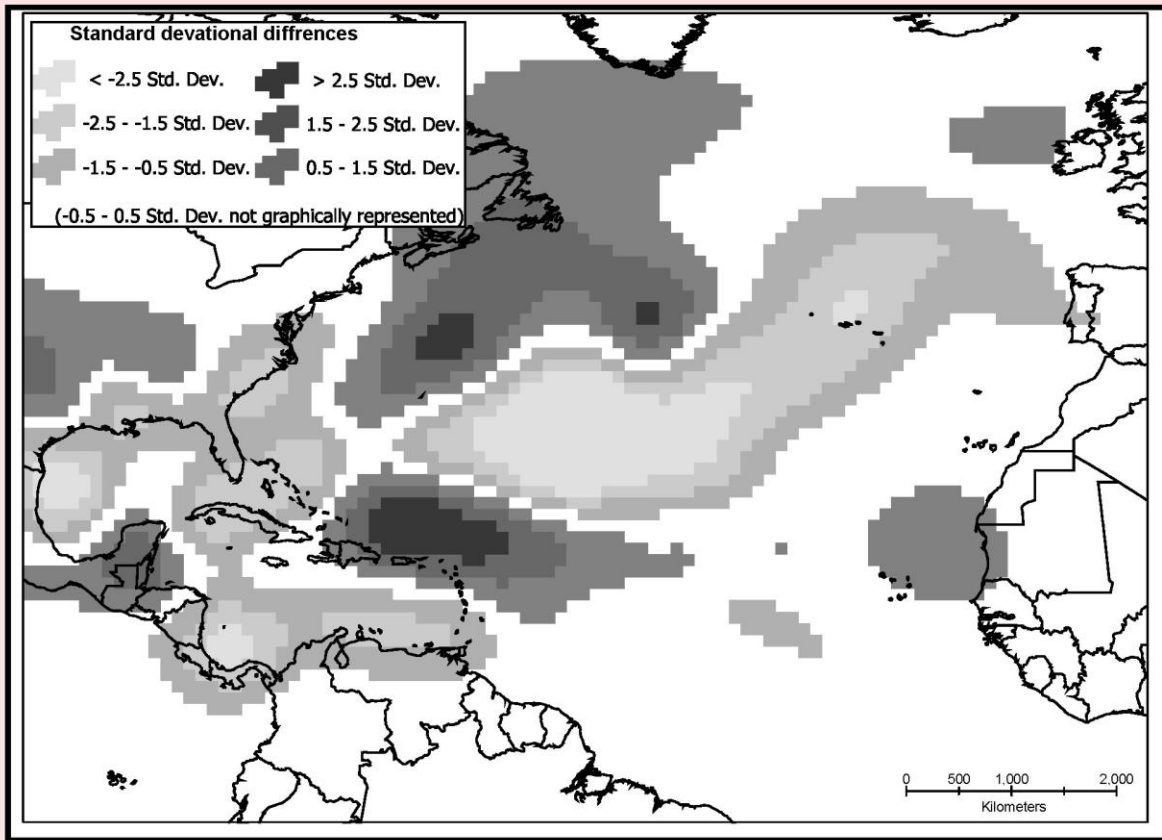
1. All segments which occurred during periods of “Extreme High” NAO ($> 2.5 \sigma$)



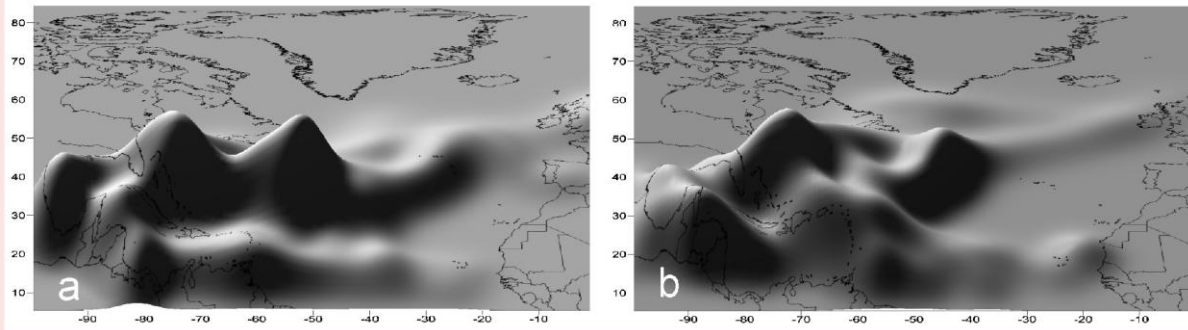
2. All segments which occurred during periods of “Extreme Low” NAO ($<-2.5 \sigma$)

Kernel density surface interpolations were applied to each group, after which the “Extreme Low” kernel density values were subtracted from the “Extreme High” kernel density values and the resulting differences plotted (**Figure 4:2**). In this figure light gray shading represents negative values, indicating areas experiencing more TCs during periods of extreme low than extreme high NAO values, while dark gray areas indicate the reverse. Perhaps the most noticeable feature of this figure is the semicircular dark gray pattern over the western Atlantic, indicating the severe recurvature of TC paths connected with high NAO values. In contrast, the light gray areas form a more horizontal band, indicating a reduced tendency to curve northeastward during periods of low NAO values. A slight northward shift of TC tracks during high NAO values is also noticeable, with the horizontal light gray band covering extreme northern South America and southern Central America indicating that the most southern tracks occur mainly during periods of low NAO values. Changes in TC frequency related to NAO values are marked along the western fringe of both the Gulf of Mexico and the Caribbean, displaying a *distinct* bimodal pattern for both high and low NAO values, with the extreme high events lying to the north of the extreme low events.

Figure 4:3 maps the geographical distribution of the TC segments occurring during extreme NAO conditions. This figure, a three dimensional surface representation based on the kernel density values of TC incidence, facilitates the visualization of the transformation of the BH from a weak horizontal trough during periods of extreme low NAO ($<- 2.5 \sigma$) (Fig. 3a) to a strong circular depression translated to the northeast during periods of extreme high NAO ($> 2.5 \sigma$) (Fig. 3b). Note the similarity in shape and spatial placement between the extreme low/extreme high surface figures here and the extreme west/extreme east tracks in **Figure 4:1**.



4.2 Plot of kernel density values of TC tracks occurring during extreme low ($< -2.5 \sigma$) NAO months subtracted from kernel density values of TC tracks occurring during extreme high ($> 2.5 \sigma$) NAO months for the period 1948-2003. Interpolation is by a 100 km bandwidth kernel density. Light gray shadings represent negative values; dark gray shadings represent positive values.



4.3 Three dimensional surface representation based on the kernel density values of occurrence incidence of all six hour storm tracks for the period 1948-2000 that occurred during periods of (a) extreme low ($< -2.5 \sigma$), (b) extreme high ($> +2.5 \sigma$) NAO. Note that the center hollow, presumably representing the BH which the TCs travel around, and not through, changes from a weak east-west trough during extreme low NAO Index values to a strong circular depression during extreme high value, while moving to the northeast.

We performed a kernel density analysis on all three storm groupings (tropical cyclones, hurricanes, and major hurricanes) for the period 1948-2003 (**Figure 4:4**). A similar pattern was found in all three cases; namely a westward path across the Atlantic from approximately the Cape Verde islands, with recurvature resulting in two main track ways, bifurcating to the northeast of the Greater Antilles. A separate cluster of tracks is found in the Western Caribbean and Gulf of Mexico. The bifurcation of the Cape Verde hurricane tracks supports the idea of the bimodal influence the BH exerts over TC paths, related to NAO values. Presumably the distinct western cluster records the Western Caribbean hurricanes.

This preliminary analysis indicates that on an inter-annual basis the strength/position of the BH (as proxied by NAO values) exerts significant control over the location of TC tracks as well as the location of hurricane landfall, as suggested by Elsner et al. (2000), with low NAO values (southwestern BH positions) corresponding to less recurved, southern tracks, and high NAO values (northeastern BH positions) corresponding to increased recurvature and more northern tracks.

4.4.2 Long Term

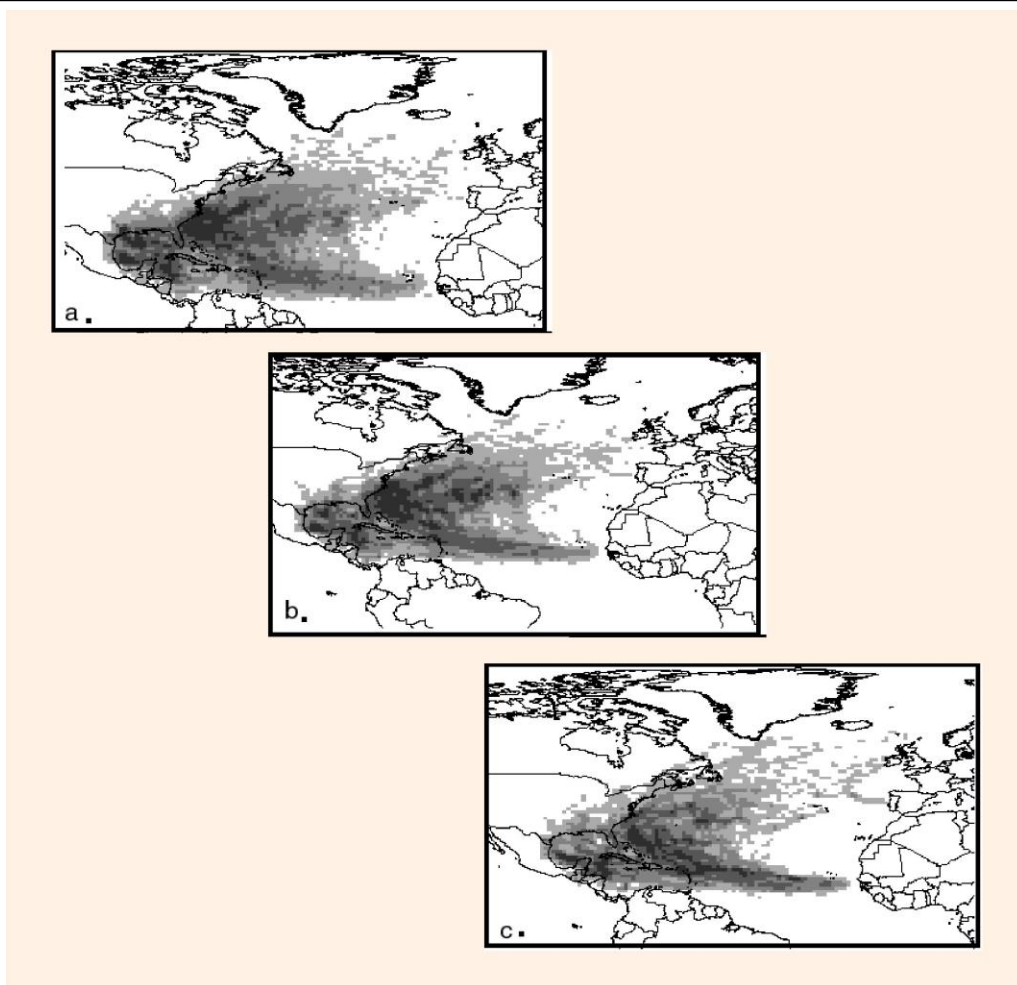
4.4.2.1 BH-TC

Sedimentary evidence indicates that the control the BH currently exerts over TCs operates over longer scales as well. Liu and Fearn (2000) have identified a period of hyperactivity on the Gulf Coast (Texas-Florida), for the period 3400-1000 ¹⁴ C yr BP., with periods of reduced activity before and after. They suggest millennial scale positional movement of the BH as the proximate cause of this oscillation in frequency of landfall, with positions to the southwest funneling storms into the Gulf of Mexico and positions to the northeast pushing the tracks along the Atlantic Coast. This implies an anti-phase relationship between the frequency of

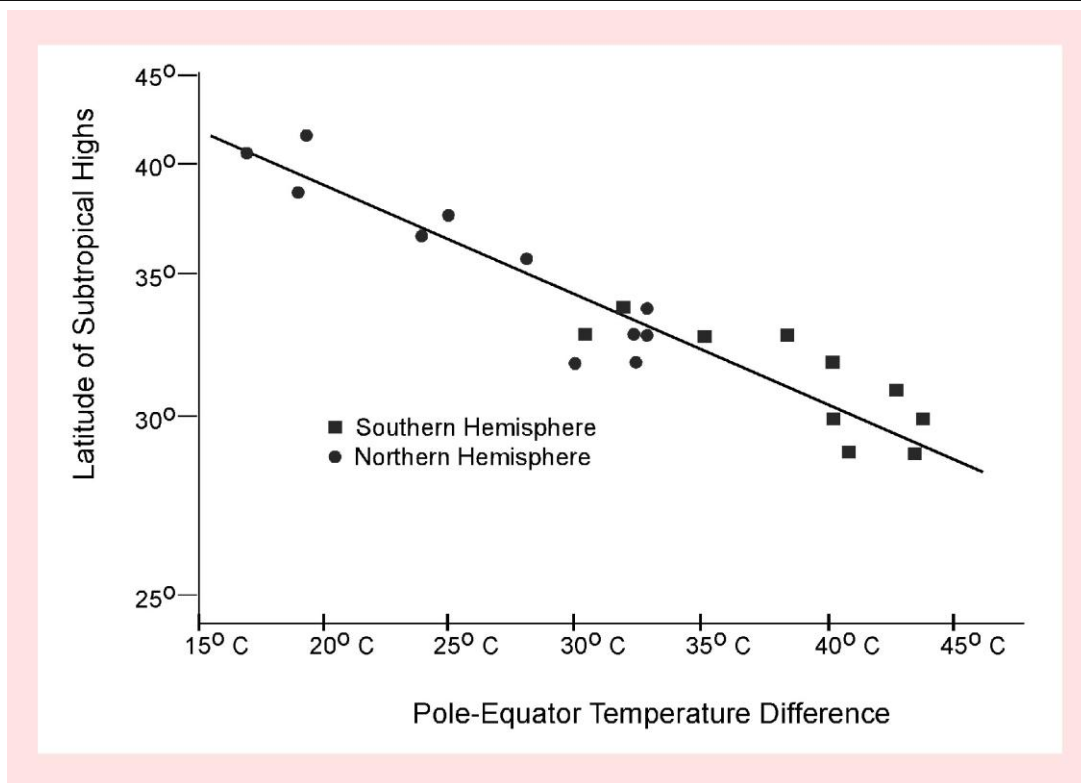
strike activity between the Gulf and Atlantic coasts, supported by results from an Atlantic Coast paleotempestology study (Scott et al., 2003), while the timing of the posited movements of the BH is supported by proxy paleoenvironmental data (Hodell et al. 1991), based on the premise that long-term residency of the BH over an area results in increased aridity.

4.4.2.2 ITCZ-BH

The long-term relationship between these two features may be more direct than the short-term, with the longer-term average annual latitude of both less affected by “noisy” short-term conditions. For both features the principal latitudinal control seems to be the Pole-Equator temperature gradient, with a steeper gradient resulting in a southern movement. For the BH this relationship is demonstrated by **Figure 4:5** (modified from Flohn, 1984), based on the monthly average positions of the subtropical highs and the Pole-Equator temperature gradient at the 300/700 mb layer. Since this gradient is primarily dependent upon polar temperatures (there being less variation in equatorial temperatures), warm (cold) periods tend to move the BH to the north (south). Flohn (1984) estimates that an increase in the average annual Arctic temperature of 7°C moves the average BH latitude 100-200 km north in the summer and 800 km north in the winter. Empirical evidence for this relationship also exists; as early as 1977 Lamb’s estimation of a paleolatitudinal record for the BH based on palynological and vegetational boundary displacement and marine microfaunal analysis evidence found significant north (south) shifts paralleling overall hemispheric heating (cooling). Much evidence, on a variety of timescales, supports temperature driven movement of the ITCZ. Modeling studies simulating polar ice cover at the Last Glacial Maximum (LGM) support a southern movement of the ITCZ (Chiang et al., 2003; Chiang and Bitz, 2005), with the increased Pole-Equator temperature gradient resulting in a 6° southern displacement of the ITCZ (Broccoli et al., 2006). Similar long-term temperature



4.4 Kernel density surface interpolation of all (a) TCs, (b) hurricanes, (c) major hurricane track sections for the period 1948-2003



driven movement of the ITCZ has occurred in both the equatorial Indian Ocean (Tiwari et al., 2006) and the eastern Pacific (Koutavas and Lynch-Stieglitz, 2004). Paleoclimatic data includes shifts in South American precipitation paralleling ITCZ movement as recorded by Andean ice cores (Thompson et al, 2000), speleothems and travertine deposits in Northeast Brazil (Wang et al. 2004), and riverine discharge (Peterson et al., 2000; Haug et al., 2001). Drought records from the western United States support northern migration of the BH during the Medieval Warm Period (Seager et al., 2007).

In addition to the average long term latitude of the two features being controlled by a single primary factor, Flohn (1984) suggests a more direct physical connection, arguing that the northern displacement of the BH resulting from a 7°C increase of average annual polar temperature alone is enough to move the ITCZ $3\text{--}4^{\circ}$ north. Theoretically, therefore, coordination of the low frequency movements of the two features seems likely.

Coordinated movement between the ITCZ and the subtropical highs implies anti-phase rainfall anomalies across the ITCZ; i.e. if the subtropical high moves in parallel with the ITCZ, southern migration of the ITCZ resulting in positive Amazonian rainfall anomalies should correlate with negative rainfall anomalies for the Caribbean. Numerous studies support this relationship during the instrumental record for the tropical Atlantic for both the Caribbean-Central American region and the Sahel to the north and Northeast Brazil to the south of the ITCZ (Hastenrath, 1976, 1985, 2000a,b; Lamb, 1978, Kapala et al., 1998; Curtis and Hastenrath, 1999). On both sides of the ITCZ movement of the ITCZ towards (away from) the location tend to result in positive (negative) rainfall anomalies on an interannual basis, indicating coordinated movement between the subtropical highs and the ITCZ. Paleoenvironmental evidence (Baker et al., 2003) for such coupling has also been demonstrated. Koutavasa and Lynch-Stieglitz (2004)

include a review of a large number of studies, based on several different proxies supporting anti-phase precipitation anomalies across the ITCZ. Since trade wind-driven upwelling provides direct evidence for the proximity of the subtropical high, anti-phase rainfall and upwelling records from the Cariacao basin provides strong support for parallel movement between the ITCZ and the BH (Haug et al., 2001).

4.4.2. 3 ITCZ-BH-TC

Marine cores from the coast of Venezuela (Haug et al., 2001) indicate that, driven by latitudinal movement of the ITCZ, the region has being alternately subject to either ITCZ-induced rainfall or BH-driven trade winds for the last 14,000 years. This suggests that the TC zone, locked in at the northern edge of the ITCZ, below the zone of intense trade winds and upwelling, has experienced a parallel migration. Based on sedimentary evidence from Saint-Martin in the French West Indies, Bertran et al. (2004) has suggested a millennial scale ITCZ driven latitudinal movement in the zone of TC activity.

4.4.2.4 ENSO and QBO

The influence of El Niño-Southern Oscillation (ENSO) on NA TC activity is well known, with El Niño (La Niña) periods reducing (increasing) overall activity, with some regional variation (Gray 1984; Richards and O'Brien 1996; Bove et al. 1998; Elsner and Kara 1999; Pielke and Landsea 1998; Bengtsson 2001; Tartaglione et al. 2003). The quasi-biennial oscillation (QBO) also influences NA TC, with the westerly phase corresponding to increases in both number of TC and major hurricanes (Gray and Shaeffer, 1991; Elsner et al., 1999; Elsner and Kara, 1999; Landsea et al., 1999; Goldenberg et al., 2001). In this paper, however, we ignore both cycles, as in effect, both of these high frequency oscillations become noise superimposed on the underlying system at the time scales (interdecadal to millennial) under consideration. The

only exception is the possibility of significant long-term variability in ENSO frequency (Haug et al., 2001; Koutavas and Olive, 2006), which potentially could affect TC frequency on the time scales of interest.

4.5 Paleo Conditions

4.5.1 ITCZ

Boundary conditions have not remained constant throughout the Holocene. Evidence from varved sediments obtained from the anoxic Cariaco Basin off the coast of Venezuela indicates significant migration of the mean latitude of the ITCZ over the last 14 000 years (Haug et al., 2001). This interpretation is based on the fluctuations in the seasonal hydrological cycle displayed in the high-resolution (subdecadal) bulk sedimentary metals record, resulting from the changing length/intensity of the annual dry and wet seasons. Intensified/lengthened wet seasons result in increased river discharge, rich in metals, while intensified/lengthened dry seasons result in increased biogenic silica, a result of increased trade wind driven upwelling on the basin.

4.5.2 BH

The chronology of the latitudinal position of the BH can be estimated from paleoenvironmental records as areas directly under its influence are dominated by subsiding dry air. Arrival of the BH over an area not previously under its influence should result in increased aridity, detectable by a variety of vegetational and isotopic proxies. Palynological studies are especially useful as their relatively low temporal resolution reduces the noise of higher frequency oscillations and are less dependent upon confounding external factors such as local salinity and hydrological changes. A large number of studies from the Central American-Caribbean region (Bradbury et al., 1981; Leyden, 1985; Hodell et al., 1991; Peterson et al., 1991; Curtis and Hodell, 1996; Islebe et al., 1996; Leyden et al., 1996; Curtis et al., 1998; Curtis et al., 1999;

Higuera-Gundy et al., 1999; Islebe and Sanchez, 2002; Nyberg et al., 2001; Rosenmeier et al., 2002) have shown low frequency environmental changes generally in temporal agreement with the ITCZ movement proposed by Haug et al., (2001). Perhaps significantly, the northwestern edge of the region (in particular the northern Yucatan peninsula) seems to demonstrate a greater variability, perhaps due to increased sensitivity to BH movement, being situated in a more ecotonal location, on the edge of the zone of influence, while larger movements would be required to leave detectable signals in locations farther south and east. Complicating these estimation however, are more general hemispheric changes resulting from variability in solar insolation due to orbital influences, especially the precessional aspects of the Milankovich cycles (Berger and Loutre, 1991; Leyden et al., 1994). Additionally, after the mid Holocene the difficulty in separating natural and anthropogenic effects increases regionally (Leyden, 1987; Leyden et al., 1998). It should be noted that only areas located directly under shifts in BH location are expected to show dramatic evidence of such shifts; far southern areas, for example, are expected to display less clear palynological responses to shifts that occur to the north, as such shifts should not result in large aridity changes at their location.

4.5.3 TC

Paleotempestology uses sedimentary evidence to establish long-term proxy hurricane strike records. In such studies, sediment cores are extracted from coastal wetlands and storm-generated layers, identified by a variety of geologic methods, are dated, permitting a chronology of site-specific landfalls (Liu and Fearn, 1993, 2000; Liu, 2004; Donnelly et al., 2001a,b, 2004; Donnelly, 2005; Donnelly and Woodruff, 2007; Scott et al., 2003). Records from several sites can be correlated to develop regional hurricane histories (Liu, 2004). Calibrations based on modern analogs indicate that the threshold storm intensity required for depositing recognizable

sedimentary signatures is roughly that of major hurricanes (category 3 or greater) (Liu, 2004; Donnelly and Webb, 2004).

Significantly, the majority of millennial scale proxy hurricane landfall records display evidence of the temporal clustering of events, often cyclic, indicating periods of hyperactivity. That these intervals are non-synchronous suggests a movement in the zone of maximum TC activity, as opposed to a basin wide frequency increase. In the United States, Liu and Fearn (1993, 2000) found evidence for a hyperactive period from 3400-1000 ^{14}C yr BP for the northern Gulf of Mexico, while Scott et al. (2003) emphasize the anti-phase timing of hyperactivity for the Atlantic coast. In the Caribbean, Bertran et al. (2004) found cyclical periods of TC activity on Saint Martin in the French West Indies, with the hyperactivity dating from ~ 4000-2300 BP; McCloskey and Keller (2009) (Chapter 6) found two periods of hyperactivity between 4500-2500 ^{14}C yr BP for the central coast of Belize, while Donnelly has found evidence for hyperactivity in Puerto Rico for the periods 5400-3600 BP, 2500-1000 BP and 250 BP to the present (Donnelly, 2005; Donnelley and Woodruff, 2007).

It should be noted that these proxy records, based only on landfall of major hurricanes, represent a minimum record of TC activity. Given the relative scarcity of major hurricanes, which currently comprise ~20% of US landfalling TCs (Landsea, 1993) it seems reasonable to assume that stratigraphic intervals providing sedimentary evidence for the increased frequency of landfalling major hurricanes do, in fact, represent extended periods of overall increase in TC activity, once geomorphological and sea level changes are controlled for. We suggest that the spatial/temporal shifts in these intervals result from the migration of the zone of maximum TC frequency.

4.6 Hindcast

By positing that the relationships between the ITCZ, BH, and TC zone have remained relatively constant over the long-term, we are able to hindcast paleopositions of the BH and the TC zone based on ITCZ position. We base our hindcast on the Cariaco record of Haug et al. (2001) due to its large amplitude, high (subdecadal) resolution and inclusion of both rainfall and trade wind data. Although the latitudinal shifts represented by the changes in metal concentrations movements have not been quantified, the difference in sign and magnitude permit rough estimations.

Based on the Cariaco record, the timing for significant changes in mean annual latitude of the ITCZ (and, by extension, location of the TC zone) are:

Northern residency: ~ 11 000-4000 BP, ~ 1100-600 BP (Medieval Warm Period)

Present position: ~2400-1100 BP

Southern residency: ~ 4000-2400 BP, ~ 400-200 BP (Little Ice Age)

A potential complication is the possibility of major change in the strength/ variability of ENSO frequency, which has been argued to have become more prevalent in the late Holocene (Haug et al., 2001; Koutavas and Lynch-Stieglitz, 2004). Although this should not affect the average latitude of the BH or TC zone, it might affect landfall frequency. However, it is possible that the apparent increased variability of ENSO suggested by Haug et al. (2001) for the interval between ~4000-2400 BP actually results from increased instability in the general atmospheric circulation system, perhaps resulting from the establishment of a new atmospheric equilibrium.

4.7 Hypothesis Testing

Evidence for/against our proposed low-frequency latitudinal oscillation of the NA circulation system requires the long-term correlation of the various components. In order to correlate low

frequency ITCZ and BH movements, it is necessary to establish an accurate proxy for BH location. One possibility is determining the zone of aridity resulting from the subsiding air issuing from the BH, recognizable palynologically by increasingly xeric taxa, or isotopically by the changing $\delta^{18}\text{O}$ ratios of closed basin lakes. However, both vegetational and isotopic proxy records are subject to a variety of local controls; additionally, they are constrained geographically as only fringe areas are directly affected by BH movements.

The correlation of ITCZ and TC zone could be more direct, based upon a basin wide paleo strike record developed from paleotempestological studies extending to the mid Holocene. With recognizable sedimentary signatures posited to be deposited only for major hurricanes, longer paleo strike records seem unlikely, since major hurricanes probably did not occur during the early Holocene due to the lowered surface sea temperatures resulting from the large volume of glacial meltwater entering the NA basin.

However, comprehensive paleostrike records do not currently exist. For the NA basin multi millennial scale proxy records are spotty at best, particularly for the Caribbean and the US Atlantic coast. However, new research may prove fruitful; if the frequency of TC-inhibiting El Niño events has increased throughout the late Holocene as posited (Clement et al., 2000; Trudhope et al., 2001; Haug et al., 2001; Moy et al., 2002; Koutavas and Lynch-Stieglitz, 2004), the resulting abundance of mid Holocene events increases the possibility that landfall patterns may be preserved in the sedimentary record.

Based on our model, increased hurricane landfall can be expected to have occurred along the northern area (US Atlantic Coast) from ~8-4000 BP, and during the Medieval Warm Period, ~1100-600 BP, while decreased landfall should have occurred ~4000-2400 BP and during the Little Ice Age, (~ 400-200 BP). The southern area (Gulf Coast and the Caribbean) should exhibit

the reverse pattern.

Obtaining evidence for/against such temporal/spatial shifts in maximum strike frequency therefore presents a means of testing this model. During periods of extreme northern/southern movement, the fringe areas, which currently experience very low levels of TC activity, may have experienced increased activity, thereby producing relatively easily recognizable sedimentary evidence for frequency changes. Due to the latitudinal smearing of TC landfall resulting from the high frequency oscillation in BH intensity, the record in central areas will quite possibly exhibit a less distinct signal. The long return intervals of major hurricanes, generally > 100 years (Elsner and Kara, 1999; Liu and Fearn, 1993, 2000; Donnelly et al., 2001a, b, 2004) makes the existence of a clear sedimentary record over short time spans somewhat problematic, thereby reducing the utility of the recent oscillations connected to the Little Ice Age and the Medieval Warm Period. It is therefore suggested that studies focusing on the period from 8000-4000 BP in the extreme north and 4000-2400 BP in the south are the most likely to produce useful information.

Obviously, there are very significant practical difficulties in obtaining proxy strike records for the suggested periods, given the magnitude of sea level raise and geomorphological changes in dynamic coastal areas. Coring submerged kettle holes in the northern area is one possibility (J. P. Donnelly, personal communication), as are study sites in areas of uplift and steep bathymetry, or areas where “keep-up” reefs/mangroves have minimized relative sea level rise.

4.8 Summary

Using both a GIS and literature based analyses of current conditions we developed a model of current TC activity for the NA basin, in which TC are latitudinally “fixed” between the ITCZ to the south and the BH to the north, with changes in the general atmospheric circulation, as

proxied by the NAO Index values, resulting in the smearing of track location and landfall across the NA.

Evidence suggests that the coordinated movement of the ITCZ and the BH has existed through the Holocene, controlled primarily by the pole-equator temperature gradient. Changes in that gradient, ultimately driven by orbital factors, have resulted in latitudinal movement of this integrated atmospheric structure on a number of time scales. As part of this structure the TC zone has migrated north and south over the Holocene in rough parallel with the ITCZ. From ~ 8000 BP on sedimentary evidence for the migration of the zone of maximum hurricane landfall has potentially been preserved. Hindcasts, based on the proxy migration record of the ITCZ, the southern edge of the structure, suggest that the zone of maximum TC activity moved significantly to the

1. North from ~ 8000-4000 BP and 1100-600 BP
2. South from ~ 4000-2400 and 400-200 BP.

By providing proxy paleostrike records, paleotempestology studies in the northern and southern edges of the TC zone provide a method of evaluating the validity of the model.

4.9 References

Bailey, T.C., and Gatrell, A., 1995. Interactive Spatial Data Analysis. Longman, Essex.

Baker, P.A., Seltzer, G.O., Fritz, S.C, Dunbar, B., Grove, M.J., Tapia, P.M., Cross, S.L., Rowe, H. G., and Broda, P.J., 2001. The history of South American tropical precipitation for the past 25,000 years. *Science* 291, 640-643.

Bengtsson, L., 2001. Enhanced: Hurricane threats. *Science* 293, 440-442.

Berger, A., and Loutre, M.F., 1991. Insolation values for the climate for the last 10 million years. *Quaternary Science Reviews* 10, 297-317.

Bertran, P., Bonnisent, D., Imbert, D., Lozouet, P., Serrand, N., and Stouvenot, C., 2004. Paleoclimat des Petites Antilles depuis 4000 BP: l'enregistrement de la lagune de Grand-Case a Saint-Martin. *Comptes Rendus Geoscience* 336, 1501-1510.

Bove, M.C., Elsner, J.B., Landsea, C.W., Niu, X.-f., and O'Brien, J.J., 1998. Effects of El Niño on U.S. landfalling hurricanes, revisited. *Bulletin of the American Meteorological Society* 76, 2477-2482.

Bradbury, J. P., Leyden, B.W., Salgado-Labouriau, M., Lewis, W.M., Schubert, C., Binford, M.W., Frey, D.G., Whitehead, D.R., and Weibezahn, F.H., 1981. Late Quaternary environmental history of Lake Valencia, Venezuela. *Science* 214, 1299-1305.

Broccoli, A.J., Dahl, K. A., and Stouffer, R.J., 2006. Response of the ITCZ to northern hemisphere cooling. *Geophysical Research Letters* 33, L01702.

Chiang, J. C. H., and Bitz, C. M., 2005. Influence of high latitude ice cover on the marine Intertropical Convergence Zone. *Climate Dynamics* 25, 477-496. DOI:10.1007/s00382-005-0040-5.

Chiang, J. C. H., Biasutti, M., and Battisti, D. S., 2003. Sensitivity of the Atlantic Intertropical Convergence Zone to last glacial maximum boundary conditions. *Paleoceanography* 18, 1094. DOI:10.1029/2003PA000916.

Climate Research Unit of East Anglia University, (<http://www.cru.uea.ac.uk/cru/data/nao.htm>).

Clement, A. C., Seager, R., and Cane, M. A., 2000. Suppression of El Niño during the mid Holocene by changes in the earth's orbit. *Paleoceanography* 15, 7317-737.

Curtis, S., and Hastenrath, S., 1999. Trends of upper-air circulation and water vapour over equatorial South America and adjacent oceans. *International Journal of Climatology* 19, 863-876.

Curtis, J. H., and Hodell, D. A., 1996. Climate variability on the Yucatan peninsula (Mexico) during the past 3500 years, and the implications for Maya cultural evolution. *Quaternary Research* 46, 37-47.

Curtis, J. H., Brenner, M., Hodell, D.A., Balser, R.A., Islebe, G.A., and Hooghiemstra, H., 1998. A multi-proxy study of Holocene environmental change in the Maya lowlands of Peten, Guatemala. *Journal of Paleolimnology* 19, 139-159.

Curtis, J. H., Brenner, M., and Hodell, D. A., 1999. Climate change in the Lake Valencia basin, Venezuela, ~12600 yr BP to present. *Holocene* 9, 609-619.

Davis, R. E., Hayden, B.P., Gay, D. A., Phillips, W. L., and Jones G. V., 1997. The North Atlantic subtropical anticyclone. *Journal of Climate* 10, 728-744.

- Donnelly, J. P., 2005. Evidence of past intense tropical cyclones from backbarrier salt pond sediments: a case study from Isla de Culebrita, Puerto Rico, USA. *Journal of Coastal Research* 42, 201-210.
- Donnelly, J. P., and Webb, T. III, 2004. Back-barrier sedimentary records of intense hurricane landfall in the northeastern United States. In Murnane R. J., and Liu K-b (eds), *Hurricanes and Typhoons: Past, Present and Future*, Columbia University Press, New York.
- Donnelly, J. P., Woodruff, J., 2007. Intense hurricane activity over the past 5000 years controlled by El Nino and the West African Monsoon. *Nature* 44, 465-468. DOI: 10.1038/nature05834.
- Donnelly, J. P., Bryant, S. S., Butler, J., Dowling, F. L., Hausmann, N., Newby, P., Shuman, B., Stern, J., Westover, K., and Webb, T. III, 2001a. A 700 year sedimentary record of intense hurricane landfalls in southern New England. *Geological Society of America Bulletin* 113, 714-727.
- Donnelly, J. P., Roll, S., Wengren, M., Butler, J., Lederer, R., and Webb, T. III, 2001b. Sedimentary evidence of intense hurricane strikes from New Jersey. *Geology* 29, 615-618.
- Donnelly, J.P., Butler, J., Roll, S., Wengren, M., and Webb, T. III, 2004. A backbarrier overwash record of intense storms from Brigantine, New Jersey. *Marine Geology* 210, 107-121.
- Elsner, J. B., and Kara, A. B., 1999. *Hurricanes of the North Atlantic: Climate and Society*. Oxford University Press, Oxford.
- Elsner, J. B., Kara, A. B., and Owen, M. A., 1999. Fluctuations in North Atlantic Hurricane frequency. *Journal of Climate* 12, 427-437.
- Elsner, J. B., Liu, K-b, Kocher, B., 2000. Spatial variations in major U.S. hurricane activity: statistics and a physical mechanism. *Journal of Climate* 13, 2293-2305.
- Flohn, H., 1984. Ice-free Arctic and glaciated Antarctic. In Flohn, H., and Fantechi, R., (eds), *The Climate of Europe: Past, Present and Future*. D. Reidel Publishing Company, Dordrecht.
- Goldenberg, S. B., and Shapiro, L. J., 1996. Physical mechanisms for the association of El Nino and West African rainfall. *Journal of Climate* 9, 1169-1187.
- Goldenberg, S. B., Landsea, C. W., Mestas-Nunez, M. A., and Gray, W. M., 2001. The recent increase in Atlantic hurricane activity: causes and implications. *Science* 293, 474-479.
- Gray, W. M., 1984. Atlantic seasonal hurricane frequency Part I-El Nino and 30 mb quasi-biennial oscillation influences. *Monthly Weather Review* 112, 1649-1668.
- Gray, W. M., Shaeffer, J. D., 1991. El Nino and QBO influences on tropical cyclone activity. In Glantz, M. H., Katz, R. W., Nichols, N., (eds), *Teleconnections Linking Worldwide Climate Anomalies*. Cambridge University Press, New York.

- Hastenrath, S., 1966. On general circulation and energy budget in the area of the Central American seas. *Journal of Atmospheric Sciences* 23, 694-711.
- Hastenrath, S., 1976. Variations in low-latitude circulation and extreme climatic events in the tropical Americas. *Journal of Atmospheric Sciences* 33, 202-215.
- Hastenrath, S., 1985. *Climate and Circulation in the Tropics*. D. Reidel Publishing Company, Dordrecht.
- Hastenrath, S., 2000a. Interannual and longer-term variability of upper air circulation in the Northeast Brazil-tropical Atlantic sector. *Journal of Geophysical Research* 105, 7327-7335.
- Hastenrath, S., 2000b. Interannual and longer term variability of upper-air circulation over the tropical Atlantic and West Africa in boreal summer. *International Journal of Climatology* 20, 1415-1430.
- Haug, G. H., Hughen, K. A., Sigman, D.M., Peterson, L. C., and Rohl, U., 2001. Southward migration of the Intertropical Convergence Zone through the Holocene. *Science* 292, 1304-1314.
- Higuera-Gundy, A. M., Brenner, M., Hodell, D. A., Curtis, J.H., Leyden, B. W., and Binford, M. W., 1999. A 10,300 ^{14}C yr record of Climate and Vegetation change from Haiti. *Quaternary Review* 52, 159-170.
- Hodell, D. A., Curtis, J. H., Jones, G. A., Higuera-Gundy, A., Brenner, M., Binford, M., and Dorsey, K. T., 1991. Reconstruction of Caribbean climate change over the past 10,500 years. *Nature* 352, 790-793.
- Hurrell, J. W. 1995. Decadal trends in the North Atlantic Oscillation and relationships to regional temperature and precipitation. *Science* 269, 676-679.
- Islebe, G. A., and Sanchez, O., 2002. History of Late Holocene vegetation at Quintana Roo, Caribbean coast of Mexico. *Plant Ecology* 160, 187-192.
- Islebe, G. A., Hooghiemstra, H., Brenner, M., Curtis, J. H., and Hodell, D.A., 1996. A Holocene vegetation history from lowland Guatemala. *Holocene* 6, 265-271.
- Jones, P. D., Jonsson, T., and Wheeler, D., 1997. Extension to the North Atlantic Oscillation using early instrumental pressure observations from Gibraltar and south-west Iceland. *International Journal of Climatology* 17, 1433-1450.
- Kapala, A., Machel, H., and Flohn, H., 1998. Behaviour of the centres of action above the Atlantic since 1881. Part II: associations with the regional climate anomalies. *International Journal of Climatology* 18, 23-36.
- Knowles, J. T., and Leitner, M., 2007. Visual representations of the spatial relationship between Bermuda High strength and Hurricane tracks. *Cartographic Perspectives* 56, 16-30.

- Koutavas, A., and Lynch-Stieglitz, J., 2004. Variability of the marine ITCZ over the eastern Pacific during the past 30,000 years. In Diaz, H. F., Bradley, R. S., (eds), *The Hadley Circulation: Present, Past and Future*. Springer-Verlag, New York.
- Koutavas, A., and Olive, G. C., 2006. Holocene modulation of ENSO by the Intertropical Convergence Zone. Joint Assembly of the American Geophysical Union; Baltimore, Maryland from 23-26 May 2006.
- Lamb, H. H., 1977. *Climate, Present, Past and Future. Volume 2 Climatic History and the Future*. Methuen and Co. Ltd, London.
- Lamb, P. J., 1978. Case studies of tropical Atlantic surface circulation patterns during recent sub-Saharan weather anomalies: 1967 and 1968. *Monthly Weather Review* 106, 482-491.
- Landsea, C. W., 1993. A climatology of intense (or major) Atlantic hurricanes. *Monthly Weather Review* 121, 1703-1713.
- Landsea, C. W., Pielke, R. A. Jr., Mestas-Nunez, A. M., and Knaff, J. A., 1999. Atlantic Basin hurricanes: indices of climate change. *Climate Change* 42, 89-129.
- Leyden, B. W., 1985. Late Quaternary aridity and Holocene moisture fluctuations in the Lake Valencia basin, Venezuela. *Ecology* 66, 1279-1295.
- Leyden, B. W., 1987. Man and climate in the Maya lowlands. *Quaternary Research* 28, 407-417.
- Leyden, B. W., Brenner, M., Hodell, D. A., and Curtis, J. H., 1994. Orbital and internal forcing of climate on the Yucatan Peninsula for the past ca. 36 ka. *Paleogeography, Paleoclimatology, Paleoecology* 109, 193-210.
- Leyden, B. W., Brenner, M., Whitmore, T., Curtis, J. H., Piperno, D. R., and Dahlin, B., 1996. A record of long- and short-term climatic variation from northwest Yucatan: cenote San Jose Chulchaca. In Fedick, S. L. (ed), *The Managed Mosaic; ancient Maya Agriculture and Resource Use*. University of Utah Press, Salt Lake City. 30-52.
- Leyden, B. W., Brenner, M., and Dahlin, B., 1998. Cultural and climatic history of Cuba', a lowland Maya city in Quintana Roo, Mexico. *Quaternary Research* 49, 111-122.
- Liu, K-b., 2004. Paleotempestology: principles, methods and examples from Gulf coast lake sediments. In Murnane, R.J., and Liu, K-b., (eds), *Hurricanes and Typhoons: Past, Present and Future*. Columbia University Press, New York. 13-57.
- Liu, K-b., and Fearn, M. L., 1993. Lake-sediment record of late Holocene hurricane activities from coastal Alabama. *Geology* 21, 793-796.
- Liu, K-b., and Fearn, M. L., 2000. Reconstruction of prehistoric landfall frequencies of catastrophic hurricanes in northwestern Florida from lake sediment records. *Quaternary Research* 54, 238-245.

- Machel, H. A., Kapala, A., and Flohn, H., 1998. Behaviour of the centres of action above the Atlantic since 1881. Part I: characteristics of seasonal and interannual variability. *International Journal of Climatology* 18, 1-22.
- Maslin, M. A., and Burns, S. J., 2000. Reconstruction of the Amazon Basin: effective moisture availability over the past 14,000 Years. *Science* 290, 2285-2287.
- Mayle, F. E., Burbridge, R., and Killeen, T. J., 2000. Millennial-Scale dynamics of southern Amazonian rain forests. *Science* 290, 2291-2294.
- McCloskey, T. A., and Keller, G., 2009. 5000 year sedimentary record of hurricane strikes on the central coast of Belize. *Quaternary International* 195, 53-68.
- Moy, C. M., Seltzer, G. O., Rodbell, D. T., and Anderson, D. M. 2002. Variability in El Nino/Southern Oscillation at millennial timescales during the Holocene epoch. *Nature* 420, 162-165.
- Neumann, C. J., Jarvinen, B. R., McAdie, C. J., and Hammer, G. R., 1999. Tropical Cyclones of the North Atlantic Ocean, 1871-1998. NOAA, Asheville, North Carolina
- NOAA website (<http://hurricane.csc.noaa.gov/hurricanes/viewer.htm>)
- Nyberg, J. B., Malmgren, B. A., Kuijpers, A., and Winter, A., 2001. A centennial-scale variability of tropical North Atlantic surface hydrography during the late Holocene. *Paleogeography, Paleoclimatology, Paleoecology* 183, 25-41.
- Peterson, L. C., Overpeck, J. T., Kipp, N. G., and Imbrie, J., 1991. A high-resolution Late Quaternary upwelling record from the Cariaco Basin, Venezuela. *Paleoceanography* 6, 99-119.
- Peterson, L. C., Haug, G. H., Hughens, K. A., and Rohl, U., 2000. Rapid changes in the hydrological cycle of the tropical Atlantic during the last glacial. *Science* 290, 1947-1951.
- Pielke, R. A. Jr., and Landsea, C. W., 1998. Normalized U.S. hurricane damages, 1925-1995. *Weather Forecasting* 13, 621-631.
- Portis, D. H., Walsh, J. E., Hanley, M. E., and Lamb, P. J., 2001. Seasonality of the North Atlantic Oscillation. *Journal of Climate* 14, 2069-2078.
- Poore, R. Z., Dowsett, H. J., Verardo, S., and Quinn, T. M., 2003. Millennial-to century scale variability in Gulf of Mexico Holocene climate records. *Paleoceanography* 18, 1048.
DOI:10.1029/2002PA000868, 2003
- Reading, A. J., 1990. Caribbean tropical storm activity over the past four centuries. *International Journal of Climatology* 10, 365-376.

- Richards, T. S., and O'Brien, J. J., 1996. The effect of El Nino on U.S. landfalling hurricanes. *Bulletin of the American Meteorological Society* 77, 773-774.
- Rosenmeier, M. F., Hodell, D. A., Brenner, M., and Curtis, J.H., 2002. A 4000-year lacustrine record of environmental change in the southern Maya lowlands, Peten, Guatemala. *Quaternary Research* 57, 183-190.
- Sahsamanoglou, H. S., 1990. A contribution to the study of action centers in the North Atlantic. *International Journal of Climatology* 10, 247-261.
- Scott, D. B., Collins, E. S., Gayes, P. T., and Wright, E., 2003. Records of prehistoric hurricanes on the South Carolina coast based on micropaleontological and sedimentological evidence, with comparison to other Atlantic Coast record. *Geological Society of America Bulletin* 115, 1027-1039.
- Seager, R., Graham, N., Herweijer, C., Gordon, A. L., Kushnir, Y., and Cook, E., 2007. Imprints for Medieval hydroclimate. *Quaternary Science Reviews*. DOI:10.1016/j.quascirev.2007.04.020.
- Tartaglione, C. A., Smith, S. R., and O'Brien, J.J., 2003. ENSO impacts on hurricane landfall probabilities for the Caribbean. *Journal of Climate* 16, 2925-2931.
- Tedesco, K., and Thunell, R., 2003. High resolution tropical climate record for the last 6,000 years. *Geophysical Research Letters* 30, 1891.
- Thompson, L. G., Mosley-Thompson, E., and Henderson, K. A., 2000. Ice-core paleoclimate records in tropical South America since the Last Glacial Maximum. *Journal of Quaternary Science* 15, 377-394.
- Tiwari, M. R., Ramesh, R., Somayajulu, B., Jull, A., and Burr, G., 2006. Correlation between the equatorial and the high-latitude climatic variations and its implications. Joint Assembly of the American Geophysical Union; Baltimore, Maryland from 23-26 May 2006.
- Trewartha, G. T., 1981. *The Earth's Problem Climates*, 2nd edition. The University of Wisconsin Press, Madison.
- Trudhope, A. W., Chilcott, C. P., McCulloch, M. T., Cook, E. R., Chappell, J., Ellam, R. M., Lea, D. W., Lough, J. M., and Shimmield, G.B., 2001. Variability in the El Nino-Southern Oscillation through the glacial-interglacial cycle. *Science* 291, 1511-1517.
- Visbeck, M. H., Hurrell, J. W., Polvani, L., and Cullen, H. M., 2001. The North Atlantic Oscillation: Past, Present and Future. *PNAS* 98, 12876-12877.
- Walsh, J. P., and Reading, A. J., 1991. Historical changes in tropical frequency within the Caribbean since 1500. *Wurzburg Geographische Zeitschrift* 80, 199-240.

Wang, X., Auler, A. S., Edwards, R. L., Cheng, H., Cristalli, P. S., Smart, P. L., Richards, D. A., and Shen, C-c., 2004. Wet periods in northeastern Brazil over the past 210 kyr linked to distant climate anomalies. *Nature* 432, 740-743.

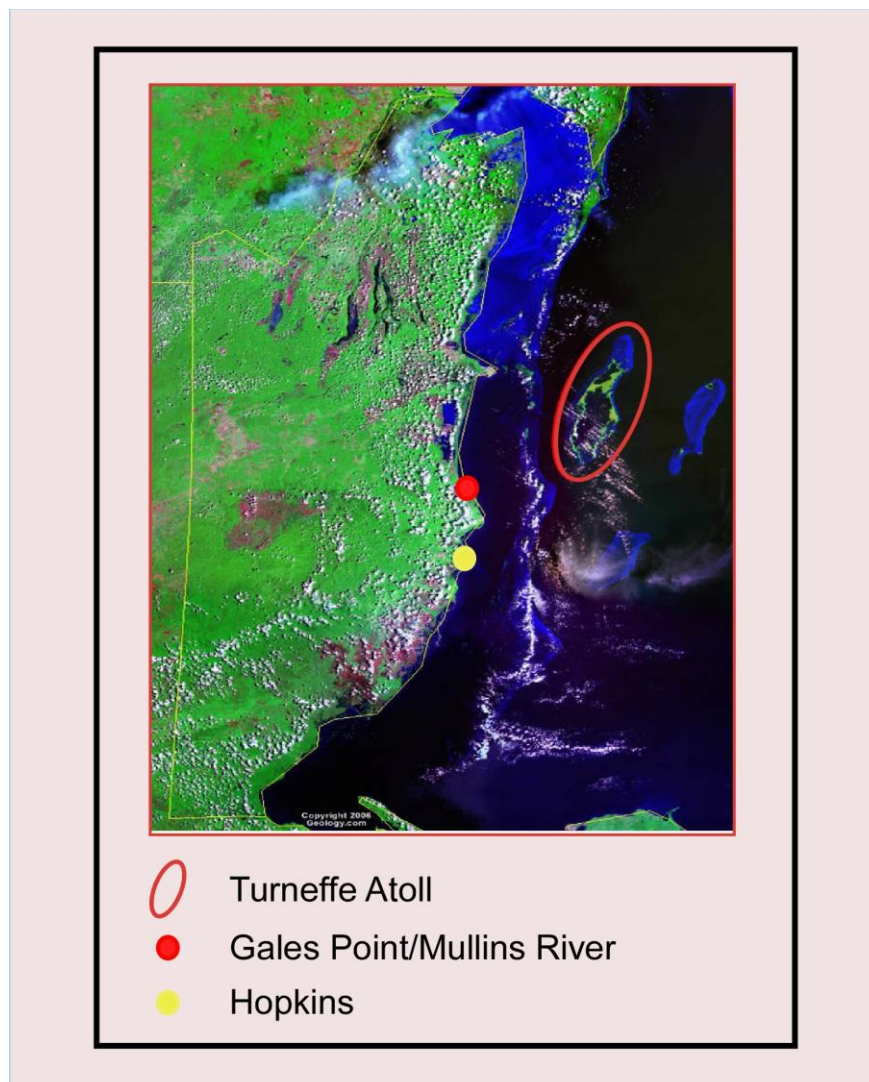
CHAPTER 5 PHYSICAL BACKGROUND, BELIZE

5.1 Background

Belize was the site of much of the work undertaken for this project. Along with general reconnaissance along the entire length of the coast (**Appendix A**), two in-depth studies were conducted on the mainland, one in the Gales Point/Mullins River area, (**Chapter 6**) and the second farther south near the village of Hopkins (**Chapter 7**) (**Figure 5:1**). A third study was conducted on six mangrove cays on the offshore Turneffe Atoll (**Chapter 8**). Due to this geographical focus, the geologic setting and history of Holocene sea level rise will be detailed for Belize.

5.2 Geologic Setting

Belize is located on the Maya block at the southern tip of the North American Plate (NAP). The Maya block is an exotic terrane, believed to have originated in the Gulf of Mexico and rotated counterclockwise to have joined to the southern part of Mexico around the Early Cretaceous (Mann et al., 2007; Alvarado et al., 2007). The southern edge of the Maya block marks the junction of the NAP and the Caribbean Plate (CAR): some few hundred kilometers to the west the northeastwardly moving Cocos Plate is subducting beneath the CAR along the Middle American Trench (Donnelly et al., 1990; McCann and Pennington, 1990) (Map-**Figure 2:15**). As described above (**Figure 2:16**), east of Belize the CAR-NAP boundary becomes lateral west of Jamaica, with two strike slips zones that merge near the Cayman Islands, and a wide transtensional belt extending in an arc along the entire northern coast of Cuba and the eastern edge of the Yucatan peninsula. Naturally, normal faulting dominates this entire area with no evidence of vertical deformation of the seafloor (McCann, 2006). Westward of Cayman Islands



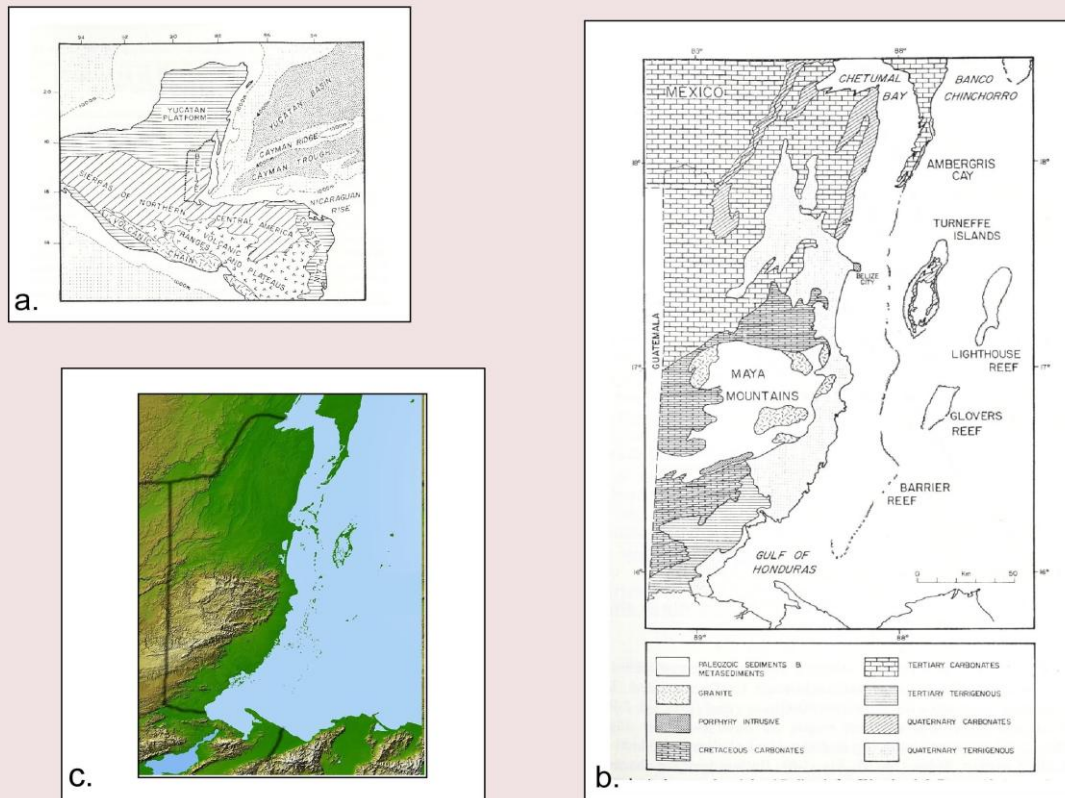
5.1 Google Earth image of Belize, showing the study sites discussed in this dissertation.

the boundary is a covered rift, marked by the Cayman Trough on the seafloor and the Motagua valley upon reaching the continent; farther westward its extension is somewhat uncertain as it is disappears under Tertiary/Quaternary volcanic cover (Weyl, 1980; McCann and Pennington, 1990).

5.2.1 Geologic History

The suturing event responsible for this rift has been dated to the late Cretaceous, probably during a Caribbean superplume event (Donnelly et al., 1990). Abundant ophiolites related to this event were overthrust during the latest Cretaceous (Campanian and Maastrichtian), and can be found on both sides of the suture zone. Although this rift, dividing both blocks and plates, is the defining geologic event in the tectonic history of Belize, several other events have produced major effects; the most important of which is the geologically driven differences between the northern and southern halves of the country. The northern half of the country (roughly from Belize City northward) is a part of the Yucatan Peninsula, a carbonate platform with very little topographic relief and slow sluggish streams which transport very low amounts of sediments. The southern half of Belize is dominated by the Maya Mountains, reaching elevations of over 1100 meters, that provide large amounts of sediments to the coast, in part due to the much higher precipitation levels (> 3750 mm/yr as opposed to ~ 1200 mm/yr in the northern half, Wantland and Pusey, 1971) (**Figure 5:2a**) These mountains consist of a metamorphic Paleozoic basement with granitic plutons of various ages, capped in many places by Cretaceous limestones, evidence of their history as a large faulted block that has experienced various cycles of uplift and subsidence (Donnelly et al., 1990).

A Permian–Triassic orogeny upthrust and deformed the Paleozoic sedimentary rocks that form the basement of the Maya Mountains, followed by the deposition of terrestrial redbeds



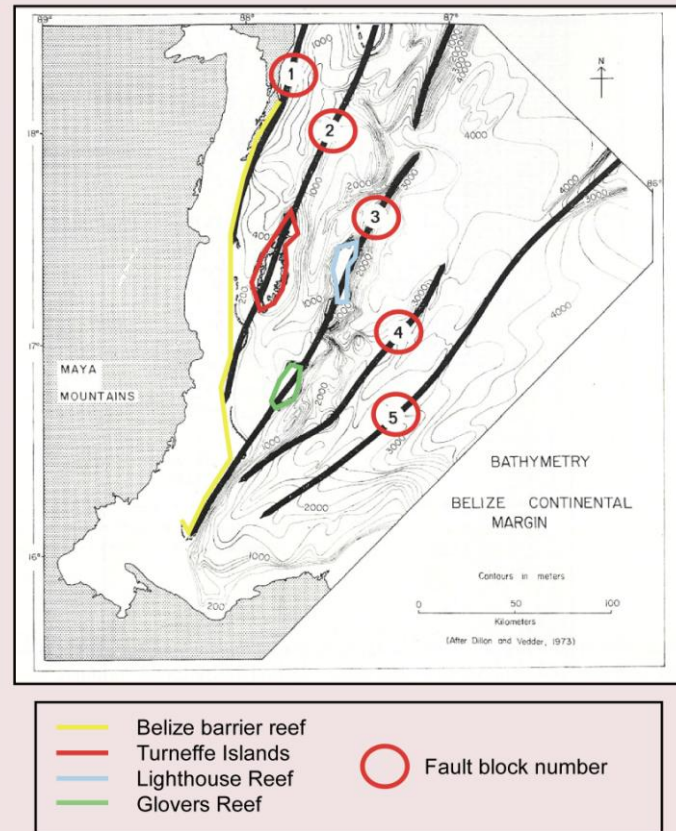
5.2 Geologic setting of Belize; (a) morpho-tectonic provinces; (b) geological map showing age of surface sediments; (c) generalized topography. (a and b) are from James and Ginsburg (1979) (c) is from <http://ambergriscaye.com/maps/art/BELIZE-incrediblepacepicsBZsm.jpg>

during the Jurassic. The Early Cretaceous was a period of general subsidence during which even the Maya Mountains were subjected to carbonate deposition. Large quantities of evaporites were deposited in the northern part of the country during the Albian-Cenomanian age, followed by a period of normal ocean deposition. In all, over 3000 m of limestone covers the Yucatan peninsula. Large karst areas have formed as a result of this thick limestone cover and heavy precipitation (Coates, 1997). As noted above, the inter-plate rifting then commenced in the Late Cretaceous, with the ensuing overthrust of the ophiolite complexes. This orogeny resulted in large quantities of clastic materials being deposited in the southern part of the country during the early Tertiary. Uplift predominated during the Tertiary, although the northern section remained submerged until the Pliocene when the entire Yucatan block tilted northward. Later a thin Quaternary veneer of terrigenous material was deposited on sections of coastal plains (**Figure 5:2b**) (Miller and Macintyre, 1977; James and Ginsburg, 1979; Donnelly et al., 1990; Lara, 1993).

5.2.2 Continental Margin

The continental margin is dominated by 5 parallel *en echelon* normal faults, each characterized by a discontinuous ridge running in a generally north-northeast direction (James and Ginsburg, 1979; Gischler, 1994) (**Figure 5:3**). The continental shelf consists of a shallow marine lagoon lying between the mainland and the barrier reef. The reef lies on top of three of the fault blocks, with the northern section on the westernmost block, the central section on the second block, and the far southern section on the third (**Figure 5:3**).

Bathymetrically the shelf divides into two distinct sections, paralleling the terrestrial division and the differing geologic history. The average depth of the northern shelf is 2.5 meters and the maximum is 5.5 meters, blocked on the east by a rather discontinuous barrier reef. To the



5.3 The continental margin of Belize, highlighting the five offshore faults. Note the generally steep dropoff along the east of each fault block. Turneffe Atoll is situated on the second fault block, with Glovers Reef and Lighthouse Reef on the third. Figure is modified from James and Ginsburg (1979).

south the shelf becomes wider and deeper (from around 6 meters near Belize City to > 65 meters in the far south). Because of this difference in depth, the southern shelf was inundated as a result of Holocene sea level rise earlier (~10,000-8,000 cal yr BP) than the northern shelf (5600-6100 cal yr BP) (Gischler and Hudson, 2004). Moving south, the barrier reef also becomes thicker and more substantial, changing from a barrier rim along the northern shelf to a barrier platform in the south (Miller and Macintyre, 1977; Purdy et al., 1975). Top and bottom salinity, bottom mud and carbonate percentages, marine facies, and many other geologic indicators differ markedly in the northern and southern shelves (Miller and Macintyre, 1977; Wantland and Pusey, 1971, 1975). The barrier reef ends in a distinctive hook some 30 kilometers north of the east-trending Guatemalan/Honduran mainland. The regional subsidence hingeline is located just off the present coast (Lomando and Ginsburg, 1996).

The Holocene barrier reef began developing ~8260 – 6680 cal yr BP (Gischler and Hudson, 2004) and is generally located over Pleistocene topographic highs, formed either by reefs (Dillon and Vedder, 1973; Halley et al., 1977; Shinn et al., 1979) or siliclastic deposits, either older channel deposits from paleodrainage systems originating in the Maya Mountains (Choi and Ginsburg, 1982; Choi and Holmes, 1982) or wedges deposited seaward of the barrier reef during Pleistocene lowstands (Ferro et al., 1999). Recent coring supports antecedent reefs, formed during the last interglacial (stage 5e) as the origin of these topographic highs (Gischler and Hudson, 2004). Lara (1993) suggests, however, that since the location of the Quaternary reefs are fault controlled, their foundations lie much deeper and in much older strata.

5.2.3 Continental Slope and Isolated Carbonate Platforms

The continental slope, beginning at the edge of the barrier reef, is marked by rapidly increasing water depths, with depths of >4000 m reached within <150 km. The steady increase,

however, is interrupted by three isolated carbonate platforms; Turneffe Atoll, Lighthouse Reef, and Glovers Reef (**Figure 5:3**). These platforms are rare Atlantic atolls, accreted coral reefs that rise from deep water (>500m west of Turneffe, and >1000 m between Turneffe and Lighthouse Reef) to the surface, where a coral rim, in some cases supporting sand and/or mangrove cays, surrounds a central lagoon. Of the global total of 425 atolls, only 15 occur in the Atlantic (Stoddart, 1965; Geister, 1983). These atolls are fault-controlled with Turneffe Atoll located on the second fault block and Glovers Reef and Lighthouse Reef on the third. All three atolls are of the “keep-up” variety, under the nomenclature devised by Neumann and Macintyre (1985).

Many similarities and differences exist between the three platforms. **Table 5:1** lists some of the important features. Glovers Reef and Lighthouse Reef are enclosed by surface breaking coral rims, while Turneffe has subaerial rims only on the east (windward) side, and submerged reefs on the leeward (Gischler, 1994). On all three atolls, the windward fore reef, composed mainly of *Acropora palmate* and *Agaricia agaricites* coral has a well developed spur and groove system. Typically, the initial slope is ~ 20-30% until reaching the brow, characterized by abundant coral, at ~ 20-40 m, after which the slope becomes vertical for “several hundreds” of m (James et al., 1976; James and Ginsburg, 1979; Gischler and Hudson, 2004). *Montastraea annularis* dominate the leeward reefs. All three have similar interior lagoons containing *Thalassia* and patch coral.

Although sharing many characteristics, there are also several important differences between the atolls. As their names imply, both Glovers Reef and Lighthouse Reef contain very little land area or mangrove development. Open circulation prevails in their interior lagoons, characterized by clear water, patch reefs, and light colored

5.1 Characteristics of the three Belizean Atolls. Information compiled from Gischler (1994); Gischler and Lomando (2000); Gischler and Hudson (1998, 2004).

Name	Size km ²	Land area %	Depth of Central Lagoon m	Circulation	Patch Reefs	Mangrove	Time of Flooding yr BP	Maximum Holocene Reef Thickness m	Surface Breaking Reefs
Turneffe Atoll	525	22	8	Restricted	Rare	Common	~6000	11.7	Windward Side
Lighthouse Reef	200	3	8 (east) 3 (west)	Open	Common, linear	Rare	~6500	7.9	All around Thinner on Leeward
Glovers Reef	260	0.2	18	Open	>860	Rare	~7500	3.8	All around Channels to Leeward

carbonate bottom sediments. Turneffe's lagoon has restricted circulation, is surrounded by large mangrove islands, resulting in darker water with *Thalassia* dominating the dark organic rich lagoon bottom. The lagoon is subject to "extreme" salinity and temperature variability (Smith, 1941; Gischler, 1994). The most obvious inter-atoll difference is the decreasing amount of land and subsequent reduction in mangroves from Turneffe Atoll through Lighthouse Reef to Glovers Reef. These differences are the result of three major controls, namely:

1. Antecedent topography
2. Holocene sea level rise
3. Wave and current regimes

5.2.3.1 Antecedent Topography

All three atolls are underlain by Pleistocene reefs formed during oxygen isotope stage 5e, as evidenced by an abundance of coring sites with a typical stratigraphic sequence of Pleistocene reefs (sometimes displaying subaerial features) followed by Holocene soil development and mangrove peat (Gischler and Hudson, 2004). Underlying this are 1030 m (Turneffe Atoll) and 560 m (Glovers Reef) of Tertiary reef and shallow water material above Cretaceous-Eocene siliclastics, as shown by deep bores drilled by Shell Oil (Gischler and Lomando, 2000; Gischler and Hudson, 2004). The Pleistocene reefs underlying fault blocks 1-3 all exhibit very distinct tilting, with the southern ends generally lying at elevations 10-20 m below the northern end (**Figure 5:4**).

Differential subsidence has been suggested as a possible cause, although no direct evidence was been found for neo-tectonics along these ridges (Gischler and Hudson, 1998, 2004; Gischler and Lomando, 2000). An alternative explanation is a steep karstification gradient. Over the mainland west of these three atolls, annual precipitation increases from 1500 mm to 4500

along a north to south transect. If a similar precipitation gradient existed throughout the Late Pleistocene, the resulting increased dissolution could account for lowered surface elevations in the south (Glovers Reef). However, it appears that the precipitation in the south is at least partially orographic in nature, with questionable applicability farther east over the open sea. Whatever the causes of this tilting, the resulting antecedent topography places Glovers Reef, Lighthouse Reef, and Turneffe Atoll at progressively higher elevations.

5.2.3.2 Holocene Sea Level Rise

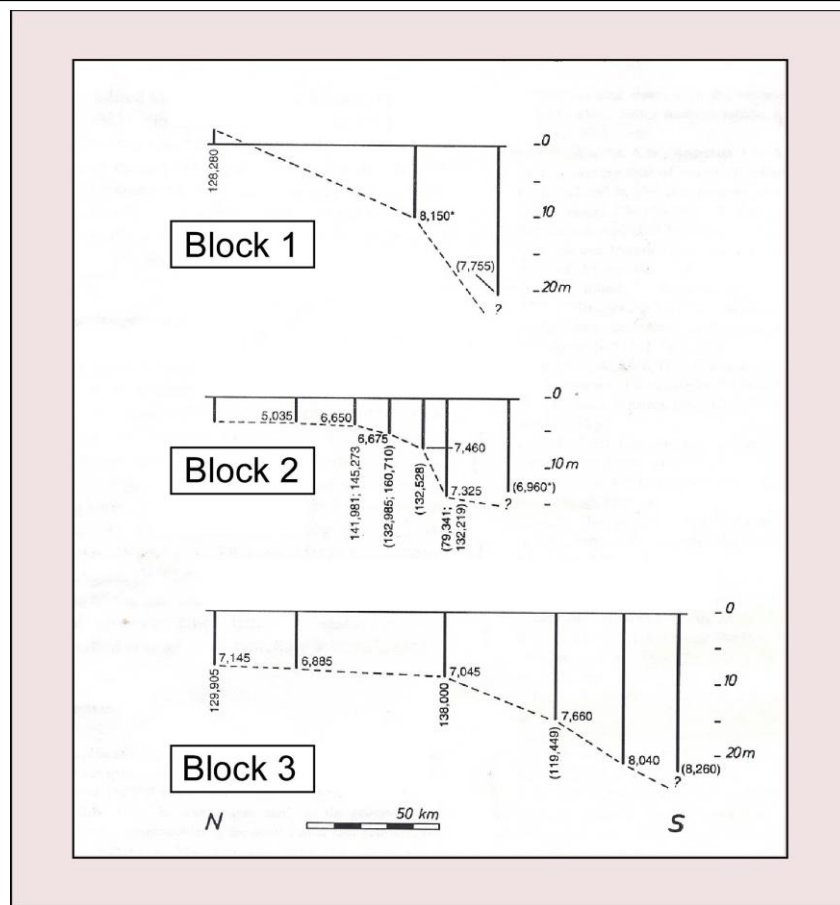
This elevational gradient results in time transgressive dates of inundation by the Holocene sea level rise, with Glovers Reef flooding ~8500 cal yr BP, followed by Lighthouse Reef ~ 7000BP cal yr and Turneffe Atoll ~ cal yr 6000 BP (Gischler and Hudson, 1998; Gischler and Lomando, 2000; Gischler, 2003). This, in turn, resulted in progressively thicker Holocene reef deposits and deeper lagoon depths across the antecedent elevation gradient.

5.2.3.3 Wave and Current Regimes

Mean wave approach for the area is 75° (Burke, 1982; Gischler, 2003; Gischler and Hudson, 1998, 2004; Gischler and Lomando, 2000), which results in differing wind regimes for the three atolls (Gischler, 2003; Gischler and Hudson, 1998, 2004; Gischler and Lomando, 2000). In particular, the southeast position of Lighthouse Reef tends to shelter the southern section of Turneffe, which has been suggested as major cause of the atoll's extensive mangrove development (Gischler, 2003; Gischler and Hudson, 1998, 2004; Gischler and Lomando, 2000) (Figure 5:5). The predominant current is an N-S countercurrent along the coast and within Glovers Reef (Purdy, 1974; Wallace and Schafersman, 1977; Gischler, 2003).

5.2.4 Tectonic Regime

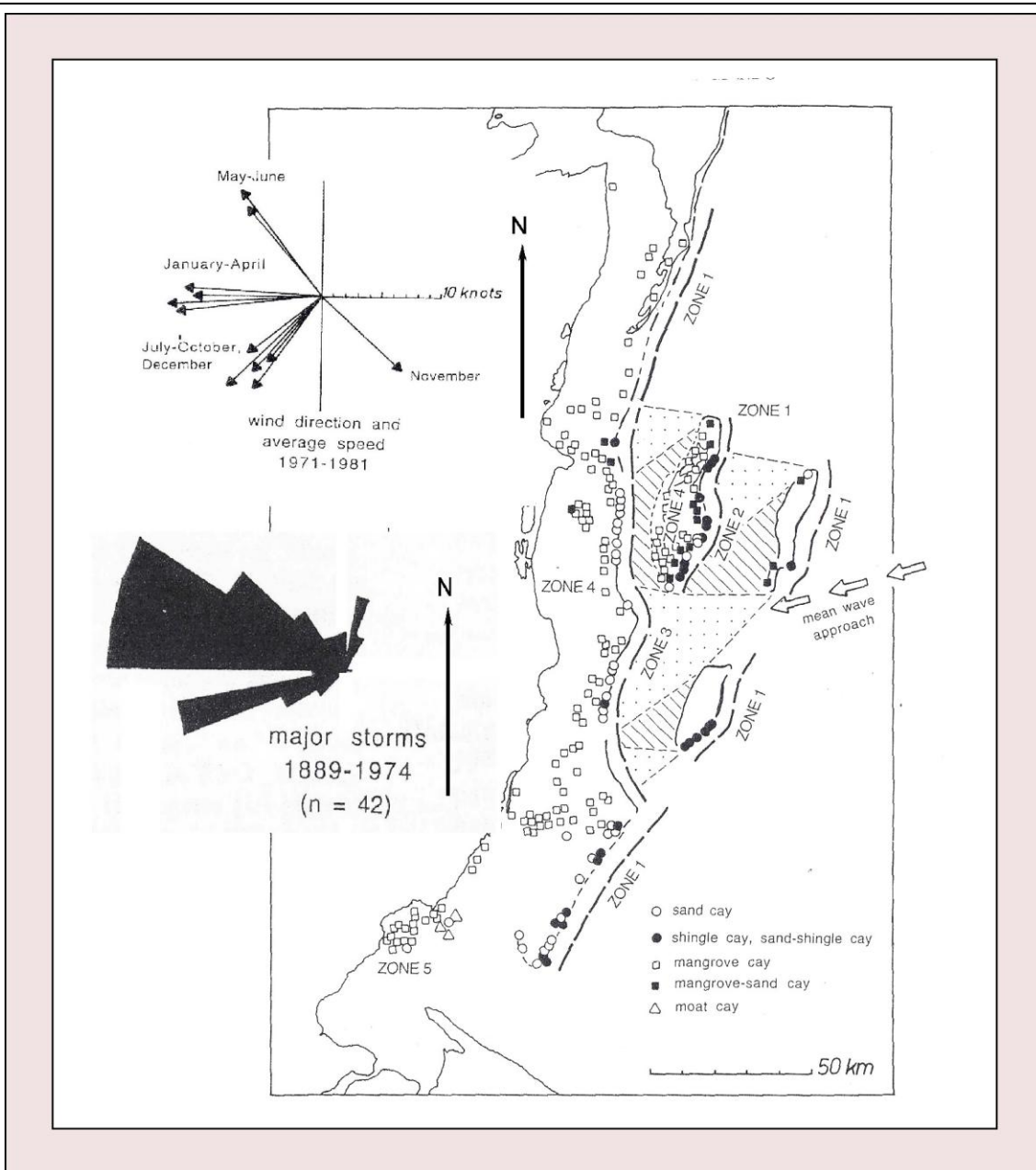
Although the Motagua is the major fault along the CAR/NAP junction in Central



5.4 Tilt of the Pleistocene basement of the continental margin. The southern ends of fault blocks 1-3 are generally 10-20 m lower than the northern end. Modified from Gischler and Hudson (2004).

America, it is not the only one, as it is paralleled by the Jocotan to the south and the Polochic to the north. The Polochic was more active in the Tertiary (particularly the Miocene), and is generally regarded as responsible for 130 kilometers of lateral offset. However, it has not been identified with any historic earthquakes (McCann and Pennington, 1990). The Motagua fault apparently absorbs ~ 20 mm/year of the relative motion of the two plates, and has experienced at least two large ruptures during historic times, in 1775 and 1976. The 1976 event was “disastrous”, resulting in ~ 2 meters of instantaneous offset, and another 2 meters of post-event creep (Donnelly et al., 1990).

Moving east off the coast, the rift becomes the Cayman Trough, a pull-apart basin, which probably opened in the middle Eocene, and has resulted in “substantial” subsidence along the Belize margin since then (Lara, 1993). She suggests a “Pliocene and/or later” tectonic episode for the southern shelf, characterized by high-angle normal faults, which she conjectures might still be active. However, there has been less dramatic modern faulting along this section than along the Motagua fault, with only a “few” small earthquakes recorded between Hispaniola and Central America between 1955-1990, although two groups of seismic activity are found, one just south of the Cayman Islands, and the other in the Swan fracture zone off the north coast of Honduras (McCann and Pennington, 1990). In 1856 a large underwater earthquake occurred in this area, accompanied by a tsunami, perhaps resulting from secondary slumping (McCann and Pennington, 1990). In general, however, these sections have experienced less seismic activity than other sections of the plate boundary (**Figure 5:6, 2:16**). A group of underwater Pleistocene age stalactites in an interstadially formed cave on Lighthouse Reef Atoll consistently incline 5-10° from the vertical (Jones and Dill, 2002). The northern inclination of these speleothems possibly results from Quaternary faulting, the geographical extent of which is not known. Since



5.5 Wave and wind regime for coastal Belize. Note the sheltered position of the southern end of Turneffe Atoll, which lies leeward of Lighthouse Reef. Wind/wave energy is greatly reduced landward of the barrier reef. From Gischler and Lomando (2004).

the Yucatan platform has been tectonically inactive for at least the late Holocene (Bonini et al., 1984; Dillon and Vedder, 1973), no historic earthquakes are shown for the northern part of the country.

5.3 Sea Level

Barring unusual local conditions, sea level rise for Belize should parallel the regional curves presented in Chapter 1 (**Figures 2:9-10, 12-14.**) In fact, several studies directly examining Post-Wisconsin sea level rise have been conducted in Belize. Macintyre et al. (1995) conducted a study based on radiocarbon-dated peat obtained in a transect taken across a small cay in the southern shelf, obtaining peat records up to 10 meters in depth. Interestingly, many cores recovered datable basal mud covering Pleistocene limestone, which permitted accurate dating of inception of the sea level rise related marine flooding of this cay. In addition, the authors compiled a specific Belizean sea level curve, based on a number of peat studies (corals were not considered), which basically reproduces the curves already discussed. Age of marine flooding of the three deep-water atolls situated on the second and third offshore fault ridges are also known, and are in basic accord with the previously examined curves (Gischler and Hudson, 1998). So, all indications are that relative sea level has risen continuously in Belize since the LGM, though probably at a decreasing rate.

However, due to their nature, such geologic proxies are best suited for delineating general trends and generally do not permit high-resolution data either spatially (vertically) or temporally. In the fact, it has been suggested that the crudeness of such proxies allow for the underidentification of small, short-term oscillations (Moerner, 1987). As discussed above, elevational control is less than perfect for biological proxies, as evidenced by *Acropora plamata* being found as deep as 17 meters, and the possible inability to accurately identify similar

mangrove species consistently. Macintyre et al. (1995) reports “extensive” fracturing and slumping of Belizean peat deposits. Radiocarbon dates do not have a one to one correspondence when calibrated to calendar years; depending upon the atmospheric level of ^{14}C for the relevant interval, and the size of the error bars, a single ^{14}C date can yield a number of possible calendar dates (CALIB5.0 program at depts.washington.edu/qil/calib/). For fairly recent time periods, other methods can be attempted to determine the date of geologic events. In Belize, with possibly the most detailed human cultural record (direct and indirect) in the western hemisphere, archeological data can possibly yield very useful, high-resolution data.

There are several studies of this nature which can be used to estimate recent sea level rise. Since the basic chronology of the ancient Maya is known, material artifacts and general cultural milestones (such as population density, relative level of deforestation) pertaining to that civilization can be used as stratigraphic markers (though not unambiguously). Perhaps the most obvious Belizean example of this is McKillop’s (2002, 1995) conclusion of a meter of sea level rise in southern Belize since the Late to Terminal Classic period (AD 700-900, or ~1300-1100 cal yr BP). The archeological evidence seems both clear and widespread, as shown by the large number of submerged sites encountered by McKillop (2002) (**Figure 5:7**).

At Wild Cane Cay offshore shovel tests at 10 meter intervals display a concentric pattern Of submerged artifacts, with midden deposits extending 1.5 m below present water level, indicating an estimated reduction of land area from 4 to 2 hectares since the Classic period (McKillop, 1995) (**Figure 5:8**). This is supported by the presence of non-salt adapted plant macrofossils at Classic period stratigraphic levels (dating was by charcoal and ceramic analysis). Similarly, in the adjoining Stingray Lagoon, artifacts from the same period are found protruding from the seafloor at depths of 0.8 meter to 1.0 meter. Evidence for similar rates of sea level rise

over the last 1000 years are found at other locations along the southern coast (McKillop, 1993, 1996, 2002).

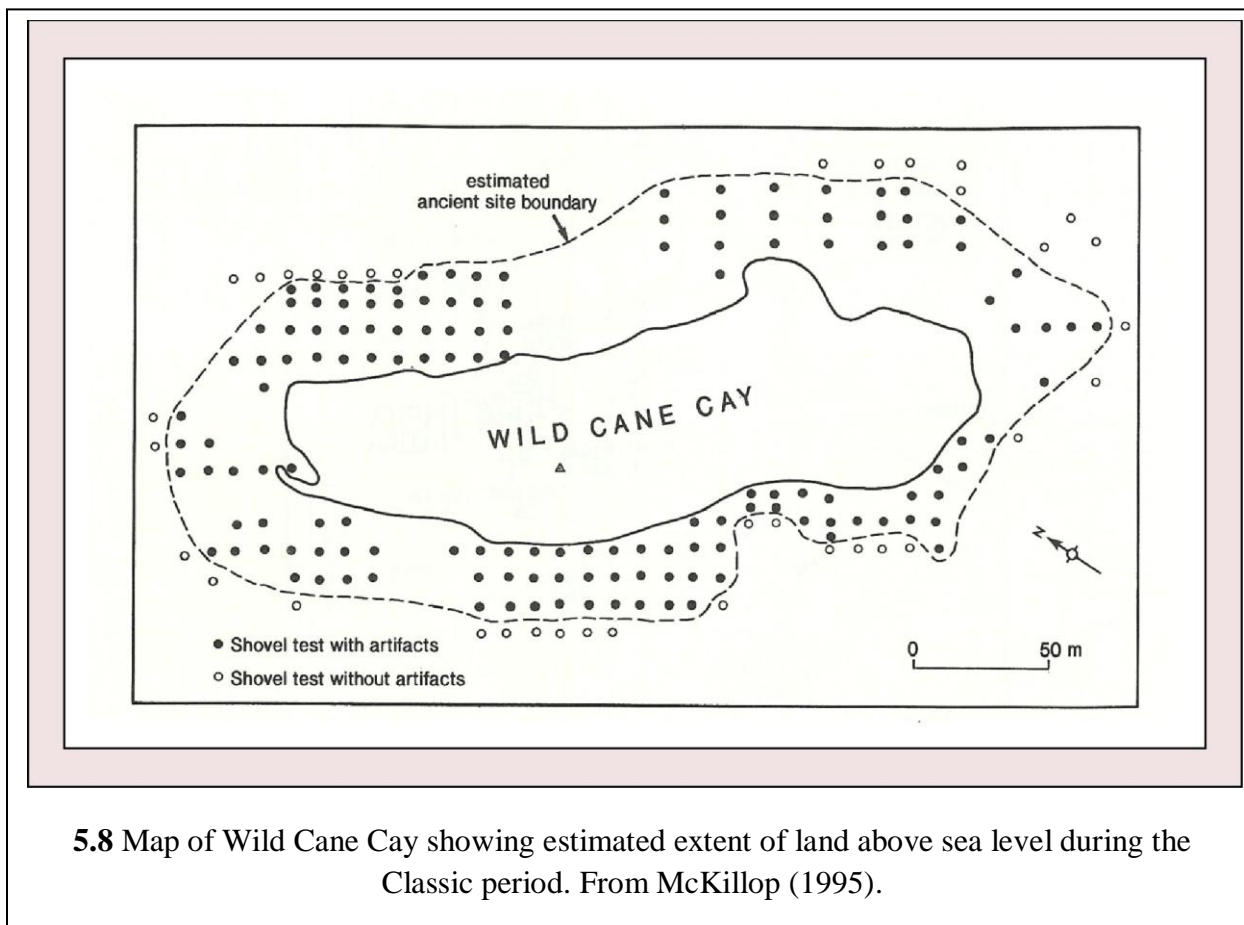
However, these findings are at odds with some archeological/geochemical results from the northern part of the country. Alcala-Herrera et al. (1994) examined lithologic changes as well as ostracod, gastropod, and foraminiferal abundances from the Cobweb swamp in northern Belize to determine the salinity changes over the last 8000 years. After an initial sea level rise-driven change from fresh to brackish conditions around 5600 cal yr BP, they found generally decreasing salinity after that period, with near limnetic conditions being established by ~ 3400 cal yr BP. This seems to indicate an original slowing in the rate of sea level rise, followed by stable conditions. This is paralleled by findings from Albion Island, which, though having a less direct connection with the sea, shows a similar decrease in salinity, beginning ~5000 cal yr BP (Bradbury et al., 1991). A similar study (Pohl et al., 1996) found sea level reaching ~1 m below present at 3000 cal yr BP. The correlation of paleosalinity levels with relative sea level rise, however, is somewhat uncertain, due to possible anthropogenic influence. The practice of wetland engineering for agricultural purposes is well-documented for Belize and the surrounding region (Pohl and Bloom, 1996; Dunning et al., 2002). Alcala-Herrera et al. (1994) consider the change from brackish to fresh water to have possibly resulted from increased freshwater input, due to deforestation and/or agricultural development. They also raise the possibility of the human damming of the swamp. In the Yucatan, similar questions have been raised concerning ancient Maya control over local water tables (Leyden et al., 1998). It should be noted that the Cobweb Swamp study was carried out in order to assess the anthropogenic impact on the environment, in the context of the adjacent archeological site of Colha. Recent research indicates that during ancient Maya times the human/climate/environment interaction was multi-directional, often

Site (Laboratory Number)	Maximum Depth below Sea Level (cm)	Cultural Context	Environmental Context	Uncalibrated Radiocarbon Age (± 1 sigma)	2 sigma Calibrated Age (95% Probability)
Stingray Lagoon (B-69869)	100	work shop	underwater	1180 \pm 50 B.P.	cal A.D. 670–870
David Westby		work shop	underwater		
Orlando's Jewfish		work shop	underwater		
Pelican (B-69905)	80	midden	below peat inundated	1400 \pm 50 B.P.	cal A.D. 450–650
Green Vine Snake	unknown*	midden	inundated		
Tiger Mound (B-37037)	80	midden	inundated	1270 \pm 60 B.P.	cal A.D. 560–800
Killer Bee	unknown*	work shop	inundated		
Wild Cane Cay (B-9095)	140	midden	inundated	1200 \pm 80 B.P.	cal A.D. 600–920
Wild Cane Cay (B-9426)	80	midden	inundated	1540 \pm 60 B.P.	cal A.D. 290–530
Wild Cane Cay (B-9425)	80	midden	inundated	1510 \pm 60 B.P.	cal A.D. 439–660
Wild Cane Cay (B-9094)	120	midden	inundated	1510 \pm 60 B.P.	cal A.D. 439–660
Frenchman's Cay	80	building foundations	inundated		
Pork and Doughboy** (B-87007)	57	midden	underwater	1270 \pm 50 B.P.	cal A.D. 665–885

* The base of the archaeological deposits was not reached in the excavations.

** The calibrated radiocarbon date for Pork and Doughboy was provided by Beta Analytic. Other dates were calibrated using the calibration curves in Stuiver and Pearson 1986.

5.7 Submerged archaeological sites in southern Belize. From McKillop (2002).



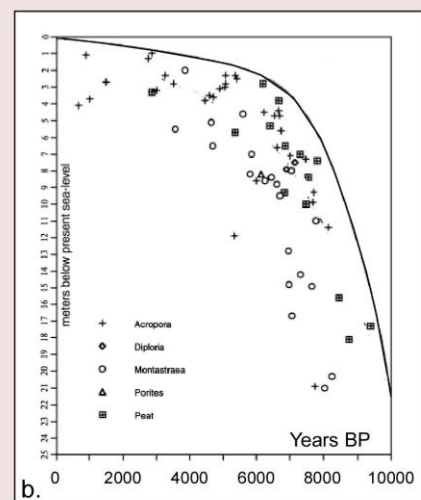
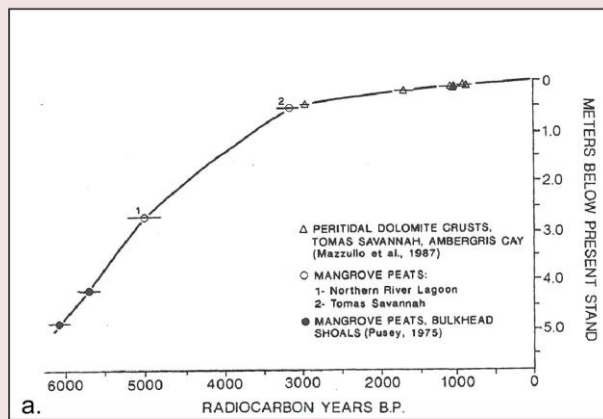
fluctuating between stable/unstable states, further complicating the geological record (Dunning and Beach, 2004).

Mazullo and Reid (1988), Dunn and Mazullo (1993), and Mazullo et al. (1987, 1992), working with cultural artifacts, corals, island stratigraphy and dolomitization of surface sediments on Ambergis Cay all found very little sea level rise over the last few millennia. Their studies indicate that by 2100 cal yr BP the sea level was within 30 cm of present MSL, which was reached ~1000 cal yr BP (**Figure 5:9a**). Mazullo et al. (1992) specifically focused on the last 410 years, through an examination of patch coral on the shelf to the east of Ambergis Cay, directly behind the barrier reef. These corals show lateral, rather than vertical accretion, which the authors attribute to the lack of accommodation space, i.e., the stability of water depth (Mazullo et al., 1992). This is specifically contrasted with patch reefs in the southern shelf, which due to their differing geologic setting/history and energy environment, have developed different community composition and growth strategies.

A recent Belize specific curve, based on 69 coral and basal peat dates, supports the view of minimal recent sea level rise, showing sea level reached 2 m below present nearly 6000 BP and 1 m below present before 3000 cal yr BP (Gischler and Hudson, 2004; Gischler, 2006) (**Figure 5:9b**).

5.4 Discussion

There are several possible explanations for this discrepancy in the recent sea level curves for Belize. The most likely is the basic differences in the geologic setting and history of the northern and southern portions of the country. In particular, the southern coast has a much higher sedimentation rate, due to both the greater topographic relief and amount of rainfall received. Because the southern shelf is so much deeper it flooded 2000-4000 years earlier than the



5.9 Belize specific sea level curves; (a) is from Dunn and Mazullo (1993), based on peritidal dolomite crusts and basal peats, including data from Mazullo et al. (1987) and Pusey (1975); (b) is from Gischler and Hudson (2004), based on basal peat and coral data.

northern shelf (Gischler and Hudson, 2004). This has led to deeper peat accumulations as well as a heavier water load on the shelf floor. This could result in increased subsidence, both through peat compaction/dewatering and hydrostatic adjustment. Although the Motagua fault is strike/slip and should not be expected to result in significant vertical displacement, activity on the scale of the 1976 event could reasonably result in slumping of deep peat deposits. Lara's (1993) conjecture that the nearly vertical normal faults in the southern shelf (her study area is only a few tens of kilometers from McKillop's) may still be active raises a more direct possibility. In fact, McKillop's (1995) reference to "the ancient submergence" of Stingray Lagoon possibly indicates a paleoseismic event. The "immediately noticeable" observation of the unusually large size of the potsherds strewn over a relatively flat submerged area there would seem more in keeping with a sudden, increase in relative sea level. Similarly, her observation of the excellent state of preservation of organic plant and animal remains at Wild Cane and Frenchman's Cays also argues for a rapid ancient submergence, which would more probably result from either a seismic event or rapid subsidence than from the slow creep of sea level rise.

In general, it seems that the Belize-specific curves of Dunn and Mazullo (1993) (**Figure 5:9a**) and Gischler and Hudson (2004) (**Figure 5:9b**) that demonstrate minimal (~1m for the last 3000 years) recent sea level rise are probably the most accurate, particularly for the northern areas, the barrier reef and the three carbonate platforms, as relative sea level raise along the deeper southern shelf may be confused by a number of non-eustatic factors.

5.5 References

Alcala-Herrera, J.A., Jacob, J. S., Castillo, M.L.M., and Neck, R.W., 1994. Holocene paleosalinity in a Maya wetland, Belize, inferred from the microfaunal assemblage. *Quaternary Research* 41, 121-130.

- Alvarado, G. E., Dengo, C., Martens, U., Bundschuh, J., Aguilar, T., and Bonis, S. B., 2007. Stratigraphy and geologic history. In Bundschuh, J., and Alvarado, G. E., (eds), Central America Geology Resource Hazards. Taylor and Francis, London. Vol. 1, 345-394.
- Bonini, W. E., Hargraves, R. B., and Shagam, R., (eds), 1984. The Caribbean-South American Plate boundary and regional tectonics. Geological Society of America Memoir. 162. Boulder, Colorado.
- Bradbury, J. P., Forester, R. M., Bryant, W. A., and Covich, A. P., 1991. Paleolimnology of Laguna de Cocos, Albion Island, Rio Hondo, Belize. In Pohl, M. D., (ed), Ancient Maya Wetland Agriculture. Westview, Boulder, Colorado. 119-154.
- Burke, R. B., 1982. Reconnaissance study of the geomorphology and benthic communities of the outer barrier reef platform, Belize. In Rutzler, K., and Macintyre, I. G., (eds), The Atlantic Barrier Reef Ecosystem of Carrie Bow Cay, Belize. Smithsonian Contributions to the Marine sciences 12, 509-526.
- Choi, D.R., and Ginsburg, R.N., 1982. Siliclastic foundations of Quaternary reefs in southernmost Belize Lagoon, British Honduras. GSA Bulletin 93, 116-126.
- Choi, D.R., and Holmes, C., 1982. Foundation of Quaternary reefs in south-central Belize lagoon, British Honduras. American Association of Petroleum Geologists Bulletin 66, 2663-2671.
- Coates, A.G., 1997. The forging of Central America. In Coates, A. G., (eds.) Central America: a Natural and Cultural History. Yale University Press, New Haven. 1-37.
- Dillon, W. P., and Vedder, J. G., 1973. Structure and development of the continental margin of British Honduras. Geological Society of America Bulletin 84, 2713-2732.
- Donnelly, T.W., Horne, G. S., Finch, R. C, Lopez-Ramos, E., 1990. Northern Central America; the Maya and Chortis blocks. In Dengo, G., and Case, J.E., (eds), The Geology of North America, Vol. H, The Caribbean region The Geologic Society of America, Boulder, Colorado. 37-76.
- Dunn, R. K., and Mazullo, S. J., 1993. Holocene Paleocoastal reconstruction and its relationship to Marco Gonzales, Ambergris Caye, Belize. Journal of Field Archaeology 20, 121-131.
- Dunning, N. P, and Beach, T., 2004. Noxious or nurturing nature? Maya civilization in environmental context. In Golden, C. W., and Borgstede, G., (eds), Continuities and Changes in Maya Archaeology: Perspectives at the Millennium. Routledge, New York. 125-141.
- Dunning, N. P., Luzzadder-Beach, S., Beach, T., Jones, J., Scarborough, G., and Culbert, T. P., 2002. Arising from the *Bajos*: the evolution of neotropical landscape and the rise of Maya civilization. Annals of the Association of American Geographers 92, 267-283.

Ferro, C. E., Droxler, A. W., Anderson, J. B., and Mucciarone, D., 1999. Late Quaternary shift of mixed siliclastic-carbonate environments induced by glacial eustatic sea-level fluctuations in Belize. In Harris, P. M., Saller, A. H., Simo, J. A., (eds), *Advances in Carbonate Sequence Stratigraphy: Application to Reservoirs, Outcrops and Models*. Special Publications-Society of Economic Paleontology Mineralogists, 63, 385-411.

Geister, J. 1983. Holozane westindische Korallenriffe: okologie und fazies. *Facies* 9, 173-284.

Gischler, E., 1994. Sedimentation on three Caribbean atolls: Glovers Reef, Lighthouse Reef and Turneffe Islands, Belize. *Facies* 31, 243-254.

Gischler, E., 2003. Holocene development in the isolated carbonate platforms off Belize. *Sedimentary Geology* 159, 113-132.

Gischler, E., 2006. Comment on “Corrected western Atlantic sea-level curve for the last 11,000 years based on calibrated ^{14}C dates from *Acropora palmate* framework and intertidal mangrove peat” by Toscano and Macintyre. *Coral Reefs* 22:257–270 (2003), and their response in *Coral Reefs*. 24:187–190 (2005). *Coral Reefs* 25, 273–279. DOI 10.1007/s00338-006-0101-1

Gischler, E., and Hudson, J. H., 1998. Holocene development of three isolated carbonate platforms, Belize, Central America. *Marine Geology* 144, 333-347.

Gischler, E., and Hudson, J. H., 2004. Holocene development of the Belize Barrier reef. *Sedimentary Geology* 164, 223-236.

Gischler, E., and Lomando, A. J., 2000. Isolated carbonate platforms of Belize, Central America: sedimentary facies, late Quaternary history and controlling factors. In Insalco, E., Skelton, P. W., and Palmer, T.J., (eds) *Carbonate Platform Systems: Components and Interactions*. Geological Society, London. Special Publications, 178, 135-146. The Geological Society of London, London.

Halley, R. B., Shinn, E. A., Hudson, J. H., and Lidz, B., 1977. Recent and relic topography in the Boo Bee patch reef, Belize. In Taylor, D. L., (ed), *proceedings third International Coral Reef Symposium*, Miami. Vol. 2, University of Miami, 29-35.

James, N.P., and Ginsburg, R.N., 1979. The seaward margin of Belize barrier and atoll reefs. *International Association of Sedimentologists*, Special Publication No. 3.

James, N.P., Ginsburg, R.N., Marszalek, D.S., and Choquette, P. W., 1976. Facies and fabric specificity of early subsea cements in shallow Belize (British Honduras) reefs. *Journal of Sedimentary Petrology* 64, 523-544.

Jones, A. T., and Dill, R. F., 2002. The Great Blue Hole of Lighthouse Reef Atoll, Belize, Central America. In Jackson, T. A., (ed), *Caribbean Geology into the Third Millennium: Transactions of the Fifteen Caribbean Geological Conference*. University of the West Indies Press, Barbados.

Lara, M. E., 1993. Divergent wrench faulting in the Belize southern lagoon: implications for Tertiary Caribbean plate movements and Quaternary reef distribution. *American Association of Petroleum Geologists Bulletin* 77, 1041-1063.

Leyden, B. W., Brenner, M., and Dahlin, B., 1998. Cultural and climatic history of Coba', a lowland Maya city in Quintana Roo, Mexico. *Quaternary Research* 49, 111-122.

Lomando, A. J., and Ginsburg, R. N., 1996. How important is subsidence in evaluating high frequency cycles in the interior of isolated carbonate platforms? *American Association of Petroleum Geologists Bulletin* 79, 1231-1232 (abstract).

Macintyre, I. G., Littler, M.M. and Littler, D. S., 1995. Holocene history of Tobacco Range, Belize, Central America. *Atoll Research Bulletin* 430, 1-18.

Mann, P, Rogers, R. D., and Gahagan, L., 2007. Overview of plate tectonic history and its unresolved tectonic problems. In Bundschuh, J., and Alvarado, G. E., (eds), *Central America Geology Resource Hazards*. Taylor and Francis, London. Vol. 1, 201-237.

Mazullo, S. J., and Reid, A. M., 1988. Sedimentary textures of recent Belizean peritidal dolomite. *Journal of Sedimentary Petrology* 3, 479-488.

Mazullo, S. J., Reid, A. M., and Gregg, J. M., 1987. Dolomitization of Holocene Mg-calcite supratidal deposits, Ambergris Cay, Belize. *Geological Society of America Bulletin* 98, 224-231.

Mazullo, S. J., Anderson-Underwood, K. E., Burke, C. D., and Bischoff, W. D., 1992 Holocene coral patch reef ecology and sedimentary architecture, northern Belize, Central America. *Palaios* 7, 591-601.

McCann, W. R., 2006. Estimating the threat of tsunamigenic earthquakes and earthquake induced- landslide tsunamis in the Caribbean. In Mercado-Irizarry, Liu. P., (eds), *Caribbean Tsunami Hazard*. World Scientific, New Jersey. 43-65.

McCann, W. R., and Pennington, W. D., 1990. Seismicity, large earthquakes, and the margin of the Caribbean Plate. In Dengo, G., and Case, J.E., (eds), *The Geology of North America*, Vol. H, The Caribbean region The Geologic Society of America. Boulder, Colorado. 291-306.

McKillop, H., 1993. Comment on Scott Atran: Itza Maya tropical agro-forestry." *Current Anthropology* 34, 691-692.

McKillop, H., 1995. Underwater archaeology, salt production, and coastal Maya trade at Stingray Lagoon, Belize. *Latin American Antiquity* 6, 214-228.

McKillop, H., 1996. Prehistoric Maya use of native palms: archeobotanical and ethobotanical evidence. In Fedick, S. L., (ed), *The Managed Mosaic: Ancient Maya Agriculture and Resource Use* University of Utah Press, Salt Lake City.

McKillop, H., 2002. Salt: White Gold of the ancient Maya. University Press of Florida, Gainesville.

Miller, J. A., and Macintyre, I. G., 1977. Field Guidebook to the Reefs of Belize. Third International Symposium on Coral Reefs. Atlantic Reef Committee, University of Miami, Miami Beach.

Moerner, N-A., 1987. Models of global sea-level change. In Tooley, M. J. and Shennan, I., (eds), Sea-level Changes. The Institute of British Geographers Special Publication Series 20. Basil Blackwell Ltd, New York. 332-355.

Neumann, A. C., and Macintyre, I. G., 1985. Reef response to sea level rise: keep-up, catch-up or give-up. In Gabrie, C., Toffart, J. I., Salvat, B., (eds), Proceedings, Fifth International Coral Reef Symposium, Tahiti. Antenne Museum, EPHE, Moore, French Polynesia. 3, 105-110.

Pohl, M., and Bloom, P., 1996. Prehistoric Maya Farming in the Northern Belize: more data from Albion Island and beyond. In Fedick, S. L., (ed), The Managed Mosaic: Ancient Maya Agriculture and Resource Use University of Utah Press, Salt Lake City. 145-164.

Pohl, M., Pope, K. O., Jones, J. G., Jacob, J.S., Piperno, D. R., deFrance, S.D., Lentz, D.L., Gifford, J.A., Danforth, M.E., and Josserand, J.K., 1996. Early agriculture in the Maya lowlands. *Latin American Antiquity* 74, 355-372.

Purdy, E.G, 1974. Karst-determined facies patterns in British Honduras: Holocene carbonate sedimentation model. *American Association of Petroleum Geologists Bulletin* 2, 1-52.

Purdy, E. G., Pusey, W. C. III, and Wantland, K. F., 1975. Continental shelf of Belize-regional shelf attributes. In Wantland, K. F., and Pusey, W. C., (eds), Belize Shelf-carbonate Sediments, Clastic Sediments and Ecology. American Association of Petroleum Geologists Studies in Geology No. 2. American Association of Petroleum Geologists, Tulsa.

Pusey, W.C., 1975. Holocene carbonate sedimentation on northern Belize shelf. In Wantland, K. F., and Pusey, W.C (eds), Belize's Shelf-carbonates Sediments, Clastic Sediments and Ecology. American Association of Petroleum Geologists Studies in Geology. No.2, Tulsa. 131-233.

Shinn, E. A., Halley, R.B., Hudson, J. H., Lidz, B., and Robbin, J., 1979. Three dimensional aspects of Belize patch reefs (abstract) SEPM Annual Meetings Abstracts with program, p. 164.

Smith, F. G.W., 1941. Sponge disease in British Honduras, and its transmission by water currents. *Ecology* 22, 415-421.

Stoddart, D. R., 1965. The shape of atolls. *Marine Geology* 3, 369-383.

Wallace, R. J., and Schafersman, S. D., 1977. Patch-reef ecology and sedimentology of Glovers Reef Atoll, Belize. In Frost, S. H., Weiss, M. P., and Sanders, J. B. (eds), Reefs and Related Carbonates-Ecology and Sedimentology. American Association of Petroleum Geologists, Studies in Geology, 4. American Association of Petroleum Geologists, Tulsa. 37-52.

Wantland, K.F., and Pusey, W.C., 1971. A guidebook for the field trip to the southern shelf of British Honduras 21st Annual Meeting of the Gulf Coast Association of Geological Societies and Gulf Coast Section of SEPM. New Orleans Geological Society, New Orleans.

Wantland, K.F., and Pusey, W.C., 1975. Belize Shelf-carbonate sediments, Clastic Sediments and Ecology American Association of Petroleum Geologists Studies in Geology No. 2. American Association of Petroleum Geologists, Tulsa.

Weyl, R., 1980. Geology of Central America. Gebrueder Borntraeger, Berlin.

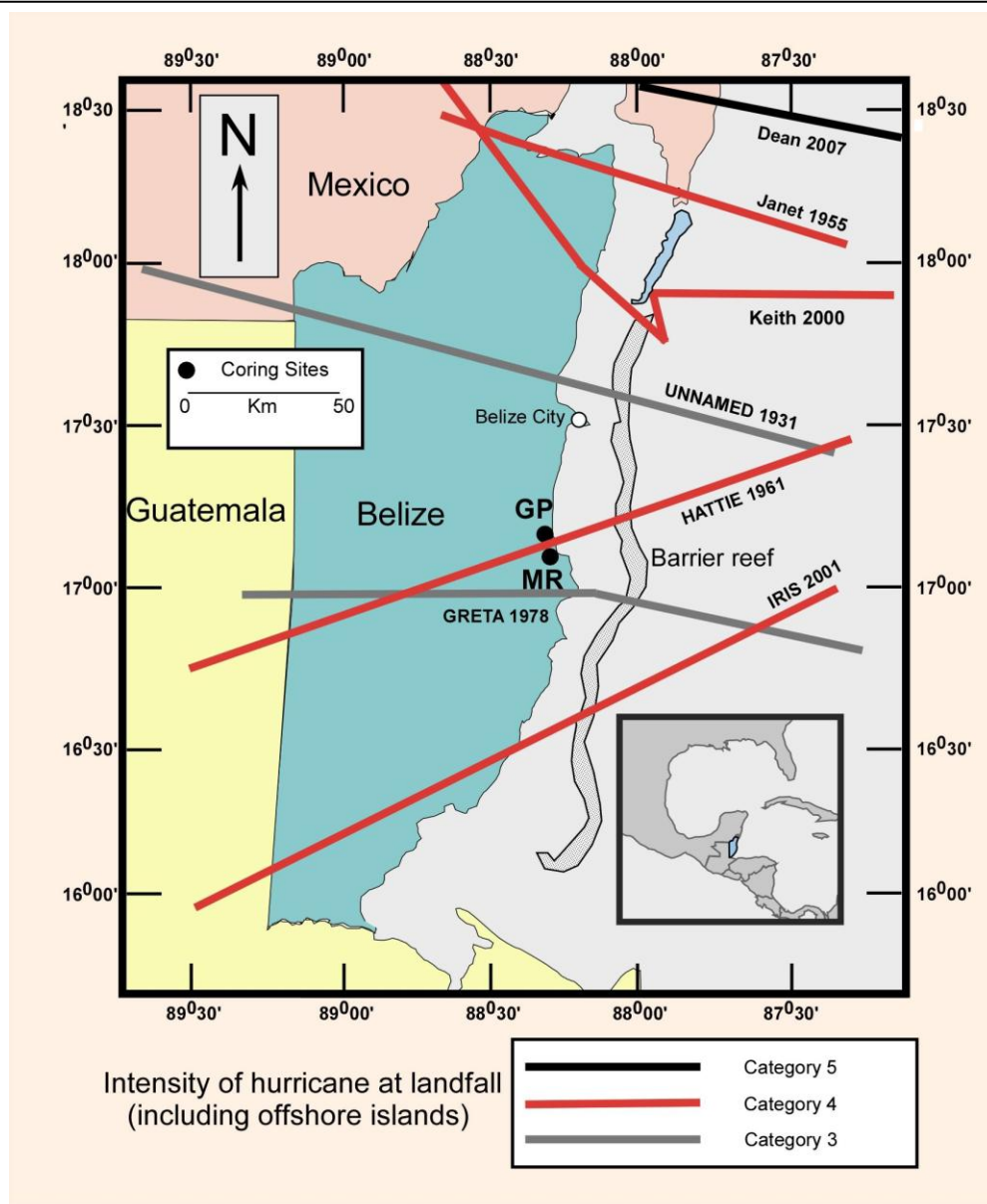
CHAPTER 6 GALES POINT-MULLINS RIVER, BELIZE*

6.1 Introduction

Hurricanes are capable of exerting tremendous societal stress. In the North Atlantic Basin, which includes the Gulf of Mexico and Caribbean Sea, hurricanes have killed 300,000 to 500,000 people over the past 500 years (Rappaport and Fernandez-Partagas, 1997). Average annual costs in the United States alone are in the billions of dollars (Pielke and Pielke, 1997). The extreme devastation inflicted on the United States during the 2004 and 2005 seasons demonstrates that hurricane-generated damages can be economically important on a national scale. The same is true for the coast of Belize, which has been subject to devastating hurricane strikes through recorded history. This includes six major hurricanes of category 3 or higher at landfall within the last 70 years. These are the unnamed hurricane of 1931, Hurricanes Janet (1955) and Keith (2000), which passed to the north of Belize City, Hattie (1961), and Greta (1978), which made landfall at Mullins River and just north of Dangriga, respectively, and Iris (2001), (**Figure 6:1**). All of these hurricanes devastated coastal towns, except for Iris (2001), which made landfall in a relatively unpopulated area near Monkey River and devastated the tropical forest. The immense human and material costs to the Belizean people are well documented.

Hurricanes were already mentioned in Maya hieroglyphics (Rappaport and Fernandez-Partagas, 1997). But it was not until 1495, when a hurricane destroyed the town of Isabella founded by Columbus on the island of Hispanola, that the earliest dated Caribbean hurricane was recorded (Rappaport and Fernandez-Partagas, 1997). However, despite ongoing improvements

*Printed by permission of Quaternary International.



6.1 Map of Belize showing coring sites and tracks of major hurricanes (category 3 or higher at landfall) since 1931

and corrections, the early historical records are still far from complete, with early storms mainly recorded from populated areas and when encountered at sea, with many records subsequently lost (Chenoweth, 2006, 2007; Garcia-Herrera et al., 2007; Mock, 2004). A fairly comprehensive list of landfalling hurricanes has been compiled since 1871 (Neumann et al., 1999), but complete and reliable records for the North Atlantic began only with aircraft reconnaissance in the 1940s. A much longer storm record can be obtained from the sedimentary record, specifically from hurricane-deposited sand layers in coastal lakes, marshes and swamps. The underlying assumption is that major or “intense” hurricanes (category 3 or greater) generate large storm surges, which crest barrier dunes and deposit sand fans landward. These sand layers become interbedded with the normally deposited coastal vegetation, which permits the establishment of multi-millennial hurricane strike records. The long-term hurricane record has been investigated in recent years by historical and geological methods as a discipline labeled paleotempestology. To date such studies have been conducted largely along the Gulf and Atlantic Coasts of the United States in an effort to understand cycles of hurricane activity and establish risk parameters for susceptible areas (Liu and Fearn, 1993; Collins et al., 1999; Liu and Fearn, 2000; Donnelly, et al., 2001a, 2001b, 2004; Scott et al., 2003). In contrast, only three published studies exist, to date, from the more often struck Caribbean (Bertran et al., 2004; Donnelly, 2005; Donnelly and Woodruff, 2007).

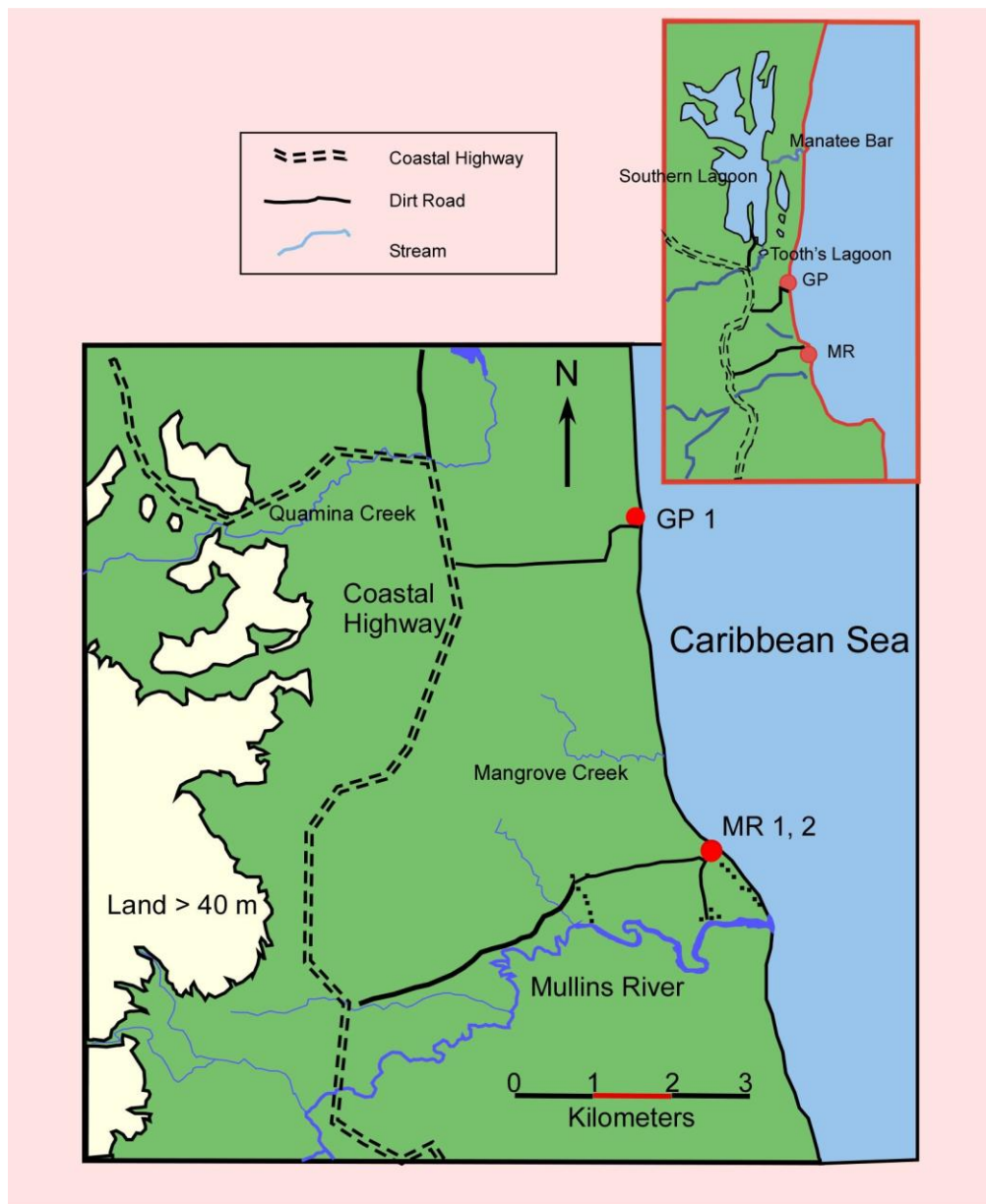
The main objective of this study is to extend the paleotempestology record to the relatively unstudied Western Caribbean region of Belize, by determining the frequency of hurricane strikes over the past 5000 years. This record can then be used to evaluate the relationship between strike frequencies in the Caribbean and other parts of the North Atlantic Basin, and to estimate the level of hurricane-generated stress upon the ancient Maya civilization.

6.2 Regional Setting

6.2.1 Geological

Both the historical frequency of hurricane strikes and the relatively stable coastal geomorphology promote the coast of Belize as a paleotempestology study site. With the offshore barrier reef acting as a buffer, the low energy wave regime inside the reef system results in highly reflective beaches, which are geomorphologically the most stable, with relatively low levels of dune destruction (Short and Hesp, 1982; Wright and Short, 1984), thereby reducing the temporal variability of site sensitivity.

The northern half of Belize is part of the low-lying carbonate Yucatan platform, while the south is dominated by the Maya Mountains, a faulted block composed of Paleozoic basement rocks and granitic intrusions, capped by Cretaceous limestone (Donnelly et al., 1990). The division between these two morphotectonic provinces occurs at the latitude of Belize City. The study sites are located slightly to the south of this division on a coastal plain formed of terrigenous Quaternary sediments, in an area of minimal topographic relief characterized by marshes, swamps, and scrubby wetlands. Drainage is minimal and low lying areas are waterlogged throughout the year; soils are typically peats and marls. The first significant topographical relief is >6 km west of the Mullins River site and ~ 4 km west of the Gales Point site (Figure 2). The Barrier reef lies ~20 km offshore, separated from the coast by a shallow shelf lagoon, which is characterized by sediments rich in quartz sand, mollusc and *Halimeda* marl, carbonate *Halimeda* sand, and *Thalassia* beds (James and Ginsburg, 1979). The Mullins River (MR) and Gales Point (GP) localities are within sight of each other along a nearly north-south running beach, which trends east near Mullins River (**Figure 6:2**).



6.2 Site map, showing coring sites (dots), buildings (squares), watercourses (solid gray lines), Coastal Highway (dashed double lines), dirt roads (solid black lines) and land over 40 m (hatched area).

6.2.2 Gales Point

The area surrounding Gales Point is particularly flat and low. An elevated road winds through >2 km of swamps and marshes with no clearly defined waterways. The nearest mapped waterway is Quamina Creek, located ~2 km from Gales Point. Quamina Creek is a small sluggish stream that emerges from the hills 4 km to the west, and drains north into the sea via Tooth's Lagoon, Southern Lagoon, and the Manatee Bar. All other drainage appears to be by sheet flow. The transect for this study is normal to the shore, with cores obtained at 10 m intervals from 60 m to 110 m from the shoreline. The elevation of the profile rises progressively inland and away from the sea, reaching a maximum of ~1.5 m on the crest of the foredune at a distance of 35 m. All surface and underlying sediments up to the foredune appear to be sand. Beyond 35 m, the elevation decreases, soil appears at about 50 m from the shoreline and the vegetation becomes progressively thicker. Beyond 95 m a hardwood swamp predominates at roughly sea level, with standing water and distinct swamp vegetation, characterized by palms and hardwoods.

6.2.3 Mullins River

The Mullins River site (MR) is on slightly higher land approximately 4.5 km to the south and 1 km north of the mouth of Mullins River, in an area of swamp, marsh, and forest. The transects' seaward edges begin in a small marsh that progressively changes inland first to tropical forest and then to thick palmetto swamp (**Figure 6:3**). Except for the marsh, which is in a shallow depression, the surface topography is generally flat at an elevation of less than 1 m up to the palmetto marsh at ~75 m. At that point the land dips abruptly to near sea level. A small dirt track runs along the shore to the nearly abandoned seaside village of Mullins River, which was destroyed during hurricane Hattie (1961). A new village was established farther inland.

6.3 Methods

For this investigation a total of 21 cores were obtained in two parallel transects at Mullins River, which marks the point of eyewall impact for Hurricane Hattie (1961). A single transect was taken at Gales Point, 4.5 km to the north. Coring was principally by Vibracorer and Russian Peat Borer, with a few initial cores obtained by means of 4.2 cm diameter galvanized steel pipes that were driven into the ground manually. Cores were obtained in parallel transects perpendicular to the coast and spaced at about 10 m, except where obstructed by vegetation. At Gales Point, cores were taken from 60 to 110 m inland. At Mullins River, two transects were cored 75 m apart starting at 15 m and 20 m from the shoreline and extending to 85 and 120 m inland. Core length is variable with most cores between 0.8 m to 1.5 m, though two cores reach 3 m. Significant sediment compaction occurred only in the manually driven steel pipes, which were adjusted for compaction or omitted from this study.

In the laboratory, the cores were split lengthwise and the sediments examined visually and optically for grain size, color, texture, composition, and lithological changes at 1 cm intervals. The sediments were classified according to the percentage of coarse, medium, and fine sand, silt, clay, and organic matter. Samples from each sand or sandy clay layer were washed through a 63-micron sieve and the dried residues examined under the microscope for marine microfossils (e.g. foraminifera, diatoms, sponge spicules, ostracodes, bivalve, and gastropod shells) as evidence of hurricane transport. Lithologs were based on these data for each core. LOI analysis was performed on each core at 4 to 5 cm intervals, with closer spacing across lithological changes in order to measure the organic content. Samples were dried overnight at 50°C, then weighed, heated in a convection oven at 600°C for three hours, then reweighed to determine the amount of organic carbon ignited (Dean, 1974).



6.3 Photo of site of Mullins River Line 2, looking from the Caribbean Sea inland, showing the transition from marsh to tropical hardwood forest. The grass in the marsh is approximately waist high. The palmetto swamp farther inland is not visible.

6:1 Gales Point chronology

Location	Depth (cm)	Material dated	^{14}C yr BP	Cal B P (2σ)	Probability (% area under distribution)
GP 13	107	grass	2130 ± 35	1998–2159	0.85
				2170–2177	0.01
				2246–2301	0.14
GP 20	74	leaf	325 ± 25	307–343	0.21
				346–464	0.79
GP 15	76	wood	2200 ± 30	2141–2324	1.00
GP 15	188	wood	3990 ± 45	4296–4331	0.04
				4348–4574	0.96
				4773–4777	0.002
GP 15	273	leaf	4700 ± 30	5321–5420	0.60
				5438–5481	0.23
				5531–5578	0.18

.Radiocarbon age control was obtained from five samples (peat layers or larger organic fragments) adjacent to sand layers identified as hurricane deposits, with the analyses performed at Woods Hole Oceanographic Institution (**Table 6:1**). Calibration of ^{14}C yr BP to cal yr BP were performed on the CALIB5.0.2 program from the Queens University Belfast's website (<http://calib.qub.ac.uk/calib/>) based on Stuiver and Reimer (1993). References for calibration datasets are from Reimer et al. (2004).

6.4 Results

6.4.1 Hurricane Events

Interbedded sand/clay layers were identified as hurricane-generated on the basis of lithologic, sedimentologic, microscopic and loss-on-ignition analyses. Major events are identified by the thickness of sand layers, presence of pebbles, marine shells, and microfossils. Events of lesser magnitude are recognized by relatively thin clastic layers and finer grained sand or silt embedded in peat. However, in some intervals the recognition of individual storm deposits is more problematic due to the absence of interbedded peat layers, possibly due to erosion by subsequent storm events, resulting in the amalgamation of events. Such amalgamation is identified by the abrupt truncation of one fining upward sequence and by the superposition of a younger sequence, commonly accompanied by visually obvious changes in structure, grain size, and color/composition. Similar amalgamation of hurricane events has been observed in the Gulf of Mexico (Keen et al., 2004).

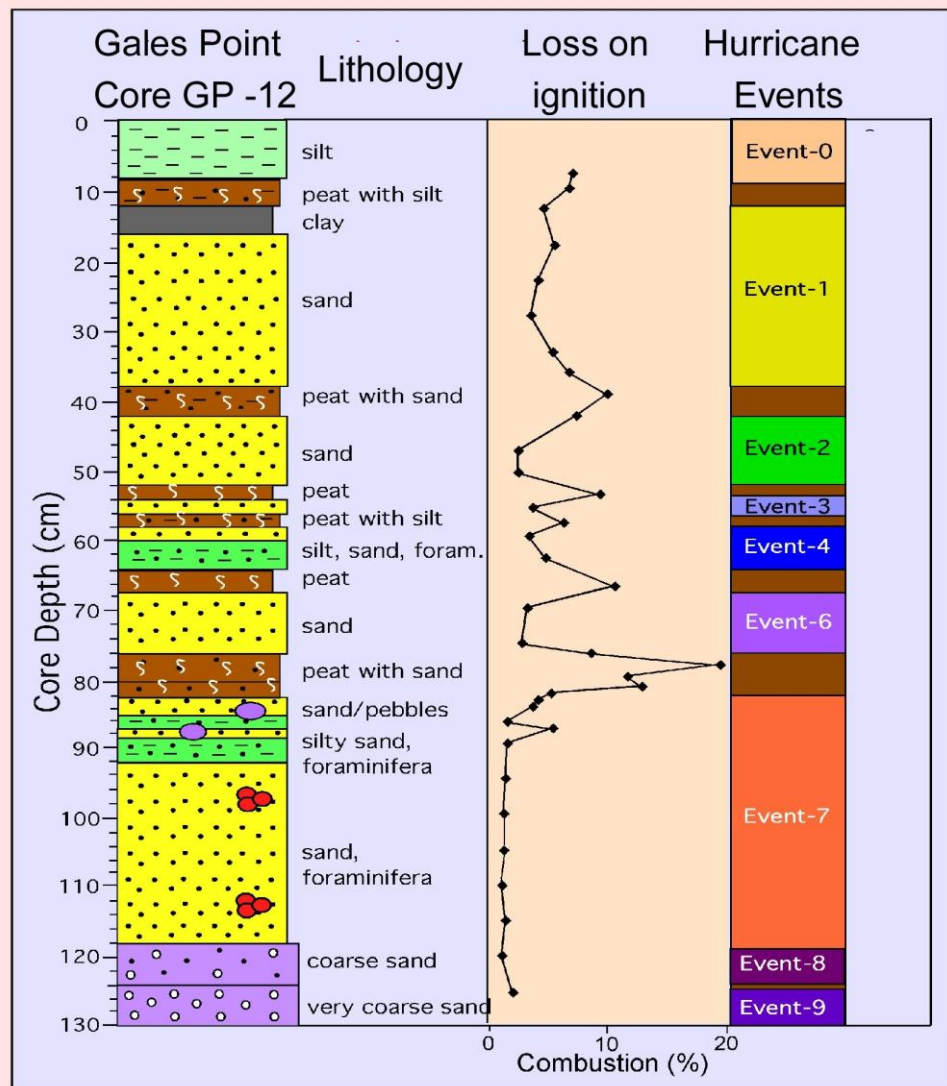
Correlation of hurricane events from core to core within and between transects was achieved by visual comparison in addition to lithological and organic (peat) contents determined from grain size and loss-on-ignition analyses. Not all transects show the same sequence of hurricane storm deposits. This is probably due to the variation in distance from the eyewall

center, local topography, and erosion patterns, and the peculiarities of the track and nature of individual storms. Here we detail cores from Gales Point and Mullins River, which represent a composite history of hurricane events for the past 5000 years.

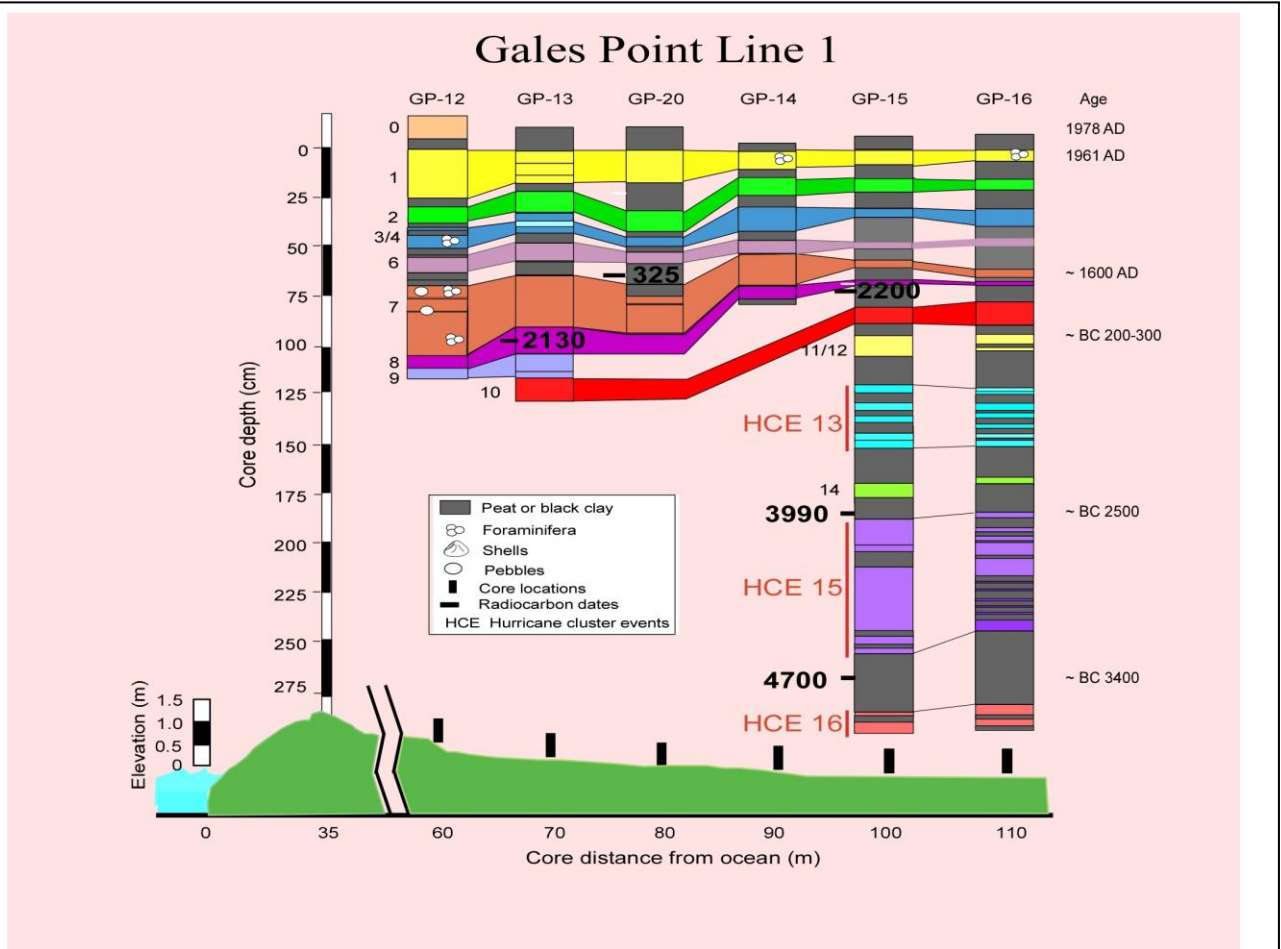
6.4.1.1 Gales Point Line 1

The most seaward core (GP-12) of Gales Point Line 1 is 60 m from the ocean. GP-12 represents a typical core litholog in that loss-on-ignition data indicate a generally close correlation between low combustion ratio (e.g. absence of peat) and intervals of marine transported materials (e.g. sand, silt, **Figure 6:4**). For most of the core, the alternating peat and sand layers clearly mark depositional intervals of normal coastal vegetation, alternating with storm transported marine material. In these intervals hurricane deposits are easily identified and correlated landward. At the bottom of the core, a sand layer (<5% organic content) shows evidence of three consecutive fining-upward sequences, each truncating the one below. This feature is interpreted as the amalgamation of three distinct hurricane events. Eight and possibly nine hurricane events can be identified in core GP-12 (**Figure 6:4**). The numbering system is not sequential in this core because it is based on the composite number of storm events identified in the three transects. Some of the events are missing in GP-12, as well as in the other cores of this transect, possibly due to erosion by subsequent hurricanes, or the limited landward extent of some hurricane deposits.

The GP-12 core litholog can be correlated with the five landward cores, which follow a gradual slope of about 2⁰ to a hardwood swamp where the last two cores (GP-15, GP-16) were drilled at 100 and 110 m from the ocean (**Figure 6:5**). The thickness of storm event layers and the grain size generally decrease with distance from the shoreline. Five radiocarbon dates derived from this transect provide age control for hurricane events.



6.4 Litholog and loss on ignition data for Core GP-12. Note that high combustion rates correspond to peat layers. The bottom sand interval is identified as three separate events on the basis of distinct structure, color and grain size.



At the top of core GP-12 is a silt layer (Event 0), which is not recognizable landward, but the underlying peat layer is present in all cores (**Figure 6:5**). Event 1 is marked by a sand layer with foraminifera, which can be recognized in all of the six transect cores. The thickness of the sand layer decreases from 22 cm in GP-12 to a few cm in GP-16 and grain size decreases. Similarly, sand layers and grain size decreases are observed for all other events (Events, 2, 4, 6, 7, 8 and 9) with distance from shore. Storm Event 3 may be present in a 2 cm thick sand layer (54–56 cm) sandwiched between two peat layers. However, this sand layer could not be differentiated consistently landward from Event 4, a 6 cm thick sand and silt with foraminifera. For this reason Events 3/4 are left undifferentiated. Event 6 (68–76 cm core depth) marks a major hurricane. A radiocarbon age of 325 ± 25 ^{14}C yr BP (2σ dates from AD 1486-1643) was obtained from the 6 cm peat layer below Event 6 in GP-20 (**Figure 6:5**). Event 7 is represented by a thick sand layer with pebbles and foraminifera (82–130 cm), which thin beyond 90 m from shore (**Figure 6:5**). Event 8 is marked by a coarse sand layer below Event 7, but is separated by a peat layer between 90-110 m inland. The absence of the peat shoreward suggests erosion. A radiometric age of 2130 ± 35 ^{14}C yr BP was obtained for Event 8 from a long grass stem in GP-13 (98-102 cm depth) that was presumably buried by the event. The peat underlying Event 8 in GP-15 yielded an age of 2200 ± 30 ^{14}C yr BP. Event 9 is marked by a coarse, pebbly sand layer (GP-12, GP-13), but core recovery failed between 80–90 m landward. Event 10 is tentatively identified by a silt layer recovered in cores GP-13, 15, and 16.

The 3 m long cores (GP-15, GP-16) recovered from the swamp depression consist mainly of peat with interlayers of silt marking storm events. In these cores, Events 11 and 12 are marked by two silt layers separated by peat in core GP-16, but not distinctly so in GP-15 (**Figure 6:5**). A cluster of five to six closely spaced, thin, alternating silt, clay, and peat layers mark a hurricane

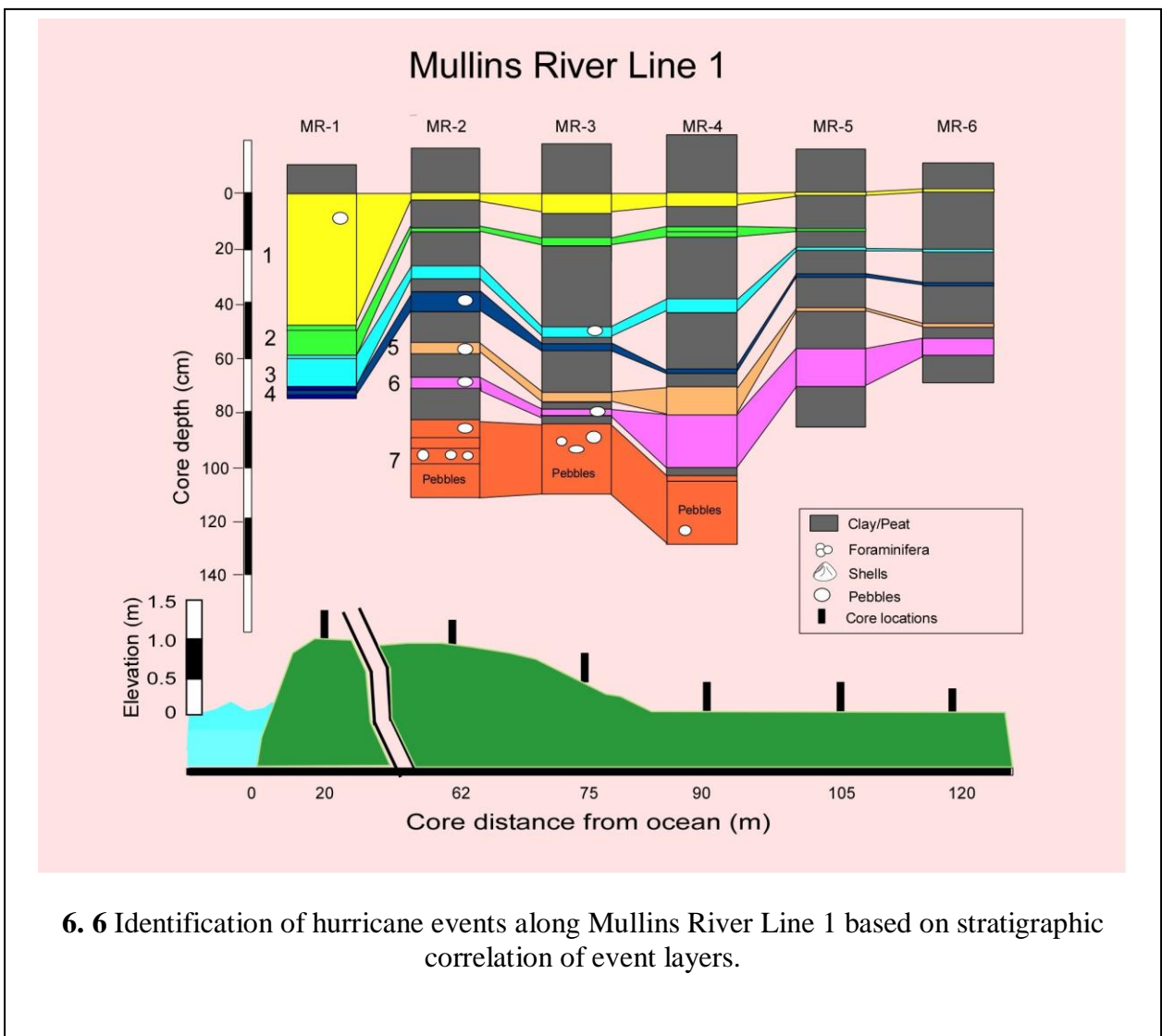
cluster event, HCE 13. Event 14 is a single event with a radiocarbon age of 3990 ± 45 ^{14}C yr BP from the underlying peat. Event HCE 15 is another cluster of hurricane events with at least 11 closely spaced clay and silt layers separated by peat or clayey peat in GP-16. Not all events of this cluster can be recognized in GP-15 due to mixing of clay and peat, possibly as a result of coring disturbance. Cluster Event HCE 16 is at the base of the core. The peat layer between cluster events HCE 15 and HCE 16 yielded a radiocarbon age of 4700 ± 30 ^{14}C yr BP (**Figure 6:5**).

6.4.1.2 Mullins River Line 1

Mullins River Line 1 reveals predominantly coarse- and finer-grained sand layers nearshore with a peat layer on top. Landward of 62 m, thick clay or peat layers alternate with thin silt or sand layers, representing storm deposits (**Figure 6:6**). In the most distant cores (105 m, 120 m), drilled in a palmetto swamp, the storm deposits are generally thinner. Event 1 is marked by a thick sand unit with pebbles nearshore (core MR-1), but rapidly thins landward, similar to Events 2-4. These are tentatively identified as the same numbered events as at Gales Point. From 62 m to 120 m inland Events 1 to 6 are recognized by relatively thin sand layers, frequently with pebbles up to 75 m inland. Event 6 shows a thicker sand layer landward of 90 m, which may be due to the local topographic depression, particularly in core MR-4. As at Gales Point, Event 7 represents the highest energy hurricane deposit characterized by thick orange-brown sand layers with pebbles and clasts ripped from the underlying clay. Large pebbles were transported at least 90 m inland. The cores in the palmetto swamp did not reach this deposit.

6.4.1.3 Mullins River Line 2

Mullins River Line 2 is 75 m south of Line 1 and spans from 15 m to 85 inland, ending in the palmetto swamp that begins at about 70 m. This transect reveals a very different



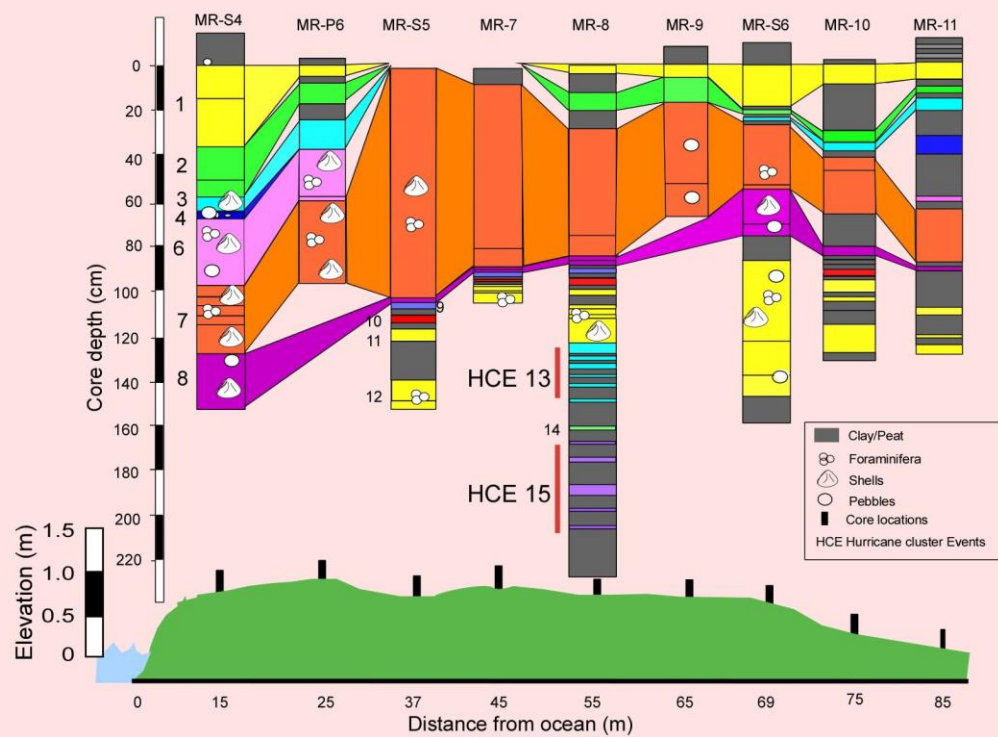
6. 6 Identification of hurricane events along Mullins River Line 1 based on stratigraphic correlation of event layers.

subsurface pattern from the nearby Line 1 or Gales Point (**Figure 6:7**). Hurricane Event 1 shows significant spatial variability as indicated by the difference in thickness between 15-25 m from shore, absence between 37–45 m, thin layers between 55-65 m, and thick deposits in the palmetto swamp at 69 m. This variability appears to be the result of erosion and non-linear distribution of sediments by the storm. Between 37–45 m inland a significant amount of surface sediments was scoured, exposing Event 7 deposits. A local survivor noted that Hurricane Hattie “scooped out” the surface sediments at this locality. Events 2 to 4 and 6 to 8 can be recognized in core MR-S4 and Events 2, 3, 6 and 7 in core MR-P6. From 55 and 69 m inland, Event 2, and Events 3-4 are present, respectively. Event 6 is marked by a 30 cm thick sand, pebble and shell layer with foraminifera (**Figure 6:7**). Event 7 is the most remarkable storm deposit encountered in all transects, but at Mullins River Line 2 this event is represented by an unusually thick coarse sand, shell and pebble layer with foraminifera that can be traced into the palmetto swamp (**Figure 6:7**). Event 8 is recognized by a sand layer. Events 9 to 10 are tentatively identified by thin sand and silt layers separated by clay or peat. The sand layers of Events 11-12 are rich in shells, foraminifera, and occasional pebbles, similar to Gales Point (**Figure 6:5**). Cluster event CE 13 and CE 15 can be recognized, as well as Event 14.

6.4.2 Geomorphic Stability

Sand layers identified as hurricane deposits can be traced inland, where with increasing distance from the shore the thickness of the sand layers and the grain size markedly decreases from coarse sand to finer sand and silt for each hurricane event (**Figures 6:5-7**). Despite a core spacing of only 10 m some variability exists in the thickness of individual sand /silt layers along each transect. This may be due to local topographic highs and lows, erosion, differential sediment dumping, and differential compaction due to sediment burial, particularly in peat

Mullins River Line 2



6.7 Identification of hurricane events along Mullins River Line 2 based on stratigraphic correlation of event layers.

layers. The composition of sediments indicates that very little geomorphological change (e.g. lateral movement of the shoreline, creation/reduction of beach ridges and tidal inlets, etc) occurred over the period under consideration.

For example, at the greatest distance from the shoreline along Gales Pont Line 1, cores GP-15 and GP-16 consist of swamp vegetation (peat) throughout, whereas shoreward cores GP-12, GP-13, GP-20, and GP-14 consistently indicate near-shore environments. Similar observations can be made in the other transects. This environmental stability probably results from the presence of the barrier reef system. During normal conditions, such a barrier reef results in very low-energy inner-reef environments, while during storms the reef's vertical seaward face and massive structure absorbs large amounts of wave energy, as well as causing earlier wave translation and reducing the fetch of waves over the inner channel, all of which act to reduce the destructive force of storms on the mainland (Hopley, 1984). These processes tend to produce geomorphologically stable reflective beach environments, because the force of both the normal and extreme weather conditions are reduced. Although erosion does occur, the long-term records of the Belize coast are not subject to the same level of geomorphological changes as those from less protected beach environments along the US Gulf and Atlantic coasts.

6.5 Discussion

6.5.1 Hurricanes and the Historical Record

All three transects in the Gales Point/Mullins River area show similar hurricane patterns. Relatively evenly-spaced events are preceded by the much larger Event 7, which is characterized by thicker sedimentary deposits with larger grain sizes, pebbles, and often abundant marine fauna (**Figures 6:5-7**). The two longest cores, (GP-15 and GP-16), show evidence of cyclic periods of increased hurricane activity. Sediment erosion prevents determination of average

sedimentation rates and hence the extrapolation of recent hurricane event dates. However, the dates for some of the hurricanes can be inferred from ^{14}C dates and the historical hurricane records. Because radiocarbon dates were obtained only from Gales Point Line 1, the correlation with Mullins River is based on the stratigraphic sequence of events and the comparison of sedimentary characteristics (lithology, grain size, marine fossils). Not all events are recorded in all transects, and the number of events above Event 7 varies from 5-6 among the three transects. Event 0, found only at the top of the most seaward core of the Gales Point transect is tentatively identified as Hurricane Greta in 1978, which made landfall about 15 km to the south near Dangriga. The sand layer labeled Event 1 is probably the result of Hurricane Hattie (1961), as it is the topmost event layer at the site of eyewall impact for this category 4 storm. Event 2 can be stratigraphically correlated with the unnamed hurricane of 1931, though no absolute dating is available for the underlying interval.

Correlations between events lower in the column and historically recorded storms are problematic due to the vagueness of the historical record, which not only fails to note point of landfall, but also fails to register maximum wind speed, and, in general, merely records the strength of storms at the major population center, Belize City. Hence discrepancies between the sedimentary and historical records are likely, as storms that made landfall south of Belize City could have left a sedimentary signature in the study sites, but may not have been recorded historically. Alternatively, some of the hurricanes historically recorded at Belize City may have been too weak or too distant to have left a clear sedimentary record farther south at the study sites.

If the widely recognized Event 3 corresponds to a historically recorded hurricane, it is most likely the unnamed hurricane of 1893, which caused severe damage in Belize City and in

the southern districts (Metzgen and Cain, 1925). Event 4 is weakly recorded or mixed with Event 3 throughout Gales Point Line 1, recognizable as a thin layer throughout Mullins River Line 1, and intermittently recorded in Mullins River Line 2. This possibly represents the storm of August 31, 1864, which passed directly over Belize City, causing a storm surge of 5 feet (Tannehill, 1938).

Event 5 is identifiable only in Mullins River Line 1, where it is present in all cores that reach sufficient depth. Stratigraphically this storm can be correlated to the hurricane of August 19, 1827, which “drove all ships on shore at Belize” (Smith, 1842, quoted in Stoddart, 1963). Since this storm predates NOAA records, the location of landfall and maximum wind speed are unknown, prohibiting a more conclusive identification.

Event 6 is present across all cores in Mullins River Line 1 that are deep enough, and in all but the most landward core of Gales Point Line 1. It is also intermittently present in Mullins River Line 2. This event was relatively forceful, as indicated by pebbles found at 62 and 75 meters inland in Mullins River Line 1, and pebbles, shells, and foraminifera at 15 and 25 m in Mullins Rivers Line 2. Based on Stoddart’s (1963) list, the first recorded hurricane, which occurred on September 2, 1787, was the most powerful of the early storms, producing a 7-8 foot storm surge, which “desolated” Belize City, killing many people, destroying all shipping, and all but one house. Since the point of landfall is unknown, it is difficult to calculate the expected sedimentary impact of this storm at the coring locations.

6.5.2 An Extreme Event

The most noticeable hurricane is Event 7. Although this event could not be dated directly, a sample from 10 cm above it has a radiocarbon date of 325 ± 25 ^{14}C yr BP, for which the 2σ date ranges correspond to calendar dates for the periods AD 1486-1604 and 1607–1643. In the

absence of other dating methods (e.g., average sedimentation rate), Event 7 can be tentatively dated to about AD 1500, assuming that the 10 cm sediment represents a significant, though undetermined, time span.

A date of 2130 ± 35 ^{14}C yr BP (2σ date ranges correspond to the periods cal BC 352–297, 228–221, and 210–49) was obtained for Event 8 sand deposits, which immediately underlie Event 7 (**Figure 6:5**). These two ^{14}C dates thus indicate a large gap in the sediment record spanning about 1750 years, (from ~ AD 1500 to ~ 250 BC) as a direct result of sediment erosion by Event 7. This suggests that Event 7 was catastrophic and removed significant amounts of surface sediments in the area of Gales Point and Mullins River. The extreme force of Event 7 is also indicated by the thickness of the deposited layers, the transport of large pebbles and shells, and the tearing of clasts from the underlying clay.

The magnitude of Event 7 is best viewed in relation to Hurricane Hattie (1961), (Event 1) whose point of eyewall impact at Mullins River (Stoddart, 1963) left a much less dramatic sedimentary profile (**Figures 6:5–7**). Nevertheless, Hurricane Hattie was one of the defining events in modern Belize history. It caused tremendous physical damage and is historically important both socially and economically in that the British government moved the colony's capital from its traditional coastal location in Belize City to the present inland site at Belmopan in order to avoid similar disasters in the future (Setzekorn, 1978).

The location of landfall for Event 7 is not known and will have to be determined by future coring. However, its thick sedimentary deposits in the Gales Point and Mullins River areas leave no doubt as to the tremendous force of this hurricane, which exceeds any other in the 5000 year history examined. Although in the coastal areas of the United States the thickness of overwash layers as a proxy for storm magnitude is dependent upon the stage of the tide at time of

landfall, this is not a factor in Belize with an average tidal range of ~0.3 m (Stoddart, 1962). Many factors, such as duration of landfall, angle of strike, coastal profile and geomorphology, and height and composition of beach barrier, can contribute to the sedimentary effect of a storm. Certainly, extent of the deposited sand layer cannot be uncritically used to determine absolute intensity. With several different proxies (grain size of transported material, thickness of deposit, amount of associated erosion, mixing of the underlying layer) over three transects spanning 4.5 km all indicating an extreme event, it seems highly likely that Event 7 was much stronger than all other storms in the record.

6.5.3 Clustered Hurricane Events

The sedimentary record extending to ~ 5000 ^{14}C yr BP was recovered in Gales Point cores GP-15 and GP-16 (**Figure 6:5**). These two cores reveal a clustering of hurricane events separated by relatively long periods of quiet peat deposition. Within each cluster the rapidly alternating peat and clay/silt/sand layers probably indicate periods of greatly increased hurricane activity. The same clustered events can be recognized in the deepest Mullins River core (MR-8, **Figure 6:7**).

In general, core GP-16, situated 10 meters farther into the swamp, presents a higher resolution record than GP-15, with a minimum of 6 events for HCE 13, 11 events for HCE 15 and 2 events for HCE 16. The improved resolution of core GP-16 is presumably due to the reduced amalgamation of the hurricane layers resulting from the increased buffering provided by the additional 10 meters of swamp vegetation.

6.5.4 Activity Regimes

A radiocarbon date obtained from 3 cm above the top of cluster HCE 15 in core GP-15 (**Figure 6:5**) provided a date of 3990 ± 45 ^{14}C yr BP, which calibrates to a number of calendar

dates between ~4300-4700 cal yr BP, with 96% of the area under the curve falling within the period 4348-4574. A second radiocarbon sample selected 15 cm below the bottom of HCE 15 provided a date of 4700 ± 30 ^{14}C yr BP, which calibrates to a number of calendar dates centered ~5300-5600 cal yr BP. These ^{14}C dates indicate that the cluster HCE 15 was deposited over a period of somewhat less than 1,000 years between ~4500-4000 ^{14}C yr BP (~5500-4500 cal yr BP). The interval covered by HCE 13 indicates a somewhat shorter time period. Lack of bracketing dates prevents precise dating of this interval, but a period of ~ 3200-2500 ^{14}C yr BP can be estimated. This indicates two separate periods of increased hurricane activity occurring between ~ 4500-2500 ^{14}C yr BP (~5500–2500 cal yr BP).

The most recent 500 years can probably also safely be regarded as an active period with 4-6 hurricanes occurring over the period. No activity regime can be determined for the preceding interval from ~500 -2200 ^{14}C yr BP, as the deposited material has been removed by erosion. The material below this level suggests a relatively Quiet period, as only 2 (possibly 3) events occur within the 46 cm interval between the sample dated to 2200 BP and the beginning of HCE 13, which, based on the trendline calculates to an interval of 592 ^{14}C yr. The calculated difference between the calibrated date ranges for the two depths is between 455-867 cal yr, indicating a longer return interval is longer than for the active periods, even using the minimum possible interval length. A summary diagram of the activity regimes is presented in **Figure 6:8**.

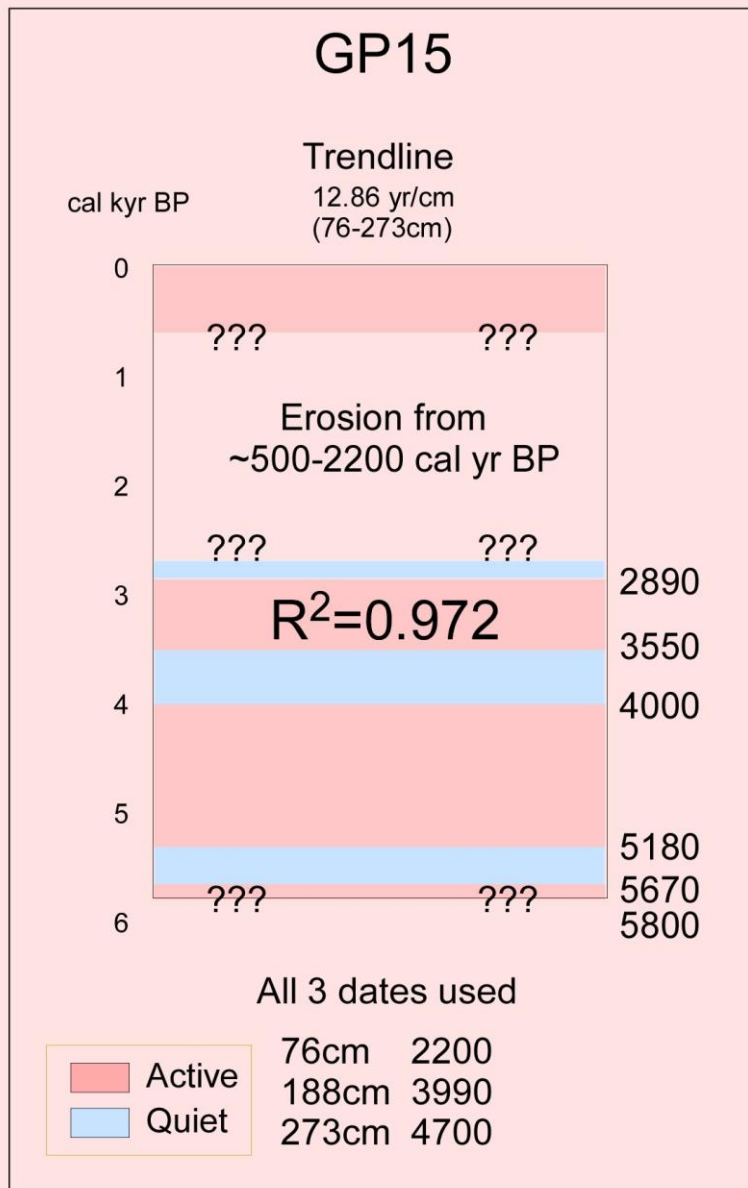
6.5.5 Sea Level Rise

Relative sea level rise is an important factor when considering paleotempestological data, particularly in an area such as Belize characterized by a shallow, low gradient continental shelf, where a rapid rise results in a large transgression of the paleoshoreline. Many sea level studies have been conducted in the Caribbean (e.g., Hendry, 1982; Lighty et al., 1982; Digerfeldt and

Enell, 1984; Digerfeldt and Hendry, 1987; Fairbanks, 1989) and several are based on data from Belize (Woodroffe, 1988; Macintyre et al., 1995, 2003; Toscano and Macintyre, 2003). These studies generally show a smooth curve, with a decreased rate of rise around 5,000-6,000 cal yr BP. In Belize, the rate of relative rise varies latitudinally, with the deeper southern shelf locations displaying rates up to 1 m over the last 1000 years (McKillop, 2002, 1995). In contrast, in the north studies show a rise of only 30 cm over the last 2100 years, with present levels reached ~1000 ^{14}C yr BP (Mazullo et al., 1992; Dunn and Mazullo, 1993). This difference probably results from greater subsidence in the southern areas due to increased water depth and thus a strengthened hydrostatic response and earlier flooding which resulted in thicker peat deposition, and, consequently, greater compaction and dewatering (see **Chapter 5**). Based on the northern curve established by Dunn and Mazullo (1993) (**Figure 6:9**), change in relative sea level should have been fairly insignificant for the last 5000 years, although between 3500–5000 ^{14}C yr BP the impact would depend on the coastal gradient. Indeed, Peltier's (1988) mathematical model predicts levels slightly higher than the present for Belize over the past 5000 years.

6.5.6 Tsunami

A related issue is the possibility of tsunami driven surges, which could mimic the sedimentary effects of a hurricane. Contradictory sedimentary differences between tsunami and hurricane deposits have been noted (Nanayama et al., 2000; Tuttle et al., 2004), making definitive differentiation between the two difficult (Donnelly, 2005). Belize lies just to the north of the junction of the Caribbean and North American Plates (Donnelly et al., 1990). The subduction of the North American Plate under the Caribbean Plate along the extreme southeast edge of the Caribbean results in the Antillean Island Arc, which includes several active volcanoes (Peter and Wertbrook, 1976; Paul, 1995) and recurrent seismic activity. A recent



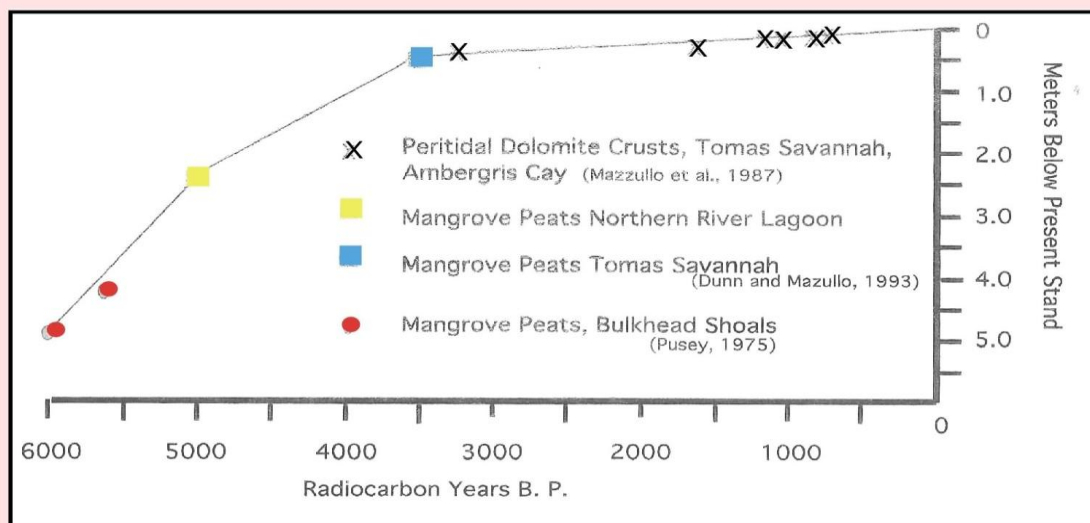
6.8 Inferred hurricane activity regimes for GP/MR area. Active periods are marked in pink, Quiet periods in blue. Dates on the left are cal kyr BP, dates on right are calculated cal yr BP dates for regime change points. ^{14}C dates for specific depths are interpolated by assuming constant sedimentation between the three measured samples listed at the bottom. These dates are then entered into the CALIB 5.0.2 program (using an error bar of 40 years), producing calibrated cal yr BP date range(s). A date in the middle of the highest probability date range(s) is selected.

work catalogues 127 Caribbean tsunami during the period 1498-1998 (O'Loughlin and Lander, 2003), resulting from a number of causes, including tectonically driven earthquakes, volcanic explosions, and subaerial and submarine slumping (Scheffers, et al., 2005).

However, near Belize, situated >3000 km northwest of the island arc, the plate junction occurs as a strike/slip fault, resulting in lateral movement between the plates. This reduces the possibility of locally generated tsunami primarily to those resulting from large-scale underwater slumping, the secondary effect of seaquakes. The possibility of teletsunami (tsunami generated >1000 km from the area of impact) is low, since those originating in the Antillean Island Arc are relatively small (Scheffers et al., 2005), and an investigation of Holocene tsunami deposits in the southern Caribbean excludes tsunami approaching from the open Atlantic as a probable cause (Scheffers et al., 2005). Therefore, the frequency of tsunami near Belize is low, with only three being recorded since 1498. All three were generated along the Honduran coast, with the 1856 event, apparently the strongest, affecting only the southernmost tip of Belize (O'Loughlin and Lander, 2003; McCann and Pennington, 1990). Thus, although the possibility exists that one or more of the suspected hurricane-generated layers actually result from tsunami, the probability is low.

6.5.7 Annual Hurricane Strike Probability

An estimate of the average annual hurricane strike probability can be made based on the ^{14}C dates. The ^{14}C date of 325 ± 25 ^{14}C yr BP obtained from between Events 6 and 7 in core GP-20 corresponds to calendar date ranges from AD 1486–1604 (78.6 % probability) and AD 1607–1643 (21.4% probability). Five and six hurricane events are recorded after that time at Gales Point and Mullins River, respectively. This indicates that the minimum average annual probability of recordable strikes is ~1–1.2 % (5 to 6 storms in ~500 years). However, to arrive at



6.9 Sea level curve for northern Belize modified from Dunn & Mazullo (1993).

an accurate risk assessment for the national coastline, the relationship between strikes occurring and strikes recorded must be determined. Cores obtained from the point of eyewall impact of Hurricane Greta (category 3, 1978) displayed only a weak, spatially confined sedimentary signal, while cores from the point of landfall of Hurricane Iris (category 4, 2001) failed to display clear sedimentary evidence of the storm. This indicates that perhaps the threshold for reliable recordation might be as high as a strong category 4.

Another important parameter is the radius within which storms are recorded. Examination of cores from a location ~15 km to the south (not shown) shows very little correspondence with the events recorded in the Mullins River/Gales Point area. Because the coastline of Belize extends ~250 km north-south, a recordation radius of 15 km (recordation diameter 30 km) results in a national exposure eight times larger than that of each individual location, assuming uniform geographic strike frequency. Based on the historical data that hurricane strike frequency increases south to north for Belize (Alaka, 1976), a probability calculation derived from the central area should be reasonably applicable for the entire coast.

These observations suggest a national exposure of roughly 8-10 major storms (category 3 or larger) every century, or roughly one per decade. This is only slightly higher than the 20th century record. Stoddart (1963) lists 13 hurricanes from 1900 through Hattie in 1961, five of which caused serious economic damage. To this list must be added the minor Hurricanes Francelia (1969) and Fifi (1974), along with Greta in 1978, for a total of 16. The NOAA record, though differing substantially from Stoddart's before 1942, records 13 hurricanes for the 1900s, five of them major hurricanes. Not included in either list for the 1900s are direct hits by two major hurricanes (Keith, 2000 and Iris, 2001), as well as near misses by two category 5 storms, the extremely large Mitch (1998) and Dean (2007).

Complicating this calculation are the uncertainties regarding the sensitivity of the recording sites. Other studies have identified hurricanes over larger distances, based on the presence of marine microfossils (Collins et al., 1999; Scott et al., 2003). The reduced recordation diameter indicated here might be due to specific characteristics of either the sites of impact for Greta and Iris or the storms themselves. Possibilities include a low percentage of clastic material in the transported material (local informants complained of the odor of the material deposited by Iris, indicating a high organic content, rather than sand) and the unsuitability of micropaleontological analysis as a diagnostic tool as calcareous materials dissolve rapidly in the acidic swamp environments (Graham, 1994).

6.5.8 Cyclicity in Hurricane Frequency

Liu and Fearn (2000) hypothesize a millennial scale oscillation in the cycle of North Atlantic hurricane activity. Based on results from a variety of sites on the US Gulf Coast, they identify a period of hyperactivity there from around ~3400-1000 ^{14}C yr BP, with periods of greatly reduced activity before and after. They have proposed shifts in the position of the Bermuda High as the causative agent of this oscillation, as over the historical period the strength/position of the Bermuda High has been shown to exert important control over location of hurricane landfall (Elsner et al., 2000). A high-resolution record based on varved sediments from the Cariaco Basin in the southern Caribbean has demonstrated significant low frequency meridional movement in the Intertropical Convergence Zone (ITCZ) over the past 14,000 years (Haug et al., 2001). If strong north/south migration of the ITCZ is accompanied by similar, if not precisely simultaneous, movements of the Bermuda High and the hurricane zone, periods of increased hurricane activity in the Caribbean should exhibit latitudinal clustering.

An investigation from St. Martin in the French West Indies (Bertran et al., 2004) suggests

increased hurricane activity there for the period 4900–~2600 cal yr BP, closely matching the record from this study (two periods of increased activity from ~5500–2500 cal yr BP). Both sites are at the same latitude (~18° N), thereby supporting the hypothesis of latitudinally coherent periods of increased hurricane activity. Furthermore, this period correlates to a period of generally southern migration of the ITCZ, while the period of hyperactivity observed by Liu and Fearn (2000) on the Gulf Coast roughly correlates to a northern movement of the ITCZ (Haug et al., 2001). This evidence, therefore, supports the idea of a climatically controlled zone of hurricane landfall slowly migrating north and south across the Caribbean. Because the position of the Bermuda High also has significant climatic implications, especially precipitation levels, the influence of such a migration on cultural development is potentially of regional importance.

However, Donnelly and Woodruff (2007) show a different pattern of hurricane activity from sediment cores in Puerto Rico. They observed increased activity from ~5400–3600, decreased activity for the period ~3600–2500 cal yr BP, increased activity again 2500–1000 cal yr BP, and 250 cal yr BP to the present. Because the most recent active period corresponds to relatively cool sea surface temperatures (SST), they conclude that warm SST are not necessary for increased hurricane activity. Coherent and interrelated atmospheric conditions, such as the El Niño/Southern Oscillation (ENSO) and the condition of the West African monsoon, they suggest, exert a more important influence over hurricane landfall than isolated conditions such as steering control and average SST. Based on data for the period 1950–2004, Bell and Chelliah (2006) make a similar argument for a coherent coupling of oceanic and atmospheric conditions as the driver of hurricane activity. Latitudinal shifts in the atmospheric circulation system could be the proximate cause of such a coherent system. Further studies covering a larger number of localities along with the use of new investigative methods, such as isotopic investigation of tree

ring and speleothem records (Frappier et al., 2007a, b; Miller et al., 2006) may help resolve this issue.

6.5.9 Hurricanes and the Ancient Maya

Several recent studies have linked cultural development of the ancient Maya with environmental conditions, in particular correlating demographic and cultural decline with periods of drought (Hodell et al., 1995; Curtis and Hodell, 1996; Gill, 2000; Hodell et al., 2001; Islebe and Sanchez, 2002; Rosenmeier et al., 2002; Haug et al., 2003), perhaps related to the 206 year solar activity cycle (Hodell et al., 2001), or changes in the intensity of the earth's geomagnetic field (Gallet and Genevey, 2007). It is possible that hurricanes also exerted an important environmental control. Certainly, the cultural, economic and agricultural destruction associated with major hurricane strikes occurring at the frequency calculated here suggests the possibility of continuing restraint on the ancient Maya civilization.

Hurricanes would have severely affected the agricultural base since the hurricane season corresponds to the most vulnerable period of the annual agricultural cycle when the major corn crop is either growing or drying in the fields. A major hurricane strike during this period would have had very significant nutritional consequences, as a large percentage of the year's grain would have been lost due to the rapid spoiling of the corn resulting from storms leveling the fields. Although some portion of the crop could potentially be salvaged if immediately collected and dried, the effectiveness of this seems rather limited, particularly given the probability of continuing precipitation and the vulnerability of thatch roofs to wind damage. Only mature corn can be dried in this manner and requires being spread out in the sun, or husked, shelled, and dried over a fire. If immature, the corn would be lost entirely. Just such a devastating effect was observed in Honduras after the passage of Hurricane Mitch (1998), which destroyed 58% and

35% of the corn and bean crops, respectively (Economic Commission for Latin America and the Caribbean, 1999; Global Information and Early Warning System, 1999). In addition, stored food crops were lost to floods, landslide, and damaged buildings (Morris et al., 2002). This threat to the national food security was severe enough to force the government to release strategic grain reserves (Mainville, 2003).

Even more important is the possible reduction of long-term agricultural resources. During periods of high population density that requires the utilization of hillsides and marginal land (McKillop, 2004), the extreme rainfall connected with hurricanes could have resulted in significant soil erosion and phosphorus burial, decreasing the area's long term carrying capacity. Although the exact nature of ancient Maya agricultural practices is under debate (Fedick, 1996), it probably shared some characteristics with present day sustainable land management (SLM) practices. These utilize a variety of non-mechanized soil conservation and agroecological methods, including agroforestry, to promote agricultural sustainability on small holdings. Holt-Gimenez (2002) shows that relative to "conventional" farms, these practices reduced the environmental damage to farmlands, such as the loss of topsoil and vegetation, landslides and erosion that were inflicted by Hurricane Mitch. However, he found that agroecological resistance "collapsed" under conditions of high stress related to extreme storm intensity. These findings combined with the widespread occurrence of landslides throughout Honduras and Nicaragua as a result of Hurricane Mitch suggest that major hurricanes could have negatively impacted ancient Maya agricultural potential on decadal to centennial timescales.

Some level of disruption of trade (particularly coastal) and overall economic stability seem implicit in large-scale hurricane strikes. Although these disruptions would have been both local and periodic, they could have resulted in chronic cultural stress. Our study suggests that

several of the prehistoric hurricanes left a sedimentary signature roughly equal to, or exceeding that left by Hurricane Hattie at landfall. The magnitude of prehistoric hurricanes, where the locations of landfalls and hence maximum sedimentary expressions are unknown, are likely underestimated in this study. The ability of large individual events to cause regional destruction was demonstrated by hurricane Katrina on the US Gulf Coast in 2005 and Hurricane Mitch in 1998, which resulted in an estimated 10,000 deaths, 3 million displaced or homeless people in Central America (Ecocentral, 1998; CRIES, 1999) and inflicted damage equal to 13.3% of Central America's GNP (Holt-Gimenez, 2002).

Of particular interest in this regard is the sheer magnitude of the extremely large prehistoric Event 7, which together with similar magnitude hurricanes could be expected to have caused devastating large-scale social disruptions. Unfortunately, sediment erosion by Event 7 removed the relevant interval that could have provided direct information concerning the relationship between hurricanes and the classic period (AD 300-900). During the subsequent collapse of the Maya civilization, lowlands in Mexico, Belize, Honduras, and coastal Guatemala were abandoned between AD 975 and 1000 (Coe, 1999).

The occurrence of multi-centennial periods of increased hurricane frequency, as suggested by clusters of events between ~ 4500–2500 ^{14}C yr BP, would have greatly increased the environmental stress, perhaps making coastal farming untenable. Future recovery of longer and more complete cores may reveal whether this clustering of events continued into the classic period, and if so, how these periods correlate with Maya cultural history.

6.6 Conclusions

1. Five to six major hurricanes were observed in the sedimentary record of the past 500 years along the central coast of Belize. This represents 1 to 1.2 catastrophic storms every 100

years in the study area. The “average” strike probability for the 250 km long coast of Belize is roughly one major storm per decade.

2. One giant hurricane, Event 7, struck the central coast of Belize sometime before AD 1500. Compared with Hurricane Hattie (category 4), Event 7 was significantly more powerful and capable of achieving catastrophic effects. Several other events appear to have been roughly equivalent to Hurricane Hattie.
3. A temporal clustering of hurricanes was observed in the study area. These periods of hyperactivity roughly match those determined for St. Martin, and precede a similar period for the US Gulf Coast. These records support a model of climatically controlled migration of the hurricane belt.

6.7 References

- Alaka, M.A., 1976. Climatology of Atlantic tropical storms and hurricanes. In Schwerdtfeger, W. (ed), *Climates of Central and South America. World Survey of Climatology (Volume 12)*. Elsevier, New York. 479-509.
- Bell, G. D., and Chelliah, M., 2006. Leading tropical modes associated with interannual and multidecadal fluctuations in North Atlantic hurricane activity. *Journal of Climate* 19, 590-612.
- Bertran, P., Bonnissent, D., Imbert, D., Lozouet, P., Serrand, N., and Stouvenot, C., 2004. *Paleoclimat des Petites Antilles depuis 4000 BP: l'enregistrement de la lagune de Grand-Case a Saint-Martin. Comptes Rendus Geoscience* 336, 1501-1510.
- Chenoweth, M., 2006. A reassessment of historical Atlantic basin tropical activity, 1700-1855. *Climatic Change* 76, 169-240.
- Chenoweth, M., 2007. Objective classification of historical tropical cyclone intensity. *Journal of Geophysical Research-Atmospheres*. 112(D5), D05101.
- Coe, M. D., 1999. *The Maya (Sixth Edition)*. Thames and Hudson, London.

Collins, E.S., Scott, D.B., and Gayes, P. T., 1999. Hurricane records on the South Carolina Coast: Can they be detected in the sediment record? *Quaternary International* 56, 15-26.

Coordinadora Regional de Investigaciones Económicas y Sociales (CRIES), 1999. Enfoque estrategico centroamericano sobre reconstrucción y transformación desde la sociedad civil organizada nacional y regionalmente. CRIES, Managua.

Curtis, J.H., and Hodell, D. A., 1996. Climate variability on the Yucatan peninsula (Mexico) during the past 3500 years, and the implications for Maya cultural evolution. *Quaternary Research* 46, 37-47.

Dean, W.G., 1974. Determination of carbonate and organic matter in calcareous sediments and sedimentary rocks by loss on ignition: Comparison with other methods. *Journal of Sedimentary Petrology* 44, 242-248.

Digerfeldt, G., and Enell, M., 1984. Paleoecological studies of the past development of the Negril and Black River morasses, Jamaica. *Petrol Corp Jamaica*, Kingston, Jamaica.

Digerfeldt, G., and Hendry, M. D., 1987. An 8000 year Holocene sea-level record from Jamaica: implications for interpretation of Caribbean reef and coastal history. *Coral Reefs* 5, 165-169.

Donnelly, J.P., 2005. Evidence of past intense tropical cyclones from backbarrier salt pond sediments: a case study from Isla de Culebrita, Puerto Rico, USA. *Journal of Coastal Research* 42, 201-210.

Donnelly, J.P. and Woodruff, J.D., 2007. Intense hurricane activity over the past 5,000 years controlled by El Nino and the West African monsoon. *Nature*, 447, 465-468.

Donnelly, J.P., Bryant, S., Butler, J., Dowling, J., Fan, L., Hausmann, N., Newby, P., Shuman, B., Stern, J., Westover, K., and Webb, T. III, 2001a. 700 year sedimentary record of intense hurricane landfalls in southern New England. *GSA Bulletin* 113, 714-727.

Donnelly, J.P., Roll, S., Wengren, M., Butler, J., Lederer, R., and Webb, T. III, 2001 b. Sedimentary evidence of intense hurricane strikes from New Jersey. *Geology* 29, 615-618.

Donnelly, J.P., Butler, J., Roll, S., Wengren, M., and Webb, T. III, 2004. A backbarrier overwash record of intense storms from Brigantine, New Jersey. *Marine Geology* 210, 107-121.

Donnelly, T.W., Horne, G. S., Finch, R.C., and Lopez-Ramos, E., 1990. Northern Central America; the Maya and Chortis blocks. 1990. In: Dengo, G., Case, J.E., (eds.) *The Geology of North America*, Vol. H, The Caribbean region. The Geologic Society of America, Boulder, Colorado. 37-76.

Dunn, R.K., and Mazullo, S. J., 1993. Holocene Paleocoastal reconstruction and its relationship to Marco Gonzales, Ambergris Caye, Belize. *Journal of Field Archaeology* 20, 121-131.

- Ecocentral, 1998. Hurricane Mitch kills 11,000, wrecks region's economy. In Noticen, 1998-11-12, <http://ladb.unm.edu/noti>
- Economic Commission for Latin America and the Caribbean, 1999. Nicaragua: assessment of the damage caused by Hurricane Mitch 1998: Implications for Economic and Social Development and for the Environment, ECLAC, Mexico City.
- Elsner, J.B., Liu, K-B., and Kocher, B., 2000. Spatial variations in major U.S. hurricane activity: statistics and a physical mechanism. *Journal of Climate* 13, 2293-2305.
- Fairbanks, R.G., 1989. A 17,000-year glacio-eustatic sea level record: influence of glacial melting rates on the Younger Dryas event and deep-ocean circulation. *Nature* 342, 637-642.
- Fedick, S.L. (ed), 1996. *The Managed Mosaic: Ancient Maya Agriculture and Resource Use*. University of Utah Press, Salt Lake City.
- Frappier, A.B., Sahagian, D., Carpenter, S.J., González, L.A., and Frappier, B.R., 2007a. A stalagmite proxy record of recent tropical cyclone events. *Geology*, 7, 111–114. DOI: 10.1130/G23145A.
- Frappier, A. B., Knutson, T., Liu, K.-b., and Emanuel, K., 2007b. Perspective: coordinating paleoclimate research on tropical cyclones with hurricane-climate theory and modeling. *Tellus Series A-Dynamic Meteorology and Oceanography* 59, 529-537.
- Gallet, Y., and Genevey, A., 2007. The Mayans: climate determinism or geomagnetic determinism? *EOS* 88, 129-130.
- Garcia-Herrera, R., Gimeno, L., Ribera, P., Hernandez, E., Gonzalez, E., and Fernandez, G., 2007. Identification of Caribbean hurricanes from Spanish documentary sources. *Climatic Change* 83, 55-85.
- Gill, R.B., 2000. *The Great Maya Droughts*. University of New Mexico Press, Albuquerque.
- Global Information and Early Warning System, 1999. Special report on Honduras. FAO/WFP Crop and Food Supply Assessment Mission to Honduras.
- Graham, E., 1994. *The highlands of the lowlands: Environment and Archaeology in the Stann Creek District, Belize, Central America*. Monographs in World Archaeology No. 19. Prehistory Press, Madison, Wisconsin.
- Haug, G.H., Hughen, K.A., Sigman, D.M., Peterson, L.C., and Rohl, U., 2001. Southward migration of the Intertropical Convergence Zone through the Holocene. *Science* 292, 1304-1314.
- Haug, G. H., Gunther, D., Peterson, L. C., Sigman, D. M., Hughen, K. A., and Aeschlimann, B., 2003. Climate and the collapse of Maya civilization *Science* 299, 1731-1735.

Hendry, M.D., 1982. Late-Holocene sea-level changes in western Jamaica. In Colquhoun D. J. (ed), *Holocene Sea-Level Fluctuations: Magnitude and Causes*. University of South Carolina. Columbia, South Carolina. 71-80.

Hodell, D.A., Curtis, J. H., and Brenner, M., 1995. Possible role of climate in the collapse of Classic Maya civilization. *Nature* 375, 391-394.

Hodell, D.A., Brenner, M., Curtis, J. H., and Guilderson, T., 2001. Solar forcing of drought frequency in the Maya lowlands. *Science* 292, 1367-1370.

Holt-Gimenez, E., 2002. Measuring farmers' agroecological resistance after Hurricane Mitch in Nicaragua: a case study in participatory, sustainable land management impact monitoring. *Agriculture Ecosystems and Environment* 93, 87-105.

Hopley, D., 1984. The Holocene "high energy window" on the central Great Barrier Reef. In Thom, B.G., (ed) *Coastal Geomorphology in Australia*. Academic Press, Sydney. 135-150.

Islebe, G. A., and Sanchez, O., 2002. History of Late Holocene vegetation at Quintana Roo, Caribbean coast of Mexico. *Plant Ecology* 160, 187-192.

James, N.P., and Ginsburg, R.N., 1979. The seaward margin of Belize barrier and atoll reefs. *International Association of Sedimentologists, Special Publication* No. 3.

Keen, T.R., Bentley, S.J., Vaughan, W.C., and Blain, C.A., 2004. The generation and preservation of multiple hurricane beds in the northern Gulf of Mexico. *Marine Geology* 210, 79-105.

Lighty, R.G., Macintyre, I.G., and Stuckenrath, R., 1982. *Acropora palmata* reef frameworks: a reliable indicator of sea level in the western Atlantic for the past 10,000 years. *Coral Reefs* 1, 125-130.

Liu, K-b., and Fearn, M.L., 1993. Lake-sediment record of late Holocene hurricane activities from coastal Alabama. *Geology* 21, 793-796.

Liu, K-b., and Fearn, M.L., 2000. Reconstruction of prehistoric landfall frequencies of catastrophic hurricanes in northwestern Florida from lake sediment records. *Quaternary Research* 54, 238-245.

Macintyre, I.G., Littler, M.M., and Littler, D.S., 1995. Holocene history of Tobacco Range, Belize, Central America. *Atoll Research Bulletin* 430, 1-18.

Macintyre, I.G., Toscano, M.A., Lighty, R.G., and Bond, G.B., 2003. Holocene history of the mangrove islands of Twin Cays, Belize, Central America. *Atoll Research Bulletin* 510.

Mainville, D.Y., 2003. Disasters and development in agricultural input markets: bean seed markets in Honduras after Hurricane Mitch. *Disasters* 27, 154-171.

- Mazullo, S. J., Anderson-Underwood, K. E., Burke, C. D., and Bischoff, W. D., 1992. Holocene coral patch reef ecology and sedimentary architecture, northern Belize, Central America. *Palaios* 7, 591-601.
- McCann, W. R., and Pennington, W. D., 1990. Seismicity, large earthquakes, and the margin of the Caribbean Plate. In Dengo, G., Case, J.E., (eds) *The Geology of North America, Vol. H, The Caribbean region*. The Geologic Society of America, Boulder, Colorado. 291-306.
- McKillop, H., 1995. Underwater archaeology, salt production, and coastal Maya trade at Stingray Lagoon, Belize. *Latin American Antiquity* 6, 214-228.
- McKillop, H., 2002. *Salt: White Gold of the ancient Maya*. University Press of Florida, Gainesville, Florida.
- McKillop, H., 2004. *The ancient Maya: New Perspectives*. ABC-CLIO, Santa Barbara, California.
- Metzgen, M., and Cain, E. E., 1925. *The handbook of British Honduras comprising historical, statistical and general information concerning the colony*. The West India Commission, London.
- Miller, D., Moro, C. I., Grissino-Mayer, H. D., Mock, C. J., Uhle, M.E., and Sharp, Z., 2006. Tree-ring isotope records of tropical cyclone activity. *Proceedings of the National Academy of Science* 103, 14294-14297.
- Mock, C. J., 2004. Tropical cyclone reconstructions from documentary records; examples from South Carolina. In: Murnane, R.J., K.B. Liu, (eds), *Hurricanes and Typhoons: Past, Present, and Future*. Columbia University Press, New York. 121-148.
- Morris, S. S., Neidecker-Gonzales, O., Carletto, C., Munguia, M., Medina, J. M., and Wodon, Q., 2002. Hurricane Mitch and the livelihoods of the rural poor in Honduras. *World Development*, 30, 49-60.
- Nanayama, F., Shigeno, K., Satake, K., Shimokawa, K., Koitabashi, S., Miyasaka, S., and Ishii, M., 2000. Sedimentary differences between the 1993 Hokkaido-nansei-oki tsunami and the 1959 Miyakojima typhoon at Taisei, southwestern Hokkaido, northern Japan. *Sedimentary Geology* 135, 255-264.
- Neumann, C.J., Jarvinen, B.R., McAdie, C.J., and Hammer, G.R., 1999. *Tropical cyclones of the North Atlantic Ocean, 1871-1998. 5th Revision*. DOC/NOAA Historical Climatology Series 6-2. National Climate Data Center, Asheville.
- O'Loughlin, K.F., and Lander, J.F., 2003. *Caribbean tsunamis: a 500-year history from 1498-1998*. Kluwer Academic Publishers, Dordrecht.
- Paul, M., 1995. Geologic and tectonic development of the Caribbean plate boundary in southern Central America. *Geological Society of America, Special Paper*, 295, XI-XXXII.

Peltier, W.R., 1988. Lithospheric thickness, Antarctic deglaciation history, and ocean basin discretization effects in a global model of postglacial sea level changes: a summary of some sources of nonuniqueness. *Quaternary Research* 29, 93-112.

Peter, G., and Wertbrook, G. K., 1976. Tectonics of the southwestern North Atlantic and Barbados Ridge Complex. *Bulletin of the Association of American Petroleum Geologists* 60, 1078-1106.

Pielke, R.A., Jr., and Pielke, R.A., Sr., 1997. Vulnerability to hurricanes along the U.S. Atlantic and Gulf Coasts: Considerations of the use of long-term forecasts. In Diaz H.F., Pulwarty, R.S. (eds), *Hurricanes, Climate and Socioeconomic Impacts*. Springer-Verlag, Berlin. 147-180.

Rappaport, E.N., and Fernandez-Partagas, J., 1997. History of the deadliest Atlantic tropical cyclones since the discovery of the New World, In Diaz H.F., Pulwarty, R.S. (eds), *Hurricanes, Climate and Socioeconomic Impacts*. Springer-Verlag, Berlin. 93-108.

Reimer, P.J., Baillie, M.G.L., Bard, E., Bayliss, A., Beck, J.W., Bertrand, C., Blackwell, P.G., Buck, C.E., Burr, G., Cutler, K.B., Damon, P.E., Edwards, R.L., Fairbanks, R.G., Friedrich, M., Guilderson, T.P., Hughen, K.A., Kromer, B., McCormac, F.G., Manning, S., Ramsey, C.B., Reimer, R.W., Remmele, S., Southon, J.R., Stuiver, M., Talamo, S., Taylor, F.W., van der Plicht, J., and Weyhenmeyer, C.E., 2004. *Radiocarbon* 46, 1029-1058.

Rosenmeier, M. F., Hodell, D. A., Brenner, M., and Curtis, J. H., 2002. A 4000-year lacustrine record of environmental change in the southern Maya lowlands, Peten, Guatemala. *Quaternary Research* 57, 183-190.

Scott, D.B., Collins, E.S., Gayes, T.S., and Wright, E., 2003. Record of prehistoric hurricanes on the South Carolina coast based on micropaleontological and sedimentological evidence, with comparison to other Atlantic Coast records. *GSA Bulletin* 115, 1027-1039.

Setzekorn, W.D., 1978. *A Profile of the New Nation of Belize, formerly British Honduras*. Ohio University Press, Columbus, Ohio.

Scheffers, A., Scheffers, S., and Kelletat, D., 2005. Paleo-tsunami relics on the southern and central Antillean island arc. *Journal of Coastal Research* 21, 263-273.

Short, A.D., and Hesp, P.A., 1982. Wave, beach and dune interactions in southeastern Australia. *Marine Geology* 48, 259-284.

Smith, T., 1842. The East Coast of Yucatan. *Nautical Magazine* 11, 334-338.

Stoddart, D. R., 1962. Three Caribbean atolls: Turneffe Islands, Lighthouse reef, and Glover's reef, British Honduras. *Atoll Research Bulletin* 87, 1-147.

Stoddart, D. R., 1963. Effects of Hurricane Hattie on the British Honduran reefs and cays, Oct.30-31, 1961. *Atoll Research Bulletin* 95, 1-142.

Stuiver, M., and Reimer, P.J., 1993. Radiocarbon 35, 215-230.

Tannehill, I.R., 1938. Hurricanes: Their Nature and History. Princeton University Press, Princeton.

Toscano, M.A., and Macintyre, I.G., 2003. Corrected western Atlantic sea-level curve for the last 11,000 years based on calibrated C-14 dates from Acropora palmate framework and intertidal mangrove peat. Coral Reefs 22, 257-270.

Tuttle, M. P., Ruffman, A., Anderson, T., and Jeter, H., 2004. Distinguishing tsunami from storm deposits in Eastern North America; the 1929 Grand Banks tsunami versus the 1991 Halloween storm. Seismological Research Letters 75, 117-131.

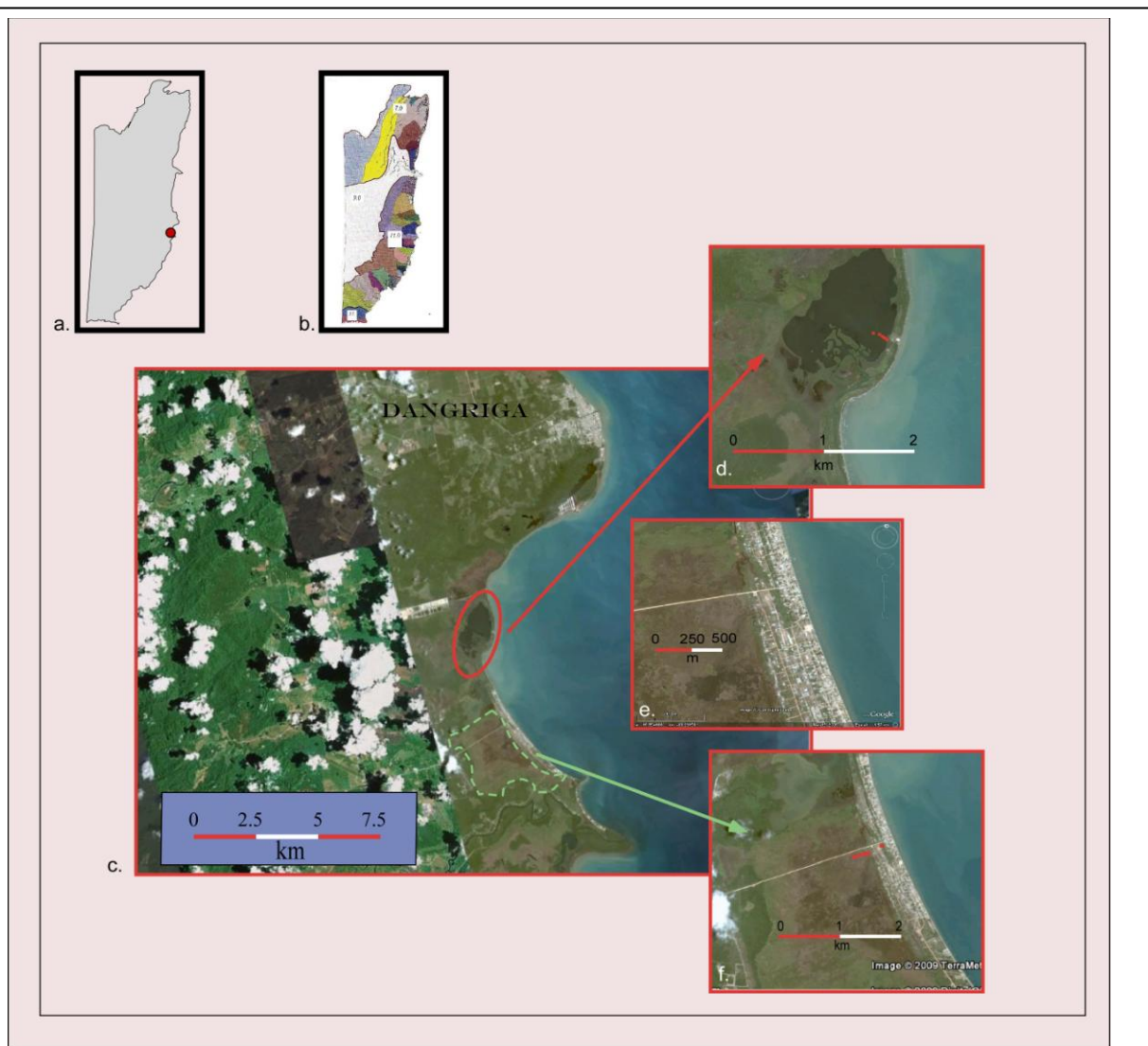
Woodroffe, C.D., 1988. Mangroves and sedimentation in reef environments: indicators of past sea-level trends? Proceedings, 6th International Coral Reef Symposium, Australia, Vol. 6, 535-539.

Wright, L.D., and Short, A.D., 1984. Morphodynamic variability of beaches and surfzones: a synthesis. Marine Geology 56, 92-118.

CHAPTER 7 COMMERCE BIGHT-HOPKINS MARSH, BELIZE

7.1 Regional Setting

As discussed in **Chapter 5**, Belize is divided into two distinct morphotectonic regions, with the division occurring at the latitude of Belize City. The northern half of the country is part of the low-lying carbonate Yucatan platform, while the southern half belongs to the northern Central American Sierra unit (**Figure 5:2**). The study sites, at ~16.9 N, 88.3 W, lies within the southern province, on a coastal plain composed of terrigenous Quaternary material eroded from the Maya Mountains to the west (**Figure 5:1**). These mountains, composed of a Paleozoic core with granitic batholiths, and capped by Mesozoic limestone, are a large faulted block, characterized by abrupt topographic relief. Victoria Peak at 1120 m lies <20 km west of the 100m contour line; Richardson Peak at 1000 m is <10 km west of the 100m contour line. Annual precipitation along the range is between 3000-5000 mm/yr (Portig, 1976), resulting in a large number of short, wide rivers draining small valleys (**Figure 7:1b**). These larger streams cut roughly parallel courses southeast across the plain to the sea, depositing alluvial material that supports tropical forests along the banks, and creating a series of small deltas composed of larger grained clastic materials along the coast (Marshall, 2007). However, drainage is poor for the non-riparian sections, which form the majority of the coastal plain, generally 10-30 km in width, which, consisting of heavily leached topsoil and acid subsoil, is unsuitable for farming and supports only a sparse pine savanna (Moberg, 1992). Approaching the coast, the land is generally low and muddy, dominated by wetlands. A thin coastal sand strip supports coconuts on the ridges and mangroves (*Rhizophora mangle*, *Avicennia germinans*, and *Laguncularia racemosa*) at sea level (Morris, 1883; Waddell, 1961; Moberg, 1992). Due to the low coastal elevation,



7.1 Site map; the location of the site along the coast is shown in (a); (b) shows drainage basins for the country. Note the extremely large number of short streams draining the eastern face of the Maya Mountains along the southern half of the coast. A Google Earth image of the Hopkins area is displayed in (c), showing the spatial relationship between (d) Commerce Bight Lagoon (CBL); (e) Hopkins village; and (f) the Hopkins marsh.

agriculture usually is avoided along the coast, beginning a few km inland. For the same reason, most villages are located not on the ocean, but some distance upstream. This has been the practice since at least the late 1800s (Morris, 1883). Various agricultural schemes have been initiated in the area in the past, the most important being a proposal just prior to World War I for a large scale (>7,500 acre estate) banana industry connected by railway to a deep water pier just south of Dangriga (Moberg, 2001). However, the project was unsuccessful, and by 1937 production and marketing problems and Panama disease combined to finally finish the industry (Stetzekorn, 1975; Moberg, 1992, 2001; Wiley, 2008), that, according to Waddell (1961), had basically collapsed even before the railroad construction was finished. In any case, the early banana industry was centered in Middlesex, ~ 30 km to the northwest, in the north Stann Creek watershed. Until very recent times, agriculture had not been an important factor in the national economy, accounting for only 14% of the colony's GNP in 1946 (as opposed to 21% for forestry products) (Waddell, 1961). As late as 1961 agriculture was characterized as "generally primitive" (Waddell, 1961, p. 99), while by the mid 1980s it was estimated that only 12-15% of the suitable land was being worked (Bolland, 1986). Generally, agriculture has had an insignificant impact on the coastal geomorphology of Belize.

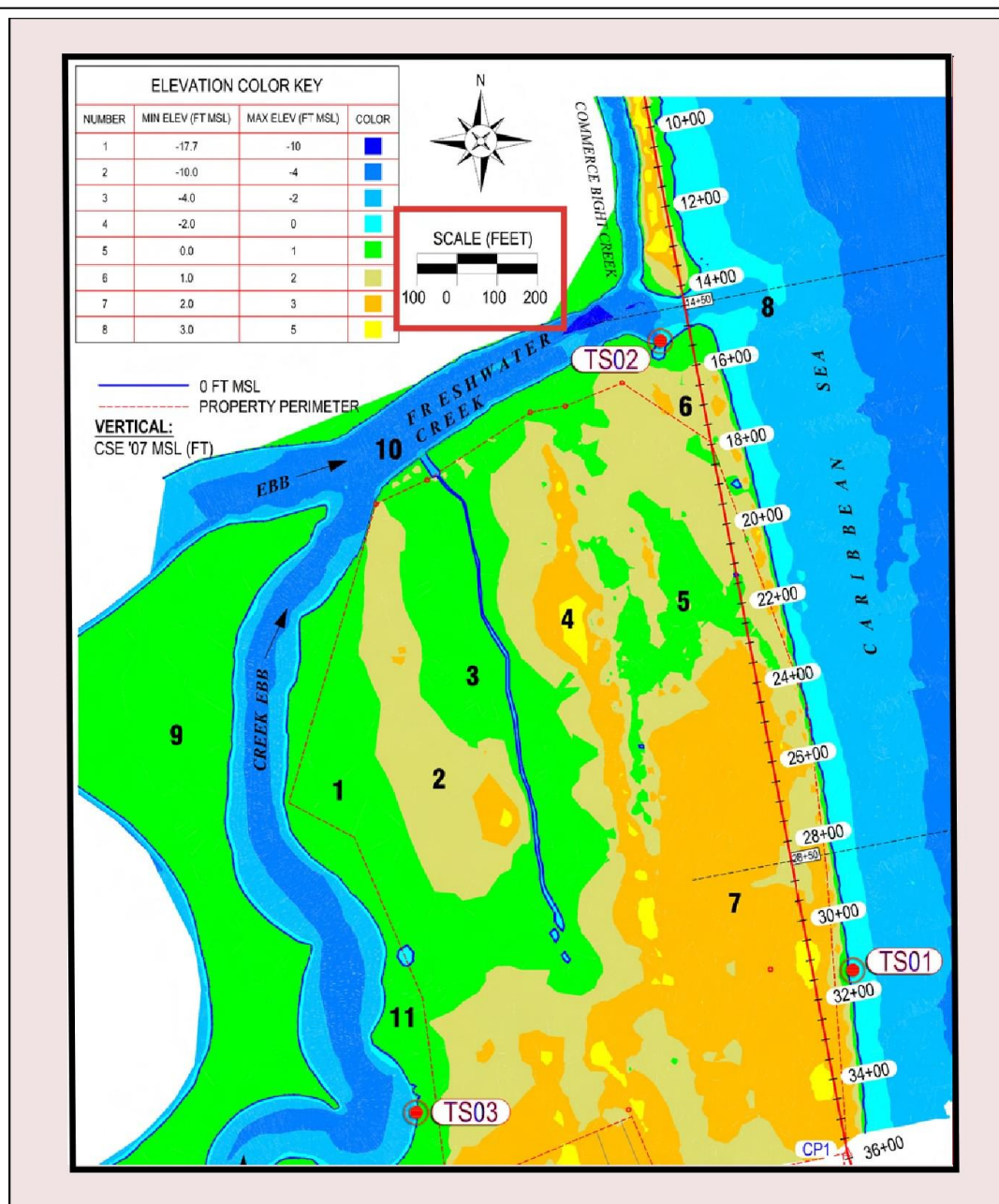
7.2 Study Sites

Our study area is located along the southern central coast of Belize, on the inner curve of a cusped bay between the headlands formed by Stann Creek to the north and Sittee River to the south (**Figures 5:1, 7:1**). The town of Dangriga is situated at the mouth of Stann Creek. The coastal plain here is ~ 10 km wide, with large wetlands covering the coast. Drainage for the immediate area is by Freshwater Creek and Black Ridge Creek, both very short watercourses that drain only the lowest elevations of the Maya Mountains, as branches of the Sittee River pass

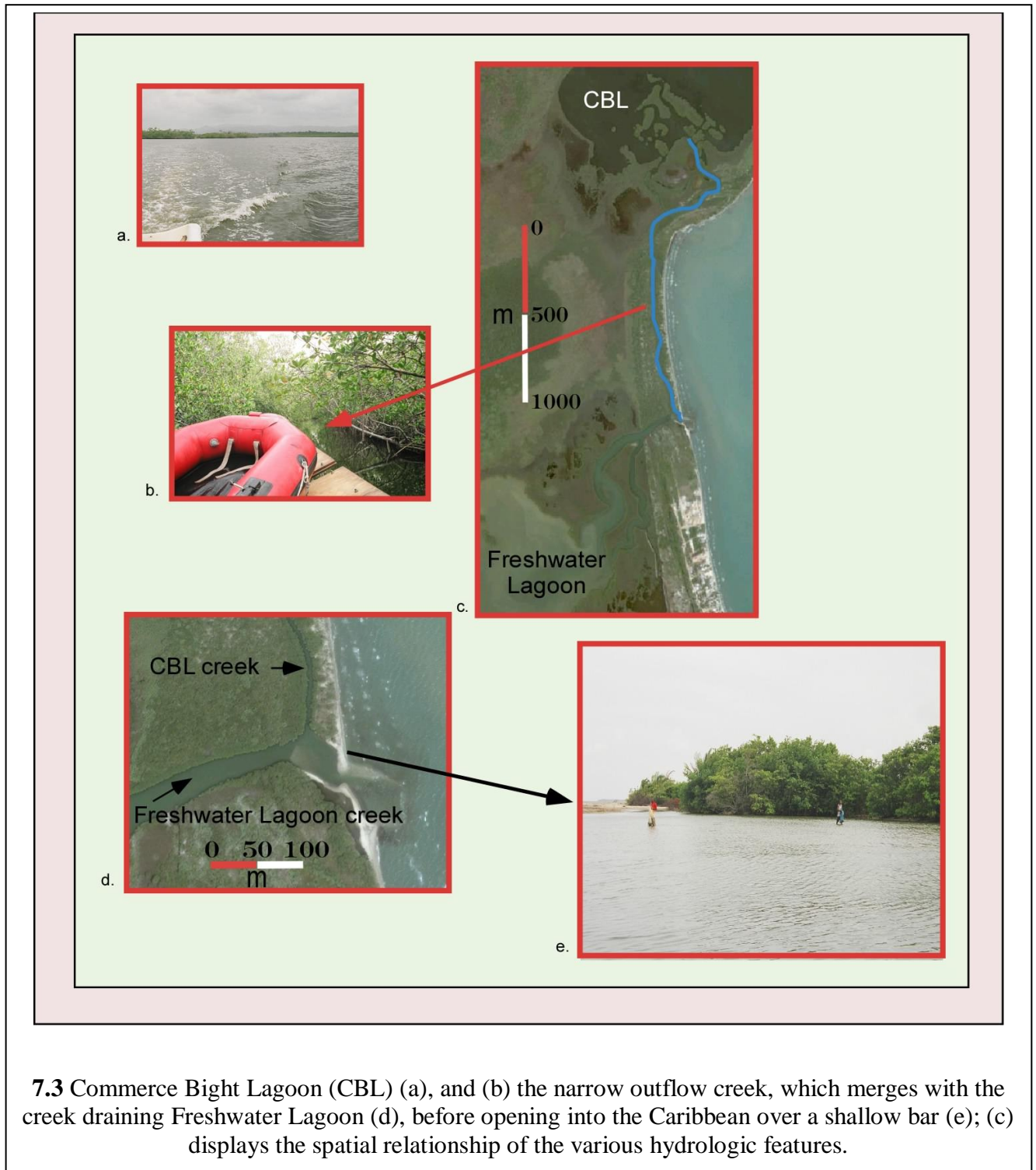
behind them, capturing the flow from higher elevation. Both creeks are small and sluggish, and each delivers its water to shallow lagoons just inland from the Caribbean Sea, with Freshwater Creek flowing into Freshwater Creek Lagoon, and Black Ridge Creek discharging into Commerce Bight Lagoon (CBL). Outflow from each is by small creeks, which discharge into the sea through a common mouth (Freshwater Creek). The land between the lagoons is low and swampy, part of a nearly continuous wetlands that extends southward >10 km, broken only by the natural levees of Sittee River. Hopkins village sits on top of a relatively high (~3 m) sand ridge between the sea and the wetlands (**Figure 7:1 a**). Offshore bathymetry is rather steep, with the 10 foot (~3 m) contour occurring within ~ 100 m (**Figure 7:2**).

7.2.1 Commerce Bight Lagoon

CBL is a shallow (<2 m) body of water separated from the Caribbean Sea by a low (<1.5 m) sand barrier ~150 m wide. A single house built on the barrier is the only visible human infrastructure; the rest of the lake is surrounded by dense vegetation, both mangroves and hardwoods (**Figure 7:3a**). Lake salinity was 21.5 ppt when we visited in the third week in June 2004, after the start of the rainy season, but before much heavy rain had fallen. Surface temperature was 30°C. Presumably temperature and salinity vary seasonally, depending on precipitation and weather. CBL is directly connected with the sea through a twisting, narrow (3-5 m wide) creek, ~2.5 km in length (**Figure 7:3b, c**). This creek runs south, generally paralleling the shoreline, perhaps following a relict swale in an antecedent dune system. This creek has a muddy bottom and banks supporting dense stands of red mangroves (*Rhizophora mangle*) (**Figure 7:3b** CBL creek). During our visit the mouth of the creek, was extremely shallow (<50 cm, **Figure 7:3e**), despite the addition of the discharge from Freshwater Lagoon. Google Earth imagery suggests that the river mouth sand bar results from alongshore drift from the north,



7.2 Hopkins topography and beach bathymetry. Both distances and elevations are in feet. The diagram is from CSE (2007).



7.3 Commerce Bight Lagoon (CBL) (a), and (b) the narrow outflow creek, which merges with the creek draining Freshwater Lagoon (d), before opening into the Caribbean over a shallow bar (e); (c) displays the spatial relationship of the various hydrologic features.

which nearly closes this opening during dry periods (**Figure 7:3d**). Presumably increased river discharge during the wet season increases the depth and width of the creek mouth.

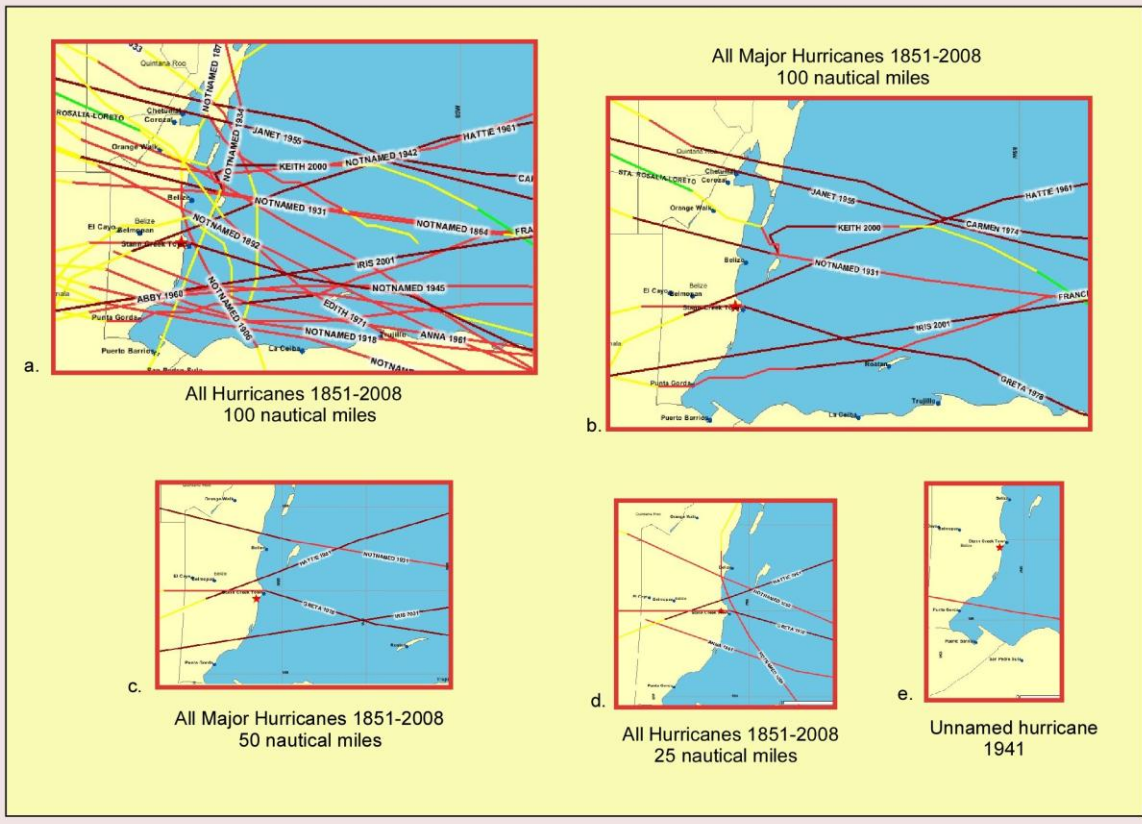
7.2.2 Hopkins Village

Hopkins is a linear village, 3-4 streets wide, fronting the Caribbean Sea (Bass, 1999). Inland from the village the elevation drops, transitioning first into a palmetto swamp ~70 m in width, and then a brackish to fresh marsh, dominated by sedges, that extends roughly 2 km to the west (**Figure 7:1**). The village was founded in 1941 by predominately Garifuna settlers, relocated from Newtown, a few miles to the north, due to destruction of that village resulting from the unnamed hurricane of September 29, 1941. Prior to that relocation, the population consisted of four families, and the higher ground was a coconut plantation, leased to an Englishman (Moberg, 1992; Bass, 1999). The village is connected with the paved road (the Southern Highway) by a gravel road built through the marsh in 1971. Previously travel was by boat, foot, or unimproved trail through the marsh during the dry season (Bass, 1999). Small subsistence-scale farming has occurred west of the marsh since the establishment of the village, access formerly being by boat up Freshwater Creek. More recently slightly larger scale citrus plantations have been planted (Bass, 1999), with the first crop produced in 1986 (Moberg, 1992).

Cores were taken from two transects, one (CB) from the eastern edge of CBL, and one (HPN) from the wetlands directly west of Hopkins village, covering the palmetto swamp and the eastern edge of the marsh (**Figure 7:1**). HPN is ~ 4.5 km south of CB.

7.3 Hurricane History

As discussed in **Chapter 6**, Belize has been struck repeatedly by hurricanes during the historic period. **Figure 7:4a** displays all hurricanes that have passed within 100 nautical miles of our study sites since 1851, based on NOAA's HURDAT ("best track") data set. Eight of these



7.4 Hurricane history based on NOAA HURDAT data. All tracks occurring since 1851 are shown for (a) hurricanes; and (b) major hurricanes passing within 100 nautical miles of the site; (c) all major hurricanes passing within 50 nautical miles of the site, (d) all hurricanes passing within 25 nautical miles of the site; and (e) the track of the unnamed hurricane of 1941.

were major hurricanes (category 3 or greater as measured on the Saffir-Simpson scale, which requires sustained winds of >111 mph [96 kt or 178 kph]) (**Figure 7:4b**). Of these, four passed within 50 nautical miles of our site (**Figure 7:4c**). In addition, three minor hurricanes, Anna (1961) and unnamed storms in 1892 and 1906, passed within 25 nautical miles. These storms are discussed in greater detail below, in order to assess their potential for having deposited identifiable sedimentary markers, as is the unnamed storm of 1941, as the literature identifies it as having caused significant geomorphic changes in the area (Bass, 1999, Moberg, 1992).

In addition to the HURDAT data set that covers the period 1851-2008, a list of hurricanes affecting Belize for the period 1787-1961 was compiled by Stoddart (1963), based on both standard texts (Poey, 1855, 1865; Tannehill, 1956) and local records (Metzgen and Cain, 1925; Burdon 1931-1935; Anderson, 1958). A comparison of the two reveals the difficulties inherent in dealing with older records. For the period 1851-1916, the two records show a total of seven events. However, only a single event (a storm that passed directly over Belize City in 1864) appears in both records as occurring in the same month, and in the same general area. Two other events are recorded as occurring in the same year in both records, but the date of occurrence varies by a month in one case, and the location of landfall by 80 km in the other. Three events appear only in HURDAT, and one only in Stoddart's list. However, for the period 1916-1961, the records show a total of 12 events, 11 of which occur in both (although the date of occurrence is off by one month in one case). One event is found in HURDAT, but not in Stoddart. The discrepancy with the HURDAT data reduces the confidence with which one can use Stoddart's list to extend the hurricane record to 1787, especially in the southern and northern zones, as his record is necessarily biased toward the Belize City area, the only population center during the colony's early history. However, it is probable that the Stoddart list tends toward undercounting,

with minor or more distant storms missed, but the major storms along the central coast described reliably.

7.3.1 Major Hurricanes

7.3.1.1 Unnamed Storm of 1931

This hurricane hit Belize City on September 10, the country's most important national holiday, catching many people out in the streets. Estimates of city death tolls range up to 2500 people, 20% of the city's population (Cain, 1933). The economic consequences of this event were considerable. Although HURDAT places landfall approximately 25 kilometers north of Belize City, popular accounts place the eye of the storm passing directly over the city (people rushed out to begin rescue operations, thinking that the storm had passed, where they were again caught in the open [Cain, 1933]). Stoddart (1963) (relying on Burdon, [1931], and Cain, [1933]) gives precise times for the lull, so it seems possible that at least a portion of the eye passed over Belize City. HURDAT lists this as a category 3 hurricane, with maximum windspeed at landfall of 110 knots (127 mph). Because the eyewall passed from 65 to 90 kilometers to the north of our study site, it is not expected that the storm's weaker left front quadrant left any detectable sedimentary signature there. Additionally, our site locations along the inner edge of a bay may significantly reduce recording sensitivity for storms passing on the north of the headland that protrudes >7 km to the east (**Figure 7:3**).

7.3.1.2 Hattie, 1961

After passing directly over Turneffe Atoll (**Chapter 8**), Hattie made landfall on the mainland near the village of Mullins Rivers (**Chapter 6**) as a category 5 hurricane with maximum sustained winds of 140 knots (>160 mph) and a minimum central pressure of 920 mb. Due to the tremendous damages, this hurricane wrecked on both the environment (Stoddart,

1963) and the national infrastructure, Hattie became one of the defining events in modern Belizean history. Following the storm the British government moved the colony's capital from its traditional coastal location in Belize City inland to Belmopan, specifically to avoid similar future disasters (Setzekorn, 1975). Although the eyewall of Hattie probably passed within 30 kilometers, our sites were on the storm's weaker left front quadrant, and more likely experienced seaward, rather than landward, movement of water. The near total destruction in Hopkins (only two buildings were left standing) (Moberg, 1992) probably results more from construction materials and practices (pole and thatch house on a sand ridge) (Bass, 1999) than high windspeed.

7.3.1.3 Greta, 1978

Greta made landfall as a medium strength category 3 hurricane, with maximum windspeed of 105 knots (121 mph) and a central pressure of 957 mb, producing tides up to 6-7 feet above MSL north of Dangriga (Lawrence, 1979), perhaps amplified by topographical/geomorphological factors, as no flooding was reported in the south part of town (Unsigned, 1978). Greta's point of landfall was ~ 10 km of our sites, again to the north.

7.3.1.4 Iris, 2001

Iris was a category 4 hurricane that made landfall with maximum sustained wind speed of 125 knots (144 mph), and a minimum central pressure of 948 mb, and predicted storm surges of 13-18 feet. However, Iris was a "very small" storm, with hurricane force winds extending only 30 km from the center (Avila, 2001; Unsigned, 2001). Iris underwent a very rapid intensification shortly before landfall, with minimum pressure dropping from 990 to 950 mb and wind speed increasing from 75-120 knots within an 18 hour period (Avila, 2001). These factors, along with a high rate of forward travel combined to severely limit both the duration and extent of hurricane

winds generated by Iris, thereby reducing the spatial extent of the storm surge. Point of landfall was near the mouth of Monkey River, roughly 60 kms south of our sites.

7.3.2 Minor Hurricanes

7.3.2.1 Unnamed Storm of 1906

HURDAT lists this storm as category 1, with maximum wind speeds of 80 knots (92 mph), with its track, passing from south to north over the sea to the east, leaving the coring sites along the weakened left front quadrant. Closest approach was probably ~ 15 km.

7.3.2.2 Anna, 1961

Anna was also a category 1 storm, with maximum wind speeds of 80 knots (92 mph). Stoddart (1963), visiting the site the following day, reported a few uprooted trees and a localized overwash event at Placencia, the point of eyewall impact, >40 km south of our sites

7.3.2.3 Unnamed Storm of 1892

This storm was a little stronger (category 2, 85 knots, 98 mph), and a little farther away, probably passing ~60 km to the north.

7.3.2.4 Unnamed Storm of 1941

While in Belize waters, this category 2 hurricane had a minimum central pressure of 992 mb and wind speeds of 90 knots, which decreased to 80 knots (category 1) at landfall. As HURDAT data places the closest approach to the study sites at > 90 km to the south, local effects could be expected to be minimal.

However, reports (<http://www.doe.gov.bz/documents/EIA/Hopkins%20Harbor>; Moberg, 1992;) state that the storm caused so much erosion at Newton, two miles north of Hopkins (very near the CB transect), that the village had to be abandoned. Although this storm achieved maximum wind speeds of 105 knots, it was a hurricane for only three days, and a major

hurricane for <24 hours, reducing to category 2 while still >450 km from Belize. Storm size or radius of hurricane strength winds are not provided; however it seems unlikely that a storm of such short duration could develop great spatial extent, especially as its track passed over land near Cabo Gracias a Dios, on the Mosquito Coast.

7.4 Methods

In addition to the standard methods described in **Chapter 2.4** and used in the other study sites, the cores from the CB transect were subjected to analysis by a GeoThek Multi-sensor Core Logger, which measured gamma density at 0.5 cm intervals (Evans, 1965), as well as grain size analysis, which was conducted by means of a series of stacked sieves.

7.5 HPN Transect

7.5.1 Results

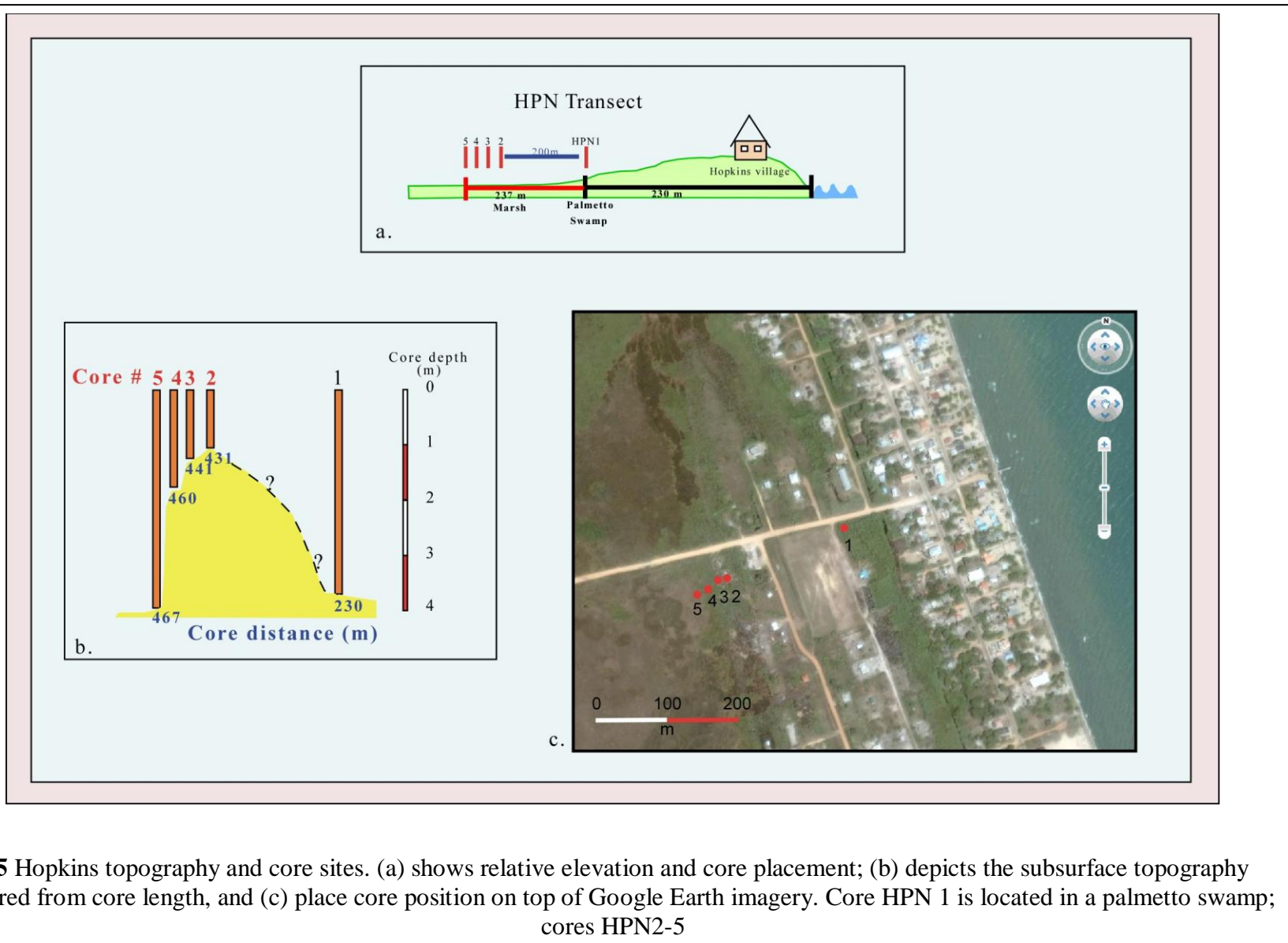
Six cores were obtained along this transect, spanning a distance of 237 m, covering from 230-437 m inland. Duplicate cores were extracted by modified Livingstone piston corer and a peat borer in the same location near the landward edge of a palmetto swamp at 230 m inland. The Livingston core displayed significant compaction and was eliminated from further analysis. The palmetto swamp is only seasonally wet, and had no standing water during our visit in June, 2004. Moving to the west, elevation rises slightly, and remains above the permanent water table for approximately 150 m, crossing the village soccer field and a secondary road. Beyond this the elevation drops and a *Cyperaceae* dominated marsh is encountered (**Figure 7:5**). Four peat borer cores were extracted from this marsh at 431, 441, 460, and 467 m from the sea. All cores were pushed until refusal; the cores at 230 and 467 m reached depths > 350 cm, while the cores at 431, 441, and 460 m inland penetrated 103, 129, and 174 cm respectively. These depths are distance below ground level; however, in the marsh the intensely matted nature of the plant roots did not

permit collection in the root zone. (Normal collection occurred in the palmetto swamp at 230 m). Sediment retrieval started at the depths of 21, 28, 50, and 20 cm respectively at 431, 441, 460, and 467 m inland (**Figure 7:4**). Transect cores were predominately peat/organic material with clay intervals, interrupted by occasional thin (generally 1-5 cm) silt and/or sand layers. Core depth suggests that the marsh is located over uneven subsurface topography, the most likely cause being a pre-existing dune and swale system (**Figure 7:5**).

7.5.1.1 Example Litholog

Core HPN5 was chosen as the example litholog for this transect. This composite core, the most inland at 467 m, consists of seven 50 cm peat borer sections. As mentioned above, the root zone (0-20 cm) was not captured by the coring device. It is not clear whether this gap actually represents missing sediment; very little soil was visually present in the material (inability to collect the material resulted from the strong connectivity of the root mass with surrounding vegetation; it did not result from the liquid nature of the soil). It is highly likely that most of the uncollected material is simply the ephemeral bottom section of the plants, which will not be preserved in the sedimentary record. Core depth reached 384 cm.

The results of LOI analysis are presented in **Figure 7:6**. Shown are the water, organic, carbonate and residual (mainly silicates) percentages as individual curves (**Figure 7:6 a,b, c, d**), a combined LOI curve (**Figure 7:6e**), and the core litholog (**Figure 7:6f**). A comparison of the data presented in **Figures 7:6 a- f** demonstrates that sedimentary features of the core can be inferred from a careful reading of the LOI diagram. High water and organic percentages (blue and green curves) represent generally organic deposition (usually peat); an example is the section from cm 20-110 (**Figure 7:6**). A sharp drop and a corresponding increase in the amount of residual material (gray curve) indicate non-organic intervals, usually light colored clastics.

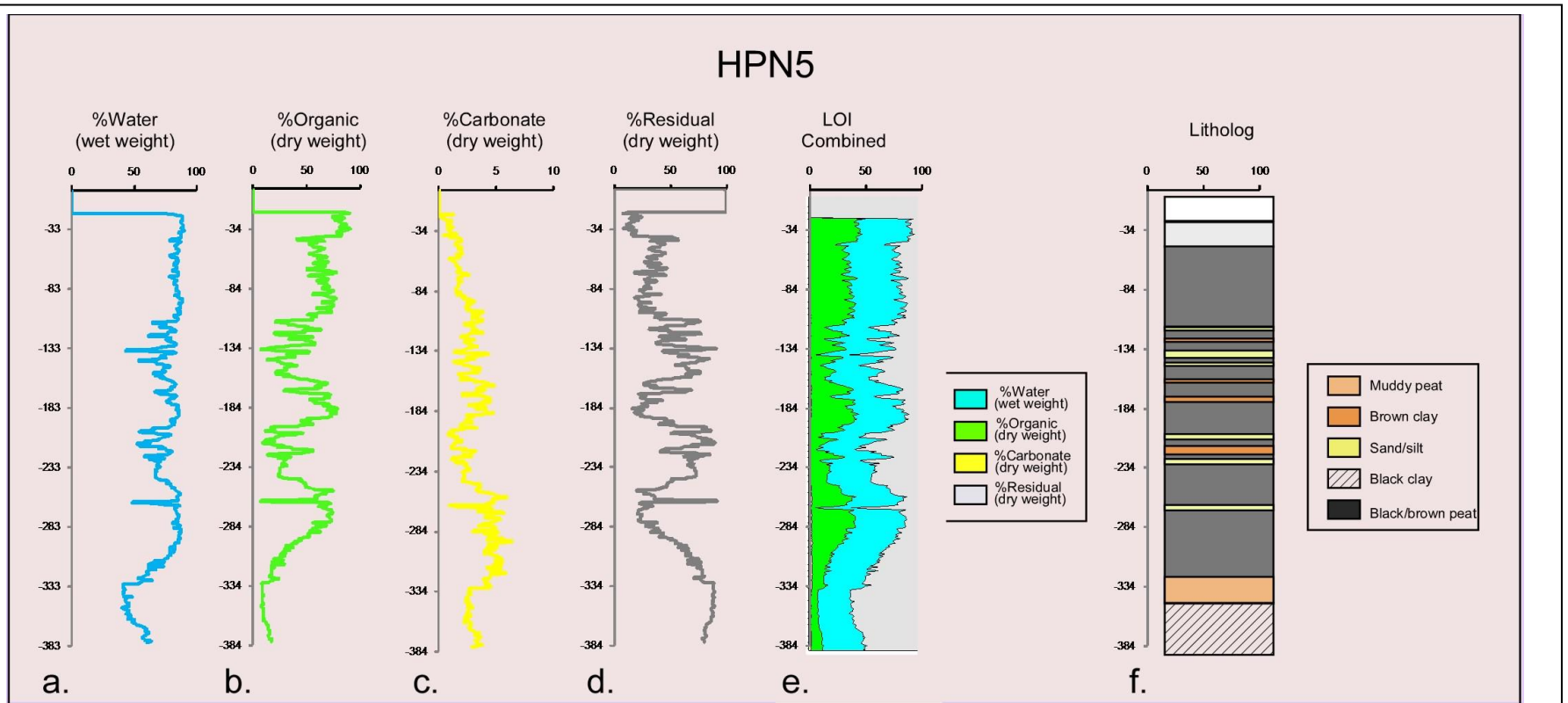


Examples are cm 111-115, 122-127, 132-136, and 264-265 (**Figure 7:6-7.7**).

Sedimentary change can occur slowly, as occurs in the interval from cm 272 to 333, during which residual values gradually increase from 22% to 88%. This increased muddiness (higher clay content), continues lower in the core, marking a slow transition from peat to clay (**Figure 7:6, 7:8**). Such incremental changes can often be used as markers of slowly changing boundary conditions, while abrupt LOI changes potentially signal discrete events. One such example is the interval from cm 262-266 where residual values increase from 36-92% and then back to 23% within 5 cm.

The core litholog (**Figures 7:6f**) can also provide important information when attempting to identify event-driven sedimentary changes. In addition to identifying clastic layers, some grain size information is provided. The yellow bands (**Figures 7:6, 7, 8**) indicate sand/silt layers, whose transportation requires a more energetic delivery process than does smaller grained material. The thinness and interbedded character of these intervals suggest short lived, high energy events as the most likely cause of deposition.

In this core water and organic content are positively correlated to each other and negatively correlated with residual content. Carbonates are a minor component, generally between 1-3%, except for a 25 cm interval beginning at 160 cm (blue box “A” **Figures 7:8d**) and a 80 cm interval beginning ~ 250 cm, (blue box “B”), where values are generally >4%, with a maximum value of 6.3%. Carbonate and water/organics have a nonlinear relationship, as displayed by the graph displaying carbonate and organic values (**Figures 7:8 d**). This graph displays a generally inverse relationship from 20-100 cm, a direct relationship from that depth until ~285 cm, below which the relationship becomes inverse until ~330cm, at which point it again becomes direct until the bottom of the core. It should be noted that, although percentages of both carbonates and organics are lower in the clastic spikes at intervals, the



7.6 Loss on ignition (LOI) curves and litholog for core HPN5. Shown are (a) water, (b) organic, (c) carbonate, and (d) residual (mainly silicate) percentages as individual curves; (e) a combined LOI curve, and (f) the core litholog.



cm 35-47



cm 111-115



cm 122-124

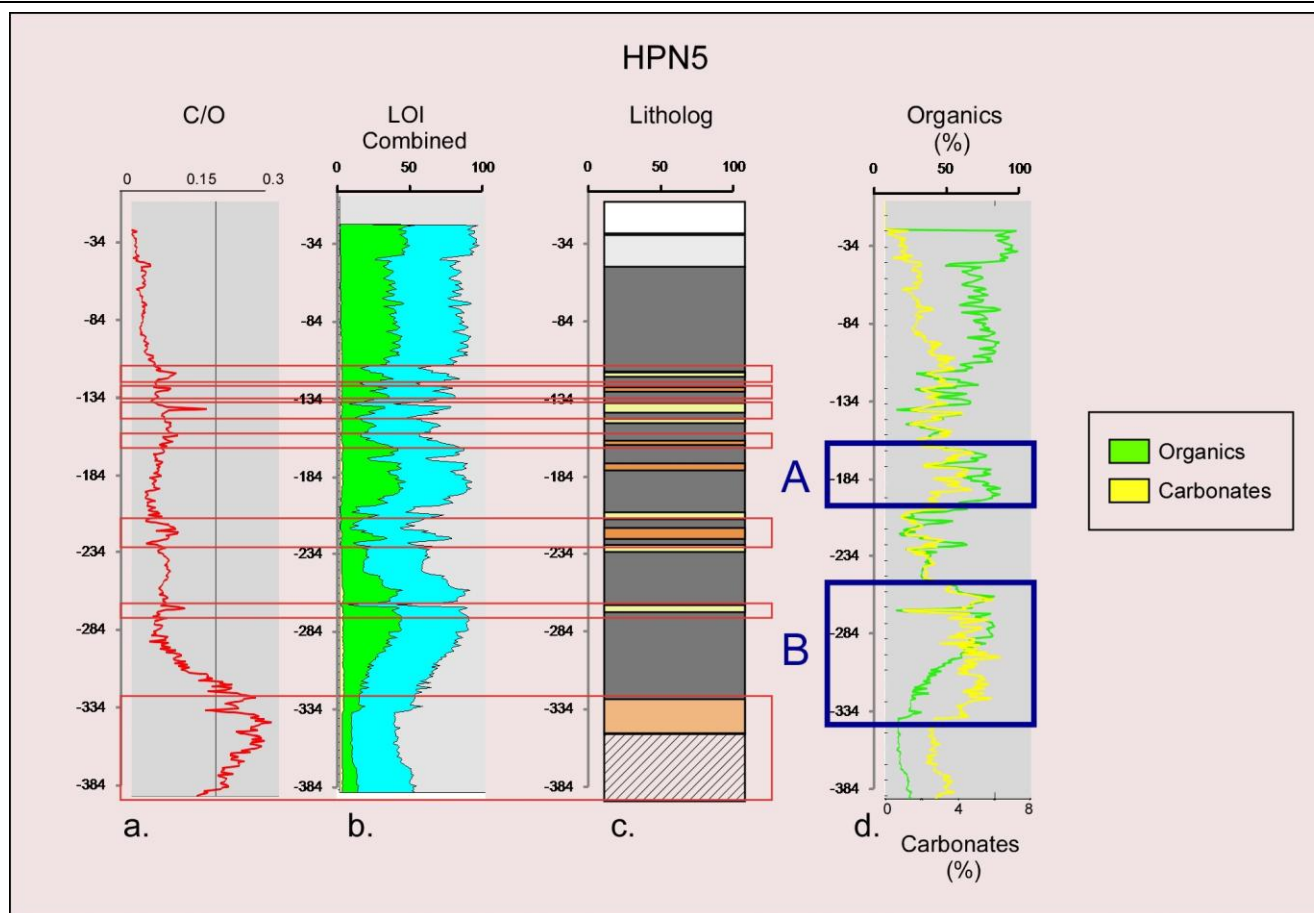


cm 132-136



cm 264-265

7.7 Photos of clastic layers occurring in core HPN5. Depth of layers are marked below each photo, these depths are measured from ground level, with sediment retrieval beginning at 20 cm (see text for fuller discussion of this issue).



7.8 The relationship between carbonate and organic values for core HPN5. As (a) is a graph of the carbonate values divided by organic values, spikes to the right indicate a relative increase in carbonates; the combined LOI curve and litholog are presented in (b, c). The nonlinear relationship (d) between carbonate (yellow) and organics (green) is clear when percentages of each are plotted against each other. The blue boxes marked A, B are the intervals of relatively high carbonate values; the C/O ratio (a) is fairly constant throughout A, but increases sharply downcore for B.

carbonate/organic ratio consistently these levels (**Figure 7:8a**), possibly marking an increase in marine material (red boxes, **Figure 7:8b**). The thick spike in this ratio below ~300 cm probably marks a slowly changing depositional environment, with a high carbonate ratio at the lower end corresponding to a deeper, more marine setting, and the upcore ratio decrease resulting from the steady development of a marsh/swamp environment.

Surprisingly, the relationship between carbonates and organics is different within the two high carbonate intervals, with the 25 cm interval beginning ~160 cm (“A”) corresponding to a relatively constant carbonate/organic ratio, while the 80 cm interval beginning ~250 cm (“B”) corresponds to a sharp downcore increase (**Figure 7:8a**). Again, this is evidence for the ability of LOI data to track sedimentary/environmental conditions accurately, with the ratio change below 250 cm most likely resulting from slowly changing environmental conditions (marsh/swamp development), while the ratio for the higher interval probably represents fairly static conditions.

7.5.1.2 Dating

Five plant/organic samples were selected from HPN5 and sent to the NOSAMS facility at Woods Hole Oceanographic Institute for AMS dating. The results are listed in **Table 7.1**. There is one date reversal, with the sample at cm 220 showing a date 440 yrs younger than the sample 89 cm higher up. The bottom two dates are overlapping at the 95% confidence interval, although separated by 82 cm.

Including all samples produces a depth/date graph with an intercept of 904 years and a R^2 value of 0.615 (**Figure 7:9a**). Removing the date for the sample at 220 cm improves the R^2 value to 0.908 and gives an intercept of 1067 years (**Figure 7:9b**), removing both that date and the one from 328 cm improves the R^2 value to 0.998 and gives an intercept of 432 years (**Figure 7:9c**),

removing the dates at 220 and 246 cm improves the R^2 value to 0.999 and gives an intercept of 1083 years (**Figure 7:9d**), removing the dates at 220 and 328 and artificially imposing an intercept of -54 yrs (AD 2004) gives an R^2 value of 0.965. Sedimentation rates for these calculations range from 0.10 – 0.06 cm/yr (9.8 – 18.1 yr/cm).

Removing the core's empty top 20 cm (the rootzone) from the calculations (in effect assuming that the depositional surface begins with the sediments, and that the root zone is irrelevant) produces increased intercept values along with identical R^2 values and depositional rates for each of the first four dating schemes (**Figure 7:10 a-d**). Forcing an intercept age of -54 years (surface = AD 2004) increases the depositional rate to 0.05 cm/yr (20.2 yr/cm) and lowers the R^2 value to 0.885 (**Figure 7:10e.**).

All of these scenarios present difficulties.

A regionally occurring type of systematic error is the hard water lake effect. This process commonly occurs in limestone areas where lake waters are depleted in ^{14}C , due to the leaching of old calcium carbonates from the surrounding limestone. This isotopic depletion is maintained in the shells of water dwelling organisms (mollusks, gastropods) formed at equilibrium with the lake water, resulting in falsely old dates. However, as all dated samples were of plant/organic origin, this type of error should not occur.

7.5 .1.3 Zonation

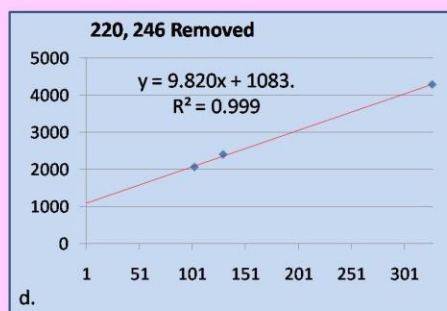
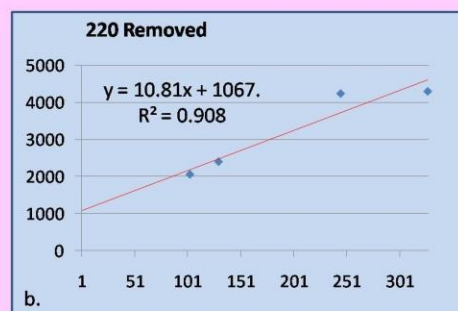
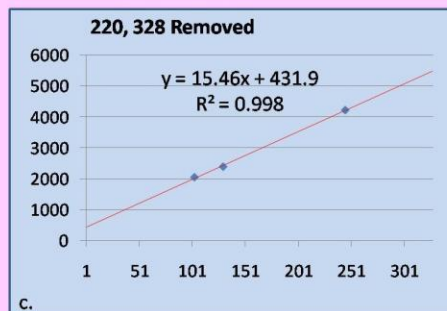
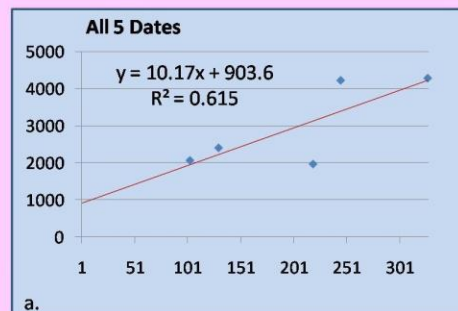
HPN5 can be divided into six zones, based on changes in the LOI curve (**Figure 7:11**). **7.5.1.3.1**

Zone 1(21-104) is generally highly organic. The upper segment, from 21-40 cm is mainly partially decomposed roots, with water values near 90% and organic content varying between 75-90%, The lower part is a black/brown peat composed of more deteriorated material, showing occasional small spikes in residual values; organics are generally >60%, but vary between 41-

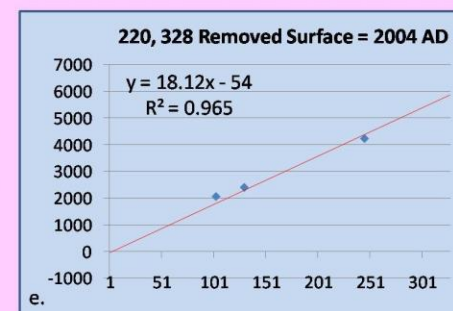
7.1 HPN5 chronology

Core	Depth cm	Material	Lab	Sample #	2 δ ¹⁴ C yr BP	2 δ Cal BP	%
HPN5B	104	Organic	WHOI	OS-72531	2060 ±30	1948-2118	1
HPN5C	131	Organic	WHOI	OS-71471	2400 ±20	2349-2486 2648-2650	0.996 0.004
HPN5D	220	Organic	WHOI	OS-71472	1960 ±20	1867-1950 1960-1971 1979-1984	0.973 0.02 0.007
HPN5E	246	Organic	WHOI	OS-72427	4230 ±50	4782-4869 4610-4768 4584-4599	0.41 0.575 0.015
HPN5F	328	Organic	WHOI	OS-71603	4290 ±20	4836-4866	1

¹⁴C yr
Age



20 cm rootzone included



Depth (cm)

7.9 Depth-date graphs for HPN5, including the root zone (i.e. sediment retrieval begins at 20 cm depth). Five inconsistent dates were recorded for the core; the graphs are based on (a) all five dates, (b) four dates, with the date from 220 cm removed; (c) three dates with the dates from 220 and 328 cm removed; (d) three dates with the dates from 220 and 246 cm removed; (e) three dates with the dates from 220 and 328 cm removed and an surface intercept of AD 2004 (date of retrieval) artificially imposed.

79% ; water values are between 79% and 89%.

7.5.1.3.2 Zone 2(105-160) is also basically black/brown highly decomposed peat, with lower organic content, interrupted by several clastic layers. Organic content in the peat layers are generally >40% and only reaches 60% for a single cm, while in the clastic layers organic content is usually <30%, reaching a low of 8% at cm 135.

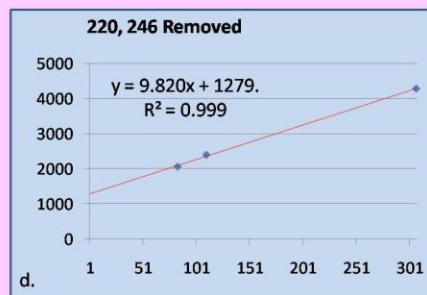
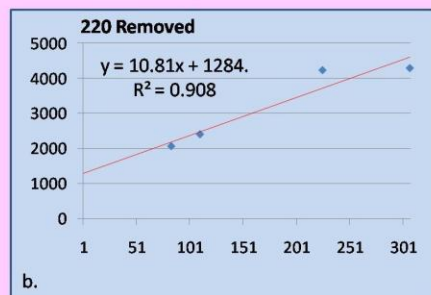
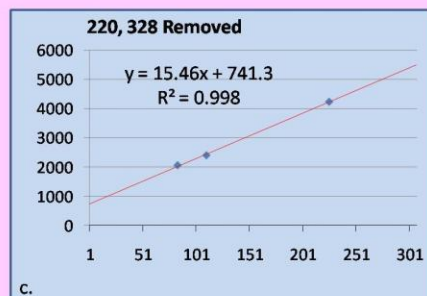
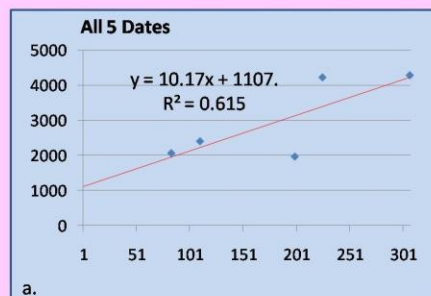
7.5.1.3.3 Zone 3(161-194) is primarily black/brown peat, with slightly elevated carbonate values. There is a single clastic layer (brown clay) at 169-172 cm where water dips to 67% and organic to 29%. Otherwise water varies between 76-87% and organics from 53-79%.

7.5.1.3.4 Zone 4(195-245) resembles Zone 2, being primarily a low organic black/brown peat, interrupted by repeated (three) clastic layers. In the peat sections water content is generally >65%, but varies from 62-84%, while organic content, generally >30%, varying between 20-56%. For the three clastic intervals (202-206 cm, 212-218,224-227), water content is generally <65%, and organic content <20%, reaching a minimum of 10%. The bottom two cm of the middle clastic layer is mixed with organics.

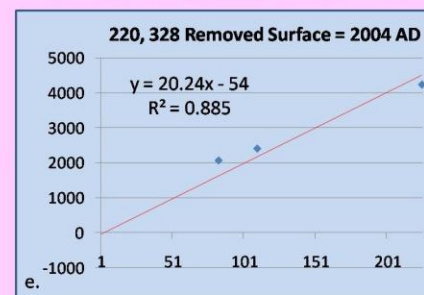
7.5.1.3.5 Zone 5(246-332) is a transition zone; the top resembles Zone 3, with high water (>80%) and organic (65%) values, apart from a single, dramatic clastic layer at cm 263-265, where water content drops to 49% and organic to 7%. From ~ cm 282 to the bottom of the zone, the material gradually becomes increasingly clastic, with water and organic values decreasing by 35% and 45%, respectively, while residuals increase ~45%. This section also exhibits slightly higher carbonate values. The division between Zones 5 and 6 is somewhat arbitrary, due to the gradual nature of the transition.

7.5.1.3.6 Zone 6(333-384) consists primarily of black clay, although organics increase near the bottom. Above cm 367 residual content remain >85 % and organic <13%, while at core bottom

¹⁴C yr
Age

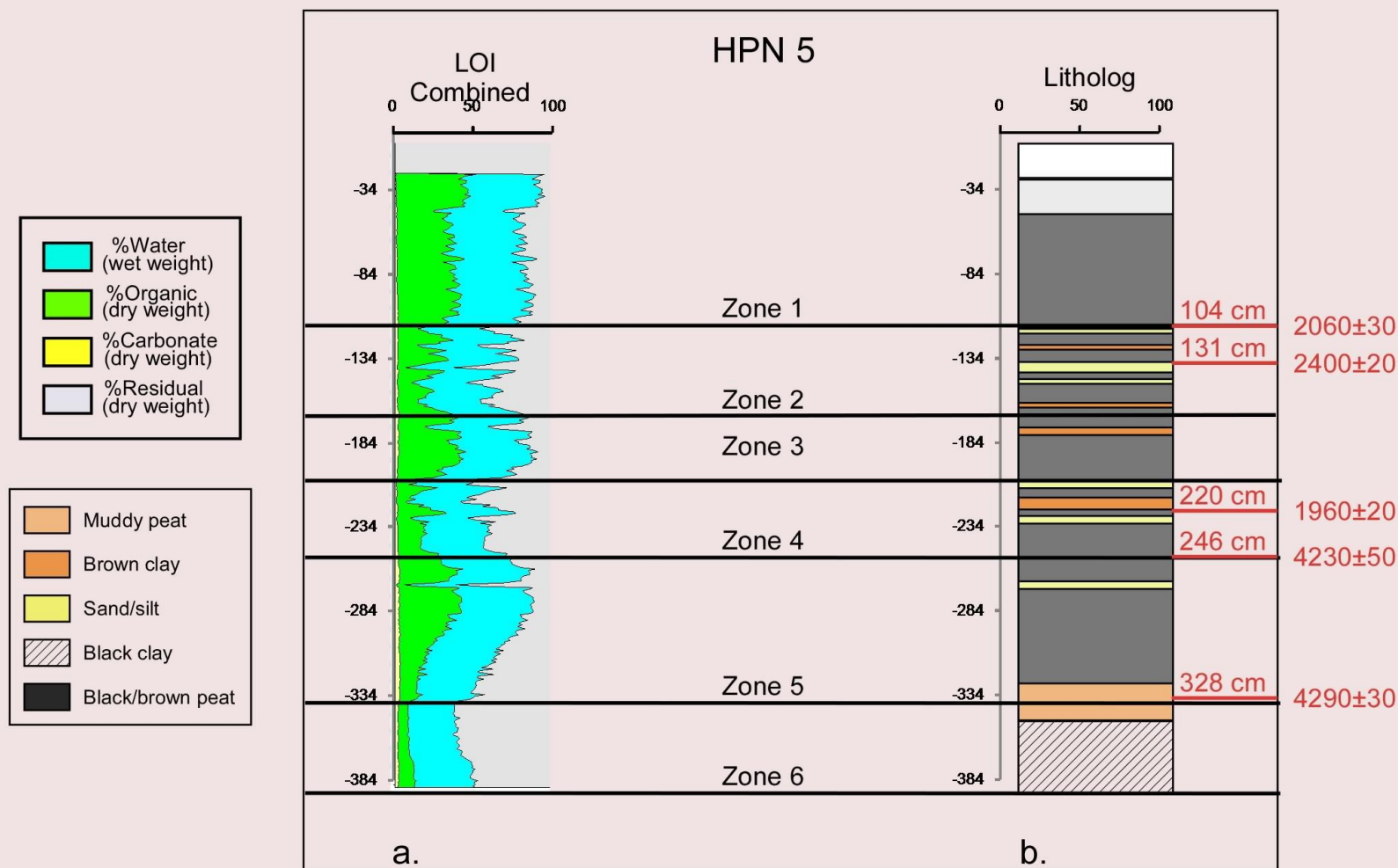


20 cm rootzone removed



Depth (cm)

7.10 As in 7:10, but with the 20 cm root zone removed; i.e. the depth that sediment retrieval begins is considered 0 cm. However, listed depths for dating samples continue under the earlier nomenclature to avoid confusion with other figures. For example, the sample referred to as “220 cm” is the same sample referred to as “220 cm” in Figure 7:10, although its measured depth is now 200 cm.



7.11 HPN5 zonation based on (a) LOI and (b) lithologic data. Depth of zone changes are given, measured from ground level, with sediment retrieval beginning at 20 cm.

the respective values are 79% and 18%.

7.5.1.4 Transect Correlation

7.5.1.4.1 HPN1

HPN 1 is the most seaward core in the transect, extracted from the palmetto swamp 230m inland from the sea. This is a composite core, consisting of seven separate peat borer sections, penetrating to a total depth of 359 cm. Core depth indicates that it is located over a depression in the antecedent dune system (**Figure 7:5**). Of particular interest is the fourth section from 155-204 cm, which is characterized by an extremely loose and unconsolidated matrix of large organic pieces, mixed with sand grains and mica (**Figure 7:12**-far left). The low density of the material is quite unusual, especially given that it covered by >1.5 m of sediments. Equally unusual are the vertically positioned undecomposed organic material >5cm in length that occur in this section. Three plant/organic samples were dated from HPN1. The results are listed in **Table 7:2**, and shown graphically in **Figures 7:12, 13**. Plotting depth vs. ^{14}C dates (**Figure 7:12 inset**) produces a graph with an unforced intercept of -54 years (AD 2004) years and a R^2 value of 0.969. It should be noted that as this core was taken in the palmetto swamp the sediments begin at ground level and there is no missing root zone. The calculated deposition rate is slightly faster than in the marsh, with 1 cm accumulating in just over 8 years (8.3 yr/cm or 0.12 cm/yr).

7.5.1.4.2 HPN2

HPN2 is a composite core consisting of two peat borer sections extracted from the marsh 431 m from the sea. The core penetrated to a depth of 103 cm. The top 21 cm (root zone) was not recovered.

7.5.1.4.3 HPN3

HPN3 is located in the marsh, 441 m from the sea. The core consists of three peat borer sections

that penetrated to 123 cm. The top 28 cm were not captured (rootzone).

7.5.1.4.4 HPN4

HPN4 consists of three peat borer sections, from 50 cm (the top 49 cm were not recovered) to 174 cm. The core location is in the marsh, 460 m from the sea.

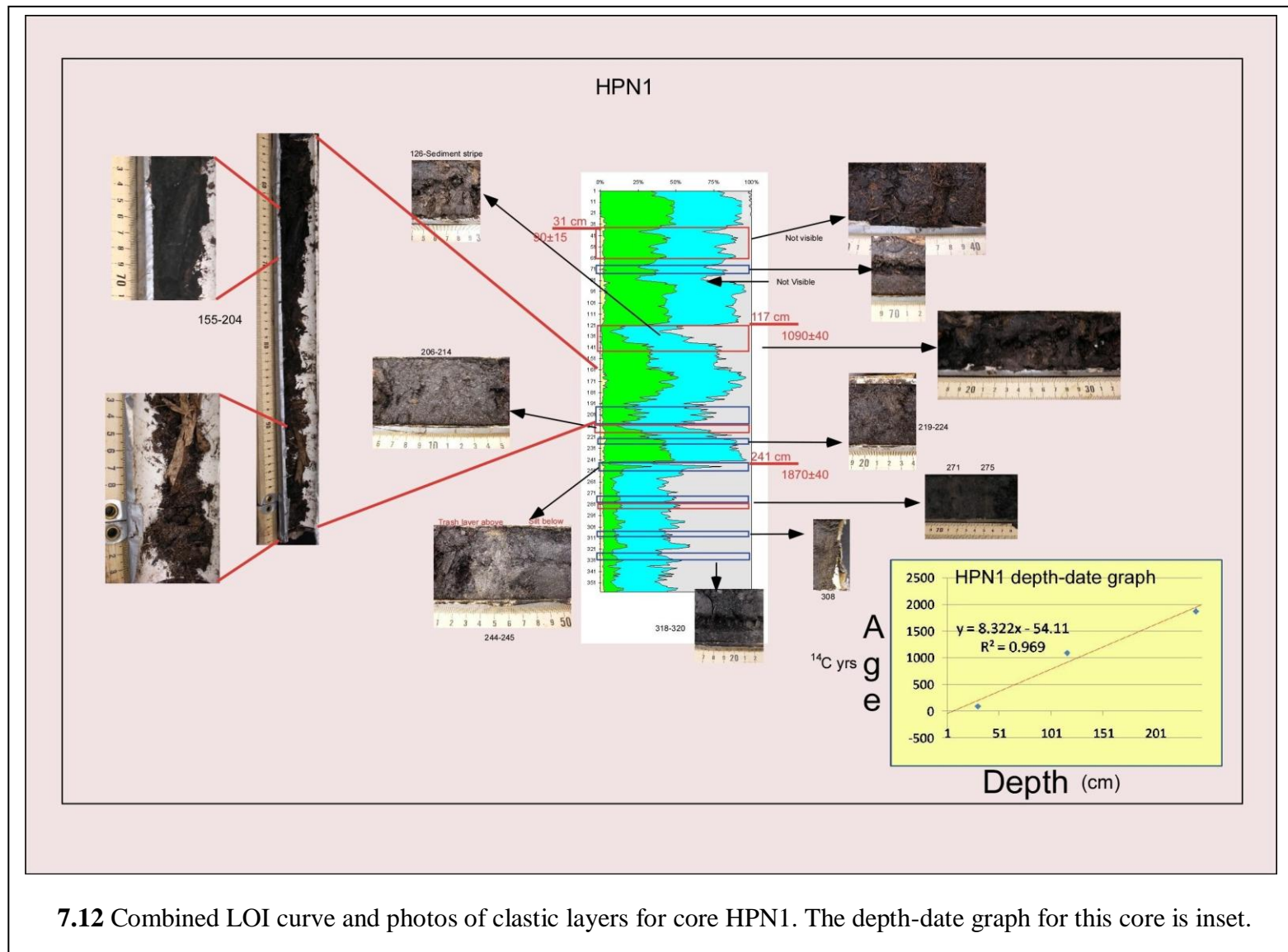
The three middle cores, HPN2, 3, 4, form a coherent grouping, as they are all relatively short (103-174 cm), end in a coarse sand layer and contain a much higher percentage of sand than do the longer cores at the transect ends, both as distinct sand layers and scattered throughout the finer material.

The radiocarbon dates and LOI curves for the HPN transect are presented in **Figure 7:13**; clastic layers are marked by red boxes.

7.5.1.5 Grain Size

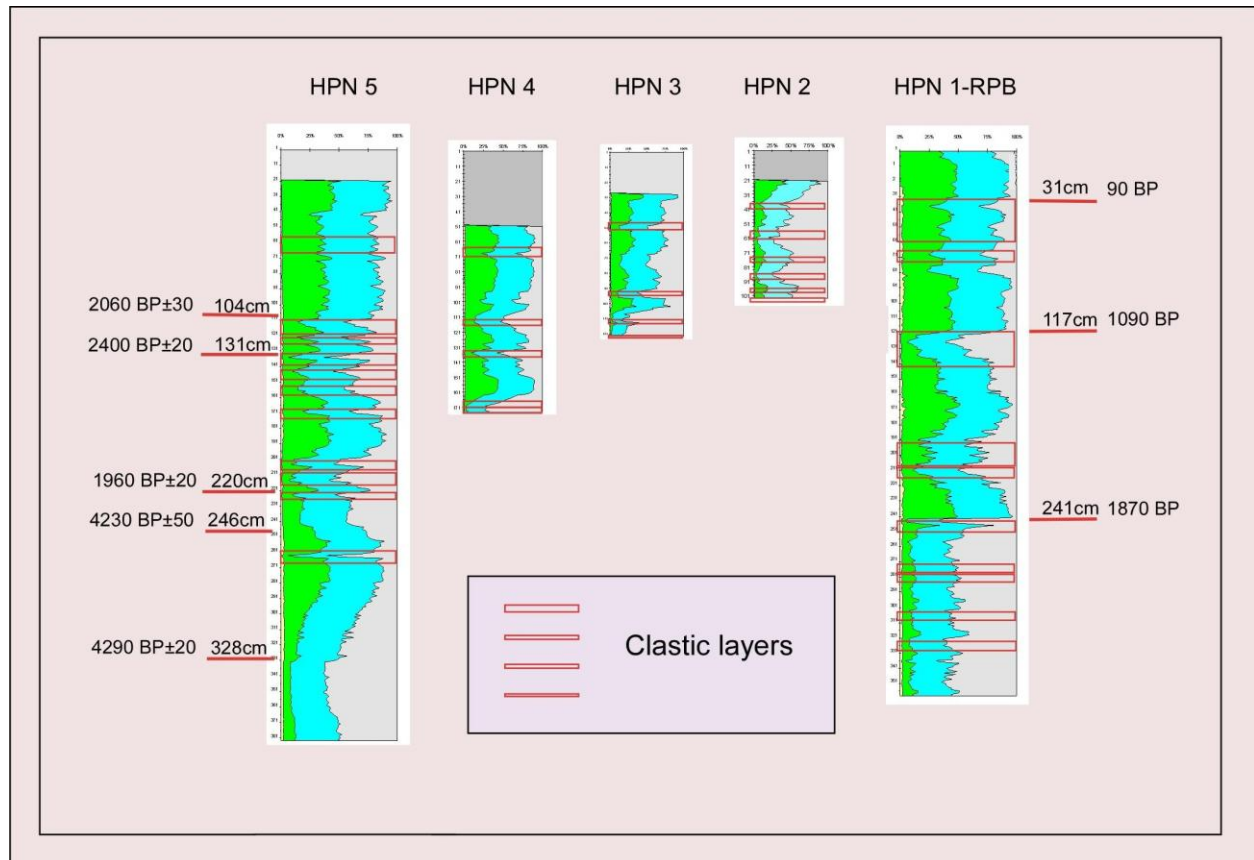
Grain size analysis was conducted on selected sand layers from HPN2 and 3, as well as a sample from the beach directly east of the transect. Because this analysis was conducted by means of a series of stacked sieves, only samples containing larger grained material were tested. Samples that contained organic materials were washed and the clay and silt size particles removed. Results are given in for phi scale, where $\phi (\varnothing) = -\log_2 d$ (where d is the diameter in mm). This means that phi values increase as grain size decreases (i.e. -1 phi is the boundary between gravel and sand, 4 is the boundary between sand and silt, and 8 the boundary between silt and clay) (Masselink and Hughes, 2003). Results are shown in **Figure 7:14**; percentages are by weight, larger grain size classes are to the left, smaller to the right.

The beach sample (red dashed line) has a bimodal distribution, with peaks in both the very coarse and coarse classes, as can be seen in both the photo and grain size graph (**Figure 7:14 a, b, c**). The distribution of the interval samples, especially for HPN2 (**Figure 7:14a**), closely



7.2 HPN1 chronology

Core #	Depth	Material	Lab	Sample#	C14 Age	Error Bar	Cal yr BP 2 σ	Probability	AD/BC
HPN1A	31	Plant/Wood	WHOI	OS- 71470	90	15	32-83	0.438	1867-1918AD
							89-91	0.002	1859-1861AD
							96-137	0.267	1813-1854AD
							223-256	0.292	1694-1727AD
HPN1C	117	Plant/Wood	Beta	212913	1090	40	928-1070	1	880-1022 AD
HPN1E	241	Plant/Wood	Beta	212914	1870	40	1712-1890	1	60-238AD



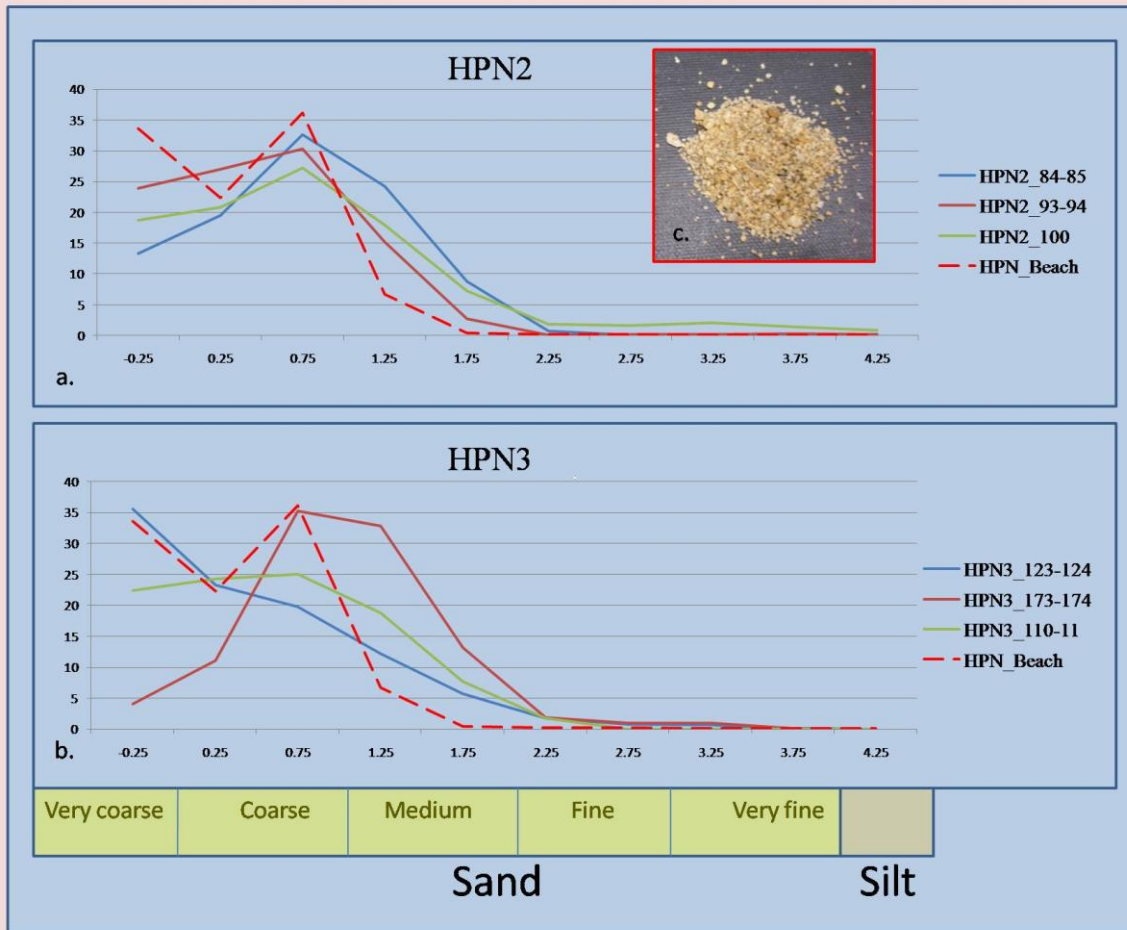
7.13 The HPN transect as depicted by combined LOI curves for each core, assuming equivalent surface elevation at each site. Radiocarbon dates are marked, using the standard depth measurement (i.e. 20 cm root zone is included). Clastic layers are marked by red boxes.

resembles that of the beach sand, once the very coarse fraction is excluded. The HPN3 intervals are generally finer (**Figure 7:14b**), however the mode for two of the samples remains within the coarse fraction, while the third sample is predominately very coarse sand.

7.5.2 Discussion

7.5.2.1 Geomorphic Controls

Unlike many coring sites, surface and subsurface topography are not parallel across this transect. The cores at either end of the transect reached depths > 350 cm, while the middle three cores penetrated <2 m cm before encountering a coarse sand layer. The depths of the three middle cores decrease seaward, suggesting they are located on the landward edge of a subsurface topographical high (**Figure 7:5**). This antecedent relief is fairly steep, as core depth increases by 210 cm over a 7 m lateral span (HPN4-HPN5). Given the inferred contours and the coarse sand encountered at the interface, the most likely cause of this subsurface topography is an antecedent dune and swale system, so common in coastal areas. A very similar topography is encountered at CBL (see below), supporting the idea that a large scale coast parallel linear dune system underlies the present surface. Further research is necessary to determine the number of dunes, as systematic probing beyond the ends of the transects was not undertaken. Because sedimentation normally occurs subaqueously, in such systems each swale may record a separate environmental history, as different swales may/may not contain water at the same time. Individual swales may be part of the same or different systems, and connectivity may change over time, depending on such factors as water level, dune height, precipitation events, and the opening/closing of barriers. In a coastal environment, dramatic variations can occur over extremely short distances, with one swale (set of swales) being influenced mainly by inland/freshwater conditions while another is driven by marine influences.



7.14 Grain size for sand samples (a, b) from cores HPN2, 3 and the beach in front of Hopkins village; a (c) photo displaying the bimodal grain size distribution for the beach sample.

In this particular case it seems possible that sedimentation was not uniform across the transect, as a sample from a depth of 246 cm in HPN5 gives a date of 4230 ^{14}C yr BP, while a sample from nearly the same depth (241 cm) from HPN1 gives a date of 1870 ^{14}C yr BP. This suggests that during at least part of the study period being studied these two locations were in separate systems, possibly recording separate histories. By their placement (only seven m separates cores HPN4 and HPN5) and the subsurface slope, it is likely that the three middle cores were on the upland seaward edge of the system containing HPN5. The bottom sand in these three cores is presumed to represent the top of the relict dune; the organic/water rise at the lower end probably represents the submergence of these locations and the inception of wetland development. The sediment records contained in these cores therefore are probably parallel to, though shorter than, those from HPN5. These shorter histories could be either abbreviated or condensed. In an abbreviated history, cores from higher elevations do not record the earlier environments, resulting in parallel sedimentation from the top down to a certain depth (the basal sand), at which point it ceases. In a condensed history, the higher cores would record the entire environmental history, but in thinner intervals.

7.5.2.2 Sedimentation Scenarios

HPN1 has a depth of 359 cm; assuming constant sedimentation, extrapolating from the dates at 117 and 241 cm gives basal dates of 3344 ^{14}C yr BP and 2786 ^{14}C yr BP respectively. Multiplying the depth by the calculated average deposition rate of 8.3 yr/cm produces a basal date of 2987 ^{14}C BP. It seems reasonable to apply a basal date of ~3000 ^{14}C yr BP to the core. Assuming an error bar of 40 years, this calibrates to a date of 3072 – 3335 cal yr BP. HPN5 has a depth of either 384 or 364 cm, depending on how the 20 cm rootzone is treated. The basal age of this core, calculated by a number of dating scenarios based on constant sedimentation and the

dated samples and average deposition rate, varies from 4809 to 7313 ^{14}C yr BP, producing a number of calibrated date ranges from 5467-8187 cal yr BP. It is reasonable to assume that the deposition began at least 5500 yr BP.

7.5.2.2.1 Scenario 1

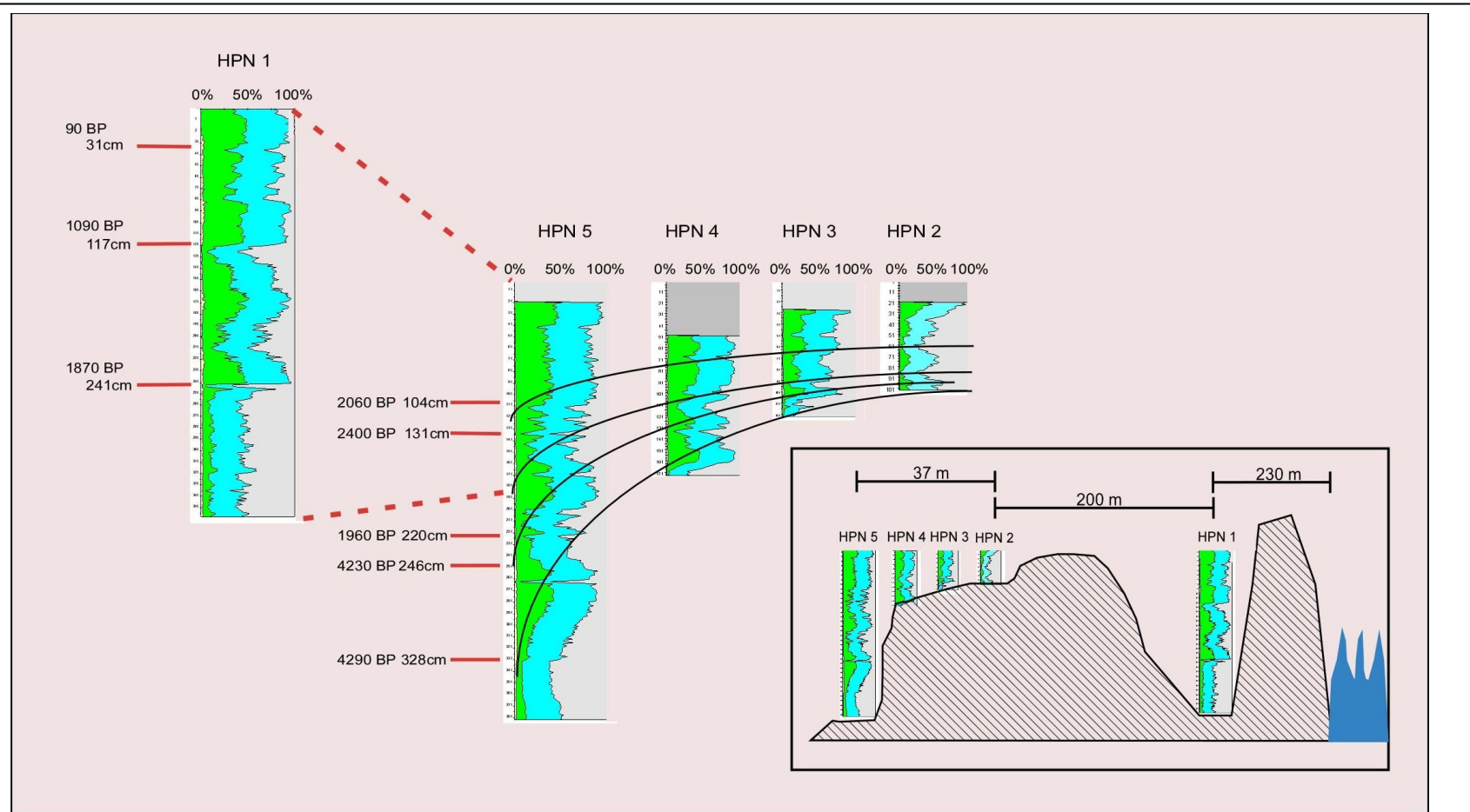
One interpretation of the effect of the subsurface topography suggests two, possibly separate, environmental records; a shorter one (~3000 years) recorded by HPN1 in a seaward swale, and a longer one (>5500 years) recorded by HPN5 in a deeper, landward swale, and by HPN 2, 3, and 4 on the swale edge. If these records are recording separate systems the dates do not require a common depth across the transect, nor need the records necessarily match. HPN1 could possibly provide a greatly expanded section correlating to the top (or missed) portion of the other cores.

Figure 7:15 is a diagram of this possibility. The curved lines are an attempt to show preferential deposition in the deeper cores, with the difference becoming less as the elevational differences reduce. This corresponds to a condensed history for the shorter cores; in the case of abbreviated histories, interval thickness would be fairly equal across the transect, but begin at a later dates at the higher sites.

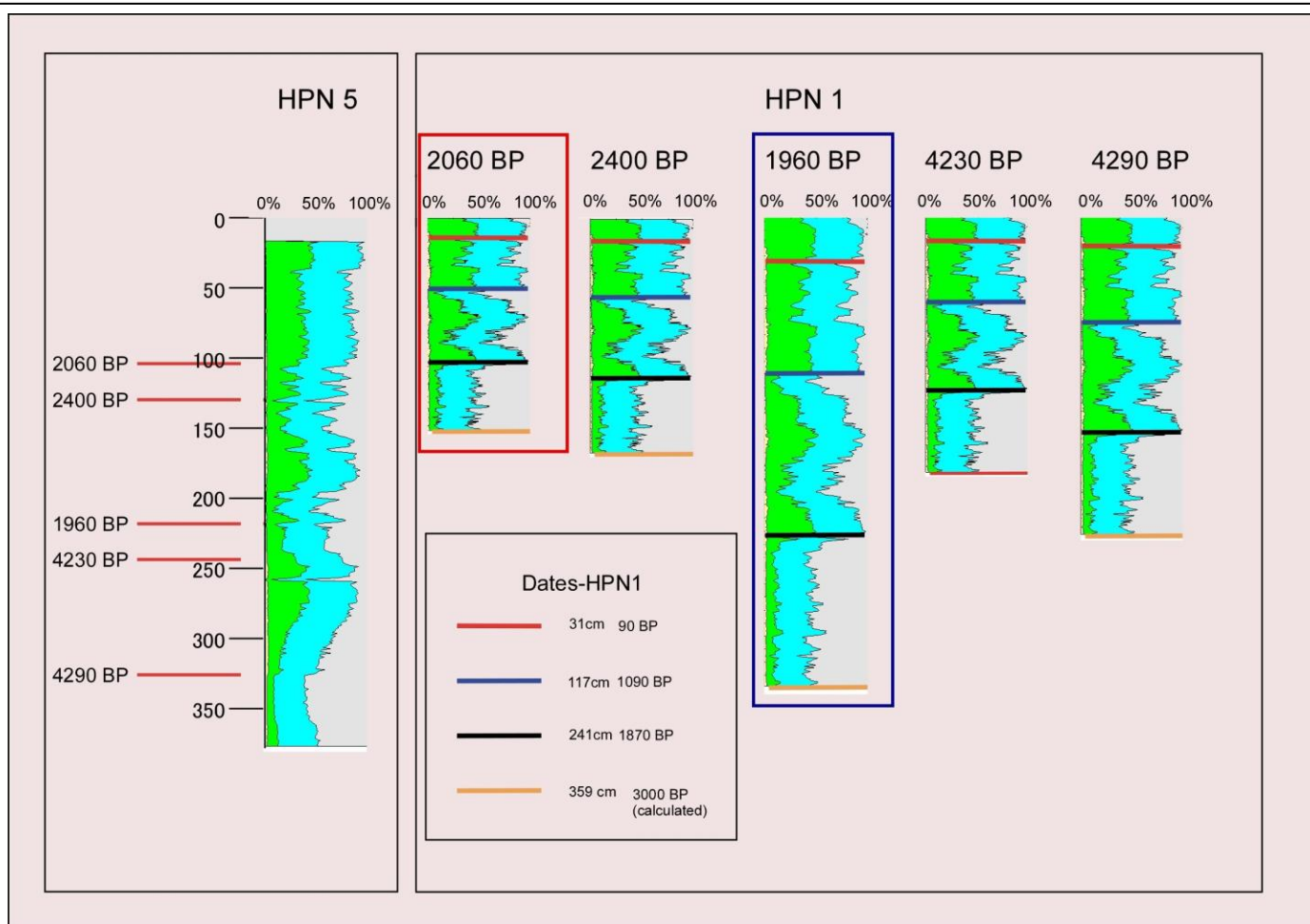
Using the basal date of 3000 ^{14}C yr BP calculated above, the HPN1 LOI curve can be stretched/contracted to correlate this date with the calculated 3000 ^{14}C yr BP depth on the HPN5 LOI curve for each of the five dated samples (**Figure 7:16**). None of these manipulations result in a very close visual match between the cores. However, if different systems are being recorded, the disjoint is not unexpected.

7.5.2.2.2 Scenario 2

An alternative possibility is that sedimentation occurred concurrently and equally across the transect, with the nonconcurrent chronologies resulting from topographically driven dating



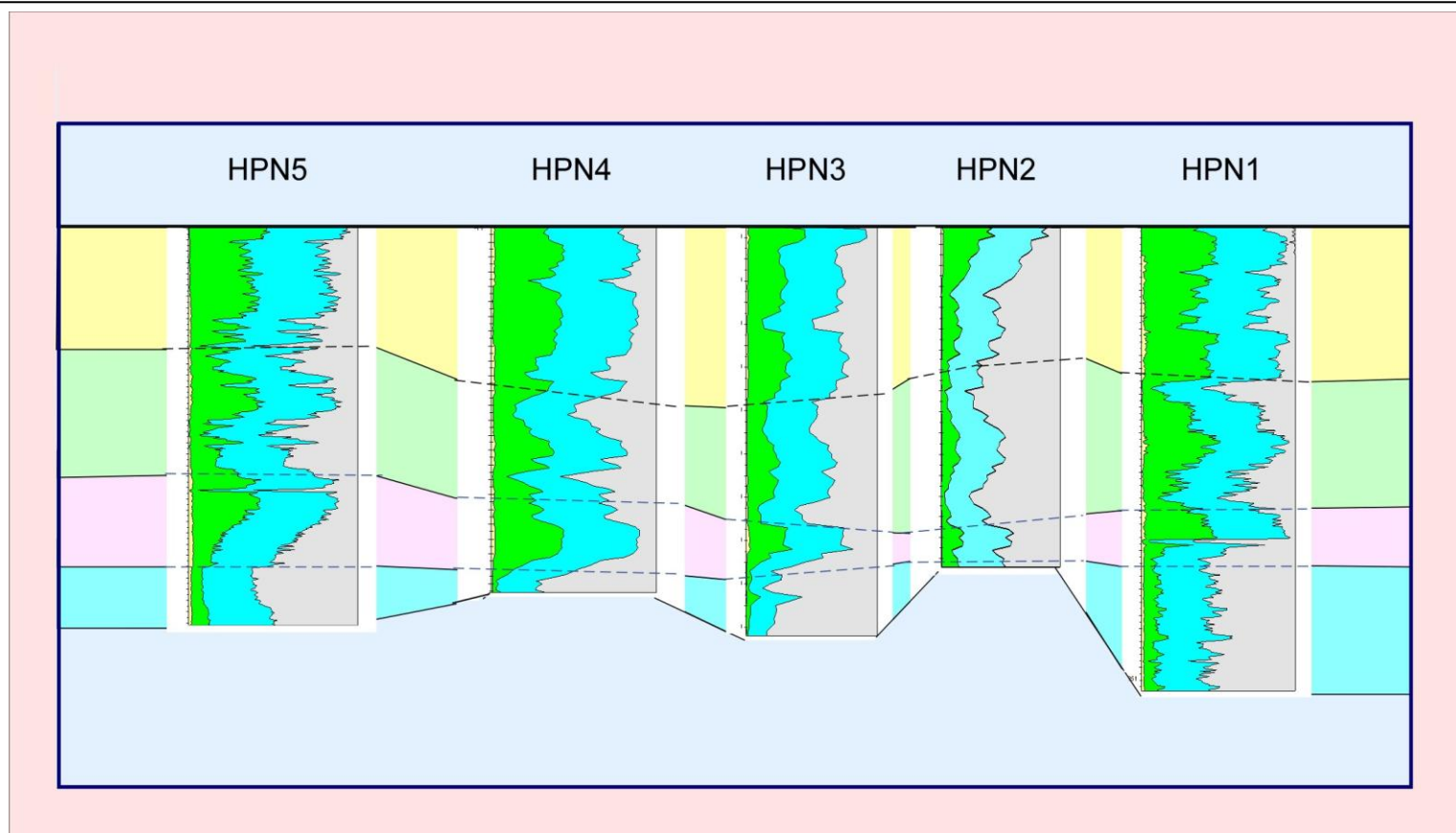
7.15 Conceptual model of possible temporal correlation of transect cores, based on separate histories for cores HPN1 and HPN2-5, derived from isolating effect of subsurface topography (inset).



7.16 Potential chronological matches between cores HPN1 and HPN5. The calculated basal age of 3000 ^{14}C yr BP for HPN1 is aligned by depth to corresponding calculated ages for each of the five dated samples from HPN5. For example, the 3000 ^{14}C basal date for HPN1 corresponds to a depth of 151 cm for HPN 1, based on the dated sample of 2060 ^{14}C for 104 cm depth (red box) and 337 cm, based on the dated sample of 1960 ^{14}C for 220 cm depth (blue box).

errors at HPN5. As discussed above, just east of HPN5 the subsurface has a 27° slope (210 cm vertical rise over 7 m horizontal distance). It is possible that this steep subaqueous slope has experienced repeated slope failure and thereby delivered extraneous material to the lower site (HPN5), contributing to the confused dated chronology. Since the relict dune would by necessity predate the current deposition such slumping would produce erroneously old dates if the dated sample contained slumped material. Under this scenario, the transect cores could be correlated stratigraphically and only the coherent HPN1 chronology used. There is some support for this view. If all the LOI curves are stretched artificially (each core stretched/contracted as a unit, thereby changing length, but maintaining shape) with all basal sand layers are set at a common depth, a fairly obvious stratigraphic parallelism can be noted (**Figure 7:17**).

One difficulty with this scenario is that parallel transect-wide deposition requires parallel transect-wide depositional environments, inferring that all sites were submerged during the entire depositional period. This would be unlikely if the >5500 year chronology from HPN 5 is correct, as sea level at the time was ~200 (Gischler and Hudson, 2004) to 500 cm (Toscano and Macintyre, 2003) below the present, meaning that the sites of the shorter cores would have probably been subaerial and less likely to accumulate sediments. However, if the entire record spans only the approximate 3000 years indicated by the HPN1 dates, this would not present a problem, as sea level rise for that period has probably only been from ~80 (Gischler and Hudson, 2004) to ~210 cm (Toscano and Macintyre, 2003). Because HPN1, which currently occupies the highest elevation of all the cores (the only one not cored in standing water) has been accumulating sediments at a steady rate as indicated by the dates, it is possible that the lower elevation cores were capable of recording throughout the period. However, there are serious difficulties in positing that sedimentation began only ~3000 years ago at HPN5, which has a



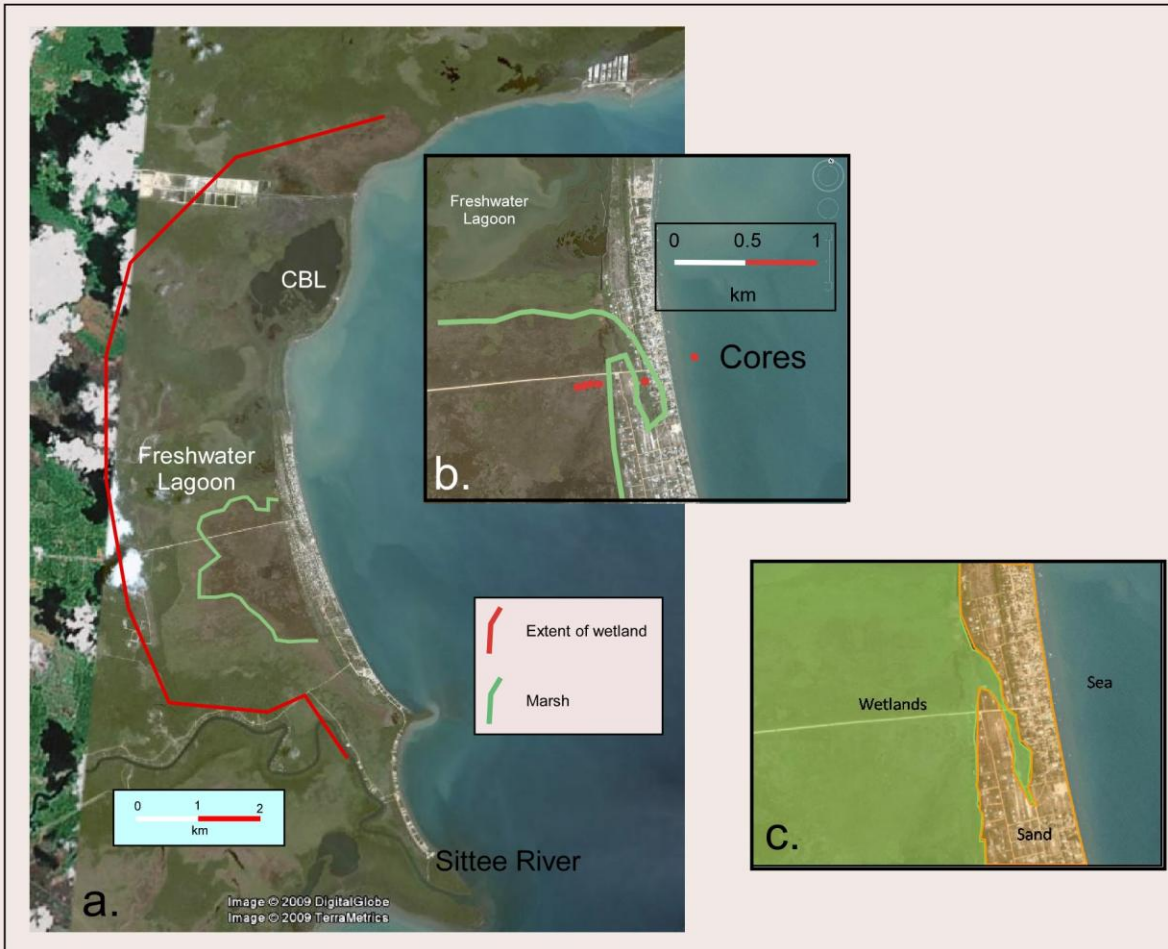
7.17 All cores in the HPN transect artificially stretched to achieve stratigraphic matching. All core tops are set at an equal depth, as are the tops the basal sand unit for each core.

depth of nearly 4 m, as it seems unlikely that such deep surfaces would not have begun accumulating material at an earlier date.

7.5.2.2.3 Scenario 3

A third possibility is that deposition ceased at some point at our inland sites, thereby explaining the large intercept dates for HPN5. Under this scenario, the sedimentation rate was greater than sea level raise from HPN2 through HPN5, with all the declivities filling with sediments until they were at sea level, after which, due to the basically static sea level and the resultant lack of accommodation space, they ceased to accrete. Date of cessation of deposition could vary between cores, depending on elevation. The date of cessation of deposition is the intercept given by the trendline, which for HPN5 is between 432 and 1284 ^{14}C yr BP, depending upon the interpretation of the 20 cm rootzone, and choice of dating scheme (**Figure 7:9, 10c, d.**). HPN1 apparently continued to receive sediments continuously through the present, as evidenced by an unforced intercept of -54 yrs, giving a surface age of AD 2004, the year in which the sample was collected. This implies that HPN1 was recording a different environment, one which remained subaqueous longer than the HPN2-5 sites. At first pass, this seems unlikely, as it has the highest elevation of all sites.

A closer look at the present surface topography perhaps can help inform on this question. As can be seen (**Figure 7:18**), a semicircular wetlands (outlined in red), ~2 km wide extends inland from north of Commerce Bight Lagoon (CBL) to the natural levee of Sittee River in the south. The deeper sections of this low area are CBL, Freshwater Lagoon, and the central section of the Hopkins Marsh (outlined in green). Present topography shows the area of the palmetto swamp (HPN1) to be a finger of the larger Hopkins Marsh (**Figure 7:18c**). It is probable that the presence of this sliver results from prior topography, with the palmetto swamp being the surface expression of a biological succession that has filled this narrow depression between two



7.18 Google Earth imagery depicting (a) HPN topography, dominated by a large wetlands (outlined in red), consisting of three deeper sections; namely CBL, Freshwater Lagoon and the Hopkins Marsh (outlined in green). (b, c) show the topographical connection between the HPN1 and HPN2-5 coring sites.

vegetated dunes, suggesting that the ancient swale over which HPN1 is located was probably previously connected to the larger marsh through a connection to the north. Depending upon the state of the connection, this small depression could, therefore, have either been part of the larger system, or have been a closed basin, recording a separate environment.

The dissimilarities between the HPN1 and HPN5 chronologies make Scenario 2 (concurrent sedimentation across the transect) unlikely. Although slope collapse provides a possible mechanism for explaining dating inconsistencies, the high R^2 values (0.998, 0.999) (**Figures 7:19, 10c, d.**) for the alignment of three HPN5 dates weakens the argument. Scenario 1 (separate histories due to independent environmental conditions) alone does not explain the large intercept values for HPN5. For these reasons we regard Scenario 3 (arrested deposition at HPN5, with a separate, shorter history at HPN1 that continued to the present) as the most likely scenario and the basis for further discussion. The stratigraphic correspondence of the LOI curves (**Figure 7:17**) supports the view that cores HPN2-4 recorded condensed versions of the HPN5 record.

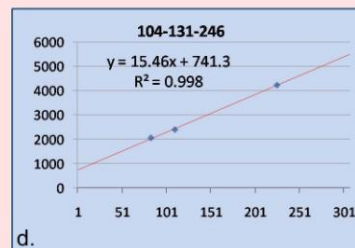
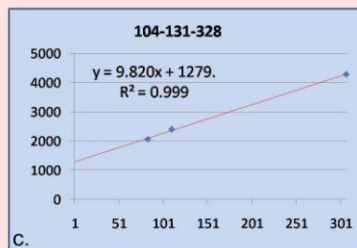
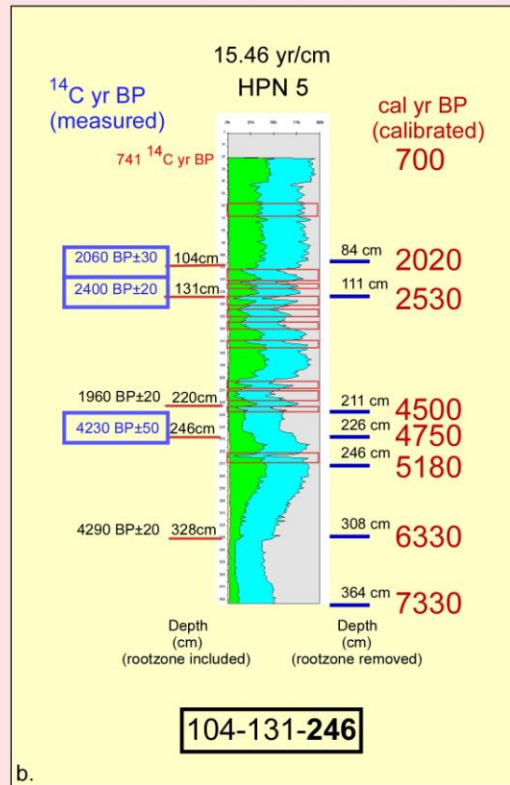
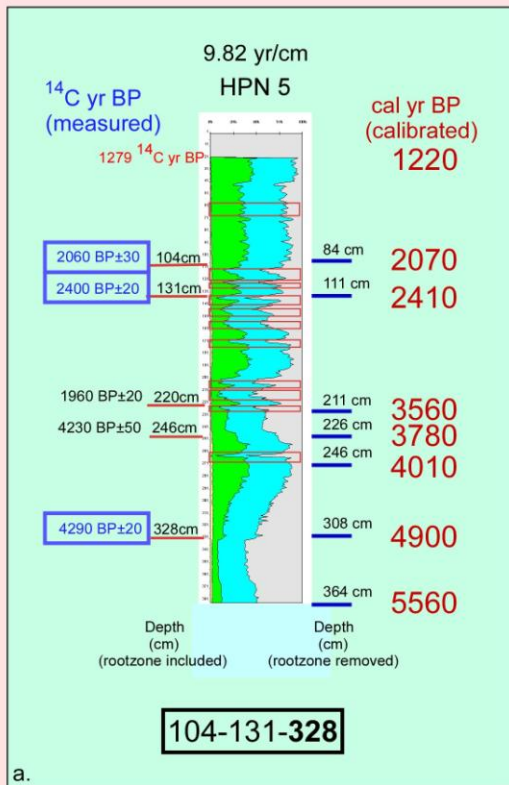
7.5.2.3 Transect Dating

7.5.2.3.1 HPN1

Given the good date-depth match for HPN1 ($R^2 = 0.969$) and the unforced surface intercept of AD 2004, it seems reasonable to accept these dates as accurate.

7.5.2.3.2 HPN5

Determining a chronology for HPN5 requires the examination of several issues. The first concerns the 20 cm deep rootzone, which can be regarded either as unrecovered (missing) sediments, or as ephemeral material, irrelevant to the paleoenvironmental record. As seen above (**Figures 7:19c, d, 10**), deleting this material increases the intercept dates, without affecting sedimentation rates or the fit of the graph. Visual inspection of the rootzone (both in the field and



7.19 Alternative HPN5 chronologies. In (a) depth dates are calculated from dated samples at 104, 131, 328 cm, while in (b) calculations are based on dates from 104, 131 and 426 cm. (c, d) are the depth-date graphs for the two scenarios.

from photos), combined with the near total lack of mineral material within the zone, lead us to believe that this zone will not be preserved in the sedimentary record, and that surface accretion results in a vertical movement of the rootzone, with sedimentation occurring below this zone at the root-soil interface. Therefore the age-depth graphs in **Figure 7:10** (top 20 cm removed from the graph) are more likely to be correct than those in **Figure 7:9** (top 20 cm left blank).

The second major decision concerns the selection of dates, as it is clear from the date reversal and two overlapping dates separated by 82 cm, that not all the dated samples can be correct. Because the dates of 2060 ^{14}C yr BP from 104 cm and 2400 ^{14}C yr BP from 131 cm match well, it seems likely that the younger date of 1960 ^{14}C yr BP from nearly a meter lower in the core (cm 220) is most likely erroneous, probably influenced by the presence of younger root material. We therefore reject this date. Farther down, at least one of the overlapping dates (4230 at 246 cm, 4290 at 328 cm) must be wrong, as it seems highly unlikely that 82 cm of sediment accumulated nearly instantaneously. The choice is not clear, both samples give extremely high R^2 values (0.998, 0.999) when against the dates from 246 and 328 cm (**Figures 7:19 c, d**).

Figure 7:19a shows the core chronology based on the dated samples from 104, 131 and 328 cm. The intercept is 1279 ^{14}C BP, with a deposition rate of 9.82 yr/cm (0.10 cm/yr) (**Figure 7:19c**). Using this deposition rate ^{14}C yr BP dates were calculated at various intervals along the core, calibrated into cal yr BP using the Calib 5.0 program (<http://calib.qub.ac.uk/calib/calib.html>), assuming a standard error of 40 years. These calibrated dates are shown in red. In order to facilitate correlation with previous diagrams in this chapter, the depths shown on the left side of the LOI diagram include the discarded 20 cm rootzone, while the depths used to produce the age-depth graph (i.e. the empty 20 cm rootzone is excluded and 0 cm marks the sediment interface where collection began) are shown on the right side. **Figure 7:19b** shows the same for the

chronology based on the dated samples from 104, 131, and 246 cm. The intercept becomes 741 ^{14}C BP, with a deposition rate of 15.46 yr/cm (0.06 cm/yr) (**Figure 7:19d**).

Similar calculations were used to determine calibrated ages for HPN1, permitting stratigraphic correlation with each of the two HPN5 chronologies (**Figure 7:20**). In both cases chronological and stratigraphic coincidence occurred, with a sharp increase in clastic layers occurring ~2000 cal yr BP in both HPN1 and HPN5. The cm depth of HPN 1 (based on the trendline deposition rate) corresponding to the intercept age for the top of HPN5 was calculated for both chronologies (157 cm for the shorter chronology (**Figure 7:20a**), and 91 cm for the longer)(**Figure 7:20b**), and inferred correlation lines drawn (dashed red lines).

The choice of dates used to create the chronology is obviously important, as the calculated HPN5 basal date changes from 5560 to 7330 cal yr BP, depending upon the date selected. The correlation with HPN1 also varies, with the section from 1-93 cm on HPN5 corresponding to either the interval from 91-245 cm or 157-245 cm for HPN1. A sample has been taken from the top of HPN5 for AMS dating to determine the intercept age in order to resolve this question. However, presently lacking such evidence, other means of date selection must be utilized. The date from the sample selected from 328 cm in the basal clay is suspect, as in other transects included in this dissertation (particularly core HJ3 from Turneffe Atoll, **Chapter 8**); incongruously young dates have resulted from samples taken in similar basal sections. This is possibly due to the ease with which younger roots can penetrate these preflooding environments, suggesting that the sample from 328 cm might be contaminated similarly. On the other hand, the date for the sample from 246 cm may be erroneously old, having resulted from the reworking of older material or the slope failure mentioned above.

Figure 7:21 shows the LOI correlations for the overlapping sections of HPN1 and HPN5, based on the two different deposition rates displayed in **Figure 7:20**. In both cases, the overlapping

section of HPN5 consists of the interval from 1-93 cm (**Figure 7:21b**). When the dates from the samples at 104, 131, and 328 are used, the intercept at the top of HPN5 is 1279 ^{14}C BP, corresponding to cm 157 on HPN1 (**Figure 7:21a**). When the dates from the samples at 104, 131, and 246 are used, the intercept at the top of HPN5 is 741 ^{14}C BP, corresponding to cm 91 on HPN1 (**Figure 7:21c**). In both cases the correlation is only extended to the first clastic layer (cm 93 HPN5, cm 245 HPN1). When the LOI curves are viewed together, it appears that the chronology based on the sample from 246 cm (**Figure 7:21c**) achieves a much closer match with HPN5. Visually the correlation is striking, particularly near the top, although HPN1 values display a much larger variability than HPN5 values. Based on this analysis, we have chosen the chronology based on the samples from 104, 131, and 246 cm (HPN5) (**Figure 7:20b; Figure 7:21c**) as our age model.

7.5.2.4 Transect Correlation

This age model provides the basis for a transect wide correlation based on the LOI curves (**Figure 7:22**). HPN5 and HPN 1 are aligned by the dating scheme described above, while HPN2, 3, and 4 are aligned with HPN5 stratigraphically. Due to our interpretation of HPN2-4 as containing condensed versions of the HPN5 history, these cores have been stretched so that the interval between the bottom of Zone 3 (the most recent zone found in all cores) and the top of Zone 9 (basal clay/sand) are of equal length in cores HPN2-5. Zone 1 occurs only in HPN1-3, Zone 2 in HPN1-4, while Zones 3-5 are found in all cores, and Zones 6-9 in HPN 2-5. This correlation supports the view of truncated deposition in certain cores, with the cessation of deposition transgressing seaward. HPN1 is apparently recording the same history from Zone 5 onward, though in an expanded form, probably indicating additional accommodation space/topographical relief.

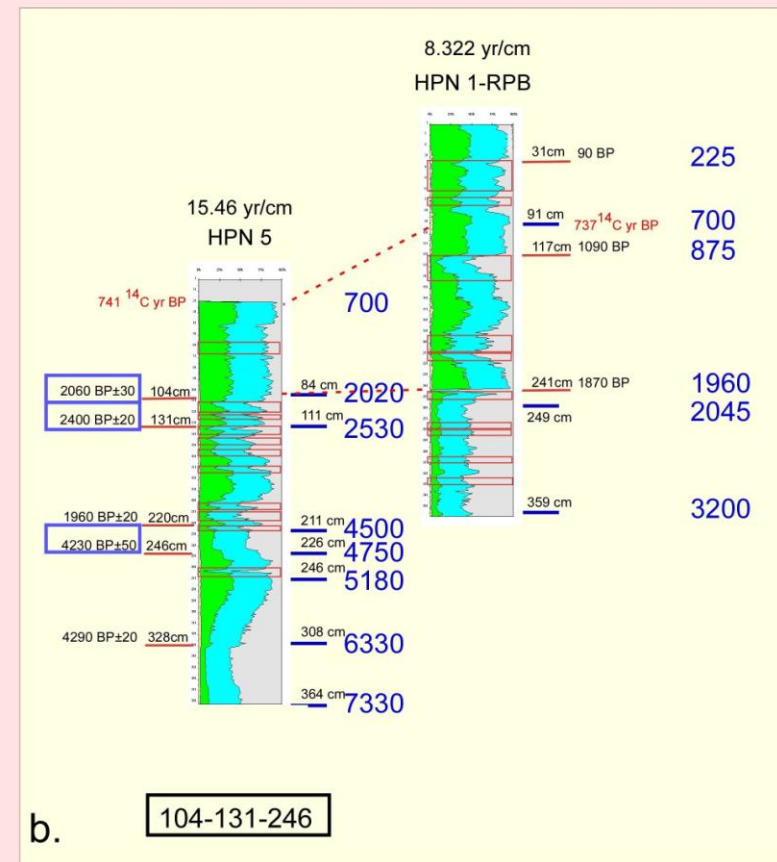
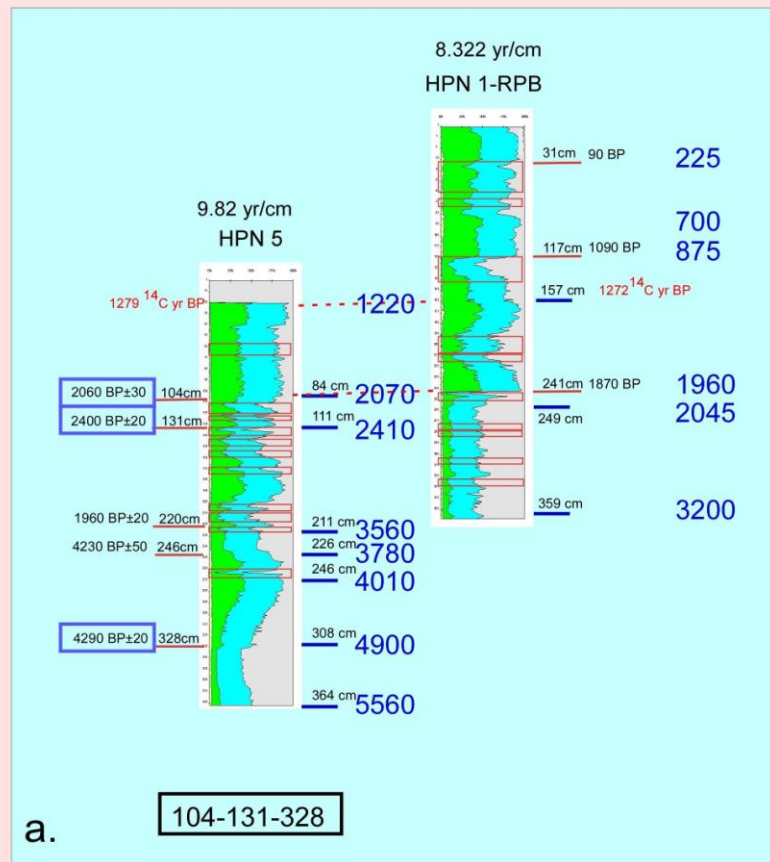
7.5.2.5 Clastic Layers

Standard deposition for the tops of all cores in this transect is organic peat, which changes to clay near the bottom of the two longer cores. All cores, however, contain a number of thin clastic layers. The clastic materials are generally sand in the three short middle cores while in the deeper cores at the transect ends they consist primarily of silt and clay, and often mica, with smaller amounts of sand. These layers are often both distinct and abrupt, usually marked by compositional and color changes, as well as sharp dips in the LOI curves (**Figures 7: 6, 7, 12**). The grain size distribution of the sand in the middle core resembles that of the beach sand, excluding the very coarse fraction (**Figure 7:14**). Removal of the extremely large grains would be expected for beach material transported so far inland. However, the lack of corresponding sand layers in HPN1 argues against the beach as the origin for all of this material. More likely is the direct transport of sand from a subaerial sandy beach ridge between HPN1 and HPN2, (this area currently supports the village soccer field, presumably indicating higher ground) or the edges of the relict dune for resuspended material. However, both HPN1 and HPN5 do contain some sand in the clastic layers. This material could have been transported from either the beach or the relict dunes.

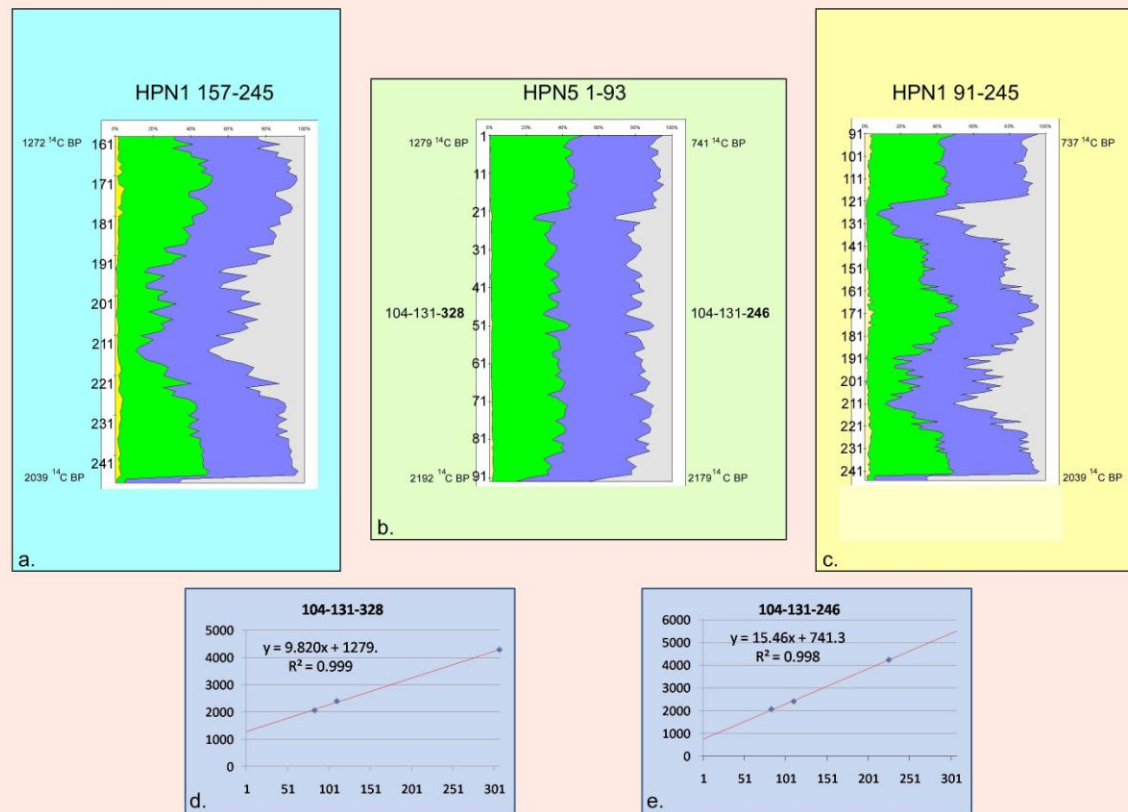
The pattern of clastic layer distribution across the transect is fairly clear, especially when the layers are superimposed on the zonation diagram (**Figure 7:23**). This figure shows clastic layers clustered in the Zones 5, 7, and 9; with exceptions being a layer near the top of Zone 4, and the middle of Zone 8 (Zone 9 lacks clastic layers in HPN5). One noticeable feature is the reduction in number of layers within the middle cores, where layer numbers are low, and occasionally missing.

7.5.2.5.1 Environmental Controls

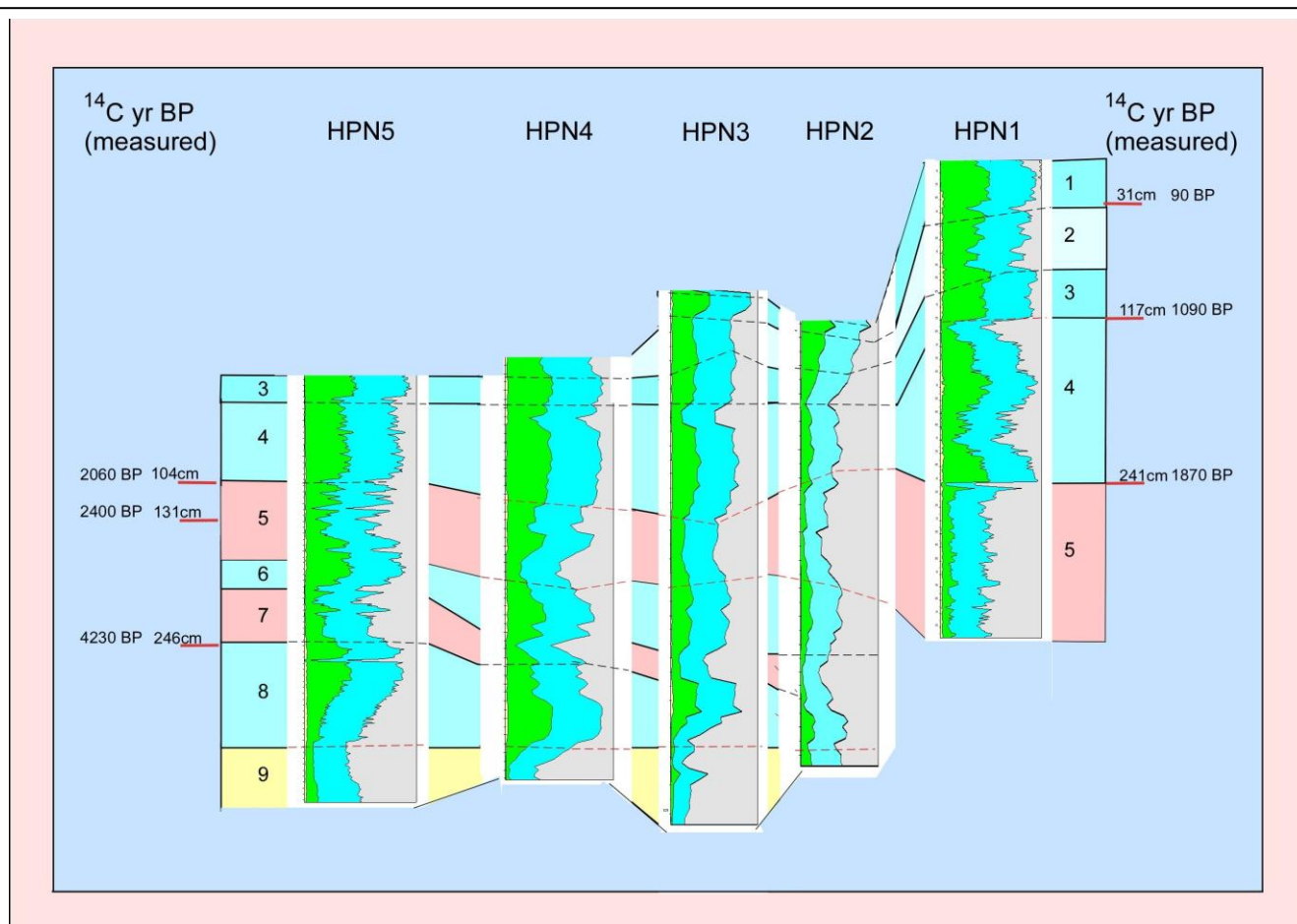
Generally in coastal wetlands where the normal deposition is organic, the presence of



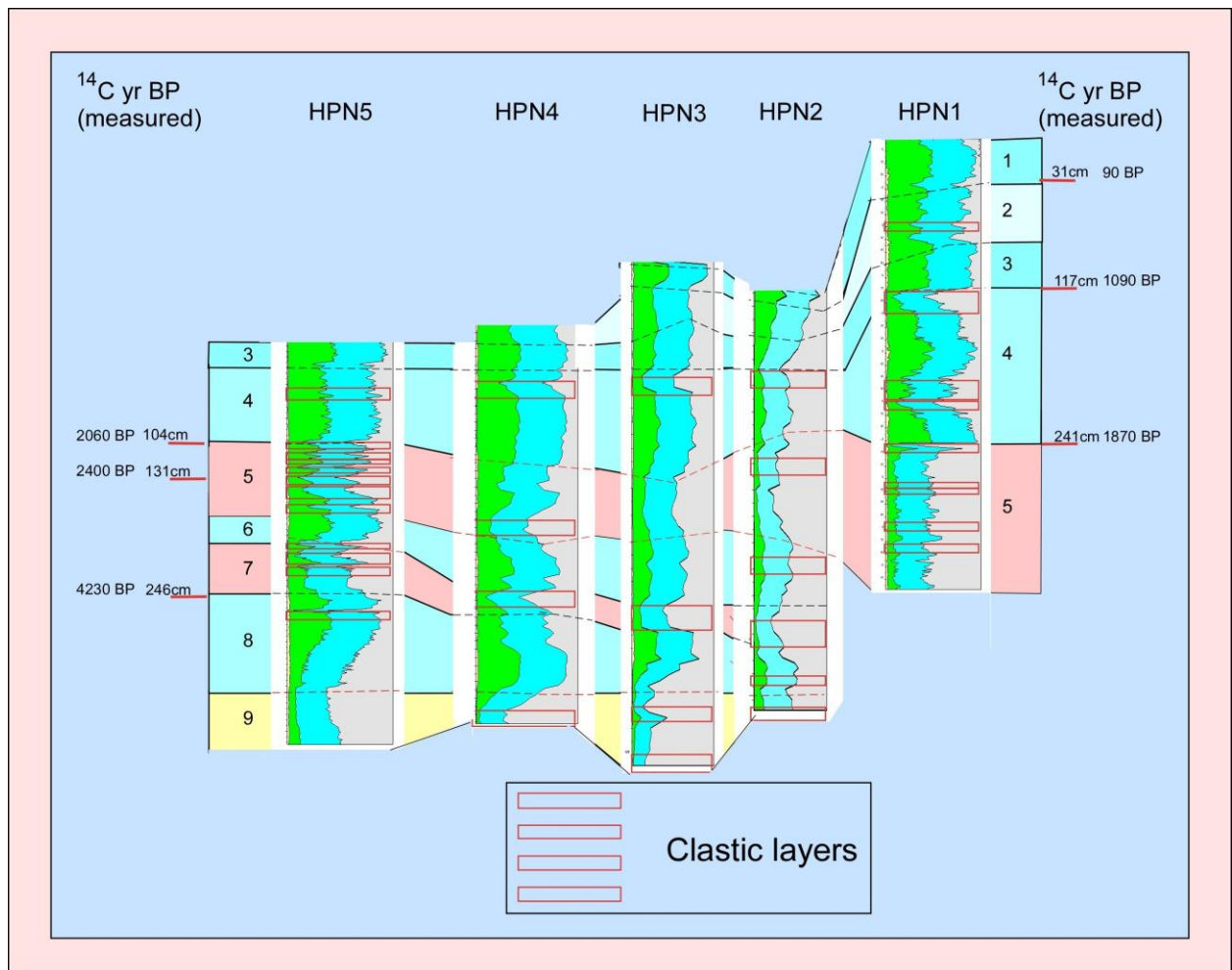
7.20 Chrono-stratigraphic correlation between cores HPN1 and HPN 5, based on the two dating scenarios presented in Figure 7:19.



7.21 Alternative stratigraphic correlation between HPN5 and HPN1, based on the two dating scenarios shown for HPN5 in Figures 7:19, 20. Dated radiocarbon ages and stratigraphic correspondence argue that cm 93 on HPN5 corresponds to cm 245 on HPN1. The calculated date for the top of HPN5 is either (a) 1279 or (b) 741 ^{14}C yr BP, depending on the dating scheme selected. These dates correspond to either (a) cm 157 or (b) 91 on HPN1. The stratigraphic correlations resulting from these two possibilities are shown. (d, e) are the depth-date graphs for the two dating schemes.



7.22 Chrono-stratigraphic correlation/zonation for the HPN transect. The dating scheme for HPN5 calculated from the dated samples at 104, 131 and 246 cm (Figure 7:20b, 7:21c) was selected, which determined the temporal relationship between HPN1 and HPN5. HPN 2-4 were then aligned by means of stratigraphic correlation.



7.23 As in Figure 7:22, with clastic layers added

clastics, especially in thin, abruptly distinct layers marks a high energy event, resulting from the transport of allochthonous material, with larger grained material indicating higher energy events. Depending upon the environmental setting, the material may be transported from either the landward or seaward side. Direction of transport can often be discerned by the sedimentation pattern, with event loads thinning and fining away from the point of origin. Determining direction of travel can help identify the nature of the event. Unfortunately in this case, the sedimentary clues do not provide unambiguous answers. It seems probable that sand available for transport is found inland of the beach, probably within the 200 m separating the locations of HPN1 and HPN2. Silt and clay may also have been present there, as well as on the beach and farther inland. The possible agents for transport are hurricanes, tsunami and rain events.

Hurricane transport would be landward, tsunami transport would be predominantly landward, followed by a possible seaward backwash, while rain events should move material from higher inland elevations toward the water courses and eventually the sea. While hurricane-generated storm surge and tsunami should be capable of moving sand, rain events in a large marsh or swamp are more likely to raise the water level, float mica and buoyant trash to the edges, and fill in low spots with clays and silts, but should not transport sand other than in water channels. The environmental settings of the coring sites during the deposition periods are key factors in determining the sedimentary effect of the various possible events. For HPN1, the geomorphological effects of sea level rise should not have had any significant impact over the period of deposition.

At 3000 cal yr BP, estimates place sea level at probably only 80 cm (Gischler and Hudson, 2004) to 210 cm (Toscano and Macintyre, 2003) below present. (As mentioned previously, the Gischler and Hudson curve [2004] seems more relevant than the Toscano and

Macintyre [2003]) curve for Belize.) The height of the ridge on which Hopkins is located is substantial, >2 meters at the beach and increasing slightly to ~m at the crest. This rather steep bathymetry continues offshore, suggesting that such relatively minor sea level change would have produced negligible lateral beach movement, particularly considering the inferred presence of an extensive, stable subsurface dune and swale system, presumably of Pleistocene age. At the initiation of deposition ~3000 cal yr BP, HPN1 was probably located in steep depression on the edge of dunes (**Figure 7:15 inset**), at approximately the same distance from the ocean as presently. As core depth is 359, stipulating 70 cm of sea level rise means that at the initiation of deposition, relative to the sea, the site was at ~3m lower elevation. The bottom section of HPN1 (<241 cm) consists of gray laminated silt, with very little organic material, lacking in *in situ* roots. This indicates an environment of fairly deep water, suggesting that water ponded at this site, probably isolated from the landward wetlands by a ridge. At ~2000 cal yr BP this ridge seemed to have failed abruptly, draining the water and initiating marsh development, which has continued through the present. If our chronology is correct, 241 cm of material has accumulated in this location over approximately the last 2000 cal yrs, a sedimentation rate nearly double that of HPN5 (0.120 m/yr vs. 0.065 cm/yr), indicating preferential deposition in a partially or wholly enclosed depression.

Given the >7000 cal yr BP basal date, much more significant geographic and geomorphological changes can be expected to have occurred for the marsh cores. At 7000 cal yr BP sea level is estimated as being 4.5 m (Gischler and Hudson, 2004) to 8 m (Toscano and Macintyre, 2003) below present. Therefore, distance to ocean and elevation relative to sea level should have been significantly greater for cores HPN2-5 during the early period, with the lower water table resulting in a drier, less vegetated environment. Just such conditions are suggested by

the cores' basal material, basically consisting of clay in HPN5 and clay and sand in HPN2-4. However, the rate of sea level rise was rapid at that point, and by 6000 cal yr BP sea level was within 2 m (Gischler and Hudson, 2004) to 5.5 m (Toscano and Macintyre, 2003) of the present. Our age model is in agreement, showing marsh development beginning at HPN5 ~6300 cal yr BP, 328 cm below current surface level. Probably by ~6000, the general environmental conditions and recording sensitivity for cores HPN 2, 3, 4, and 5 were comparable to the present. Then, as now, for these cores, currently 430-467 m from the sea, the sedimentary effects of oceanic events would most likely be driven by activity in the back barrier area, rather than direct overwash, reducing the significance of site-to-ocean distances.

Approaching the present, cessation of sedimentation progressed seaward from HPN5. HPN5, the most inland core at 467 m, records only until ~700 cal yr BP, during Zone 3. HPN4, at 460 m continued recording through Zone 2, while HPN2 and 3 at 441 and 431 m respectively, recorded through Zone 1 (**Figure 7:22, 23**). This is somewhat surprising, as the number of zones recorded is exactly inverse to core length, and therefore antecedent topography and initial accommodation space. A normal expectation is that increased accommodation space would result in more complete histories, with the shallower declivities filling up first. Perhaps in this case, on the edge of the marsh, deposition is mainly event driven, with flood-generated deposition remaining at the higher elevation, but removed by receding water levels at lower elevations.

Environmental conditions vary considerably between sites, resulting in very different depositional regimes and event responses. HPN1 is closer to the sea, at a higher elevation, and has a less direct connection with the larger back bay wetlands, most likely isolated behind a ridge until ~2000 cal yr BP. HPN2, 3, 4, and 5 are located on the seaward edge of that wetlands, with

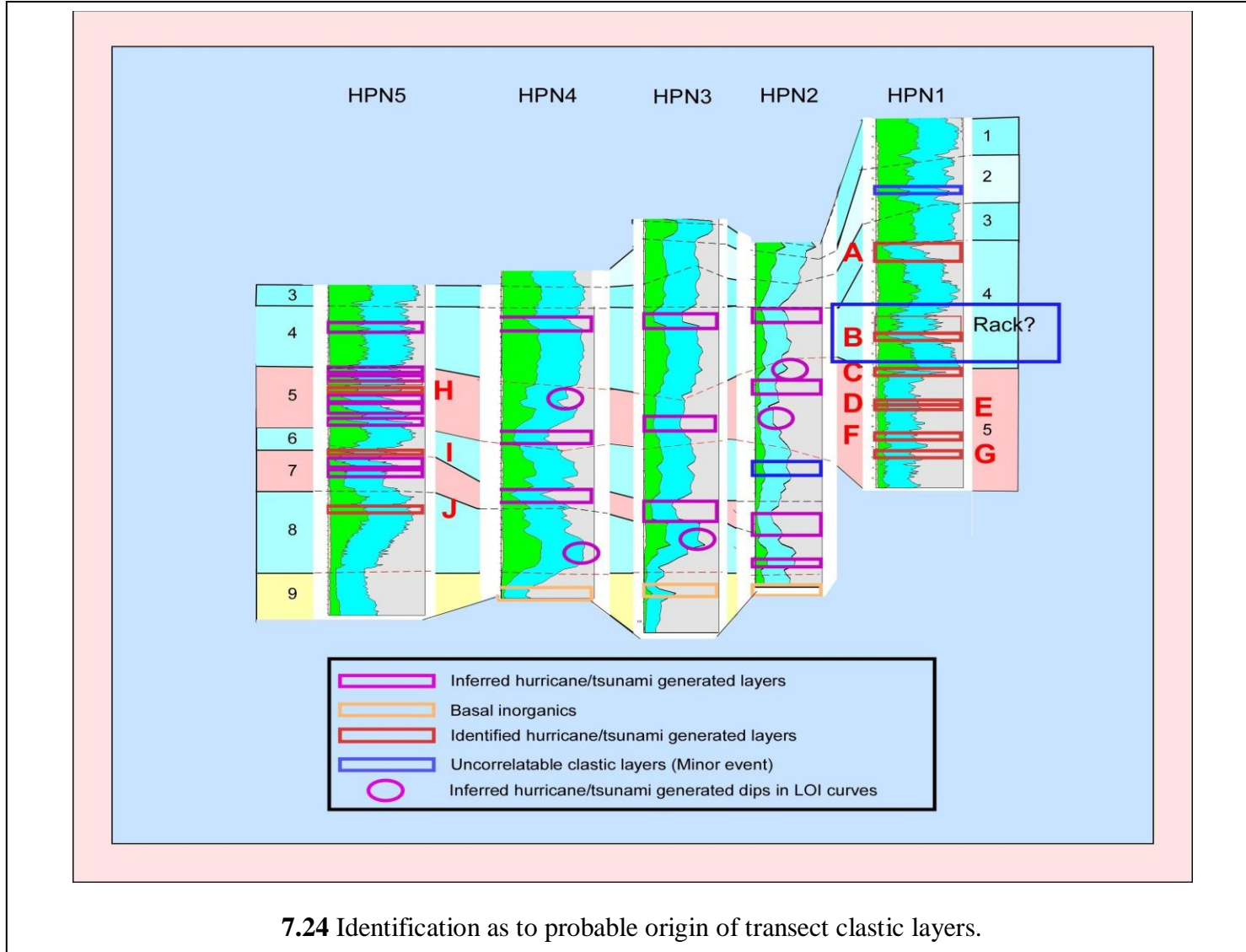
HPN 2, 3, and 4 on the landward slope and HPN5 on the bottom surface, all primarily influenced by processes occurring upon the wetlands, with differential sedimentation occurring as a result of the elevational differences. For hurricanes, HPN1 would be more susceptible to overwash and direct action by hurricane-generated waves, probably resulting in the deposition of clays and/or sand from either the beach or the surrounding dunes. During the early ponded period these storm layers could be expected to be distinct, but relatively tranquil, as water depth would inhibit chaotic resuspension of materials. During the shallow water marsh period (~2000 cal yr BP to the present), water velocity, due to the funneling of energy into the narrow dead end swale, should have been higher and more turbulent, leading to increased local erosion and resuspension of previously deposited storm layers, possibly resulting in the deposition of larger grained sediments. With an open connection to the backbarrier, the percentage of marsh material should also increase. Hurricane-generated deposition at HPN2-5 should be controlled by back barrier processes, especially flooding, and therefore be more sedate. At HPN5 this should consist primarily of clay particles settling out of the water column mixed with the occasional sand grains rolling down from the steep slope to the east. HPN 2, 3, and 4, being on the sand slope itself, which is dominated by the transport of larger grained material, are probably relatively unresponsive to small events, with clay settling preferentially at the lower locations. These locations should exhibit an exaggerated response to any event energetic enough to move sand grains, thereby further obscuring the small event layers. Response to large rainfall events would be nearly the inverse; HPN5 is perhaps capable of recording large rainfall events if sufficient clays were eroded and transported into the wetlands, while, due to its higher elevation at the eastern end of the wetlands, HPN1 should not normally be marked by these events. Due to their position on the slope, HPN2, 3, 4 should contain much less distinct (if any) records of such

events. Maximum rainfall events, of course, are usually associated with hurricanes (Riehl, 1979; Gupta, 1988; Scatena and Larsen, 1991; Unsigned, 1998; Bales et al., 2000). A tsunami wave large enough to top the barrier bridges and roll over the back barrier wetlands would likely produce hurricane-like effects at HPN1 and distinctly anomalous erosion and deposition at HPN, 2, 3, 4, and 5. Backwash traces would be a possibility at those sites.

These depositional constraints can be used to create a rudimentary model of event-generated clastic layer characteristics across the transect. Theoretically, hurricanes would leave nearly horizontal clay/sand layers at HPN1 during the ponded period, and more chaotic layers, perhaps including larger sediments and an increase in back barrier wetland material since that period. Hurricanes should be marked at HPN5 by smaller, less turbulent clay layers, and at HPN2, 3, and 4 by either sand layers or no distinguishable layers, dependent on event magnitude. Large rainfall events would be most likely to be recorded at HPN5, and tsunami should leave hurricane like signatures across the transect, probably distinguishable by erosional features.

7.5.2.5.2 Candidate Event Layers

Sedimentary evidence argues that at least some of the clastic layers result from hurricanes or tsunami. For HPN1, sand (grains, not distinct layers) occurs at 194-202 cm (“B” in **Figure 7:24**). Associated with this section, from 155-204 cm, is a very anomalous mixture of, extremely large, unconsolidated and sometimes vertically oriented organic pieces, sand grains and mica, which is probably best explained as a rack layer (**Figure 7:12**). Light colored clastics in a band from cm 206-211 probably marks the event. Sharp dips in the LOI curve and visual analysis identify the layers centered at 126 (“A”) and 244 (“C”) as probably hurricane or tsunami generated. Four clay/silt/mica layers occur in the ponded environment (Zone 5), centered at 271 (“D”), 275 (“E”), 306 (“F”) and 323 (“G”) cm. They have been identified as event layers due



to their abrupt transitions and distinct mineral composition. In HPN5 sand grains occur in layers centered at 145 (“H”), 203 (“I”) and 264 (“J”).

These 10 intervals are outlined in red (**Figure 7:24**) and display a close correspondence between cores HPN1 and 5, with their clustering in Zones 5. Clastic layer correspondence across the transect is also fairly good. The earliest event (“A”), at the very top of Zone 4 in HPN1, matches up with sand layers in all the short cores and a very distinctive visible clay layer in HPN5. Multiple dips in the LOI curves and clastic layers in cores across the transect correlate to the Zone 5 and 7 and 8 events (“C”-“J”) The corresponding layers are outlined in purple, and the LOI dips circled in order to represent probable correlation with hurricane/tsunami events. A number of clastic layers lacking sand occur in Zones 5 and 7 of HPN5. These layers are typically thin, and very distinct visually, marked by abrupt color and compositional changes, consisting of brown/orange/white/gray and/or silt, sometimes with mica. As these match our modeled sedimentary hurricane signature at HPN5, these are also outlined in purple.

As the stratigraphic correlation is based on the matching of basal inorganic layers, the cores’ bottom clastic layers can be regarded as pre-existing and irrelevant in regard to event identification. They are outlined in orange.

The event at the bottom of Zone 4 (“B”) seems anomalous, as it does not correlate to layers in any other core. It, as well as two other clastic layers that do not correlate across the transect are outlined in blue.

There is little or no evidence to support any of the clastic layers as tsunami generated. Certainly a large tsunami could be expected to have left a more distinctive signal in HPN5, probably a clear sand layer, chaotic and/or vertical deposition, and other evidence of a highly turbulent event, probably with evidence of erosion, as well as possible backwash. Similar

disturbance signatures should have occurred in HPN2, 3, and 4. A small tsunami, producing a wave roughly equivalent to a hurricane-generated storm surge, and probably producing similar effects, cannot be eliminated. As there is no obvious tsunami source inside the Belize reef, any tsunami large enough to be recorded here must have been fairly large and generated outside of the reef, and should therefore be recorded regionally. None appear in the record. However, similar difficulties in separating small tsunami/large hurricanes in other locations could mask their presence regionally. Thus, although small tsunami cannot be ruled out, they are unlikely from general geologic conditions (**Chapter 5**). For this reason, we will refer to the tsunami/hurricane layers as hurricane layers as a simplification, but it is important to remember the possibility of tsunami generation.

7.5.2.5.3 Clastic Summary

The cross transect correlation is imperfect in regard to number of events recorded. At HPN5 seven clastic layers occur in the Zone 5, whereas only five (“C” - “G”) occur in HPN1, and one to three in the middle cores. This is not unexpected as not only does our model calls for larger, more distinct layers at HPN1; it is unknown whether the entire Zone 5 is recorded at HPN1, as Zone 6 is not reached. Another possibility is that the extra layers result from smaller storms, capable of producing backbarrier flooding, but of insufficient magnitude to produce overwash deposits at HPN1. As modeled, clear storm signatures would be recorded in the middle core only under the highest energy events, as smaller events would either go unmarked or obscured by reworking by the more powerful events. The representation of the entire Zone 7 as a single dip in cores HPN2, 3, and 4 support this second view.

After correlating identified and inferred hurricane-generated layers, and eliminating the basal clastic layers, only three clastic layers remain unaccounted for (blue boxes, **Figure 7:24**).

The first of these, at 68 cm in Zone 2, HPN1, is recognizable only as a light colored band <1 cm in width producing a small dip on the LOI curve. It is most likely a minor event, perhaps corresponding stratigraphically to very small dips in Zone 2 in HPN2, 3, and 4. The same is probably true for the thin layer in Zone 6 of HPN2, possibly corresponding to dips in HPN 3 and 4. More enigmatic is the deposition at the bottom of Zone 4 in HPN1, especially as it is associated with the highly anomalous low density debris layer described above (**Figure 7:12**). The unique nature of the large, loose, and undecomposed material immediately above it suggests an equally unique cause. This material is possibly a large pile of organic flotsam trapped against vegetation on the edge of the marsh, perhaps resulting from some sort of anthropogenic disturbance. At 200 cm, the calculated date for the bottom of the debris layer is 1664 ¹⁴C yr BP. Assuming a 40 year error bar, this calibrates to four date ranges between AD 256-532, during the Classic period of the ancient Maya. Perhaps this interval represents some minor use of the area, for agricultural or resource gathering purposes. Whatever the cause, as this event does not correspond stratigraphically to other clastic layers across the transect, it is unlikely to mark a large hurricane, so is removed from the strike record.

7.5.2.6 Paleostrike Record

Displaying all events attributed to hurricanes permits a zonation based on hurricane activity regimes (**Figure 7:25**). Such a zonation shows a low level of activity from the present to ~2000 cal yr BP, preceded by increased activity until ~5200 cal yr BP. Lower in the core, activity decreases, until the basal unit, probably non-recording, is reached. Of particular interest is the correspondence between the Active period in cores HPN1 and 5. Over this period, HPN1 appears to have been a small pond, isolated from the back barrier environment, while HPN 5 was situated at the edge of the backbarrier wetlands, at a lower elevation and much greater distance

from the sea. That both environments display similar event records supports the view that these are accurate representations of storm activity for the period. Perhaps significantly, the failure of the isolating ridge at HPN1 is temporally associated with one of the larger events (“C”, **Figure 24**), suggesting that a high energy storm contributed to the breaching of that barrier.

The strike record suggests the following activity regimes (dates in calendar years)

(Figure 25b):

Quiet- Present- ~2000 BP

Active- ~2000- ~5200 BP

Quiet- ~5200- ~6300 BP

Unknown- <~6300 BP.

Two short periods (~3400-3800, 4500-4800) of reduced activity occur within the Active period (hatched boxes). These corresponds to Zone 6 and the Zone 7-8 transition in **Figure 7:23, 24**).

7.5.2.7 Recording Sensitivity/Modern Analog

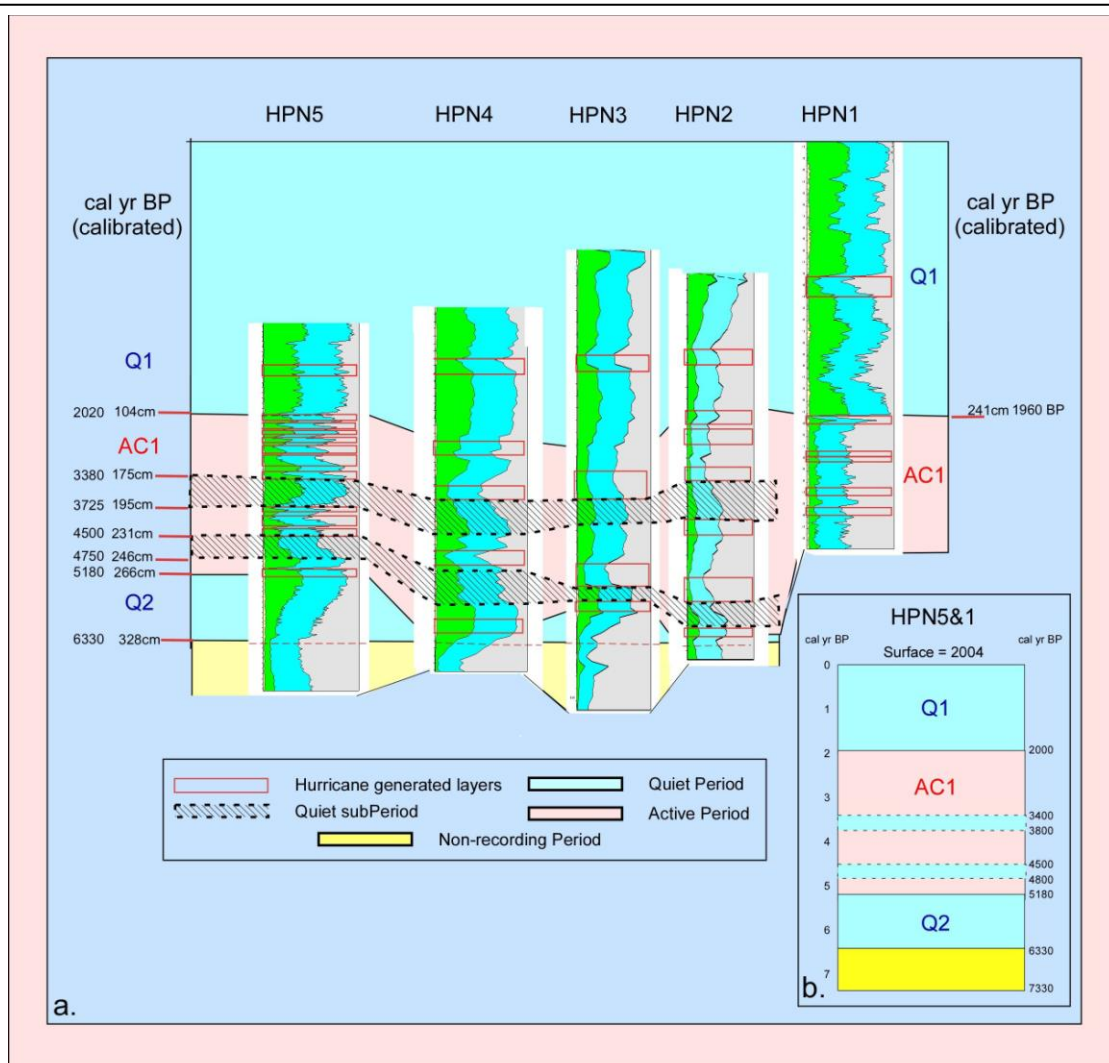
Despite the high level of damage done to the village infrastructure by recent storms and the relatively large number of hurricanes, including eight major hurricanes which have passed within 100 nautical miles of the site since 1851, there is little sedimentary evidence of any recent hurricanes within the HPN cores. HPN 1, 2, and 3 all record Zone 1, although it is not certain that HPN2 and 3 record the entire zone. Again, given the unforced intercept of AD 2004 for HPN1, we are assuming that the core was recording up to the time of extraction. In fact, the only suggestion of recent event deposition is a dip in the LOI curve at the very top of HPN1. HPN1 also displays a small LOI dip ~ 68 cm, previously identified as a minor storm. Applying our standard dating methodology, this depth corresponds to a ^{14}C age of 566, which calibrates to two date ranges from 519-650 cal yr BP or AD 1300-1431, predating both the HURDAT dataset and

the one compiled from local records by Stoddart (1963) that extends to 1787. This supports the view that no signatures of any of the multitude of historical hurricanes are present in the sedimentary record. By this analysis, site sensitivity is low, as neither a category 3 storm (Greta, 1978) passing ~10 km kilometers to the north nor a category 4 storm (Iris, 2001) passing ~ 60 km to the south, left a recognizable signature.

The geographic constraints related to track location offer a partial explanation for this lack of recent recordation, as the potential hurricane effects for Hopkins are far greater than those associated with any historic storms. Protected by the headlands to the north, maximum local effects would result from a large hurricane approaching from the southeast and making landfall either directly at, or slightly to the south of the village. On such a track, in addition to lying along the storm's powerful right front quadrant, the shape and orientation of the bay would tend to funnel and perhaps maintain wave energy in the area. Storm surge and overall energy with specific track patterns could be far greater than that experienced in the historical record. A contributing factor is the possible systematic reduction in sedimentary effect related to the reduction in topographical relief. As the bottom of the swales filled with sediments, rising water level submerged the sandy slopes and the gradients from the topographic highs reduced, less material became available for suspension and deposition. This suggests the possibility that site sensitivity has reduced slightly over time, resulting in earlier storms having left a larger sedimentary signature than equivalent recent storms, or that the magnitude of the recording threshold has increased. The effect of this process is probably minor, and is probably offset by the reduced site-to-sea distances.

7.5.2.8 Return Interval

Although the number of clearly indentified clastic layers attributed to hurricanes varies



7.25 Paleostrike record (a) for the HPN transect, with activity regimes identified; (b) is a summary regime diagram. Radiocarbon dates are interpolated from dated samples, and then calibrated to cal yr BP by means of the CALIB 5.0 program, with a median date of the high probability date ranges selected.

across the transect, rough return intervals can be calculated. For HPN1, six events are recorded over 3200 years, giving a return interval of 533 years. For HPN5, the other dated core, 12 events of varying magnitude are recorded over 7330 years, producing a return interval of 610 years. The presence of distinct activity regimes, however, requires separate calculations for each. For the recent Quiet period (Q1), extending to ~ 2000 cal yr BP, both HPN1 and 5 show a single event, or a return period of 2000 years (annual probability of 0.05%). For the preceding Active period (AC1), HPN1 shows five events over 1200 years, or a return interval of 240 years (annual probability of 0.4%), while HPN5 shows 12 events over 3200 years, or a return interval of 267 years (annual probability of 0.4%). For the ~1100 year Q2, no events are recorded, which, of course, gives an infinite return period. Thus, the regime change at ~2000 cal yr BP decreased average annual probability by ~ an order of magnitude.

These return intervals and annual probabilities are lower than those recorded at other Belizean sites (**Chapter 6**), and are considered conservative estimates, based on the site's very high recordation threshold, estimated at > category 4.

7.6 CBL Transect

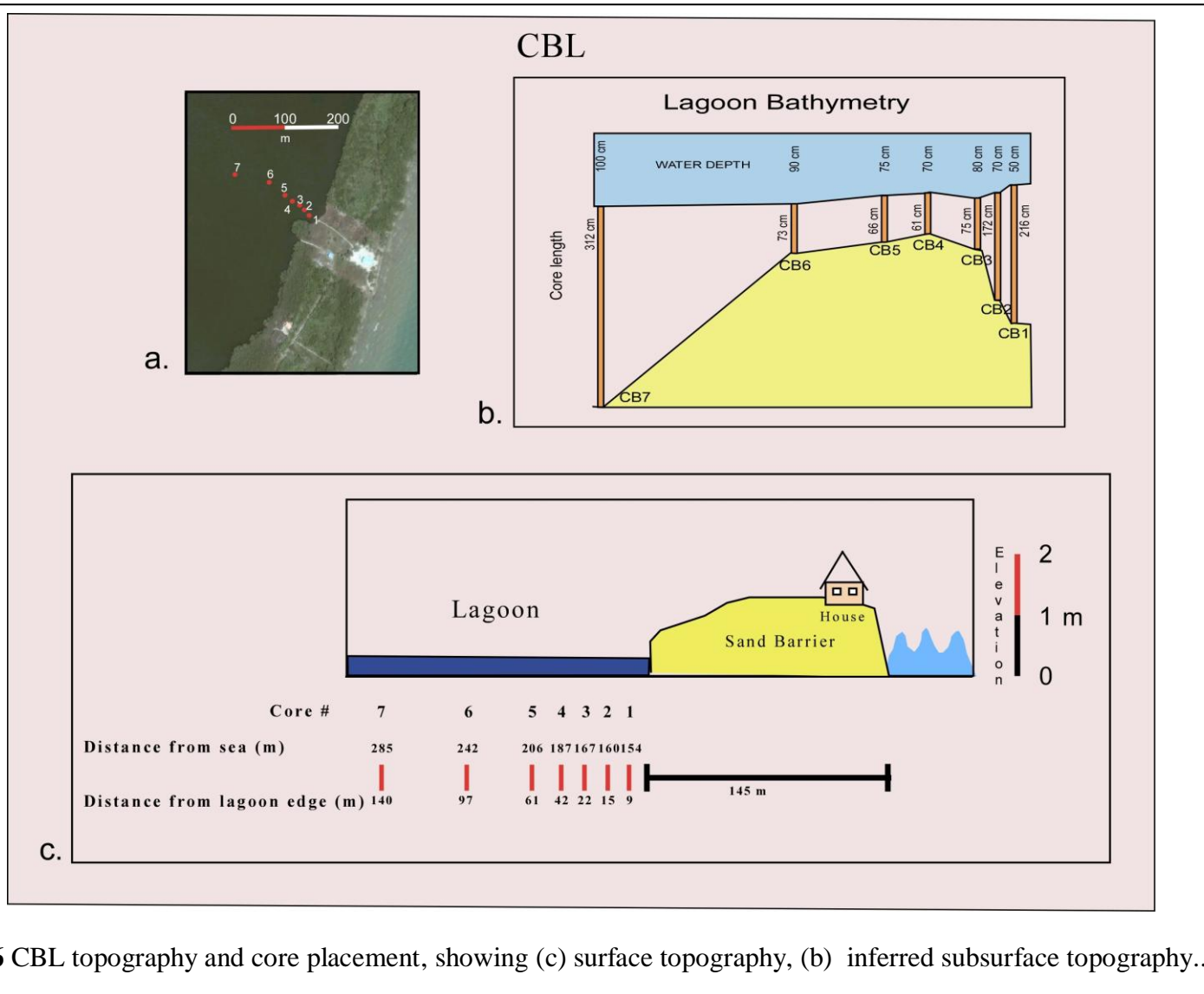
7.6.1 Results

Seven cores were obtained from the eastern (seaward) edge of CBL, spanning a distance of 131 m (**Figure 7:1, 7:26a, c**). All extraction was by modified Livingstone piston corer which was pushed until refusal. Core length was significantly longer at the transect ends; CB 1, 2, and 7 are between 172 and 312 cm in length, while CB2, 3, 4, 5, and 6 penetrated only to 61-75 cm (**Figure 7:26b**). All cores ended in either sand and/or pebbles, indicating that the pre-lagoon basal unit was reached. Core depth suggests that CBL is located over uneven antecedent topography, the most likely cause being a pre-existing dune and swale system (**Figure 7:26b**).

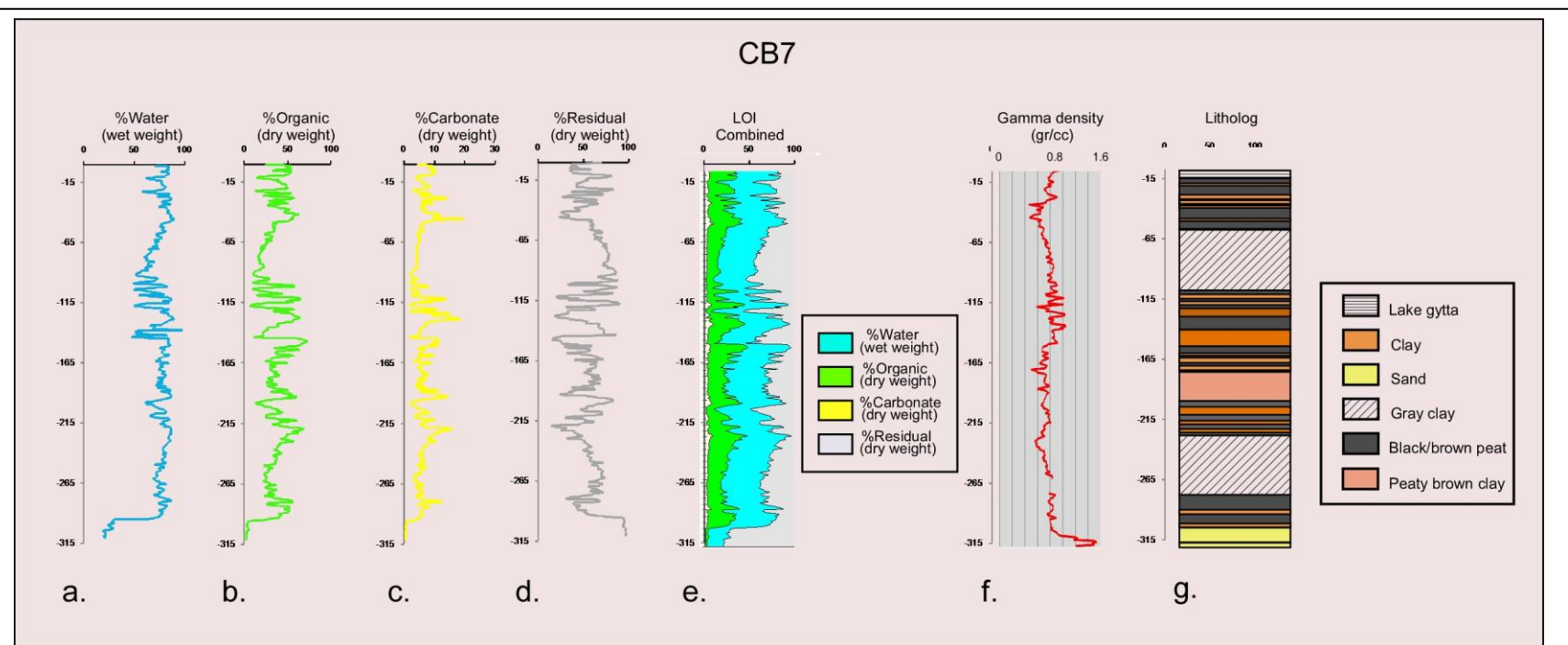
7.6.1.1 Example Litholog

Core CB7 was chosen as the example litholog for this transect. Achieving a depth of 312 cm, it is the longest and farthest inland, located 140 m from the eastern edge of CBL; 285 m from the sea. This is a composite core, composed of three piston sections. Due to the possibility of contamination of the tops of the second and third sections, a careful combination of visual inspection and LOI matching was employed at the section joints.

The results of LOI and grain size analyses are presented in **Figure 7:27**. Shown are the water, organic, carbonate, and residual (mainly silicates) percentages as individual curves (**Figure 7:27a, b, c, d**), a combined LOI curve (**Figure 7:27e**), gamma density (**Figure 7:27f**), and core litholog (**Figure 7:27g**). Gamma density was determined by running the unopened core tubes through a Geotek MultiSensor Core Logger which uses a 10 milli-curie ^{137}Cs source (<http://www.geotek.co.uk/ftp/manual.pdf>) to measure the transmission of gamma photons. Material taken from the core shoes (i.e. not contained within the tubes) could not be included in this analysis, which results in small gaps in the gamma density curves. A comparison of the data presented in **Figures 7:27a-g** demonstrates that the LOI diagram can be used to infer sedimentary features of the core. Intervals characterized by high water and organic percentages (blue and green curves), and low residual percentages (gray curve) represent generally organic deposition, an example being the peat interval from 38-48cm, where water content is > 80% , organic content ranges from 46-63%, and residuals from 24-47%. Clastic layers are marked by reversed relative values. An example is the clearly visual clay interval (**Figure 7:28**) at 116-119cm (layer H), where water content is <61%, organics ranges from 8-17% and residual values vary from 80-90%. The sand interval at the bottom of the core (296-311 cm) is marked by distinctly low water and organic values (1% and 2-6% respectively) and extremely high



7.26 CBL topography and core placement, showing (c) surface topography, (b) inferred subsurface topography..



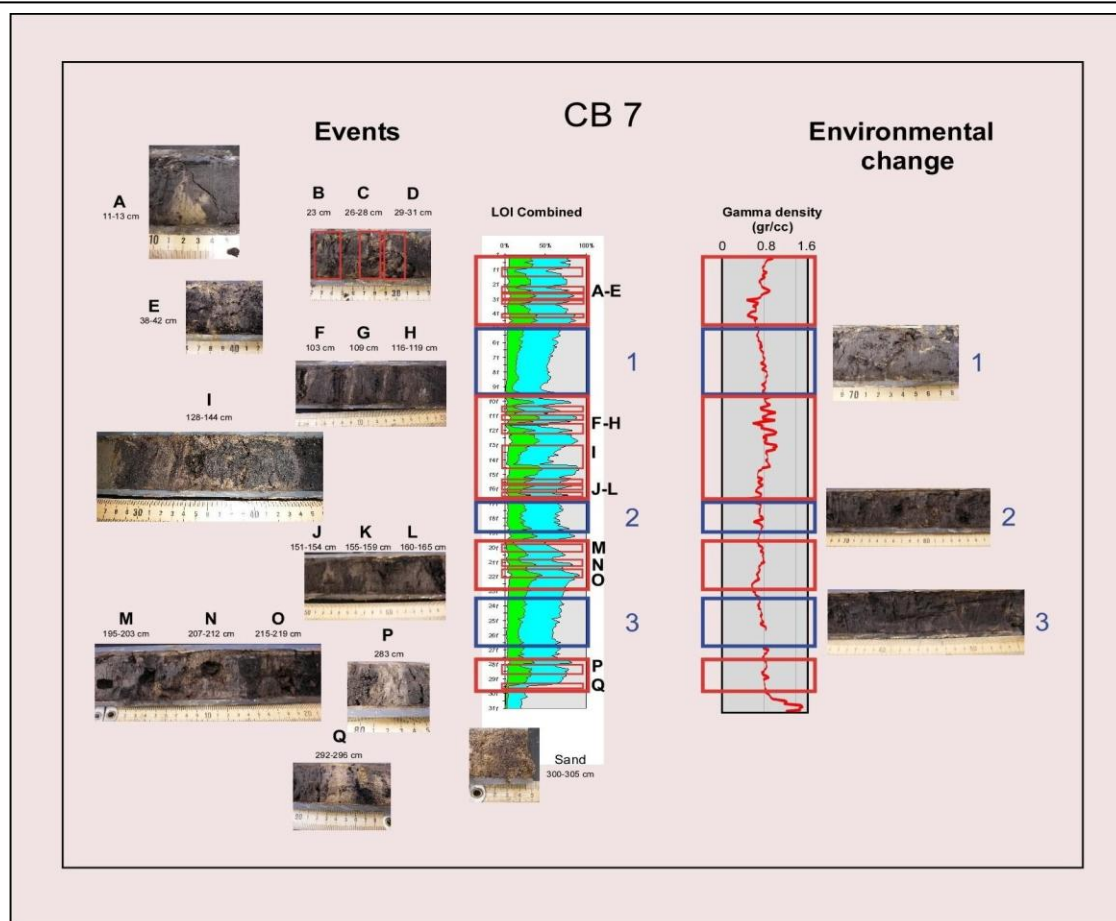
7.27 LOI curves and litholog for core CB7. Shown are (a) water, (b) organic, (c) carbonate, and (d) residual (mainly silicate) percentages as individual curves; (e) a combined LOI curve, and (f) the core litholog.

residual values (>93%) (**Figure 7:28**).

Sedimentary change can occur either abruptly or gradually. Examples of short, abrupt changes are the many narrow clay layers (layers A-Q) marked on the litholog (**Figure 7:27**) and corresponding to the visual compositional changes seen in **Figure 7:28**. An example of more gradual and long lasting change is the gray clay layer from 49-99 cm (band 1), where water (50-80%) and organic (11-38%) values remain low and fairly constant, with correspondingly high and stable residual values (57-87%). Similarly thick intervals of a slightly more peaty clay are found between 166-186 cm (band 2) and 222-265 cm (band 3). Differences in the style and rapidity of lithologic change can often indicate whether the change is being driven by slowly changing boundary conditions or by short term disruptions of the depositional environment.

Structure can also aid in distinguishing these differences, as chaotic/vertical deposition is commonly associated with relatively instantaneous high energy events, while laminated and/or uniformly horizontal deposition usually indicate low energy deposition under stable conditions, laminations usually indicating subaqueous deposition. Examples of the former are the many thin, uneven, non-horizontal clay bands (layers A-Q, red boxes in **Figure 7:28**); examples of the latter are the thicker, more homogeneous gray clay and peaty clay intervals (bands 1-3, blue boxes in **Figure 7:28**).

The abruptness of contact between layers can also provide useful information, as sharper contacts are more usually associated with event driven changes, as is evidence of erosion. Particularly abrupt compositional changes are seen at the bottoms of layers H and I. The gamma density curve can be similarly employed as intervals of larger grained materials (higher gr/cc values, spikes to the right) can be both identified and the abruptness of change noted, with abrupt, short-lived spike in grain size suggesting higher energy depositional scenarios (i.e.



7.28 Photos of clastic layers occurring in core CB7; depth of layers are marked. Red boxes mark thin, abrupt layers generally displaying sudden grain size changes, probably associated with high energy events, while blue boxes mark thicker, more homogeneous layers characterized by gradual sedimentological changes and relatively constant grain size, probably resulting from environmental conditions.

events). Examples of such intervals for CB7 include the clay layers B-L and, to a lesser extent bands M-Q, whereas bands 1-3 display relatively small and stable grain size (**Figure 7:28**).

In this core water, organic and carbonate are all positively correlated to each other and negatively correlated with residual content. Carbonates are present at a relatively constant rate throughout the core, ranging from 2-18% until the basal sand (296-312 cm), at which point their percentage drops to <1. There does not seem to be any clear relationship between the carbonate and organic values, with neither the spikes nor carbonate/organic ratio showing any correspondence with the occurrence of clastic layers (not shown).

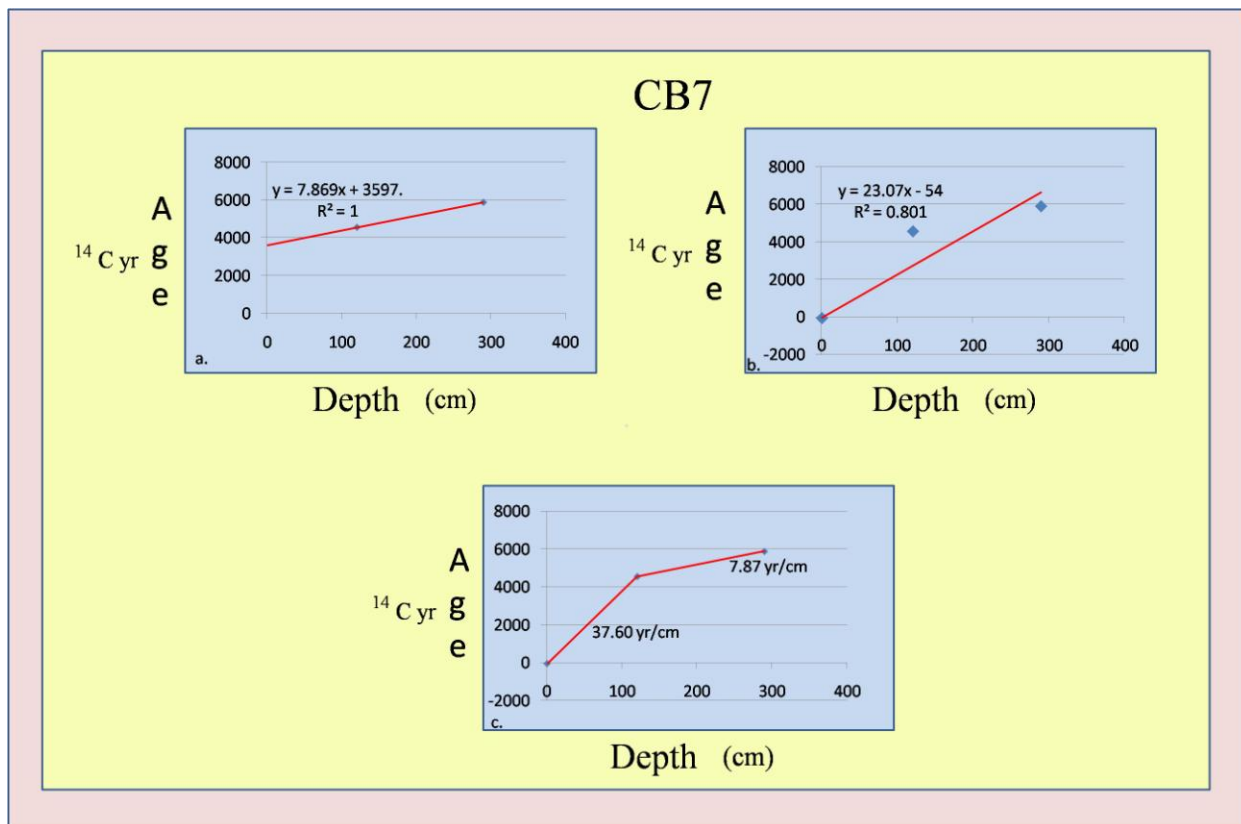
7.6.1.2 Dating

Two plant/organic samples were selected from CB7 and sent to the National Ocean Sciences Accelerator Mass Spectrometry Facility (NOSAMS) at Woods Hole Oceanographic Institute for AMS dating. The results are listed in **Table 7:3**.

Plotting the ^{14}C dates against depth produces a graph with a sedimentation rate of 0.13 cm/yr (7.87 yr/cm) and an intercept of 3597 ^{14}C yr BP years (**Figure 7:29a**). Artificially adding an age of AD 2004 at the surface produces a depth graph with a much slower sedimentation rate (0.04 cm/yr; 23.07 yr/cm) and an intercept of -54 yrs (AD 2004), with an R^2 value of 0.801 (**Figure 7:30b**). Permitting sedimentation rates to vary produces the graph in **Figure 7:30c**, in which an initial rate of 0.13 cm/yr (7.47 yr/cm) from 5880-4550 ^{14}C yr BP is followed by a much slower rate of 0.026 cm/yr (37.7 yr/cm) from then to the present with the older sedimentation rate being 5.0 times as fast as the newer rate. A third sample from 6 cm has been sent to the NOSAMS facility at Woods Hole Oceanographic Institute to resolve this issue.

7.3 CB7 chronology

Core #	Depth	Material	Lab	Sample#	C14 Age		Cal yr BP	%	AD/BC
CB7A	121	Organic	WHOI	OS-71604	4550	±20	5066-5111	0.261	BC 3162-3117
							5120-5169	0.31	BC 3220-3171
							5173-5182	0.011	BC 3233-3224
							5272-5315	0.419	BC 3366-3323
CB7C	290	Organic	WHOI	OS-71605	5880	±25	6659-6743	1	BC 4794-4710



7.29 Depth-date graphs for core CB7; (a) displays straight correlation; (b) a forced surface intercept of AD 2004 (year of extraction) imposed; (c) shows independent sedimentation rates between dated samples.

7.6.1.3 Zonation

CB7 can be divided into nine zones, based on changes in the LOI curve (**Figure 7:30**).

7.6.1.3.1 Zone 1(1-10) is moderately organic (25-55%), characterized by a distinctive greenish mud (layer A). Water values are between 71% and 84%, with moderate carbonate values (5-10%).

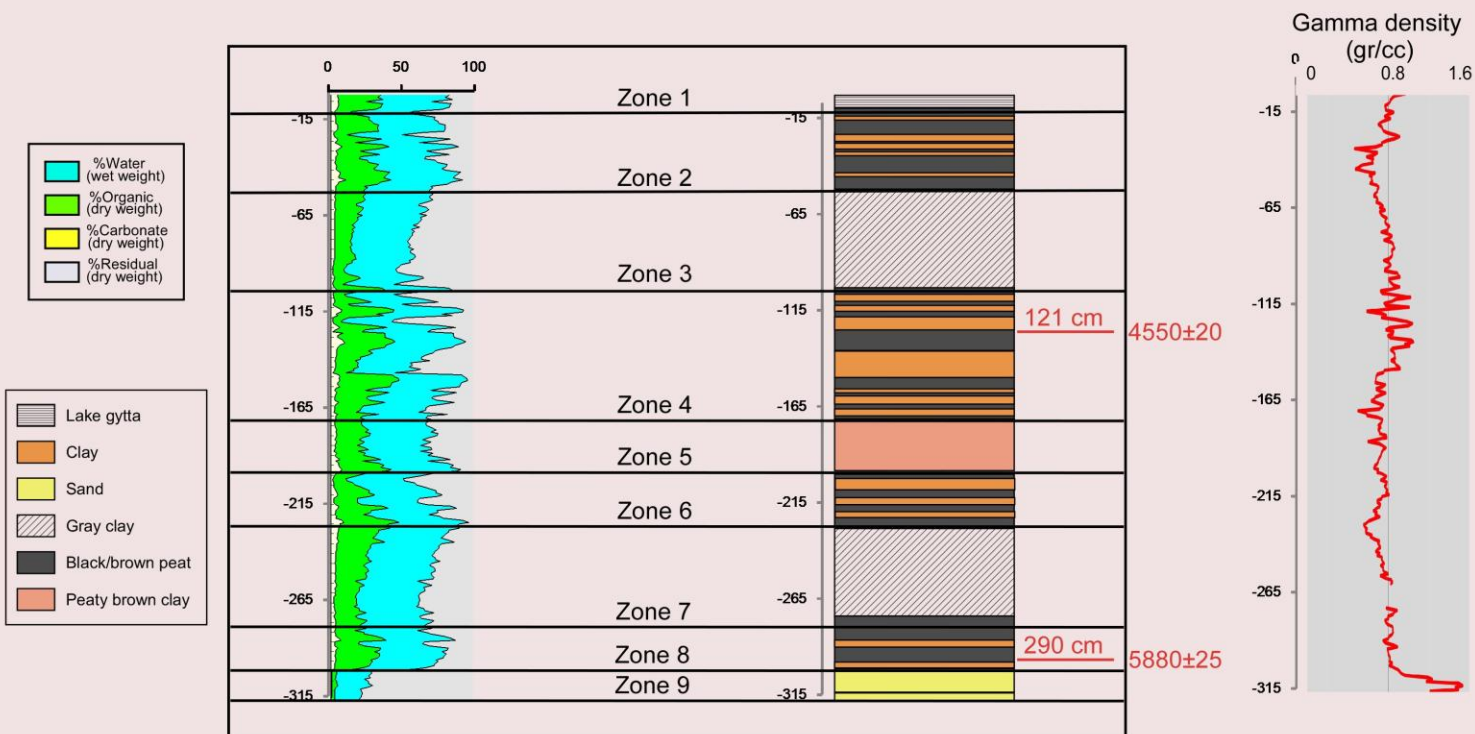
7.6.1.3.2 Zone 2(11-48) is a black/brown moderately organic peat, interrupted by several clastic layers (layers B-E). In the peat layers organic content is generally >40%, and water values >75% (maximum >90%), while in the clastic layers organic content is usually <30%, reaching a low of 14% at cm 23 (layer C).

7.6.1.3.3 Zone 3(49-100) is a massive gray clay (band 1), which is tinted brown below cm 87. Sedimentation is uniformly horizontal, with very little color change. The material becomes increasingly clastic downcore, with the grain size gradually increasing and residual values increasing from 56 to 86%, accompanying by corresponding drops (>25%) in water and organic content. Below cm 92 conditions reverse, becoming more organic.

7.6.1.3.4 Zone 4(101-165) resembles Zone 2, being primarily a low organic black/brown peat interrupted by repeated (seven) clastic layers (layers F-L). In the peat sections water content is generally >80%, but varies from 67-89%, while organic content, while generally >50%, varies between 39-72%. Of the seven clastic intervals (103-106, 109-110, 116-119, 135-144, 152-154, 156-158, and 161-164 cm), the upper four are less organic with water content generally <65%, and organic content <30% (minimum 8%), while for the bottom three clastic layers the values are higher (water generally <80%, organics generally < 40%). Grain size changes abruptly several times throughout this zone.

7.6.1.3.5 Zone 5(166-194) is a peaty brown/gray clay (band 2), becoming peatier below 187 cm.

CB 7



7.30 Zonation for core CB7, based on (a) LOI and (b) lithologic data.

Sedimentation is uniformly horizontal, with relatively constant grain size. Water (73-88%), and organic (26-61%) content are moderate, and gradually increase downcore.

7.6.1.3.6 Zone 6(195-218) consists of three distinct light colored clay sections (layers M-O), separated by thin organic intervals. All three clastic layers display abrupt color and compositional changes. Residual values vary from 31-83%, with organic content dropping as low as 15%.

7.6.1.3.7 Zone 7(219-277). Below a thin peat layer (15% residual) at the top, zone 7 is basically a gray clay, (band 3), which, moving downcore, shows first a reduction, and then an increase in organic content, with residual values changing from 27-74-60%. Sedimentation is primarily horizontal, exhibiting basically constant color and grain size.

7.6.1.3.8 Zone 8(278-295) is a muddy peat, interrupted by two clastic layers (P, Q). Organic values range from 22-56%, water from 71-86%. The two clastic layers are both visually distinct.

7.6.1.3.9 Zone 9(296-312) consists of sand, which becomes very coarse and stained (red) at the bottom. Residual values are >93%.

7.6.1.4 CB Transect

7.6.1.4.1 CB1

CB1 is the easternmost core, 9 m from the edge of CBL, and 154 m from the Caribbean Sea. This core, which consists of two piston sections with a 6 cm overlap, penetrated 216 cm of sediments, under 50 cm of water, indicating that it is located over a seaward swale of the antecedent topography (**Figure 7:26**). This location is similar to that of CB7, the example core, which probably lies in a landward swale. LOI and gamma density data for the core (shoe data not included in the gamma density graph), as well as depths (marked by red boxes) and photos of the prominent clastic layers are presented in **Figure 7:31**. Clastic layers are usually visually obvious,

generally correlating with increased grain size. Material was collected from the core shoe for each section and included in the LOI diagram, but is missing from the gamma density graph. Two plant/organic samples were selected from CB1 and sent to the NOSAMS facility at Woods Hole Oceanographic Institute for AMS dating. The results are listed in **Table 7:4** and shown graphically in **Figures 7:31**.

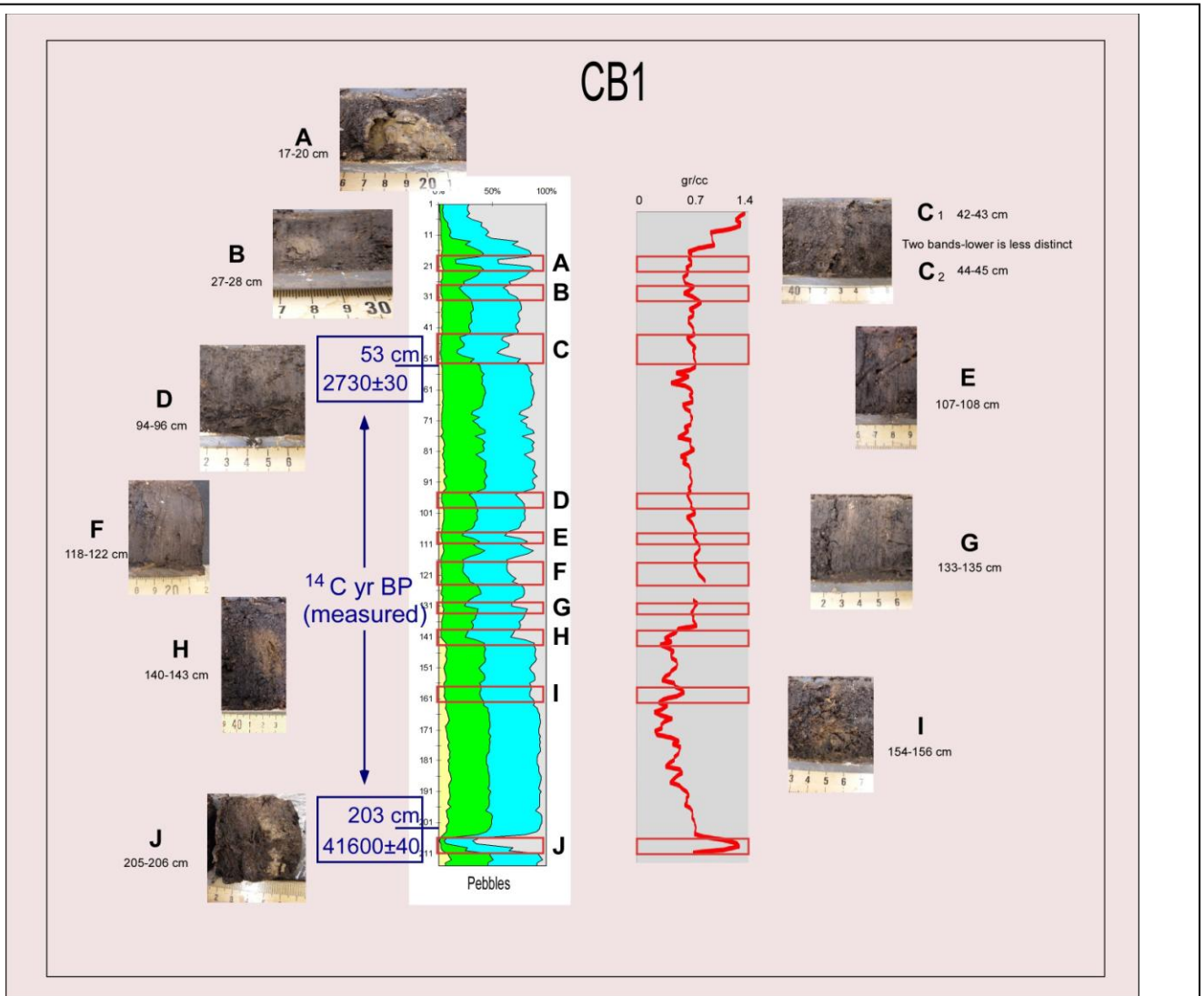
The depth/date graph of these dates shows a sedimentation rate of 0.10 cm /yr (9.5 yr/cm) and an intercept of 2234 years (**Figure 7:32**). Forcing the trendline to intercept at -54 ¹⁴C yr BP (AD 2004, the year the core was extracted) produces an R² value to 0.711 and a deposition rate of 0.04 cm/yr (22.78 yr/cm). Assuming a varying sedimentation between dates gives two very different rates; 0.02 cm/yr (51.51 yr/cm) from the surface to 53 cm and 0.10 cm/yr (9.53 yr/cm from 53-203 cm), with the older sedimentation rate being >5 times as fast as the younger rate. The similarities between the depth/date graphs for CB1 and C7 (**Figure 7:29**) are striking. As with CB7, a sample from 15 cm has been sent to the NOSAMS facility at Woods Hole Oceanographic Institute in order to establish an accurate chronology.

7.6.1.4.2 CB2

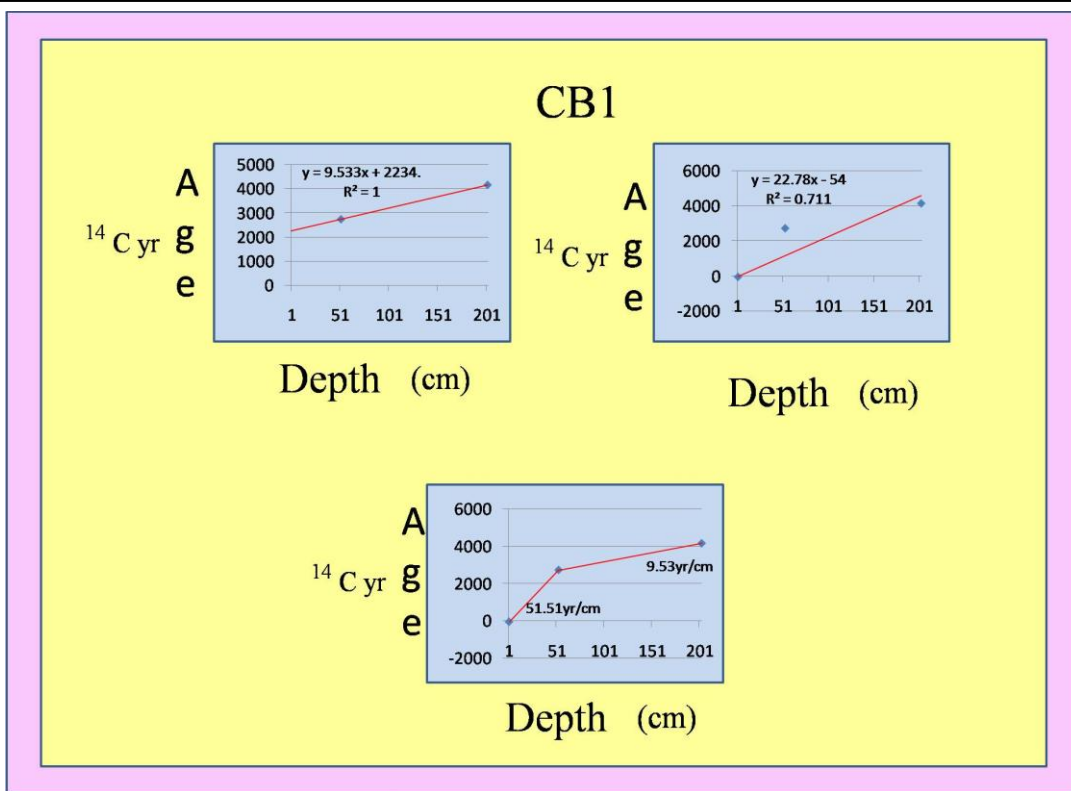
Core CB2 is the second-most seaward core in the transect, located 15 m from the eastern edge of CBL; 160 m from the Caribbean Sea (**Figure 7.26**). This core was taken in 70 cm of water and penetrated 171 cm of sediments in two sections, with a 6 cm overlap. Material was collected from the core shoe for each section and included in the LOI diagram, but is missing from the gamma density graph. The results of LOI and grain size analyses are presented in **Figure 7:33**. Shown are the water, organic, carbonate, and residual (mainly silicates) percentages as individual curves (**Figure 7:33a, b, c, d**), a combined LOI curve (**Figure 7:33e**), gamma density (**Figure 7:33f**), and core litholog (**Figure 7:33g**).

Table 7.4 CB1 chronology

Core #	Depth	Material	Lab	Sample#	C14 Age	Error Bar	Cal yr BP δ	Probability	AD/BC
CB1A	53	Plant/Wood	WHOI	OS-74106	2730	30	2761-2877	0.998	BC 928-812
							2914-2916	0.002	BC 967-965
CB1B	203	Plant/Wood	WHOI	OS-74107	4160	40	4571-4831	1	BC 2882-2622



7.31 Photos of clastic layers occurring in core CB1, depth of layers are marked. Red boxes mark thin, abrupt layers generally displaying sudden grain size changes, probably associated with high energy events. Radiocarbon ages for the two dated samples are shown.



7.32 Depth-date graphs for core CB1; (a) displays straight correlation; (b) a forced surface intercept of AD 2004 (year of extraction); (c) shows independent sedimentation rates between dated samples.

Core CB2 must be discussed in some detail, as accurate transect correlation possibly depends upon correctly interpreting an unusual sedimentary interval found from 72-99 cm within this core. This section consists of extremely unusual material, distinctly different from all other sediments in any of the cores in any of the transects covered in this dissertation. Starting at cm 72 the black/brown peat becomes increasingly muddy and mixed with gray clay; by cm 76 this becomes a chaotic mixture of light organic matter, mica, gray clay, and silt, with no clear depositional direction or consistency (**Figure 7:34d**). The bottom of the section is a thin band of mica. Immediately below this mica band, at 98 cm, is a highly organic interval, which produces dramatic excursions on all the LOI curves (**Figure 7:33 a-e**). This organic interval correlates with a slight increase in grain size, demonstrating that the section immediately above, though clearly less organic, does not consist of larger grained clastic materials. Indeed, the section from 72-97 cm is particularly light and unconsolidated, readily noticeable by the easy penetration of the sampling tool.

The physical and visual characteristics of this interval have led us to conclude that it most likely results from post-depositional disturbance. One possibility is that some large organism (human or animal) stepped in this location when the water-covered surface was ~ core depth 70 cm. This pressure would have compacted the top organic sediments and pushed it downward (accounting for the highly organic interval at cm 98), and leaving a hole which then filled with a random mixture of floating material, thereby explaining both the high percentage of mica and the unconsolidated nature of the material. Following this scenario, the mixed but increasingly horizontal, top section (72-76 cm), consisting of sediments more closely resembling higher core sections, would have resulted from the gradual resumption of normal sedimentation.

Supporting this interpretation is the close match of the LOI curves when the interval 72-99 is removed (Figure 7:34e-f). This interpretation of the section as resulting from disturbance, and therefore basically irrelevant/extraneous to transect correlation, will be considered during transect correlations. The core will be presented both as recorded and with this section removed.

7.6.1.4.3 CB3, 4, 5, 6

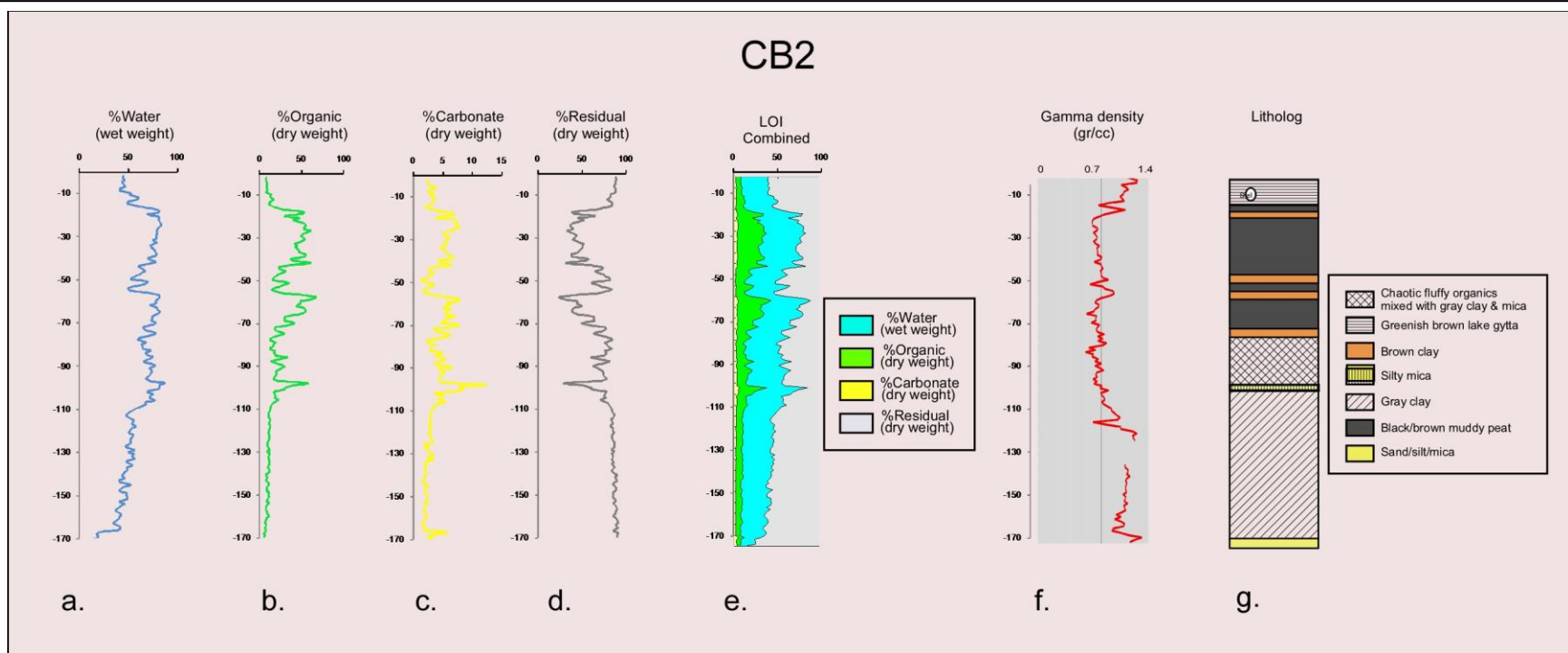
These cores will be considered as a unit, as they are all of the same approximate length, and are located within a 75 m span and exhibit very similar sedimentary patterns. The general grain size in all four of these short cores is much larger than in the longer cores (CB1, 2, 7) from either end of the transect. The material includes a significant amount of sand, from fine to coarse, both in distinct layers and more generally mixed within the sediments. LOI and gamma density graphs are provided for these four cores in **Figure 7:35** (shoe material is not included in the gamma density graphs). As in the other cores, clastic layers generally coincide with positive spikes in the gamma density graph. However, due to the somewhat random presence of sand within even the organic layers, LOI data blurs the visually obvious inter-core sand layer correlation. For this reason, a combined photo (**Figure 7:36**) will be used rather than the usual LOI diagrams for the purpose of establishing transect zonation.

7.6.1.5 Transect Zonation

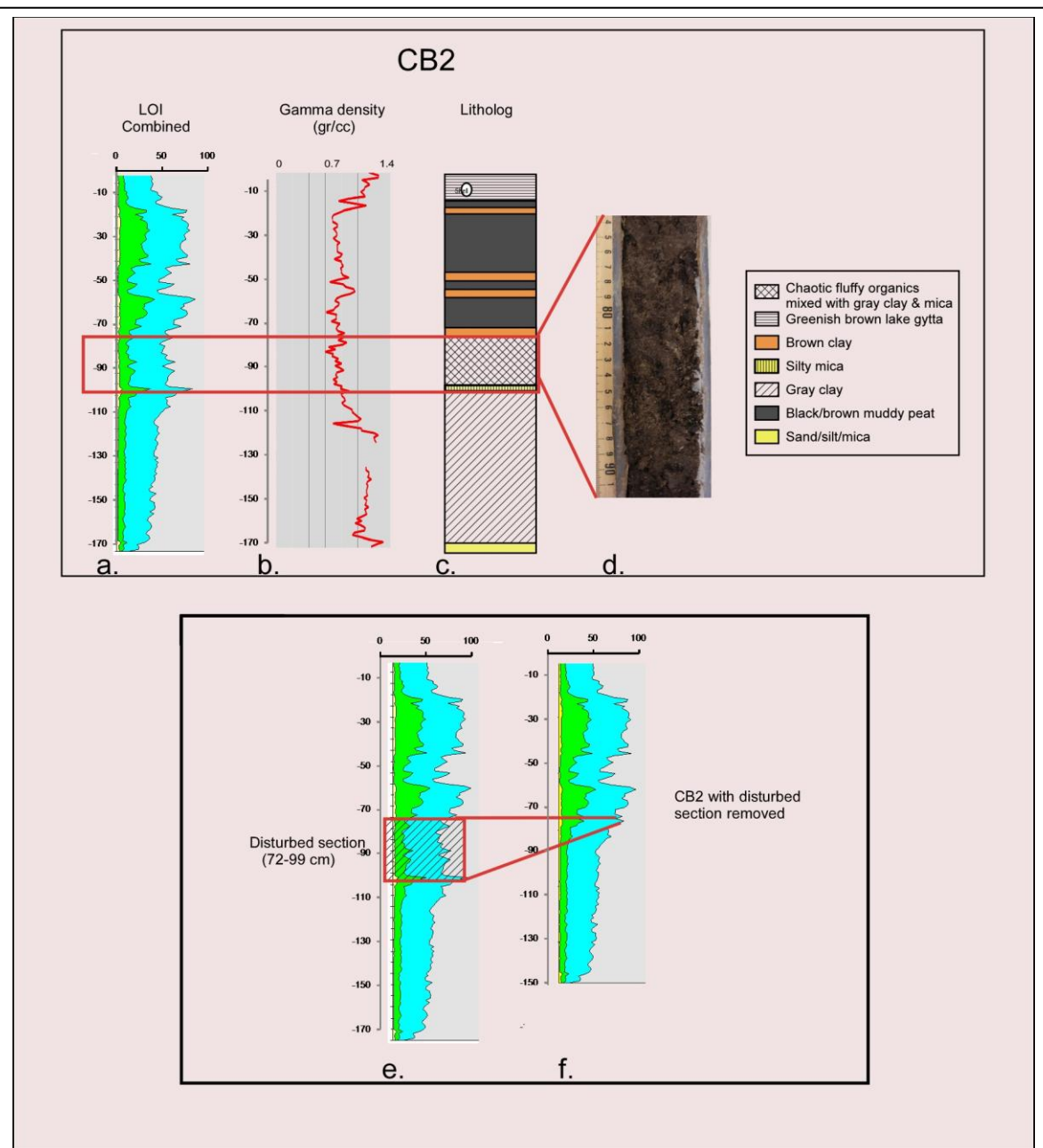
This transect cannot be correlated until the chronology is established.

7.6.1.6 Grain Size

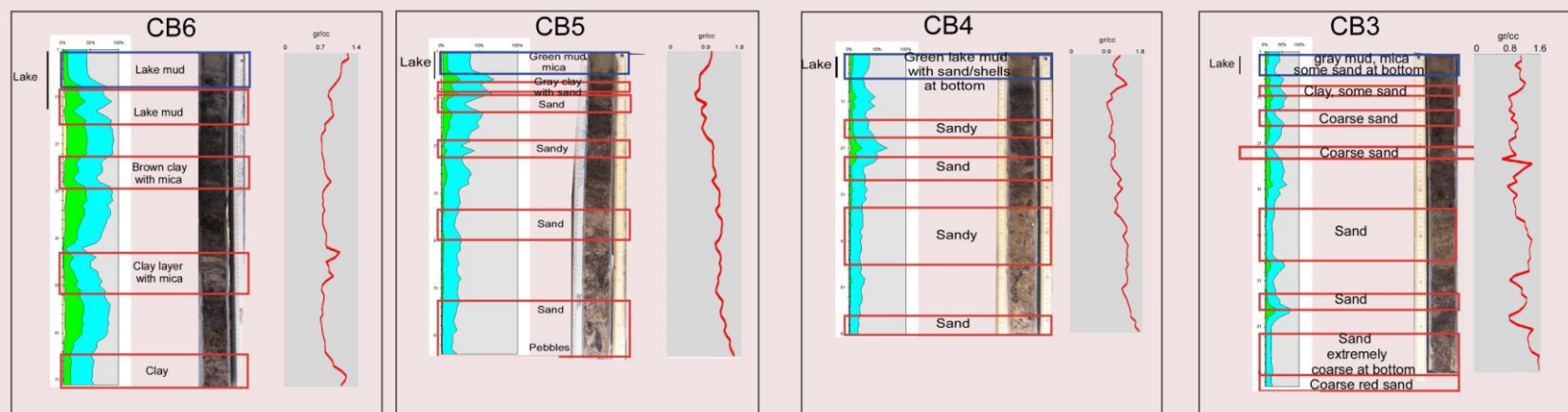
Grain size characteristics were calculated for material from the both the CBL environment and selected clastic intervals within the cores using the stacked sieve method, which is not effective for silt and clay particles. The finer material was removed prior to sieving so results show only the percentage by weight of the sand size particles, given by phi size. Results



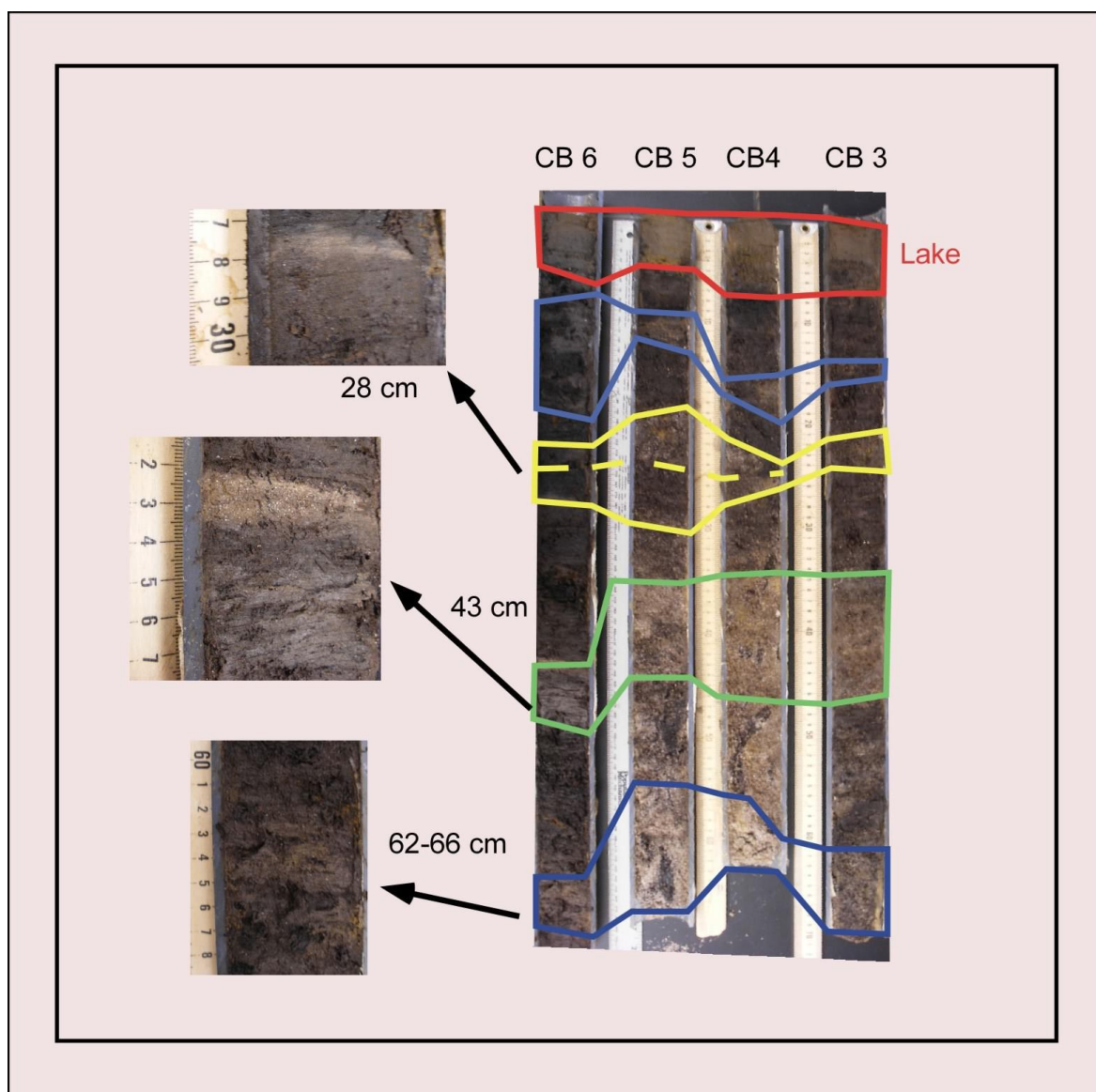
7.33 LOI curves and litholog for core CB2. Shown are (a) water, (b) organic, (c) carbonate, and (d) residual (mainly silicate) percentages as individual curves; (e) a combined LOI curve, (f) gamma density, and (g) the core litholog.



7.34 Core CB2, showing (a) LOI curve; (b) gamma density; (c) litholog, (d) photo of an anomalous sedimentary interval, and LOI curve (e) with, and (f) without the interval from 72-99 cm.



7.35 Cores CB3, 4, 5, and 6, showing LOI curve and gamma density. Red boxes mark clastic layers.



7.36 Photos of cores CB3, 4, 5, and 6. Colored boxes show inferred correlation of clastic layers between cores.

are shown in **Figure 7:37, 38**; larger grain size classes are to the left, smaller to the right. The beach samples show a progressive coarsening moving onshore (**Figure 7:37**).

7.6.1.5 Transect Zonation

This transect cannot be correlated until the chronology is established.

7.6.1.6 Grain Size

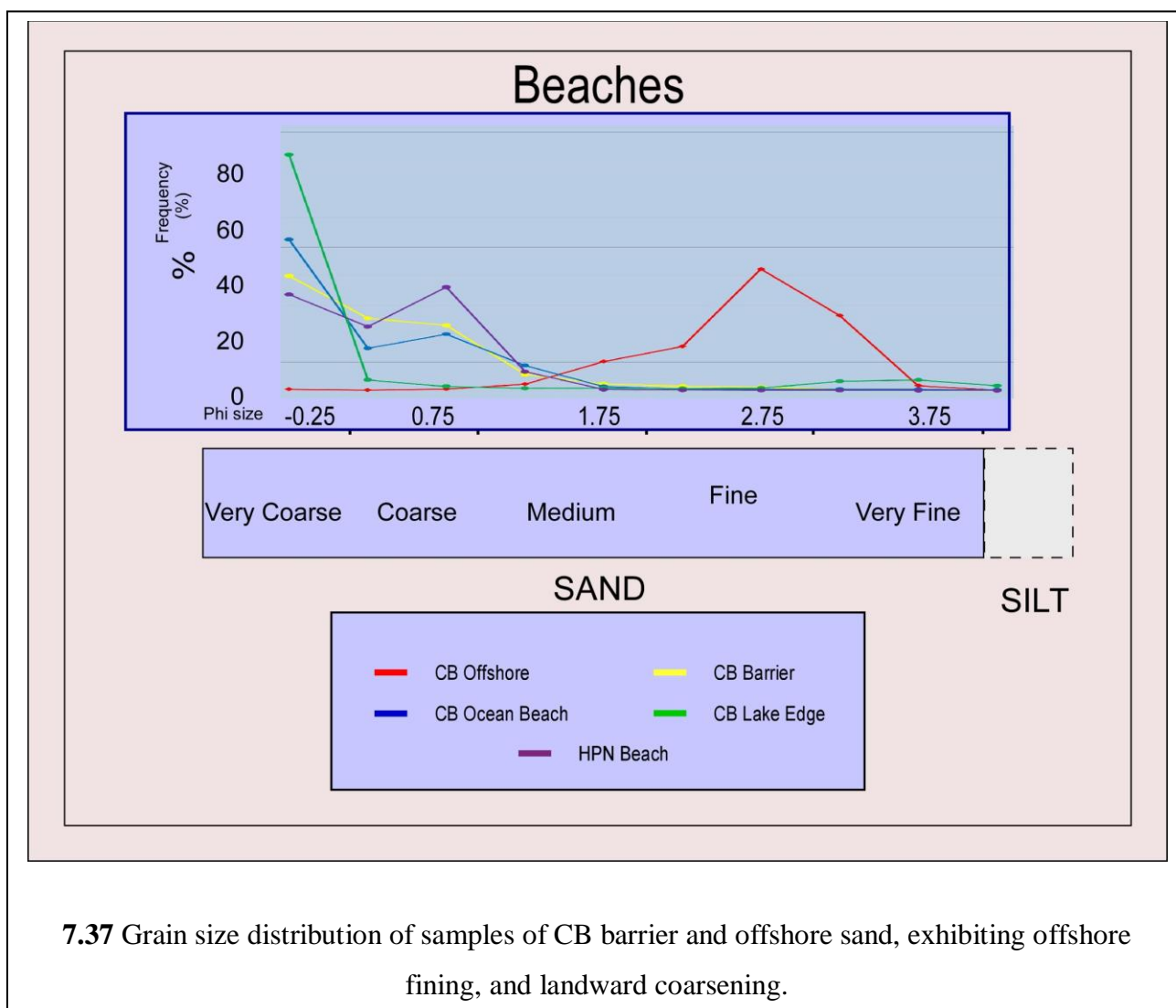
Grain size characteristics were calculated for material from the both the CBL environment and selected clastic intervals within the cores using the stacked sieve method, which is not effective for silt and clay particles. The finer material was removed prior to sieving so results show only the percentage by weight of the sand size particles, given by phi size. Results are shown in **Figure 7:37, 38**; larger grain size classes are to the left, smaller to the right. The beach samples show a progressive coarsening moving onshore (**Figure 7:37**).

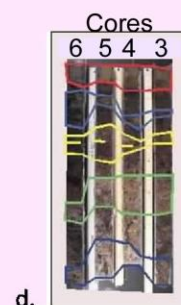
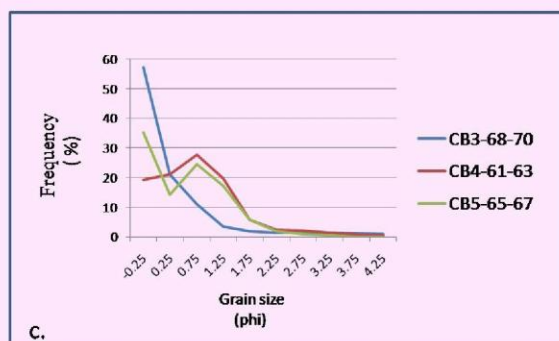
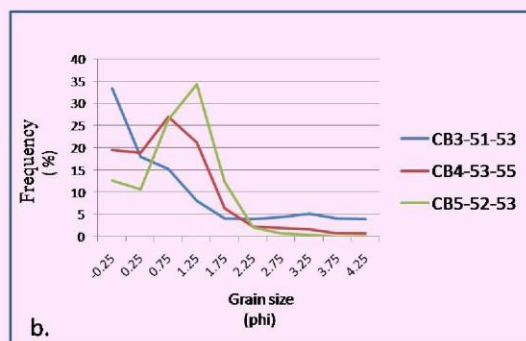
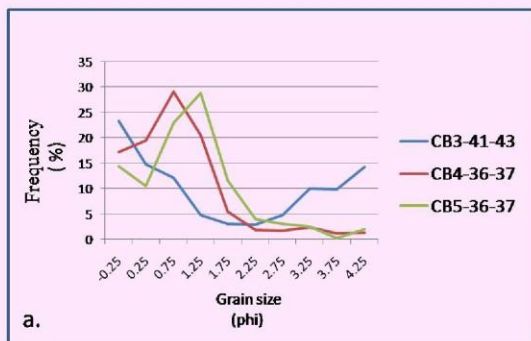
A sample taken from 25 m offshore shows the smallest grain size (red line), while the sample from the barrier (blue, yellow lines) itself are intermediate. For all three barrier from the lake edge (western edge of the barrier) (green line) shows the largest; the two samples samples the phi class with the largest percentage is very coarse sand (< 0 phi); for the lake edge sample this class constitutes $> 80\%$ of the sample. The phi class with the largest percentage for the offshore material is fine sand. A beach sample from Hopkins beach is also shown (purple line), with a mode of coarse sand.

Clastic intervals for these analyses were selected from the sandy sections of the middle cores (CB3, 4, 5). **Figure 7:38** displays grain size data from the green interval (a), and the top (b) and bottom (c) of the blue interval, as marked in (d) and **Figure 7:36**.

7.6.1.7 Clastic Layers

In CB 3, 4, and 5 the clastic intervals are usually sand (**Figures 7:35, 36**), whereas in CB





7.38 Grain size distribution of sand samples from (a) the green interval, and the top (b) and bottom (c) of the blue interval, as marked in (d). When correlated across cores CB3, 4 and 5, a general inland fining can be observed.

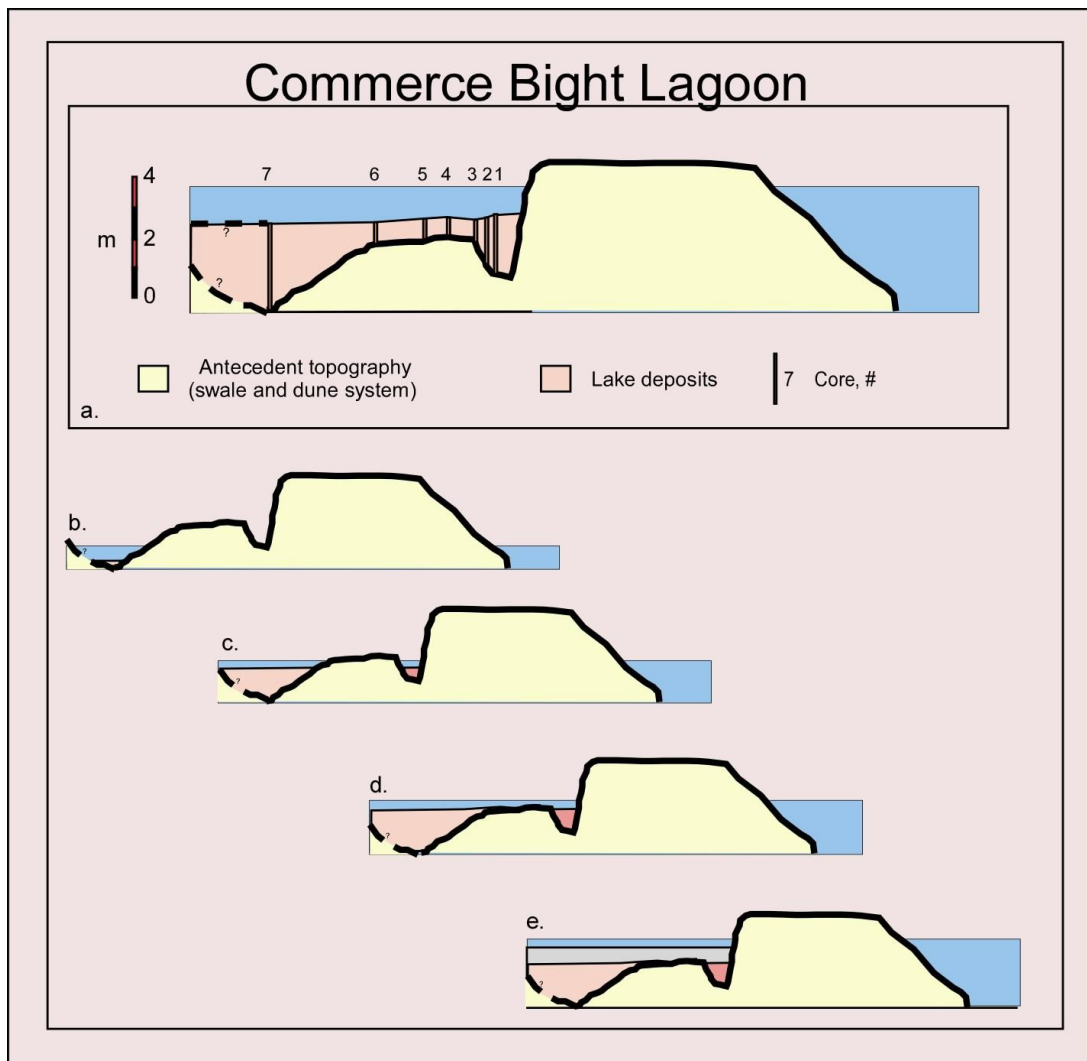
1, 2, 6, and 7 they are silt, clay, and mica except for the basal sand. In CB1, 2, and 7 the clastic layers are generally thin (<5 cm), highly visual due to their light coloration, and usually abrupt, although occasionally somewhat indistinctly mixed with the surrounding sediments (**Figure 7:28, 31**).

7.6.2 Discussion

7.6.2.1 Geomorphologic Controls

Lake bathymetry and antecedent topography play important roles in the sedimentation occurring across this transect. Lake sediments here has almost undoubtedly not been deposited uniformly in horizontal layers across the transect. Although all cores were pushed to refusal, stopped in all cases by impenetrable sand and/or pebbles, core lengths differ by a factor of 5 (61 cm–312 cm), indicating that an antecedent swale and dune system underlies the present sediments, similar to that found for the HPN transect (**Figure 7:39**). The presence of this subsurface topography may well result in different sections of the transect having different sedimentary histories, as the sand ridge beneath cores CB 3,4,5,and 6 may have effectively separated the transect into distinct environments. During periods of low water (**Figure 7:39b**) the location of cores CB1-6 could have been subaerial (non recording); slightly higher water levels could result in subaerial locations, for CB 3,4,5,and 6 and subaqueous locations for CB1, 2 on the seaward end and CB7 on the landward end, probably in unconnected systems (**Figure 7:39c**). A more unified sedimentation would occur during periods of higher water levels (**Figure 7:39d, e**). Because water level is controlled by a number of factors beyond the post glacial sea level rise, including climatic and geomorphic conditions, episodes of separate recording basins could have occurred several times throughout the history.

The underlying relict sandy beach ridge provides a possible explanation for the



7.39 Conceptual model of the potential isolating effects of the subsurface topography.

abundance of sand in cores CB 3, 4, and 5. This ridge also provides a source for larger grain material to be transported inland by storms, particularly during subaerial periods. A location on such a topographical high argues for a much shorter depositional history, as these sites would have been submerged (subject to deposition) much later than the lower elevations. In all events it is to be expected that sedimentation began first in the deeper locations, with CB7 having the longest history, followed by CB1, and 2 with shorter histories. CB 3,4,5, and 6 should have the shortest, and perhaps most intermittent, records.

7.6.2.2 Zone 1

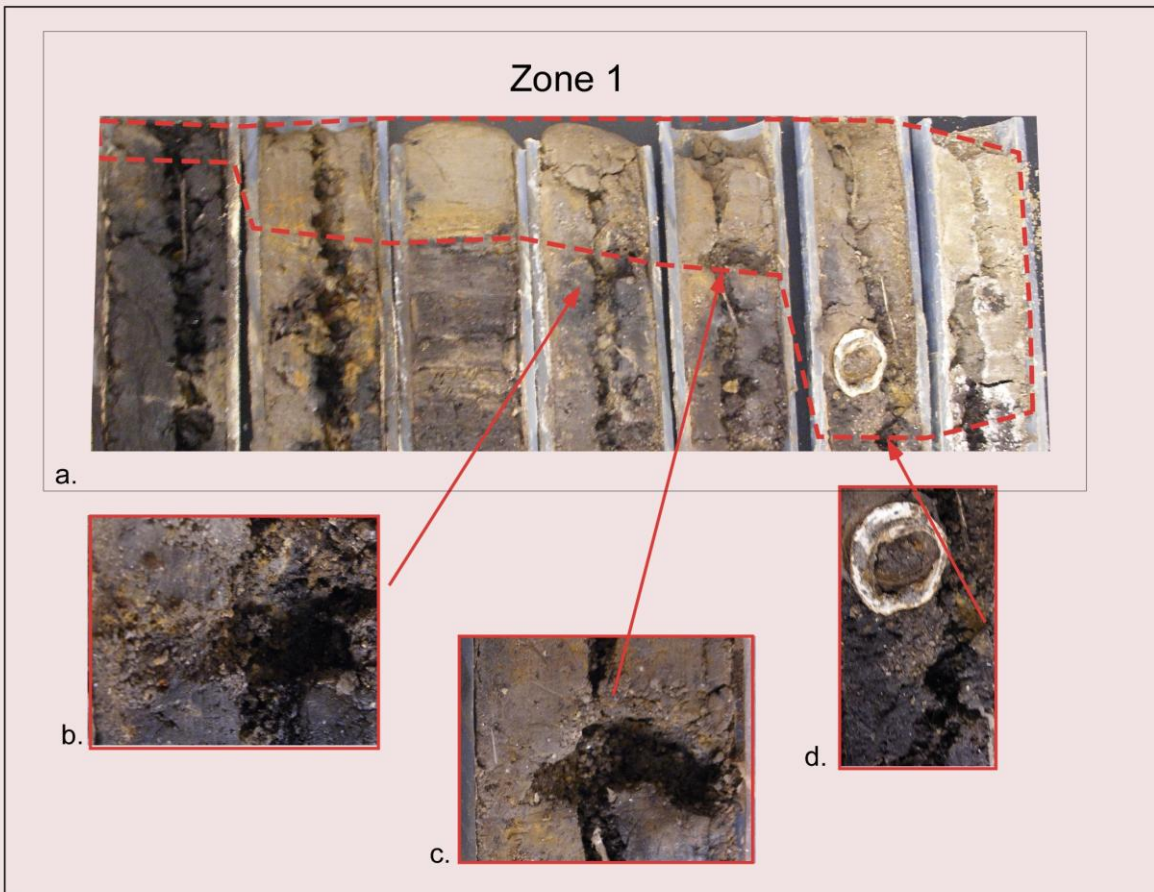
An extremely anomalous layer (Zone 1), is found at the top of all cores in this transect. The color, texture, and presence of large shells makes this layer very distinctive, to the degree that if it appeared lower in the sediments it would be used as a stratigraphic marker. The material is basically a lightly laminated, horizontally deposited clayey gyttja, which is in accordance with the location's present condition as a saline lake (**Figure 7:40**). This dramatic compositional change from the underlying sediments suggests that this material marks a major environmental change. Deeper sediments suggest periods of marsh/swamp wetlands (high organics) alternating with periods of deeper water (gray clay), none of which appears to be marine. Therefore, it appears that some energetic event caused the formation of a saline lake. The laminated, non chaotic nature of this layer supports this view, as does the layer's landward thinning; a change from marsh to lake restricts sedimentation sources to the allochthonous marine material, with preferential deposition occurring to the seaward. The abruptness of the change suggests that the change occurred quickly, while the presence of a sand/silt layer at the bottom of this interval across the transect suggests the causative agent was a high energy event. One possibility is that the event lowered/opened the barrier, increasing marine influence, and perhaps opening the area

to wave action, at least occasionally. A second possibility is that the fluvial connection with the Caribbean was opened/widened/deepened, thereby permitting more rapid outflow of freshwater during the wet season and easier inflow by marine waters during the dry. The most obvious candidate for the high energy event is a hurricane, especially given the presence of the sand/silt layer at the bottom of the interval (**Figure 7:40**).

Many Central American lakes show periods of dramatically increased clay deposition, attributed to anthropogenic causes, mainly deforestation and agricultural activity. In Lake Salpeten, Guatemala, nearly seven meters of “Maya clay” were deposited during the period of maximum disturbance associated with the ancient Maya (Leyden, 1987; see **Chapter 2**). However, that does not seem to be the cause of the Zone 1 clay layer. Firstly, the layer thins landward, which is the reverse pattern for an inland agricultural source. Secondly, until very recently (<30 years) all agriculture was of the small scale, subsistence variety, and located a several km inland, separated from CBL by substantial wetlands.

7.6.2.3 Transect Chronology

Although the shapes of the LOI curves are quite different for CB1 and CB7, the striking similarity between their depth/date graphs (**Figures 7:30, 31**) suggests that similar temporal controls influenced deposition at both sites. Straight-forward age plotting results in large intercepts for each core (2234 ^{14}C yr BP for CB1; 3597 ^{14}C yr BP for CB7), and similar sedimentation rates (0.10 vs. 0.12 cm/yr). Artificially forcing surface intercept dates of AD 2004 for the two cores yield near identical sedimentation rates of 0.04 cm/yr and similarly lowered R^2 values. When sedimentation rates are considered separately between dated samples, both cores show a five fold increase after the first sample. It seems unlikely that such close correspondence is coincidental. We have decided to accept the dates (and the subsequent intercept points) as



7.40 Photos of Zone 1 across the transect. Clear sedimentological differences appear above and below the Zone I boundary (dashed red line). (b, c, and d) show a sand and/or silt layer that commonly occurs at the base of Zone 1.

accurate, meaning that the tops of CB1 and CB 7 correspond to 2234 and 3597 ^{14}C yr BP respectively.

The most reasonable explanation for the cessation of deposition is that the sites became subaerial. However, currently the surfaces of CB1 and CB7 are, respectively, 50 and 100 cm below the lake surface. Although elevation could not be accurately checked, visual estimation put the present lake surface at roughly MSL. Geomorphologically, this seems likely as it is separated from the Caribbean Sea by only a narrow (~ 150 m) barrier, presumably consisting of porous sand. Given sea level history, it is not unreasonable that the depths of these core tops were at approximate sea level, or even higher, at 2200 and 3400 ^{14}C yr BP. However, as sea level rose, the backbarrier should have accreted, both from allochthonous marine input over the barrier and the autochthonous deposition of organic material.

However, if a high and durable barrier permitted lake level to exceed MSL (particularly during the wet season) it is possible that the locations were able to accrete above sea level. If the barrier height/impermeability was then reduced, this material could have eroded.

The hypothetical events explaining the dating dilemma runs as follows. During early periods, due to high lake levels, both CB1 and 7 could have accreted above sea level, with deposition continuing beyond the intercept dates. An abrupt lowering of the lake level, resulting from the opening/reduction of the barrier and/or deepening of the outflow stream would have then resulted in the removal of the topmost material. A high energy event, either then or later, could have removed enough material to lower the elevation below MSL, thereby turning the wetlands into a lake. Scouring could have been more extensive at CB7 than at CB1, explaining the lower surface level and the older intercept date.

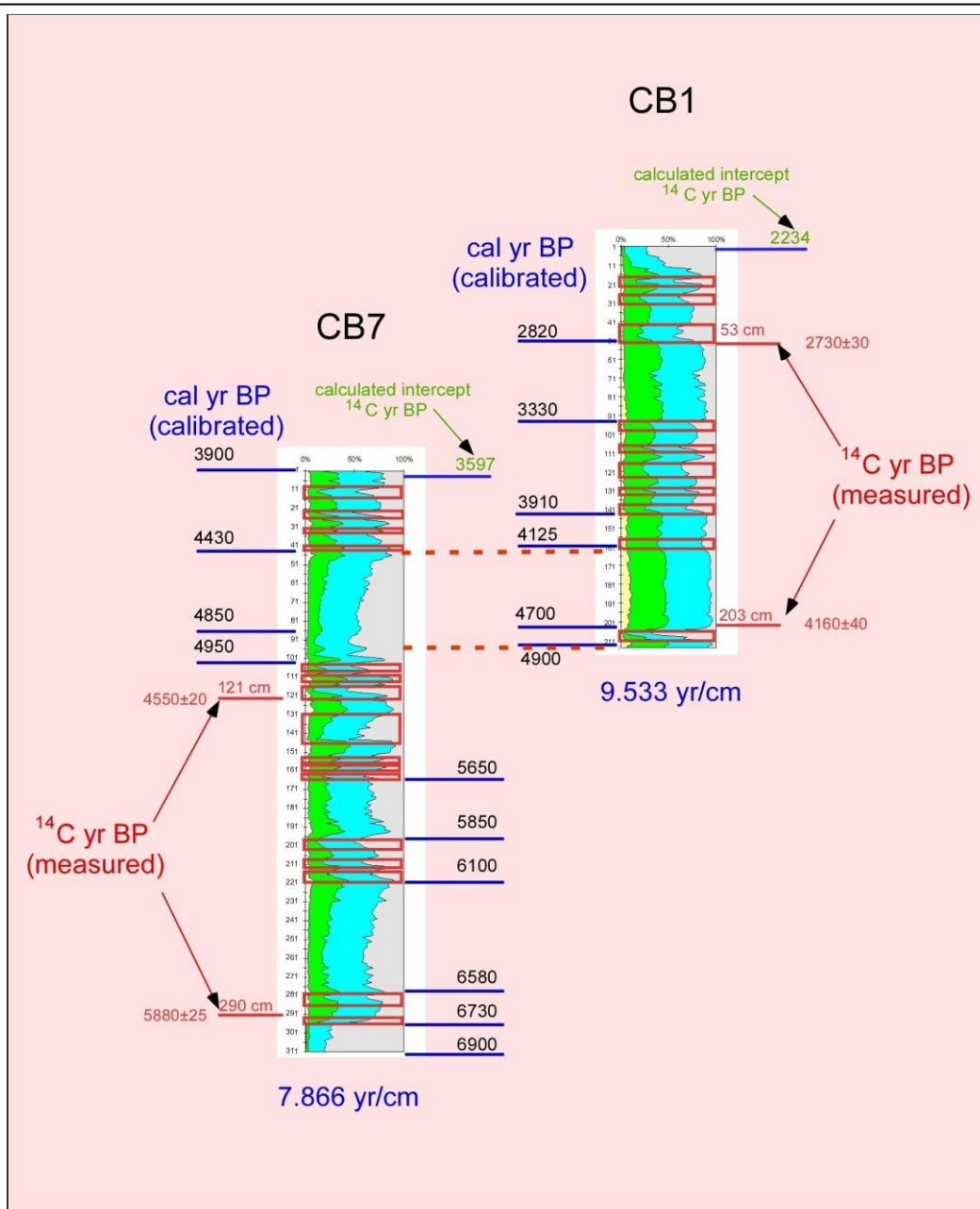
Evidence of just such an event is presented by Zone 1, which apparently marks the

location's transition from wetlands to lake. Unfortunately, the age of the hypothesized event can probably not be dated accurately, as, following our reasoning, it rests on top of eroded material. However, it cannot have occurred earlier than the most recent sediments, with a calculated age of 2234 ^{14}C yr BP (top of CB1). Assuming that the wetland surface at the time of the event approximates current lake level, ~ 50 cm of material was eroded at CB1, which, at constant sedimentation, calculates to 476 ^{14}C years, or a date of ~1700 ^{14}C yr BP. (Of course, it is possible that deposition had ceased previous to the event.) Thus, an extremely rough estimate is that the event responsible for the formation of CBL as a lake occurred sometime ~ 1700 ^{14}C yr BP. Samples have been selected for dating near the core tops of both CB1 and 7 to test our chronology hypothesis.

The chronological correlation between CB1, 7, based on truncated sedimentation, is presented in **Figure 7:41**.

7.6.2.4 Transect Zonation

Excluding the problematic core CB2 produces a coherent zonation across the transect when cores CB1, 3-6 are plotted by depth, and then correlated stratigraphically with CB7 under the chronology adopted above (Figure 7:42). Including CB2 produces several zonation possibilities (Figure 7:43a, b, c). Using the complete CB2 core, the zonation is nearly horizontal throughout the transect (Figure 7:43a), however Zone 4 in CB2 does not much resemble Zone 4 in either CB1 or CB7 due to a lack of clastic layers. Figure 43b presents an alternative zonation using the complete CB2, that leaves Zone 4 greatly condensed and Zone 5 correspondingly expanded compared to CB1, 7. In Figure 7:43c, the suspect interval (72-99cm in CB2) is treated as extraneous disturbance and is removed from the LOI diagram. This results in an expanded Zone 3 for CB2. It is possible that due to some extremely local geomorphologic condition that



7.41 Chrono-stratigraphic correlation between cores CB1 and CB7, supported by chronological and stratigraphic correspondences.

the bottom section of CB2 was located in deeper water, and is simply recording a separate environment. Although all three scenarios present difficulties, we will use the scheme presented in **Figure 7:43a** in further discussion, as it presents the most coherent stratigraphic correlation. In fact, however, the general transect pattern seems clear from the other cores, making the selection subcritical.

Zone 1 is temporally discontinuous with the other zones, as, according to our analysis it has been superimposed on top of eroded material, explaining why it is located immediately above Zone 2 in cores CB1-6, but above Zone 4 in CB7. Zone 2 appears in all cores except CB7, Zone 3 only in CB1, and 2. Zone 4 occurs in CB1, 2, and 7. Zones 5, and 6 are found in CB1, and 7, while Zones 7-9 only occur in CB7 (**Figure 7:43a**).

7.6.2.4.1 Zone 1 is a greenish brown clay, occasionally containing shells, distinctly different from any other sediments within the transect. This zone thins landward across the transect, but generally begins abruptly, usually with a sand/silt base.

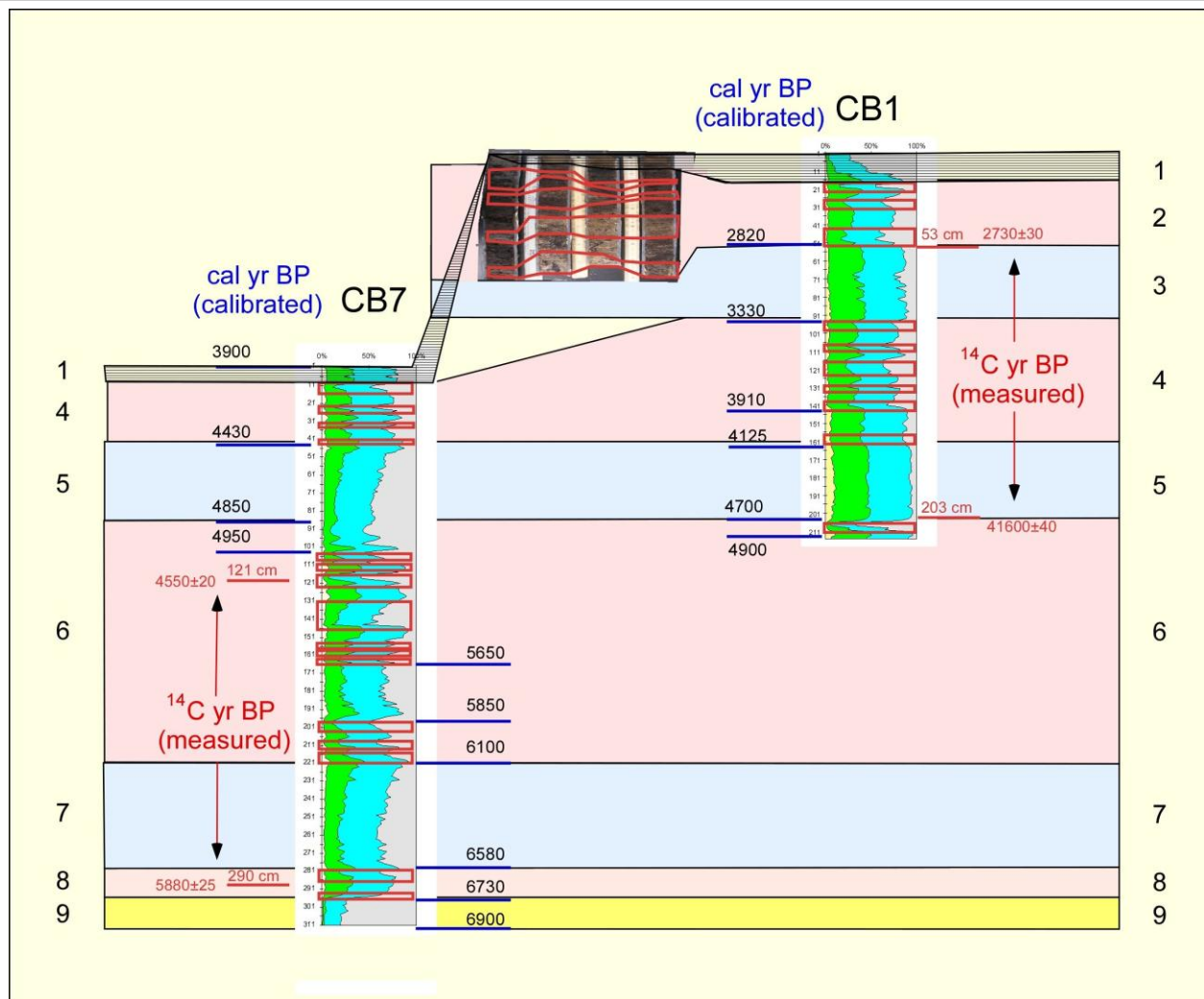
7.6.2.4.2 Zones 2, 4, 6, 8 are generally organic intervals, interrupted by repeated clastic intervals.

7.6.2.4.3 Zones 3, 5, 7 generally lack the abrupt clastic layers. The organic values are generally low when these Zones occur in CB2, and 7 and high in CB1.

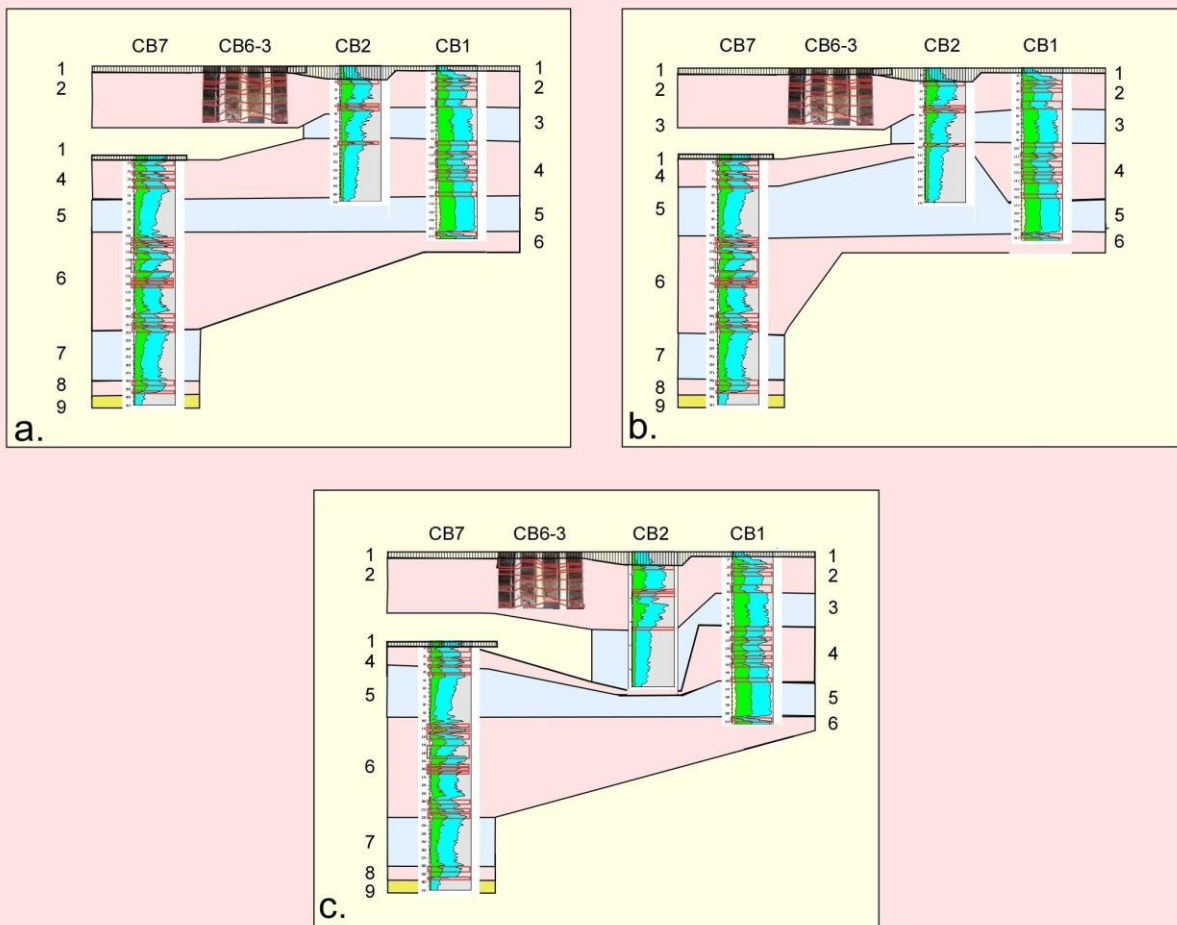
7.6.2.4.4 Zones 9 is sand, probably predating the formation of the wetland.

7.6.2.5 Clastic Layers

Clastic layers in this transect occur in two easily distinguishable general forms. The first is a thick, massive gray clay which occurs over extended intervals, and displays incremental compositional and/or color change and relatively stable grain size. This is interpreted as resulting from slowly changing environmental conditions, probably related to water depth. The second type are thin, visually distinct layers exhibiting abrupt bottom contact, dramatic



7.42 CB transect zonation, excluding core CB2.



7.43 Three alternative zonations for the CB transect, depending upon the treatment of core CB2.

color/compositional changes, and abrupt grain size spikes, all characteristic of sudden changes in the depositional environment, and therefore interpreted as event generated. Perhaps the most intriguing feature of this transect is the periodic occurrence of event layers. The composition of these intervals varies from sand in CB 3, 4, and 5 to silt, clay, and mica in CB 1, 2, 6, and 7. Sand intervals in the middle cores display a consistent geographical pattern. **Figure 7:38a** shows that for the interval outlined in green (**Figure 7:36, 38d**) grain size progressively decreases landward. The same is true for the top of the blue event (**Figure 7:38b**), and generally true for the bottom of that event (**Figure 7:38c**), although grain size is slightly larger for CB5 than CB4. Comparison between **Figures 7:38b** and **c** show that fining upward occurs for the interval. Because landward and upward fining is an expected result of landward transport, this evidence supports a seaward sand source. Due to the general lack of sand in the two most seaward cores, the most likely source candidate is the relict dune underlying these middle cores. Presumably, sand is readily accessible along the seaward edge of the antecedent dune, which *is* resuspended in storms and moved inland. Higher elevations on the seaward section of the relict dunes could have remained subaerial throughout much of the period and provided a source of sand to be transported landward by storm surges. The beach, consisting of clean (98% residual), poorly sorted, very coarse sand is another potential source. Direct fluvial delivery of coarse sand from the land side of CBL is unlikely, given the low gradient and extensive wetlands to the west, the distance to the western edge of CBL, and the fining pattern mentioned above. Although the beach sand originates in the interior highland, it is most likely delivered to the ocean by the larger streams and then moved latitudinally by longshore transport and pushed onshore by wave action.

One potential source of the silt, clay, and mica is the beach barrier, across which the surface sediments vary dramatically, transitioning from clean sand to sand in an organic muddy

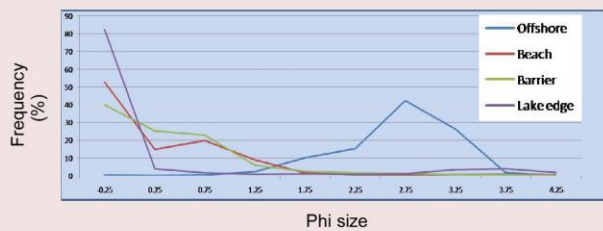
CBL sand samples

25 m offshore

Ocean beach

Barrier

Lake edge



Loss on ignition

	% Water	% Organic	% Carbonate	Residual
Offshore	0	1	1	98
Beach	9	1	1	98
Barrier	44	17	1	82
Lake edge	11	5	1	94

7.44 Grain size distribution and photos of CBL barrier and offshore sediment samples.

matrix that becomes increasingly organic (**Figure 7:44**). Mica is present in all of the barrier samples. The low barrier surface is probably regularly affected by waves, wind, changing vegetation patterns, and bioturbation, resulting in the spatial heterogeneity and the chaotic mixture of dissimilar and poorly sorted material seen in **Figure 7:44**. Offshore, a rapid fining of material occurs; the sample taken from at 25 m is mainly (>86%) fine to very fine sand. Grain size commonly reduces through silt to clay farther offshore (Open University, 1999). Large storm surges can therefore be expected to entrain and transport a great variety of material that spans the grain size spectrum, from offshore through dune zones. Upon reaching the deeper waters of CBL, standard settling processes, resulting in an inverse relationship between grain size and distance transported, should dominate, meaning that larger material should be preferentially deposited over distance inland, creating the fining inland pattern observed in the sand samples.

This pattern is not as obvious for the smaller grained intervals, particularly given that Zone 4, and 6 are the only clastic dominated zones that occur in both CB1 and 7 (**Figure 7:42**). The top of Zone 4 is probably missing in CB7, and only the extreme top of Zone 6 is present in CB1, making transect-wide correlation of the deeper clastic layers infeasible. However, the thin, abrupt nature of these layers argues that these, like the sand layers, are event-generated.

Although CBL's watershed is small and flat, extremely large precipitation events may be capable of transporting silts and clays from the lagoon's western edge and depositing them in the core locations (a distance of ~ 1km), especially the flat mica flakes. The effectiveness of such transport depends, of course, on the existent hydrodynamics, determined by factors as such water depth, water movement, and vegetative regime. Coastal impacts of hurricanes generally result from a combination of the effects of storm surge, wind speed, and precipitation, which do not

necessarily have a direct relationship. During hurricanes producing large storm surges (direct hits) landward sediment transport would be relatively more important, while the reverse would be true for storms with relatively large precipitation totals and smaller surges. Such a bi-directional transport system would act to mask landward interval event thinning, and complicate cross-transect correlation.

In my opinion, the cause of the clastic layers is most likely intense tropical storms. Apart from tsunami, hurricane-generated storm surge is basically the only plausible agent for the landward transport of very coarse sand and their deposition in distinct layers, as this material is too large for easy movement by aeolian processes. Storm surge will certainly transport the barrier's silt and clay material, as well, while the associated erosion and rainfall is the most likely source of the extreme conditions necessary for the transportation and deposition of inland clays in the core locations. Although it is impossible to exclude all non-hurricane severe weather events, typically the largest rainfall events result from hurricanes. For example, in North Carolina the near simultaneous passage of three events brought "unprecedented" rainfall, delivering up to 85% of the annual precipitation in some locations (Bales et al., 2000). Similar effects occur in the tropics, with individual events commonly producing > 500 mm of rain (Riehl, 1979), with totals of >2000 mm having been recorded (Gupta, 1988). In Puerto Rico individual storms since 1899 have produced 5-40% of the average annual rainfall at specific locations (Scatena and Larsen, 1991), while in Nicaragua the rainfall associated with Hurricane Mitch (1998) has been the largest single precipitation event in >100 years (Unsigned, 1998). Due to the close stratigraphic correlation in both depth and number of clastic layers between CB3, 4, 5, and 6 and Zones 1 and 2 of CB 1, the four middle cores have been treated as a holding abbreviated records and assigned to the top two zones. However, as no samples have been dated

from these cores, the possibility exists that in fact these cores contain a shortened, comingled record of the entire history, with each of the four clastic layers being condensed versions of Zones 2, 4, 6 and 8. Due to the thin depositional layers, the apparently shallow water depth and lack of fine grain sediments, repeated storms powerful enough to move and resuspend sand grains could easily turn the signature of several closely spaced storms into a single indistinguishable storm layer. However, we consider this a less likely scenario, and unless additional dating proves otherwise, we will consider these cores to have recorded only the most recent history.

Although the clastic layers behave similarly (disappearing) in Zones 5 in both CB1 and CB7, the surrounding environment appears to be very different for the two locations (**Figure 42**). In CB1 these zones are marked by high water and organic values, suggesting lush wetlands, while the values are much lower in CB7, suggesting deeper water or bare vegetation. The differing environmental conditions suggest that during this period the cores locations were in separate hydrological systems, divided by the relict dune below cores CB3, 4, 5, and 6. This is reasonable, as aligning the cores by depth shows that the bottom of the middle cores (i.e. the surface of the relict dune) corresponds roughly to the bottom of Zone 2 in CB1 (**Figure 7:42, 43**). It is possible that until the water table reached this level this ridge formed the division between a fluvial/precipitation based freshwater wetlands to the west and a beach and dune system to the east. In that case, CB1 would have been located in a shallow swale, functioning as a salt/brackish marsh or swamp, while CB7 would have been located at the bottom of a wetlands deep enough to prevent *in situ* plant growth. The fact that clastic layer occurrence continued in parallel through unrelated systems argues that the process generating these layers was external to the systems.

7.6.2.6 Hurricane Activity

Regarding the lettered clastic layers as hurricane-generated allows us to establish a proxy hurricane strike record, with each strike represented as a red box (**Figure 7:45**). However, as the youngest extant material below the lake interval (Zone 1) appears to be at least 2000 years old, there is no possibility of identifying any historical storms. Like the HPN transect, the multitude of historic events is not present in the sedimentary record, suggesting either very low site sensitivity, or, more likely, a non-recording environment.

By combining the information from CB1 and 7 the record extends from ~6900 – 2400 cal yr BP, with calculated cal yr BP dates for each regime changes marked in black (**Figure 7:45a**). These calculations are based on an assumption of constant sedimentation at the rate indicated by the trendlines (0.105 cm/yr for CB1, 0.127 cm/yr for CB7). The most striking feature of this record is the clustering of events, resulting in clearly distinguishable regime shifts between Active and Quiet periods, until environmental changes ~6700 BP probably render the proxy inarticulate (non-recording). When the dates are rounded off to the nearest 100 years, and adjustments made between the overlapping sections, the following pattern presents itself (years in cal yr BP) (**Figure 7:45b**):

Active – 2200-2800

Quiet – 2800 – 3300

Active – 3300 – 4300

Quiet – 4300 – 4800

Active – 4800 – 6100 (possibly containing a short [~200 years] Quiet period beginning ~5600

Quiet – 6100 – 6600

Active – 6600 – 6700

Nonrecording – 6700 – 6900

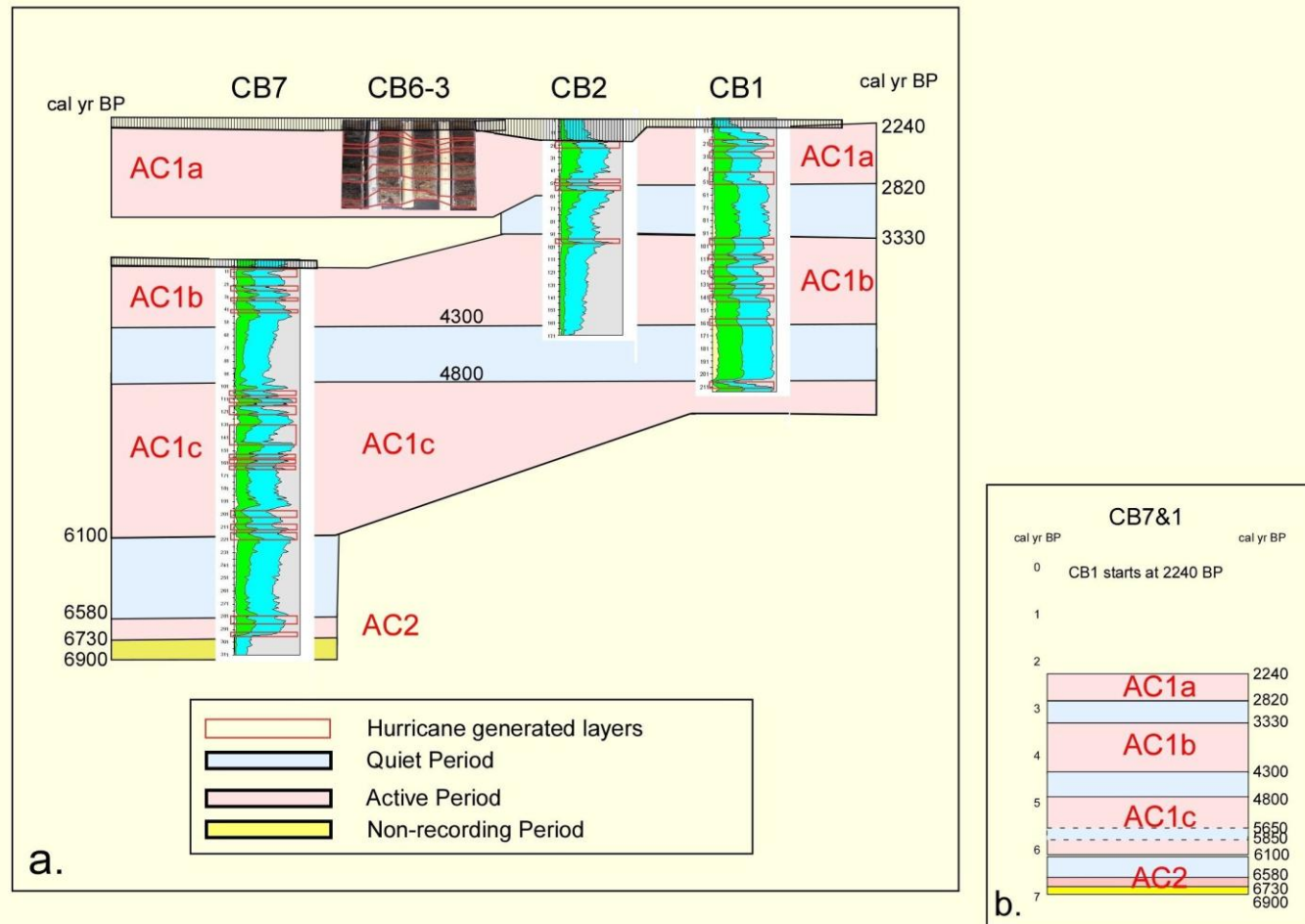
7.6.2.7 Return Intervals

Return intervals can be calculated for several of the activity zones. Three events occur over ~600 years in AC1a of CB1, while in CB3-6 there are four events during what is perhaps the same interval, giving a return interval of 150-200 years (**Figure 7:42**). For AC1b, CB1 shows evidence of six events over ~1000 years, while CB7 indicates four events in ~500 years, giving return intervals of 125-167 years. AC1c shows a return interval of 130 years at CB7, with 10 events in ~1300 years. The short and truncated AC2 shows two possible events in ~150 years or a return interval of 75 years. Thus, return intervals for the Active Periods have remained fairly constant over time, ranging from 75-200 years, but clustering around 150 years, equivalent to a 0.6% annual average strike probability. No events are recorded for the quiet periods. These return intervals are roughly of those half of those calculated for the Active Period for the HPN transect. These relatively short return intervals, combined with the lack of sedimentary evidence for historic storms, argues that site sensitivity has dropped dramatically, either due to complete cessation of deposition and/or the replacement of a wetlands by a lake.

7.6.2.8 Environmental Stability

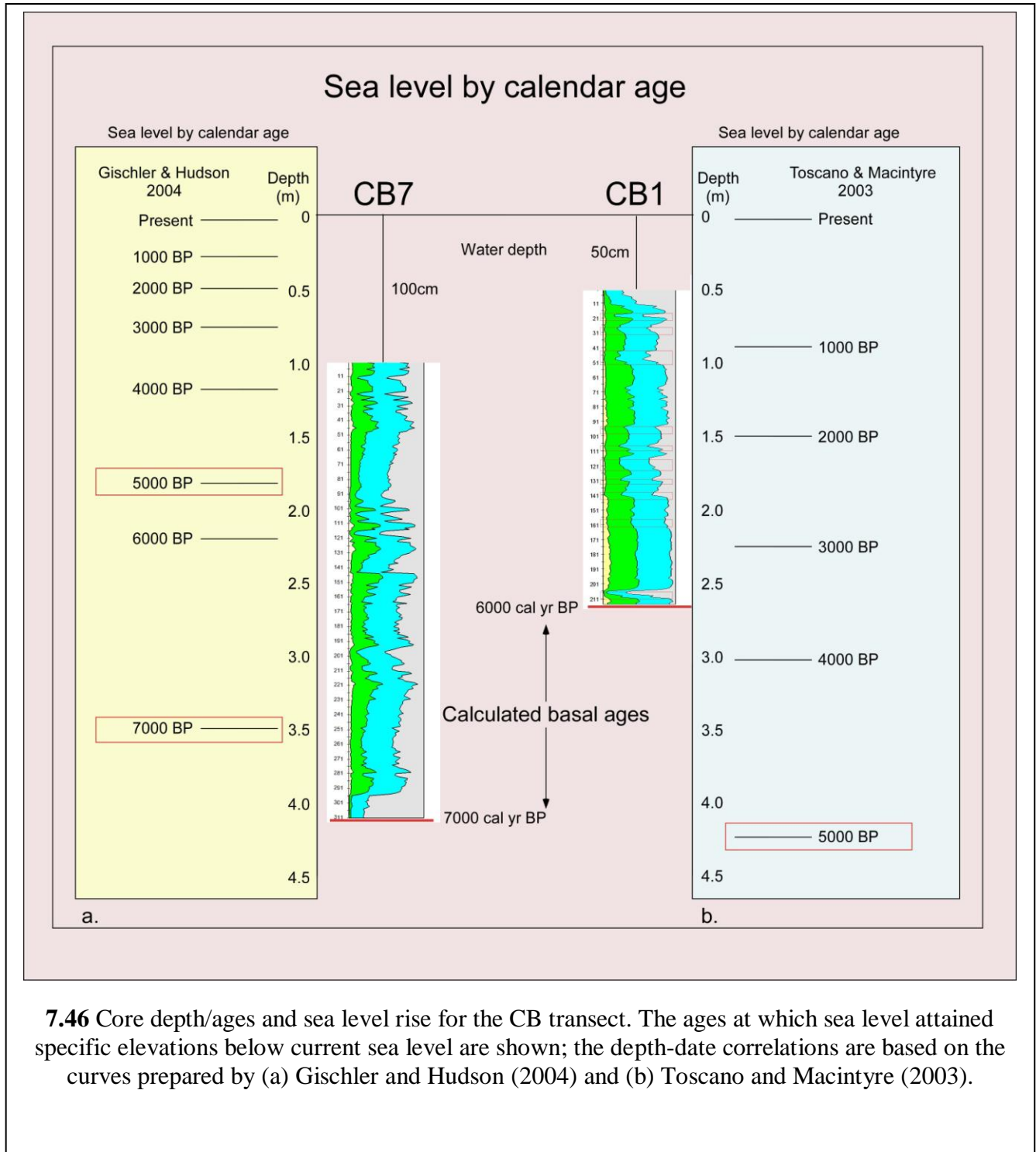
With calculated basal dates of for 4900 and 6900 cal yr BP, the significance of environmental change that may have occurred over the record must be considered. Accepting the visual estimation that the surface of CBL was approximately at MSL at time of coring, the bottom of core CB7 lies >4 m below present sea level (100 cm depth of lake water column plus 312 cm of sediments), while the bottom of core CB1 lies >2.5 m below present sea level (50 cm of lake water plus 216 cm of sediments).

At 7000 cal yr BP sea level had not yet slowed and was from 3.5 m (Gischler and



7.45 Paleostrike record (a) for the CB transects, with activity regimes identified; (b) is a summary regime diagram. Radiocarbon dates are interpolated from dated samples, and then calibrated to cal yr BP by means of the CALIB 5.0 program, with a median date of the high probability date ranges selected.

Hudson, 2004) to 7 m (Toscano and Macintyre, 2003) below present, while at 5000 cal yr BP the rate had slowed and sea level was from < 2 m (Gischler and Hudson, 2004) to slightly > 4 m (Toscano and Macintyre, 2003) below present. Displaying calendar ages and estimated sea levels on a common platform with core depths (**Figure 7:46**) demonstrates that, according to the Gischler and Hudson (2004) curve, both cores should have been below sea level at the calculated date of the initiation of deposition, while the Toscano and Macintyre (2003) curve places both far above contemporary sea level. In either case, if eustatic sea level was the sole controlling factor, sedimentation should have continued to the present. However, water depth within the back barrier environment may not have been identical to sea level. Perhaps significantly, the top of CB7, with a calculated date of 3900 cal yr BP, terminates slightly above what the Gischler and Hudson (2004) curve indicates was sea level at 4000 cal yr BP. If barrier height had permitted back barrier deposition to exceed sea level, then a rupturing of the barrier and a return to sea level for back barrier water table around that time could account for the cessation of deposition. The correspondence between Gischler and Hudson's (2004) estimated sea level and cessation is just as close for CB1, with deposition apparently ceasing ~ 2240 cal yr BP, and core height matching a sea level date of ~2000 cal yr BP. As mentioned earlier, the Gischler and Hudson curve, derived from Belizean data, seems to be the most appropriate curve for the country. As initial site elevation relative to sea level was probably not significantly different than at the present, any change in site sensitivity probably results from a combination of lateral beach movement and barrier height. Given the relatively steep offshore bathymetry, a 3 m drop in sea level only moves the shoreline ~100 m seaward (CSE, 2007) (**Figure 7:2**). Under such conditions at 7000 cal yr BP CB7 would be in a position roughly analogous to the present position of HPN5, while at 5000 cal yr BP the Gischler and Hudson (2004) sea level curve shows



the base of CB1 slightly below sea level about 250 m from the sea, similar to the present position of HPN1. Modeling the system at the time on the present functioning of the HPN back barrier environment, it seems likely that, as found, hurricane events should have been recorded as clay layers, with perhaps some diminishing sensitivity related to the greater site-sea distance. In general, although distance has decreased over time, it probably resulted in little overall change in site sensitivity, as long as deposition continued. However, as the last ~2200 years do not seem to have been recorded at this site, no estimation of the threshold level is possible.

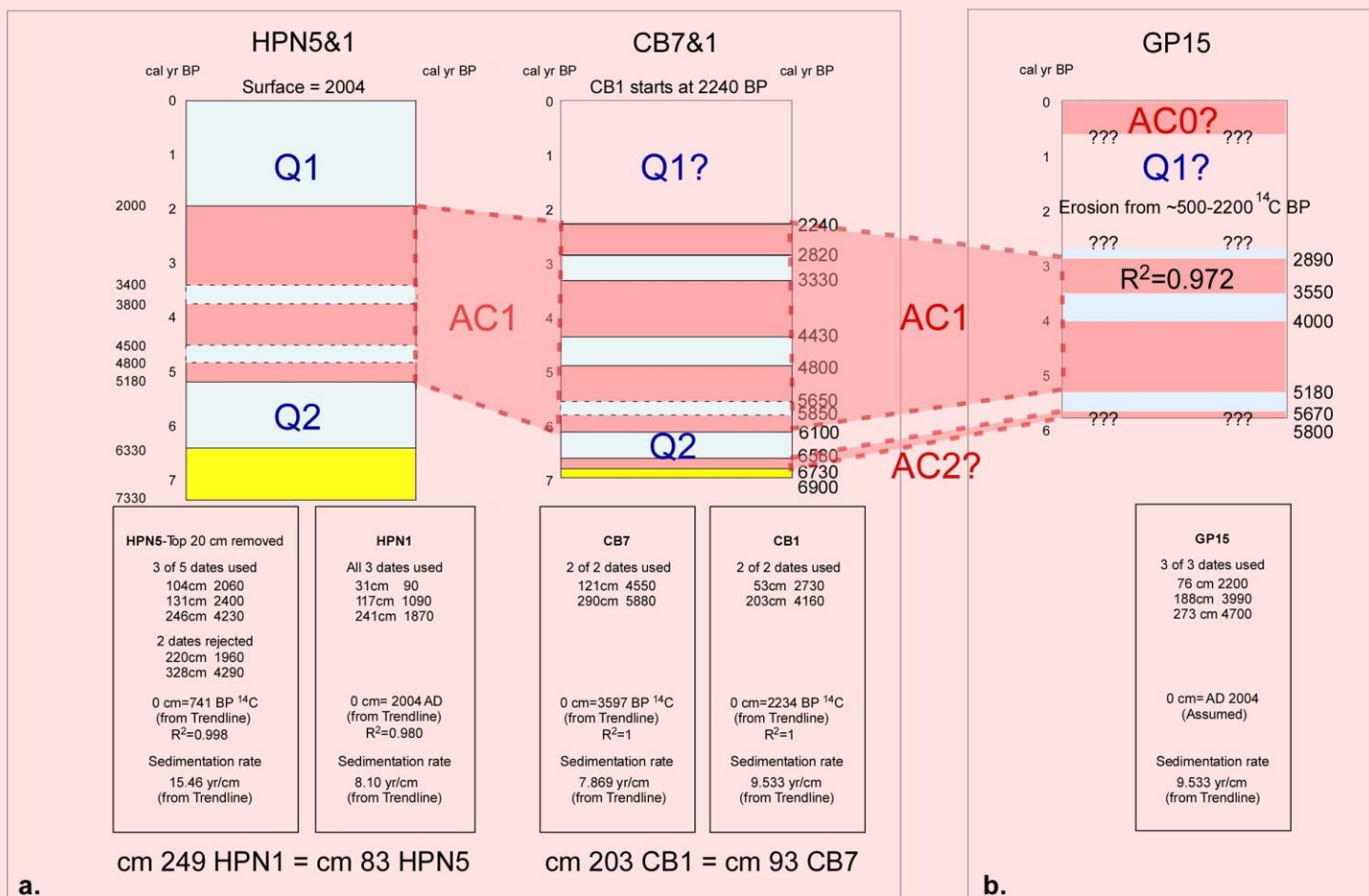
7.7 Overall Summary

7.7.1 CB-HPN-GP/MR Hurricane Activity Correspondence

There is good correspondence between the HPN and CB transects in terms of the dating of hurricane activity regimes (**Figure 7:47a**). Both sites show an extended AC1, punctuated by two-three short periods of reduced activity, which is preceded by Q2, extending until the basal, nonrecording, period. Q1 shows reduced activity for the past 2000 years at HPN; this part of the record is missing for CB. Although the regime pattern is similar, there are some temporal discrepancies, as the AC1 extends ~ 1000 years farther into the past at CB than for the HPN transect.

The return intervals during Active periods are roughly twice as long for HPN as for CB, probably indicating a higher minimum recording threshold for at HPN. Because of the less frequent sedimentary signatures, the identification of short Quiet subperiods within Active periods is more problematic for HPN.

These activity regimes match fairly well with the those inferred from the Gales Point/Mullins River record discussed in **Chapter 6 (Figure 7:47b)**, which show a punctuated AC1 from ~5200 – 2900 cal yr BP, with the suggestion of an earlier one (AC2) beginning ~ 5700



7.47 Hurricane activity regimes for mainland Belize sites; (a) HPN, CB (this chapter), and (b) GP/MR (Chapter 6).

cal yr BP (**Figure 7:47b**), as does CB. The identification of AC2, however, rests on a small number of events at the bottom of the cores and possibly results from the water table rise associated with post glacial sea level rise. The brief recent Active period (AC0) (~the last 500 years) observed in the GP transect was not found at HPN (CB was non-recording during the period), and has therefore been marked with a question mark.

7.8 Conclusions

The HPN and CB transects share similar subsurface topography, most likely a Pleistocene age dune and swale system, with long end cores apparently located over antecedent swales and shorter middle core located on sand based topographic highs. Due to this topography, multiple occasionally isolated, environmental systems probably existed at times along both transects, resulting in nonuniform sedimentation. In the HPN transect the middle cores apparently recorded a complete, though condensed sedimentary history, whereas in the CB transect the middle cores probably captured only the most recent history. Cessation of deposition apparently occurred in both transects, with the sedimentary record terminating before the present in specific cores. Because of the elevational differences resulting from the nonuniform antecedent topography, depositional responses to high energy events varied by location.

Although relative relief is similar between the transects, absolute relief is different. The present surface of the HPN transect is higher, and has captured the last ~5000 years, while the present surface of the CB transect is below sea level, containing a record from ~7000 – 2400 cal yr BP. In both cases, for different reasons, site sensitivity is low and has probably remained fairly constant throughout the periods recorded. Neither site has captured sedimentary signatures of any historic storms, although the tracks of several major hurricanes have closely approached the site during the historical period. This is as expected at CB, which has not been recording for

the past two millennia. For HPN this indicates that site sensitivity is probably on the catastrophic level (possibly >category 4), although track location is of great importance, as a narrow geographic window controls storm surge effects. Return intervals at HPN during Active Periods have been on the order of 250 years, nearly twice that for CB. For this reason, we can assume that site sensitivity was greater at CB, although threshold storm magnitude cannot be estimated.

Despite the low sensitivity the sedimentary both transects record hurricane landfalls and show clear evidence of multi-centennial to millennial scale variability in hurricane activity. The records for the two sites are in general agreement, although timing is not completely consistent, as the Active Period extends farther into the past at CB. Combining the two records produces the following activity regimes record (dates are in cal yr BP, and rounded to the nearest century):

Quiet- Present- ~2000

Active- ~2000- ~5200 (HPN), or 6100 (CB)

Quiet- < ~5200 (HPN), 6100 (CB)

Unknown- <~6300 (HPN), 6700 (CB)

The long Active period is punctuated by a two-three shorter, ill-defined quiet subperiods. This activity regime record is in general accord with that produced from the GP/MR site (**Chapter 6**), although timing is not exact. The recent Active Period (~ the last 500 years) found there is not observed in this record.

Further samples have been sent for AMS dating in order to resolve chronological inconsistencies.

7.9 References

Anderson, A. H., 1958. Brief Sketch of British Honduras. Belize. Government Printer. London.

Avila, L. A., 2001. Tropical cyclone report: Hurricane Iris 4-9 October 2001. National Hurricane Center. <http://www.nhc.noaa.gov/2001iris.html>. Accessed April 9, 2009.

Bales, J. D., Oblinger, C. J., and Asbury H. Sallenger, Jr., A. H., 2000. Two months of flooding in eastern North Carolina, September - October 1999: hydrologic water-quality, and geologic effects of Hurricanes Dennis, Floyd, and Irene. Water-Resources Investigations Report 00-4093. Raleigh, North Carolina 2000.

Bass, J. O., 1999. Garifuna seashore, Creole riverside: an ethnographical investigation of two Belizean villages. Unpublished Masters Thesis, Louisiana State University.

Bolland, O. N., 1986. Belize: A New Nation in Central America. Westview Press, Boulder and London.

Burdon, J. A., 1931. Hurricane in British Honduras. Blackwood's Magazine 230, 547-585.

Burdon, J. A., 1931-1935. Archives of British Honduras, Edited with an historical note by John Alden Burdon. 3 volumes. London.

Cain, E. E., 1933. Cyclone! Being an Illustrated Official record of the Hurricane and Tidal wave which Destroyed the City of Belize (British Honduras) on the Colony's Birthday, 10th September 1931. Arthur H. Stockwell, Ltd, London.

Coastal Science & Engineering (CSE), 2007. Supplemental coastal engineering report: Shoreline assessment and preliminary design for waterfront improvements, Hopkins Bay Resort, Hopkins, Belize, CA. Coastal Science & Engineering (CSE), Columbia, South Carolina.

Evans, H.B., 1965. GRAPE - A device for continuous determination of material density and porosity. Proceedings of 6th Annual SPWLA Logging Symposium. 2, 25.

Gischler, E. and Hudson, J. H., 2004. Holocene development of the Belize Barrier reef. Sedimentary Geology 164, 223-236.

Gupta, A., 1988. Large floods as geomorphic events in the humid tropics. In Baker, V. R., Kochel, R. C., and Patton, P. C., (eds) Flood Geomorphology. John Wiley and Sons, New York, 310-315.

Lawrence, M. B., 1979. Atlantic hurricane season of 1978. Monthly Weather Review 107, 477 - 491.

Leyden, B. W., 1987. Man and climate in the Maya lowlands. Quaternary Research 28, 407-417.

Marshall, J. S., 2007. Geomorphology and physiographic provinces. In Bundschuh, J., and Alvarado, G. E., (eds), Central America Geology Resource Hazards. Taylor and Francis, London. Vol. 1, 75-122.

Masselink, G., and Hughes, M.G., 2003. Introduction to Coastal Processes and Geomorphology. Arnold Publishing, London.

Metzgen, M. S., and Cain, E. E., 1925. The Handbook of British Honduras Comprising Historical, Statistical and General Information concerning the Colony. The West India Committee, London.

Moberg, M., 1992. Citrus, Strategy, and Class: The Politics of Development in southern Belize. University of Iowa Press, Iowa City.

Moberg, M., 2001. Responsible men and sharp Yankees, the United Fruit Company, resident elites, and colonial state in British Honduras. In Striffler, S., and Moberg, M., (eds), Banana Wars: Power, Production and History in the Americas. Duke University Press, Durham, North Carolina.

Morris, D., 1883. The Colony of British Honduras. Harrison and Sons, London.

Open University, 1999. Waves, Tides and Shallow-water Processes, Second Edition. ButterworthHeinemann, Milton Keynes, England.

Poey, A., 1855. A chronological table comprising 400 cyclonic hurricanes which have occurred in the West Indies and in the North Atlantic within 362 years, from 1493 to 1555. Journal of the Royal Geographic Society 25, 291-328.

Poey, A., 1865. Bibliographie cyclonique. Annal Hydrographica 28, 305-396.

Portig, W. H., 1976. The climate of Central America In Schwerdtfeger, W., (ed), Climates of Central and South America, World Survey of Climatology, 12. Elsevier, New York. 405-478.

Riehl, H., 1979. Climate and Weather in the Tropics. Academic Press, New York.

Scatena, F. N., and Larsen, M. C., 1991. Physical aspects of Hurricane Hugo in Puerto Rico. Biotropica 23, 317-323.

Setzekorn, W. D., 1975. A profile of the New Nation of Belize, formerly British Honduras. Ohio University Press, Columbus.

Stoddart, D. R., 1963. Effects of Hurricane Hattie on the British Honduran reefs and cays, Oct.30-31, 1961. Atoll Research Bulletin 95, 1-142.

Tannehill, I. R., 1956. Hurricanes. Ninth edition. Princeton University Press, Princeton, New Jersey.

Toscano, M. A., and Macintyre, I. G., 2003. Corrected western Atlantic sea-level curve for the last 11,000 years based on calibrated C-14 dates from *Acropora palmate* framework and intertidal mangrove peat. Coral Reefs 22, 257-270.

Unsigned, 1978. Preliminary Report Hurricane Greta (& Hurricane Olivia) September 13-23, 1978. http://www.nhc.noaa.gov/archive/storm_wallets/atlantic/atl1978-prelim/greta/prelim01.gif. Accessed April 9, 2009.

Unsigned, 1998. Mitch vs. las lluvias provocadas durante el period de affectation de otros huracanes. In *Las Lluvias del Siglo en Nicaragua* INETER. Instituto Nicarauense de Estudio Territoriales. Managua, Nicaragua. 43-45.

Unsigned, 2001. Hurricane Iris advisory Number 17. Nationa Weather Service, Miami, FL. <http://www.nhc.noaa.gov/archive/2001/pub/all12001.public.017.html>. Accessed April 9, 2009.

Waddell, D. A.G., 1961. *British Honduras: a Historical and Contemporary Survey*. Oxford University Press, London.

Wiley, J., 2008. *The Banana: Empire, Trade Wars, and Globalization*. University of Nebraska Press, Lincoln and London.

CHAPTER 8 TURNEFFE ATOLL, BELIZE

8.1 Introduction

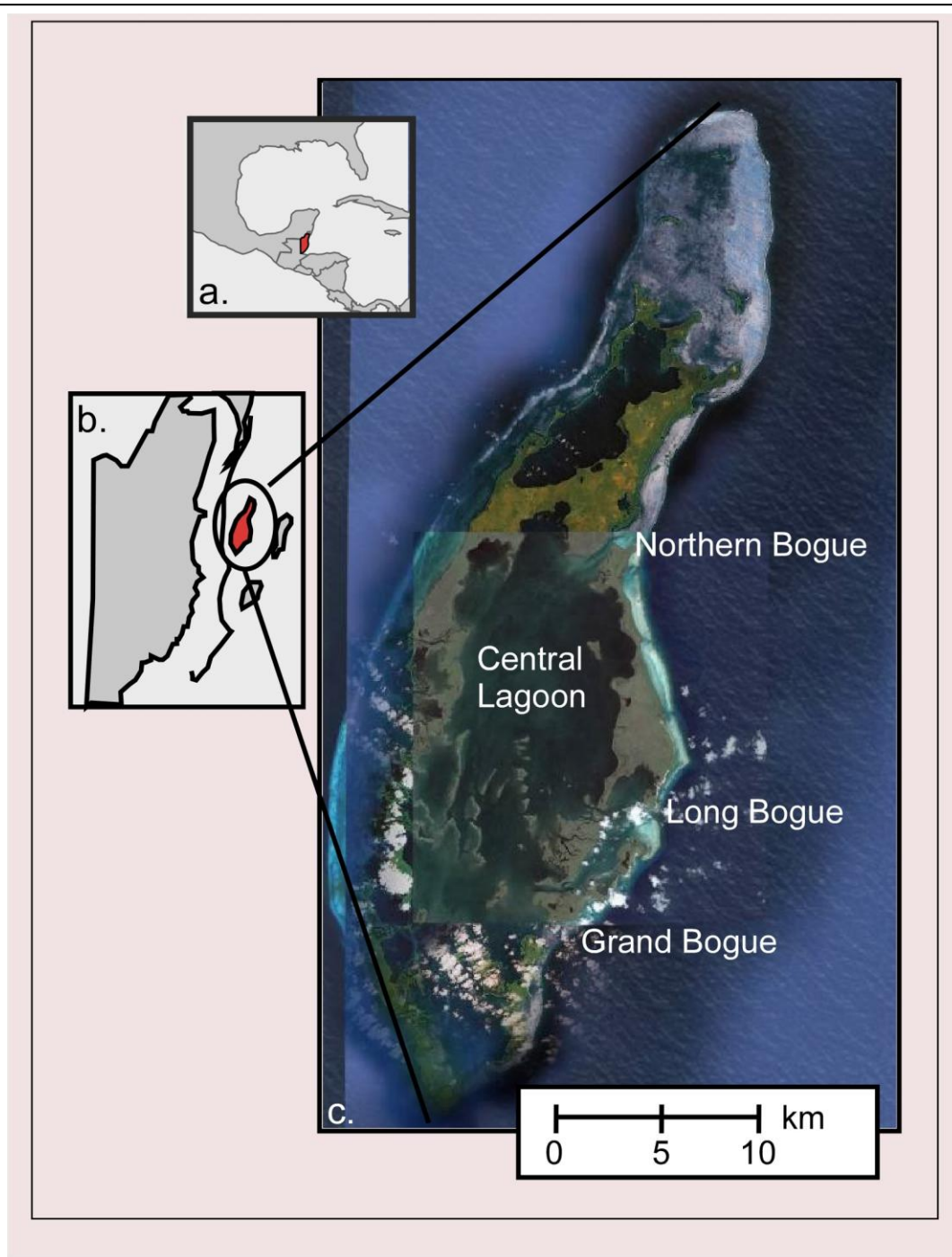
Relative sea level changes can complicate the determination of paleohurricane strike records, particularly along low gradient coasts as small rises can result in large coastal transgressions, thereby changing site-to-sea distances, perhaps dramatically, over relatively short periods. In order to negate this effect of Holocene sea level rise Turneffe Atoll, one of the three carbonate platforms offshore of Belize, was chosen as a study site, as the Atoll is dominated by reefs and mangroves that have kept up with sea level rise. The basic geological framework of these carbonate platforms has been studied in some detail (Gischler, 1994, 2003; Gischler and Hudson, 1998; Gischler and Lomando, 2000; Lomando and Ginsburg, 1998; Stoddart, 1962) and shows the three platforms to have been successively flooded, with Turneffe being the last, at around 6000 BP. The coral on all three platforms have kept up with sea level rise since the time of flooding, even though the temporal differences in initiation of flooding have resulted in different platforms experiencing different rates of sea level rise (Gischler and Hudson, 1998). The extensive mangrove cays found on Turneffe Atoll have similarly kept up with sea level, due probably in part, to a relatively late date for flooding and higher antecedent elevation (Gischler and Hudson, 1998). The mangrove cays have therefore remained basically at sea level since the mid Holocene, potentially preserving a direct archive of hurricane strikes since that period, that do not need to be normalized for shoreline movement.

8.2 Setting

Offshore the continental margin of Belize is characterized by 5 parallel *en echelon* normal faults running to the north-northeast (James and Ginsburg, 1979; Gischler, 1994)

(**Figure 5:3**). Turneffe Atoll is located on the second fault ridge, separated from the barrier reef by water depths of >400 m. The ocean floor drops eastward and depths of >1000 m are encountered between Turneffe and Lighthouse Reef and Glovers Reef, both situated on top of the third fault ridge (**Fig.5:3**). Turneffe Atoll is somewhat elliptical with the long axis running north-south. Maximum distances are ~50 km n-s and 16 km e-w (**Figure 8:1**).

The eastern face of the atoll is basically a vertical wall hundreds of meters in height, topped by a nearly continuous wave breaking rim of coral. This rim is broken by a small number of openings, the most important of which, from north to south, are Northern Bogue, Long Bogue, and Grand Bouge. Lying behind the rim in most places is a reef flat < 400 m wide covered by a few tens of centimeters of water. Small sandy cays, formed by the accumulation of water driven sand, often occur along the eastern edge of the reef-flat, while the western edge generally terminates in mangrove cays. The center of the atoll is the Central Lagoon, dotted with mangrove cays that rise steeply from the lagoon floor. Circulation is restricted. Maximum lagoon depth is 8 m; the floor is densely covered by sea grass (*Thalassia*) and the calcareous algae *Halimeda*, along with sponges (*Spherospongia* species) and occasional coral, mainly (*Porites* species and *Manicina areolata*). Seafloor sediments are dark, stained by the decaying organic matter washed off the mangrove cays and are dominated by *Halimeda* debris (Gischler and Hudson, 1998; Gischler, 2003). Water temperature has a normal annual range of 27°-29°C, but as a result of the restricted circulation, can display dramatic shifts, as can salinity, with extremes of 31°C and 70 ppt being recorded in 1939 (Smith, 1941). The atoll's western edge is dominated by encircling mangrove cays, and the fringing coral rim, which is lower than the eastern rim, commonly subaqueous (**Figure 8:1, 2**). The northern section has a more open circulation and a smaller percentage of land. Tidal range is 30 cm (Gischler, 2003).



8.1 Map of (c) Turneffe Atoll, showing geographical relation to (b) Belize mainland, and (a) the Caribbean.

Atoll vegetation is dominated at by mangroves. At low elevations red mangroves (*Rhizophora mangle*) dominate, with dwarf *Rhizophora* forests developing under higher saline conditions (usually resulting from lack of flushing). Mangrove zonation is common, with fringing *Rhizophora* at the lowest levels, with bands of first black (*Avicennia germinans*) and then white mangroves (*Laguncularia racemosa*) forming behind the red (McKee, 1995; McKee and Faulkner, 2000; Murray et al., 2003). *Batis maritima* and *Sesuvium* species are short ground cover commonly associated with the mangrove zones. Small sections of cay forest consisting of such broadleaf trees as *Bursera simaruba*, *Metopium brownei*, *Cardia sebestena*, *Ponteria campechiana*, *Bumelia retusa*, and *Coccoloba uvifera* occupy the higher elevations and can reach heights of 15 m (Minty et al., 1995). Monospecific stands of coconut trees, generally lacking in understory plants, are commonly found on the beach ridges (Garcia and Holtermann, 1998). Mangroves typically form on peaty soils, and the coconut and cay forests on sandy soils (Stevely and Sweat, 1994; Minty et al., 1995) (**Figure 8:2**).

Sand is produced by the powdering of coral on the reef face and flats; autochthonous carbonate production, mainly by *Halimeda* (mollusks dominate in the open circulation of the other carbonate platforms) dominate the lagoon floor sediments (Gischler and Hudson, 1998; Gischler, 2003). Subaerial sand is most common on the eastern reef flat, either in piles as sandy cays along the inside coral rim or as beaches on the eastern edges of the facing mangrove islands. Beaches are commonly lacking on the interior mangrove islands, which generally rise steeply from the lagoon floor and consist of muddy peat right to the island edge.

Animal species include the American crocodile (*Crocodylus acutus*), manatee, marine turtles, an endemic snake, and many bird species (Meerman, 2006; Platt et al., 2004).

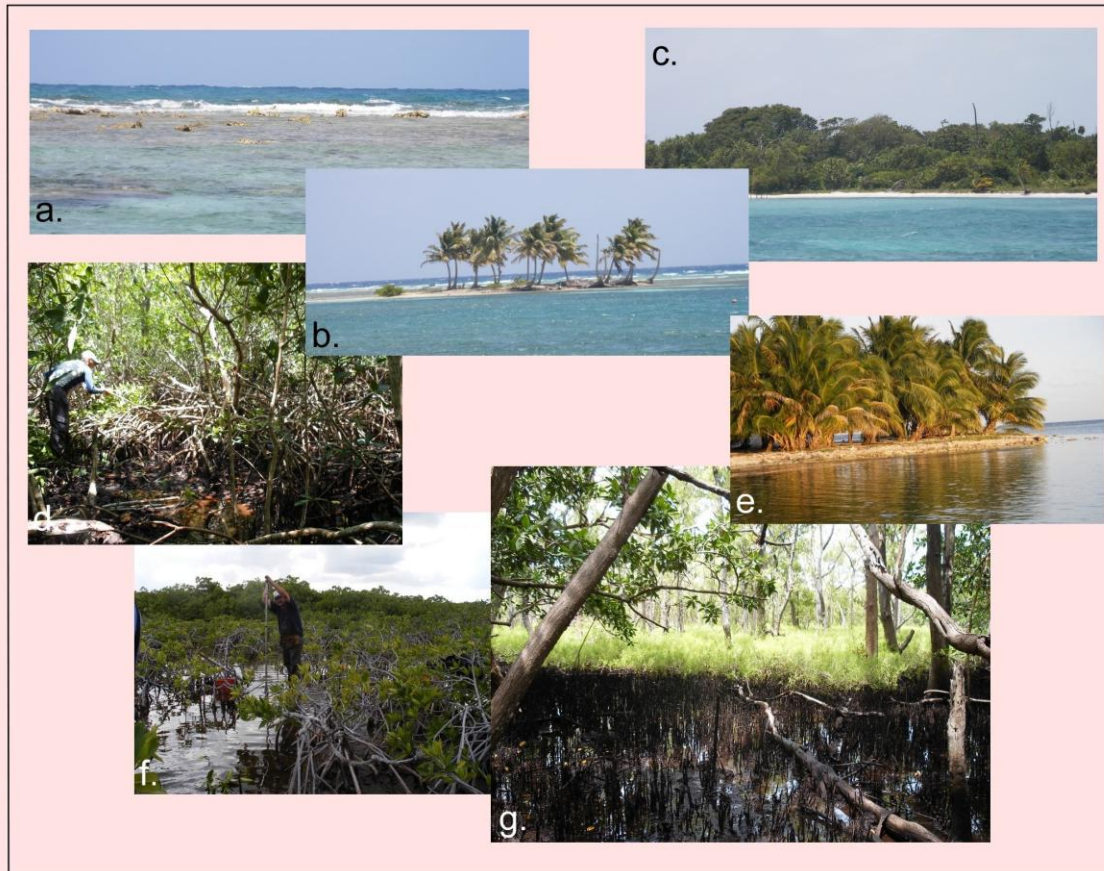
8.3 Study Sites

Cores were extracted from six mangrove cayes; four facing the reef-flat along the eastern edge of the atoll, one in the channel of Long Bogue and one from the Central Lagoon (**Figure 8:3**). The first five sites were chosen to match areas recorded as having received maximum damage from Hurricane Hattie (1961), based on Stoddart's (1963) damage assessment map, while the sixth was used as a control (**Figure 8:3a**). The overall transect covers a 30 km n-s span; individual site transects extend from the sea up to 150 m inland.

8.3.1 GC The farthest north, this site is situated on the eastern edge of a large mangrove cay, directly across the reef flat from Grassy Cays, a group of small sand cays up against the inside rim of the fringing coral. Very tight fringing *Rhizophora mangle* extended into the water beyond the edge of the island; there was no beach. Cores were extracted at 64, 89, and 125 m inland.

8.3.2 Blackbird Cay This transect was taken from the eastern edge of Blackbird Cay, ~ 500 m north of the small airstrip used by one of the tourist operations on the cay. The reef flat is especially wide in this location (>750 m), and there is a wide sandy beach, behind which our transect passed through the *Rhizophora* - *Avicennia* - cay forest zones. Canopy height was ~10-15 m. A total of 12 cores reaching 165 m inland were taken; apart for one long core (360 cm) at 90 m, core length was between 50 and 150 cm. Not all cores were kept.

8.3.3 HJ Cay Three cores were taken from a small mangrove cay approximately 3 km west of the coral rim. The cay's position blocking the channel makes it a likely location to record storm surge funneled down the Long Bogue. Like most of the mangrove cays located off the reef-flats this cay raises very steeply from the lagoon floor, with water depth reaching 4 m less than 10 m offshore. Cores were taken at 1, 29, and 69 m inland, with vegetation changing from thick,



8.2 Physical characteristics of Turneffe Atoll. (a) Wave breaking eastern coral rim and reef flat; (b) a small sandy cay, formed by the accumulation of water driven sand, located along the eastern edge of the reef-flat; (c) cay forest with broadleaf trees; (d) fringing red mangrove (*Rhizophora mangle*) forest; (e) coconut dominated beach ridges; (f) dwarf red mangrove forest in a nutrient poor interior of a mangrove cay; (g) black mangrove (*Avicennia germinans*) trees, with thick *Batis maritima* ground cover.

medium tall (<5m) *Rhizophora* at the first two sites to dwarf (<1 m) *Rhizophora* at 69 m. Core lengths were all >400 cm.

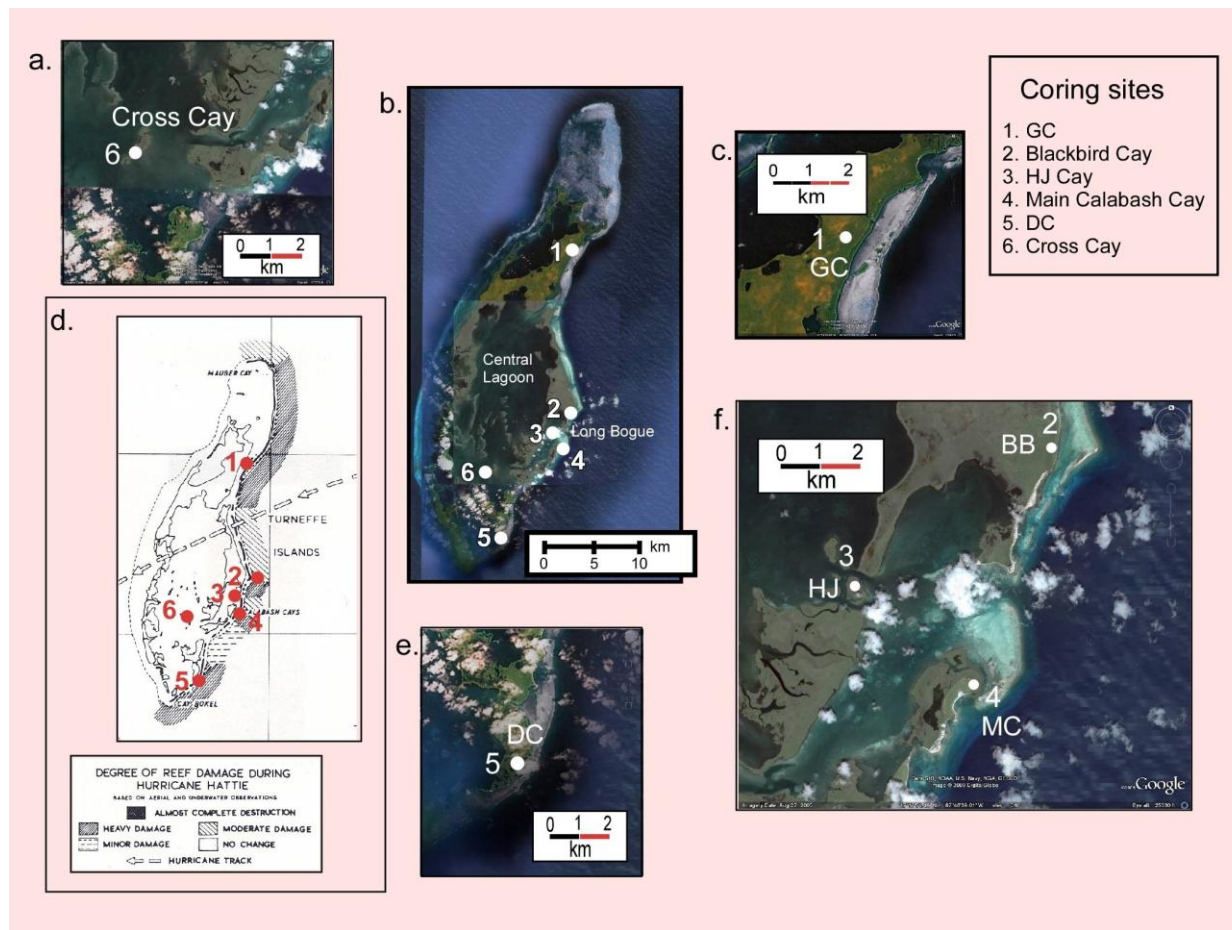
8.3.4 Main Calabash Cay This is a sandy cay on the reef flat, just south of the mouth of Long Bogue. Three short cores (<150 cm) were taken within the *Avicennia* zone along a cusped transect paralleling the northern rim of the cay. The cores were photographed and stratigraphic information recorded, but the cores were not transported to the United States.

8.3.5 DC This site is on a medium size mangrove cay near the south end of the atoll. The reef flat is narrow at this point, ~ 40 m of shallow (>1.5 m) water separates the cay from Deadman's IV, a member of a group of small sand cays on the seaward edge of the reef flat. A single core (353 cm) was extracted from the interior edge of the *Rhizophora* zone, 82 m inland from the sea. A tall *Avicennia* forest begins a few m farther inland, marked by a large number of old (pale, bleached) downed trees, generally pointing toward the northeast.

8.3.6 Cross Cay This site is located on a small mangrove cay in the southern section of the Central Lagoon. A single core, 463 cm in length was extracted from the *Rhizophora* zone, 42 m inland.

8.4 Hurricane History

The tracks of all (a) hurricanes and (c) major hurricanes (category 3 or higher) passing within 65 nautical miles (120 km) of 17.5°N, 87.8 °W (within Turneffe Atoll) from 1851-2008, as recorded by NOAA's HURDAT dataset are shown in **Figure 8:4**. It is basically the same set of storms noted as affecting the mainland sites mentioned in **Chapters 6 and 7**. What is striking about this list is the number of catastrophic storms; five storms achieve at least category 4 within a 65 nm radius with Janet (1955), and Hattie (1961) reaching category 5. Three major storms, the unnamed hurricane of 1931, Hattie (1961) and Keith (2000) all passed



8.3 Study site map. The spatial distribution (b) of the six coring sites (numbered and marked by white dots in Turneffe Atoll): (a., c, e, f) close up Google Earth images of each coring site showing their position relative to atoll geography, especially their proximity to the reef flat. Sites were chosen to correspond to areas suffering maximum damage from Hurricane Hattie, which passed directly over the Atoll in 1961 (d).

extremely close to the atoll.

8.4.1 Unnamed hurricane of 1931

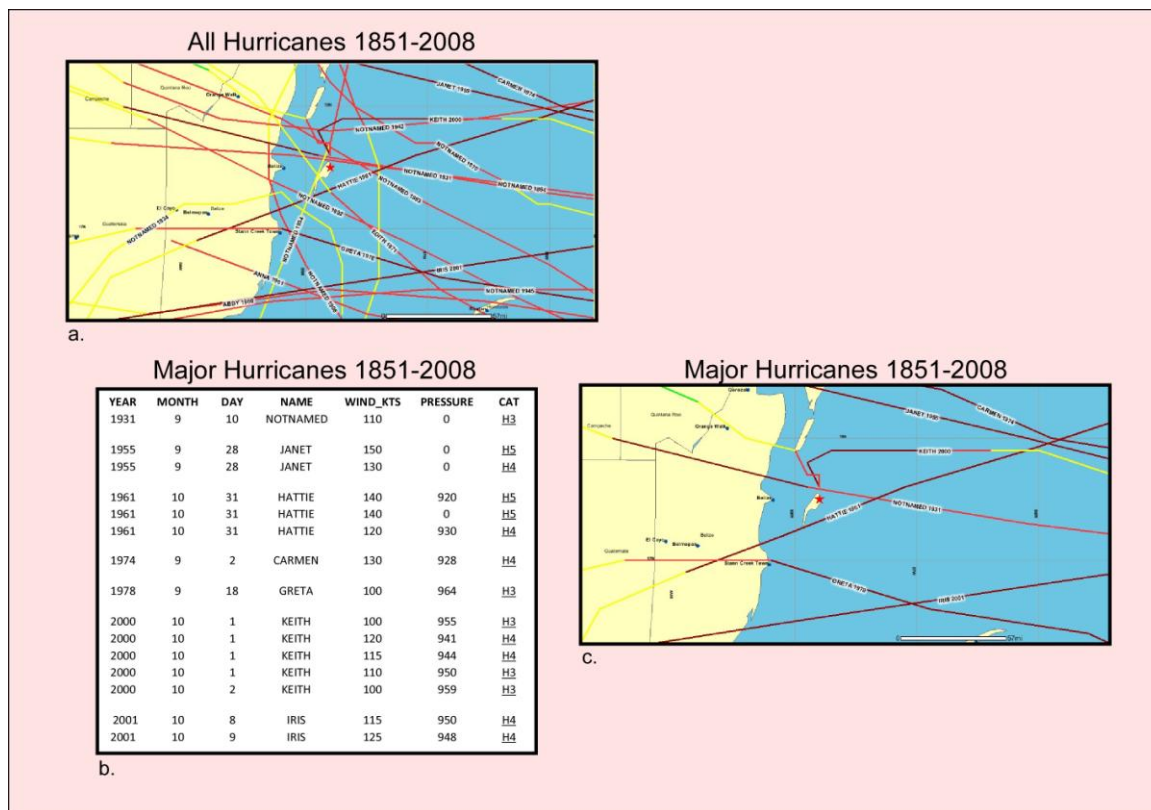
This hurricane's effect on the country of Belize was discussed above (**Chapter 7**). Specific damages to Turneffe are not recorded. HURDAT records show a maximum sustained wind speed of 110 knots (127 mph; 204 kph) as the storm passed slightly to the north of Turneffe.

8.4.2 Hurricane Hattie (1961)

Hattie was a category 5 hurricane with maximum sustained windspeed of 140 knots (161 mph; 259 kph) as it passed over Turneffe. Although NOAA data shows the track passing over the southern tip of the atoll, calculations by Stoddart (1963), based on damage, tree fall and associated data, puts the path farther north, with the eye passing just to the south of Northern Bogue. Much damage was inflicted on the human population, after which the cay was abandoned for many years, partly in response to the destruction of the coconut plantations which were the community's economic backbone (Garcia and Holtermann, 1998). Hattie caused tremendous ecological and geomorphic changes, as detailed by Stoddart (1963). He reports widespread death and defoliation of trees, massive sand movement including the building/removal of beach ridges, extensive scour pits, and a large crack ("several" 100 m long, "several" m wide and >six m deep) that opened in the lagoon floor, accompanied by the emergence of an array of sand banks and shoals, some reaching above sea level.

8.4.3 Hurricane Keith (2000)

Keith became a category 4 hurricane with maximum sustained winds of 120 knots (138 mph; 222 kph) just north of Turneffe. Due to a high pressure system over the Gulf of Mexico and a low pressure system over western Cuba, Keith stalled and remained in the area for > two



8.4 Hurricane history for Turneffe Atoll. The tracks of (a) all hurricanes , and (c) major hurricanes passing within 65 nautical miles (120 km) of the point marked by the red star according to the NOAA HURDAT (“best track”) dataset covering the period 1851-2008, are shown, as are (b) the physical details of the major storms.

days (Beven, 2001). Negative storm surges were reported along the Belizean coast, and the floor of the Bay of Chetumal on the Mexican border was exposed. A small (<2 m) storm surge, that approached from the mainland was reported for Cay Caulker, to the north of Turneffe (Beven, 2001). Rainfall was torrential with 83 cm falling at the Belize City airport (Beven, 2001). Keith very severely impacted the Turneffe mangroves, damaging ~ 4000 hectares or 35% of the land area (Meerman, 2006).

8.5 Methods

Methods followed are those described in **Chapter 2.4**. In addition, a preliminary palynological analysis was conducted. Pollen was processed using the procedures described by Faegri and Iverson (1989).

8.6 Results

8.6.1 HJ Cay

Three cores were extracted by Russian peat borer along this 69 m transect, all within the monospecific *Rhizophora* zone. HJ3 was located in a few cm of water on the island's edge, HJ2 among medium height (< 5 m) forest, and HJ1 in a flooded dwarf zone. Dwarf *Rhizophora* are typically associated with inland locations where less regular tidal flushing results in reducing soil conditions, higher soil toxicity and salt levels (Feller, 1995; Mendelsohn and McKee, 2000). All cores were pushed until refusal, with both HJ1, 3 penetrating to the basal clay; core lengths were between 433-449 cm. Transect cores show a common pattern, with a thin basal clay followed by a thick peat layer, then a very thick carbonate layer (which may/may not be sandwiched between a chaotic mixture of interbedded peat and inorganic layers), followed by a thick peat layer extending to the surface.

8.6.1.1 Example Litholog

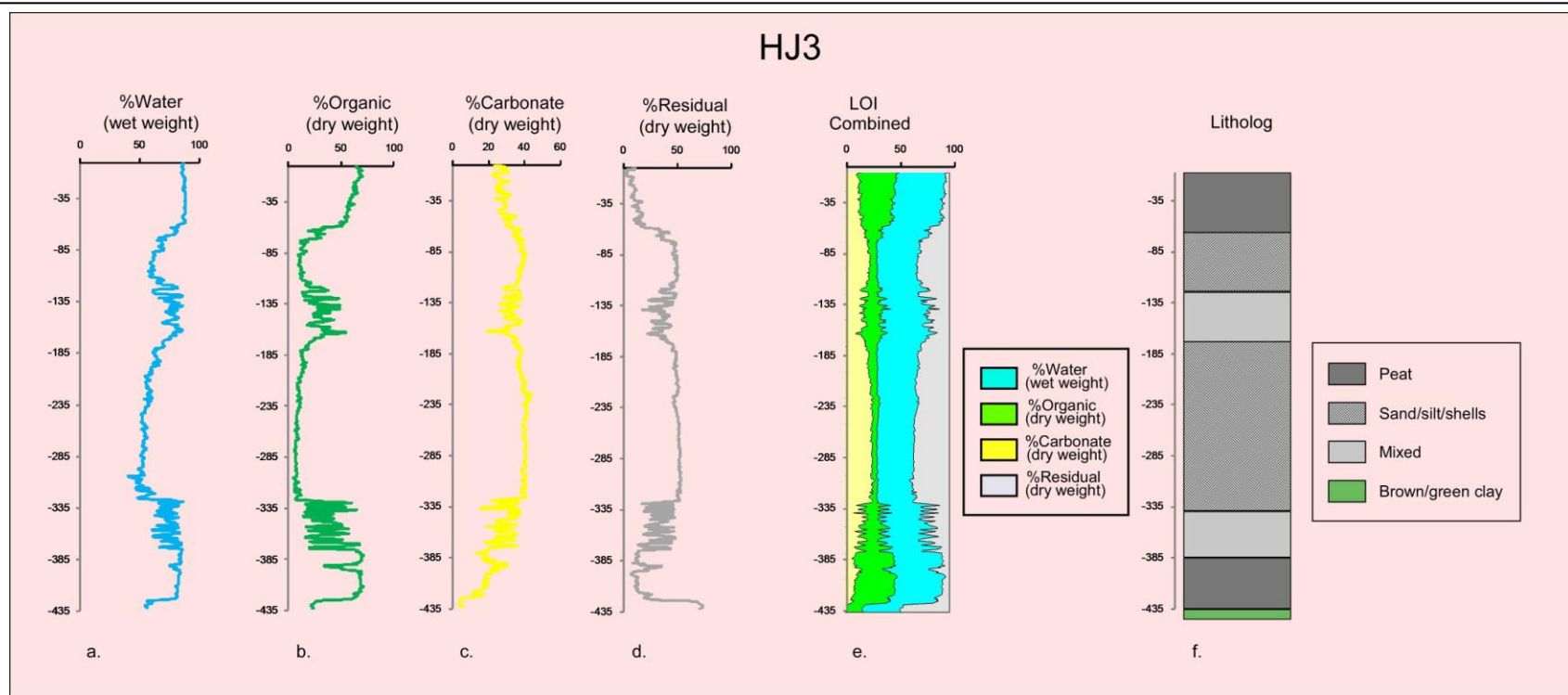
Core HJ3 was chosen as the example litholog for this transect. This composite core, taken from the extreme seaward edge of the island, consists of nine 50 cm peat borer sections with a 14 cm overlap between the two bottom sections. Core depth is 433 cm.

The results of LOI analysis are presented in **Figure 8:5**. Shown are the water, organic, carbonate, and residual (mainly silicates) percentages as individual curves (**Figure 8:5 a, b, c, d**), a combined LOI curve (**Figure 8:5 e**), and the core litholog (**Figure 8:5 f**). A comparison of the data presented in **Figures 8:5 a- f** demonstrates that the LOI diagram can be used to identify the four basic sedimentary units found in this core reliably (**Figure 8:6**).

8.6.1.1.1 Peat High water and organic accompanied by moderate (generally between 25-35%) carbonate and low residual percentages identify organic deposition (peat); an example is the section from cm 1-59.

8.6.1.1.2 Sand/Silt/Shells (s/s/s) A sharp drop in water and organics and a moderate and large increase in the carbonate and residual percentages respectively mark the carbonate layers, which here occurs between 60-114 and 175-329 cm. These layers consist of a structureless mixture of sand, silt, and shells. The material is relatively unconsolidated, as evidenced by the ability to penetrate these thick layers.

8.6.1.1.3 Mixed This unit is marked by rapid variation between clumps of material composed of the two previously described materials, with abrupt dips/spikes in all four curves, over which water and organic values rise and dip in parallel, precisely in the inverse with carbonates and residual values. Such units occur from 115-162 and 330-378 cm. The most distinctive feature of this unit is the extremely chaotic nature of the different sediment types, possibly a result of some manner of high energy disturbance.



8.5 LOI curves and litholog for core HJ3. Shown are (a) water, (b) organic, (c) carbonate, and (d) residual (mainly silicate) percentages as individual curves; (e) a combined LOI curve, and (f) the core litholog.

8.6.1.1.4 Clay A brown/green clay, occurring at the base of several cores extracted from Turneffe Atoll, can be recognized by low organic and carbonate percentages combined with intermediate water, and high residual values. In HJ3 this occurs below 425 cm.

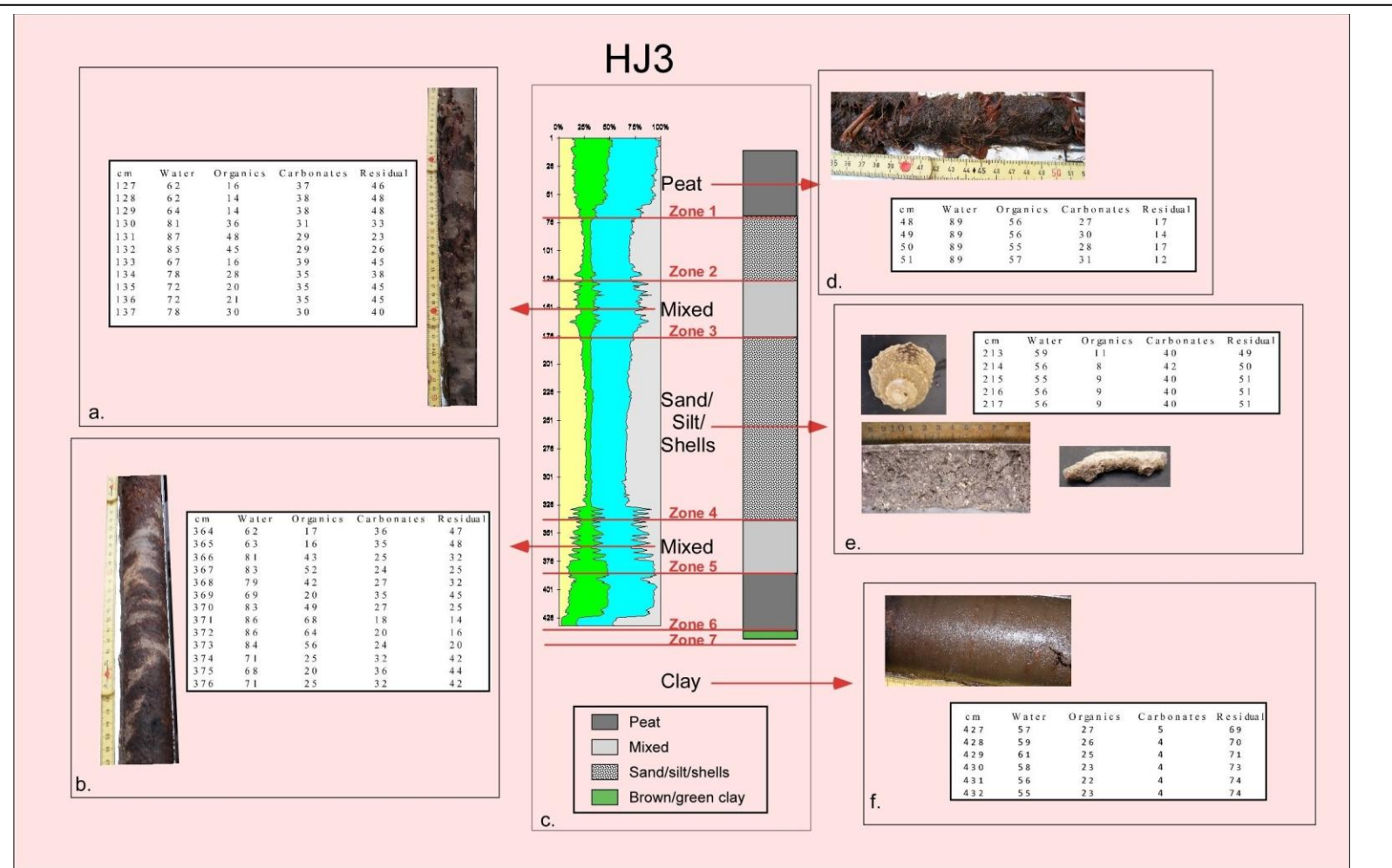
8.6.1.2 HJ3 Zonation

Based on the identification of stratigraphic units, HJ3 can be divided into seven zones (**Figure 8:6**). The peat, s/s/s and clay zones are distinct and unambiguous. The mixed layers are exactly that, a chaotic mixture of peat and s/s/s layers. These layers are not interbedded horizontally and do not seem to represent a succession of tranquil shifts between depositional environments alternately favoring organic and inorganic material. Rather the vertical orientation and general depositional incoherency of much of the material suggests simultaneous deposition (possibly redeposition of transported material) of the two drastically different sediments. For this reason, the mixed layers are treated as a single zone, reflecting a particular deposition style, and not as a number of separate zones, each reflecting a stable depositional environment.

8.6.1.2.1 Zone 1(1-59cm) is mainly brown, partially decomposed plant material and peat. Water (>86%) and organic (49-74%, decreasing at the bottom) values are high, residuals are low (0-18%), carbonates are moderate (22-32%).

8.6.1.2.2 Zone 2(60- 114cm) is an s/s/s layer. The first 13 cm are transitional, with decreasing organic and water values. Below 72 cm organic values are <20%, dipping below 10%; with carbonate values between 36-41% and residuals slightly higher (41-51%).

8.6.1.2.3 Zone 3(115-162) is a mixed layer. Values fluctuate dramatically; water varying from 62-87%, organics from 13-50%, carbonates from 27-39%, and residuals from 17-48%. Sedimentation is often vertical and chaotic.



8.6 HJ3 sedimentological units and zonation. Pictures and identifying LOI characteristics are presented for the four sedimentological units present in HJ3; (d) peat; (e) shells/silt/sand; (a) mixed (a chaotic combination of the two previous units) (a, b); and (f) a basal clay. (c) The core's seven zones are shown

8.6.1.2.4 Zone 4(163- 329cm) is an s/s/s layer. There is a transition zone from 163-174, marked by a peat layer at 163-165, then decreasing organic content to 174 cm, below which organic never reach 20% and reach a low of 5% , while carbonates range from 34-45%.

8.6.1.2.5 Zone 5(330-378) is a mixed layer, similar to Zone 3, with a similar range of water, organic, carbonate and residual values.

8.6.1.2.6 Zone 6(379-424cm) is a dark brown/black well-rotted peat, with a small, less organic section from 391-395. Except for that section, and cm 424 which is the transition to Zone 7, organic content ranges from 62-72% while carbonate remains below 27%, decreasing to 11%.

8.6.1.2.7 Zone 7(425-433cm) is the basal clay. Residuals reach 74%, while water, organic, and carbonate values are low.

8.6.1.3 Dating

Three plant/organic and two bulk sediment samples were selected from HJ3. Three samples were sent to Beta Analytic and two to the NOSAMS facility at Woods Hole Oceanographic Institute for AMS dating. The results are listed in **Table 8:1**, and shown graphically in **Figures 8:8**).

There is a single date reversal as the sample from 430 cm (basal clay layer) is dated 900 years younger than the sample 15 cm above it. The basal date is most likely incorrect, with penetration by younger roots into the clay layer resulting in a falsely younger date. The age/depth graph for this core shows very good correspondence, with high R^2 values (0.95-0.99) for all scenarios (**Figure 8:7**). The three graphs on the left plot ^{14}C age vs. depth for all five dates, showing linear trendline and R^2 values for (a) straight plotting, (b) with a forced intercept of zero, and a moving average (c), which assumes changing sedimentation rates between dated samples. The three graphs on the right are the same with the date for 430 cm excluded. An

assumption of constant sedimentation produces calculated sedimentation rates between 0.07 and 0.08 cm/yr (12.19-14.76 yr/cm), with intercepts of -374 (when the basal date is included) to -586 years (when that is removed). Postulating a slightly faster sedimentation rate (0.1 cm/yr) for the top 163 cm and a slightly slower rate (0.06) from 163-415 cm, and excluding the basal date produces an intercept of zero (**Figure 8:7f**).

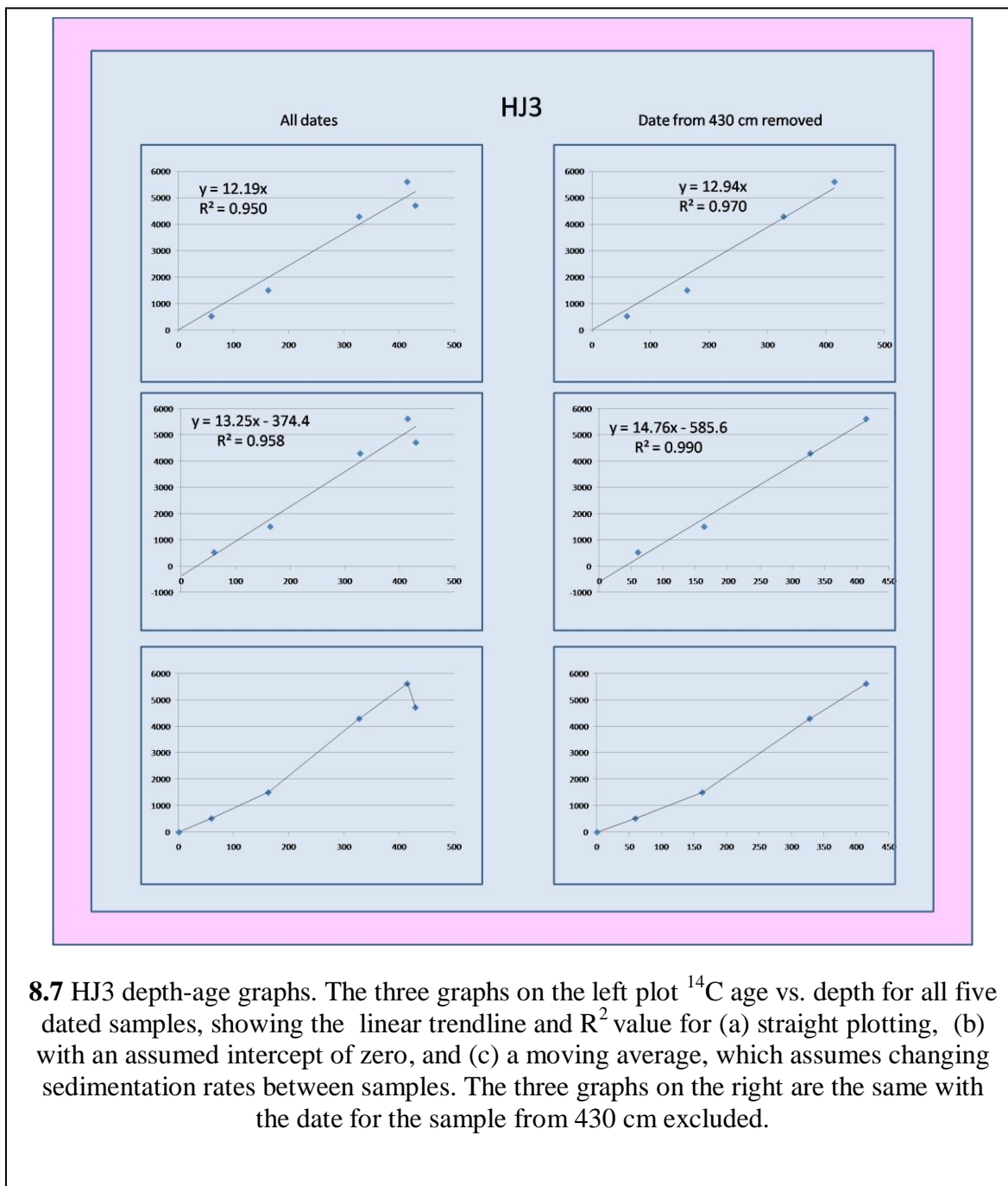
8.6.1.4 Pollen

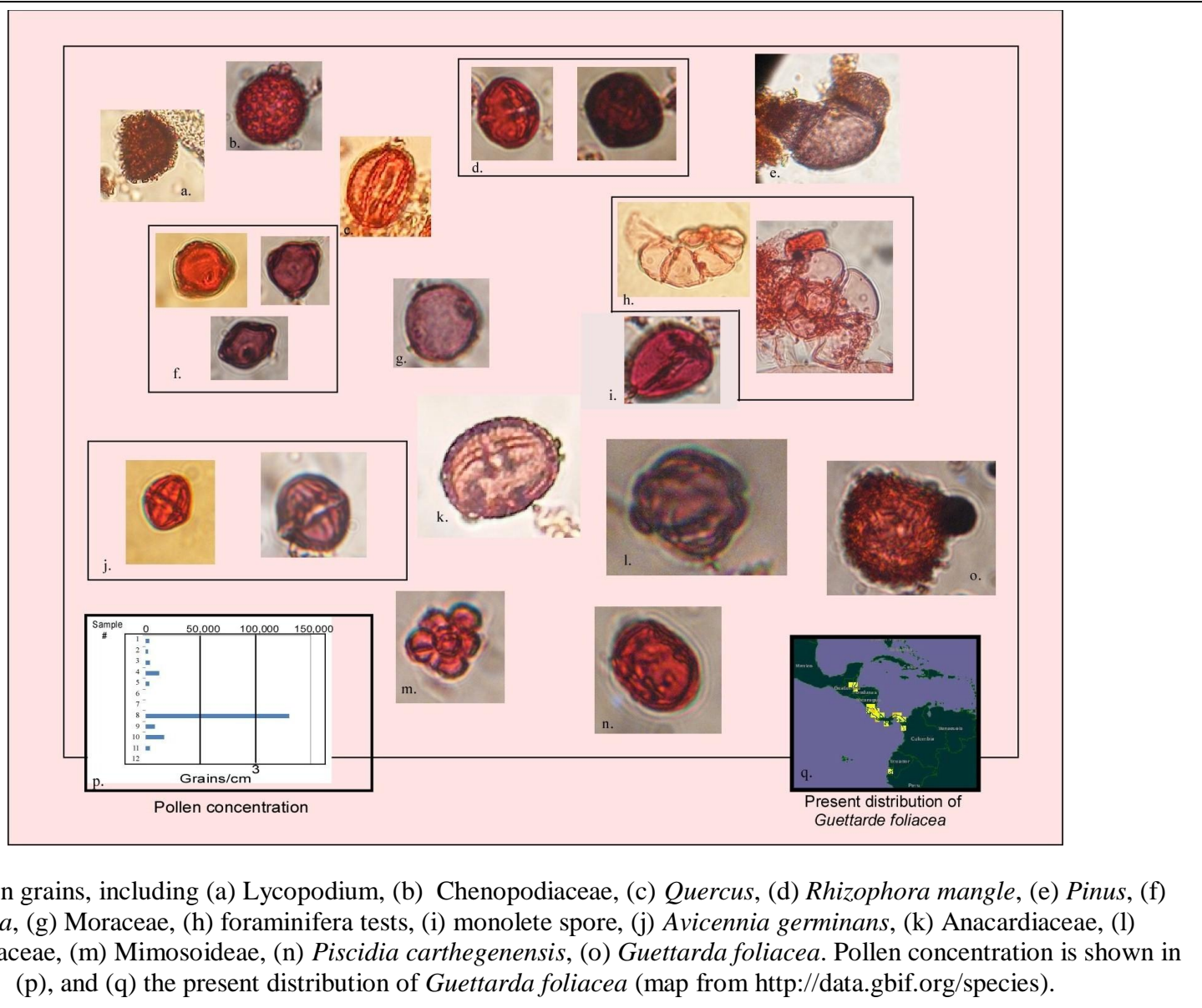
The pollen concentration was low throughout, as has been found to occur in cores from similar environments. Wooller et al. (2007) were unable to count more than 100 pollen grains at several levels in a peat dominated core from Twin Cays, Belize; Torrescano and Islebe (2006) experienced similar difficulties when counting pollen from a swamp located on the Belize-Mexican border some 120 km to the northwest, being unable to achieve the 200 grains at several levels. The pollen was especially sparse in the carbonate layers (**Figure 8.8p**). Samples were taken for counting at 12 depths; six samples came from peat intervals, four from carbonate layers and two from the basal clay.

Three pollen groupings were identified, correlating to the three sediment types (**Figure 8:9**). The six peat samples were dominated by *Rhizophora mangle* (red mangrove), with a substantial Cheopodiaceae component, while the inorganic layers were dominated by Cheopodiaceae. The pollen in the basal clay was almost exclusively *Guettarda foliacea*, a member of the Rubiaceae family. This plant is a rather inconspicuous neotropical understory plant (no common name), currently occurring along both the Caribbean and Pacific coasts from Belize to Peru (<http://data.gbif.org/species/14241908>) (**Figure 8.8q**, map from Global). Monolete spores and foraminifera tests were found throughout, trilete spores were less common.

8.1 HJ3 chronology

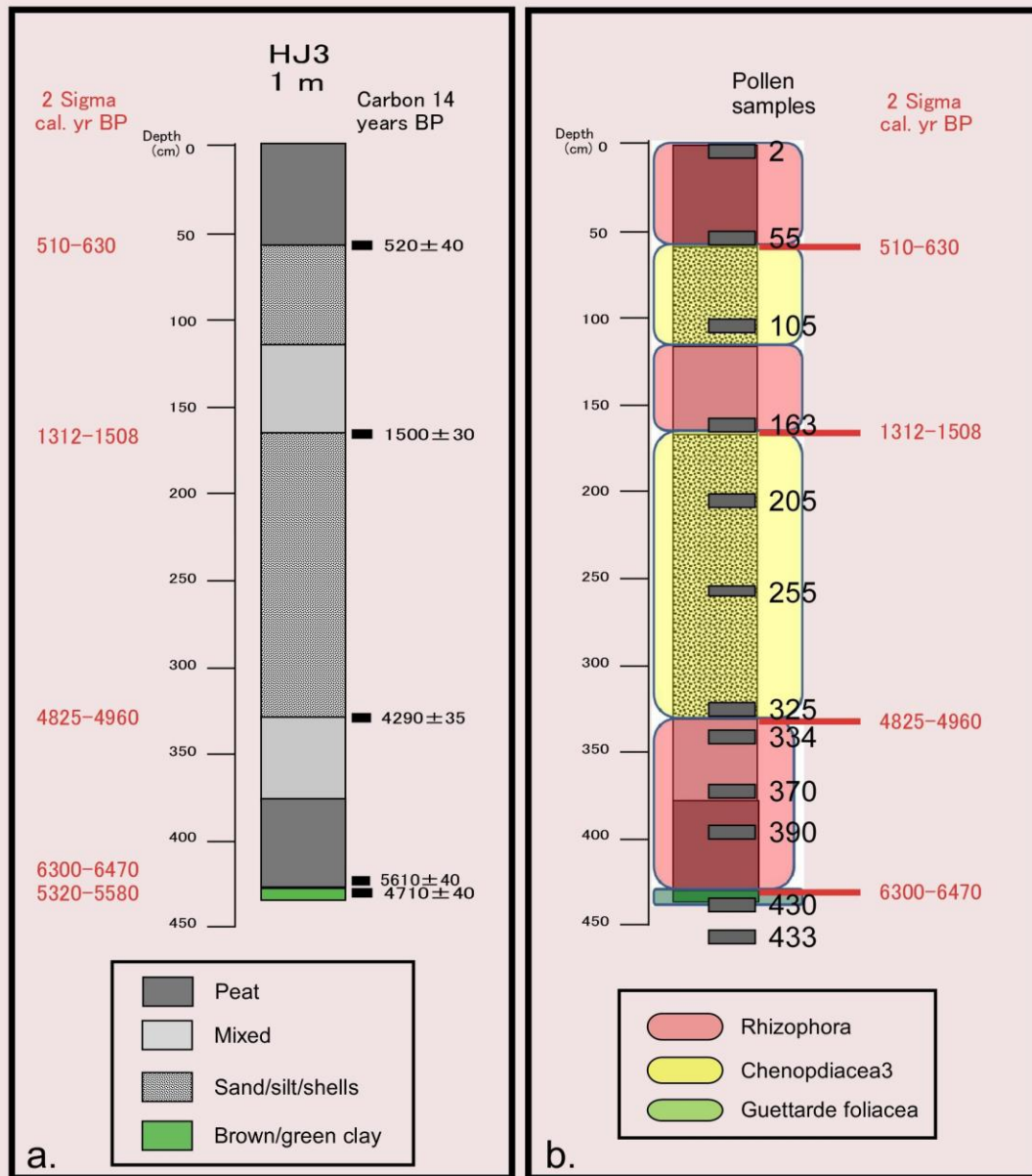
Depth cm	Material	Lab	Sample#	C14 Age	Error		Cal yr BP $\pm 2\sigma$	%	Cal yr AD/BC
					Bar				
60	Plant/wood	Beta	2E+05	520	± 40	600-630	0.22		1316-1355 AD
						510-560	0.78		1388-1447 AD
163	Plant/wood	WHOI	63006	1500	± 30	1312-1417	0.934		533-638 AD
						1466-1490	0.045		460-484 AD
						1495-1508	0.021		442-455 AD
328	Plant/wood	WHOI	63028	4290	± 35	4825-4893	0.868		2944-2876 BC
						4897-4960	0.132		3011-2948 BC
415	Bulk Sed	Beta	2E+05	5610	± 40	6300-6470	1		4519-4356 BC
430	Bulk Sed	Beta	2E+05	4710	± 40	5320-5580	0.487		3471-3372 BC
							0.222		3538-3489 BC
							0.291		3633-3557 BC





8.8 Pollen grains, including (a) *Lycopodium*, (b) *Chenopodiaceae*, (c) *Quercus*, (d) *Rhizophora mangle*, (e) *Pinus*, (f) *Myrica*, (g) *Moraceae*, (h) foraminifera tests, (i) monolete spore, (j) *Avicennia germinans*, (k) *Anacardiaceae*, (l) *Melastomaceae*, (m) *Mimosoideae*, (n) *Piscidia carthagenensis*, (o) *Guettarda foliacea*. Pollen concentration is shown in (p), and (q) the present distribution of *Guettarda foliacea* (map from <http://data.gbif.org/species>).

HJ3



8.9 Litholog of core HJ3 showing (a) stratigraphy, depth of samples chosen for radiocarbon dating (black bars), the conventional ^{14}C dates (black), and calibrated calendar ages; (b) depths of pollen samples (black bars), and pollen groupings (transparent colored boxes).

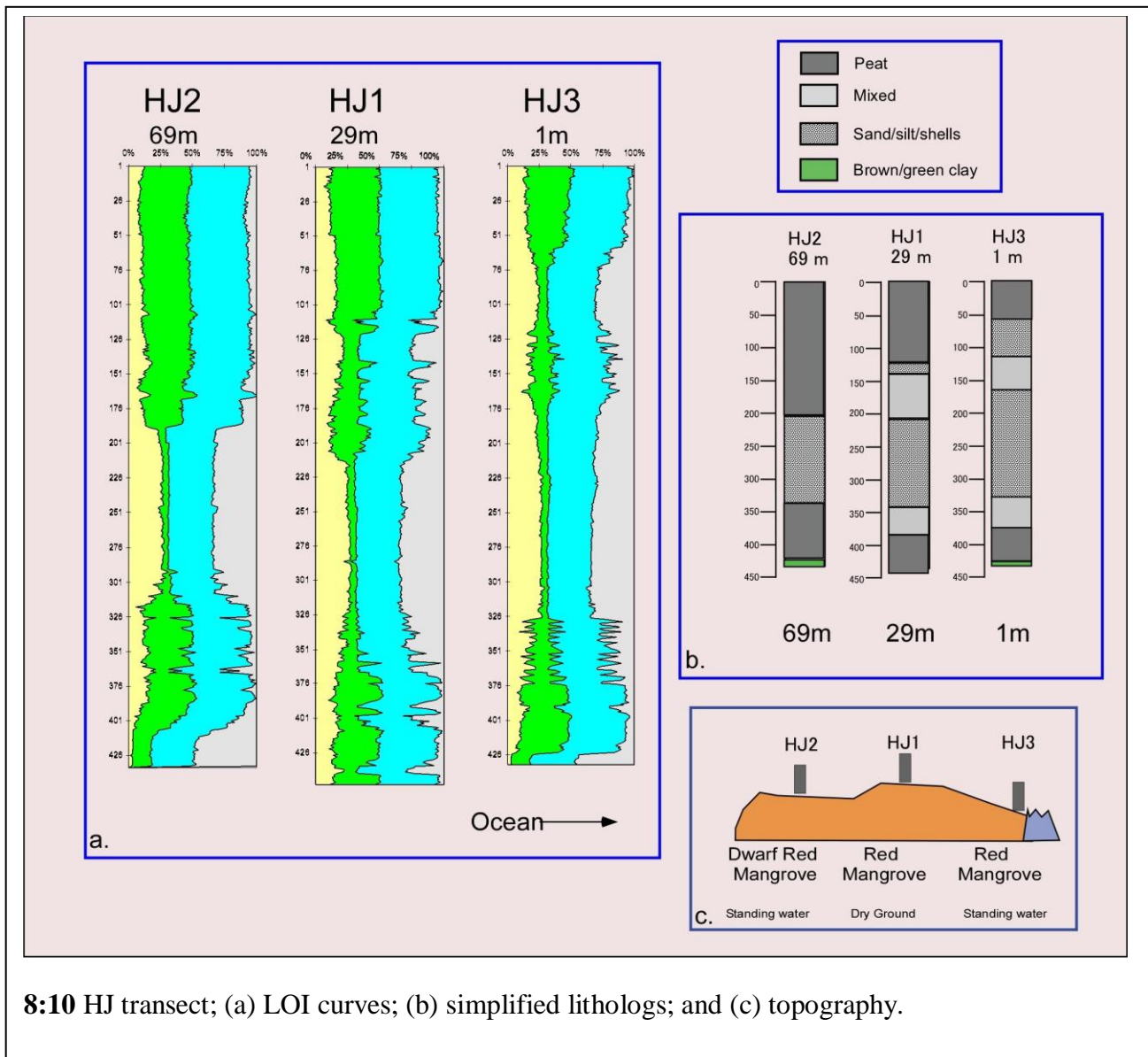
Several other pollen types, generally mixed forest taxa, are present, including *Pinus*, *Quercus*, Anacardiaceae, Moraceae, Melastomaceae, *Ambrosia*, *Mimosa*, *Myrica*, and *Piscidia cartegensis* (Leguminosae) in the peat intervals. Moraceae and Melastomaceae are also present in a sample from a carbonate interval, and a single grain of Malpighiaceae is found in the basal clay (**Figure 8:8**). Abundance of these taxa is generally greater near the top, possibly due to enhanced preservation. *Pinus* is present from the top until at least 370 cm and *Quercus* to 334 cm.

8.6.1.5 HJ Transect

All three cores display a similar sedimentary progression, as shown in both the LOI diagrams and core lithologs (**Figure 8:10**). Above the basal clay, (which HJ 1 does not reach), all cores show a thick peat section, followed by a thick carbonate interval, which changes to peat/organic at the top. The carbonate layer is more complicated closer to the shore with thick mixed layers bracketing the lower s/s/s layer, as well as the occurrence of a second s/s/s layer higher up in the core. (**Figure 8:10 a, b**). The topography and vegetation changes are displayed in **Figure 8:10 c**. HJ1 displays zones 1 -6, missing only the basal clay. HJ2 contains zones 1, 4, 6, and 7, lacking the mixed zones (zones 3, and 5) and the top s/s/s zone (zone 2). In general the s/s/s zones decrease in thickness moving inland.

8.6.2 GC

Three cores were extracted by Russian peat borer and modified Livingstone piston corer along this 151 m transect. GC2 was obtained 64m from the water in the fringing *Rhizophora* zone, consisting of dense, medium height (<4m) monospecific *Rhizophora*. GC1 was located at 89 m inland, at the landward edge of the exclusive *Rhizophora* zone. Trees here were taller and less dense, with abundant *Batis maritima* groundcover. GC3 was extracted 125 m inland in a



8:10 HJ transect; (a) LOI curves; (b) simplified lithologies; and (c) topography.

mixed forest, dominated by *Rhizophora*, but including *Avicennia* and several varieties of hardwoods and palms. All cores were pushed until refusal; only GC1 penetrated to the basal clay. Core lengths were between 360-454 cm. GC1, and 2 consist of a thick carbonate layer sandwiched by peat; GC 3 is consistently peat.

8.6.2.1 Example Litholog

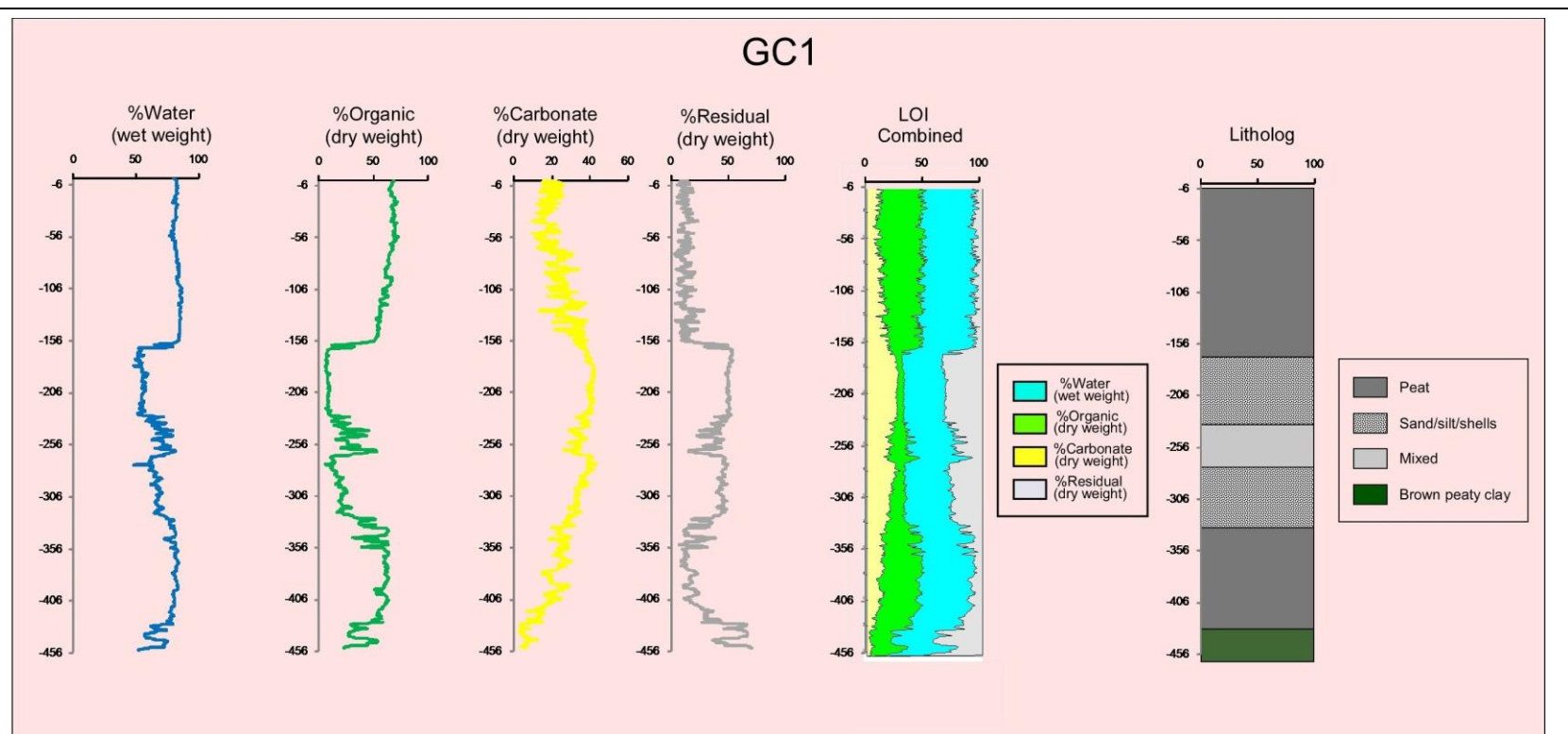
Core GC1 was chosen as the example litholog for this transect. This is a composite core, consisting of eight 50 cm peat borer sections and a single 90 cm piston corer (from 96-182 cm), all with 5 cm overlaps. Core depth is 454 cm.

The results of LOI analysis are presented in **Figure 8:11**. Shown are the water, organic, carbonate, and residual (mainly silicates) percentages as individual curves (**Figure 8:11 a, b, c, d**), a combined LOI curve (**Figure 8:11 e**), and the core litholog (**Figure 8:11 f**). The same four sedimentary units found in core HJ3 (**Figure 8:6**) are found in this core, As in the HJ transect, they can be identified readily using the LOI diagram (**Figure 8:12**). They are:

8.6.2.1.1 Peat High water and organic accompanied by moderate (generally between 15-30%) carbonate and low residual percentages identify organic deposition (peat); an example is the section from cm 1-156.

8.6.2.1.2 Sand/Silt/Shells (s/s/s) A sharp drop in water and organics and moderate and large increases in the carbonate and a residual percentages (respectively) signal these layers, which occur between 159-229 and 268-327 cm. These layers consist of a mixture of sand, silt and shells.

8.6.2.1.3 Mixed This unit is marked by rapid alternations between the two previously described sedimentary types, with abrupt dips/spikes in all four curves, over which water and organic



8.11 LOI curves and litholog for core GC1. Shown are (a) water, (b) organic, (c) carbonate, and (d) residual (mainly silicate) percentages as individual curves; (e) a combined LOI curve, and (f) the core litholog.

values rise/dip in parallel to each other, but inversely with carbonates and residual values. The mixed section in this core is from 230-267 cm.

8.6.2.1.4 Clay This core reaches the basal clay, which, though more organic and less greenish, is similar to that encountered in the HJ transect. This clay can be recognized by low organic and carbonate, intermediate water, and high residual percentages. In this core this unit occurs below 426 cm; some organically enriched sections occur within this interval.

8.6.2.2 GC1 Zonation

Based on the identification of stratigraphic units, GC1 can be divided into six zones (**Figure 8:12**). The zones are generally distinct, although short transitional intervals do occur. The basal clay is slightly less distinct than in the HJ transect, as the color change from the following peat interval is less dramatic, and higher organic values persist into the clay. Nonetheless, the change is marked easily, both visually and by the texture change from rough organic particles to smooth sticky clay. The mixed layer, as in the HJ transect, is treated as a single unit, and not as a series of rapidly oscillating depositional environments, as visual inspection indicates chaotic, vertical mixing, as opposed to tranquil, horizontal changes (**Figure 8:12**).

8. 6.2.2.1 Zone 1(1-155cm) is mainly brown, partially decomposed plant material and peat. Water values are generally > 80%, with maxima of 88%; organic values begin near 70%, decreasing to 51% at the bottom, residuals are low (generally <20%), and carbonates are moderate (20's-30's %).

8.6.2.2.2 Zone 2(156-229cm) is an s/s/s layer. The first 8 cm are transitional, with decreasing organic and water values, with an organic peak at 162-163. Below 163 cm organic values are <12%, with carbonate values between 36-43%, while residuals increase to 48-54%.

8.6.2.2.3 Zone 3(230-267) is a mixed layer. Values fluctuate dramatically; water varying from 58-82%, organics from 14-53%, carbonates from 26-40%, and residuals from 16-50%.

Sedimentation is often vertical and chaotic (**Figure 8:12**).

8.6.2.2.4 Zone 4(268-327 cm) is an s/s/s layer. Water content is between 62-75%; organics, which reach a low of 6% are generally < 20%, though increase to 33% at the bottom, while carbonates range from 29-43%, decreasing downcore. Residuals vary from 39-50%.

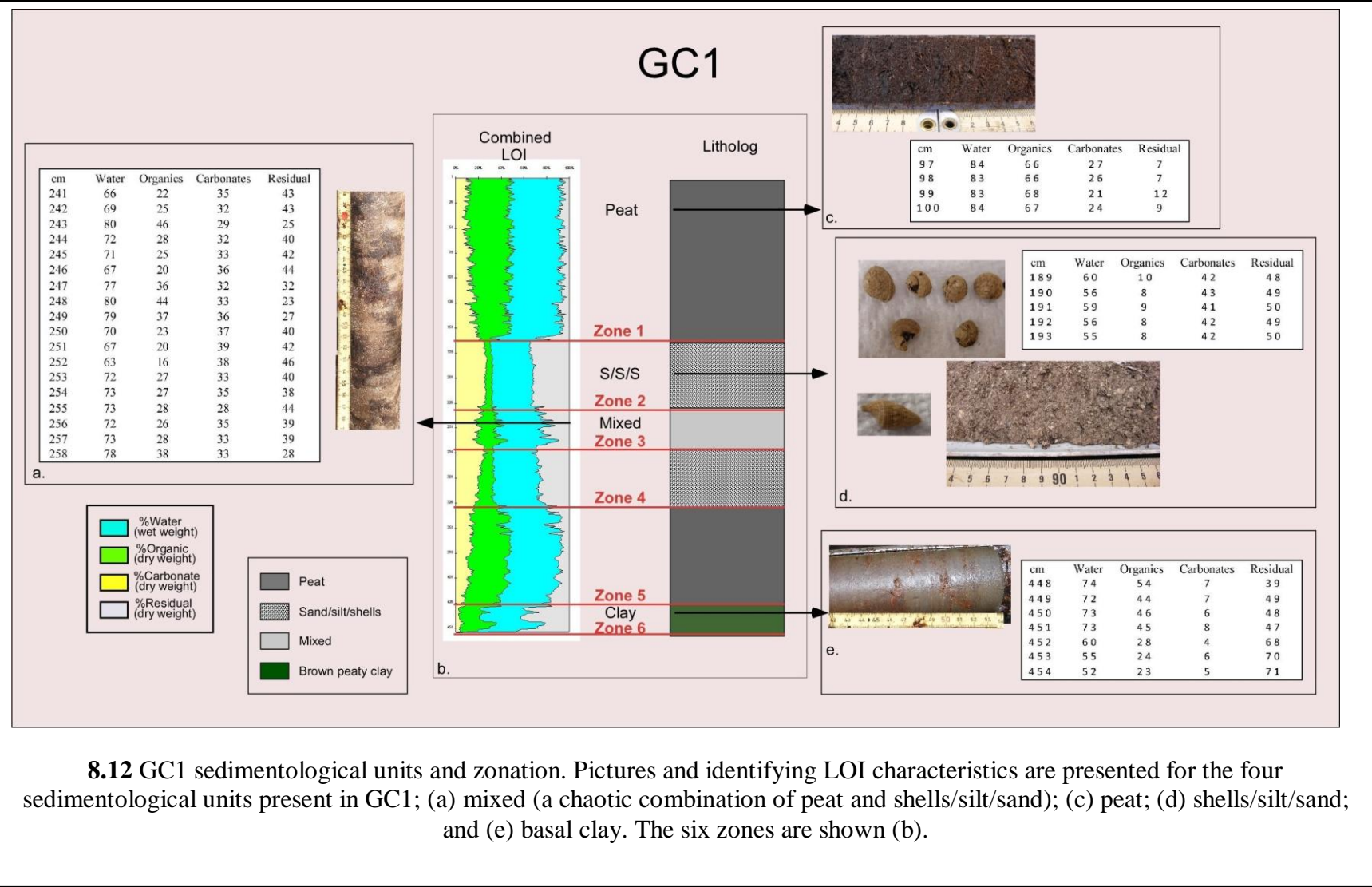
8.6.2.2.5 Zone 5(328-429cm) is a dark brown/black well-rotted peat, with a few small, mostly horizontal lower organic sections. Even with those sections, water content never dips below 73% and is mostly >80%. Although dipping to 35% in the less organic sections, organic percentages are generally >60%, while carbonates remain below 32%, decreasing to 7% at the bottom. Residuals are generally low, ranging from 8-43%, increasing downcore.

8.6.2.2.6 Zone 6(430-454cm) is the basal clay. Residuals reach 71%, while water is moderate (52-76%), and organic (23-54%) and carbonates (<12) values are low.

8.6.2.3 GC Transect

A LOI diagram was not produced for GC 3, which was photographed and described, but not brought back to the United States. Apart from the basal clay, which GC2 did not reach, GC1, 2 display similar sedimentary progressions, changing from peat to the carbonate rich s/s/s layers and then back to peat. The carbonate layer thins across the transect, being both thinner and patchier in GC1, and missing in GC3 (**Figure 8:13**). Elevation consistently increases landward across this transect, with GC3 being beyond the monospecific *Rhizophora* zone in an area of mixed forest (**Figure 8:13c**).

GC2 displays zones 1, 2 and 5, while GC3 consists entirely of Zone 1. This zonation (presence/absence of the mixed inorganic layers) is probably spatially, as opposed to



temporally, controlled, with sedimentary changes dependent upon proximity to sea and not changing environment.

8.6.3 BB

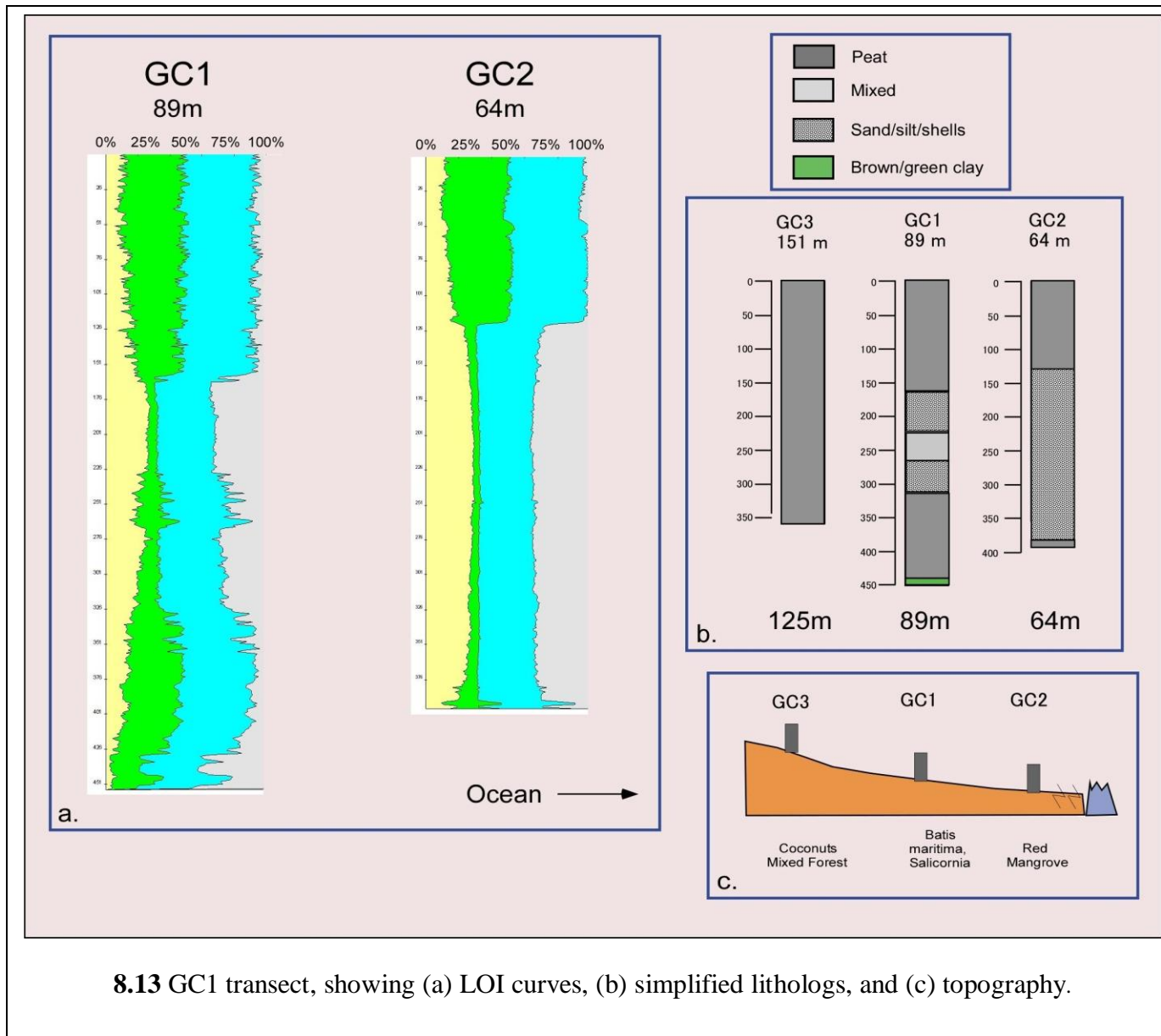
A total of 12 cores was extracted by Russian peat borer along this 165m transect. BB1 reaches a depth of 372 cm (**Figure 8:14**), the length of the other cores vary from 50 to 150 cm. All cores were photographed and described, though not all were brought to the United States and subjected to LOI. As the fringing monospecific *Rhizophora* zone was very narrow in this location, this transect started at 80 m in a tall, (canopy >10 m) somewhat open mixed forest (mainly *Rhizophora* and *Avicennia*), and ended in a cay forest with hard woods and coconuts.

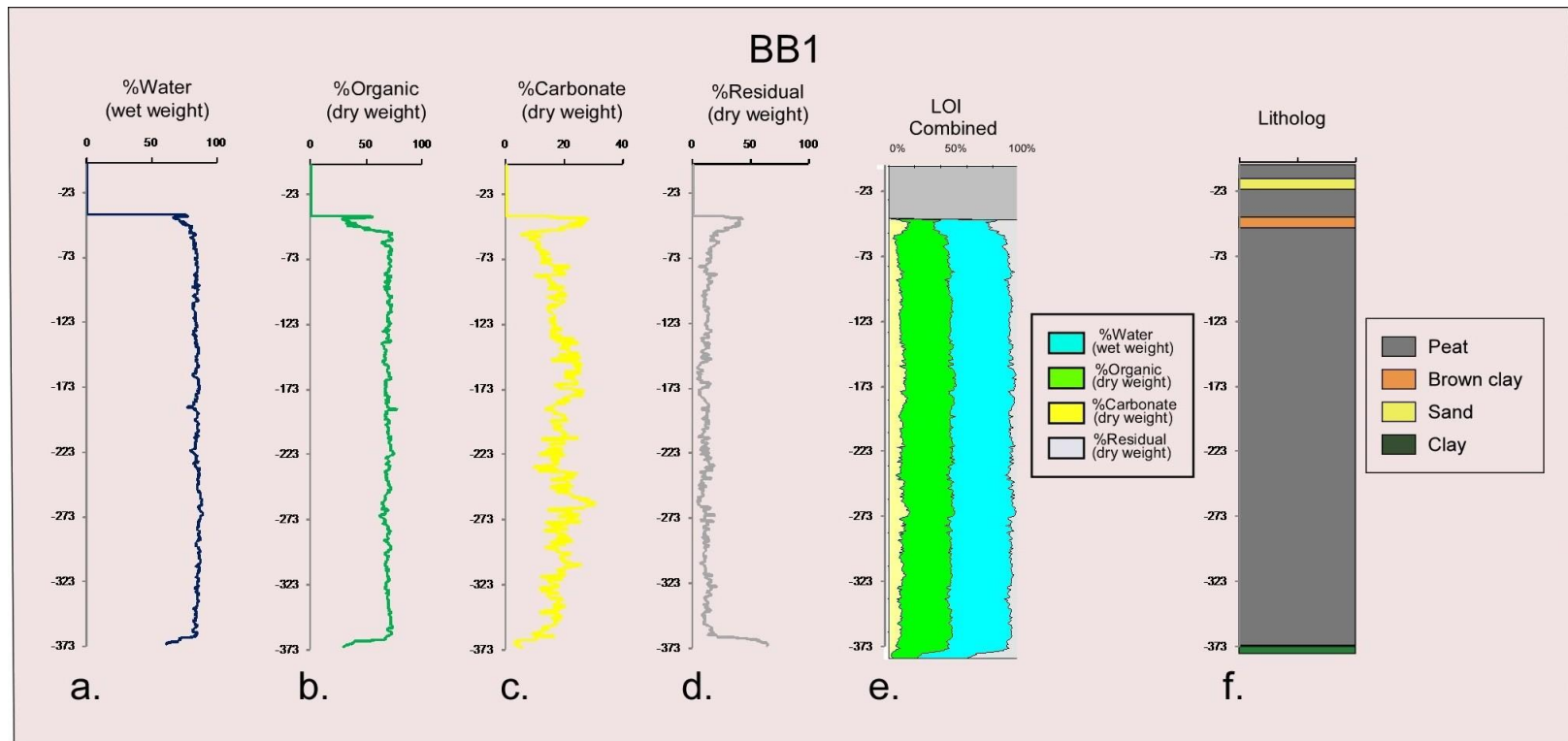
8.6.3.1 Example Litholog

BB1 was chosen as the example litholog for this transect. This is a composite core, consisting of eight 50 cm peat borer sections with 5 cm overlaps, taken from adjacent holes in a depression under a tall mixed mangrove forest. location, this transect started at 80 m in a tall, (canopy >10 m) somewhat open mixed forest (mainly *Rhizophora* and *Avicennia*), and ended in a cay forest with hard woods and coconuts.

The results of LOI analysis are presented in **Figure 8:14**. Shown are the water, organic, carbonate, and residual (mainly silicates) percentages as individual curves (**Figure 8:14 a, b, c, d**), a combined LOI curve (**Figure 8:14 e**), and the core litholog (**Figure 8:14 f**). LOI data is missing for the top 40 cms, as this core section is being preserved for ^{137}Cs dating. BB1 is almost entirely peat above a thin basal clay layer. Two narrow clastic layers occur near the top; a distinct sand layer from 12-18 cm and a clay layer from 40-48 cm (**Figure 8:14**). The peat, clastic, and clay layers are easily identifiable from the LOI data (**Figure 8:15**).

8.6.3.1.1 Peat High water and organic accompanied by moderate (<30%) carbonate and low





8.14 LOI curves and litholog for core BB1. Shown are (a) water, (b) organic, (c) carbonate, and (d) residual (mainly silicate) percentages as individual curves; (e) a combined LOI curve, and (f) the core litholog.

residual percentages identify organic deposition (peat). This is the principal component of the core.

8.6.3.1.2 Clastic Layers LOI was not performed on the sand layer, the clay layer displays lower water and organic content and increased carbonate and residual.

8.6.3.1.3 Clay This core reaches the basal clay, which is somewhat mixed with roots. As with the other basal clays, it can be recognized by low organic, carbonate, and water percentages, and high residual values.

8.6.3.2 Zonation

BB1 consists of only two zones.

8.6.3.2.1 Zone 1 (1-368cm) is peat. The degree of decomposition is not entirely constant, but most is well-rotted. Water content is generally ~ 85%, organics ~ 70%, carbonates between 10-30%, with very low residual values (generally <20%, and often <10%). The two clastic layers which appear at the top will be discussed in more detail below.

8.6.3.2.2 Zone 2 (368-372cm) is the basal clay, recognizable by texture, grain size, composition, color, and the characteristic LOI signature of low values for all but residuals.

8.6.3.3 BB Transect

BB1 is the only core in this transect that penetrates to Zone 2. The other 11 cores were taken in an attempt to map the geographical limits of the large clastic layer at the top of BB1. In order to ensure broad spatial coverage, multi-directional transects were employed, with two cores each extracted at 100, 110, 115, and 130 m (**Figure 8:16b**). Due to transportation limitations the second peat borer section (50-100 cm) of several cores were left in Belize. As there is no LOI data for these core sections, lithologs, based on visual observation, photographic evidence, and written descriptions were used in constructing the transect diagram.

The LOI curves for the relevant cores are included in **Appendix A**. Only the top 150 cm of BB1 is shown.

The clastic layers found near the top of BB1 appear in several other cores.

8.6.4 Main Calabash Cay

Three short cores were obtained from this cay. All three cores were taken in the *Avicennia* zone, landward of the *Rhizophora*, approximately 150 m from the southern edge of Long Brogue. The transect is curvilinear and parallels the northern edge of the cay. No LOI data exist for these cores, as they were photographed and described, but not taken out of the country. All cores are composite, taken by Russian peat borers pushed to refusal. MC1 consists of two sections, MC2 and 3 of three sections each, all with a minimum overlap of 10 cm. The transect lithologs are presented in **Figure 8:17**, as well as a site photo showing the tall *Avicennia* and *Batis maritima* groundcover. The photo is taken looking toward the north, in the direction of Long Bogue.

8.6.4.1 Zonation

All three cores consist of two zones.

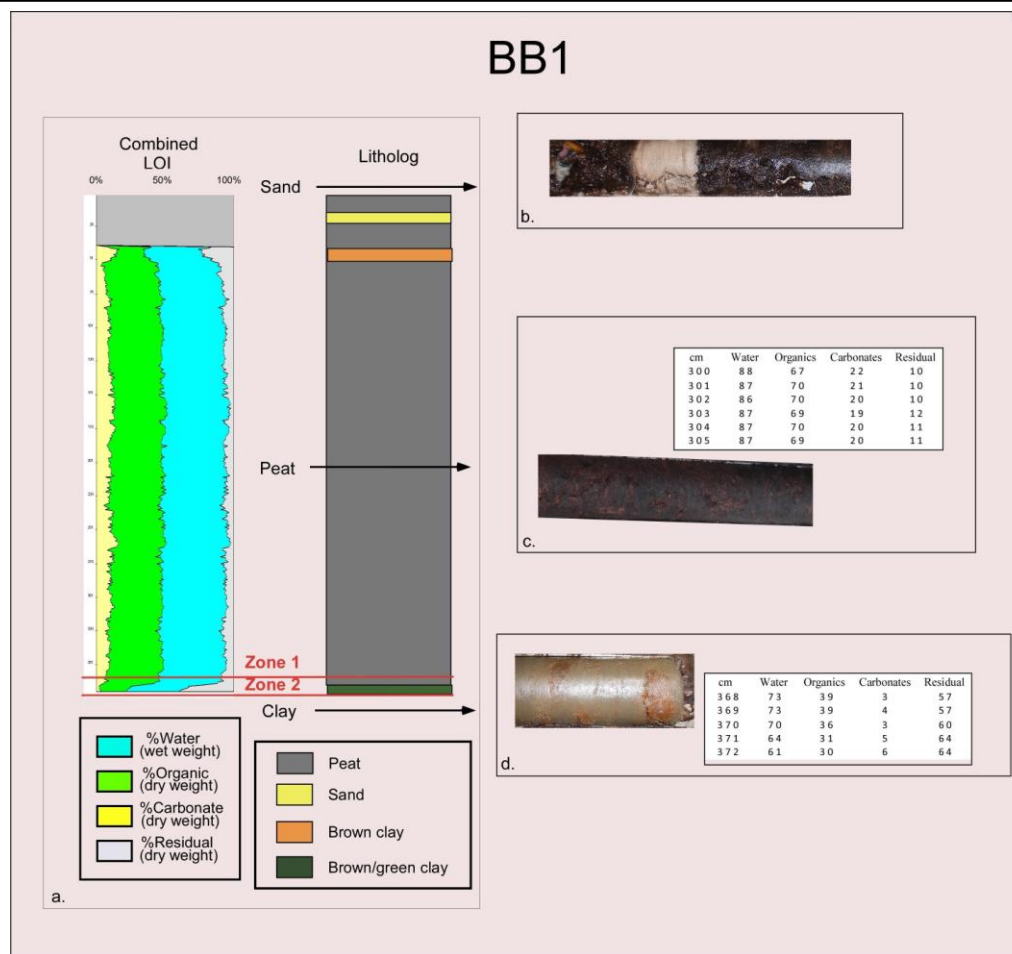
8.6.4.1.1 Zone1 Peat

8.6.4.1.2 Zone 2 s/s/s

These two zones match the top two zones from the HJ and GC transects. The material in the s/s/s zone strongly resembles that from similar HJ and GC zones, consisting of light colored sand, silt, and shells, with an abundance of *Halimeda* flakes (**Figure 8:17**).

8.6.5 DC

A single composite core consisting of seven Russian peat borer sections, reaching a depth of 353 cm, was raised from this southern cay. Core location was 82 m from the sea in a



8.15 BB1 sedimentological units and zonation, showing (a) LOI curve, litholog, and zonation. Pictures and identifying LOI characteristics are presented for the three sedimentological units present in BB1; (b) a prominent sand layer near the top; (c) peat; and (d) basal clay.

very tight, medium height (<4 m) fringing *Rhizophora* zone, in standing water. The core is highly organic, generally consisting of dark, well-rotted peat from the core top until ~ 300 cm, when water, organic, and carbonate values drop sharply and the material transitions into clay. A brown/clay clay, similar to that encountered in other Turneffe locations, predominates below 310 cm. A distinctive sound, indicating that the final penetration push hit rock, suggests that this clay directly overlays coral bedrock (**Figure 8:18a**).

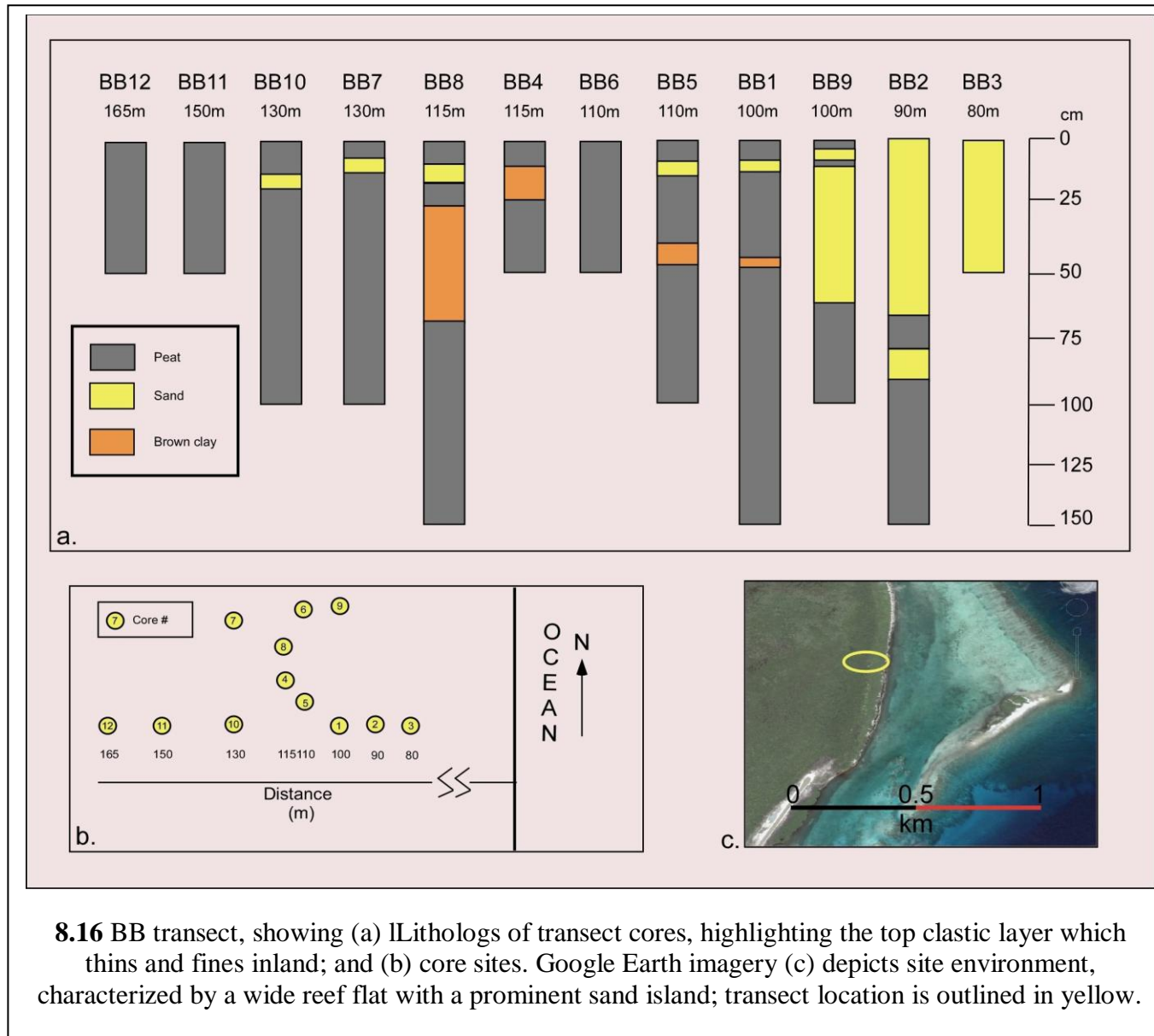
8.6.5.1 Zonation

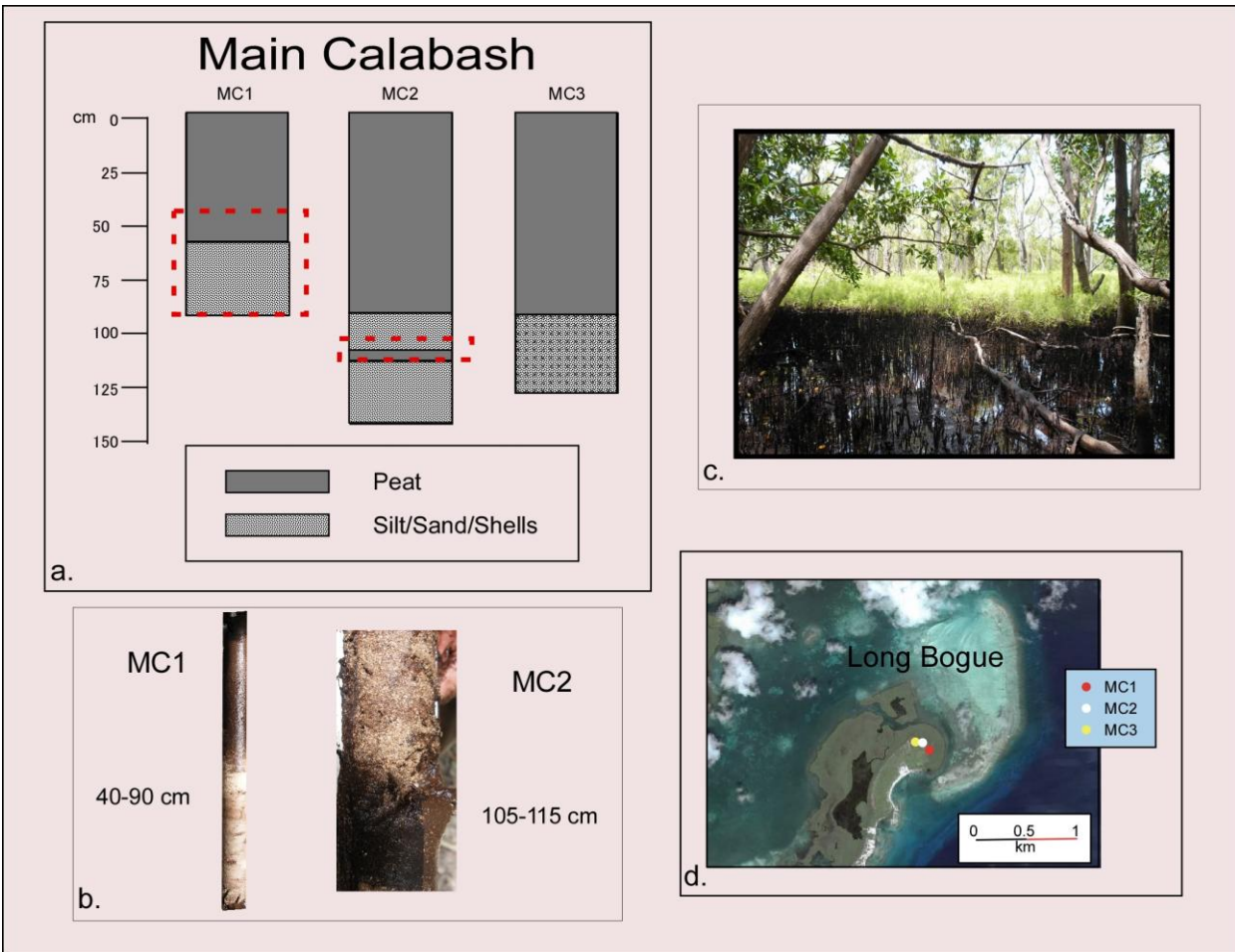
8.6.5.1.1 Zone 1 (1-296cm) Organic peat, marked by high water and organics, moderate carbonates (usually < 20%, though decreasing down core), and low residuals (usually <20% above 250 cm).

8.6.5.1.2 Zone 2 (297-353cm) 297-310cm is a transitional dark, peaty clay; below 310 cm the material becomes predominately clay, with residual values hovering near 70%.

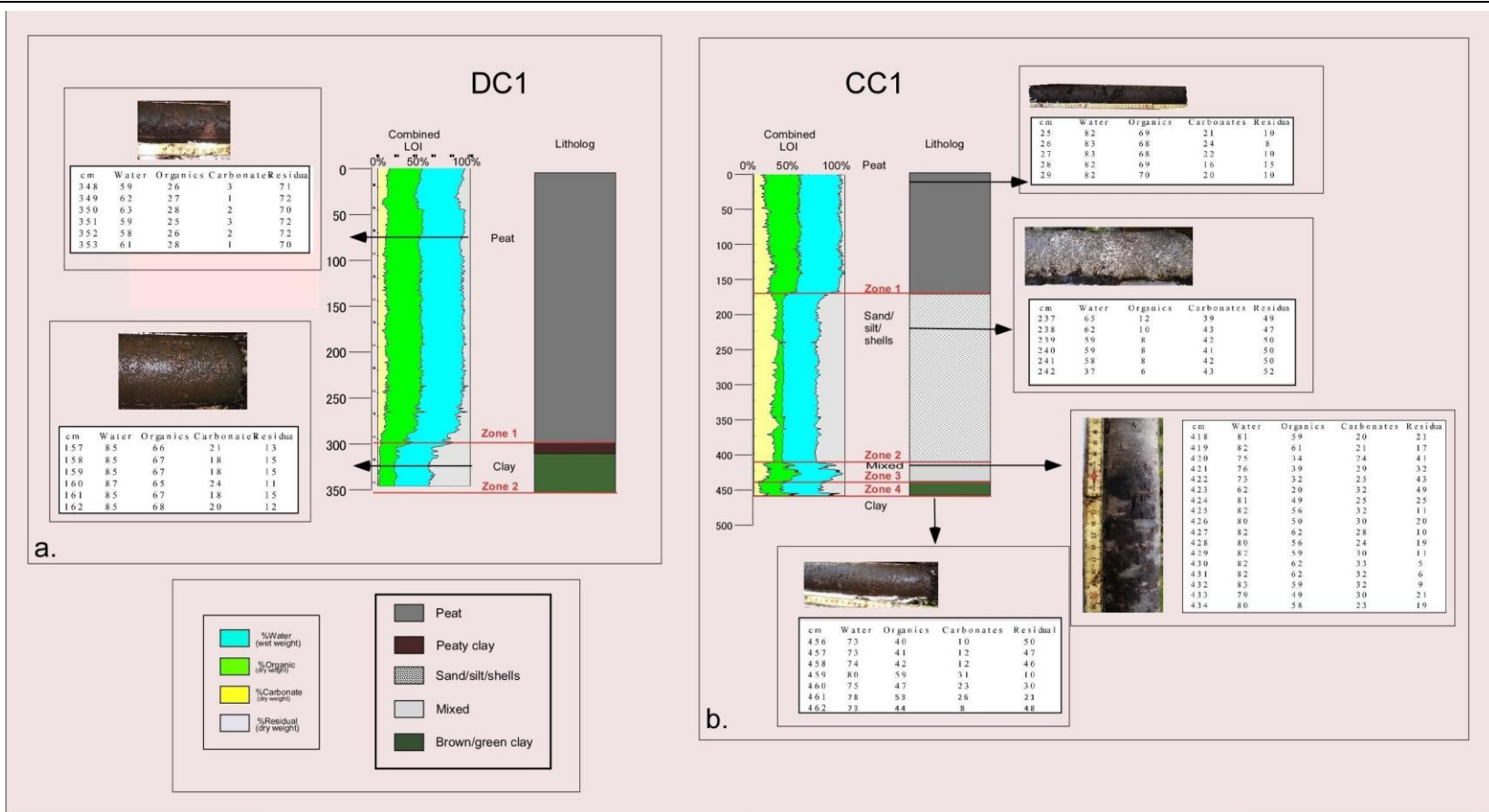
8.6.6 Cross Cay

A single composite core consisting of ten Russian peat borer sections, reaching a depth of 462 cm, was extracted from Cross Cay, a mangrove cay in the south central section of the Central Lagoon. Core location was 42 m from the sea, just beyond the fringing *Rhizophora* zone in a fairly open area dominated by slightly taller *Avicennia*. The core is highly organic at the top, consisting of very dark, well-rotted peat. Below this the sediments abruptly change to a thick carbonate-rich layer containing many shells and *Halimeda* flakes, very similar to those observed in other transects; although basically structureless, indications of horizontal deposition exists. Below this there is non-horizontally structured mixed layer, composed of small, incoherent clumps of the material from the two previous sediment types. The core bottom consists of the familiar brown/green clay (**Figure 8:18b**).





8.17 MC transect, showing (a) lithologs of transect cores, (b) core photos with abrupt sedimentological changes, and (c) coring site. Google Earth imagery (d) shows transect location in an *Avicennia germinans* forest (c) landward of the fringing *Rhizophora mangle* zone on the northern perimeter of the island, suggesting that hurricane flooding possibly approaches from Long Bogue in the north northeast. Red dashed boxes in (a) outline the core sections portrayed in the photos in (b).



8.18 DC1 and CC1 sedimentological units and zonation. Pictures and identifying LOI characteristics are presented for (a) the two sedimentological units (peat and clay) present in DC1, and (b) the four units (peat, mixed, shells/silt/sand and basal clay) occurring in CC1.

8.6.6.1 Zonation

8.6.6.1.1 Zone 1 (1-171cm) Dark, well-rotted peat, with high water and organic content, moderate carbonates, very small residual percentages (generally <15%).

8.6.6.1.2 Zone 2 (171-414cm) s/s/s interval. Moderate water and residual, high carbonate, low organic percentages.

8.6.6.1.3 Zone 3 (415-440 cm). Mixed, with rapid fluctuation between peat and s/s/s sediments.

8.6.6.1.4 Zone 4 (441-462) Basal clay, more organic than in other sites.

8.7 Discussion

8.7.1 Hurricane Hattie

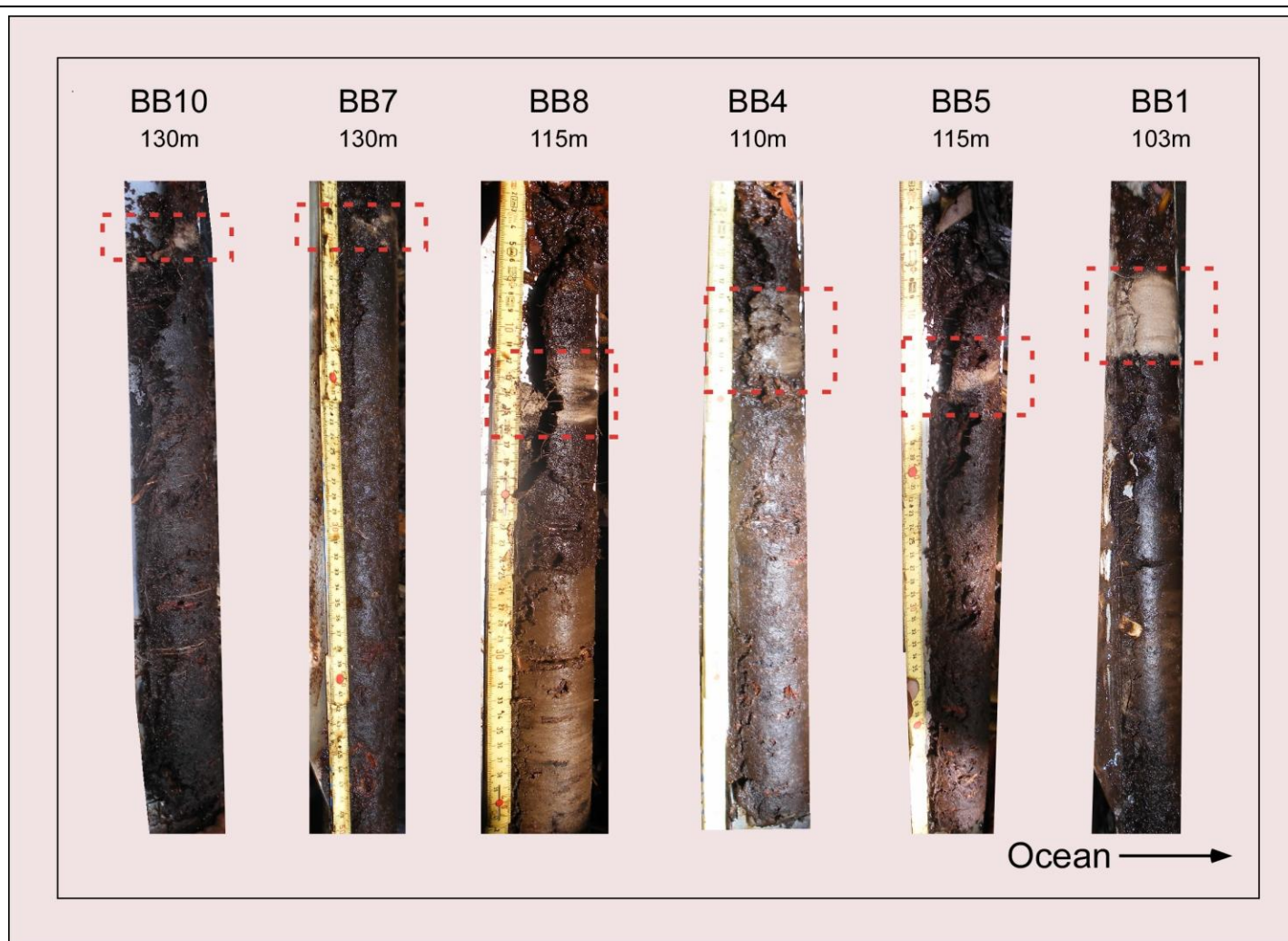
As the most important hurricane to strike the country of Belize in recorded history, the characteristics and effects of Hurricane Hattie have been discussed in several previous chapters. It was expected that Hattie, passing directly over Turneffe Atoll as a category 5 storm, would have left a clear sedimentary signal throughout the atoll. This was not the case, probably due to the fact that Turneffe's geologic framework reduces the sediment supply needed to produce the expected sedimentary signature. As an isolated carbonate platform, rising nearly vertically from depths of >1000 m, there is an extremely limited amount of mobile sand. There are no offshore sand bars to supply sediment to be transported inland by storm surge and very few sand beaches within the atoll itself. The entire sand supply consists of that produced by the wearing of coral on the narrow reef flat along the eastern edge of the atoll. This sand is generally moved along the inside of the fringing coral rim by currents, where it collects in the form of sandy cays. Some sand is moved across the reef flat to provide narrow beaches along the eastern edge of the mangrove cays sitting on the inner edge of the reef flat. Presumably some sand is lost over the eastern rim either directly or by tidally driven transport through the

bogues. Transport from the rim to the Central Lagoon is “restricted”, with non-skeletal grains “absent” on the lagoon floor (Gischler, 1994). While coral rubble is the most common bottom material along the atoll’s eastern edge, the lagoon bottom consists (in order of magnitude) of *Halimeda* flakes, mollusk shells, fine grained sediments, and foraminifera particles (Gischler, 1994).

Except for the mangrove cays sitting on top of the eastern reef flat, all mangrove cays are mounds rising steeply up off of the lagoon floor, thereby severely restricting transport of the bottom material onto the cays. These conditions severely limit the availability of materials to be moved by storm surge. A location downwind of one of the transient sand cays has the greatest potential for recording the passage of a hurricane.

The BB transect seems to have been in such a position during Hurricane Hattie. A very distinct sand layer (at times reducing to silt/clay) has been preserved across the top of this transect, as can be seen both visually (**Figure 8:19**) and from the LOI diagrams (**Figure 8:16**). The layer is clearly recognizable from 100 to 130 m inland. Closer toward the sea, the Hattie layer cannot be distinguished reliably from the beach facies that dominate the core tops (BB3, BB2, and BB9). The layer was not visually present at cores at 150 and 165 m (BB11 and BB 12). Some spatial variability is seen within the sand sheet, as it thinned from ~ 7 to 1 cm over the 30 m transect, and was completely missing at a site at 110m (BB6), while fining to clay at a 115 m site (BB4). Although this layer has not yet been subjected to ^{137}Cs analysis, its position near the core top, landward thinning and fining and distinct and abrupt compositional change makes its identity certain.

An earlier hurricane is possibly marked by the lower clay layer marked in cores BB1, 4, 5, and 8. Cores BB2 and 9 also show a lower sand layer, but, as with the Hattie layer, their



8.19 BB transect top clastic layer. Photos of core tops across the transect cores, highlighting the clastic layer which thins and fines inland.

proximity to the beach makes the identification questionable. If this lower layer is the signature of a historical storm, the unnamed hurricane of 1931 is the most likely candidate.

Sedimentary evidence for any other historically recorded hurricanes is lacking, including Greta (1978), the eyewall of which passed ~ 20 km south of Turneffe and Keith (2000), which grazed the atoll's northern edge.

An examination of the transect lithologs (**Figure 8:16**) supports the idea that the availability of mobile sand is highly variable temporally. There is a sharp compositional change from sand to peat in the lower sections of both BB2 and 9. Since beach translation, not being controlled by sea level rise, should be minimal, the abrupt appearance of sand probably indicates the formation of the sandy cay on the reef flat to the east of the site. This illustrates the transient nature of the sand supply and explains the paucity of events in the proxy record.

Hurricane Hattie does not seem to have left a recognizable sedimentary signal in any other location, including those from the GC and DC sites, which, like BB were situated directly across the reef flat from a group of sandy cays. Stoddart (1963) shows Hattie passing through the center of the atoll, putting the GC site near the eyewall on the right front quadrant; NOAA records show Hattie passing farther south, putting the DC site in a similar position. Whichever track is correct, it would be expected that at least one of the sites would have been in optimal location to have recorded the storm.

8.7.2 Regional Paleoenvironmental History

Sediment cores have been taken from a number of neighboring environments, including the coral rims and lagoon floors of all three carbonate platforms as well as numerous mangrove cays inside the barrier reef (Halley et al., 1977; Gischler, 1994, 2003; Gischler and Hudson, 1998, 2004; Gischler and Lomando, 2000; McKee and Faulkner, 2000; Jones and Dill, 2002;

Gischler et al., 2008, Wooler et al., 2004, 2007). The stratigraphic sequence normally encountered from these mangrove islands is basal limestone, followed by soil (clay), and then peat to the surface, with peat sequences up to 10 m thick having been recovered (Macintyre et al., 1995). Cores extracted from the lagoon floors show a similar limestone-clay-peat bottom sequence, above which the peat is abruptly replaced by carbonate deposition, either *Halimeda* (Turneffe) or mollusk-dominated (Lighthouse Reef and Glovers Reef) (Gischler, 2003). These sequences have been interpreted as directly resulting from regional environmental history. During the last glaciation the Belize shelf (currently a shallow marine lagoon between the barrier reef and the mainland) and the three carbonate platforms were above sea level. The platforms were dish shaped limestone islands, while the limestone shelf was connected to the mainland, cut by river channels, the topography controlled at depth by faults, and more superficially by the antecedent topography imposed by a series of Pleistocene reefs, themselves possibly sited on top of earlier topographic highs based on siliclastic river deposits (see **Chapter 5**). Glacial melting and eustatic sea level rise drove a rise in the water table, leading to soil formation in most locations. As sea level continued to rise, both the shelf and the platforms flooded, leading to mangrove development in intertidal areas and vertical accretion by coral along the rims (Gischler and Hudson, 1998, 2004; Gischler, 2003). As the coral rims built up, interior water depth increased, drowning the mangroves in lower areas and where accretion was slow. These flooded areas formed the floor of either the shelf or atoll lagoons, depending on location. With the replacement of mangrove peat deposition by the slower accretion rate associated with carbonate production, the drowned areas fell farther below sea level. On the carbonate platforms accommodation space has increased since flooding, with lagoonal floor sedimentation lagging far behind the vertical accretion of the coral rim (Gischler

and Hudson, 1998, 2004; Gischler, 2003). On the other hand, “keep-up” mangroves, often starting on antecedent highs (Halley et al., 1977), have kept pace with sea level, building ever thicker peat sequences that support the steep sided mangrove cays that presently dot the shelf lagoon and atolls. This results from continuous near-sea level mangrove production as the cays accrete upward, remaining within the upper tidal zone as the sea level rises (Woodroffe, 1981, Ellison, 1993; Macintyre et al., 1995; McKee and Faulkner, 2000; Wooller et al., 2007).

It is this regional environmental progression that has lead to the two standard stratigraphic sequences;

1. Limestone - brownish/greenish clay- mangrove peat
2. Limestone - brownish/greenish clay- mangrove peat-carbonates

Where mangroves have kept up with sea level, peat deposition continues to the present (Scenario 1); where they have not, an abbreviated peat layer becomes overlaid by carbonate-dominated sands and silts (Scenario 2).

Time of flooding varied with elevation. The general n-s tilt of the Pleistocene basement (**Figure 5:4**), resulting from tectonics and/or preferential meteoric dissolution caused generally earlier flooding for southern locations. As sea level rise was not constant over time (**Chapter 3**), location, along with a host of local factors, exerts an important control over the ability of reefs and mangroves to keep up with sea level rise. In general, the higher northern locations flooded later, during periods of slower sea level rise, and therefore favored continued mangrove development (Gischler and Hudson, 1998, 2004; Gischler, 2003). It is probably due to the late date of flooding, combined with the sheltered position downwind from Lighthouse Reef, that mangrove development has been so successful on Turneffe Atoll, with 22% of the atoll existing as land, compared to 3% and 0.2% respectively for Lighthouse Reef and Glovers Reef

(Gischler, 1994; Gischler and Lomando, 2000; Gischler and Hudson, 1998, 2004). Gischler (2004) shows a steady decrease in mangrove coverage for Glovers Reef from 8000-6000 BP (at which time mangroves essentially disappeared) and from 6000- to the present for Lighthouse Reef, as progressively fewer locations were able to keep up with sea level rise.

8.7.3 Inferred Local Paleoenvironmental History

Of the six sites cored in this study, two parallel Scenario 1, none parallel Scenario 2, and four follow a third scenario, in which the top interval of Scenario 2 (carbonates) are followed by at least a single return to peat. This sedimentary succession is unusual; with the resumption of peat deposition after a period of carbonate deposition otherwise unknown in the literature. In fact, the most striking features of these cores are these thick carbonate layers, bracketed by peat.

The minimum spatial coverage of this unique stratigraphy is 25 km, the distance that separates sites 1 (GC) and 6 (Cross Cay). However, the occurrence is not spatially coherent, as site 2 (BB) shows no carbonate layer, although such layers occur at the nearby sites 3, and 4 (HJ Cay and Main Calabash) (**Figure 8:20**). The carbonate layers display a specific spatial orientation, characterized by inland thinning. At HJ Cay and GC this is a narrowing of the layer, with the bottom and top of the layer converging across the transect. At Main Calabash Cay, the short core lengths only permit examination of the top of the layer, which deepens from 60-90 cm moving inland. There is some indication in these three transects of upper and lower carbonate layers, with the ability to distinguish the two changing spatially. Beginning and end of these layers is often abrupt, (GC1, 2; HJ2; MC 1, 2; CC1) and/or associated with a chaotic mixing of peat and carbonate clumps (HJ1, 3; CC1). The depth of the bottom of the carbonate

layers (presumably related to time of initiation) is nearly identical for GC2, HJ1, HJ3, and only slightly deeper for CC1.

Age and environmental information were obtained only for core HJ3, which contains two extensive carbonate intervals. The most obvious result of a rudimentary palynological investigation was the distinct pollen grouping common to each of the three sediment types. Although the extremely low pollen concentrations and incompleteness of the study render any interpretation somewhat suspect, it seems probable that three distinct vegetation groupings exist. The oldest and simplest occurred during the deposition of the basal clay, previous to ~6500 BP. This period is dominated by a terrestrial plant, *Guettarda foliacea*, a member of the Rubiaceae family. The only other pollen encountered for this interval is a single grain of Malpighiaceae, probably from a tree species. The provisional identification of this interval as a terrestrial period, with very low plant diversity seems reasonable. Due to the rather restrictive pollination requirement for *Guettarda foliacea* (big birds and mammals according to the Smithsonian Tropical Research Institute, <http://striweb.si.edu/esp/tesp/details.php?id=4622>), a high concentration of this plant suggests a lack of competition. The interpretation of this interval as a species poor, clay-based terrestrial environment is in keeping with previous descriptions of Turneffe prior to flooding as a mud covered limestone island (Gischler and Hudson, 1998; Gischler, 2003). The duration of this period is unknown, but presumably covers an extended period from the start of deposition (phreatic water rise) until time of flooding, evidently a period of very low sedimentation rates.

The peat intervals seem to represent vegetation conditions very similar to the present, mainly red mangrove forests. Presumably the Chenopodiaceae pollen derives from *Batis maritima*, which is currently extremely wide-spread. The upper peat section has a larger

number of forest taxa, while the sample from 370 cm, in the bottom peat section, contains *Pinus*, *Mimosa*, and a few *Guettarda foliacea* grains. Based on an assumption of constant sedimentation as supported by the age/depth graph (**Figure 8:7**), the duration of the peat regimes seemed to have lasted ~ 500 years for each of the top two intervals, and around 1500 years for the bottom sequence. Compositionally, the peat sections within the mixed layers resemble the top and bottom peat intervals; it is their stratigraphic incoherency that sets them apart.

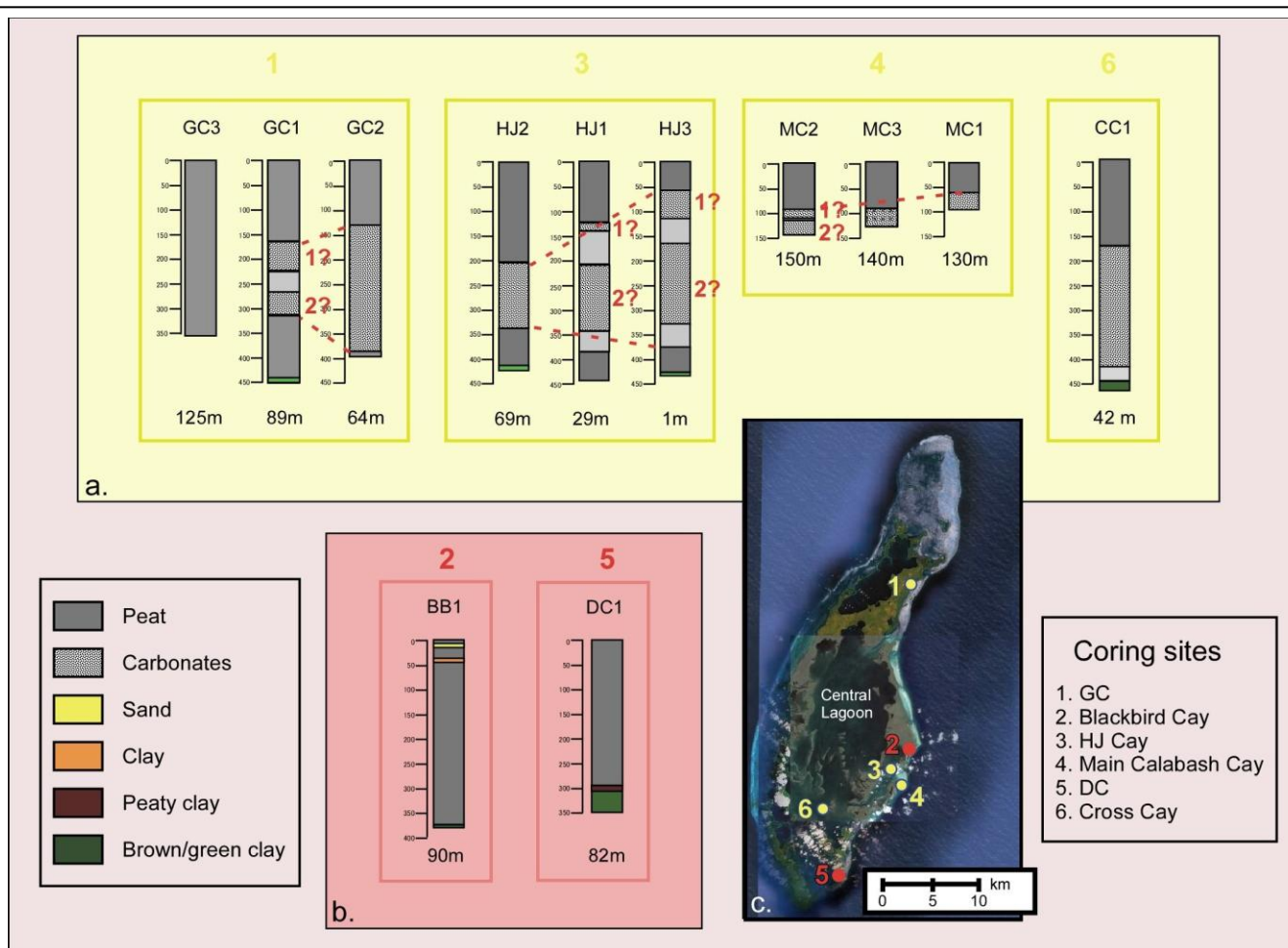
There are two carbonate intervals in this core, the more recent of which probably lasted ~ 500 years, while the thicker bottom interval appears to cover a period of ~3500 years (**Figure 8:21**).

The classification of these intervals presents difficulties. The preponderance of Chenopodiaceae pollen, presumably *Batis maritima*, suggests a salt marsh or mud flat.

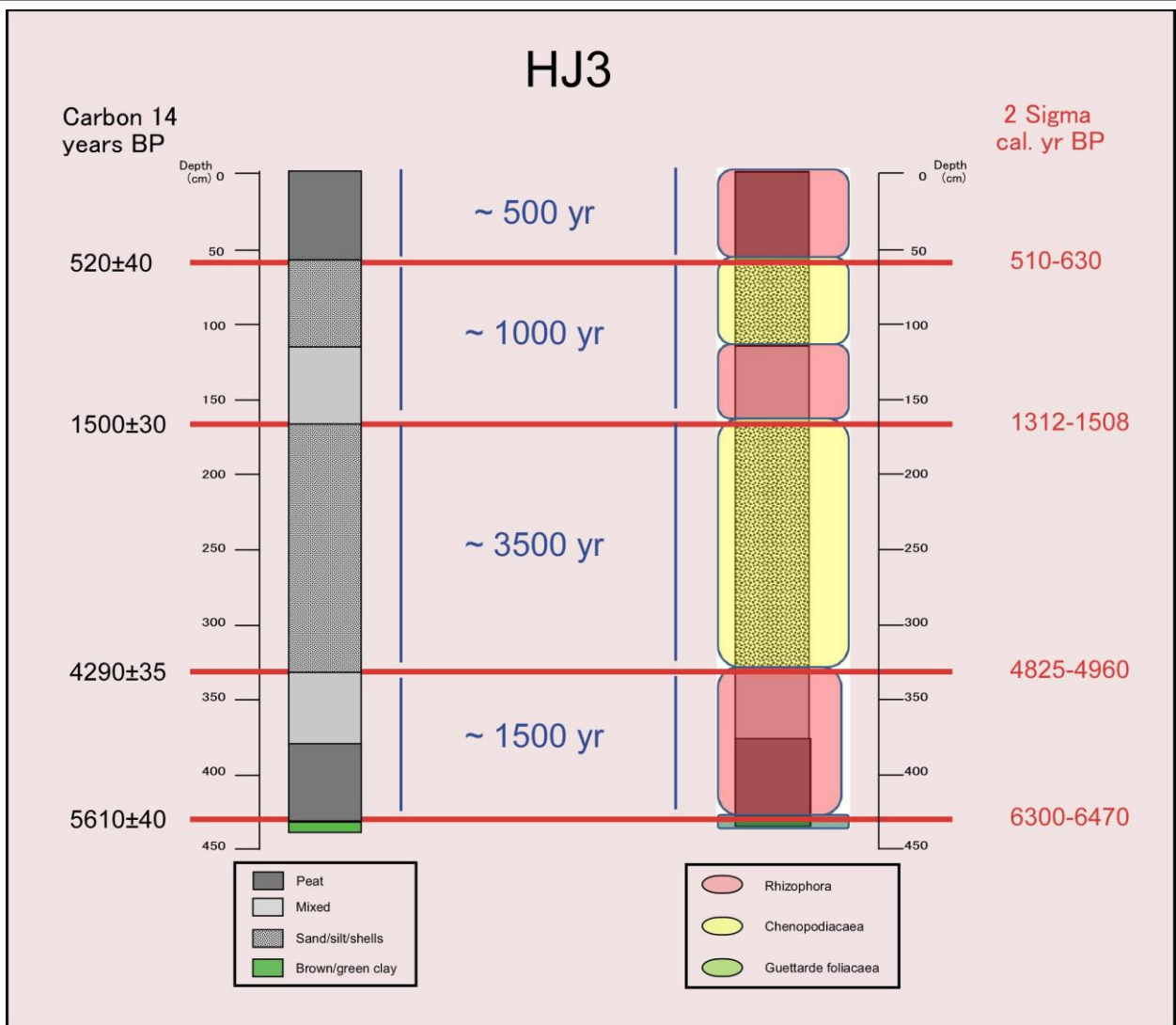
However, under current conditions *Rhizophora* is nearly always present in such areas, at the minimum forming a surrounding fringe. Because *Rhizophora* is a proliferate pollen producer (Ramcharan and McAndrews, 2006), one would expect a significant *Rhizophora* pollen

component at these depths. However, *Rhizophora* pollen is noticeably lacking. This is particularly puzzling given the presence of less expected taxa, such as Moraceae,

Melastomaceae (205 cm), *Pinus*, and *Quercus* (105, 205 cm). Indeed, *Pinus* is more abundant than *Rhizophora* at 105 cm in the upper carbonate section. The high abundance of *Halimeda* flakes as well as overall appearance, composition and structure suggest a flooded period with deposition resembling that occurring on the lagoon floor. The bottom of some carbonate layers (HJ3, MC3) include a shell and/or *Halimeda* flake layer, as commonly occurs at the beginning of lagoon floor carbonate layers (Gischler, 2003). The gradual secular downcore decreases in organic content for both carbonate layers are more indicative of slow deposition during gradual



8:20 Combined transects. The lithologs from (a) four coring locations, [site numbers corresponding to yellow numbers in (c)], display thick carbonate layers, while lithologs from (b) two locations, numbered in red (c). A landward thinning of the carbonate layers is noticeable across the GC, HJ and MC transects (a), as is the separation of the layers into upper and lower units. Transects that do/do not contain these carbonate layers do not fall into distinct geographic groupings.



8.21 Duration of ecological periods. Litholog of core HJ3 showing stratigraphy and pollen groupings (transparent colored boxes); measured radiocarbon dates are listed in black and the calibrated calendar ages in red. Estimations of the duration of specific ecological periods are in blue in the center of the diagram.

environmental change than instantaneous event-generated deposition. The interpretation of these intervals as submerged periods would explain the abundance of *Chenopodiaceae* (surrounding salt marshes in flooded areas), the lack of *Rhizophora* (too deep), and perhaps the rather random nature of the water-borne pollen grains that happened to be preserved. It is possible that the resulting environment (a shallow flooded island top composed of soft carbonate material), which currently has no analog on Turneffe (the only shallow water areas being reef flats), led to a no analog vegetation assemblage. Presently *Thalassia* dominates the lagoon floor, but at significantly greater (5-8 m) depths.

An alternative explanation is that some event instantaneously deposited these large carbonate layers on the cays, thereby dramatically increasing elevation and drainage, allowing a mixed forest to establish itself, replacing the mangroves, with *Batis maritima* present as a groundcover. Surface elevation above mean high tide could account for low pollen concentrations, rising sea level would eventually submerge the location, leading to the reestablishment of mangroves. Hurricanes are certainly capable of increasing a cay's elevation through the deposition of overwash sandlayers, an example being the augmentation of a beach in the northern section of Turneffe by Hurricane Keith (Platt et al., 2004). However, the nature of the sediments argues against this, as they do not resemble event layers, particularly in regard to their unconsolidated nature. We were able to core through >160 cm of this material at HJ3, while typically even a few cm of an event generated sand layer prevents penetration. Perhaps the slow subaqueous accumulation, mixed with occasional periods of resuspension and/or bioturbation results in a less consolidated mix than that produced by pounding of storm storm waves.

The history inferred from HJ3 follows the regional history from clay covered limestone

island, through flooding and mangrove development to carbonate dominated flooded period. At this point it diverges, displaying a second cycle of mangrove development, flooding, and return to mangrove. Although no pollen was examined from other cores, it seems reasonable to assume similar histories for those areas displaying this peat-carbonate-peat stratigraphy. Visual recognition of *Rhizophora* detritus and the distinctive mangrove based peat throughout the length of the two cores lacking carbonate intervals (BB1, DC1) support a standard Scenario 1 environmental history for those locations.

Core lengths varies by only 15 cm across the HJ transect, with both HJ 2 and 3 reaching the basal clay. As evidenced by the lack of standing water, surface level was slightly higher for the longest core, HJ1, further reducing bottom depth differences. Although no clay was recovered from HJ1, penetration refusal indicates that either stiff clay or the bedrock base was encountered directly below the deepest recovered material. This suggests that the islands' antecedent base was relatively flat, and that the accretion probably proceeded equally across the island, implying minimal shoreline movement.

Core analysis indicates two distinct environmental histories for Turnelle Atoll mangrove cays over the last 6000+ years. Although all progressed from bare limestone through a species-poor terrestrial environment to *Rhizophora*-dominated mangrove forest, at some point several of the islands show a transgressive carbonate interval(s), probably lasting for 1000s of years, followed by a return(s) of mangroves. The processes responsible for producing the stratigraphies occurring in the cores lacking the carbonate layers seem straight forward (Scenario 1). Identifying the processes involved in creating the bracketed carbonate layers is not, but is essential for understanding the atoll's environmental history.

8.7.4 Carbonate Layers

8.7.4.1 Possible Causes

As in nearly all geological investigations dealing with sedimentary change, possible causes fall into two broad categories; gradual (resulting from slow changes in the boundary conditions) and rapid (event driven). We will examine each group of causes in turn.

8.7.4.1.1 Gradual

Gradual changes in boundary conditions in coastal environments are usually driven by climate and/or sea level changes. These, in turn, can affect conditions either directly or indirectly through such mediums as secular geomorphologic or vegetation changes. For example, a climatic change (altered strength/direction of the dominant wind) can affect back barrier depositional regime by changing dune height, while changing sea level can affect back barrier depositional regime through alterations to the water table. The effects of such large changes are usually regional in scale, often larger, and should be observable across several parallel proxies. For example, eustatic or isostatic sea level raise will not be expressed solely as increased marsh accretion in a single bay; increased precipitation should show up in number of different records (palynological, isotopic, sedimentological, chemical) over a broad area.

I can identify no climate-driven mechanism capable of causing the abrupt depositional reversals seen in these cores. The lack of corresponding shifts in the regional record further negates this possibility. Similar arguments apply to the identification of absolute sea level changes as the responsible agent. Although sea level rate has not been constant, and can be used to explain the ability (or lack thereof) of mangroves and corals to keep up with rising water levels, the timing of such rate changes are not at all consistent with the changes seen in the cores. Drowning of mangrove should correspond with faster rates and their reestablishment

with slower rates. This is not what we see in the case of HJ3, the only dated core. In general, sea level rise slowed appreciably around 5000-6000 BP, and has continued to slow since, showing almost insignificant rise over the last 2000 years (**Chapters 2, 5**). In HJ3, however, the bottom carbonate interval begins ~5000 BP, just as sea level rise is slowing. There is no apparent correspondence between the end of that period, or the following peat-carbonate-peat period with the regional sea level curve. Neither do these changes match other regional records. HJ2, cored in standing water, is at a lower elevation than HJ1 but shows reduced layer thickness, indicating that layer transgression is based on proximity to the sea, rather than elevation, as it would be if driven by sea level change. The observed sedimentary changes are simply too large, too abrupt and too local to have been driven by such large scale drivers as climate or sea level changes.

8.7.4.1.2 Event Driven

Potential event driven causes of these thick carbonate layers include hurricanes, tsunamis, tectonic subsidence, and platform slumping.

8.7.4.1.2.1 Hurricanes

Hurricanes are clearly capable of causing both great ecological damage (Craighead and Gilbert, 1962; Lugo, et al., 1983; Brokaw and Walker, 1991; Frangi, and Lugo 1991; Gresham et al., 1991; Lodge and McDowell, 1991, Reilly, 1991; Tanner et al., 1991; Boose, et al., 1994; Bellingham, et al., 1995; Meerman., 2001,2006; Boose, 2003; Cahoon et al., 2003) and geomorphologic changes (Chabreck and Palmisano, 1973; Gayes, 1991; Scatena and Larsen, 1991; Scoffin, 1993; Cahoon et al., 1995; Dawes et al., 1995; Dingler and Reiss, 1995; Jackson et al., 1995 ; Goodbred and Hine, 1995 ; Tedesco et al., 1995; Risi et al., 1995; Kang and Trefry, 2003; Keen and Stone, 2000). When the interaction with fire is considered the

resulting changes can have long term effects (Liu et al., 2003, 2008), perhaps lasting hundreds of years (Urquhart, 2009). The usual coastal effects of hurricanes are tree damage (defoliation, limb breakage, uprooting), flooding and inland sand transport. The intrusion/ponding of marine waters can also lead to plant mortality (Bianchette et al., 2009).

However, as discussed above, Hattie's signature in the Turneffe sedimentary record is spatially sparse and sedimentarily unspectacular, and does not in any way resemble the carbonate layers observed in our sites. However, severe ecological/geomorphologic consequences have been recorded as a result of intense hurricane strikes within the region. Cahoon et al. (2003) reported "virtually complete" mortality for mangroves from Hurricane Mitch (1998) on Guanaja, one of the Bay Islands of Honduras, with no regrowth and a complete absence of propagules at the site 27 months after the storm. Of particular importance is the observed peat collapse and a measured elevation loss for 11 mm/yr for the period, with model simulations calculating additional losses of 56 mm over the following 7 years (Cahoon et al., 2003).

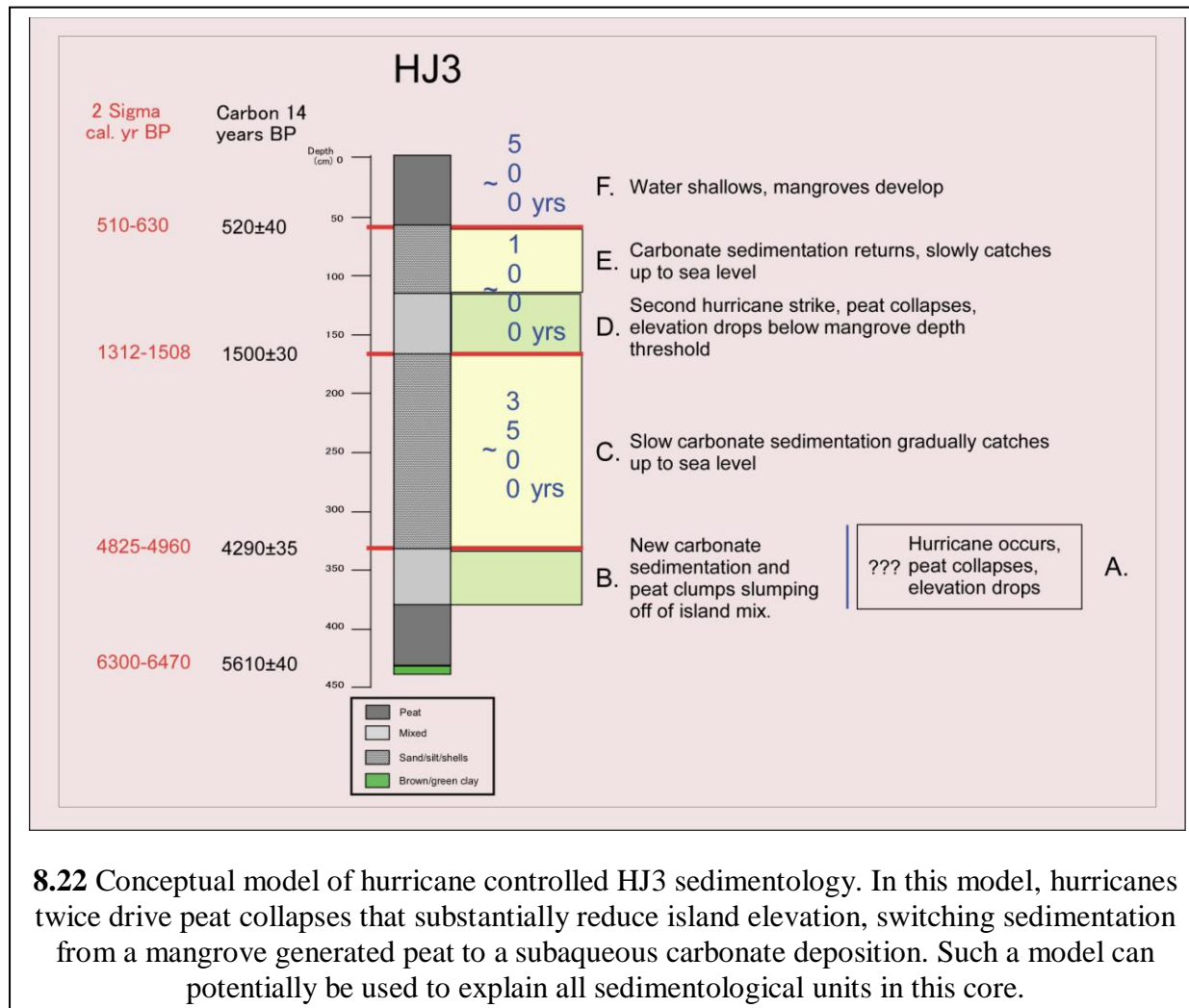
Supporting the view that tree death and subsequent root decomposition can result in lowered elevation, McKee and Faulkner (2000) demonstrate that, as leaf litter is susceptible to both tidal export and biological consumption, peat accumulation and vertical accretion are dominated by root production. Indeed, they document an interior pond on their study site, a Belizean cay, with large, submerged *Avicennia* stumps. Because *Avicennia* typically occupies slightly higher, elevations, this indicates a lowering of surface elevation following tree death.

As mangroves have a water depth threshold, beyond which they cannot survive, these studies suggest that hurricanes are potentially capable of causing long-term removal of mangroves from a site through reducing surface elevation. Where the elevation decrease is

large, the change could theoretically be permanent, depending upon sedimentation rate, and the direction and rate of sea level change. A complicating issue is the source of propagules, the availability of which can be limited by current direction (Hensel and Proffitt, 2002), particularly important for Turneffe, given the atoll's oceanic location.

In the case of HJ3, there are upper and lower carbonate layers separated by a mixed layer. A hurricane based explanation of the stratigraphy is illustrated in Figure 8:22. In this scenario mangroves begin developing at the site shortly after flooding, resulting in peat deposition, when at some undated point an extremely large hurricane hits (**A**), resulting in complete mangrove mortality, peat collapse, and elevational decrease. The island surface is eroded to the peat at 378 cm core depth. As the water is now too deep for mangrove growth (aggravated by lack of propagules), lagoon bottom style carbonate sedimentation begins, with the carbonate material chaotically mixed with large clumps of mangrove peat eroded off the island edge during and/or after the event (**B**). Around 5000 cal yr BP the island stabilizes (**C**) and peat clasts no longer intrude into the depositional regime. Standard carbonate sedimentation continues for the next 3500 years, raising the surface level by 166 cm, thereby gaining approximately 50 cm on sea level, which increases by ~1 m during the period) (**Figure 5:8**). The minimum threshold depth for mangrove growth is now met, and they develop rapidly (**D**). A second storm now hits and the process is repeated (**D, E**), with mangroves reestablishing themselves ~ 500 BP (**F**).

An extrapolation of this scenario, though possible, seems an unlikely explanation for the existence of the atoll-wide carbonate layers. First, it should be noted that Mitch was an extremely large and powerful storm that stalled off the coast of Honduras and hovered over the Bay Islands for more than two days (Guiney and Lawrence, 1999; Hensel and Proffitt 2002).



Mitch's minimum central pressure (905 mb) and the 15 hours of sustained winds of >155 knots (178 mph, 287 kph) make it one of the strongest North Atlantic hurricanes on record. Hurricane force winds and tropical storm force winds extended up to 110 and 280 km from the center, respectively (<http://lwf.ncdc.noaa.gov/oa/reports/mitch/mitch.html>, <http://www.nhc.noaa.gov/archive>). The effect of Mitch on Guanaja was probably exceptional, resulting from a combination of the storm's large size, extreme magnitude, and slow translational speed. Neither Hurricane Keith nor Hattie had such devastating effects on Turneffe, although both were powerful storms that passed close by. Like Mitch, Keith's forward movement stalled near Turneffe, increasing the duration of its interaction with the atoll. In general, the tremendous geomorphologic changes that Hurricane Mitch visited on Guanaja do not seem to be applicable to Turneffe Islands.

A second consideration is the area over which such destruction occurred. Although the mangrove devastation was near complete in the highly impacted areas of Guanaja, medium and low impact sites were located ~ 30 km distance on the neighboring island of Roatan, (Hensel and Proffitt, 2002). At these sites tree mortality was less and recovery faster. It is not clear whether mangroves exist at intermediate distances, and if so, the level of their destruction. In any case, it is difficult to envision a storm capable of complete ecological/geomorphological destruction across the distances separating our coring sites. The alternative explanation of a series of extreme storms at various sites during the same general time period also seems unlikely.

The question of propagule availability is valid, and could conceivably limit recovery. However, Lighthouse Reef and Glover Reef lie to the east and southeast respectively. Both currently have mangroves (though very restricted amounts on Glovers Reef); with

paleoecological reconstruction suggesting increased mangrove coverage before ~ 5000 BP (Gischler, 2003). A multitude of mangrove cays exist to the west, behind the barrier reef, which itself possibly supported mangroves during the period in question. *Rhizophora* can apparently establish itself without any obvious propagule source, as is evident in the case of Barbados, which has mangroves despite being much more isolated, more removed from major currents, and possessing rather inappropriate geomorphological constraints (Ramcharan, 2005). Even in the unlikely case of a paleohurricane causing the complete destruction of the entire mangrove community on Turneffe Atoll, a lack of propagules should not have prevented their reestablishment for 3500 years.

If the carbonate layers result from hurricane(s), the responsible mechanism must be elevational decrease, driven by peat collapse resulting from near total tree mortality. As this process does not seem to have occurred on Turneffe during historical hurricanes, hurricanes are unlikely to be the cause of the layers.

8.7.4.1.2.2 Tsunami

Tsunami are potentially capable of causing massive damage, as there is an extremely large upper size limit; the larger the force of an object causing a sudden vertical displacement in a body of water, the greater the resulting wave. Although the background discussion (**Chapter2**) outlines general tsunami characteristics and Caribbean causes and risks, Turneffe presents a special case. Most of the work done on tsunami focuses on their effects on continental margins or large oceanic islands. As these shores are generally characterized by relatively low gradient bathymetry, and the size/shape/destructive power of tsunami waves is controlled by the mechanics of their shoaling, the effect on vertical oceanic atolls is not well known, and possibly significantly different.

For this reason a recent study on the effects of the Sumatran tsunami (December 26, 2004) on an atoll within the Maldives archipelago is very informative (Kench et al., 2006, 2008). The Maldives archipelago consists of almost two dozen atolls and reef platforms stretching ~750 km n-s along a broad carbonate bank in the Indian Ocean. The atolls are aligned in two parallel chains along the eastern and western rim of the archipelago. The study atoll was the South Maalhosmadulu atoll near the northern end of the western chain. The Sumatran tsunami originated ~2500 km to the southeast, generated by a from a 9.3 Mw seaquake (Stein and Okal, 2005). The main tsunami waves passed directly over the Maldives, losing 0.5m in wave height in the process (Titov et al., 2005), entering the archipelago through a 60 km gap along the eastern edge. After crossing ~ 50 kilometers of open water (2000 m depth) the waves were “allowed” to enter the South Maalhosmadulu atoll through the large (4500 m wide, 40 m deep) gaps in the atoll’s coral rim (Kench et al., 2008). Due to the rapid shoaling and/or restricted entrance, the tsunami’s expression within the atoll was relatively gentle, consisting of “rising tidal surges” and not the pounding waves commonly associated with tsunami.

In general, the tsunami power was greatly reduced, with overall geomorphologic effects to South Maalhosmadulu atoll described as “relatively minor” (Kench et al., 2008). Principal geomorphologic effects included overwash deposition and shoreline erosion along island fronts, and deposition and spit formation along the back, with all 11 islands exhibiting some level of both deposition and erosion. Unlike Turneffe, this atoll has a large supply of mobile sand surrounding most islands, which led to the deposition of impressive overwash sand sheets. Sand sheets were 1-30 cm thick, and reached up to 60 m inland. Material was primarily medium to very coarse beach sand, with a small admixture of reef sediments and island soil.

Internal stratification occurred only in the thickest deposits. Terminal *Halimeda* drapes occasionally occurred. Coral rubble strandlines were created and isolated clasts as large as 2 x 1.4 x 0.5 m transported inland (Kench et al., 2006, 2008). Erosion along the island fronts, usually in the form of scarping, was common, affecting up to 54% of the shorelines on individual islands (Kench et al., 2006, 2008). Due to the islands' small size and low elevation, backwash generally did not occur, with the tsunami waves generally either rolling completely across the islands or percolating downward. An unusual erosional feature were seepage gullies, formed when ponded water in the generally dish shaped islands eventually broke through the rim and flowed back to the sea (Kench et al., 2006, 2008).

Despite the level of described geomorphologic change, the authors conclude that this event will not be preserved in the sedimentary record. Due to monsoonal effects, the strong seasonal variability in wind and ocean conditions drives high-amplitude annual cycles in sand movement and depocenter location. The authors found that the geomorphic effect of the tsunami was smaller than the annual seasonal effect, and that subsequent annual cycles will mask the tsunami derived changes. They particularly note that tsunami do not lead to island instability (Kench et al., 2006, 2008).

There are several reasons why tsunami probably are not the agent responsible for the creation of the carbonate layers. The most important is the bathymetry of the atoll, which rises almost vertically from a 1000 m floor (**Figure 8:3**). It is the effect of shoaling, which changes the wave energy from translational to transitional, which focuses the energy on the landform; in the open ocean tsunami waves are barely noticeable. The integrity of the eastern coral rim, broken only by the three narrow, shallow bogues (10's of m wide x <10 m deep) should further reduce wave energy in the lagoon by blocking the entrance. It appears that nearshore depth and

rim gaps are of primary importance in determining wave energy. The hardest hit islands in the Maldives study were those that met both of the following conditions;

1. Open exposure (behind km wide gaps in the atoll rim that let the energy in)
2. Extended shoaling (wide reef flats that permitted earlier shoaling and greater wave energy).

Although the mathematics of tsunami wave energy generation on deep water atolls have not been studied, it seems likely that Turneffe is fairly well protected from tsunami from the expected (eastern) direction of approach (**Chapter 2**), both by the steep bathymetry and the integrity of the coral rim. This should reasonably result in a tsunami's energy being expressed as a gradual inundation rather than steep breaking waves. In fact, there is a good chance that the atoll geology renders tsunami risk "negligible" (Brander, personal communication).

A second argument against tsunami as the responsible agent is the lack of correspondence with neighboring proxy records, as any tsunami approaching from the east large enough to significantly impact Turneffe should have had regional effects. The age of the extremely large sedimentary signature associated with Event 7 from the Gales Points/Mullins River transects (**Chapter 6**) approximately match the date of the beginning of the upper carbonate layer in HJ3, but there is no matching event from the Hopkins/Commerce Bight transects (**Chapter 7**). Nor does the bottom layer correspond to any large event in from the mainland records.

Tsunami approaching from the west would be less hindered due to both a shallower ocean floor (~500m) and a lower, less continuous rim, and would not require parallel records from mainland cores, as the energy would be propagated eastward, into Turneffe and the open ocean and not westward over the shelf. Approach from the west would have to originate from

the outside the barrier reef, probably from the shelf edge situated ~15-20 km to the west of Turneffe. Due to the proximity and high angle dip (40^0) (Garcia and Holtermann, 1998), this location is potentially capable of producing a localized, possibly intense tsunami.

In general, however, there is very little geomorphologic resemblance between the effects of the Sumatran tsunami on the Maldives atolls and the carbonate layers observed from Turneffe Atoll. Although some characteristics such as landward thinning, the presence of coral clasts and widespread erosion are similar, the overall effects are very different. On Turneffe the grain size is much smaller (probably due more to sediment source than depositional mechanics, however), the layers are much thicker, extend much farther inland, generally do not show internal stratification, lack terminal drapes, and often show gradual secular compositional change. No evidence for the transport of large coral blocks exist on Turneffe and the dating makes instantaneous deposition unlikely. As mentioned above, the carbonate layers more closely resemble lagoon floor bottoms than event layers, including occasional basal shell layers. Certainly, identifying these layers, which apparently changed the sites' depositional regimes for thousands of years, is not in agreement with the finding from the Maldives that tsunami effects would neither be preserved in the sedimentary record or have any significant negative impact on island stability.

8.7.4.1.2.3 Seismic Activity

Although situated only ~150 km north of the plate boundary, Turneffe is not especially subject to tectonic disturbances, due mainly to the boundary's strike/slip nature (**Chapter s 2, 5**). However, tectonic activity does occasionally occur in the area, as evidenced by the 7.3 seaquake that occurred 125 km NNE of La Cieba, Honduras on May 28, 2009 (<http://earthquake.usgs.gov/eqcenter/recenteqsww/Quakes/us2009heak.php>). A lack of tectonic

activity however, does not rule out small scale seismic events, particularly on the carbonate platforms. Similar small scale events have already been suggested as the explanation for abrupt relative sea level rises in the southern shelf lagoon (**Chapter 5**). As Turneffe consists of a series of Holocene and Pleistocene reefs built over Tertiary reef and shallow water material above Cretaceous-Eocene siliclastics, occasional settling of this tall tower seems likely. Some tangential evidence for such movement exists. The top of the Pleistocene reef for the first three fault blocks all show a distinct southern dip, with the northern ends elevated 10-20 m above those of the south (**Figure 5:4**). A possible explanation for this tilt is differential weathering. Presently, on the mainland, the precipitation gradient increases sharply to the south, driven by the orographic effects of the Maya mountains. It is unclear, however, whether this gradient persists offshore, or whether similar conditions prevailed throughout the Pleistocene. If precipitation was greater in the south during the Pleistocene, this could have resulted in increased dissolution of the reefs, thereby accounting for the lowered elevations. An alternative explanation is a tilting of the ridges, although no direct neo-tectonic evidence was been found for this (Gischler and Hudson, 1998, 2004; Gischler and Lomando, 2000). More direct evidence for platform movement comes from a group of stalactites in a speleothem gallery at around 40 m depth in the Great Blue Hole, a submerged sinkhole in Lighthouse Reef, ~25 km east of Turneffe. 22 of the 29 stalactites in the gallery show a northern tilt of 5-10°, some with bends and spiral structure, indicating a tilt of the platform as they formed (Dill, 1977; Jones and Dill, 2002).

Either overall platform tilting or settling of different platform sections provide reasonable scenarios for explaining the presence of the carbonate layers. A small vertical drop or slightly larger tilting could lower island surfaces far enough below sea level to either kill the

existing mangroves and/or inhibit new mangrove growth, after which normal lagoon floor style sedimentation would commence. Either the disturbance caused by the movement itself or the resulting peat collapse could explain the intrusion of the large organic clasts into the carbonate material. Such a scenario also explains the inland thinning of the layers, as the more inland cores sites would be exposed to shallower water. In the case of HJ3, core stratigraphy would follow the scenario outlined in **Figure 8:22**, with seismic movement instead of hurricane induced peat collapse driving the abrupt increases in water depth. Both Littler et al. (1995) and Macintyre et al. (1995) report the presence of large blocks of peat slumped off of submerged sections of cay walls in the Tobacco range. They attribute this slumping to undercutting, resulting from the action of “severe storms and earthquakes” (Macintyre et al., 1995). This supports the view that events can cause slumping and lateral/vertical movement of peat deposits on cay edges, neatly explaining the large organic clasts in the mixed layers.

The spatial gaps in layer presence are less troubling if tilting is the responsible agent, as, depending upon location of the hingeline, movement could be of differing magnitude and even direction at the various coring sites. For example, a tilt to the north could result in a preferential lowering, and therefore a thick carbonate layer, of the northern site (GC), while raising the elevation of the southern site (DC), thus accounting for that site’s lack of the carbonate layer. The reef flat is exceptionally broad in front of the BB transect (**Figure 8:3**), perhaps indicating greater structural strength and less vertical mobility, and thereby explaining the lack of carbonate layers in the BB transect cores. Subsidence to the northwest could also explain spatial differences. Of course, platform movement could cause the slumping of individual cays, which may or may not be expressed in a spatially consistent manner.

Spatial consistency is also not required if the movement resulted from small

intra-platform subsidence or realignments. The slumping of individual cays from purely local factors also provides a possible answer. This explanation is less likely, however, as there is no record of slumping-related elevational reduction in other cays, even in peat deposits as thick as 10 m. The slumping reported for the Tobacco range is attributed to undercut walls and does not suggest that locations up to 89 m inland can be driven below sea level by similar processes.

The apparent repetition of the peat-carbonate-peat sequence in the GC, HJ, and MC transects suggest that small scale subsidence may be a reoccurring event. If so, there are fairly significant potential societal consequences, especially given the increasing use of the atoll as a tourist destination (Pat, 2001).

8.7.4.2 Carbonate Layer Summary

Sedimentologically, the carbonate layers do not appear to be event layers, as they generally lack the chaotic nature, occasionally vertical deposition and overall structure (upward fining) usually associated with instantaneous high energy deposition. The thickness is also beyond the usual event parameters as is the unconsolidated nature of the material. The most likely depositional environment for the layers is a subtidal surface too deep to permit mangrove development.

However, stratigraphically, the layers do resemble event layers due to their landward thinning, general atoll-wide temporal correspondence, the chaotic nature of the lower contact between the peat and carbonate layers, especially for HJ1 and 3, GC1, and CC1. The extreme vertical mixing and general incoherency of the depositional pattern at these levels argues for some type of high- energy disturbance.

A likely resolution to this paradox is to view the layers as event generated, with the important effect of the event being a rising of relative sea level for the sites, with the layer itself

consisting of normally deposited material. Once water depth surpasses mangrove depth restrictions, sedimentation can switch abruptly from organic to carbonate. The answer, therefore, lies in identifying a process capable of producing abrupt relative sea level rise within the spatial and temporal parameters of our sedimentological results.

Slow acting environmental changes do not seem capable of producing the required water depth increases. Neither do hurricanes. Although the hurricane-driven reduction of surface elevation through peat collapse has been recorded in the area, this response has not been observed for historical events on Turneffe, and does not seem capable of operating at the necessary spatial scale. Tsunami also seem an unlikely candidate, as not only does atoll geology limit their geomorphologic effects, regional records show no corresponding event. A tsunami resulting from a localized collapse of the Belize shelf remains a possibility. Local seismic activity, probably a shifting of all or part of the platform, is the process that can most successfully explain abrupt (probably repeated) relative sea level rise in a wide-spread but spatially spotty manner.

8.7.5 Forest Taxa

Many examples of forest taxa that are not currently present on Turneffe Atoll were found in the preliminary pollen survey conducted on core HJ3. The source of these grains and their importance to the paleoenvironmental history of the atoll are interesting questions.

Two of the most common non-resident pollen types are *Pinus* and *Quercus*. The presence of *Pinus* is probably the result of regional transport, as it is a common species found in mainland savannas, approximately 35 km to the west. *Pinus* is more common in the samples from 163 cm to the top, in agreement with Wooller et al. (2004, 2007) who report a sharp increase of *Pinus* pollen at around the same depth from, which they date to around 3500 BP.

Similar increases have been observed as occurring from other regional locations for the same approximate period (Islebe et al., 1996, Wahl et al., 2006). *Quercus* also seems to be slightly more common over the top 163 cm. Wooller et al. (2007) attribute the *Pinus* increase to climatic change, with warmer and wetter conditions forcing a mainland shift from savanna to forest, supported by regional data (Markgraf, 1993; Leyden, 2002).

An alternative explanation is a change in wind direction/strength resulting in enhanced regional transport from the mainland. Being under the influence of the trade winds, the predominate wind direction on Turneffe Atoll is from the northeast, blowing toward, rather than from, the mainland, as indicated by the wind rose for both normal weather and for major storms (**Figure 5:5**). Episodic occurrences of El Niño conditions and the strengthening of low level westerlies can be perhaps be invoked to explain upwind transport from the mainland, especially for the vesticulate taxa. Therefore, it is possible that increased El Nino frequency, which in fact seems to have occurred during the period between ~4000-2400 BP (Haug et al., 2001), might also be at least partially responsible for the increase seen in pine, and possibly oak.

However, it is more difficult to support regional transport as the sole mechanism responsible for the presence of some of the other forest and mixed pollen, which includes Anacardiaceae, Moraceae, Melastomaceae, *Ambrosia*, *Mimosa*, *Myrica* and in the peat intervals. The Anacardiaceae and Melastomaceae pollen seem particularly compact and dense for regional transport (**Figure 8:8k, l**). Moraceae and Melastomaceae are present in a sample from an inorganic interval, and a single grain of Malpighiaceae is found in the basal clay. It seems likely that some of these plants were physically present on the atoll, although water transport is also a possibility. *Myrica* is commonly reported from similar locations (Islebe and

Sanchez, 2002; Torrescano and Islebe, 2006), while Moraceae is a common regional forest species. Hardwood cay forests exist on higher elevations on the larger cays, but are of very limited area.

There exists a reasonable potential for deliberate human transport of useful species, and inadvertent transport of others, for at least for the last millennia. Although little archeological work has been done on the atoll, pottery shards from along the eastern edge indicate that Maya people were present since at least the 8th and 9th centuries AD, and possibly much earlier (MacKie, 1963; Chi, personal communication). By the late 18th century various groups were making use of the islands, by the time of Hurricane Hattie (1961) there were 7-8 small settlements on the atoll, and many types of mainland species were reported to have been taken to the atoll during this period. Anthropogenically-driven vegetation change was presumably large as the population engaged in agriculture, and a fairly large-scale planting/maintenance of coconut palms. Chickens, dogs and pigs were kept (Stoddart, 1963). Pine is mentioned as definitely being present during this period, with some remnant individuals still existing (Chi, personal communication). Turneffe Atoll became completely depopulated following Hurricane Hattie; Stoddart (1963) expected this state to continue for “several” years. Currently the atoll has a very small permanent population, although regularly visited by fishermen, and, more recently, tourists. Possibly early pine and other forest pollen represent similar ancient Maya use of the islands. However, it seems unlikely that human use was of much significance before ~2000 BP.

8.7.6 Carbonate-Organic Relationship

Both carbonate and organic values (% of dry weight) are calculated for each cm of core length during the LOI process. These values can be plotted against each other and their

mathematical relationship classified as either positive or inverse. There is some indication that these relationships can be used to mark shifts in the depositional environment, with a direct relationship indicating stronger terrestrial influence and an inverse relationship stronger marine influence (McCloskey, 2006). The argument is that depositional mechanics differ during marine and terrestrial dominated periods in the near tidal zone. During more terrestrial periods (lower relative sea level, periods of beach progradation, increased fluvial influence, etc.) deposition is additive, with carbonates and organics increasing/decreasing in parallel as input is received from both sources. During more marine (submerged) periods, however, the depositional environment is dominated by zero sum mechanics; i.e. during calm periods authochthonous organic deposition dominates while the import of allochthonous carbonates dominates during storms. Thus, the relationship between carbonates and organics should be inverse (either/or deposition) for marine periods, and direct (neither/both) for terrestrial periods.

Plotting carbonate and organic values in parallel enables the relationship type to be recognized visually (**Figure 8:23a, b**). This operation was performed on all Turneffe cores for which LOI data was generated, permitting the identification of positive and inverse intervals. These intervals were separated and classified according to their sediment type as determined from the core. Possible classifications were:

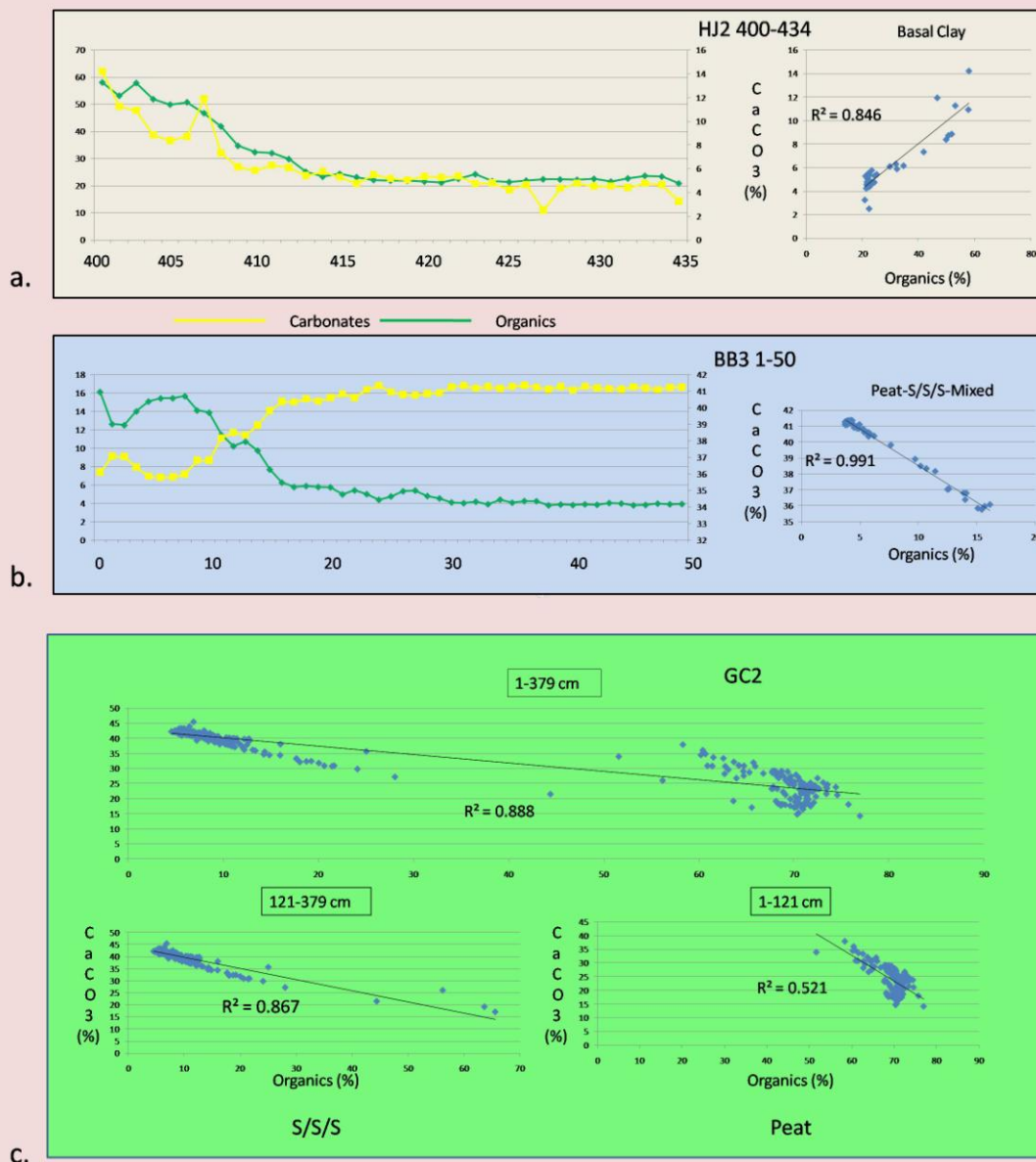
1. Peat- S/S/S-Mixed (16 sections)
2. Basal Clay (6 sections)

Organic values (X axis) were plotted against carbonate values (Y axis) for all sections, trendlines were selected and the coefficient of determination (R^2) values were generated. In all cases Peat-S/S/S-Mixed layers recorded negative trendlines (inverse relationships), while all

Basal Clay intervals recorded positive trendlines (direct relationships). Samples sections are shown in **Figure 23b**). Basically, this process divided the sediments into two groups; the basal clays, and everything higher up in the cores. Since the clay intervals have been identified as representing terrestrial environments and everything else as marine, this analysis supports the carbonate-organic hypothesis. It is significant that the carbonate-organic relationship is inverse for all non-clay layers, which includes such different sediment types as peat, carbonates, a mixture of the two and even the event layer from the BB transect. Core GC2 provides a good example (Figure 23c). The top graph displays the scatterplot for the entire core; despite two distinct groupings by sediment types, the overall inverse relationship is very clear, with an R^2 value of 0.888. The bottom two graphs show the scatterplots for each sediment type separately; the s/s/s interval from 121-379 cm on the left is characterized by high carbonate and low organic values, while the peat grouping (cm 1-120), on the right shows lower carbonate and much higher organic values. Yet the carbonate-organics relationships are strongly inverse in both (R^2 values of 0.867 and 0.521). The strong inverse relationship (R^2 of 0.991) displayed in Figure 8:23 b is from BB3, a core consisting entirely from beach sand. Thus we have three separate sedimentary facies, peat, carbonates, and sand, all showing inverse relationships between carbonate and organic values, while all the basal clay relationships are direct. Perhaps significantly, the non-clay intervals that show the weakest inverse relationships are cores BB1 and DC1, the two cores that do not contain any carbonate layers, and presumably experienced the weakest marine influence.

8.8 Conclusions

1. Cores extracted from six mangrove cays suggest that reliable long term proxy hurricane strike records do not exist in the sediments forming the mangrove cays in Turneffe Atoll,



8.23 Organic-carbonate relationship. LOI organic and carbonate values are generally direct for (a) the basal clays, and inverse for (b) all sediments higher in the core, regardless of composition, as evidenced by (c) two distinct groupings of the peat and carbonate (shells/silt/sand) intervals in core GC2.

Belize. The general paucity and transitory nature of mobile sand resulting from the atoll's deep water location severely limit the ability of hurricane derived storm surges to generate overwash lobes. Several historic storms have left no discernible sedimentary signal.

2. Hurricane Hattie (1961), a well documented category 5 hurricane deposited an easily recognizable sand layer at a single coring site. This sedimentologically distinct layer was encountered from 100-130 m inland, thinning from 7 to 1 cm over the distance. The presence of this layer is attributed to the fortuitous presence of a sand cay to the windward during the passage of Hattie.

3. Palynological and sedimentary evidence indicate that the Turneffe Atoll mangrove cays share a common ecological history, with basal clay, probably representing a species poor terrestrial environment being replaced by a *Rhizophora mangle* forest shortly after flooding resulting from post glacial sea level rise. This was dated to ~ 6500 BP at the HJ site.

4. At two sites the peat deposition, presumably representing *Rhizophora mangle* forest continues through the present, having maintained a roughly static elevation relative to sea level over the mid to late Holocene.

5. In four sites the continuous peat deposition is interrupted by thick carbonate intervals, which possibly lasted several thousands of years. The carbonate intervals have very low pollen concentrations, dominated by Chenopodiaceae, and generally lack *Rhizophora* pollen. The ecosystem represented by the pollen assemblage does not seem to match current conditions, while the sedimentary conditions probably represent subaqueous deposition below the maximum depth at which mangrove can survive.

6. The origin of these intervals has not been resolved, but they probably result from event-driven increases in relative sea level. Candidate events include hurricanes, tsunamis, random

island slumping, and seismic activities. Hurricanes probably lack the necessary geomorphologic power or spatial coverage to have been responsible. Not only are appropriate tsunami missing in the regional record, geologic factors, principally the atoll's vertical eastern and intact rim, probably reduce tsunami energy below the requisite levels, although a local event, approaching from the west cannot be eliminated. Individual island slumping would produce neither the required result, nor necessarily explain the apparent temporal coincident of events. Seismic activity, accentuated by associated island slumping, produced by a movement of all or parts of the carbonate platform itself has the best chance of reasonably explaining the phenomena.

7. If seismic activity is the responsible agent, there is a need for risk assessment, as sedimentological evidence suggests at least two incidents.

8. Low quantities of mixed forest taxa are present throughout the core. Although regional transport can plausibly explain the presence of the more buoyant taxa, the possibility exists that forest species not currently present on the atoll were formerly present, perhaps introduced anthropogenically.

9. These cores exhibit systematic variation between LOI determined carbonate and organic values. The relationship is positive (direct) for all basal clays and inverse for all other material, including peat, carbonate, sand layers, and mixed material. The relationship type possibly correlates with strength of terrestrial vs. marine influence during deposition.

8.9 References

Beven, J., 2001. Tropical Cyclone report Hurricane Keith 28 September – 6 October 2000. http://www.nhc.noaa.gov/2000keith_text.html.

Bellingham, P. J., Tanner, E.V.J., and Healey, J. R., 1995. Damage and responsiveness of Jamaican montane tree species after disturbance by a hurricane. *Ecology* 76, 2562-2580.

- Bianchette, T. A., Liu, K.-b., Lam, N. S.-n., and Kiage, L. M., 2009. Ecological effects of Hurricane Ivan on the Gulf Coast of Alabama: a remote sensing study. *Journal of Coastal Research* SI 56, 1622-1626.
- Boose, E., Foster, D. R., and Fluet, M., 1994. Hurricane impacts to tropical and temperate forest landscapes. *Ecological Monographs* 64, 369-400.
- Boose, E., 2003. Hurricane impacts in New England and Puerto Rico. In Greenland, D., Goodin, D., and Smith, R. C., (eds), *Climate Variability and Ecosystem Response to Long-term Ecological Research Sites*. Oxford University Press, Oxford, 25-41.
- Brokaw, N.V. L., and Walker, L. R., 1991. Summary of effects of Caribbean hurricanes on vegetation. *Biotropica* 23, 442-447.
- Cahoon, D. R., Reed, D. J., Day, J. W., Steyer, G. D., Boumans, R. M., Lynch, J. C., McNally, D., and Latif, N., 1995. The influence of Hurricane Andrew on sediment distribution in Louisiana coastal marshes. In Stone, G. W., and Finkl, C. W., (eds), *The Impact of Hurricane Andrew on the Coastal Zones of Florida and Louisiana: 22-26 August 1992*. *Journal of Coastal Research* SI 21, 280-294.
- Cahoon, D. R., Hensel, P., Rybczyk, J., McKee, K. L., Proffitt, C. E., and Perez, B. C., 2003. Mass tree mortality leads to mangrove peat collapse at Bay Islands, Honduras after Hurricane Mitch. *Journal of Ecology* 91, 1093-110.
- Chabreck, R. H., and Palmisano, A. W., 1973. The effects of Hurricane Camille on the marshes of the Mississippi River delta. *Ecology* 54, 118-1123.
- Craighead, F. C., and Gilbert, V. C. 1962. The effects of Hurricane Donna on the vegetation of southern Florida. *Quarterly Journal of the Florida Academy of Sciences* 25, 1-28.
- Dawes, C. J., Bell, S. S., Davis, R. A., McCoy, E. D., Mushinsky, H. R., and Simon, J. L., 1995. Initial effects of Hurricane Andrew on the shoreline habitats of southwestern Florida. In Stone, G. W., and Finkl, C. W., (eds), *The Impact of Hurricane Andrew on the Coastal Zones of Florida and Louisiana: 22-26 August 1992*. *Journal of Coastal Research* SI 21, 103-110.
- Dill, R. F., 1977. The blue holes: geologically significant submerged sinkholes and caves off British Honduras and Andros, Bahamas Island. In Taylor, D. L., (ed), *Proceedings of the Third International Coral Reef Symposium, Miami*. 2, 237-242.
- Dingler, J. R., and Reiss, T. E., 1995. Beach erosion on Trinity Island, Louisiana caused by Hurricane Andrew. In Stone, G. W., and Finkl, C. W., (eds), *The Impact of Hurricane Andrew on the Coastal Zones of Florida and Louisiana: 22-26 August 1992*. *Journal of Coastal Research* SI 21, 254-264.
- Ellison, J. C., 1993. Mangrove retreat with rising sea-level, Bermuda. *Estuarine, Coastal and Shelf Science* 37, 75-87.

Faegri, K. and Iversen, J. 1989. Textbook of Pollen Analysis. John Wiley and Sons, Chichester, UK.

Feller, I. K., 1995. Effects of nutrient enrichment on growth and herbivory of dwarf red mangroves (*Rhizophora mangle*). *Ecological Monographs*, 65, 477-505

Frangi, J. L., and Lugo, A. E., 1991. Hurricane damage to a flood plain forest in the Luquillo Mountains of Puerto Rico. *Biotropica* 23, 324-335.

Garcia, E. and Holtermann, K., 1998. Calabash Caye, Turneffe Islands Atoll, Belize.

CARICOMP-Caribbean coral reef, seagrass and mangrove sites. Coastal region and small island papers 3, UNESCO, Paris.

Gayes, P. T., 1991. Post-hurricane Hugo nearshore side scan sonar survey: Myrtle to Folly Beach, South Carolina. *Journal of Coastal Research* 8, 95-111.

Gischler, E., 1994. Sedimentation on three Caribbean atolls: Glovers Reef, Lighthouse Reef and Turneffe Islands, Belize. *Facies* 31, 243-254.

Gischler, E., 2003. Holocene development in the isolated carbonate platforms off Belize. *Sedimentary Geology* 159, 113-132.

Gischler, E., and Hudson, J. H., 1998. Holocene development of three isolated carbonate platforms, Belize, Central America. *Marine Geology* 144, 333-347.

Gischler, E., and Hudson, J. H., 2004. Holocene development of the Belize Barrier Reef. *Sedimentary Geology* 164, 223-236.

Gischler, E., and Lomando, A. J., 2000. Isolated carbonate platforms of Belize, Central America: sedimentary facies, late Quaternary history and controlling factors. In Insalco, E., Skelton, P. W., and Palmer, T.J., (eds), *Carbonate Platform Systems: Components and Interactions*. Geological Society, London. Special Publications, 178, 135-146. The Geological Society of London, London

Gischler, E., Shinn, E. A., Oschmann, W., Fiebig, J., and Buster, N., 2008. A 1500-year Holocene Caribbean climate archive from the Blue Hole, Lighthouse Reef, Belize. *Journal of Coastal Research* 24, 1495-1505.

Gresham, C. A., Williams, T. M., and Lipscomb, D. J. 1991 Hurricane Hugo wind damage to southeastern U.S. coastal forest tree species. *Biotropica* 23, 420-426.

Goodbred, S. L., and Hine, A. C., 1995. Coastal storm deposition: salt-marsh response to a severe extratropical storm, March 1993, west-central Florida. *Geology* 23, 679-682.

Guiney, J. L. and Lawrence, M. B., 1999. Preliminary Report Hurricane Mitch 22 October-05 November 1998. <http://www.nhc.noaa.gov/1998mitch.html>. Accessed May 30, 2009.

Halley, R. B., Shinn, E. A., Hudson, J. H., and Lidz, B., 1977. Recent and relict topography of Boo Bee Patch reef, Belize. In Taylor, D. L., (ed), Proceedings of the Third International Coral Reef Symposium, Miami. 2, 29-35.

Haug, G. H., Hughen, K. A., Sigman, D. M., Peterson, L. C., and Rohl, U., 2001. Southward migration of the Intertropical Convergence Zone through the Holocene. *Science* 292, 1304-1314.

Hensel, P. and Proffitt, C.E., 2002. Hurricane Mitch: acute impacts on mangrove forest structure and an evaluation of recovery trajectories: executive summary: USGS Open File Report 03-182, 25 p.

Islebe, G. A., Hooghiemstra, H., Brenner, M., Curtis, J. H., and Hodell, D. A., 1996. A Holocene vegetation history from lowland Guatemala. *The Holocene* 6, 265-271.

Islebe, G. A., and Sanchez, O., 2002. History of Late Holocene vegetation at Quintana Roo, Caribbean coast of Mexico. *Plant Ecology* 160, 187-192.

Jackson, L. L., Foote, A. L., and Balistrieri, L. S., 1995. Hydrological, geomorphological, and chemical effects of Hurricane Andrew on coastal marshes. In Stone, G. W., and Finkl, C. W., (eds), *The Impact of Hurricane Andrew on the Coastal Zones of Florida and Louisiana: 22-26 August 1992*. *Journal of Coastal Research* SI 21, 306-323.

James, N.P., and Ginsburg, R.N., 1979. The seaward margin of Belize barrier and atoll reefs. *International Association of Sedimentologists, Special Publication No. 3*.

Jones, A. T., and Dill, R. F., 2002. Great Blue Hole of Lighthouse Reef Atoll, Belize, Central America: deep technical diving to collect sea-level records. In Jackson, T. A., (ed), *Caribbean Geology: Into the Third Millennium*. Fifteenth Caribbean Geological Conference. University of the West Indies Press, Kingston, Jamaica. 181-193.

Kang, W.-j., and Trefry, J. H., 2003. Retrospective analysis of the impacts of major hurricanes on sediments in the lower Everglades and Florida Bay. *Environmental Geology* 44, 771-780.

Keen, T. R., and Stone, G. W., 2000. Anomalous response of beaches to hurricane waves in a low energy environment, northeast Gulf of Mexico, U. S. A. *Journal of Coastal Research* 16, 1100-1110.

Kench, P. S., McLean, R. F., Brander, R. W., Nichol, S. L., Smithers, S. G., Ford, M. R., Parnell, K. E., and Aslam, M., 2006. Geological effects of tsunami on mid-ocean atoll islands: the Maldives before and after the Sumatran tsunami. *Geology* 34, 177-180.

Kench, P. S., Nichol, S. L., Smithers, S.G., McLean, R. F., and Brander, R. W., 2008. Tsunami as agents of geomorphic change in mid-ocean reef islands. *Geomorphology* 95, 361-383.

Leyden, B. W., 2002. Pollen evidence for climatic variability and cultural disturbance in the Maya lowlands. *Ancient Mesoamerica* 13, 85-101.

Littler, M. M., Littler, D. S., Macintyre, I. G., Brooks, B.L., Taylor, P. R., and Lapoint, B. E., 1995. The Tobacco range fracture zone: a unique system of slumped mangrove peat. *Atoll Research Bulletin* 29, 73-91.

Liu, K.-b., Lu, H., and Shen, C., 2003. Assessing the vulnerability of the Alabama Gulf coast to intense hurricane strikes and forest fires in the light of long-term climatic changes. In Ning, Z. H., Turner, R. E., Doyle, T., and Abdollahi, K., (eds), *Integrated Assessment of the Climate Change Impacts on the Gulf Coast Region*. Gulf Coast Regional Climate Change Council and LSU Graphic Services, Baton Rouge, La., 223-230.

Liu, K.-b., Lu, H., and Shen, C., 2008. A 1200-year proxy record of hurricanes and fires from the Gulf of Mexico coast: testing the hypothesis of hurricane-fire interactions. *Quaternary Research* 69, 29-41.

Lodge, D. J., and McDowell, W. H., 1991. Summary of ecosystem-level effects of Caribbean Hurricanes. *Biotropica* 23, 373-378.

Lomando, A. J., and Ginsburg, R. N., 1996. How important is subsidence in evaluating high frequency cycles in the interior of isolated carbonate platforms? *American Association of Petroleum Geologists Bulletin* 79, 1231-1232 (abstract).

Lugo, A. E., Applefield, M., Pool, D. J., and McDonald, R. B., 1983. The impact of Hurricane David on the forest of Dominica. *Canadian Journal for Forest Research* 13, 201-211.

Macintyre, I. G., Littler, M. M. and Littler, D. S., 1995. Holocene history of Tobacco Range, Belize, Central America. *Atoll Research Bulletin* 430, 1-18.

MacKie, E. W., 1963. Some Maya pottery from Grand Bogue Point, Turneffe Islands, British Honduras. Appendix to Stoddart, 1963. 131-135.

Markgraf, V., 1993. Climatic history of Central and South America since 18,000 yr B.P.: comparison of pollen records and model simulations. In Wright, H. E., Kutzbach, J. E., Webb, T. III, Ruddiman, W.F., Street-Perrott, F. A., and Bartlein, P. J. (eds), *Global Climates since the Last Glacial Maximum*. University of Minnesota Press, Minneapolis, 357-385.

McCloskey, T. A., 2006. Paleo hurricanes on the Coast of Belize. Annual Meeting, Association of American Geographers, Chicago.

McKee, K. L., 1995. Mangrove species distribution patterns in a Belizean mangrove forest: an exception to the dominance-predation hypothesis. *Biotropica*, 27, 334-345.

McKee, K. L., and Faulkner, P. L., 2000. Mangrove peat analysis and reconstruction of vegetation history at the Pelican cays, Belize. *Atoll Research Bulletin* 468, 45-58.

- Mendelssohn, I. A., and McKee, K. L., 2000. Saltmarshes and mangroves. In Barbour, M. G., and Billings, W. D., (eds), North American Vegetation. Cambridge University Press, New York.
- Meerman, J. C. 2001. A first Assessment of damage to terrestrial ecosystems in Southern Belize as caused by Hurricane Iris of October 8, 2001. Report prepared for the Belize Forest Department. Belmopan, Belize.
- Meerman, J. C., 2006. Mangrove and conservation value assessment at northern Turneffe. Report to the Belize Forest Department of the Ministry of Natural Resources. Belmopan, Belize.
- Minty, C. D., Murray, M. R., and Zisman, S. A., 1995. Turneffe terrestrial resource reconnaissance report to Coral Caye Conservation Ltd. Marine Research Centre, University College of Belize, Technical Report Series No. 2.
- Murray, M. R., Zisman, S. A., Furley, P. A., Munro, D. M., Gibson, J., Ratter, J., Bridgewater, S., Minty, C. D., and Place, C. J., 2003. The mangroves of Belize: Part 1: distribution, composition and classification. *Forest Ecology and Management*. 174, 265-279.
- Pat, W., 2001. Case study: tourism and biodiversity (ecotourism- a sustainable development tool, a case for Belize. Ministry of Tourism and Youth, Government Printers, Belmopan, Belize.
- Platt, S. G., Rainwater, T. R., and Nichols, S., 2004. A recent population assessment of the American Crocodile (*Crocodylus acutus*) in Turneffe Atoll, Belize. *Herpetological Bulletin* 89, 26-32.
- Ramcharan, E. K., 2005. Late Holocene ecological development of the Graeme Hall swamp, Barbados, West Indies. *Caribbean Journal of Science* 41, 147-150.
- Ramcharan, E. K., and McAndrews, J. H., 2006. Holocene development of coastal wetland at Maracas Bay, Trinidad, West Indies. *Journal of Coastal Research* 22, 581-586.
- Reilly, A., 1991. The effects of Hurricane Hugo in three tropical forests in the U.S. Virgin Islands. *Biotropica* 23, 414-419.
- Risi, J. A., Wanless, H. R., Tedesco, L. P., and Gelsanliter, S., 1995. Catastrophic sedimentation from Hurricane Andrew along the southwest Florida coast. In Stone, G. W., and Finkl, C. W., (eds), *The Impact of Hurricane Andrew on the Coastal Zones of Florida and Louisiana*: 22-26 August 1992. *Journal of Coastal Research* SI 21, 83-102
- Scatena, F. N., and Larsen, M.C., 1991. Physical aspects of Hurricane Hugo in Puerto Rico. *Biotropica* 23, 317-323.
- Scoffin, T.P., 1993. The geological effects of hurricanes on coral reefs and the interpretation of storm deposits. *Coral Reefs* 12, 203-221.

- Smith, F. G.W., 1941. Sponge disease in British Honduras, and its transmission by water currents. *Ecology* 22, 415-421.
- Stevely, J. M., and Sweat, D. E., 1994. A preliminary evaluation of the commercial sponge resources of Belize, with reference to the location of the Turneffe Islands Sponge Farm. *Atoll Research Bulletin* 424, 1-14.
- Stein, S., and Okal, E. A., 2005. Global reach of the Sumatran tsunami. *Nature* 434, 581-582.
- Stoddart, D. R., 1962. Three Caribbean atolls: Turneffe Atoll, Lighthouse Reef, and Glovers Reef, British Honduras. *Atoll Research Bulletin*. 87, 1-151.
- Stoddart, D.R. , 1963. Effects of Hurricane Hattie on British Honduras reefs and cays. *Atoll Research Bulletin* 95, 1-120.
- Tanner, E. V. J., Kapos, V., and Healey, J. R., 1991. Hurricane effects on forest ecosystems in the Caribbean *Biotropica* 23, 513-521.
- Tedesco, L. P., Wanless, H. R., Scusa, L. A., Risi, J. A., and Gelsanliter, S., 1995. Impact of Hurricane Andrew on South Florida's sandy coastlines. In Stone, G. W., and Finkl, C. W., (eds), *The Impact of Hurricane Andrew on the Coastal Zones of Florida and Louisiana: 22-26 August 1992*. *Journal of Coastal Research* SI 21, 59-82.
- Titov, V., Rabinovich, A. B., Mofjeld, H. O., Thomson, R. E., and Gonzalez, F. I., 2005. The global reach of the December 26 2004 Sumatra tsunami. *Science* 309, 2045-2048.
- Torrescano, N., and Islebe, G., 2006. Tropical forest and mangrove history from southeastern Mexico: a 5000 yr pollen record and implications for sea level rise. *Vegetation History and Archaeobotany* 15, 191-195.
- Urquhart, G. R., 2009. Paleoecological record of hurricane disturbance and forest regeneration in Nicaragua. *Quaternary International* 195, 88-97. DOI:10.1016/j.quaint.2008.05.012.
- Wahl, D., Byrne, R., Schreiner, T and Hansen, R., 2006. Holocene vegetation change in the northern Petén and its implications for Maya prehistory. *Quaternary Research* 65, 380-389.
- Woodroffe, C. D., 1981. Mangrove swamp stratigraphy and Holocene transgression, Grand Cayman Island, West Indies. *Marine Geology* 41, 271-294.
- Wooller, M. J., Morgan, R., Fowell, S., Behlig, H. and Fogel, M., 2004. Mangrove ecosystem dynamics and elemental cycling at Twin Cays, Belize during the Holocene. *Journal of Quaternary Science* 19, 703-711.
- Wooller, M. J., Behlig, H., Smallwood, B.J., and Fogel, M., 2007. A multiproxy peat record of Holocene mangrove palaeoecology from Twin Cays, Belize. *The Holocene* 17, 1129-1139.

CHAPTER 9 SOUTHERN CARIBBEAN COAST, NICARAGUA

9.1 Geographic Setting

Nicaragua is located in Central America, south of Honduras and north of Costa Rica. The country's Caribbean coast runs almost directly north-south at 83° W, lying between 10.8 - 15.0°N. This is below the main belt of current hurricane activity, making it a likely location to pick up southern movement in hurricane activity.

9.2 Geologic Setting

9.2.1 Chortis Block

Nicaragua is located on the Chortis block, the northernmost block on the continental section of the Caribbean Plate (CAR) (**Figure 2:15**). This block is an exotic terrane, formerly adjacent to the Guerrero block along the southwestern coast of Mexico. Although subject to some disagreement (Lara, 1993), it is generally accepted that during the Mesozoic and Tertiary the block translated eastward and rotated counterclockwise before accreting to what is now Mexico and Guatemala in the Miocene (Mann et al., 2007; Alvarado et al., 2007). The lateral displacement between the Chortis and the Maya block to the north is not clear, with estimates varying from 120-1000 km (Coates, 1997).

The basement of the Chortis block contains Precambrian-Paleozoic rock, the only pre-Mesozoic rock on the CAR (Donnelly et al., 1990) and, along with the Maya block, forms the base of nuclear Central America (Alvarado et al., 2007). The block has been tectonically active almost continuously since the Early Cretaceous, with the Mesozoic magmatism probably related to the Laramide orogeny (Donnelly et al., 1990). The Chortis block contains five separate morphotectonic regions (Weyl, 1980; Donnelly et al., 1990; Coates, 1997; Mann et al., 2007),

the result of various collisions occurring since the Mesozoic, including accretions of oceanic islands, island arcs and an area of magmatic overprinting (James, 2007; Mann et al., 2007). The northern boundary with the Maya plate lies in the Motagua valley of Guatemala, as discussed in **Chapters 2 and 5**; the exact location of the Chortis' southern boundary with the neighboring Chorotega block is not physically obvious, as it is covered by alluvium and late Cenozoic volcanics. However, the division, as first proposed by Dengo (1985), is usually accepted as running from the Santa Elena fault zone on the Pacific to the Hess Escarpment in the Caribbean (Escalante, 1990; Mann et al., 2007) (**Figure 2:15**). This also the point of lowest relief (45m) for a Caribbean-Pacific transect of Central America (Coates, 1997).

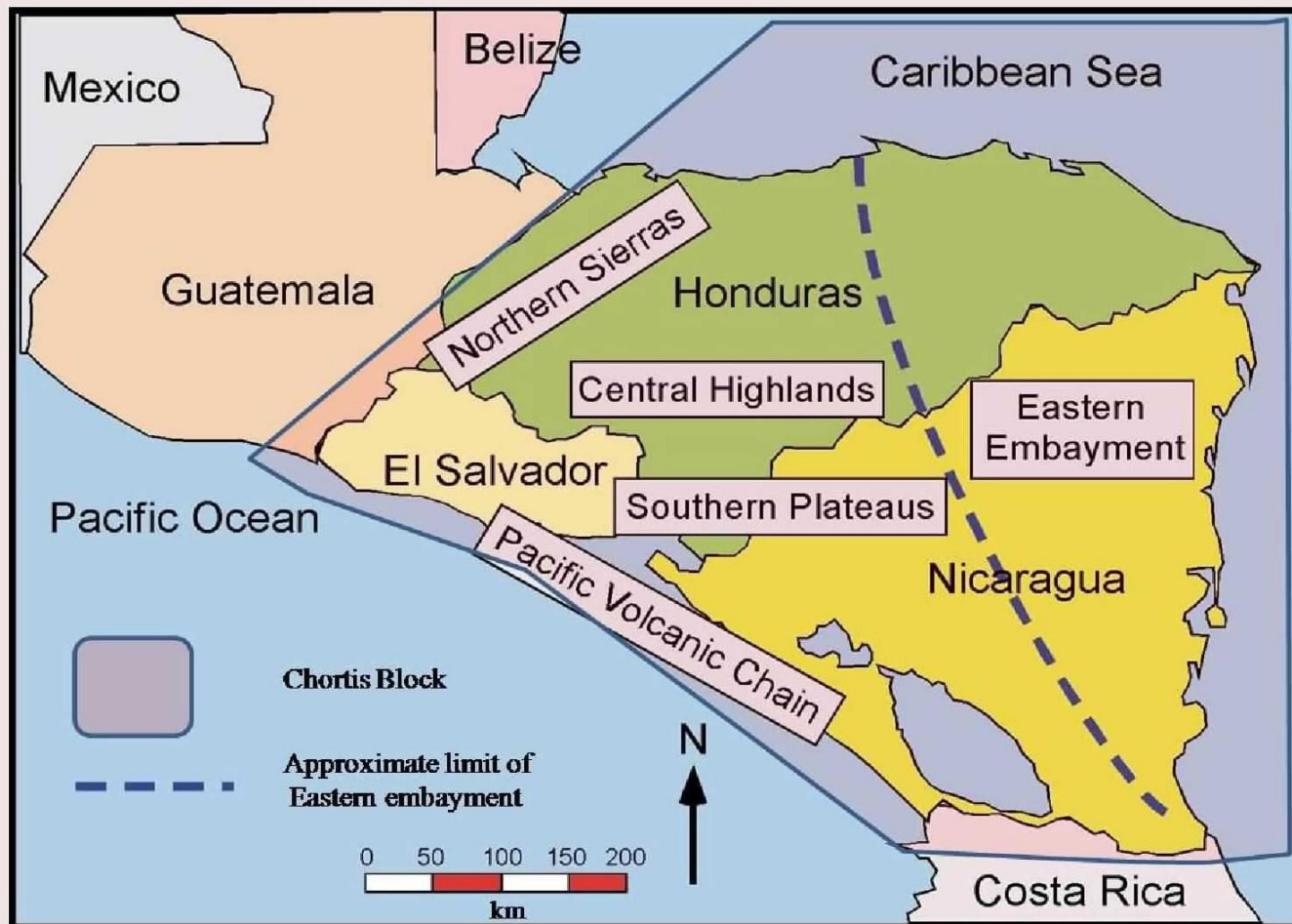
9.2.1.1 Moskito Coast Lowlands

The five morphotectonic regions are (**Figure 9:1**):

1. Northern Sierras
2. Central Highlands
3. Eastern Embayment
4. Southern Plateaus
5. Pacific Volcanic Chain

(Donnelly et al., 1990).

The eastern embayment, also referred to as the Moskito coast lowlands, the Moskito coast, the Mosquito coast or La Mosquitia (Marshall, 2007; Dodds, 2001), is a vast coastal plain covering most of the eastern parts of both Honduras and Nicaragua, which continuing off shore as the Nicaragua Rise (or Mosquito Banks) reaches nearly to Jamaica (Mills and Hugh, 1974), supporting extensive sea grass beds and scattered coral reefs (Wallace, 1997). Along this rise, the largest carbonate platform in the southern Caribbean (Cortes, 2007), the continental shelf



9.1 Geologic setting I. Nicaragua is located on the Chortis block, which consists of five distinct morphotectonic provinces.

extends ~ 250 km offshore, with maximum water depth at the shelf edge of less than 45 m (Mills and Hugh, 1974). During the Holocene sea level rise the surface of this platform has not raised significantly, due to “highstand shedding”, the relatively instantaneous removal of large amounts of carbonates (1300-2000 mm/ky) from the platform tops to the upper slopes (Glaser and Droxler, 1991; Schlager et al., 1994).

This entire eastern embayment has been receiving sediments since the formation of the geosynclinal Mosquitia basin in the Triassic (Mills and Hugh, 1974; Mills et al., 1967; Weyl, 1980). The Pliocene-Pleistocene delta of the Coco River, several dozens of km in extent, is an example of the vast amount of materials that has been eroded from the highlands (Marshall, 2007). Although uplift of the Coco River ridge in the Cretaceous and stream piracy in the headwater area during the Pleistocene has resulted in some locational shifts of the deposition centers, deposition has been continuous (Mills and Hugh, 1974; Rodgers, 1998). Petroleum wells show >2000 m of Mesozoic and 5000 m of Tertiary materials (Mills and Hugh, 1974; Weyl, 1980; Donnelly et al., 1990), mostly shallow marine material mixed with some larger-grained terrestrial clastics resulting from the rapid erosion following uplift of the highlands during the late Tertiary (Mills and Hugh, 1974; Marshall, 2007). The topmost formation is the Quaternary Bragman’s Bluff, again shallow marine and terrestrial sandstone and gravel (Mills and Hugh, 1974). Post Wisconsin sea level rise has driven the deposition shoreward resulting in abundant sediment supply and open beaches along almost the entire coast (Marshall, 2007). Longshore current is generally to the south (Cortes, 2007), resulting in linear sand barriers forming to the south of river mouths (Marshall, 2007).

9.3 Environmental Setting

The Miskito coast lowlands are dominated by wide (up to 150 km), low-gradient alluvial

plains, covered by pine savanna and crossed by large sluggish rivers, while mangrove swamps, wetlands, and barrier beaches fronting extensive tidal lagoons characterize the coast (Parsons, 1955; Wallace, 1997; Christie, 2000; Marshall, 2007). The pines (*Pinus caribaea* var. *hondurensis*), the most equatorward naturally-occurring pines in the western hemisphere, dominate the coastal savannas, finally disappearing just north of Bluefields Bay. The savannas are subjected to frequent fires, with annual occurrence probability estimates ranging from 33-100% (Christie, 2000). Rainfall is heavy, often exceeding 5000 cm/yr (Marshall, 2007), divided into a wet season from June through January and a dry season from February through May. During the dry season, evaporation can exceed precipitation (Brenes et al., 2007).

Population is racially and ethnically mixed, and very low, generally restricted to small coastal villages and isolated communities scattered along the navigable rivers (Christie, 2000; Herlihy, 2001; Dodds, 2001). South of Puerto Cabezas in Nicaragua, villages may be separated by as much as 10 km. Larger towns include Puerto Lempira in Honduras and Puerto Cabezas and Bluefields in Nicaragua. Total population of La Mosquitia is around 40,000, for Honduras (Milligan, 1997), and slightly less than 300,000 for Nicaragua (UNHCR, 2003). In Nicaragua the Caribbean coast is divided into two political divisions, the Region Autonomista Atlantico Norte (RAAN) in the north, and the Region Autonomista Atlantico Sur (RAAS) in the south.

9.4 Study Sites

Our study area was in the central section of RAAS (**Figure 9:2**). Core transects were taken from two locations in Bluefields Bay (BB) and one ~ 65 km to the north near the village of Tasbapauni on the eastern edge of the Laguna de las Perlas (Pearl Lagoon, PL)(**Figure 9:2**). Both BB and PL are large, shallow, turbid, microtidal (22 cm) estuarine lagoons, controlled by large fluvial inputs. Both are connected to the sea by restricted entrances that exhibit standard

two layer flow (outgoing fresh water on top, with denser marine water entering below (Brenes et al., 2007). Salinity and depth are seasonally variable in both systems, with rapid flushing rates. Precipitation is ~4500 mm/yr (INETER, 2000), while mean relative humidity ranges from 86-93% (Christie, 2000). Sedimentation rates are increasing in both areas, attributed to anthropogenic influences (Christie, 2000; Brenes et al., 2007).

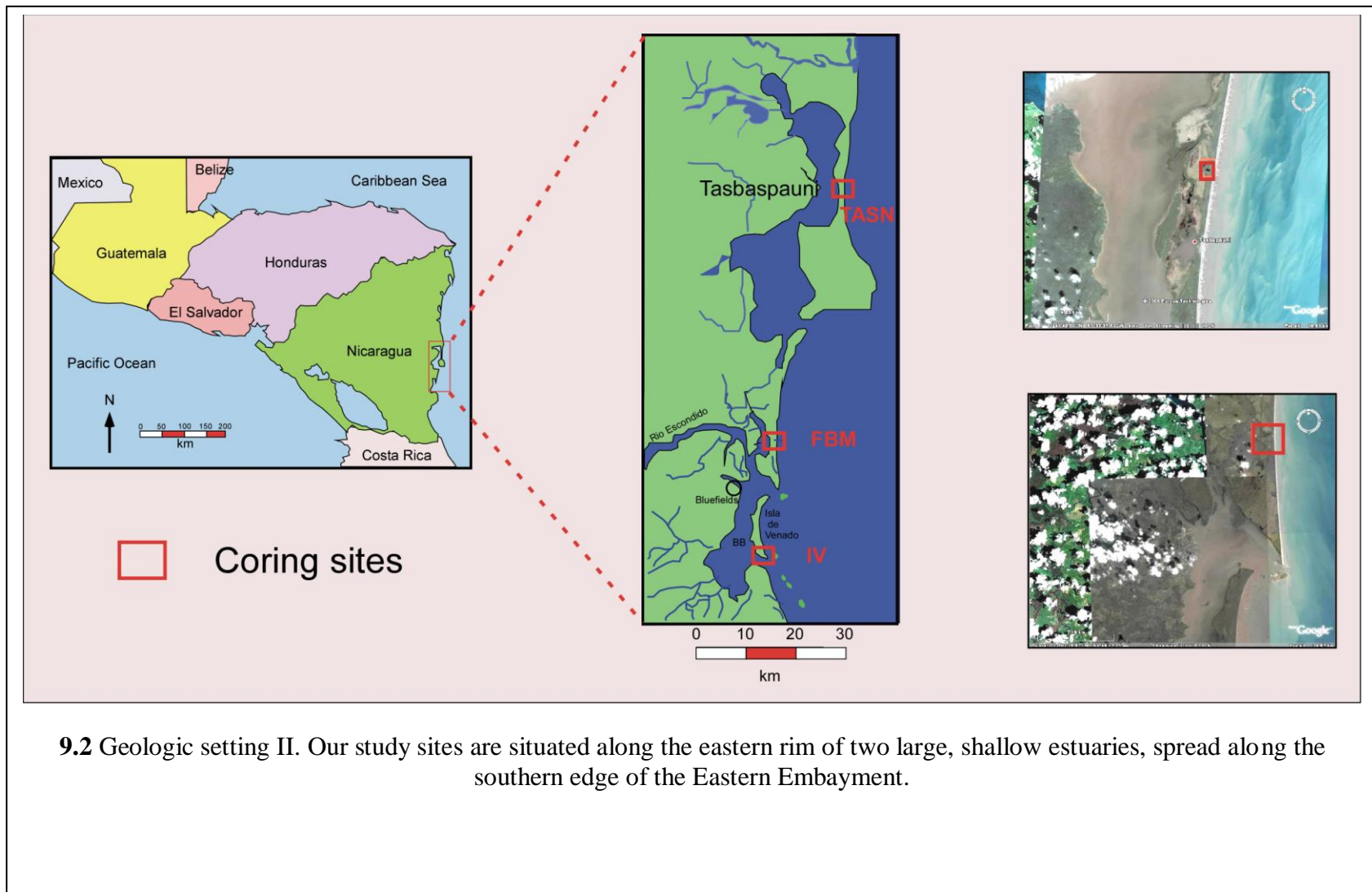
9.4.1 Bluefields Bay

Bluefields Bay has a surface area of ~ 176 km² (CIMAB, 1996), and a mean low water depth of 1 m. Freshwater input is from precipitation and four rivers, the largest of which, the Rio Escondido provides 50-75% of the volume (Brenes et al., 2007). A two year study (2000-2002) showed an unstratified water column with water temperatures varying between 22-29⁰ C, and water transparency from 0.3-1.8 m (Dumailo, 2003). Bay waters are dark due to the large amount of upland erosion, which sedimentation rates show to have been keeping pace with the exploding human population (Dumailo, 2003). Seasonal variation is dramatic, as during the wet season water depth increases, total freshwater influx nearly quadruples, salinity drops from 17.5 ppt to 0.2 ppt, and flushing time is halved from 4 to 2 days (Brenes et al., 2007).

Unlike the majority of the Mosquito lowlands, there is significant topographical relief around BB, with the town of Bluefields sitting on a large hill. The uneven topography continues into BB, which is studded with small red clay (presumably Pleistocene) islands rising a few meters above sea level (**Figure 9:3a**). In general, BB appears to be a drowned river valley, with recent sea level rise having flooded a rather uneven antecedent landscape.

9.4.1.1 Isla del Venado (IV Transect)

The eastern edge of Bluefields Bay is blocked by Isla del Venado, a large forested island. Isla del Venado is ~ 15 km long and generally between 1-2 km wide, big and high



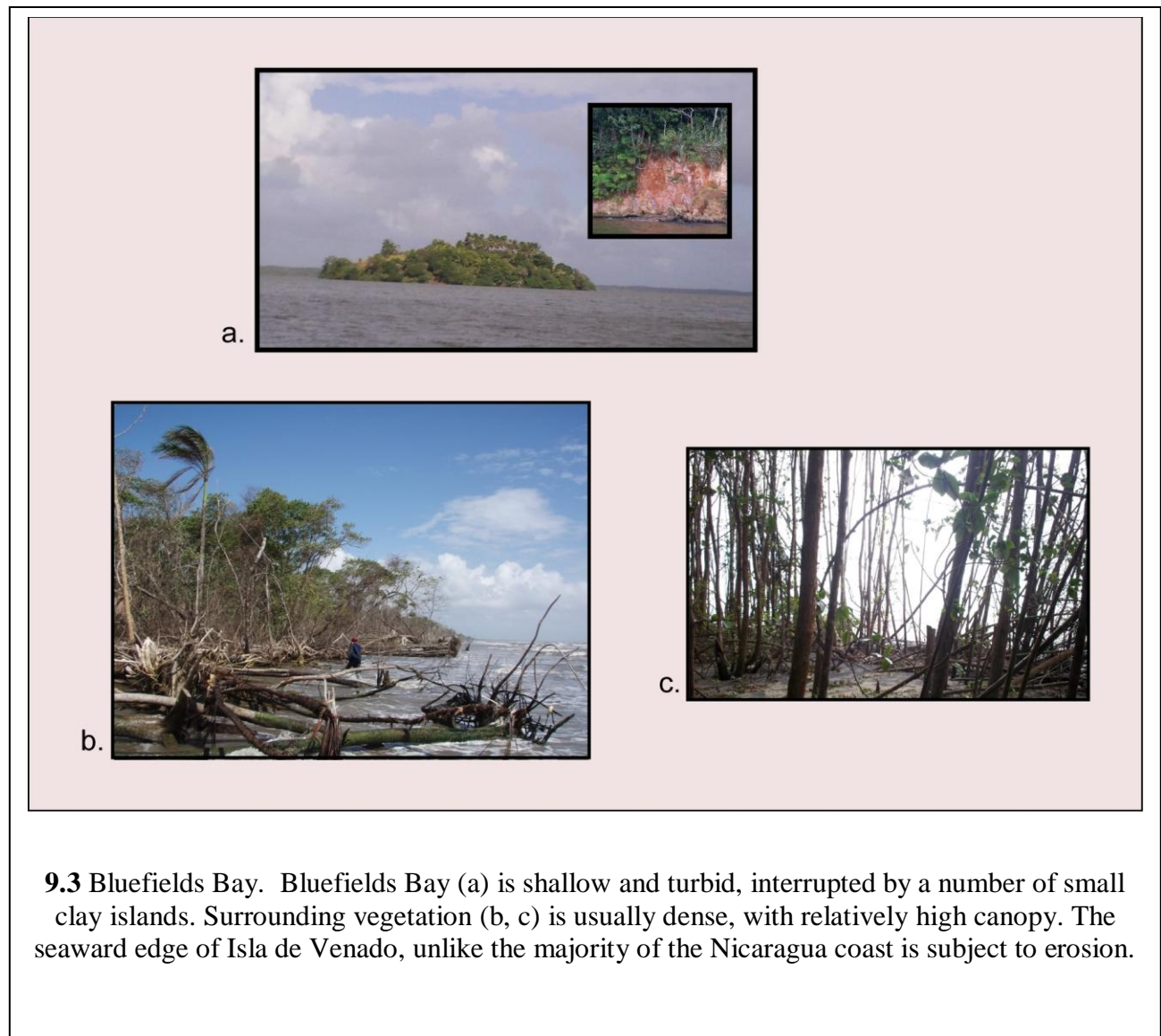
enough that it is used for farming. The position of this island shelters Bluefields Bay from the usual north east trade winds; wave energy drops dramatically from the wild eastern side to the low energy BB. Mangroves dominate the shore areas, with hardwood evergreen forest occurring on the higher elevations. The island appears to be another topographical high in this drowned estuary, composed of the same red clay as the other protruding islands. BB's only connections with the sea are at the north and south ends of this island, where the entrances, with depths ~3-4 m, are the deepest parts of the bay (Brenes et al., 2007). Unlike most areas along the Caribbean coast of Nicaragua, the eastern edge of IV shows severe coastal erosion (**Figure 9:3b**), with no beach and a continuous band of uprooted trees laying in the water, pointing toward the shore, which is covered by a line of dead and dying trees. Presumably this results from the disruption of the longshore transport by the open water gap between the mainland and the northern edge of IV.

A transect of five short cores was obtained from the southeastern edge of this island in a tall (>10 m) black mangrove (*Avicennia germinans*) forest.

9.4.1.2 Falso Bluff Marsh (FBM Transect)

Although the boundaries of the southern section of Bluefields Bay are fairly distinct, the northern end dissolves into a maze of river channels, creeks, wetlands, and second and third order bays (**Figure 9:2**). The Rio Escondido, the major source of fluvial input, has developed a delta within the northern end of the bay, where it discharges through a number of confused distributaries. Smokey Lane Lagoon (Laguna Linea Ahumada) is situated in the farthest northeast corner of this system, receiving Rio Escondido water through a number of distributaries including Guana Creek, Gilbert Creek, Top Creek, Deer Creek, and Found Out Lagoon (Laguna el Encuentro).

.



A forested barrier of varying width separates Smokey Lane Lagoon from the sea. The bay side of this barrier is covered by a thick growth of tall red mangroves (*Rhizophora mangle*), with hardwood forest occurring on the higher elevations. Falso Bluff Creek, 2-3 meters wide and a few cm deep, crosses this barrier at its narrowest point. Near the Caribbean side the red mangroves change to a dense stand of *Raphia* palms (*Raphia taedigera*). The east-west barrier thickness at the FBM transect is 730 m.

The barrier's eastern edge is a sandy beach with a low berm, ~ 1 m, behind which is a flat, grassy area with coconut trees (**Figure 9: 4b**). Approximately 70 m inland from the sea, elevation drops and a line of thick, dense low-stature bush ~ 8 m wide is encountered, behind which is an extensive cattail (*Typha*) marsh (**Figure 9: 4c**). We extracted a transect of four cores from this marsh.

9.4.2 Laguna de las Perlas

The southern end of the irregularly shaped PL is located ~ 35 km north of the town of Bluefields. Maximum north-south dimension of the lagoon is ~60 km, with a maximum east-west distance ~ 15 km. Surface area is 571 km² (Roullot, 1980), mean low water depth is 2.5 m (Brenes et al., 2007). Of the four rivers discharging into PL, the Rio Grande de Matagalpa provides 60-90% of the fluvial input (Brenes et al., 2007). This discharge is through a navigation channel dug in the 1960s connecting PL with the Matagalpa. However, the main channel of the Rio Grande de Matagalpa (~0.5 km wide) empties into the Caribbean a few km to the north (**Figure 9:2**). During wet season water depth increases, freshwater input more than doubles, and salinity drops from 18 ppt to 1.0 ppt, while flushing time reduces slightly (from 17 to 14 days) (Brenes et al., 2007). Water temperature and transparency ranges are similar to BB; dissolved oxygen levels are 3-8 mg/l (Christie, 2000; Molina, 2001). The only connection with

the sea is Bar Mouth, a small (200m wide, 5m deep) opening at the southeast end (Christie, 2000). Lagoon substrate is mostly mud and sand with a few rocks and oyster reefs. Sea grass beds, mainly *Rupia* and *Halodule* occur (Christie, 2000). Extensive flooding of the surrounding countryside occurs during heavy rains.

Twelve multi ethnic (Mestizo, Creole, Miskito, Garifuna) communities with a total 1995 population of >6000 are situated on the edges of PL (Christie, 2000).

9.4.2.1 Tasbapauni (TASN Transect)

Like BB, PL is separated from the Caribbean by a long forested barrier of varying width, the Caribal Peninsula, which consists of a sandstone base covered by more recent materials (Radley, 1960; Christie, 2000). The dumbbell shape, presence of linear shore-parallel topographic features, the abundant sediment supply, and general current direction all suggest that the unconsolidated materials forming the top of this barrier result from southern longshore drift of the sediments discharged from the mouth of the large Rio Grande de Matagalpa, located <15 km north of the northern end of PL. The village of Tasbapauni sits on the narrowest section (~400 m) of this barrier stretching from the Caribbean on the east to a small shallow extension of the of PL on the west (**Figure 9:2**). As can be seen from the GoogleEarth imagery in **Figure 9:2**, the sediments in Pearl Lagoon, including the small subbay reaching to Tasbapauni, are mainly darker fine grained mud, while along the Caribbean shore the sediments are mainly lighter colored sand. A transect of seven cores was extracted from a hardwood swamp ~ 3km north of the village.

9.5 Sea Level

No Holocene sea level curve based specifically on Nicaraguan data seems to exist. Reconstruction of sea level history for the study sites therefore relies on the more general



b.



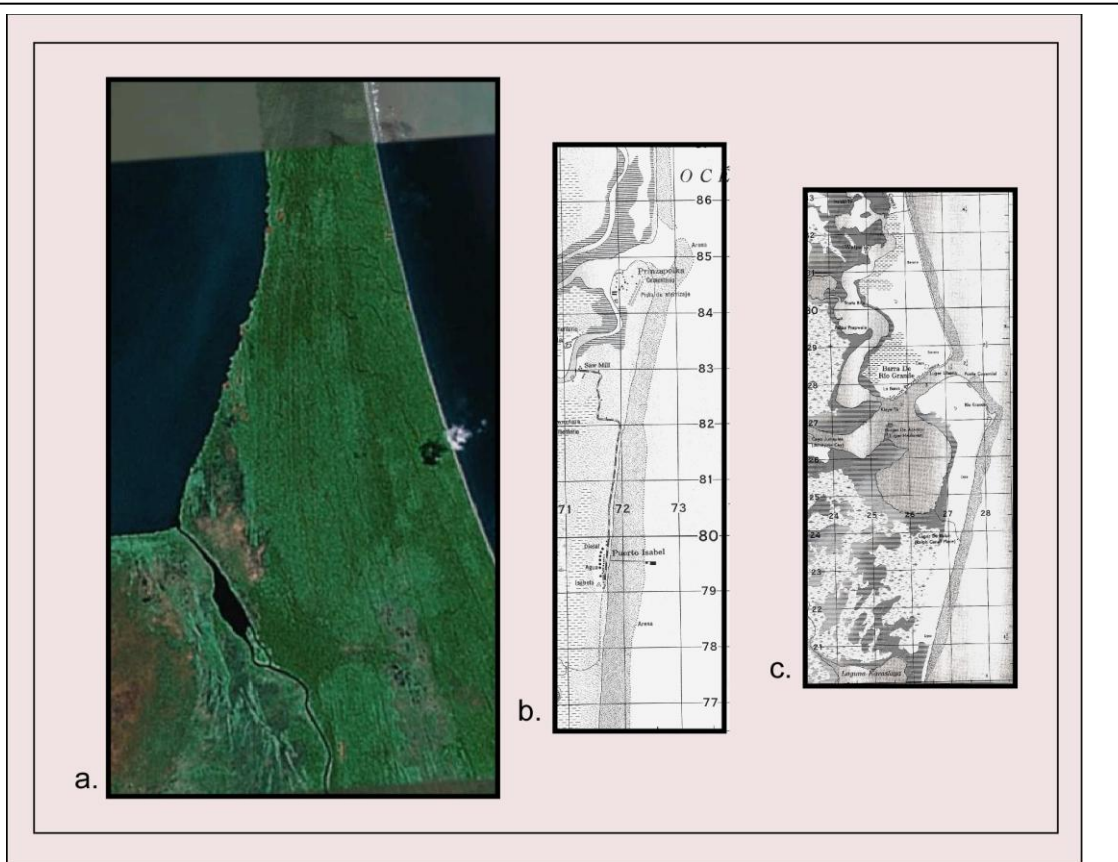
c.



9.4 Falso Bluff coring site; (a) beach, (b) open beach ridge, (c) *typha* marsh in a depression, circled in red.

western Atlantic curves (Toscano and Macintyre, 2003; Gischler and Hudson, 2004). Because the Caribbean coast of Nicaragua is geographically simple; basically a straight north-south line unconfused by extensive reefs, complex bathymetry or intricate coastal geomorphology, the local curve should parallel regional eustatic rise lacking significant geologic complications. The geologic stability resulting from millions of years of near perfect horizontal marine sedimentation, as shown by seismic profiles (Mills and Barton, 1996) argue against dramatic vertical surface movement, although a slow subsidence is probable. Tectonically, James (2007) describes the subunit of the Chortis block which contains the Mosquito coast lowlands as “stable”, with no major faults in the southern section.

Of probably greater importance is the vast amount of material eroded from the central highlands. As sea level has risen, the deposition of this material has transgressed across the shelf; currently these sediments are being deposited both as river mouth deltas (Marshall, 2007) and all along the coast. The presence of this material as a wide band of sand southward of all major rivers is immediately obvious in both satellite imagery and on maps (**Figure 9:5**). Unlike many areas where rising sea level has resulted in coastal erosion and a tangle of fallen trees, a strand of unvegetated sand along almost the entire coast, makes the Nicaragua’s Caribbean beach easily transversable on foot. Given the microtidal nature of the coast, this feature suggests a constant deposition of fresh sediments. The positioning of villages, commonly found on sand barriers in front of lagoons, and the clear linear beach features (**Figure 9:5a**) also suggest that these barriers are not disappearing under rising sea levels. It is possible that rising sea level has primarily pushed the nearshore sediments upward and landward, incrementally raising the beaches/barriers. The rate of shoreline retrogression/progradation would depend on local conditions. Under such a scenario, the distance from each coring site to the sea has probably



9.5 Coastal sediment supply. Vast amounts of sediments are eroded off of the central highlands of Nicaragua and transported to the Caribbean coast, resulting in a tremendous sediment supply available for coastal deposition, as is clear from (a) the large linear beach ridges, and (b, c) the wide sand deposits (stippled areas) issuing from the mouths of nearly all river along the coast.

reduced slightly for the period being investigated, while barrier height and wave energy required to deposit marine material in the back bay environment has probably remained relatively constant.

9.6 Hurricane History

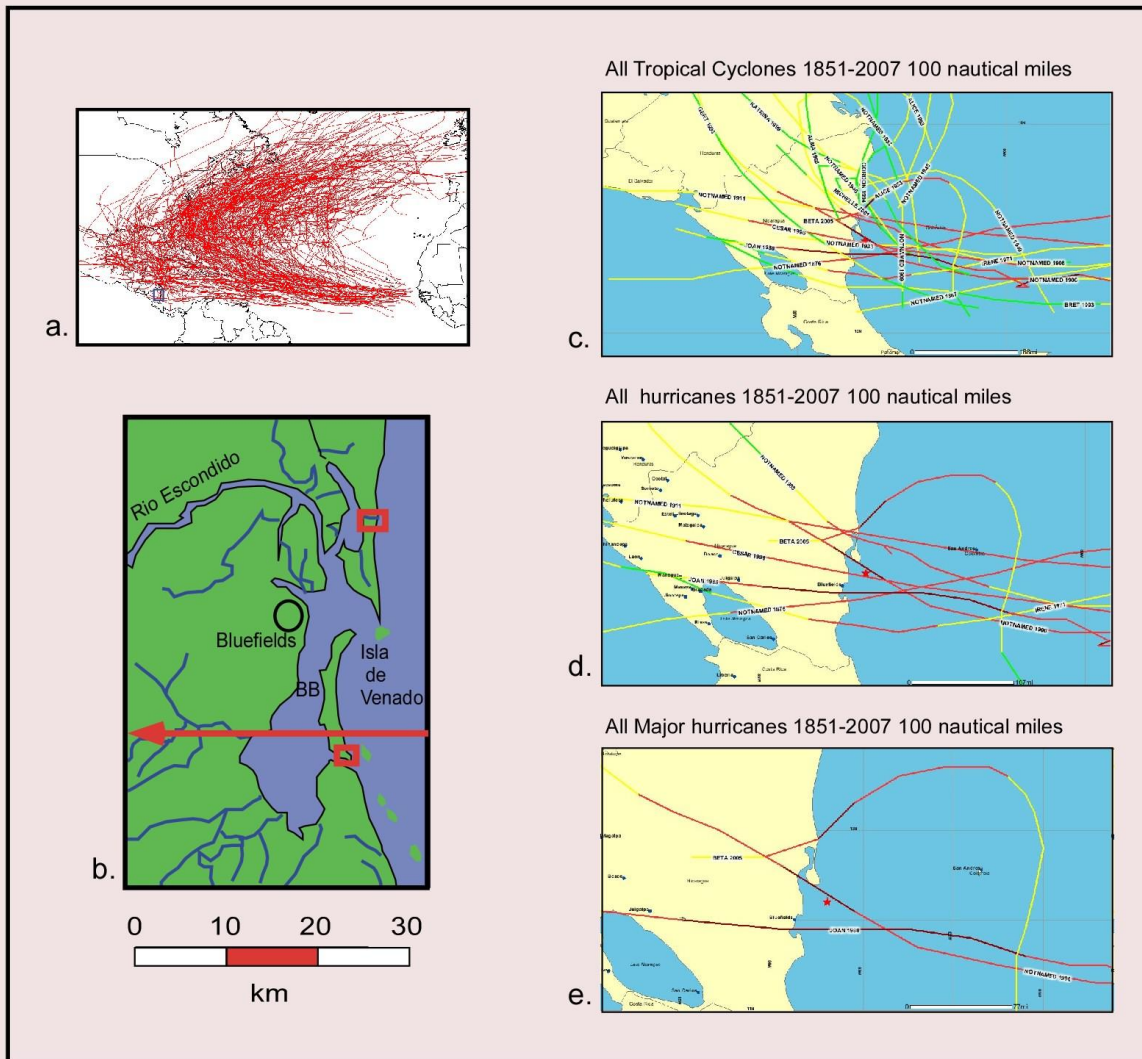
Laying between 11.9-12.7° N our study sites are on the far southern fringe of the historic hurricane belt, with hurricanes occurring much less frequently than elsewhere in the Caribbean, Gulf of Mexico, and the Atlantic coast of the United States (**Figure 9:6a**). For the 157 year period between 1851 and 2007, NOAA records show only 13 tropical storms, and nine hurricanes passing within 100 nautical miles of the front of BB. Only three of the hurricanes were major (category 3 or above) (**Table 9:1**). Although the increased frequency of recent tropical storms/depressions is probably due to improved instrumentation, the number of landfalling hurricanes, especially major hurricanes, is probably not severely underestimated for the early part of the record. The lack of recorded hurricanes for the 60 year period 1911-1971 is probably accurate, as several earlier events, including tropical storms, are recorded.

9.6.1 Hurricane Joan

Hurricane Joan impacted BB on October 22, 1988, passing over the southern edge of Isla de Venado and crossing the mainland coast near the mouth of the Kukra River in the south part of the bay (**Figure 9:6b**). Due to rapid intensification just prior to landfall, Joan hit as a category four storm with maximum sustained wind speeds of 125 knots (231 km/h) and a central pressure of 932 mb (Lawrence and Gross, 1989). Joan devastated not only the town of Bluefields, but much of Nicaragua, killing 148 people and inflicting ~\$1 billion (1988 dollars), out of a regional total of 216 deaths and \$2 billion in damages (Lawrence and Gross, 1989). After entering the Pacific, Joan was renamed Tropical Storm Miriam, persisting until November 3

9.1 List of tropical cyclones passing within 100 nautical miles of the front of Bluefields Bay since 1851.

Storm Classification	Name	Year	Maximum Wind Speed (knots)	Central Pressure (mb)	Category
Tropical Storm Depression (13)					
	Not Named	1887	40	Unknown	TS
	Not Named	1909	40	Unknown	TS
	Not Named	1933 (A)	35	Unknown	TS
	Not Named	1933(B)	35	Unknown	TS
	Not Named	1940(A)	40	Unknown	TS
	Not Named	1940(B)	35	Unknown	TS
	Not Named	1945	35	Unknown	TS
	Alice	1953	40	Unknown	TS
	Alma	1966	25	Unknown	TD
	Bret	1993	40	1001	TS
	Gordon	1994	30	1007	TD
	Katrina	1999	35	999	TS
	Michelle	2001	30	1004	TD
Minor Hurricanes (6)					
H1	Not Named	1855	70	Unknown	
H2	Not Named	1876	90	Unknown	
H2	Not Named	1908	90	Unknown	
H2	Not Named	1911	85	Unknown	
H1	Irene	1971	70	989	
H1	Cesar	1996	70	990	
Major Hurricanes (3)					
H3	Not Named	1906	105	Unknown	
H4	Joan	1988	125	932	
H3	Beta	2005	100	962	



9.6 Hurricane history for the Caribbean coast of Nicaragua. A display (a) of all NA TCs from 1947-2008 from the NOAA HURDAT (“best track”) data shows that the Nicaraguan coast lies to the south of the main area of hurricane activity. A display of (c) all TCs, (d) hurricanes, and (e) major hurricanes passing within a 100 nautical miles of 12°N, 83.5°W (front of Bluefields Bay). (b) Hurricane Joan, a category 4 storm passed directly over Bluefields Bay in 1988.

(http://www.nhc.noaa.gov/archive/storm_wallets/atlantic/atl1988-prelim/joan/prelim02.gif).

Joan caused “severe” damage to over 500,000 ha of tropical forest (Boucher, 1990; Boucher et al., 1990; Vandermeer et al., 2000). Much of the damaged area burned the following dry season (Christie, 2000; Urquhart, 2009).

9.6.2 Hurricane Beta

Hurricane Beta made landfall near the mouth of the Rio Grande de Matagalpa as a category two storm with 90 knots maximum wind speed on October 30, 2005. The location of landfall was just to the north of the Tasbapauni coring site (Beven, 2006; Pasch and Roberts, 2006). Widespread forest damage was reported (ACT, 2005)

9.7 Methods

Methods followed are those described in **Chapter 2.4**.

9.8 FBM Transect

9.8.1 Results

Five cores were obtained along a transect from the location described above. A single short core was extracted at 70 m inland from a narrow band of short trees and shrubs. Four longer cores were extracted from a *typha* marsh at 100, 120, 132, and 156 m inland from the sea. A modified Livingstone piston corer was used to extract the cores at 132 and 156 m; a peat borer was employed at the other three spots. All cores were mostly peat and clay with occasional sand layers.

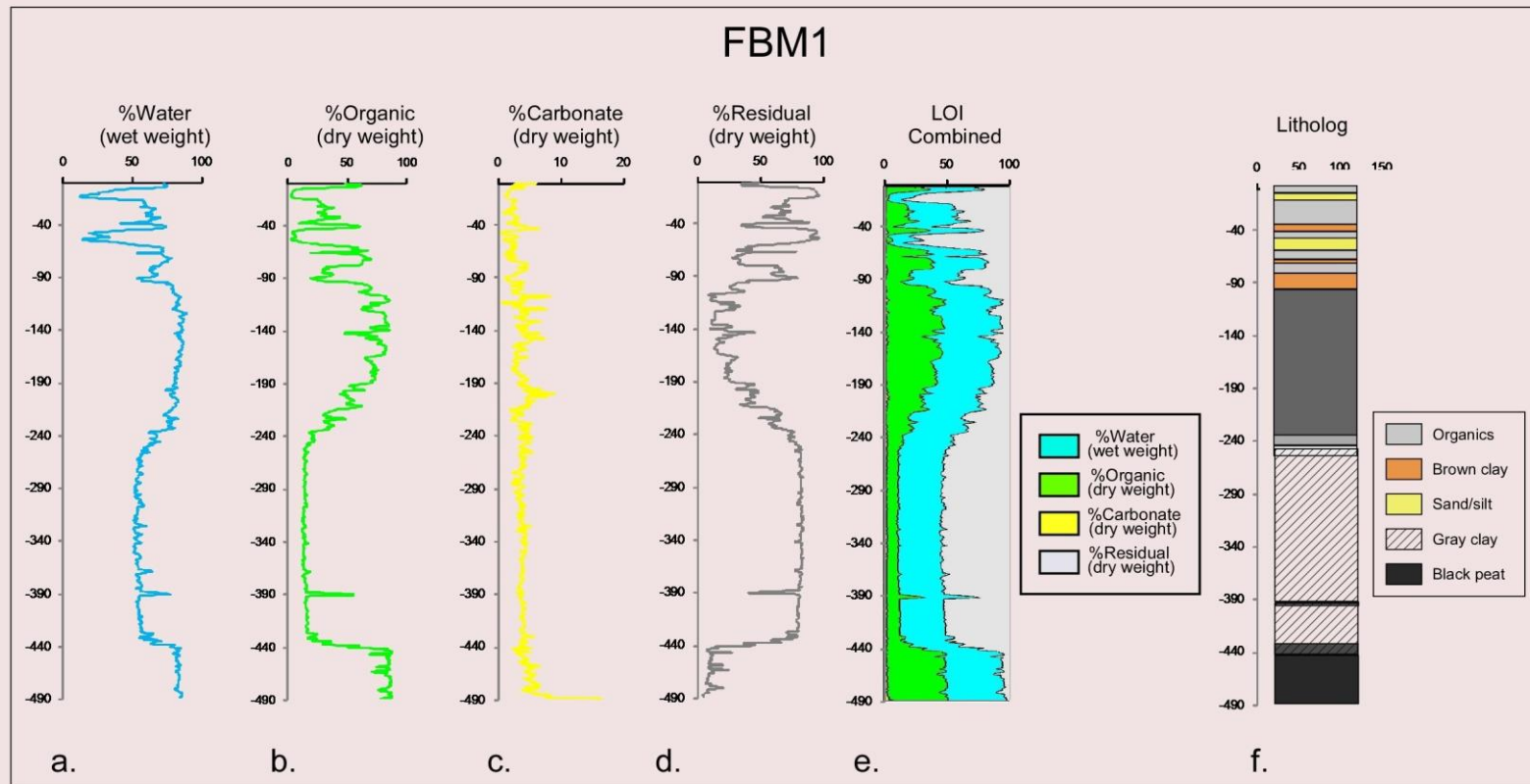
9.8.1.1 Example Litholog

Core FBM1 was chosen as the example litholog for this transect. It is a composite core consisting of eleven 50 cm sections taken from slightly offset holes with 5 cm overlaps. Located 100 m inland, it is the most seaward and longest of the marsh cores, reaching a depth of 489 cm.

The results of LOI analysis are presented in **Figure 9:7**. Shown are the water, organic, carbonate, and residual (mainly silicates) percentages as individual curves (**Figure 9:7a, b, c, d**), a combined LOI curve (**Figure 9:7e**), and the core litholog (Figure 9:7f). **Figure 9:8** is a composite photo of the core.

In this core carbonates are a very minor component, generally between 2-4%, while water and organic content are positively correlated to each other and negatively correlated with residual content. An examination of the data presented in **Figures 9:7a- f** demonstrates that sedimentary features of the core can be inferred from a careful reading of the LOI diagram. A sharp drop in water and organic percentages (blue and green curves) and a corresponding increase in the amount of residual material (gray curve) indicates non-organic intervals, usually light colored clastics. Examples are cm 5-16, 36-40, 45-57, 66-68, 80-94 (**Figure 9:9**). Sand layers can usually be distinguished from clay layers, as, due to differing porosity, their typical LOI signatures differ noticeably. For example, the visually obvious change from clay (top) to sand (bottom) over the interval between cm 7-15 is equally obvious when the LOI values are examined (**Table 9:2a**, red box). Cm 10 (clay) has a much higher (25.6 % vs. 14.7%) water content than does cm 14 (sand), even though the organic percentages are similar (3.2 % vs. 3.3%) . The sharpness of contact between dissimilar materials is typically clearly noticeable on the LOI curve, an example being the abruptness drop in water and organic content and corresponding increase in residual percentages between cm 44 and 4 (**Table 9:2b**, blue box), as seen in **Figure 9:9**. Similarly, the width of such interbedded layers can be assessed accurately, and even very thin layers identified, as occurs at cm 67 (**Table 9:2c**, green box).

In backbarrier locations, normally dominated by dark, horizontally deposited organic material, the presence of light-colored clastic intervals can indicate extremely short-term, event

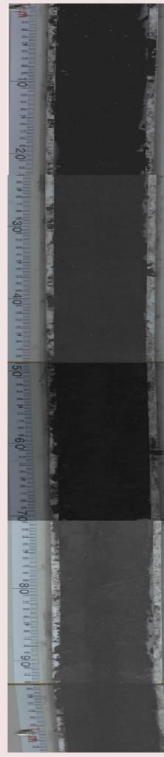


9.7 LOI curves and litholog for core FBM1. Shown are (a) water, (b) organic, (c) carbonate, and (d) residual (mainly silicate) percentages as individual curves; (e) a combined LOI curve, and (f) the core litholog.

FBM 1



1-100 cm



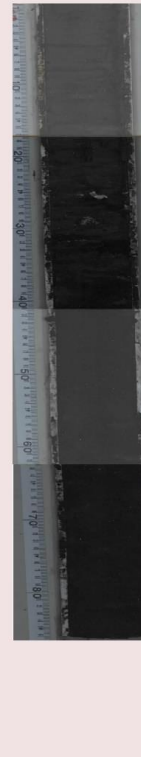
100-200 cm



200-300 cm



300-400 cm



400-485 cm

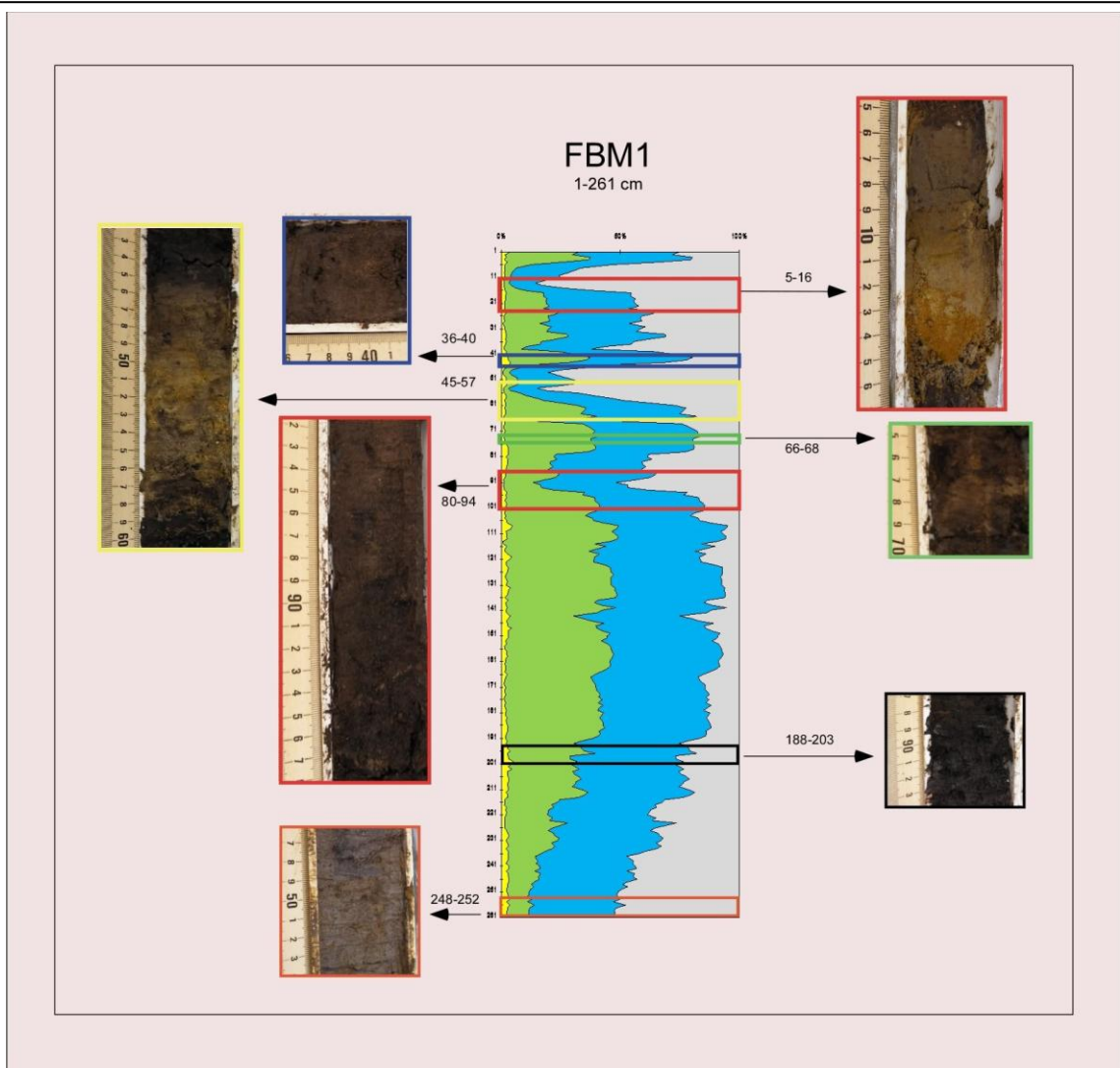
9.8 Core photo for FBM1.

9.2 Selected examples from the LOI data demonstrating the determination of sedimentological features by a careful reading of LOI values. (LOI sampling starts at the top of the core, so cm 1 starts at 0, ends at 1 cm-therefore the LOI interval 7-15 begins at cm 6, and ends at cm 15.)

Sample #	% Water	% Organic	%Carbonate	Residual		
6	52.4	16.5	2.3	81.2		
7	37.7	6.8	1.9	91.3		
8	34.5	5.0	1.8	93.2		
9	30.6	4.1	1.6	94.3		
10	25.6	3.2	1.7	95.2		Clay
11	26.5	3.3	1.7	95.0		
12	17.6	2.8	1.3	95.8		
13	12.5	2.4	1.1	96.5		
14	14.7	3.3	1.4	95.3		Sand
15	24.0	5.7	1.5	92.8		
16	38.5	11.3	1.9	86.8		a.
43	73.3	57.0	4.8	38.2		
44	68.1	40.9	6.5	52.5		
45	48.7	14.7	4.2	81.1		
46	39.4	8.8	3.0	88.1		
47	26.2	4.4	1.1	94.5		b.
65	72.7	67.5	1.8	30.8		
66	70.6	56.9	1.3	41.8		
67	53.6	19.1	2.3	78.6		
68	71.4	55.9	2.5	41.6		
69	72.6	61.6	1.1	37.3		c.

9.2 continued

188	81.4	70.0	4.6	25.4		Peat
189	80.9	71.3	4.0	24.7		
190	82.0	70.7	3.2	26.0		
191	80.9	65.9	3.3	30.8		
192	80.3	56.4	4.3	39.3		
248	62.3	16.2	4.1	79.7		Clay
249	65.1	18.6	3.9	77.5		
250	62.1	16.3	3.4	80.3		
251	60.0	14.9	3.5	81.6		
252	58.6	14.1	4.3	81.6		d.
423	56.4	16.2	3.8	80.0		Clay
424	57.2	17.0	3.4	79.5		
425	56.5	15.9	3.6	80.5		
426	56.5	16.2	4.2	79.7		
427	58.0	16.2	3.8	80.1		
448	84.0	85.9	3.7	10.4		Peat
449	84.2	85.0	4.0	11.0		
450	82.2	83.3	4.5	12.2		
451	82.4	85.3	4.1	10.7		
452	81.9	84.1	4.8	11.1		e.
387	56.0	15.6	3.7	80.7		
388	56.3	15.0	4.0	80.9		Clay
389	67.1	30.6	3.0	66.5		
390	73.8	48.0	3.6	48.3		Peat
391	77.7	54.7	3.9	41.4		
392	56.5	17.1	3.4	79.6		Clay
393	55.2	15.2	3.8	81.0		f.



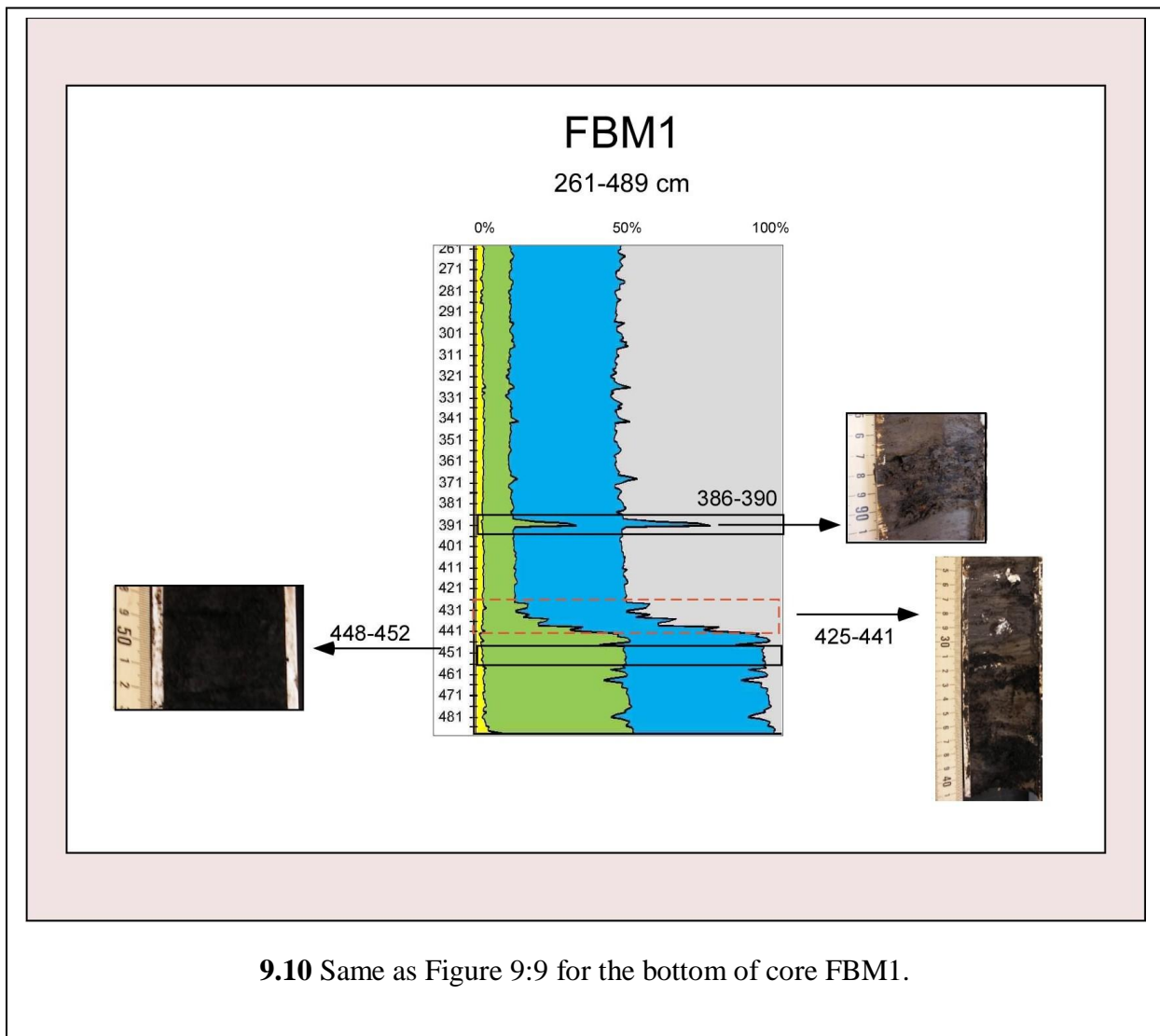
9.9 Matching of LOI curve and sedimentological data for the top of core FBM1. Photos of different units display how sediment type can be inferred from LOI curve; colored boxes mark specific clastic layers.

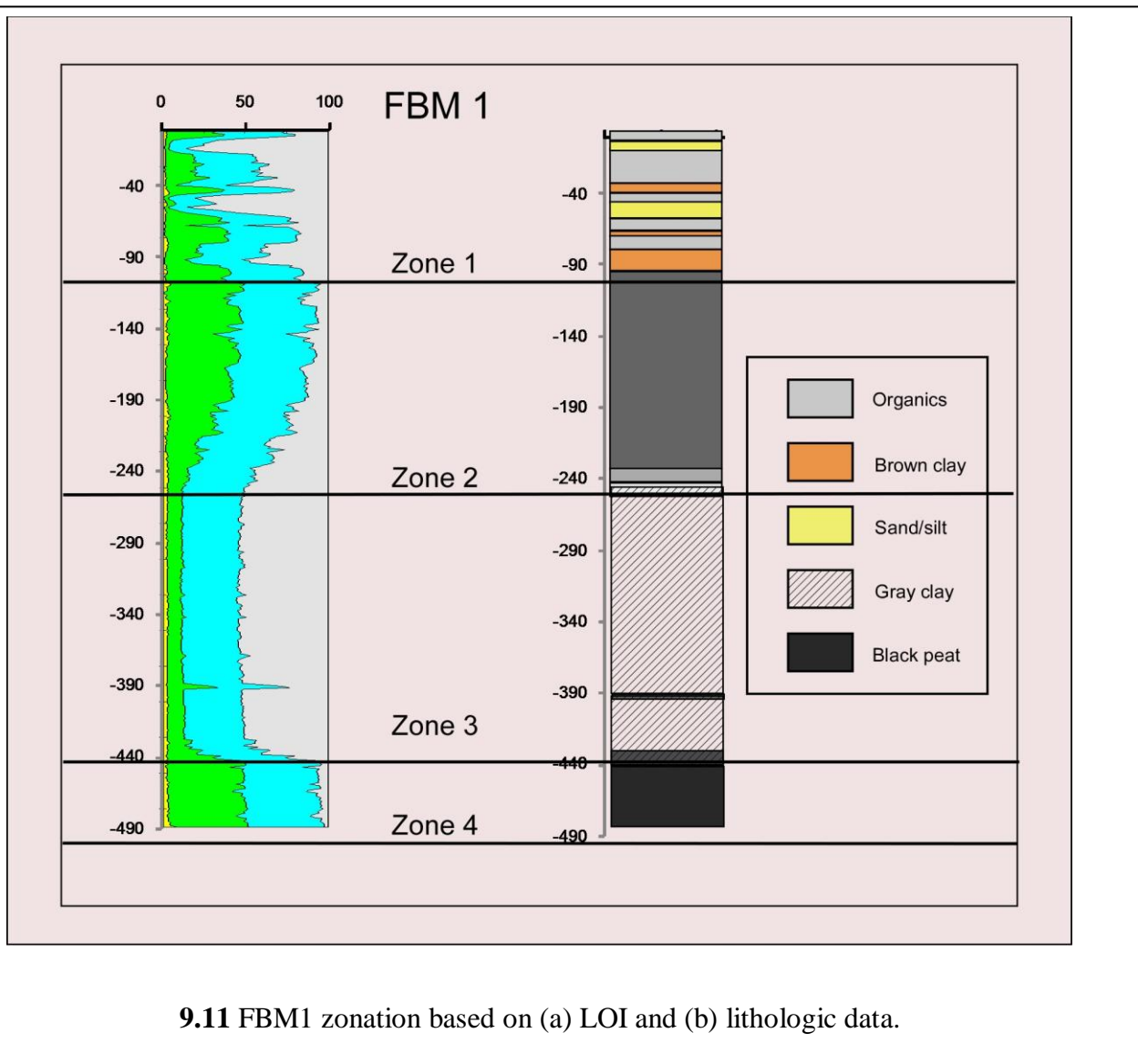
driven changes in deposition regime. Other markers of event-driven deposition are chaotic or vertical deposition, upward fining sequences, and macrofossils of exotic (marine or dune) origin. Close examination of the LOI curve also facilitates identification of more gradual changes in depositional regimes, usually resulting from one or more significant alterations in the supporting environmental framework. Examples from backbarrier locations vary from the local (inlet opening/closing) to regional (increased/decreased precipitation) to global (eustatic sea level rise). The LOI diagram can also provide information on the rate of such changes, which can vary from instantaneous to gradual. The interval from ~190 cm to 250 cm on core FBM1 (**Table 9:2-d**, pink box) provides examples of both. From ~cm 190-250 both the water and organic content slowly decrease (from >70% to <15%) as the residual content increases correspondingly (from <25% to >80). Over this 60 cm interval the sediments slowly change from mainly organic (peat) to mainly inorganic (clay). This no doubt represents a slow environmental change for the site, the exact reverse of which occurs, more rapidly at the bottom of the core between cm 420-450, though less unilinearly (**Table 9:2e**, turquoise box; **Figure 9:10**). An extremely rapid clay-to-peat-clay cycle occurs within a few cm at a depth of 390 cm (**Table 9:2f**, purple box).

9.8.1.2 Zonation

FBM1 can be divided into four zones, based on changes in the LOI curve (**Figure 9:11**).

9.8.1.2.1 Zone 1(1-98cm) shows generally high percentages of water and organic (peaty and/or organic intervals), interrupted by intervals of very high residual content (sand/silt/clay). Above 60 cm, the organic intervals generally consist of a brownish muddy peat, containing some large, partially-decomposed organic material, often recognizable as individual leaves, roots, etc. Water content varies between 58%-73%, and organic contents between 24%-69%. Below cm 60 the silt to clay, and color from brown to orange to white. Water content drops as low as 14% and





organic material becomes darker and more decomposed, with higher water (>70%) and organic (>50%) content. The clastic layers show great variability, with composition varying from sand to organic content to 2% within these clastic layers.

9.8.1.2.2 Zone 2 (99-250cm) is similar to the organic intervals of Zone 1. Between 99 and 190 cm the material is decomposed black peat; water and organic values are consistently >80 and 70% respectively. Below 190 cm the peat becomes increasingly inorganic and lighter colored, changing to muddy peat ~ 230 cm and peaty clay ~240. By 250 cm the water content has reduced to 62% and the organic to 16%. Within Zone 2 the organic material is well-rotted fibrous peat, with occasional larger pieces. The selection of 250 cm as the lower boundary is somewhat arbitrary as it is at cm 251 that water content first drops below 60%. Two bands with mildly elevated residual values occur within this zone, at 135-145 and 198-206 cm depth. These bands are much less distinct than those in Zone 1, mainly consisting of a thin admixture of brownish clay. For the higher band, water content remains > 80%, although the organic content drops to 48% at cm 143. The lower layer is visually obvious as a brown band, and organics show a >10% drop from the surrounding material, although water values show very little change.

9.8.1.2.3 Zone 3 (251-435 cm) is almost entirely a featureless, unlaminated gray clay. Apart from the narrow peat band centered at 390 cm, water and organic content remain remarkably consistent throughout the interval, hovering a few percentages above/below 55% and 15% respectively. The dramatically different peat band (**Figure 9:10**) is 3 cm thick, and contains some larger organic pieces. The transition to Zone 4 is not simple; between 425 and 441 the sediments change from clay to peat to clay to peat (**Figure 9:10**).

9.8.1.2.4 Zone 4 (436-489) is basically very well-rotted black peat, with both water and organic percentages near 85%. The few narrow drops in these levels (organic drops to 70% at cm 464)

are not visually noticeable.

9.8.1.3 Dating

Four plant/organic material samples were selected from FBM1 and sent to the National Ocean Sciences Accelerator Mass Spectrometry Facility (NOSAMS) at Woods Hole Oceanographic Institute for AMS dating. The results are listed in **Table 9.3**, and shown graphically in **Figures 9:12, 13, and 14**.

The graph (**Figure 9:12a**) produced by plotting depth (X axis) against ^{14}C age (Y axis) for these samples shows a R^2 value of 0.997 and an intercept of -26 (AD 1976), which suggests that the dates are probably correct.

9.8.1.4 Transect Correlation

The FBM transect consists of five cores. FBM3 is a short core (118 cm), consisting of three overlapping Russian Peat borer sections, taken 70 m from the sea in an area of low shrubs at the seaward rim of the *typha* depression. This core contains an expanded clastic layer and has not been subjected to LOI in order to avoid contamination for a pending ^{137}Cs analysis. FBM 2 consists of three overlapping peat borer sections reaching a depth of 126 cm. FBM4 and FBM5 each consist of two overlapping piston corer sections in adjacent holes reaching depths of 194 and 256 cm respectively.

Three plant/organic samples were selected from these cores and sent to the NOSAMS facility at Woods Hole Oceanographic Institute for AMS dating. The results are listed in **Table 9:4**, and shown graphically in **Figures 9:13, 14, and 15**.

Plotting depth against ^{14}C ages for FBM 5 shows that the dates are probably reasonable; a linear trendline shows a sedimentation rate of 0.075 cm/yr (13.34 yr/cm), but with an intercept of 128 yr (AD 1822) (**Figure 9:12c**). Artificially imposing a surface date of AD 2007 reduces

the sedimentation rate slightly to just under 0.07 cm/yr (14.51yr/cm), and yields an R^2 value of 0.995 (**Figure 9:12b**). No depth/date graph can be produced for the single sample from FBM4, but the sedimentation rate is much faster (0.15 cm/yr; 6.52 yr/cm, based on 2007 as the surface date). Cores in the FBM transect were correlated stratigraphically, based on analysis of the LOI curves as described above, and correlated with the zones described for FBM1. Zones 1 and 2 extend across the transect; Zone 3 appears only in the longer cores (100 m and 156 m), and Zone 4 only at 100m (**Figure 9:13**). Zone 1 exhibits fairly uniform thickness across the transect, being ~100 cm thick at 100, 120, thickening to ~140 at 132 m, and thinning ~ 70 cm thick at 156 m. Zone 2 shows similar thickness at 100 (~150 cm) and 156 m (~125 cm); the cores at 120m and 132m do not penetrate deep enough to encounter the bottom of Zone 2. Zone 3 is ~185 cm thick in core FBM1, the only core in which its base is encountered. Zone 4 is found only in the core at 100m, which did reach the bottom of the zone.

9.8.1.5 Zone 1 Clastic Layers

Several of the individual clastic layers in Zone 1 can be traced reliably across the transect, based on thickness, composition, and color. The five most prominent ones have been assigned letter names (**Figures 9: 14, 15**).

9.8.1.5.1 Clastic Layer A (red)

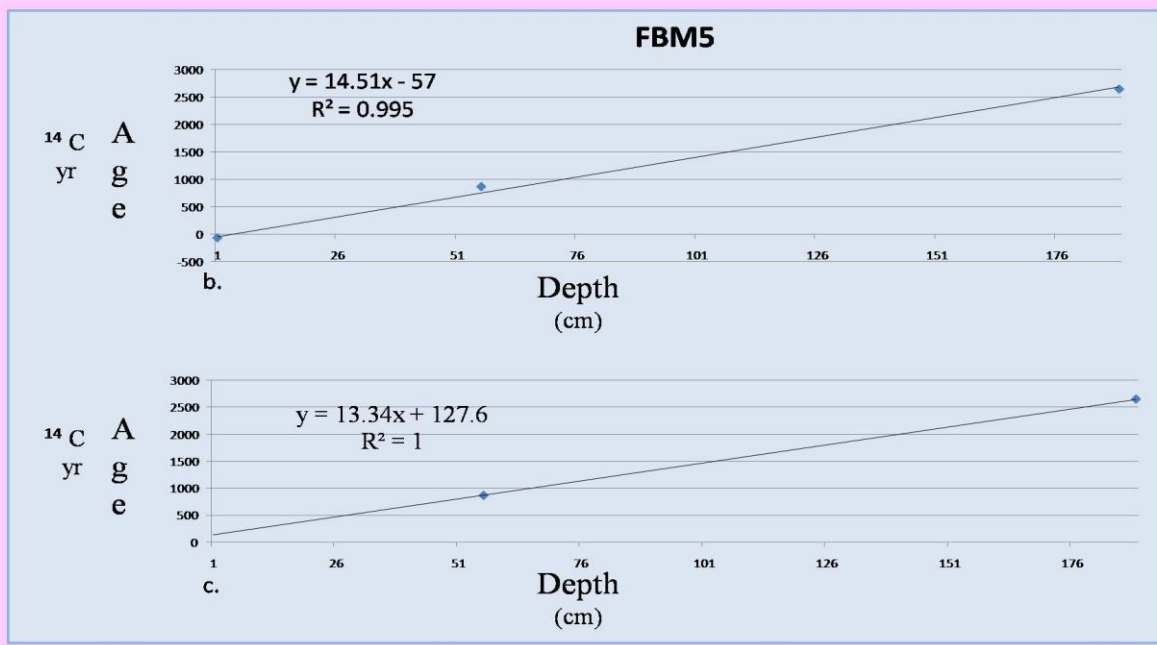
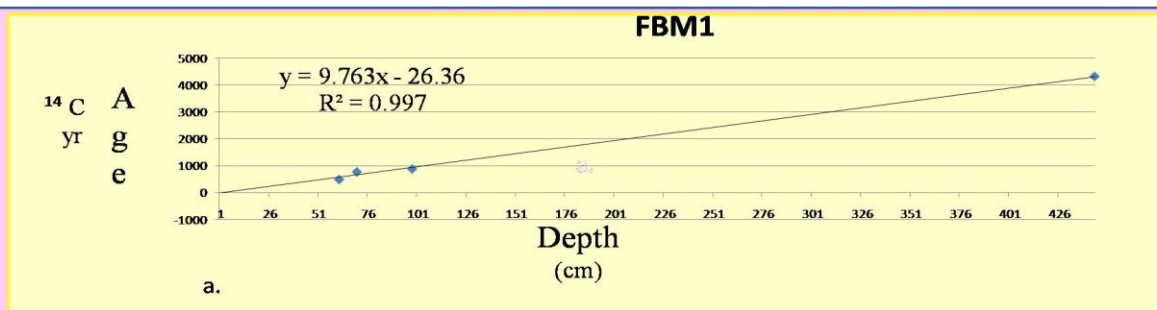
This top clastic layer is large and stratigraphically complex. From 100- 132 m it is nearly 10cm thick, thinning to >5 cm at 156 m. At 100 and 120 m it fines upward, changing from sand to silt to clay. At 132 and 156 it is a distinct gray silt/clay layer.

9.8.1.5.2 Clastic Layer B (blue)

This layer is 2-5 cm thick and is composed of brown clay except at 132 m, where the clay is gray and 8 cm thick.

9.3 FBM1 chronology

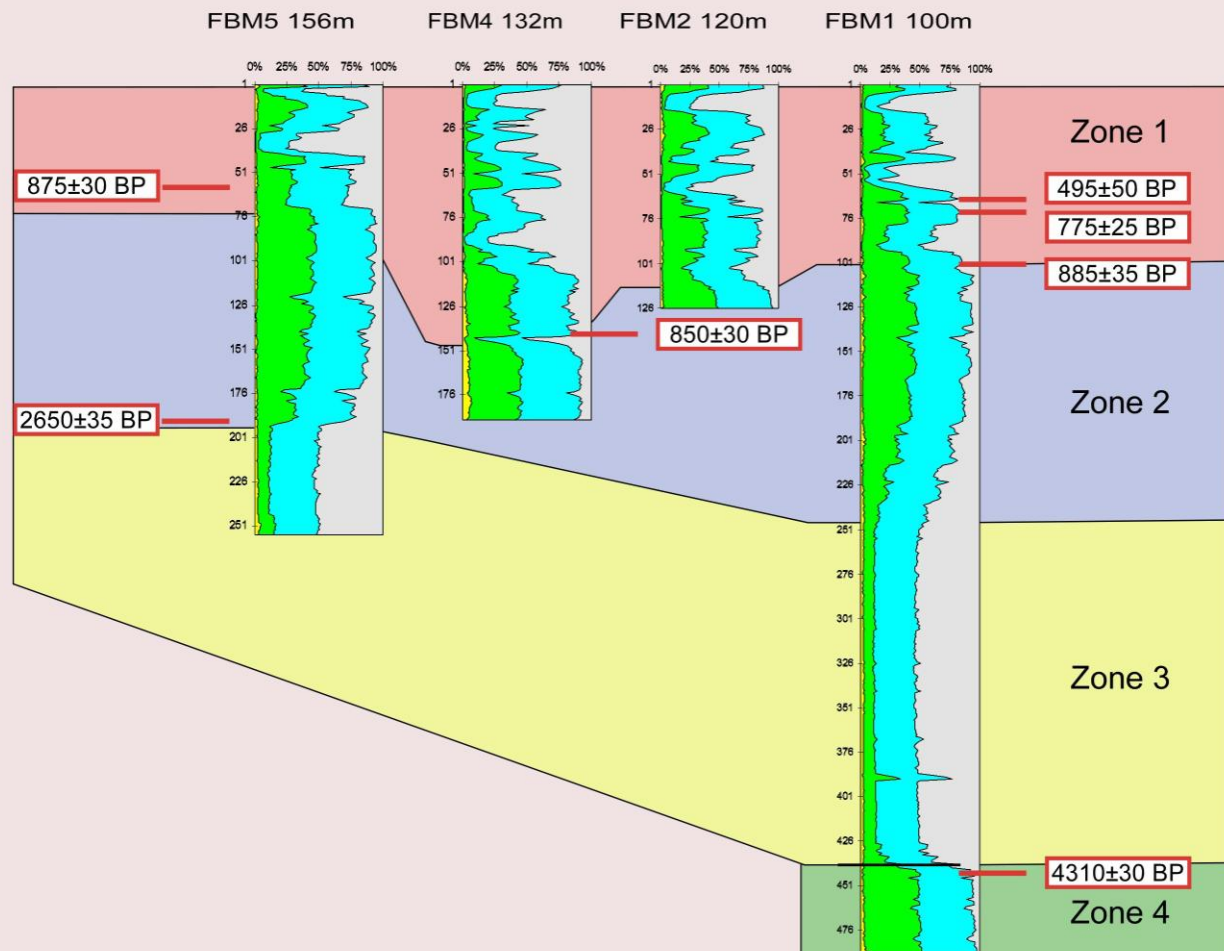
Core	Depth	Material	Lab	Sample#	C ¹⁴ yr	BP	Cal yr BP	%
FBM1B	61	Plant/Wood	WHOI	OS-70924	495	±50	465-564 589-641	0.845 0.155
FBM1B	70	Plant/Wood	WHOI	OS-70861	775	±25	673-731	1
FBM1C	98	Plant/Wood	WHOI	OS-70926	885	±35	730-910	1
FBM1K	444	Plant/Wood	WHOI	OS-70862	4310	±30	4835-4893 4897-4960	0.767 0.233
FBM5A	56	Plant/Wood	WHOI	Os-70707	875	±30	726-832 846-907	0.762 0.238



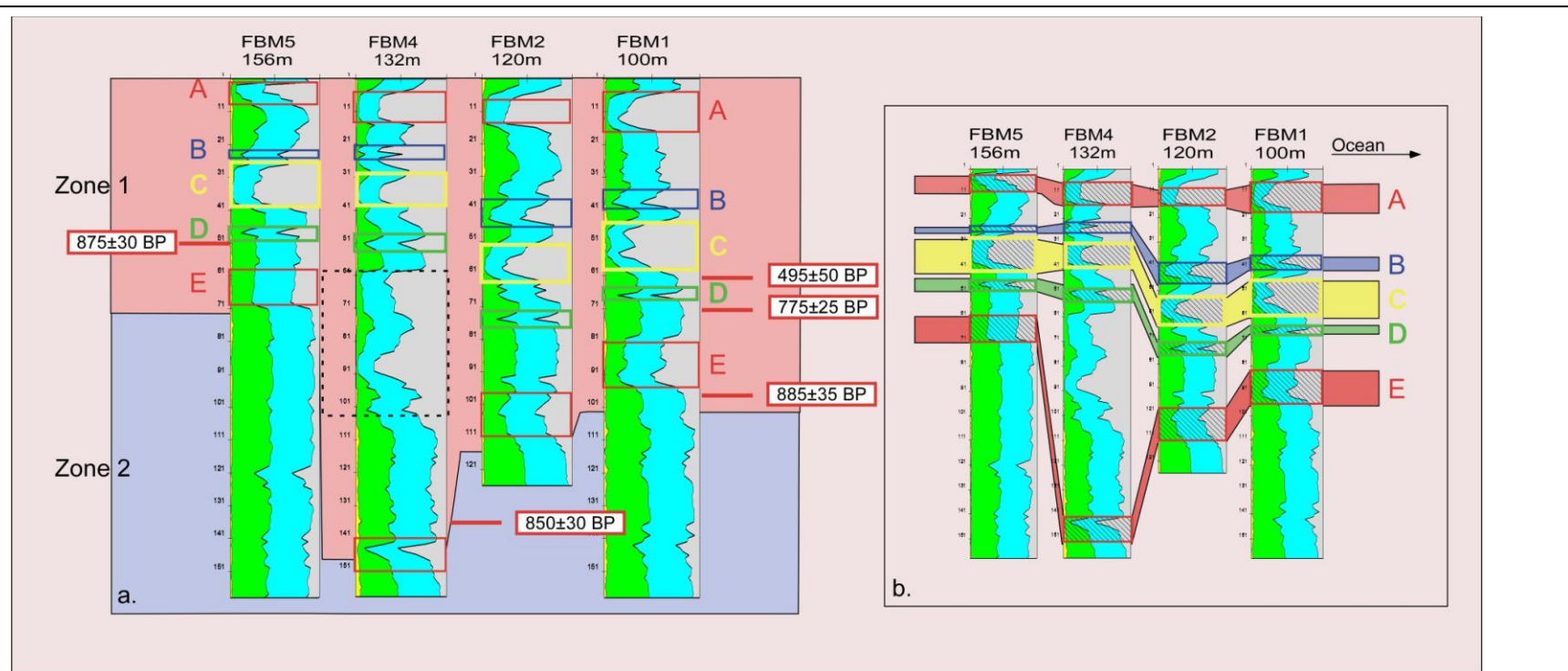
9.12 Depth-age graphs for FBM1 and FBM5, showing the linear trendline and R^2 value for (a) straight plotting for FBM1 and (c) FBM5; and for (b) FBM5 with a forced surface intercept of -57 years (corresponding to AD 2007, the year the core was extracted).

Nicaragua

Falso Bluff



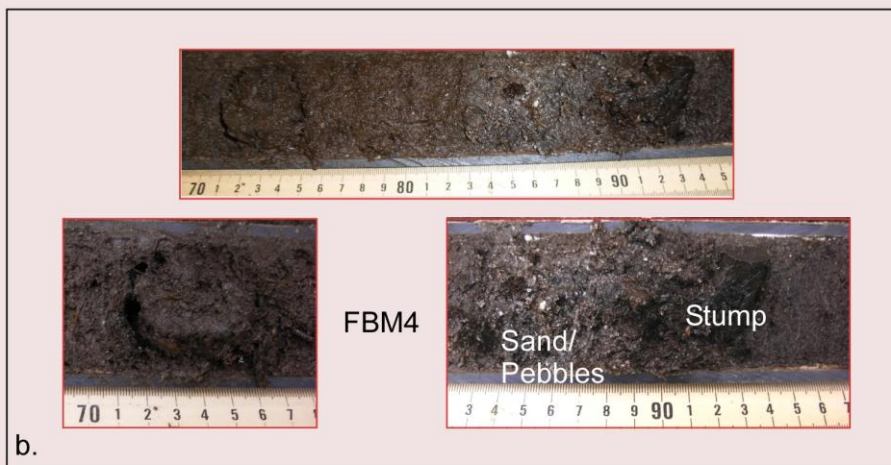
9.13 FBM transect zonation based on LOI data. Radiocarbon dates are boxed in red.



9.14 FBM transect clastic layers. Zone 1 clastic layers (a), can be correlated across the transect (similar colored boxes and capital letter designations indicate probable correspondence) from which (b) a summary diagram was created. Dashed black box indicates an anomalous interval in core FBM4, possibly a result of disturbance. Photos of this interval are presented in Figure 9:15b.

9.4 FBM4 and FBM5 chronologies

Core	Depth	Material	Lab	Sample#	C ¹⁴ yr BP		Cal yr BP	%
FBM4B	139	Organic	WHOI	OS-72533	850	±30	870-898	0.1
							818-821	0
							689-797	0.9
FBM5A	56	Organic	WHOI	OS-70707	875	±30	726-832	0.8
							845-907	0.2
FBM5B	189	Organic	WHOI	OS-73423	2650	±35	2736-2812	0.9
							2816-2844	0.1



9.15 Photos (a) of the clastic layers identified in the previous figure, using the same color scheme; (b) photos of the disturbed interval from FBM4. The radiocarbon dates are placed vertically in accordance with their stratigraphic correspondence to the clastic layers.

9.8.1.5.3 Clastic Layer C (yellow)

This layer is 9-14 cm thick, consisting of brown and/or gray clay.

9.8.1.5.4 Clastic Layer D (green)

A thin (2-3 cm) brown clay layer in all cores.

9.8.1.5.5 Clastic Layer E (red)

Across the transect this layer varies in thickness (<5-14 cm in thickness) and color (from gray to brown clay).

9.8.1.5.6 Core FBM4

Zone 1 is much thicker in this core than in the other FBM cores. Although the top events in FBM4 align well with the other cores stratigraphically (**Figure 9:14a**), and bear striking sedimentological resemblance (**Figure 9:15**), there is an anomalously large gap between Events D and E. Both LOI and sedimentary analyses show that this section, from approximately cm 60-100, marked by a black dashed box in **Figure 9:14a**, does not match the other cores, consisting of a mixed section of sand, pebbles, and organics. A large (~ 2 cm diameter) trunk that appears to be cleanly cut and lying in a downward pointing position occurs at 90-94 cm, anchoring the bottom of the section. A jumbled interval of poorly-sorted large-grained silica and carbonate material abruptly begins immediately above this trunk, while some 20 cm higher, at 70 cm an unusual organic clump 4 cm in diameter occurs, lying discontinuously within the surrounding well-rotted brown peat (**Figure 9:15b**). It is our opinion that this entire section results from disturbance. The simultaneous age of Event E is documented by three overlapping dates across the transect, yet at FBM4 it occurs 30-70 cm deeper than in the surrounding cores, suggesting that this site was a topographic low, perhaps making it subject to rapid filling. The stratigraphic correspondence both above and below, the radiocarbon dating, and the unit's sedimentological

features of all argue that this is an extraneous interval, resulting from some local disturbance. Although the cause of the disturbance is unknown, the cleanly cut nature of the thick bottom trunk suggests possible anthropogenic activity.

9.9 IV Transect

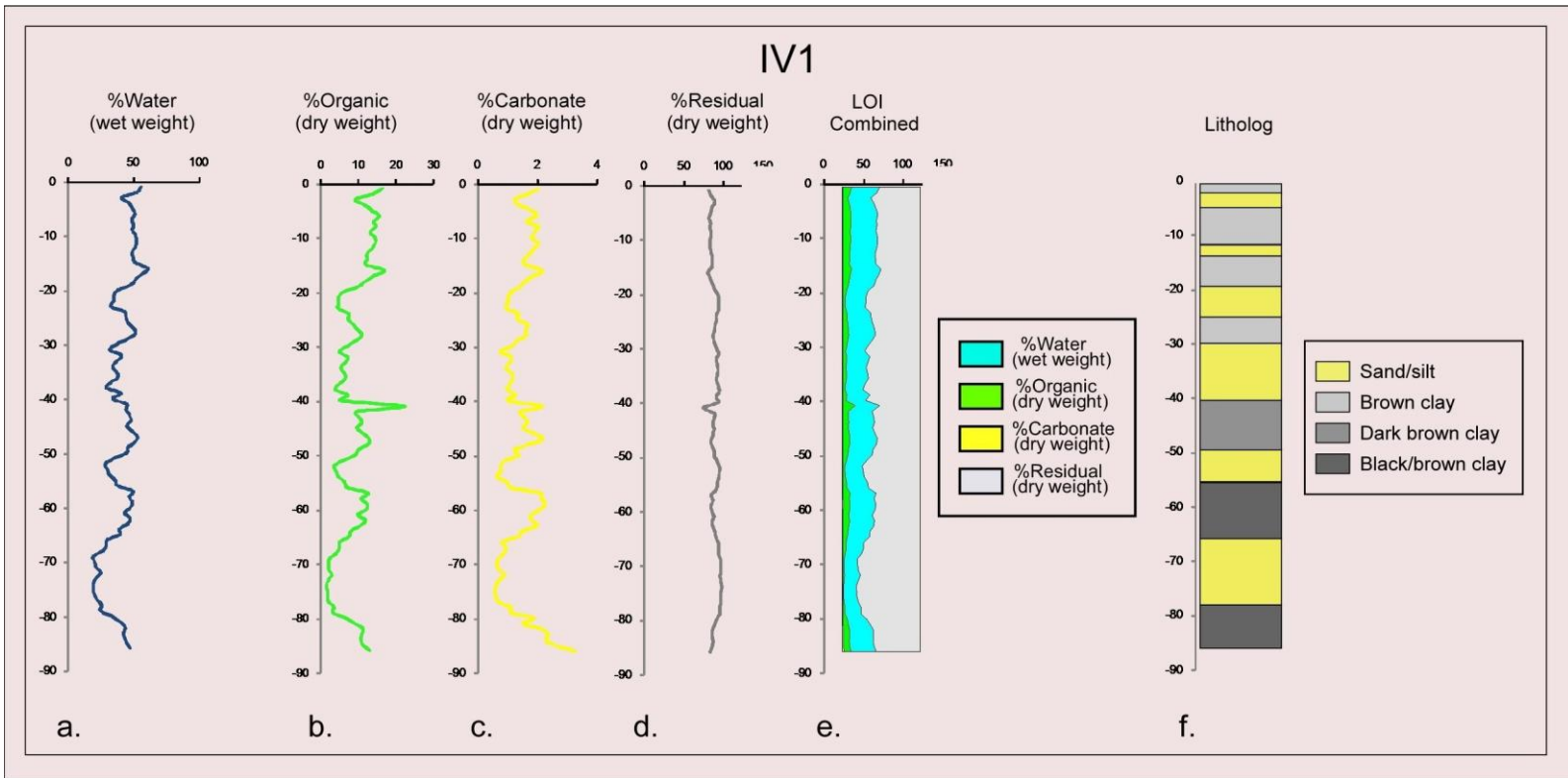
9.9.1 Results

A transect of five cores from 30-90 m inland were taken from a tall (>10 m) mixed red/black mangrove forest on the southeastern edge of Isala del Venado. Although elevation could not be measured precisely, the site consists of a level plain ~ 0.75 above MSL with minimal (<25 cm) topographic relief. No barrier berm is present. All cores are composite, combining results from two overlapping peat borer pushes. Penetration depth of the cores varies from 72 to 86 cm, indicating an impenetrable horizontal antecedent topography, presumably the prevalent red Pleistocene clay, buried under ~ 80 cm of more recent material.

9.9.1.1 Example Litholog

Core IV1 was chosen as the example litholog for this transect. IV1A reached a depth of 47 cm, which IV1B extended to 86 cm, with an 11 cm overlap.

The results of LOI analysis are presented in **Figure 9:16**. Shown are the water, organic, carbonate, and residual (mainly silicates) percentages as individual curves (**Figure 9:16a, b, c, d**), a combined LOI curve (**Figure 9:16e**), and the core litholog (**Figure 9:16f**). The core is characterized by a low organic brown clay interbedded with sand layers. Even the non-sand layers represent a basically mineral deposition, as water content varies from 19%-61%, organics from 1.6%-17% and carbonate content, apart from a single exception, remains below 2%, and reaches a minimum of 0.6%.



9.16 LOI curves and litholog for core IV1. Shown are (a) water, (b) organic, (c) carbonate, and (d) residual (mainly silicate) percentages as individual curves; (e) a combined LOI curve, and (f) the core litholog.

9.9.1.2 Zonation

Assuming that the sand layers result from transported material, the autochthonous deposition at this site is a sticky brown mud, which darkens and consolidates toward the bottom. The number of roots, and the percent and size of organic material increase toward the top. Because the general compositional conformity of this core argues against the occurrence of any significant change in the environmental boundary conditions for the site over the period of deposition, the entire core is recognized as a single zone of clay deposition, interrupted by frequent occurrences of transported clastic material (**Figure 9:17**).

9.9.1.3 Dating

A single plant/organic sample was selected from 83 cm near the bottom of IV1 and sent to the NOSAMS facility at Woods Hole Oceanographic Institute for AMS dating. The results are shown in **Table 9:5**, and in **Figures 9:17, 18**.

Assuming relatively constant deposition, the calculated sedimentation rate is 0.06 cm/year (17.23 yr/cm), slower than that calculated from the FBM transect.

9.9.1.4 Sand Intervals

Sand intervals are identified and lettered following the scheme used for the FBM transect (**Figure 9:17**). This does not imply that similarly lettered events are the same in different transects.

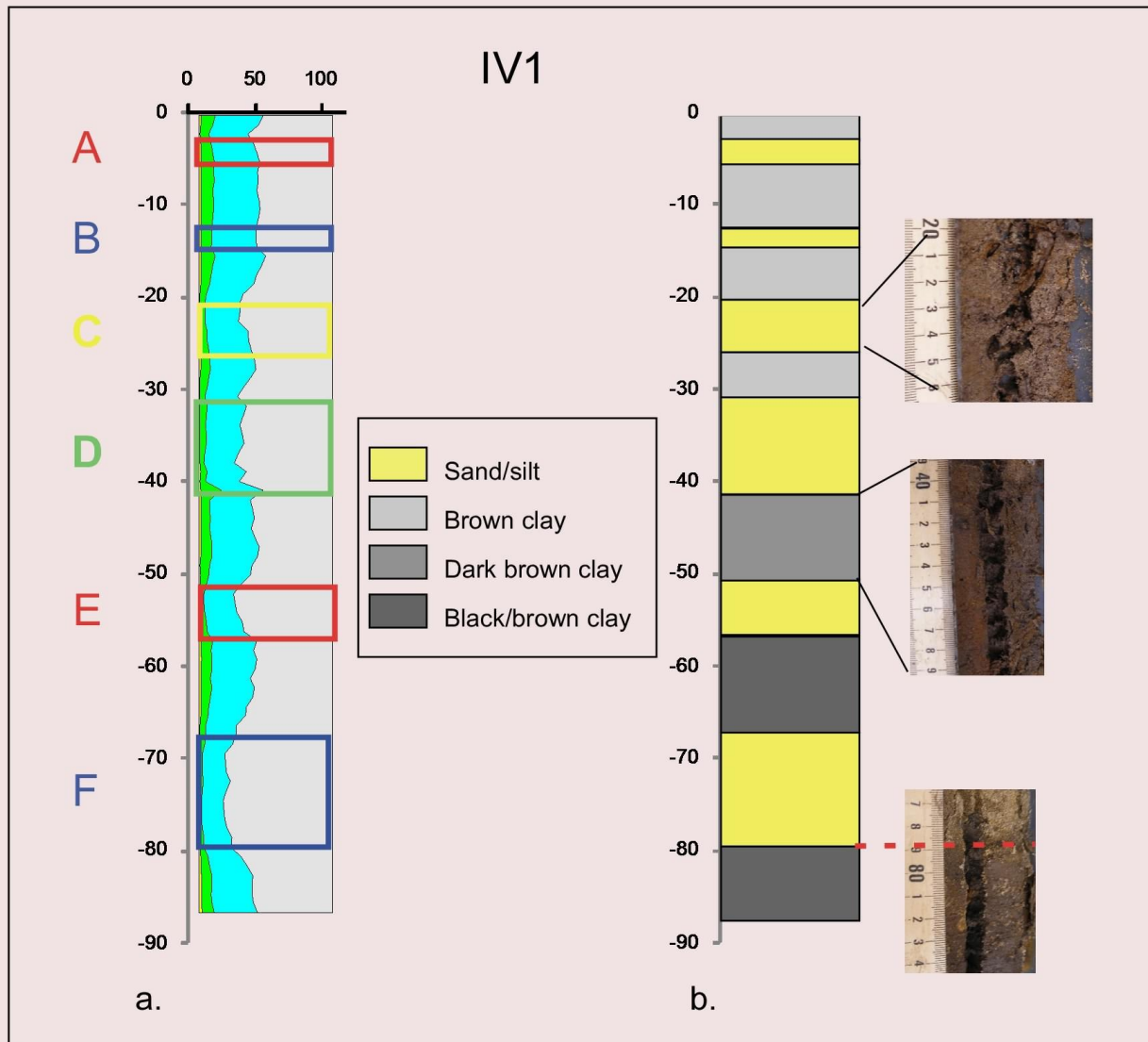
9.9.1.4.1 A (2-4cm) fine to medium sand, mixed with brown mud, not especially distinct

9.9.1.4.2 B (13cm) fine to medium sand, mixed with brown mud, not especially distinct

9.9.1.4.3 C (19-25 cm) white medium sand

9.9.1.4.4 D (30-40 cm) white medium sand, a clear bottom contact.

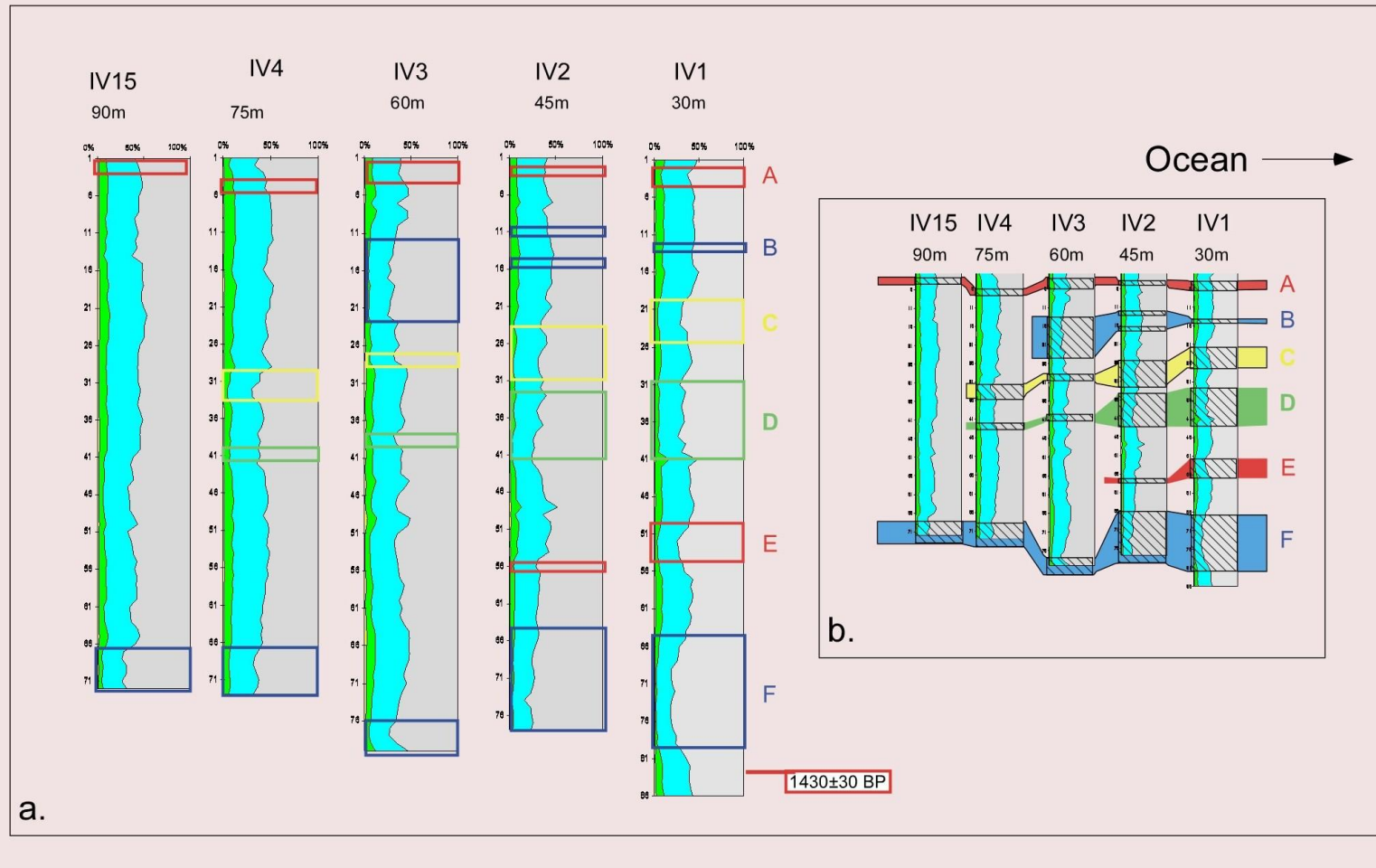
9.9.1.4.5 E (49-54 cm) white medium sand, mixed with dark mud, a distinct interval, with fairly



9.17 IV1 clastic layers. Clastic layers in IV1 (a) are marked by boxes and lettered in corresponding colors; (b) core litholog and photos of representative sedimentological units, with the abrupt compositional change at cm 79 marked by a dashed red line.

9.5 IV1 chronology

Core	Depth	Material	Lab	Sample#	C ¹⁴ yr BP		Cal yr BP	%	AD/BC
IV1B	83	Organic	WHOI	OS-73424	1430	±30	1293-1376	1	574-657AD



9.18 IV transect elastic layers. Zone 1 clastic layers (a) can be correlated across the transect (similar colored boxes and capital letter designations indicate probable correspondence), used to create which a (b) summary event diagram.

clear top contact, and less distinct bottom contact.

9.9.1.4.6 F (65-78 cm) medium white to tan clean sand, with a very distinct with sharp bottom contact, less clear top contact.

9.9.1.5 Transect Correlation

The sand layers identified in IV1 can be traced across the transect for varying distances. Sand layers A and F are found in all cores, C and D to 75 m, B to 60 m, and E to 45 m (**Figure 9:18**). Sand layers generally thin moving inland, with the exception of Layer B, which progressively thickens at 45 and 60 m. The sand layers are roughly evenly distributed by depth. All layers are primarily sand, easily distinguishable from the interbedded clay. Photos are not presented of the sand layers as the particularly viscous quality of the site's clay not only required extensive scrapping to remove, but also randomly stained some of the underlying layers. Although the composition of all layers could be determined adequately, as could the sharpness of contact between layers, the color, composition, and structure of the sand layers were not uniformly preserved, reducing the value of visual comparisons.

9.10 TASN Transect

9.10.1 Results

A seven core transect, starting at 70 m and extending to 200 m, was extracted from a hardwood swamp on the narrow forested barrier a few km north of the village of Tasbapauni (**Figure 9:2**). Although elevation could not be determined precisely, the swamp appears to be at or near sea level, behind a slightly higher beach ridge. Core penetration depths indicate that an antecedent topographical high extends at least 100 m inland (cores TASN 5, 4, and 3), beyond which the antecedent elevation drops, producing the small basin in which the swamp has developed. Westward of the ridge forming the back edge of the swamp basin, elevation continues

a very gradual decrease through a mosaic of dense mangrove forest and flooded areas which extend to the eastern edge of Pearl Lagoon, approximately 2000 m to the west (**Figure 9:2**). Tree species at the coring site included *Pachira aquatica*, *Pterocarpus*, *Elaeis oleifera*, and the swamp shrub *Spathiphyllum friedrichsthalli*. Cores at 70, 90, 100, 150, 170, and 200 m were extracted by peat borer; a modified Livingstone piston corer was used at 125 m. All cores were primarily black or brown peat and clay with occasional sand/silt layers.

9.10.1.1 Example Litholog

Core TASN1 was chosen as the example litholog for this transect. It is a composite core consisting of two Livingstone sections from slightly offset holes with a 10 cm overlap. Located 125 m inland, it is the longest core, reaching a depth of 239 cm.

The results of LOI analysis are presented in **Figure 9:19**. Shown are the water, organic, carbonate, and residual (mainly silicates) percentages as individual curves (**Figure 9:19a, b, c, d**), a combined LOI curve (**Figure 9:19e**), and the core litholog (**Figure 9:19f**). In this core carbonates are a very minor component, generally between 1-7%, with a 1 cm wide spike to 13% at 197 cm. Water and organic content are positively correlated to each other and negatively correlated with residual content.

9.10.1.2 Zonation

TASN1 can be divided into three zones (**Figure 9:20**).

9.10.1.1 Zone 1(1-73cm) Except for the top 8 cm, which has extremely high organic values (77%-91%), Zone 1 consists of black to brown peaty mud, interrupted by intervals of higher residual content. The peaty mud intervals show generally high percentages of water (>80%) and moderate organic levels (35%-70%), with few large organic pieces. The less organic sections represent increased amounts of brown clay. The top section (8-23 cm) is a distinct clay band,

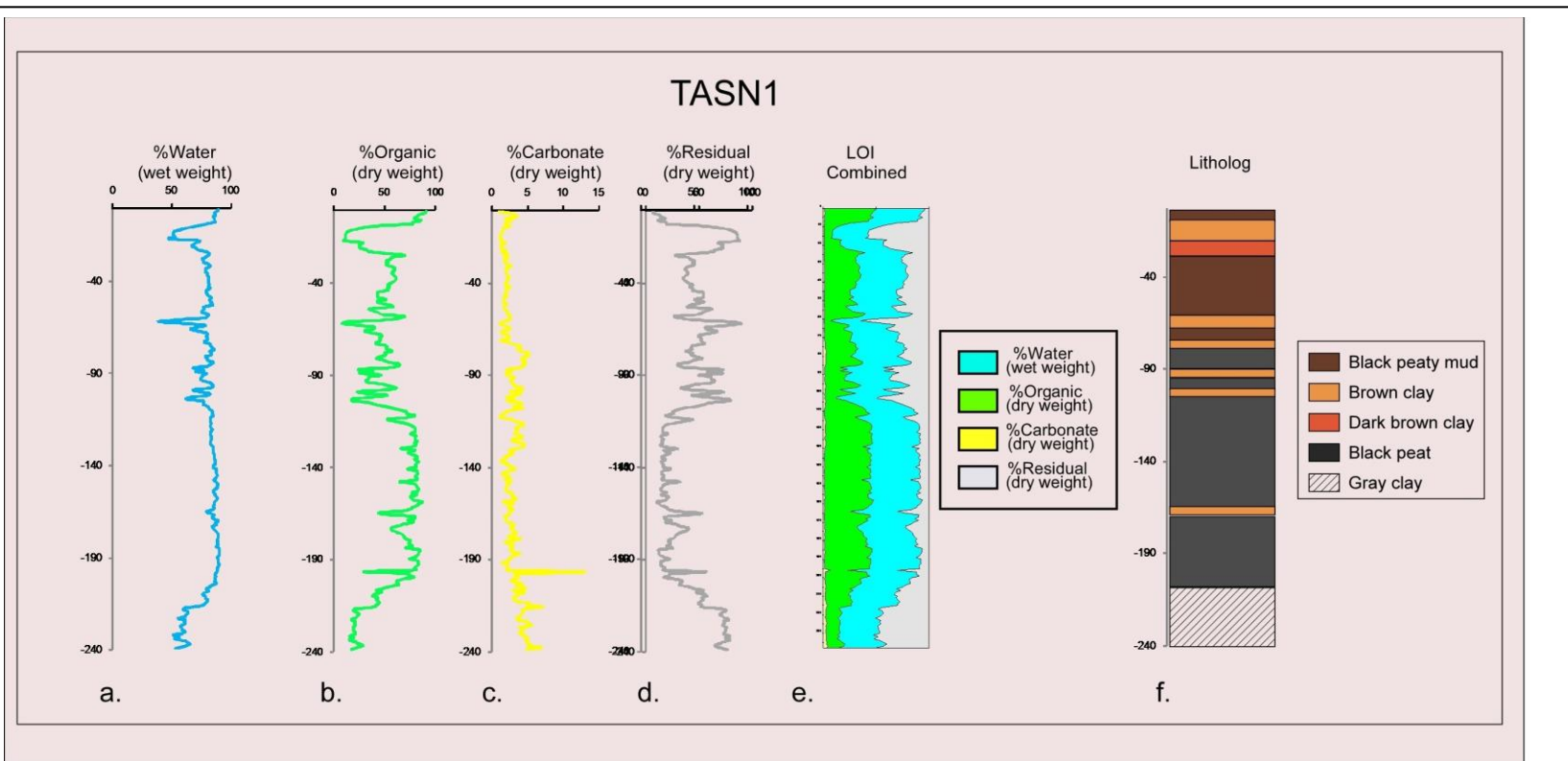
grading from dark to light brown from bottom to top. Water and organic content drop below 50% and 10% respectively. The two lower clay bands are similar, but slightly less distinct, with water, and water and organic percentages dropping below 40% and 10% respectively. At cm 73 there is a distinct change from clay to peat (**Figure 9:20**).

9.10.1.2 Zone 2 (74-216 cm) consists almost entirely of well-rotted dark brown to black peat, becoming darker at the bottom. Water and organic levels are generally >80%, with water occasionally >90%. There are three brown clay layers within this zone, at cm 87-89, 99-107, 164-167. The organic values reach lows of 24%, 17%, and 44% respectively for these intervals. A sharp spike in the carbonate percentage (to 13%) with corresponding decreases in organic and residual occurs at 197 cm. As neither water content nor visual inspection show any significant differences with the surrounding material, it is probable that this spike results from the anomalous inclusion of a carbonate rich macrofossil (shell) in the sample. Although visually the transition to Zone 3 appears to begin quite abruptly at cm 216 (**Figure 9:20**), LOI data indicate that the change is more gradual as the organic percentage drops below 80% at cm 198 and continues to fall, reaching 42% at cm 216.

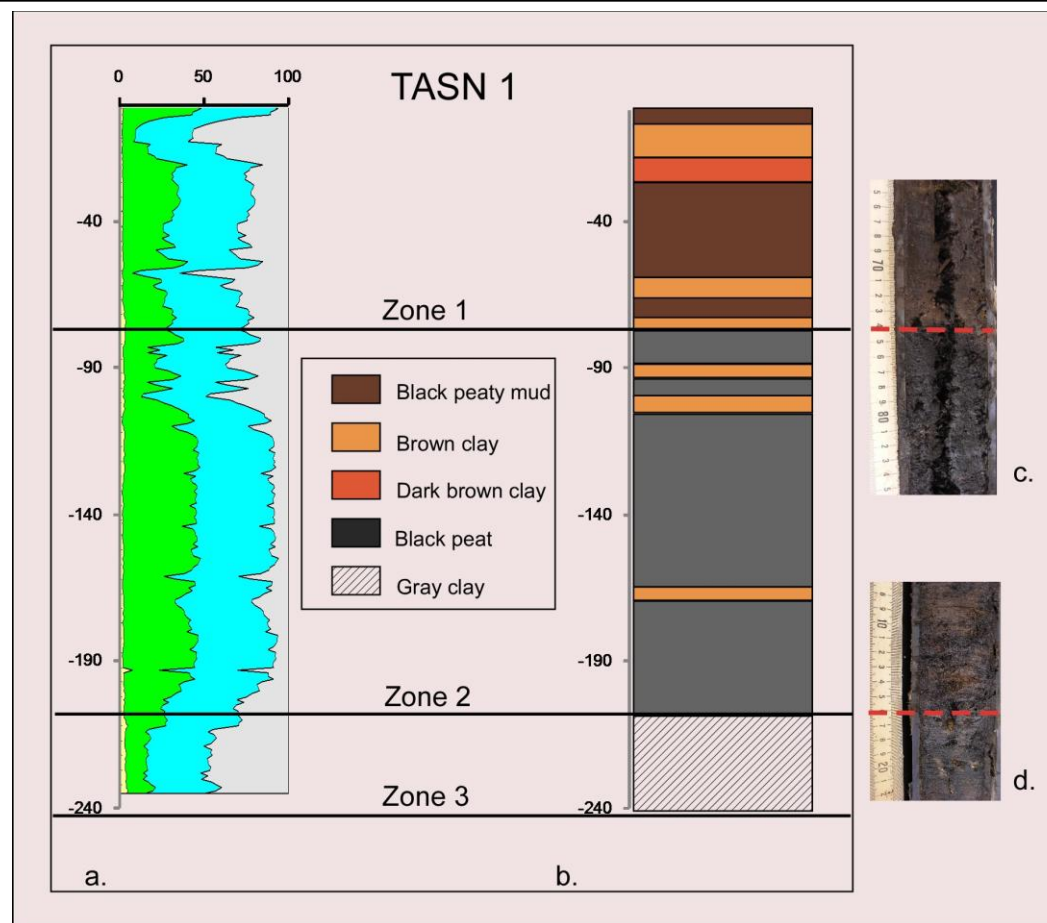
9.10.1.3 Zone 3 (217-239 cm) is an unlaminated gray clay, similar to Zone 3 in the FBM transect. Water content varies from 53%-69%, and organic content varies from 15%-29%.

9.10.1.3 Dating

Two organic samples were sent to the NOSAMS facility at Woods Hole Oceanographic Institute for AMS dating. The results are listed in **Table 9.6** and shown graphically in **Figure 9:21**. These two dates are reversed, with the top sample producing a date 107-578 calendar years older than the sample 40 cm lower in the core. Clearly, at least one of the dates must be wrong.



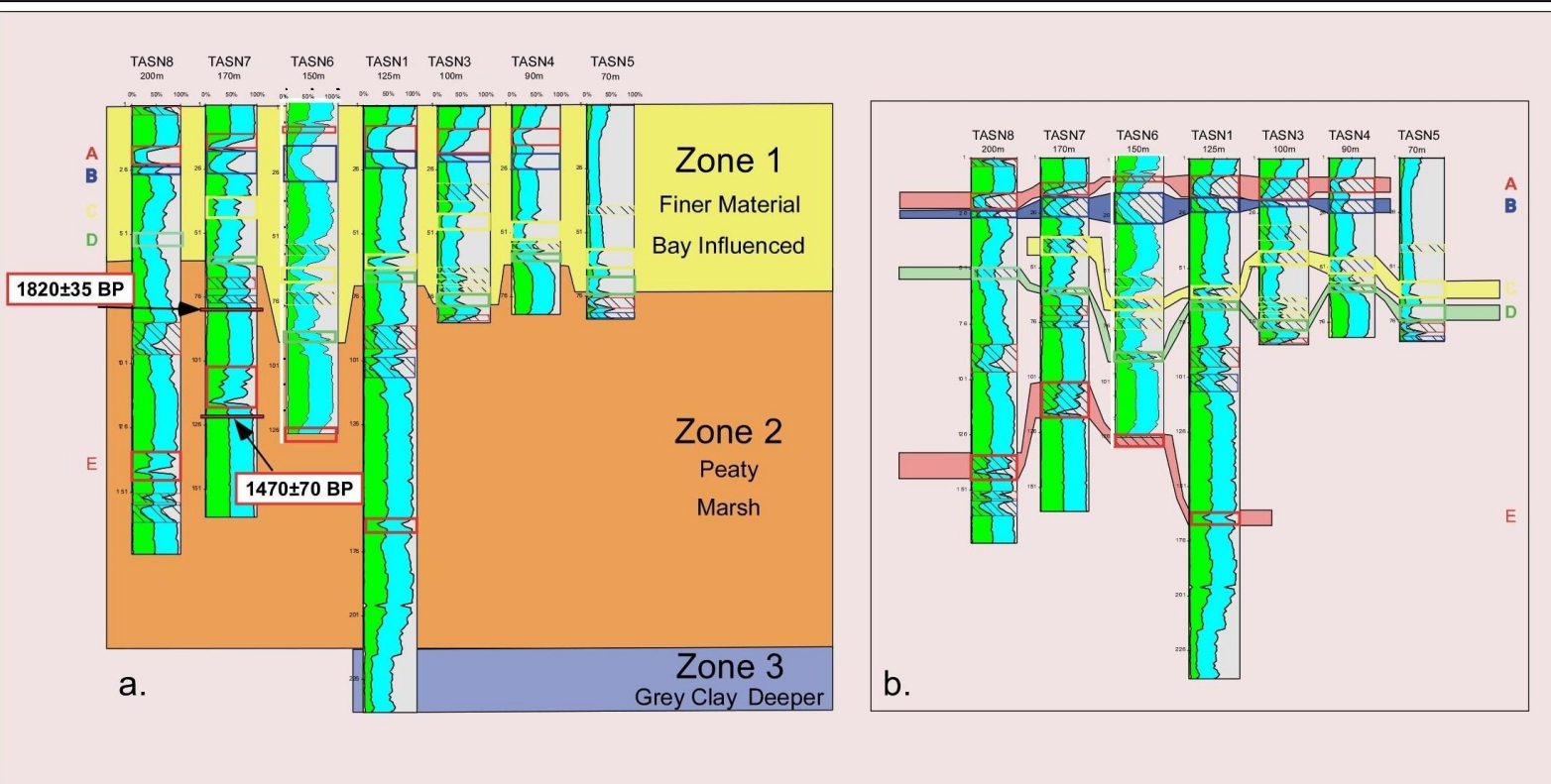
9.19 LOI curves and litholog for core TASN1. Shown are (a) water, (b) organic, (c) carbonate, and (d) residual (mainly silicate) percentages as individual curves; (e) a combined LOI curve, and (f) the core litholog.



9.20 TASN1 zonation based on (a) LOI and (b) lithologic data. Distinct compositional changes(c, d) at zone boundaries are marked by red dashed lines.

9.6 TASN7 chronology

Core	Depth (cm)	Material	Lab	Sample#	C ¹⁴ yr BP	Cal yr BP	%	AD/BC
TASN7B	81-83	Organic	WHOI	OS-72532	1820±35	1841-1864	0.03	86-109AD
						1691-1830	0.92	120-259AD
						1628-1654	0.05	296-322AD
TASN7C	122	Organic	WHOI	OS-70923	1470±70	1286-1521	1	429-664 AD



9.21 TASN transect zonation. Clastic layers (a) are correlated across the transect (similar colored boxes and capital letter designations indicate probable correspondence) though correlation is much less certain than in FBM and IV transects; used to create (b) a summary event diagram.

9.10.1.4 Transect Correlation

The zones delineated for core TASN 1 extend across the transect (**Figure 9:21**). Zones 1 and 2 appear in all cores. The transition between these zones is sharp throughout the transect, and occurs at roughly similar depths. These depths are:

TASN 5 -74 cm

TASN4 - 64 cm

TASN 3-80 cm

TASN1-74 cm

TASN6-90cm

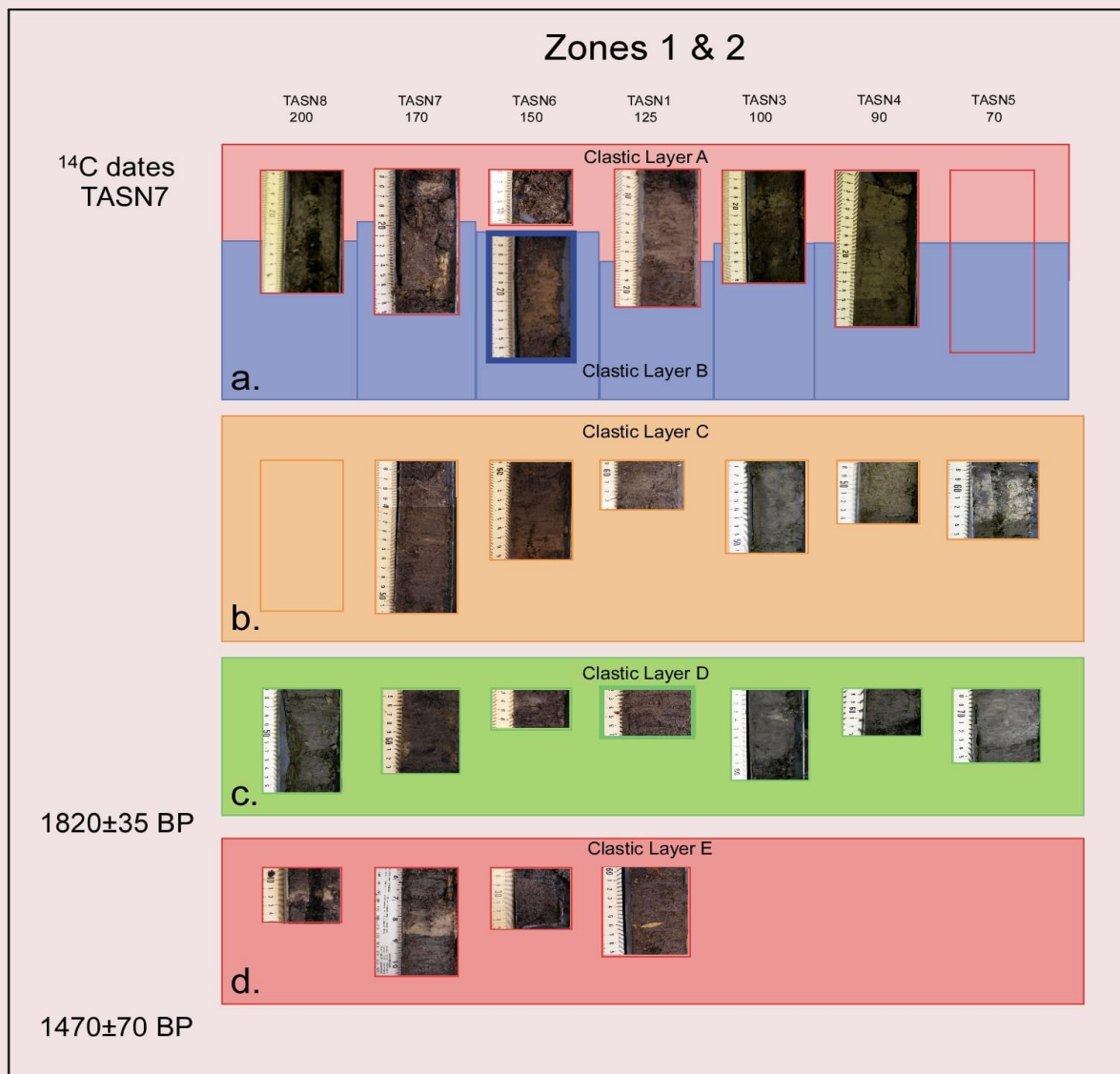
TASN7-61 cm

TASN8-61 cm

Zone 3 appears only in TASN1.

In situ plant roots in both Zones 1 and 2 suggest a shallow swamp or marsh. Zone1 is much muddier than Zone 2, suggesting increased influence/connection with the muddy PL. The reduction/lack of plant roots in Zone 3 suggests deeper water, more lacustrine environment during the time of deposition.

Clastic layers occur across the transect, frequently in Zone 1, and occasionally in Zone 2. These layers generally present as brown or gray clay in the more landward cores (TASN1,6,7, and 8) and as larger grain material in the seaward cores TASN 5, 4, and 3 (**Figure 9:22**). Stratigraphic coherency between these layers is much lower than in the FBM transect, probably due to the spatial and temporal variability resulting from the uneven sedimentation caused by the swamp's patchiness. Nevertheless, **Figure 9:21b** is an attempt at correlation of the more prominent/distinctive layers, based on visual properties, and stratigraphic positioning. Higher



9.22 Photos of the clastic layers (a) identified in the previous figure, using the same color scheme; the radiocarbon dates are placed vertically in accordance with their stratigraphic correspondence to the clastic layers.

probability correlations are marked by similarly colored boxes with thick margins, while uncorrelatable/problematic layers are marked by hatched, thin-walled boxes. For simplicity, the same color scheme is used as in the FBM and IV transects, but does not necessarily imply inter-site correlation.

The two top layers are easily distinguishable throughout. Assuming simultaneous occurrence across the transect of the abrupt change in depositional regime marked by the sharp transition from Zone 2 to Zone 1 allows the temporal correlation of a rather indistinct clastic layer immediately above this transition in all cores. This layer has somewhat arbitrarily been designated as Layer D. Layer C is much less distinct, and may be represented by any (or none) of the layers below B and above D in each core. Layer E occurs in all of the deeper cores, and is often visually distinct (**Figure 9:22d**).

9.10.1.5 Zone 1, 2 Clastic layers

9.10.1.5.1 Clastic Layers A, B (red,blue)

It is not always possible to separate these two layers, as A occurs immediately above and occasionally intermingled with B. Together they form a very distinctive unit, easily identifiable visually (**Figure 9:22a**).

9.10.1.5.2 Clastic Layer C (orange)

The correlation of this layer across the transect is extremely problematic, as a varying number of layers (none in TASN8 to five in TASN) of varying thickness occur between layers B and D. The thickest/most distinct layer in this interval for each core has been selected as the most likely candidate, marked by a thick-walled yellow box, but the identification is very weak.

9.10.1.5.3 Clastic Layer D (green)

As stated above, this layer, identified by its stratigraphic position immediately above the

abrupt transition between zones 1 and 2, is rather indistinct in the cores beyond 100m, while from 70-100m it is rather thick and large grained, consisting of sand (**Figure 9:22c**).

9.10.1.5.4 Clastic Layer E (red)

This layer is a thick and distinctive layer, especially at 170 and 200 m (**Figure 9:22d**).

9.11 Discussion

9.11.1 FBM Transect

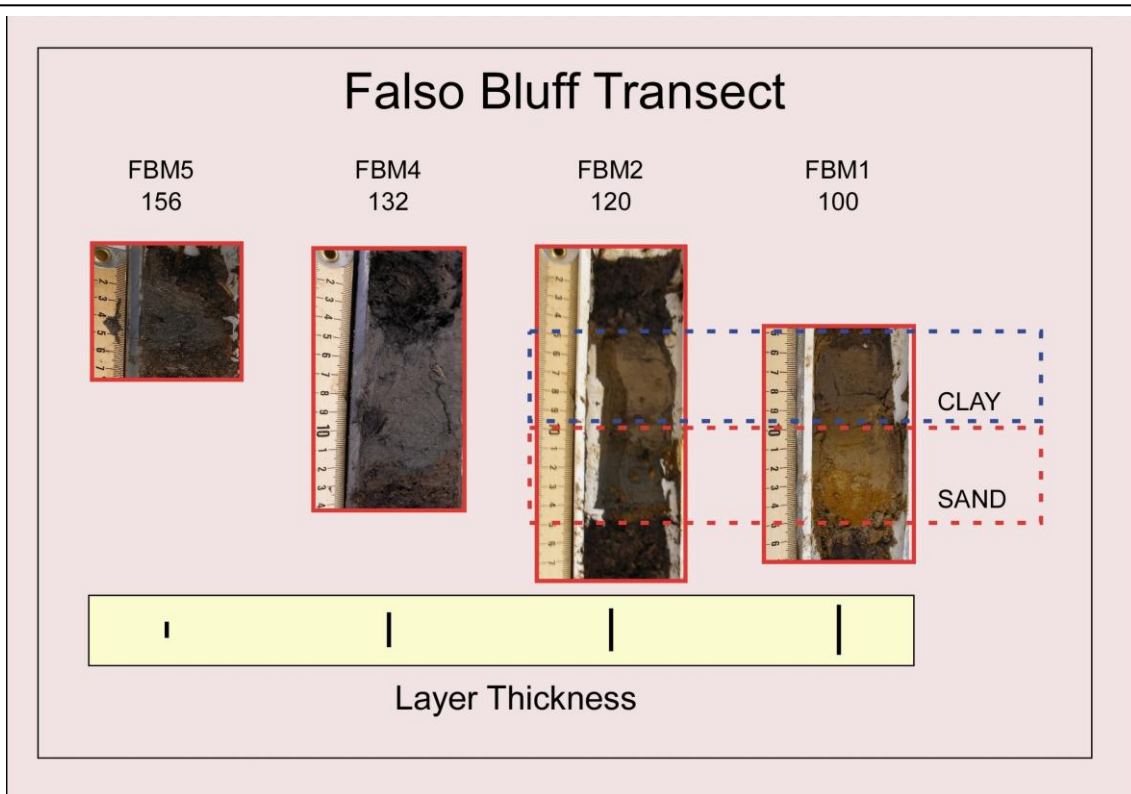
The current deposition regime in FBM marsh favors a highly organic black muddy peat; the clastic layers, particularly the larger grained material (sand) are allochthonous materials. The most likely source of this material is the sea, a few tens of meters to the east. The only stream, Falso Bluff Creek, ~100 meters to the north, is short (<800 m), narrow (< 2 m), shallow (<0.5 m) and tranquil. It has no direct connection with upland sediments, serving merely as tidal connection between the Caribbean and the sheltered back bay, the bottom material of which is almost entirely silt -size or smaller. The most likely candidate process for the transportation of large-grained marine material into the marsh environment is the storm surge associated with a hurricane. Although the beach barrier is low, the extremely dense marsh vegetation should quickly filter out any sand resulting from wave action from minor storms. Based on this reasoning, Clastic Layer A is proposed as having resulted from the passage of Hurricane Joan in October of 1988. Although ¹³⁷Cs analysis has not yet been performed to confirm the date, the layer's position near the core top and its internal stratigraphy argue for a recent overwash event, of which Joan is the most recent and intense. A visual examination of the layer (**Figure 9:23**) shows both the landward thinning and fining and upward fining associated with overwash fans. At 100 m the layer is ~10 cm thick, with a sand base topped by brownish gray silt/clay. At 120 m, although the layer is the same approximate thickness, both the units have reduced grain size,

although the upward fining is still immediately obvious. At 132 m the layer thickness has reduced, and the larger grain material has fallen out. At 156 m the layer thickness has reduced to ~ 4 cm, and the material is finer. A sharp bottom contact occurs in all cores.

Flooding from Joan was severe, washing out >400 miles of roads and 30 bridges (36 more were severely damaged) (Gerrish, 1988). Eyewitnesses of Hurricane Joan report that following the storm Bluefields Bay “turned red”, presumably from the vast amount of clay eroded from the uplands as a result of the torrential rains. It is worth remembering that the watershed for the bay is large enough that even during normal rainy seasons fluvial input reduces the salinity of BB to 1 ppt. Given the closed nature of the bay, blocked in front by Isla del Venado and the peninsula upon which the FBM transect is located, it is very possible that the (mainly fresh) water trapped in BB slowly drained to the sea over these barriers. This could account for the bimodal stratigraphy found in the cores. Following this argument, the basal sand would have been deposited during the storm by the storm surge, while the finer-grained top material could have settled out of the water column over a period of days. The location of the site in a depression would have favored the retention of water and the slow settling of silt/clay materials.

The same arguments that favor Clastic Layer A’s identification as Joan’s sedimentary signature can be applied to the deeper clastic layers. The only possible source of sand is the sea; although alternative processes capable of transporting this sand into the marsh are possible (discussed below), the most likely process is hurricane-driven storm surge. Although smaller grained clastic material might result from back bay flooding rather than storm surge, the rarity of the tremendously large rain fall anomalies required to produce such events suggest an association with the region’s largest rainfall producers, which, of course, are hurricanes (INETER, 1999).

It should be mentioned that not all drops in the LOI curve are identified as resulting from

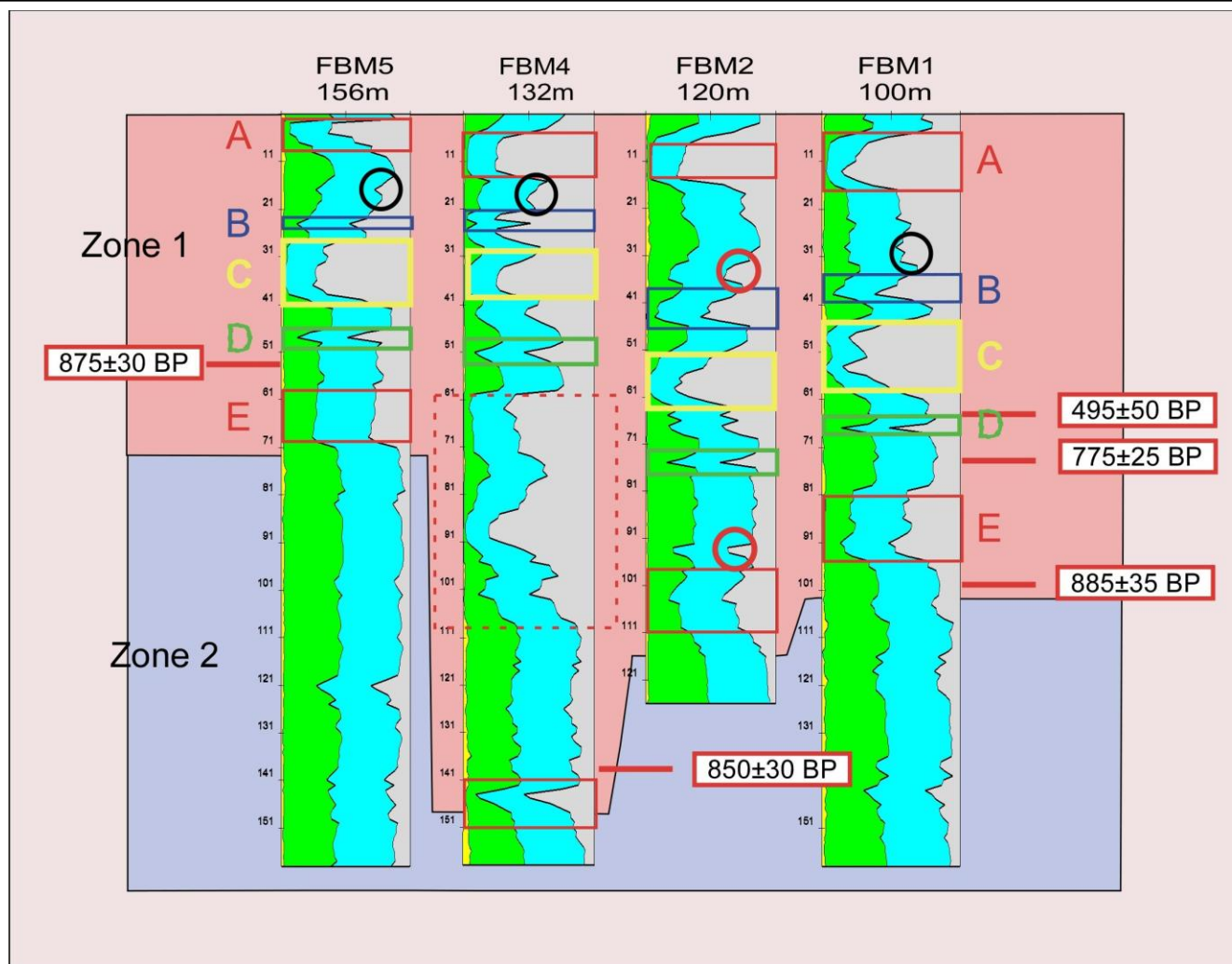


9.23 Photos of the top FBM clastic layer, displaying inland thinning and fining, as well as upward fining within cores FBM1 and FBM2. Sedimentological considerations cause us to identify Hurricane Joan (1988) as the most probable source of this layer. The complicated stratigraphy of the layer in cores FBM1 and 2 possibly results from differing immediate and delayed depositional modes associated with Joan.

hurricanes, nor do all correlate perfectly across the transect. Examples are noticeable dips in the LOI data for core FBM2 at cm 34-36 and cm 93-95 (red circles) (**Figure 9:24**). The dip at 34-36 actually correlates quite well with smaller dips in the other three cores of the transect (black circles), indicating that this is probably a minor event. The lower dip is quite obvious both visually and in the combined LOI curve; however there is no correlation with the other cores. Presumably this is the result of some local disturbance. A series of similarly uncorrelatable dips occurs from ~60-100 cm in core FBM4, which we have previously identified as probable disturbance (red dashed box).

Based on LOI data and visual analysis, we have identified Clastic Layers A-E as hurricane-generated. Radiocarbon dating supports this view. Samples from the top of Layer E from FBM5 and FBM4 and the bottom of the layer from FBM1 produced overlapping radiocarbon dates, implying that the intervals, up to 14 cm thick, was deposited almost instantaneously. By comparison, the 9 cm interval between the two samples taken from higher in FBM1 spans a 110 year interval. As indicated by the layer thickness, water, organic, and residual values, Layers A (red), C (yellow), and E (red) appear to have resulted from more powerful events than Layers B (blue) and D (green). Below Zone 1, an additional clastic layer (Layer F) occurs in Zone 2 in cores FBM1 and 5 (**Figure 9:25**). (Cores FBM2 and FBM4 do not penetrate to this level). This has also been interpreted as resulting from a hurricane, particularly due to the abruptly distinct lithological changes in cores FBM5.

Combining this information produces a hurricane strike record (**Figure 9:25**) for the site of five events, all identifiable in all cores across the transect since 885 ± 35 ¹⁴ C yr BP. Calibrating this date to calendar years produces a single date range of 730-910 cal BP (present being AD 1950) , or the period AD 1040-1220. Three of the storms left significantly larger



9.24 Non-event clastic layers for the FBM transect. The circles represent small clastic layers that probably represent minor event (black circles, upper red circle in core FBM2), or some type of local disturbance (lower red circle, core FBM2). The dashed red box in core FBM4 most likely results from anthropogenic disturbance.

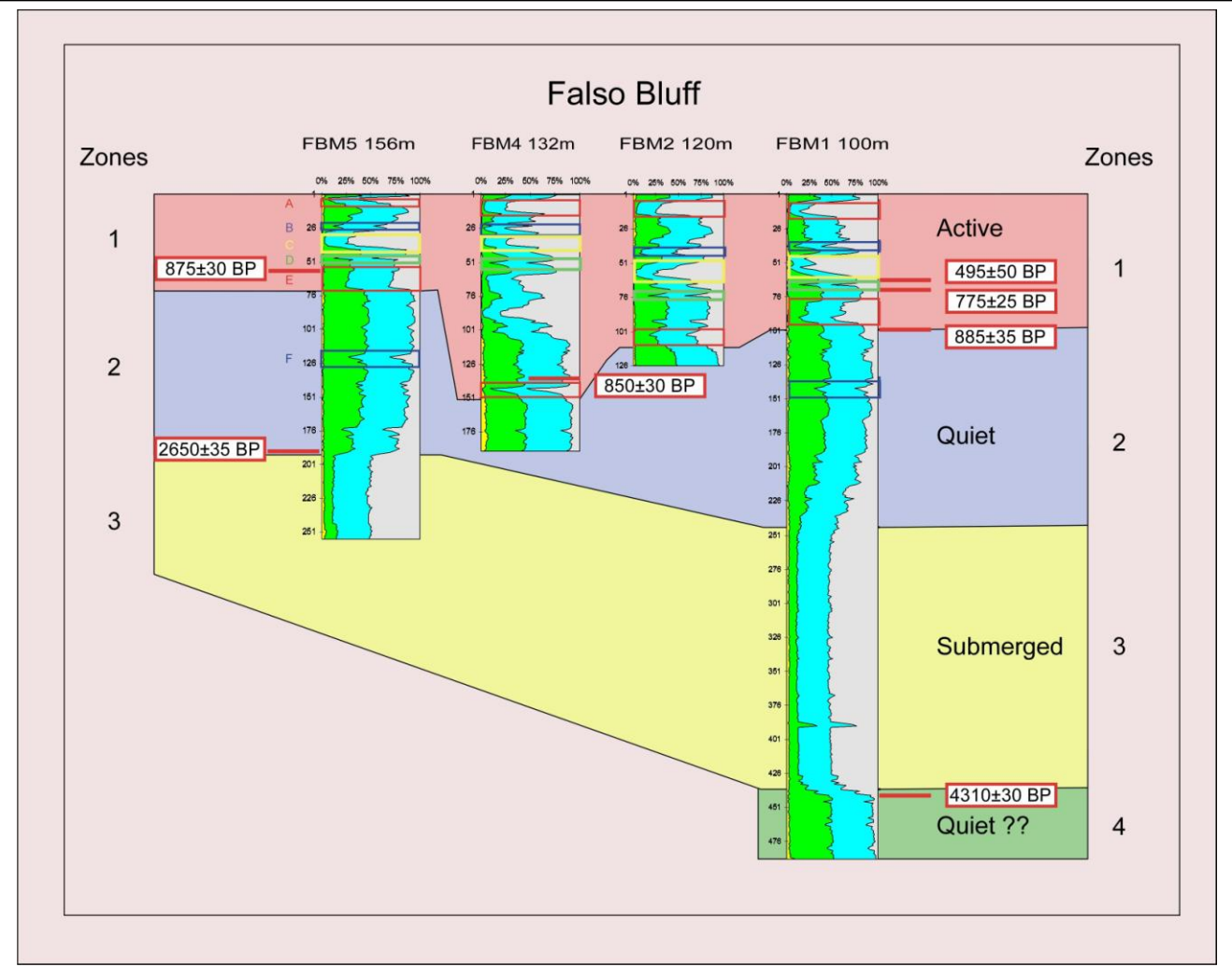
sedimentary signatures than the other two. Return interval can be calculated as between 160-200 years.

There is no basic sedimentary difference between zones 1 and 2, other than the frequency of the clastic layers. This indicates that general environmental/depositional boundary conditions remained relatively constant for the site since the beginning of Zone 2. Because the presence of Layer F in Zone 2 indicates that the site was capable of recording hurricane events during this period, the reduction in strike frequency for the zone is probably an accurate reflection of hurricane activity. For this reason, the boundary between zones 1 and 2 marks the regime change in hurricane activity from “Active” to “Quiet” (**Figure 9:25**).

The return interval for Zone 2 can be calculated using the date supplied by the sample from the bottom of Zone 2 from core FBM5. The ^{14}C date of 2650 ± 35 calibrates to two date ranges, from 2736-2844 BP, or ~ 2000 years older than the top of the Zone. Since only a single hurricane is recorded for this period, the return period is ~ 2000 years, or 10-12 times longer than for Zone 1. The annual average probability of landfall therefore increases by an order of magnitude, roughly two to three the increase found for activity regime changes along the northern coast of the Gulf of Mexico (Liu, 2004). Naturally, however, precise statistics cannot be generated from a data set of one.

Zone 3 has a very different environmental/depositional environment. The lack of *in situ* plant roots and the general aspect of the material indicate that water depth was deeper during this period. Because sand transport often stops abruptly when encountering a water barrier (**Appendix B**) it is unlikely that hurricane-generated washover lobes would have been recorded during this period, as seems to be the case.

Zone 4 is very similar to Zone 2, and could be expected to record hurricane strikes, depending upon proximity to the sea. This period ended shortly after 4310 ± 30 ^{14}C yr BP, which calibrates to two date ranges from 4835-4960 cal BP, or BC 2886-3011. No hurricane strikes are



9.25 Paleostrike and activity regime record for the FBM transect.

recognized for this period. This lack of storm signal could result from either lack of strikes, or reduced site sensitivity, possibly related to an increased distance from the sea resulting from lowered sea level. Barring unusual local factors, at 5000 BP sea level should have been within 4 m of the present (Toscano and Macintyre, 2000) and possibly within 2 m (Gischler and Hudson, 2004). Because the dated sample was extracted at a depth of 444 cm, the elevation of the site relative to sea level at the time was probably at least as low, and possibly considerably lower than at present. Although detailed information is lacking, best estimations of shore translation favor minimal lateral movement, supported by the LOI similarities between Zones 1 and 4 suggesting similar environments, hence similar distances to the beach. A palynological examination of the zones could perhaps clarify this situation. The evidence therefore supports the view that the lack of clastic intervals in Zone 4 result from lack of hurricane activity and not reduced sensitivity.

9.11.1.1 Recording Sensitivity

An important factor in establishing a paleostrike record is the determination of a site's recording sensitivity, particularly in order to establish the minimum storm intensity required to deposit a recognizable sedimentary signal. Such determination usually requires the examination of the sedimentary effects of a modern analog, i.e a historical storm of known intensity. Layer A is a fairly representative of the six identified layers, generally thicker than Layers B, D, and F and roughly equal to Layers C and E. Identifying this layer as Joan thereby establishes the other five events as having been of roughly similar or slightly lower intensities. This is a conservative estimate, as due to the slowly rising sea level, the distance to sea has probably decreased slightly for each core over time, with earlier events having to have transported material over slightly larger distances to achieve the same sedimentary event. A further consideration is possible

compaction of the event layers deeper in the cores. These factors, however, are counterbalanced by the larger grain size evident in Layer A. It is not unreasonable to assume that the site is capable of recording high category three storms and above. It should be noted that height of storm surge is not directly related to intensity classification, as storm size, duration, and angle of approach are also important. Although Joan was a category four storm at landfall, that was primarily a result of rapid intensification immediately prior to eyewall impact. The storm did not necessarily generate as large a storm surge as a larger lower category storm, or a storm of similar size that maintained a similar intensity for a longer period of time.

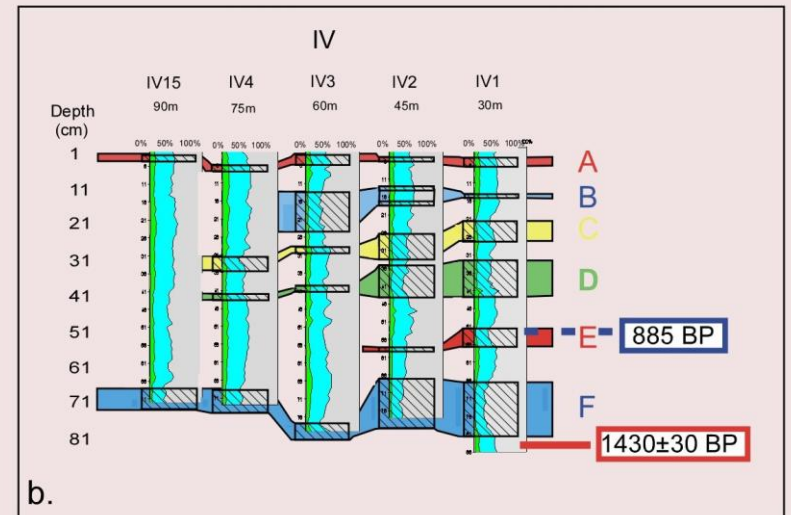
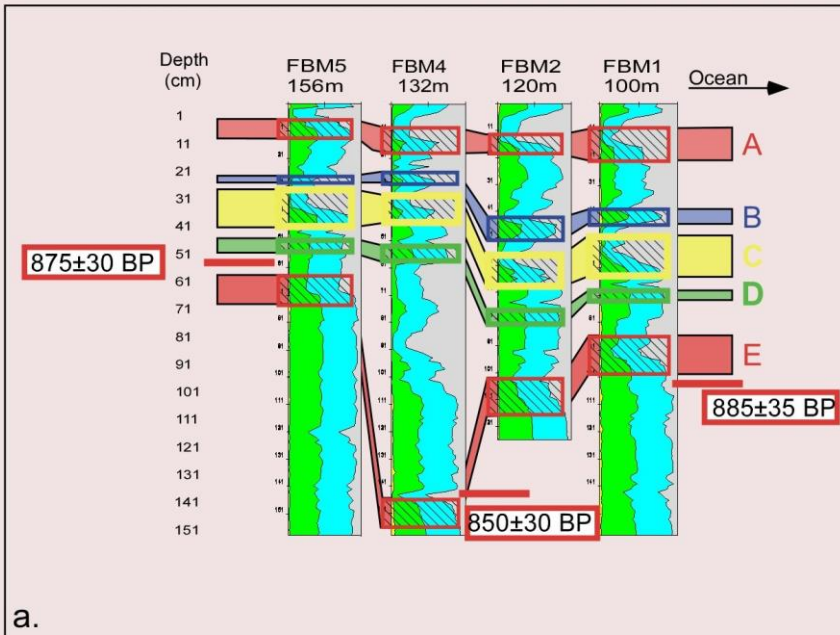
9.11.2 IV Transect

The IV transect is located ~ 26 km south of the FBM site, very close to the location of eyewall impact for Hurricane Joan (**Figure 9:6**). The presence of visual sand layers, distinctly different from the surrounding clay sediments and their landward thinning suggest that these layers are hurricane generated. The layers are relatively evenly distributed vertically, indicating a constant hurricane regime. Layer A, presumed to have resulted from Joan, due to its stratigraphic location, is, rather surprisingly, one of the thinner layers. Layers D and F have significantly larger sedimentary signatures.

The striking similarity in patterns between these layers and the Zone 1 clastic layers from FBM (**Figure 9:26**) suggest that they are recording a very similar set of events. The ^{14}C date from the bottom of core IV1 offers some support for this view and permits some speculative correlation between the FBM and IV transect strike records. The date of ~ 885 ^{14}C BP for Event E is marked by three overlapping dates along the FBM transect. Assuming constant sedimentation, this age corresponds to cm 51 on IV1, given an age of 1430 ^{14}C BP for cm 83. On **Figure 9:26** this depth is marked by a blue dashed line, and occurs within Event E on that core.

If this calculated date is correct, a very nice correlation is established between the strike records from the two sites, with both sites showing five storms over the period. Although similar coloring and numbering is employed for the two sites, this does not imply that an identical set of events are being recorded at both FBM and IV. It should be stressed that the accuracy of the calculated date is far from certain, given the vagaries of the relationship between radiocarbon and calendar ages and the inconstancy of deposition, particularly in an event-driven environment. However, with the dating available, aided by the fact that the ^{14}C age calibrated to a single date range in this case, the best estimate draws a parallel between the activity shown in the core tops.

Some further general observations can be made between the two sites. The clastic layers are generally thicker along the FBM transect and are present at greater distances inland, though grain size is often smaller. This can perhaps be explained by site differences. FBM sits behind a well developed beach and a relatively high vegetated ridge that has developed enough soil to support coconuts and grass (**Figure 9:4**), while the IV transect consists of a thin (>90 cm) clay cover over a stiff subsoil, which lacking a beach, opens directly unto the sea. At IV, as there is no loose surface soil or beach sand, the only material available for landward transport is sand eroded from below sea level. The larger grain size and reduced availability results in limited amount/distance of transport. At FBM, the availability of unconsolidated dune sand and soil means a greater transport load consisting of mixed material. Upon encountering the thick marsh vegetation the sand quickly settles out, while the silt and clay are transported farther inland. Post event settling from clay-rich BB waters draining out over the blocking landmass, resulting in the clay cap seen in FBM Layer A, is not likely at IV, as its proximity to the southern bay entrance would presumably result in a rapid outward flow, possibly even removing sand deposited during the storm surge. The combination of these factors would tend to reduce the sedimentary



9.26 Strike record correlation between the (a) FBM and (b) IV transects.

signatures of hurricanes in this location.

Based purely on layer thickness, the lower layers represent more intense storms than the top event layer, provisionally identified as Joan. Since it is unlikely that the site was the location of eyewall impact for all the other storms, as it was for Joan, this would mean that the storms were all extremely powerful, possibly category 5. However, at this site, intensity of storm/surge height is perhaps better estimated by extent of spatial coverage, given the grain size available for transport. Events A and F appear in all cores along the transect, whereas none of the other four appear beyond 75 m. It is also possible that recent erosion has removed significant amounts of beach and foreshore sand, thereby reducing the sedimentary signatures of more recent storms. Following this reasoning, Event F presents extremely large due to an abundant sand supply, which later became unavailable. It is essential to remember Isla de Venado's anomalous lack of beach sand, presumably caused by the disruption in alongshore transport resulting from the open water at the northern end of the island.

In addition to the presence of the very large sand layer (Event F) at the bottom of the IV transect, other pattern differences between the FBM and IV can be noted. If, in fact, these strike records are recording the same storm set (uncertain), some inferences concerning track locations can be made. At FBM, Layer C has a larger sedimentary profile than Layer D, while the reverse is true at IV, suggesting a more northern track for C and a more southern track for D. Event E has a very pronounced signature all across the FBM transect, yet is relatively insignificant at IV, only extending to 45 m. If this is the same event at both locations, it is reasonable to assume that the track passed closer to FBM than IV. Event B has a rather unusual signature across the IV transect, as it appears as two separate sections at 45 m and thickens significantly at 60m. It is possible that this is the result of the mingling of the sedimentary signature separate events

occurring in relatively rapid succession. We have previously suggested that a small dip directly above Event B in all the FBM cores might represent a minor event. Possibly this event left a slightly larger, though spatially sporadic mark at the IV site, combining with Event B to fill a topographic low at 60 m, while separated by intervening sediment at 45m.

9.11.2.1 Strike Record

The evenly-spaced vertical distribution of sand layers across this transect indicates that hurricane landfall activity has been fairly constant at this site throughout the period investigated. Transect zonation therefore consists of a single Active Period, extending over the last 1500 years. Temporally, this does not match with the FBM record, which shows a transition from Active to Quiet ~ 1000 BP. The stratigraphic position of Event F at the bottom of the cores presents the possibility that the sand is actually basal, formed as a result of much earlier environmental conditions, not overwash, thereby resolving this differences in activity regimes. However, this is probably not the case. Although penetration did not process beyond the Event F sand layer in cores IV2, 3, 4, and 5, in IV1 at least 6 cm of visually different material, with higher water, organic, and carbonate values are encountered below Event F. Additionally, the underlying substrate, obvious along the eroded edge of the island is the ubiquitous stiff red clay, not sand.

Several possible explanations for the differences in activity regimes between FBM and IV exist. Perhaps the ^{14}C date is incorrect, a result of the sample including older reworked material eroded from the bank and deposited onshore by a storm. Possibly sedimentation is basically storm derived-meaning that sedimentation rates are extremely slow during inactive periods and that the short interval between the sample and the bottom of Event F represents a relatively long period of time. In any case, the discrepancy depends upon the presence of a single

event, which limits its statistical significance. It is possibly significant that the date obtained from slightly below Event F (1430 ± 30 ^{14}C yr BP) in IV1 overlaps with the date (1470 ± 70 ^{14}C yr BP) obtained from just below the single event that occurred during the Quiet Period in core TASN7.

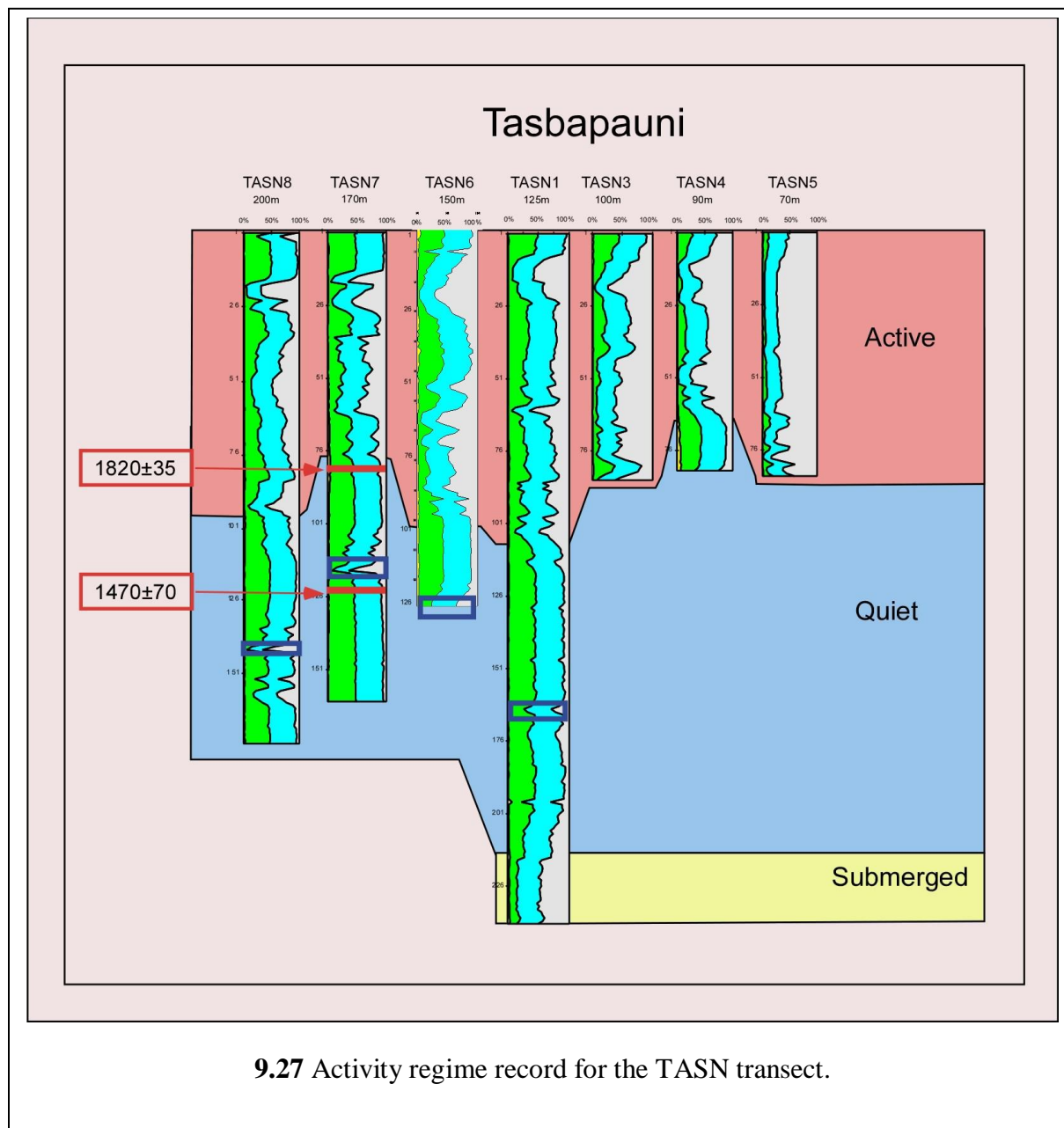
9.11.3 TASN Transect

The clastic layers in the Tasbapauni transect are generally identified as hurricane-generated, following the same arguments advanced for the FBM and IV sites. One important feature of this transect is the number of uncorrelatable clastic layers, which occur with much greater frequency than in the other two transects (**Figure 9:21**). Underlying geological and biological factors offer a possible explanation for this stratigraphic heterogeneity. Even though the entire area can be classified as “hardwood swamp”, considerable vegetational variation exists across the transect. Cores TASN 5, 4, and 3 are short, meeting refusal between 82-86 cm, indicating a sill of stiff material that forms the seaward lip of an antecedent depression, now slowly being infilled by the decaying swamp vegetation. Along the transect maximum depth occurs near core TASN1, after which the base rises landward. Within this depression, vegetation changes from low bush (TASN 5, 4, and 3) to dense low palms (TASN1 and 6) to taller hardwood species (TASN 7 and 8). In the latter two areas the swamp is patchy, with wet, low, soft spots alternating with more solid “islands” of much firmer soil centered on the root systems of the larger trees. It seems quite likely that sedimentation does not occur evenly over the entire swamp; material dropped onto the small tree islands (a few m^2 in area) will be washed into the topographical lows-the soft wet sections. Random variations in the location of trees over time (and the infilling of the hollows left as they decay) can be expected to have introduced a significant amount of variability into core stratigraphy.

The division between Zones 1 and 2 is sharp, marked by a visually obvious increase in muddiness in Zone 1. However, this boundary change is not readily apparent in the LOI, as both the clastic and organic intervals are very similar in both zones. The most likely explanation for the muddy texture of Zone 1 is increased influence of the PL sediments. PL is very turbid, with transparency values between 1.8-3 m (Dumailo, 2003), with the dark suspended sediments visible even in aerial photos (**Figure 9:2**), while the Caribbean side of the peninsula is dominated by light colored sand. This is reflected in the cores, as the clastic layers in the cores seaward of the sill often contain sand, while from 125 m landward the material is almost entirely clay. The abrupt increase in bay mud around 70 cm depth across the transect must reflect a significant geomorphological event. Two obvious possibilities present themselves. The closure or heightening of the narrow connection with the sea in the southeast corner would raise PL water levels, leading to more frequent /higher elevation flooding of the surrounding land (**Figure 9:2**).

Another possibility is the sudden increase in freshwater influx to the lagoon, particularly if the Rio Grande de Matagalpa, a very large river that passes a few km to the north of PL, changed course and began discharging through PL. One investigator has suggested that PL was formed as the Matagalpa river valley during an earlier course change (Radley, 1960).

Whatever event or process(es) caused the sedimentation change, it did not affect the sensitivity of the site significantly, as clastic layers are recorded on both sides of the zone boundary (**Figure 9:21**). As a result, hurricane activity zones can be established through Zone 2 (**Figure 9:27**). As at FBM, due to changed boundary conditions, hurricanes were probably not recorded during Zone 3. In Zones 1 and 2, 5-7 events are found between the core tops and Layer E (**Figure 9:21**), although the spacing and number of events are highly variable by core, as discussed above.



9.11.3.1 Strike Record

The discrepancy in the two radiocarbon dates makes the determination of return intervals and annual strike probabilities highly problematic.

Two distinct sets of calculations follow, based on the two different radiocarbon dates.

9.11.3.1.1 Cm 122- 1470 \pm 70 ^{14}C yr BP

This date comes from a sample taken slightly below Layer E in TASN 5. At the 95 % confidence level this date calibrates to a single date range of 1286 - 1521cal BP (present being AD 1950), or the period AD 429-664. Simply dividing these numbers by 5-7 events produces an average return interval from 180 to 300 years. However, this calculation is probably invalid as it incorporates data from two distinct activity regimes (**Figure 9:27**).

Moving backward from the present, the transect displays an active period, preceded by a quiet period marked by a single event, and finally a submerged period, which probably does not record events. This pattern is very similar to that exhibited in the FBM transect (**Figures 9:25, 26**). It should be noted that the active period extends beyond Zone 1 into Zone 2 in all cores except TASN4. Although the Active/Quiet boundary has not been dated, a simple calculation based on constant sedimentation produces a date of 928 ^{14}C yr BP for the regime boundary (77 cm) in core TASN5. This date is within a few years of the 885 \pm 35 date established for the Active/Quiet boundary along the FBM transect. Calibrating this date with a 35 year error bar produces a date range from 766-926 calendar years before AD 1950 or ~the last 800-1000, basically identical to the regime transition date for FBM. Counting 4-6 hurricanes for the period gives an average return period of 133-250 years. The return period for the lower inactive period is much longer, with one event occurring over an estimated (based on constant sedimentation and

the regime change date as above) 700-1000 years for TASN1. The landfall probability therefore increases ~3-6 times across the regime change.

9.11.3.1.2 Cm 83- 1820± 35 ¹⁴C yr BP

This date comes from a sample 22 cm below the sedimentary (mud/peat) transition, and six cm below the activity regime (Active/Quiet) transition. The date calibrates to three separate date ranges (**Table 9:6**), ranging from 1628-1864 cal yr BP. However, as 92.2% of the area under the curve occurs during the period 1691-1830 cal yr BP (AD 120-259), the sample most likely can be attributed to that period. Dating the regime change to ~ 1800 cal yr BP gives an average return interval of 300-450 years for the active period.

Assuming constant sedimentation, the bottom of TASN7 at 162 cm corresponds to an age of 3596 ¹⁴C yr BP; subtracting the 1800 year age for the end of the Active period gives the Quiet period a minimum duration of ~1800 years. With a single storm for the period, the return interval is 1800 years. In this case landfall probability during the active period is ~ 4-6 times as high as during the Quiet period, similar to the change calculated under the alternative dating scenario.

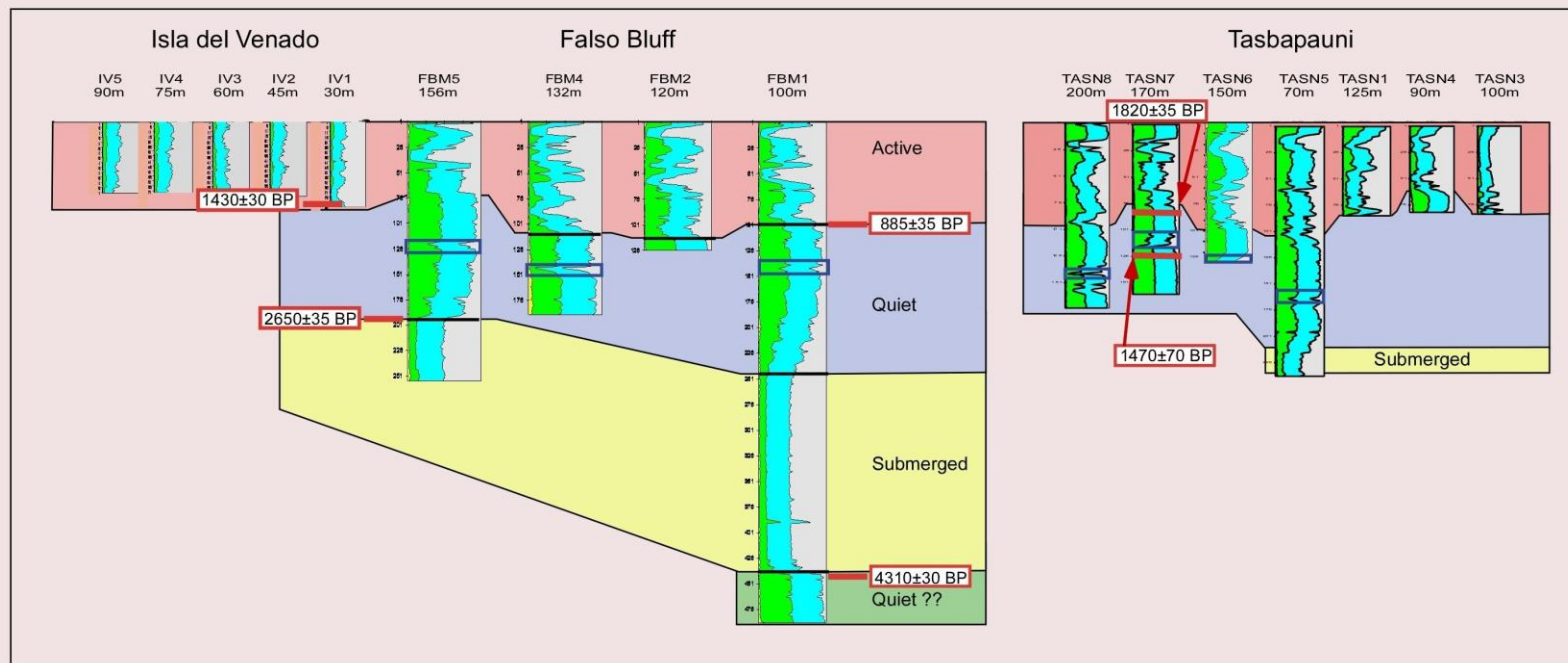
These calculations should be regarded with skepticism, as, even without reversed dates the assumption of constant sedimentation may introduce error, especially in locations dominated by event-driven deposition. Possible erosion/compaction of material can further reduce the reliability of such calculations. Clearly, there is a large difference in the annual strike probability depending upon the date used; just as clear, however, is the difference in activity across the regime change, regardless of the numbers. Regime change is clear; the dating of the change remains murky. A more accurate chronology can help resolve this issue, though care must be taken.

9.11.3.2 Recording Sensitivity

Establishing either the threshold storm intensity necessary for creating a storm signal or estimating the magnitude of the paleostorms for TASN site is difficult, due to a lack of a modern analog. Hurricane Beta made landfall as a category 2 storm with maximum sustained wind speeds of 90 knots near the mouth of the Rio Grande de Matagalpa on October 30, 2005 (Pasch and Roberts, 2006) (**Figure 9:6**), ~17 months before we cored the site. However, Beta was a rather compact storm, with hurricane-force winds extending only 30 km and tropical storm-force winds only 95 km from the center (NWS, 2005), and had already begun dissipating before making landfall. Although the TASN transect is within 30 km of the location of landfall, no sedimentary evidence of the storm was found, with the possible exception of a small subvisual dip at the top of TASN 8. From the condition of the forest and verbal reports from the nearby village of Tasbapauni, Beta did not have severe local impacts, possibly due to the area's location along the storm's weaker left front quadrant. This track location would more likely result in flooding from the PL side (perhaps explaining the dip in TASN8, the most bayward core) and very little onshore transport from the Caribbean. Beta's inability to leave a sedimentary footprint can be used as evidence to exclude small category two storms passing to the north. A rough estimate would therefore place the threshold value at either the major or catastrophic (category 3 or 4) storm level.

9.11.4 Integrated Site Correlation

Combining the three transects, by arranging them from north to south on a common vertical scale, produces a strikingly coherent picture of hurricane activity for the area (**Figure 9:28**). Regime changes, both from Active to Quiet and from Quiet to Submerged occur at almost identical depths for the FBM and TASN transects. Dates also agree, when using the TASN7 date



9.28 Activity regime record for the IV, FBM, and TASN transects, set at a uniform vertical scale.

from 122 cm (1470 ± 70 BP), which fits in at near perfect depth with the five dates from FBM. As shown above, an interpolated date, based on constant sedimentation, places the hurricane regime change as occurring at TASN within a few decades of the transition at FBM. Using the TASN8 date from 83 cm (1820 ± 35 BP) complicates the issue and argues for elevational disequilibrium regarding marsh/swamp accretion. The IV transect has excellent stratigraphic correlation with the FBM transect clastic layers at the top, perhaps recording some of the same events. However, activity at this site (in the form of a single, large storm) continues beyond the beginning of the Quiet Period at FBM.

Based on the dates from FBM, which has the most complete and consistent chronology (R^2 values of 0.995, 0.997), the pattern that emerges from combining the transect data is:

0-1000 cal yr BP – Active period

Return interval-133-250 years

1000-~3000 cal yr BP – Quiet period

Return interval -2000 years

~3000-5000 cal BP – Non-recording, (submerged)

<5000 cal BP – Unknown, (Quiet or non-recording)

Changes in return intervals imply that the regime change from Quiet to Active increases landfall probability by a factor of 3-6 at TASN and 10-12 at FBM. This is at least as large as the increase associated with a similar regime change for the northern Gulf of Mexico (Liu, 2004).

9.11.5 Regional Constraints

As TASN is > 65 km north of FBM, which is > 25 km north of IV, the complete transect spans > 90 km, much greater than the maximum distance over which a single storm will usually generate overwash deposits. This suggests that inter-site correlations reflect patterns in regional

hurricane activity, and are not merely duplicate records of the same storm set, although there is probably some overlap, particularly between the FBM and IV.

Neither do geomorphological conditions seem to be exerting significant control over clastic layer frequency changes across the activity regimes. In the FBM transect, clastic layer frequency changes significantly despite a constant (high organic/marsh) depositional environment, whereas at TASN clastic layers continue at a relatively constant rate across a marked change (peat to clay) in the depositional environment. Both transects, however, display similar clastic layer frequency changes at the same approximate depth and age, although dating is somewhat tenuous for the TASN transect. This supports the view that the frequency changes in clastic layer deposition are being driven by change in hurricane activity, not geomorphic conditions.

A possible alternative explanation is that hurricane activity remained constant while lowered sea levels reduced the site sensitivity in lower sections of the cores due to increasing distance to the sea. This seems unlikely for two reasons. First, a distinct clastic layer is found in the Quiet Period in both transects, indicating that events were, in fact, being recorded. There is no particular evidence supporting this event as exceptionally large in either transect. Secondly, minimal sea level change has occurred during the period; the date of 1430 ¹⁴ C yr BP in the middle of Zone 2 (TASN transect) correlates to sea level drop of between ~ 50 cm (Gischler and Hudson, 2004) and 1 m (Toscano and Macintyre, 2003), not enough to significantly alter recording sensitivity. Given the core depth of the dated sample (122 cm), the core site may have actually been at a lower elevation relative to MSL than at present. The distance to the sea at that time depends on a number of unknown factors, primarily the transgressive/progressive nature of coastal morphology, controlled by the relationship between sea level rise and sediment supply. If

the accumulation rate of the delivered sediment is greater than the rate of sea level rise, then the coast will prograde and core-sea distances may actually be increasing. No clear evidence exists to support coastline movement in either direction, which in any case, would exhibit both temporal and spatial variation. Because the current rate of sea level rise is probably the highest of any period during the late Holocene, the existence of an open beach along almost the entire Nicaraguan coast, despite microtidal conditions, suggests that coastal elevation is/has probably been matching sea level rise. It is possible to imagine scenarios in which the relative height, and location of the barrier has remained fairly constant, with higher sea levels driving offshore sands higher unto the barrier, and building the barrier vertically, and not horizontally. This is particularly likely in the case of the Tasbapauni transect, which is located on a barrier built on top of a stationary sandstone core (Radley, 1960; Christie, 2000).

The ability to distinguish between hurricane and tsunami generated layers remains rather problematic. Large tsunamis can often be identified reliably due to their ability to transport large material farther inland and/or to higher elevations than hurricanes (**Chapter 2**). Generally lacking reefs, however, there is very little large material available for landward transport along the Nicaraguan coast, and very few areas of higher elevations to which it can be transported. Smaller tsunami events can perhaps be confused with hurricanes, particularly from the limited evidence available in 2'' diameter cores. However, geological characteristics greatly reduce the probability of tsunami strikes for the area. As discussed in **Chapter 2** and shown in **Figure 2:16**, earthquake-generated tsunami risk for the Caribbean is greatest in the northeast area, while volcanic-generated tsunami risk is greatest to the southeast. Both areas are > 2000 km from the coring sites. Although transAtlantic teletsunamis have been reported for the Bahamas and the Lesser Antilles (Scheffers et al., 2002; Kelletat et al., 2004; Scheffers and Kelletat, 2006), the

configuration of the Greater Antilles generally blocks their path to Nicaragua. Submarine slumping of relatively high angle normal faults along the Cayman Trench presents the only nearby source of tsunamis. However, the offshore bathymetry greatly reduces the tsunami threat posed by all of these sources. As discussed above (**Figure 2:15**), the Nicaraguan Rise extends nearly to Jamaica, deepening to only to 45 m 250 km offshore. Due to the extremely long wave length of tsunamis (Masselink and Hughes, 2003)), and wave mechanics which force waves to begin breaking when the bottom depth is half the wave length, tsunami waves will break 100's of km offshore, minimizing their coastal impact. Due to these geologic features, tsunami-generated clastic layers should be extremely infrequent for the area, and therefore not likely to obscure hurricane landfall activity patterns, even if occasionally misidentified.

The apparent age/sediment depth coherency exhibited between the FBM and TASN transects is surprising, particularly as the sites are associated with different estuarine systems. If further dating supports this coherency, a regional scale control over sedimentation rates is implicated. The obvious candidate is sea level, meaning that wetland surface elevations can be utilized as sea level proxies. A related concern is that the rather abrupt onset and termination of the submerged period from 3000-5000 BP cannot be easily explained by unidirectional sea level rise.

9.12 Conclusions

Clastic layers, identified as hurricane-generated overwash fans resulting from major hurricanes, appear in three transects covering >90 km of coastline covering two unrelated estuarine systems. These clastic layers show frequency changes at similar depths and ages for two of these transects (results from the third are inconclusive, as the record only extends slightly beyond the date of regime change, perhaps obscured by the presence of a single hurricane).

These frequency changes are unlikely to have resulted from regional geomorphologic control, or the random temporal spacing of a single set of hurricane landfalls.

These frequency changes most likely reflect a regime change in regional hurricane activity. Activity regimes are:

0-1000 cal yr BP – Active period

Return interval-133-250 years

1000-~3000 cal yr BP – Quiet period

Return interval -2000 years

Regime change (Quiet to Active) results in an estimated 3-12 fold increase in major hurricane landfall, matching or surpassing estimates from the northern coast of the Gulf of Mexico.

Earlier activity levels can not currently be accessed due to

1. Important geomorphic changes
2. Uncertain recording sensitivity resulting from unresolved core-to-ocean distance issues

9.13 References

- ACT (Action by Churches Together International), 2005. ACT appeal Nicaragua-Hurricane Beta-Lace 53.
<http://www.reliefweb.int/rw/rwb.nsf/db900SID/EVOD-6J9KK8?OpenDocument>. Accessed 03-01-09.
- Alvarado, G. E., Dengo, C., Martens, U., Bundschuh, J., Aguilar, T., and Bonis, S. B., 2007. Stratigraphy and geologic history. In Bundschuh, J., and Alvarado, G. E., (eds), Central America Geology Resource Hazards. Taylor and Francis, London. Vol. 1, 345-394.
- Beven, J. L. 2006. Blown away; the 2005 Atlantic hurricane season. *Weatherwise* 59, 32-44. DOI:10.3200/WEWI.59.4.32-44.

Boucher, D.H., 1990. Growing back after hurricanes. *Bioscience* 40, 163-166.

Boucher, D.H., Vandermeer, J. H., Yih, K., Zamora, N., 1990. Contrasting hurricane damage in tropical rain forest and pine forest. *Ecology* 71, 2022-2024.

Brenes, C. L., Hernandez, A., and Ballestero, D., 2007. Flushing time in Perlas Lagoon and Bluefields Bay, Nicaragua. *Investigaciones Marinas* 35, 89-96.

Christie, P., 2000. The people and natural resources of Pearl Lagoon. In Christie, P., Bradford, D., Garth, R., Gonzalez, B., Hostetler, M., Morales, O., Rigby, R., Simmons, B., Tinkham, E., Vega, G., Vernooy, R., and White, N., (eds), *Taking Care of What We Have: Participatory Natural Resource Management on the Caribbean Coast of Nicaragua*. IDRC Books, Ottawa, 17-46.

CIMAB, 1996. Centro de Ingenieria Manejo Ambiental de Bahias y zonas Costeras. Estudio de caso: La Laguna de Bluefields Nicaragua, bases para la formulacion de un plan de manejo ambiental. Proyecto Regional PNUMA CAR/P/CR/5101-90-05(2494). La Habana, Cuba.

Coates, A.G., 1997. The forging of Central America. In Coates, A. G., (ed) *Central America: a Natural and Cultural History*. Yale University Press, New Haven. 1-37.

Cortes, J., 2007. Coastal morphology and coral reefs. In Bundschuh, J., and Alvarado, G. E., (eds), *Central America Geology Resource Hazards*. Taylor and Francis, London. Vol. 1, 185-200.

Dengo, G., 1985. Mid America; tectonic setting for the Pacific margin from southern Mexico to northwestern Colombia. In Nairn, A. E. M, and Stehli, F. G., (eds), *The Ocean Basin and Margins*. Plenum Press, New York, Vol. 7, 123-180.

Dodds, D. J., 2001. The Miskito of Honduras and Nicaragua. In Stonich, S.C., (ed), *Endangered Peoples of Latin America: Struggles to Survive and Thrive*. Greenwood Press, Westport, CT, 87-99.

Donnelly, T.W., Horne, G. S., Finch, R. C, Lopez-Ramos, E., 1990. Northern Central America; the Maya and Chortis blocks. In Dengo, G., and Case, J.E., (eds), *The Geology of North America*, Vol. H, The Caribbean region. The Geologic Society of America, Boulder, Colorado. 37-76.

Dumailo, S., 2003. Evaluacion de la problematica ambiental por medio del estudio de algunos aspectos de sedimentacion y contaminacion en la Laguna de Bluefields, RAAS, Nicaragua. Unpublished Masters Thesis, Universidad Nacional Autónoma de Nicaragua-Centro para la Investigación en Recursos Acuáticos de Nicaragua, Managua, Nicaragua.

Escalante, G., 1990. The geology of southern Central America and western Colombia. In Dengo, G., and Case, J.E., (eds), *The Geology of North America*, Vol. H, The Caribbean region The Geologic Society of America, Boulder, CO. 201-230

Gerrish, H. P., 1988 . Preliminary Report: Hurricane Joan 10-23 October 1988.
http://www.nhc.noaa.gov/archive/storm_wallets/atl. Accessed 03-15-09.

Gischler, E. and Hudson, J. H., 2004. Holocene development of the Belize Barrier reef.
Sedimentary Geology 164, 223-236.

Glaser, K.S., and Droxler, A. W., 1991.High production and highstand shedding from deeply submerged carbonate banks, northern Nicaragua Rise. *Journal of Sedimentary Research*. 61, 128-142. DOI:10.1306/D42676A4-2B26-11D7-8648000102C1865D.

Herlihy, P. W., 2001. Indigenous and Ladino-speaking peoples of the Río Plátano Biosphere Reserve, Honduras. In Stonich, S.C., (ed), *Endangered Peoples of Latin America: Struggles to Survive and Thrive*. Greenwood Press, Westport, CT. 101-120.

INETER, 1999. Características e impactos meteorológicos del Huracán Mitch en Nicaragua. Mapping Interactivo. Article # 589. http://www.mappinginteractivo.com/plantilla-ante.asp?id_articulo=589. Accessed 03-15-09.

INETER, 2000. Instituto Nicaragüense de Estudios Territoriales. Dirección de Meteorología. Informe escrito.

James, K. H., 2007. Structural geology: from local elements to regional synthesis. In Bundschuh, J., and Alvarado, G. E., (eds), *Central America Geology Resource Hazards*. Taylor and Francis, London. Vol. 1, 277-321.

Kellett, D., Scheffers, A., Scheffers, E and Scheffers, S., 2004. Holocene tsunami deposits on the Bahaman islands of Long Island and Eleuthera. *Zeitschrift für Geomorphologie* 48, 519-540.

Lara, M. E., 1993. Divergent wrench faulting in the Belize southern lagoon: implications for Tertiary Caribbean plate movements and Quaternary reef distribution. *American Association of Petroleum Geologists Bulletin* 77, 1041-1063.

Lawrence, M. B., and Gross, J.M., 1989. Annual summaries Atlantic hurricane season of 1988. *Monthly Weather Reviews* 117, 2248-2259.

Liu, K-b., 2004. Paleotempestology: principles, methods and examples from Gulf coast lake sediments. In Murnane, R.J., and Liu, K-b., (eds), *Hurricanes and Typhoons: Past, Present and Future*. Columbia University Press, New York, 13-57.

Mann, P, Rogers, R. D., and Gahagan, L., 2007. Overview of plate tectonic history and its unresolved tectonic problems. In Bundschuh, J., and Alvarado, G. E., (eds), *Central America Geology Resource Hazards*. Taylor and Francis, London. Vol. 1, 201-237.

Marshall, J. S., 2007. Coastal morphology and coastal reefs. In Bundschuh, J., and Alvarado, G. E., (eds), *Central America Geology Resource Hazards*. Taylor and Francis, London. Vol. 1, 185-200.

Masselink, G., and Hughes, M. G., 2003. Introduction to Coastal Processes and Geomorphology. Arnold Publishing, London.

Milligan, T., 1997. "No tech" technical diving: the lobster divers of Mosquitia. South Pacific Underwater Medical Society Journal 27, 147-148.

Mills, R. A., and Barton, R., 1996. Geology of the Ahuas area in the Mosquitia Basin of Honduras: preliminary report. The Association of American Petroleum Geologist Bulletin 80, 1627-1640.

Mills, R. A., and Hugh, K.E., 1974. Reconnaissance group map of Mosquitia region, Honduras and Nicaragua Caribbean coast. The Association of American Petroleum Geologist Bulletin 58, 189-207.

Mills, R. A., and Hugh, K.E., Feray, D.F., and Swolfe, H.C., 1967. Mesozoic stratigraphy of Honduras. AAPG Bulletin 51, 1711-1786.

Molina, J., 2001. Características físicas, químicas y del fitoplancton en la Laguna costera "Laguna de Perlas" (RAAS), con énfasis en la Calidad de Agua. CIRA-UNAN. Datos no publicados.

NWS TPC/National Hurricane Center, Miami, FL., 2005. Hurricane Beta intermediate advisory number 13A. http://www.nhc.noaa.gov/archive/2005/pub/al262005.public_a.013.shtml?. Accessed on line 03-15-09.

Parsons, J. J., 1955. The Miskito pine savanna of Nicaragua and Honduras. Annals of the Association of American Geographers 45, 36-63.

Pasch, R. J., and Roberts, D. P., 2006. Tropical Cyclone Report: Hurricane Beta 26-31 October 2005. http://www.nhc.noaa.gov/pdf/TCR-AL272005_Beta.pdf. Accessed 3-02-09.

Radley, J. 1960. The physical geography of the east coast of Nicaragua. Unpublished Masters thesis. University of California at Berkeley, USA.

Rodgers, R. D., 1998. Incised meanders of the Rio Patuca, stream piracy and landform development of La Mosquitia, Central America. Fifteenth Caribbean Geological Conference, Kingston, Jamaica, June 29-July 2, 1998, Articles, Field Guides & Abstracts: Contributions to Geology, Vol 3. University of the West Indies, Kingston. 92.

Roullot, J., 1980. Informe de la mission en la Laguna de Perlas, Nicaragua. Programa Interregional de Ordenacion y Desarrollo Pesquero. Informe WE-CAF 34.

Scheffers, A., and Kelletat, D., 2006. New evidence and dating of Holocene paleo-tsunami events in the Caribbean (Barbados, St. Martin and Anguilla). In Mercado-Irizarry, A., and Liu, P., (eds), Caribbean Tsunami Hazards. World Scientific Press, New Jersey. 178-202.

Scheffers , A., Scheffers, S., and Kelletat, D., 2002. Paleo-tsunamis on the southern and central Antillean island arc. *Journal of Coastal Research* 21, 263-273.

Schlager, W., Reijmer, J. G.J, and Droxler, A.W, 1994. Highstand shedding of carbonate platforms. *Journal of Sedimentary Research*. B64, 270-281. DOI:10.1306/D4267FAA-2B26-11D7-8648000102C1865D.

Toscano, M. A., and Macintyre, I. G., 2003. Corrected western Atlantic sea-level curve for the last 11,000 years based on calibrated C-14 dates from *Acropora palmate* framework and intertidal mangrove peat. *Coral Reefs* 22, 257-270.

UNHCR, 2003. Minorities at Risk Project, Assessment for Indigenous Peoples in Nicaragua, 31 December 2003. Online. UNHCR Refworld, available at: <http://www.unhcr.org/refworld/docid/469f3ab8c.html>. Accessed 02-24-09.

Urquhart, G. R., 2009. Paleoecological record of hurricane disturbance and forest regeneration in Nicaragua. *Quaternary International* 195, 88-97. DOI:10.1016/j.quaint.2008.05.012.

Vandermeer, J. H., Granzow de la Cerda, I, Boucher, D., Perfecto, I., and Ruiz, J., 2000. Hurricane disturbance and tropical tree species diversity. *Science* 290, 788-790.

Wallace, D. R., 1997. Central American landscapes. In Coates, A. G., (ed) *Central America: a Natural and Cultural history*. Yale University Press, New Haven. 72-96.

Weyl, R., 1980. *Geology of Central America*. Gebrueder Borntraeger, Berlin
http://www.nhc.noaa.gov/archive/storm_wallets/atlantic/atl1988-prelim/joan/prelim02.gif
Accessed 02-25-09.

CHAPTER 10 ST. LAWRENCE GAP, BARBADOS

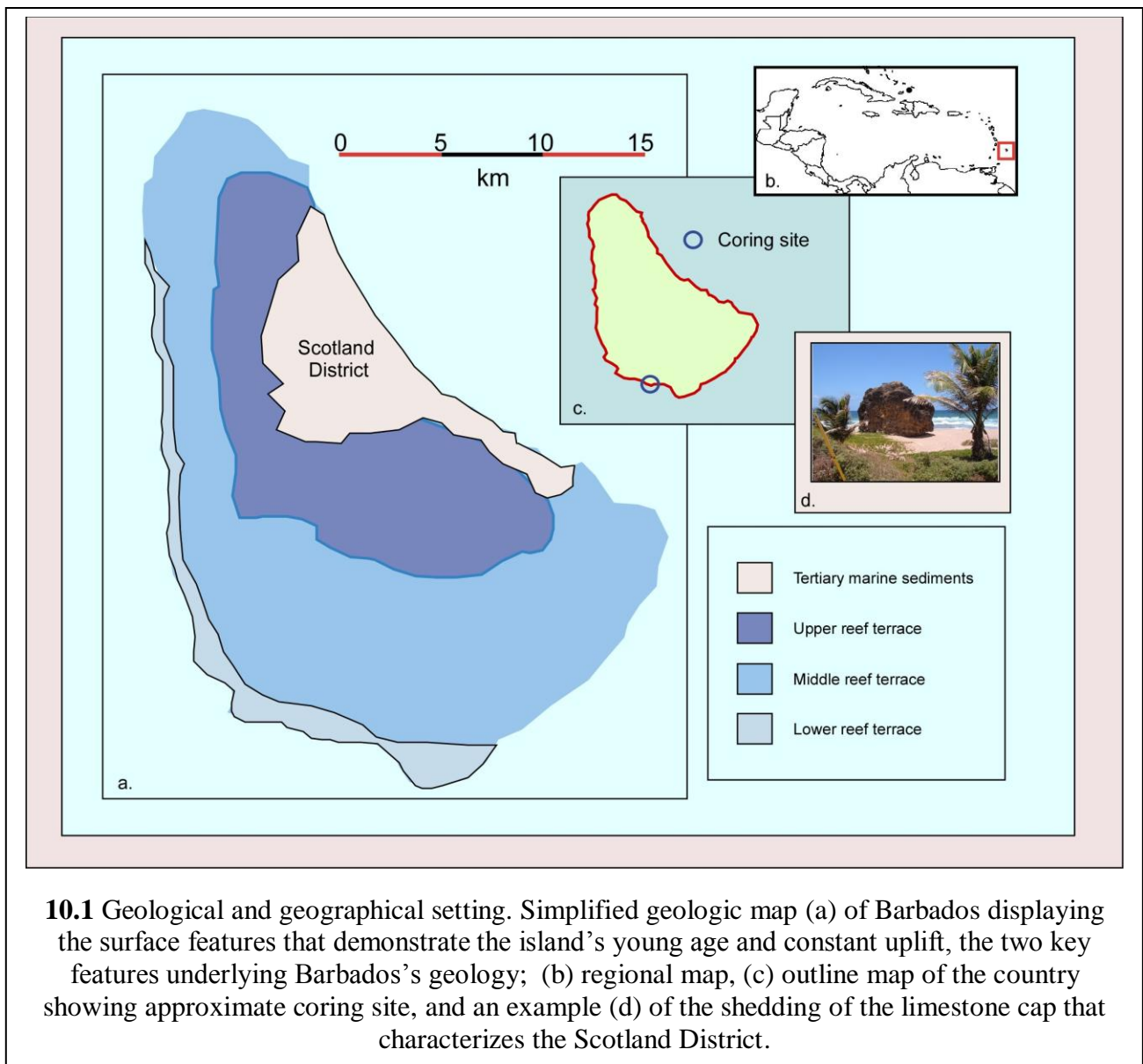
10.1 Geographic Setting

Barbados was chosen as a study site due to its location as the easternmost Caribbean island, ~160 km east of the St. Vincent and the Grenadines, the closest of the Lesser Antilles (**Figure 10:1b**). This forward placement positions Barbados to record clearly the passage of Cape Verde type hurricanes, which form off the coast of Africa and move westward across the Atlantic. Lying between 13.04° and 13.33° north latitude, Barbados is somewhat to the south of the current zone of hurricane activity (**Figure 9:6**). That, combined with the island's small size (430 km^2), means that direct hits during the instrumental period have been rare. However, even a small southern movement of the hurricane zone could dramatically increase the probability of landfall, potentially resulting in a marked and easily observable change in the sedimentary record.

10.2 Geologic Setting

The geology of Barbados is complex, but relatively short and well-studied. Non-volcanic in origin, the island consists of a mix of oceanic and terrestrial Tertiary sediments, pushed up from the ocean floor as the only subaerial portion of the Barbados Ridge accretionary prism (Speed, 1986). Island wide, these material are overlain by domed Pleistocene age coral reefs, except for the Scotland District in the northeastern part of the country, where large sections of the reef deposits have broken off and rolled down the greasy Tertiary clays into the sea (Poole and Barker, 1983) (**Figure 10:1d**).

The Eocene base of Barbados, which reaches depths $>4500 \text{ m}$, consists of a mix of terrestrial turbidites originating on the South American shield and hemipelagic rock, mainly



radiolarites. This material was accreted by offscraping of the forearc toe, over which a layer of Miocene to Oligocene sedimentary material was deposited. Reverse thrusting then covered this material with 350-700 m of older (Eocene to Miocene) oceanic materials. These oceanic clays are mixed with five distinct *mélange* units resulting from late Miocene mud diapirism (Speed, 1986). Following its emplacement, this material was folded and shear faulted by a late phase of the Andean progeny during the late Tertiary/early Quaternary. This was followed by a sedimentary hiatus, until the deposition of the Pleistocene coral (Poole and Barker, 1983). This coral is nearly identical with modern coral, containing lithofacies recognizable as reefcrest, channel cuts, and upper and lower reef fronts, dominated by such readily identifiable species as *Acropora palmata*, *A. cervicornis*, *Montastraea*, and *Diploria* (Poole and Barker, 1983). Due to uplift the oldest coral limestone is found at the highest elevations (surrounding Mt. Hillaby, 343 m), with age decreasing concentrically to the coasts. Corresponding with a series of cliffs, the limestone has been divided into Lower (<127,000 years), Middle (127,000< >484,000 years), and Upper (484,000< > 700,000 years) groups (Poole and Barker, 1983).

Fairbanks' (1989) classic paper based on radiocarbon dates from *Acropora palmata* deposits on three ridges offshore of Barbados used a calculation of a constant uplift rate of ~34 cm/kyr to determine postglacial sea level rise. Although recent research has indicated that, due to the complexities of anticlinal warping, the uplift rate may in fact not have remained constant over the entire 500,000 year span (Radtke and Schellmann, 2006), such calculations are probably accurate for the Holocene, thereby providing a sound sea level framework for the island.

10.3 Environmental Setting

Barbados lies within the influence of the northeast trades, experiencing near constant

wind along the eastern coast. Annual precipitation is divided into wet (June-December) and dry (January-May) seasons, with average annual rainfall varying from 1000 mm along the northern and southeastern coast to 2000 mm/ at the highest points at the center of the island (Jones and Banner, 2003). Temperatures are relatively constant throughout the year, with Bridgetown monthly minima ranging only from 21-23°C, and monthly maxima from 28-31°C (<http://www.bbc.co.uk/weather>).

Due to the limestone cap, Barbados has almost no surface streams and generally gradual topographic relief. The exceptions are the soft folded/eroded oceanic materials in the Scotland District and the cliffs separating the three marine terraces. Although a small amount of forest cover remains (2000 hectares, or 4.7% of national area) (<http://www.fao.org/forestry/4142/en/>), none of it is primary, as native forests had been mainly eliminated by 1665 (Krech et al., 2003). Due to the lack of estuaries and somewhat steep bathymetry, Barbados has very limited amounts of coastal wetlands. The country's only surviving mangroves are in the Graeme Hall Nature Sanctuary (Ramcharan, 2005), a dredged wetland constructed in a 35 hectare sinkhole, which recently closed due to economic constraints (<http://www.graemehall.com>). Compounding the natural scarcity is the high level of human disturbance inherent to such a small, isolated oceanic island. The first settlers were members of the Saladoid-Barrancoid Amerindian group from the Orinoco basin who migrated to the island in several waves beginning ~ AD 350. Living in seaside fishing villages and farming small plots, these people were so devastated by Spanish slave raids that the island was virtually uninhabited by the time British colonists arrived in 1627 (Beckles, 1990). Deforestation quickly followed the British as tobacco, cotton, and indigo agriculture followed a boom and bust pattern; by the 1640s sugar became the country's economic mainstay and thereafter dominated the colony's economy for centuries (Beckles, 1990). Sugar

remained more important economically than either manufacturing or service industries until the 1990s (<https://www.cia.gov/library/publications/the-world-factbook/geos/bb.html>). A high population density (<http://www.census.gov/ipc/www/idb/country/bbportal.html>) (>650 people /km² countrywide) has been exacerbated by Barbados's development as a major tourist destination. The country receives almost 1.2 million visitors annually, nearly evenly divided between stopover tourist visits and cruise passengers, achieving a total tourist expenditures of \$1,200 million USD in 2007 (Caribbean Tourism Organization, 2007, 2009; Ministry of Finance, Economic Affairs, and Energy, 2008). The tourism industry is now the backbone of the national economy, accounting for > 13% of the GDP, and employing >10% of the labor force (Ministry of Finance, Economic Affairs and Energy, 2008; Barbados Statistical Service, 2008). The island's intense human land use has stressed and altered many natural systems. Relevant examples include the historical development of "shooting trays", in which natural wetlands are dug out and diked to produce geometrically shaped shallow water-filled enclosures aimed at attracting water fowl for hunting purposes. This has occurred in parts of Graeme Hall swamp and Chancery Lane swamp on the southeast coast. Other wetlands have either disappeared under development (Inch Marlowe Swamp) or been channelized, thereby rendering their sedimentary records worthless.

10.4 Study Sites

Our study site is the St. Lawrence Lagoon (SLL), a small freshwater pond a few meters from the sea on the southwest coast (**Figure 10:2**). Immediately to the northwest is Graeme Hall swamp for which a 1400-year paleoenvironmental history has been reconstructed (Ramcharan, 2005). (We did not core Graeme Hall swamp, as we were informed by the management that it had been dredged, presumably after the coring [undated] undertaken by Ramcharan). SLL is

contained within the St. Lawrence Gap, a narrow depression of Lower coral reef, surrounded by higher, Holocene-age marine reef and modern dune deposits (Poole and Barker, 1983) (**Figure 10:3**). SLL is approachable only on foot, as it is enclosed on all sides by houses, businesses, and hotels, all with their backs to the SLL. There is no direct connection with the sea, as the seaward end is 2-3 m lower than the surrounding land. Salinity was 1.2 ppt at the time of our visit in late April (nearing the end of the dry season). Grasses and sedges dominated the vegetation; we cored through a floating marsh. Water depth was <1 m. Despite the site's location as a neglected, unseen depression at the back of a developed area, whose upper edges are collecting debris, human disturbance seemed minimal in the pond itself. When questioned, a local business owner said that SLL has never dried up, and that due to the extreme softness of the surrounding mud the center has remained undisturbed. Apart from the top few centimeters, internal evidence generally supports this view.

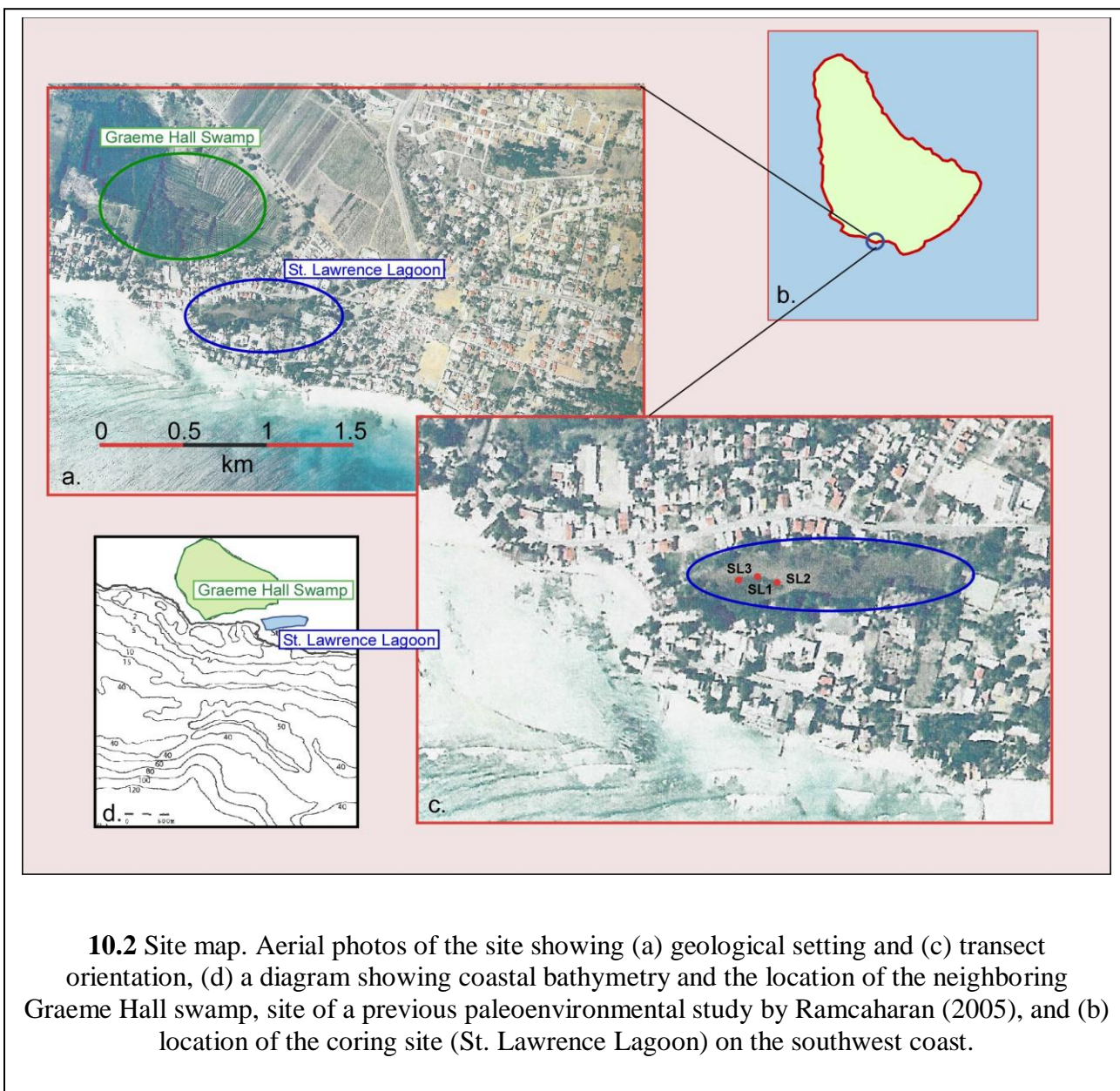
10.5 Sea Level

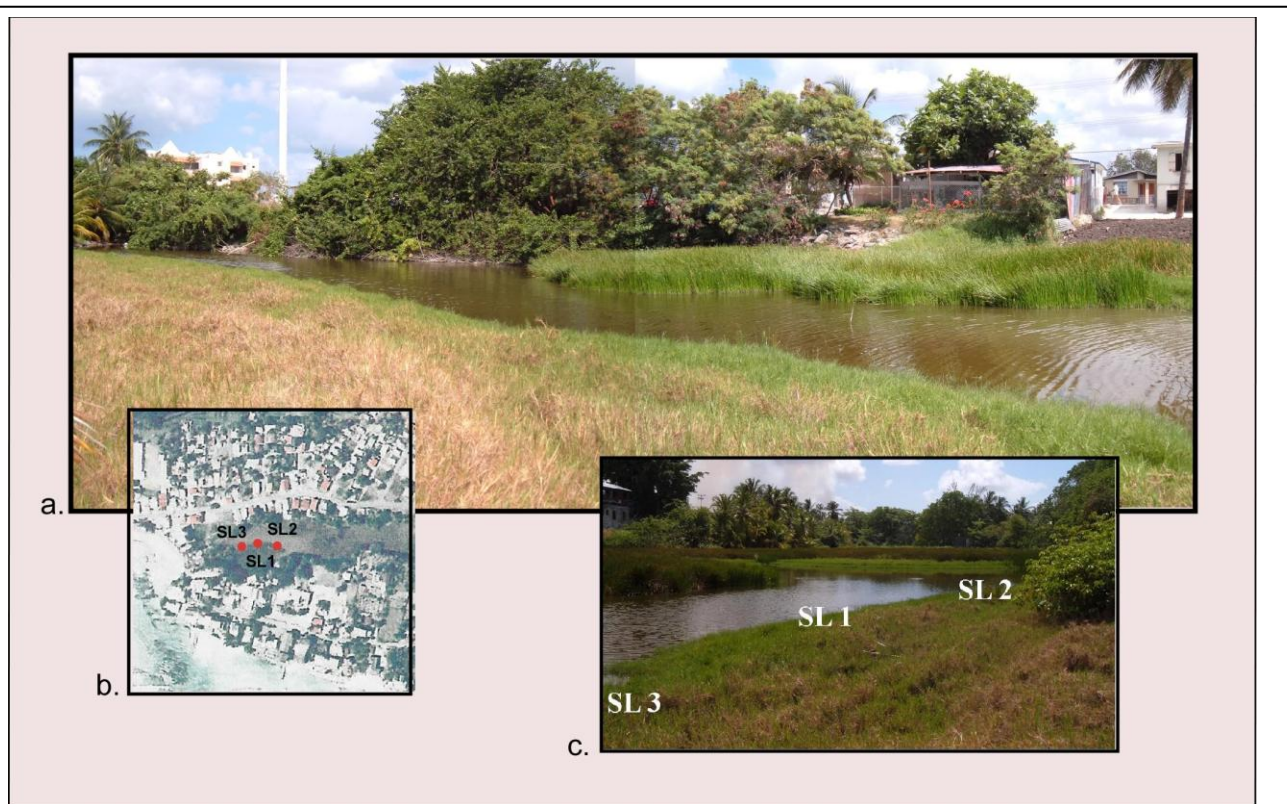
As mentioned above, pioneer eustatic sea level rise studies were based on data from Barbados, and are some of the best known/accepted in the world.

10.6 Hurricane History

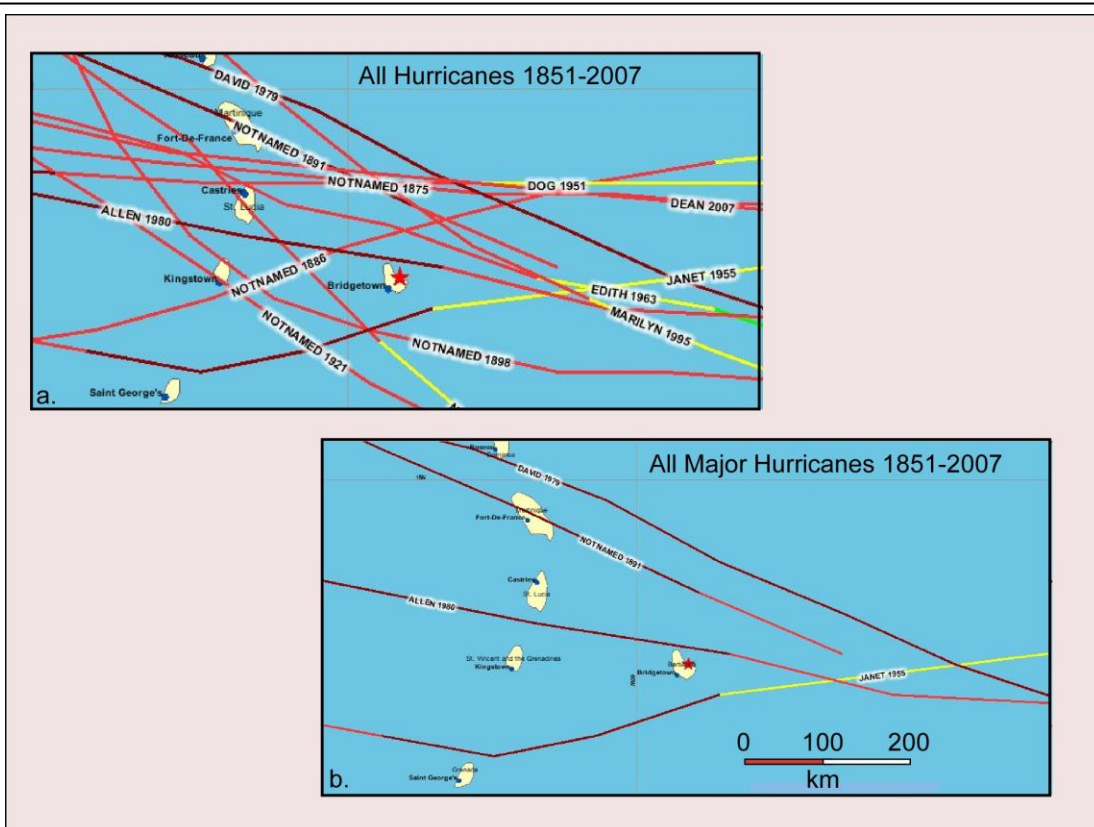
The tracks of all hurricanes (a) and major hurricanes (b) passing within 65 nautical miles of the island are shown in **Figure 10:4**). Although Barbados has not received a direct hit from a hurricane during the length of NOAA records (1851-present)

(<http://maps.csc.noaa.gov/hurricanes/viewer.html>), two hurricanes have caused significant social damage during the period. The unnamed storm of 1898 caused >100 deaths and left 50,000 homeless (Carpenter, 1899). This was a category 2 hurricane, with maximum sustained winds of 95 knots, which passed ~ 40 km south of Barbados, exposing the island to the strong right front





10.3 Coring transect. Site photo (a) showing floating marsh surrounding the small wetland situated in a narrow depression in the limestone bedrock, (c) core locations. Aerial photo(b) showing the developed nature of the area. Ocean is to the left, immediately beyond and below the tall white utility pole in (a).



10.4 Hurricane history. The tracks of (a) all hurricanes, and (b) all major hurricanes passing within 65 nautical miles of the island since 1851, based on the NOAA HURDAT ("best track") data set.

quadrant. Hurricane Janet in 1955 passed slightly closer to the island, also to the south, causing 38 deaths (Dunn et al., 1955). Although Janet developed into a very dangerous hurricane and caused tremendous damage farther west, when passing Barbados it was an immature storm, with a “very small” windfield and a 20 mile (36 km) eye, with maximum sustained wind speeds of 105 knots (category 3) (Dunn et al., 1955). As maximum wind speed had been only 50 knots the previous day, it seems likely that Joan generated only a small wave field.

Due to the long British occupation of the island, hurricane records extend to at least 1667 (Schomburgk, 1848). Between that time and the start of the NOAA records, two hurricanes stand out for their devastation; Hurricane San Calixto II of 1780 which killed >4000 people and the Great Barbados Hurricane of 1831, which killed over 1500. Category and windspeed for these storms are not known.

10.7 Methods

Methods followed are those described in **Chapter 2.4**.

10.8 Results

10.8.1 SL Transect

Three cores were obtained from the southern edge of SLL through a floating marsh and ~70 cm of water. Locations are shown in **Figure 10:3**. SL1 is a composite core; two Livingstone core barrels were pushed to a total depth of 208 cm with a 6 cm overlap, below which two Russian peat borer sections were extracted, reaching a total depth of 309 cm. SL2, taken 25 m to the east (landward), consists of four Russian peat borer sections reaching a depth of 196 cm. SL3, taken 25 m west (seaward) of SL1 (50 m west of SL2), consists of five Russian peat borer sections, reaching a depth of 226 cm. All cores were pushed to refusal. The cores generally

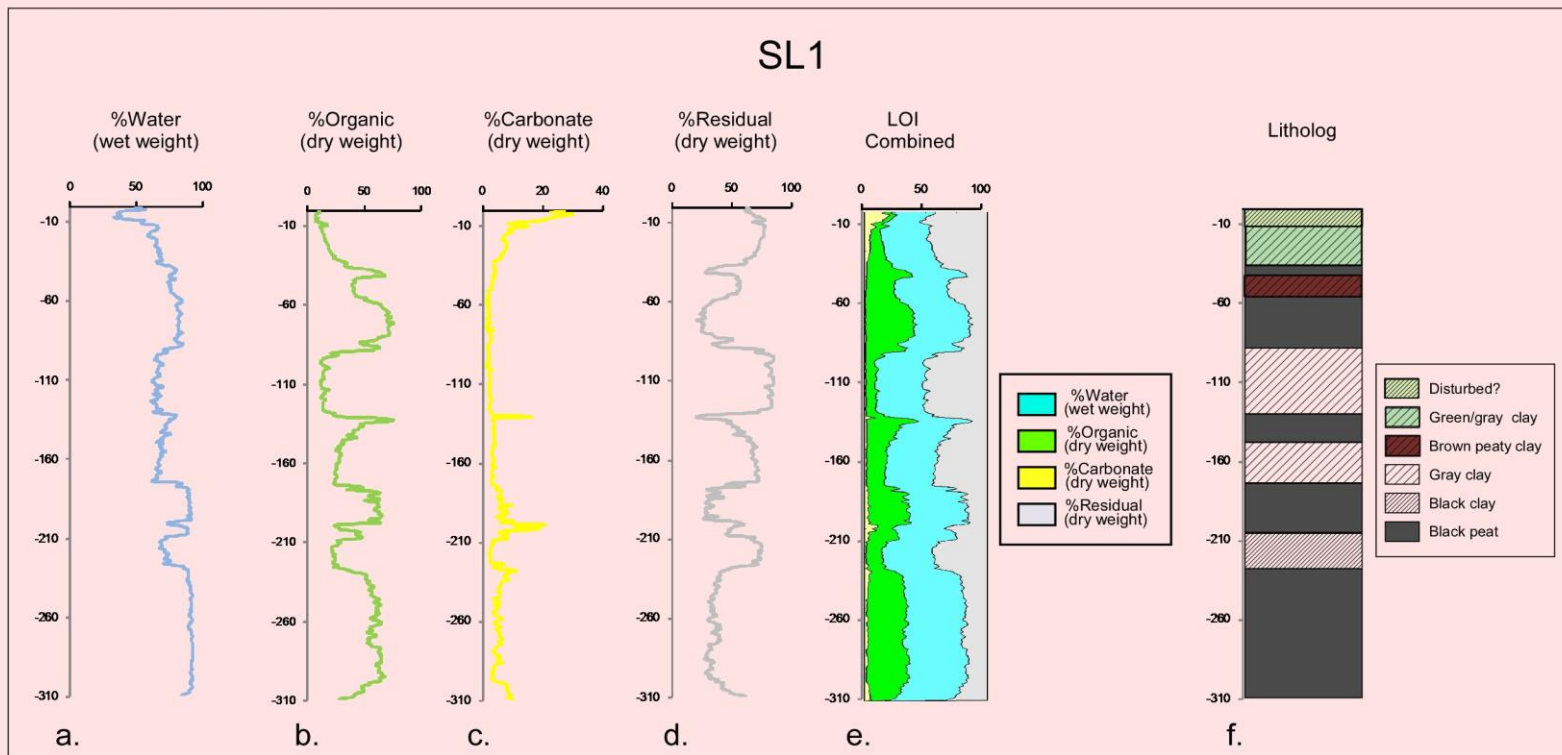
consist of alternating sections of gray/black clay and black peat.

10.8.1.1 Core SL1

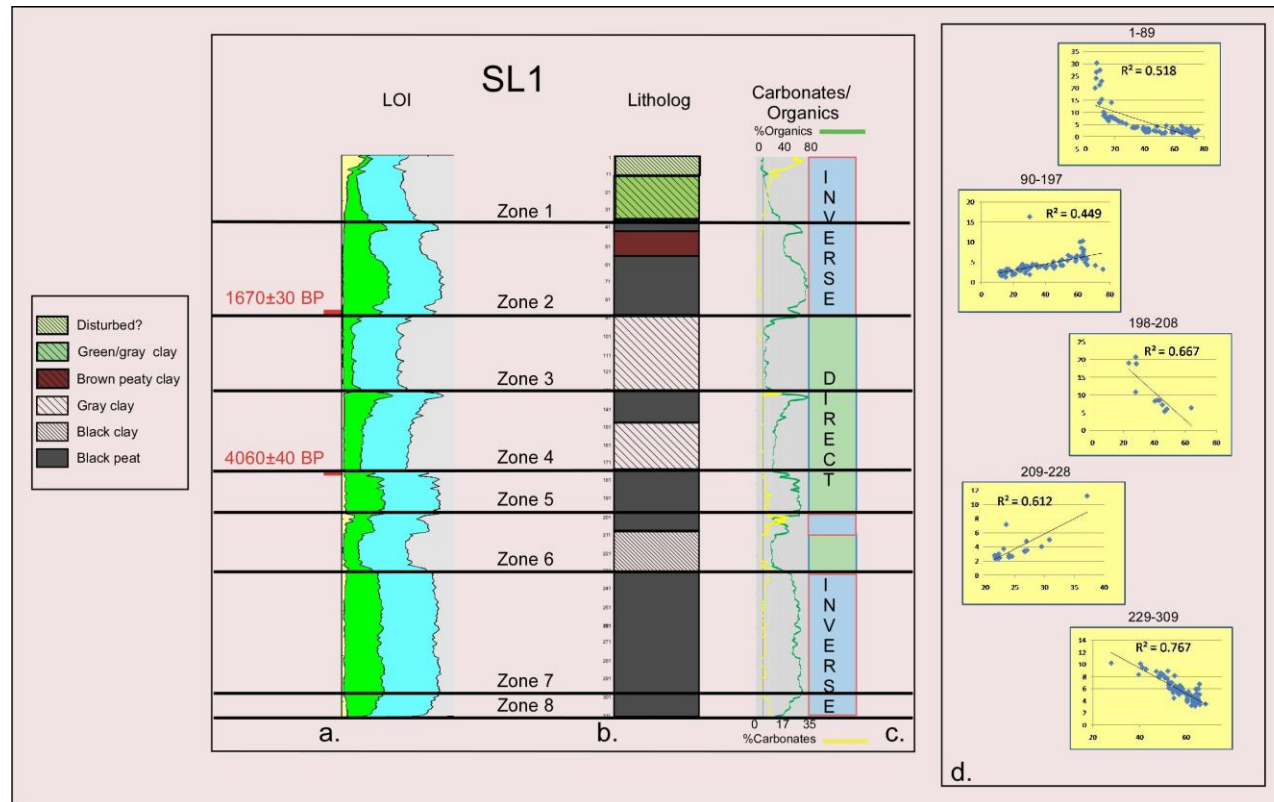
10.8.1.1.1 Example Litholog

The longest core, SL1, located 125 m inland in the middle of the transect was chosen as the example litholog. The results of LOI analysis are presented in **Figure 10:5**. Shown are the water, organic, carbonate, and residual (mainly silicate) percentages as individual curves (**Figure 10:5 a, b, c, d**), a combined LOI curve (**Figure 10:5 e**), and the core litholog (**Figure 10:5f**). As can be seen, sediments alternate between thick clay and peat intervals, with compositional changes distinctly marked by corresponding changes on the LOI curves. The peat intervals correspond to high water (blue) and organics (green) curves (59-89, 175-208, 229-309 cm), while clay intervals correspond to high residual (gray) curves, as from 90-131, 146-174, 209-228 cm. Intermediate values can indicate mixed sediments, an example being the peaty clay interval from 43-59 cm. Sedimentary change can be either rapid or gradual; an extremely abrupt change occurs over the five cm interval from 87-91 cm, during which the organic value drops from 64-21%, while residual increases from 34-77%. A slower change of the same approximate magnitude (organics increase from 16-68%, residuals drop from 76-29%) occurs over a 23 cm interval from 20-42 cm.

As usual, water and organics values have a positive relationship, and vary inversely with residual values. Carbonate values are particularly interesting in this core. Carbonate and organic values (set at separate scales to increase visibility) were plotted on the Y axis for the length of the core (**Figure 10:6c**), from which intervals of inverse and direct variation were selected visually. Each core was divided by this method at specific points (no overlaps or excluded sections), the paired carbonate/organic values for each centimeter were plotted against each



10.5 LOI curves and litholog for core SL1. Shown are (a) water, (b) organic, (c) carbonate, and (d) residual (mainly silicate) percentages as individual curves; (e) a combined LOI curve, and (f) the core litholog.



10.6 SL1 zonation based on (a) LOI and (b) lithologic data. The complicated relationship between carbonate and organics, based on their LOI values, is shown in (c), displaying alternating direct and inverse patterns, with (d) examples of each pattern. Radiocarbon dates are shown in red.

other, by section, and linear trendlines were drawn (Figure 10:6d). The carbonate/organic relationship displays abrupt and dramatic reversals, changing from an inverse relationship at the top (1-89cm), middle (198-208), and bottom of the core (228-309 cm), to a direct relationship for two sections in the middle (90-197 cm, 209, 228) (Figure 10.6d). The high R^2 values (0.449-0.767) support the view that these reversals are not random.

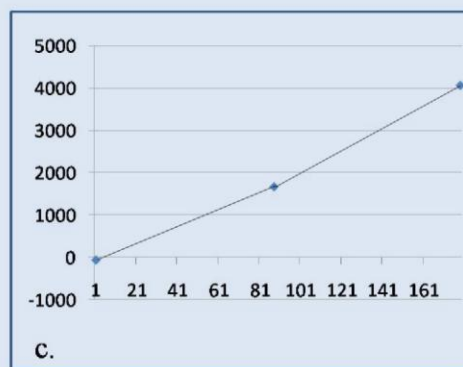
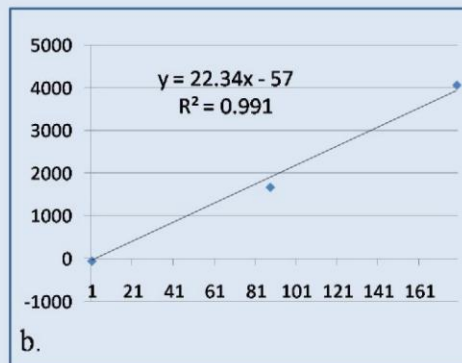
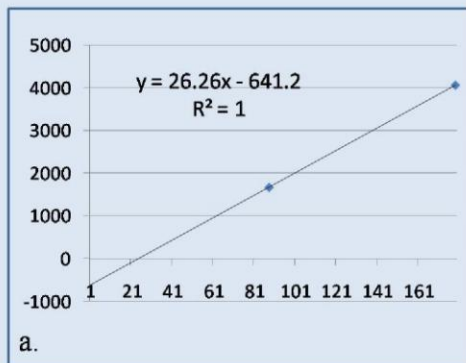
10.8.1.1.2 Dating

Two plant/organic samples were selected from SL1 and sent to the National Ocean Sciences Accelerator Mass Spectrometry (NOSAMS) facility at Woods Hole Oceanographic Institute for AMS dating. The results are listed in **Table 10:1**, and shown graphically in **Figures 10:6, 10:7**. The sample from 88 cm was dated to 1670 ± 30 ^{14}C yr BP, and the sample from 179 cm dated to 4060 ± 40 ^{14}C yr BP. The calculated date for the core bottom (309 cm) based on the assumption of constant sedimentation is 7008 ^{14}C yr BP.

Because there are only two data points, plotting depth (X axis) is against ^{14}C age (Y axis) results in a straight line ($R^2 = 1.00$) with a sedimentation rate of 0.038 cm/yr (26.26 yr/cm) and an intercept of -641 yrs (**Figure 10:7a**). In order to reduce this unacceptably large intercept date, a surface date corresponding to AD 2007 (the year of sampling) was artificially imposed (b). The resultant graph gives a slightly faster sedimentation rate of (0.045 cm/yr-22 yr/cm) with an R^2 value of 0.991. Allowing for changing sedimentation rates shows a slightly slower sedimentation rates for the more recent period (c). As ^{14}C dates do not have a linear relationship with calendar dates, changes in calculated sedimentation rates are not unexpected, particularly as recent radiocarbon dates (>2000 yrs) are older than the corresponding calibrated calendar ages, while older radiocarbon dates are younger. Because the dated material consisted of terrestrial wood and plant material, anomalous dates cannot be explained by the presence of “old” depleted

10.1 SL1 chronology

Core	Depth	Material	Lab	Sample#	C ¹⁴ yr BP		Cal yr BP	Probability	AD/BC
SL1A	88	Organic	WHOI	OS-73646	1670	±30	1652-1692	0.103	258-298AD
							1520-1631	0.897	319-430AD
SL1B	179	Organic	WHOI	OS-73641	4060	±40	4761-4801	0.107	2852-2812BC
							4675-4693	0.024	2744-2726BC
							4425-4645	0.869	2696-2476BC



10.7 Depth-age graphs for SL1; showing (a) straight plotting , a (b)forced surface intercept of AD 2007, and a (c) variable sedimentation rate.

carbon from the surrounding limestone.

10.8.1.1.3 Zonation

SL1 can be divided into eight zones, based on changes in the LOI curve (**Figure 10:6**).

10.8.1.1.3.1 Zone 1 (1-37cm) is basically a clay layer, consisting of soft green/black/gray clay.

Water (34-70%) and organic (7-39%) content are generally low, with correspondingly high residual values (57-79%). Carbonate values (4-30%) in this section are the highest for the core.

The top 12 cm differ significantly from the bottom of the zone, and probably represent disturbance, though it is unclear whether this is anthropogenic or natural. The top 2 cm are a soft green/gray clay, preceded by a visual sand/silt layer ~ 1cm thick (**Figure 10:8**). Below this are nine cm of soft clay, changing from green to greenish black, mixed with rocks, pebbles, and sand. Some of the material consists of cemented sand/silt and shells, rough on one side, and a smooth white on the other (**Figure 10:8**). It is unclear whether this cementation is natural.

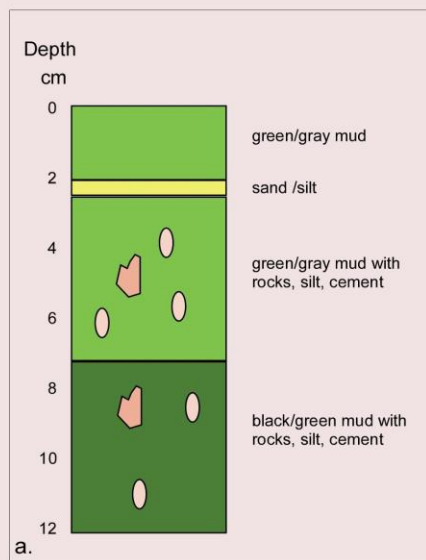
Although the smooth surface suggests a thin layer of paint or plaster, the grain size is much smaller than normally used in concrete mixtures, and the smooth layer is extremely thin. The extremely large size of the pieces of this material suggests deposition by a high-energy event, as does the stratigraphy, with the larger pebbles at the bottom. Human disturbance (dumping of construction materials, for example) could produce the same effect. Both naturally cemented rocks and broken chunks of concrete could be delivered by either method.

10.8.1.1.3.2 Zone 2 (38-89cm) is mainly black peat, sandwiching a muddier interval. Water (74-86%) and organic (39-74%) values are high, residuals are low (21-58%).

10.8.1.1.3.3 Zone 3 (90- 131cm) is grey clay, as evidenced by the residual values, which except the first and last samples, are >70%.

10.8.1.1.3.4 Zone 4 (132-174). The top is a peat section, which becomes increasingly clayey, as

SL1



10.8 Probable disturbance at the top of core SL1. The top 12 cm of core SL1 probably represents a disturbed interval, as evidenced by the litholog (a), and the presence of large pieces of cemented material, rough on one side (b, top) and smooth on the other (b, bottom). This material does not appear elsewhere in the transect.

shown by the organic decreasing from 76-25%, matched by a residual increase from 30-72%.

10.8.1.1.3.5 Zone 5 (175-198) is a peat interval. The peat consists of fairly large pieces, perhaps indicating rapid sedimentation. Organic and residual values are nearly even, inversely ranging from ~ 40-65%.

10.8.1.1.3.6 Zone 6 (199-228) begins with a clastic layer at 199-202cm, followed by 6 cm of low organic peat, and then black clay. The clastic/peat layer from 198-208 occur during a short period when the carbonate/organic relationship becomes strongly negative (R^2 value of 0.667). Although the clastic and clay intervals have similar organic percentages (<30%), the clastic layer stands out for the very high (11-21%) carbonate percentages. The organic content of the peatier section they sandwich is between 43-48%.

10.8.1.1.3.7 Zone 7 (229-298) is black, well-rotted peat, with uniformly high water (mostly >93%) and organic (mostly >60%) percentages.

10.8.1.1.3.8 Zone 8 (299-309) is also black peat, although slightly less organic, with water content between 84-93% and organic content 28-54%.

10.8.1.2 Transect Correlation

Due to a lack of cross core dating, transect zonation is based on visual similarities in the LOI curves, especially the matching of the distinctive spikes and dips. Zones 1-5 extend across the transect; Zones 6-8 appear only in SL1, the core with the deepest penetration (**Figure 10:9**). The sedimentary similarities between the three cores are obvious, especially when they are artificially stretched/condensed so that the spikes/dips occur at similar depths (**Figure 10:9b.**) This argues for lack of significant disturbance at the site, despite intense human activities in the area for several centuries.

10.9 Discussion

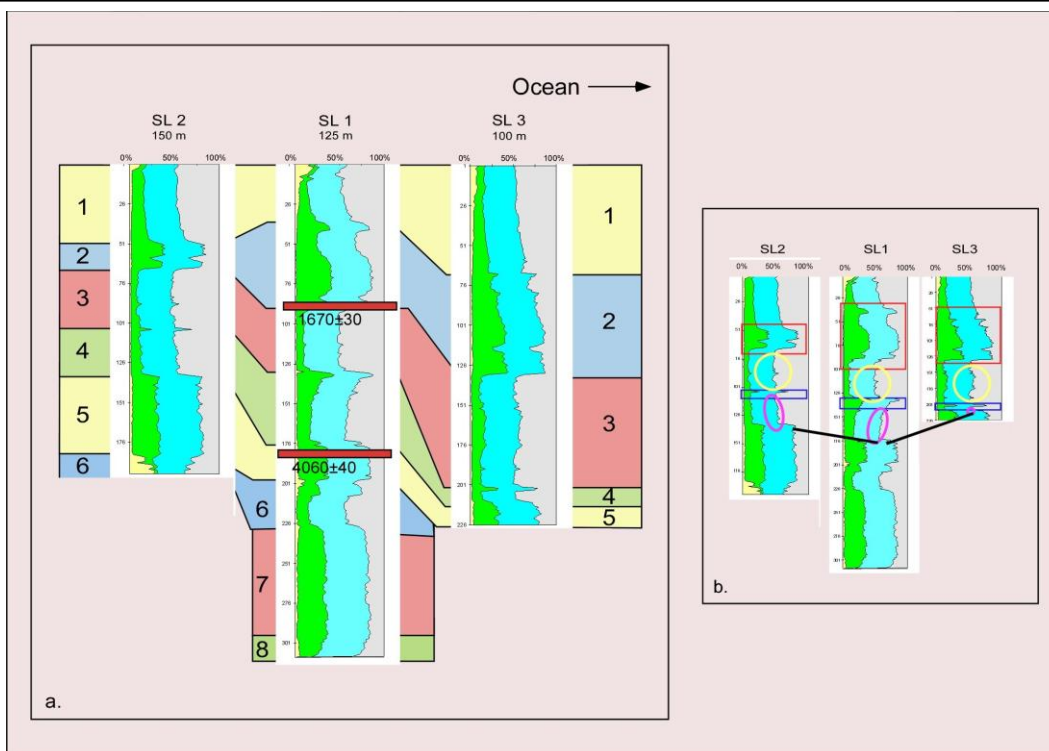
10.9.1 SL transect

10.9.1.1 Zone 1

The LOI and lithologic features associated with the top 12 cm of SL1, earlier identified as possible disturbance, are replicated in SL2 and 3, both of which show similar, though slightly less distinctive, characteristics. In these cores this layer has generally low water and organic values, high carbonate content, and presents as a gray/green/brown clay containing sand/silt/shells/pebbles and larger chunks of cemented beach material.

It seems clear that some important event accounts for this distinct sedimentary layer. The questionable nature of the material and the prevalence of extremely large-sized material present the possibility that the seaward ridge that closes off St. Lawrence Gap was raised by human action, possibly to accommodate the road that it now supports. The use of beach sand/coral blocks for fill would explain the dramatic increase in carbonates at the core tops and the presence of the larger material. Presently, the St. Lawrence Gap is completely separated from the sea, with the western (seaward) end terminating at a soil bank some 2-3 m high, westward of which one encounters a parking lot, buildings, the road and the sea. Due to the developed nature of the area (famous for the nightlife, restaurants, and upscale shopping) (www.barbados.org), it was difficult to determine how much of the present topography has been derived from human engineering. However, judging from the age of the buildings, the present topography has been in places for at least a few decades.

A second possibility is that this layer represents beach and building debris washed over the separating ridge and into SLL, as a result of natural processes, probably a powerful storm. The position of this layer at the very top of the core makes Hurricane Janet (1955) the most



10.9 SL transect zonation (a) based on LOI data. Radiocarbon dates are marked by red bars; parallel stratigraphies as indicated by LOI curves argue for uniform transect history, supporting a view of generally undisturbed deposition. In (b) the three cores have been stretched/compressed so that the bottoms of Zone 4 (marked by purple circles) in each cores are set at a common depth. Cores have been stretched/compressed as a unit so that the shapes of the curves have not been distorted.

likely candidate. However, since SLL is on the southwest coast, with the ocean to the west, Janet's east to west track, passing to the south, should have driven water out of the bay during the period of closest approach. Although subsequent landward storm surge could have occurred, the southeastern trending coast line should have dampened the magnitude. It seems unlikely that Janet was responsible for creating this layer given the hurricane's distance, size, strength, and phase of development.

Considering the area's hurricane record and the size and composition of the deposited material, this interval most likely results from human activity, probably construction.

10.9.2 Carbonate-Organic Ratio

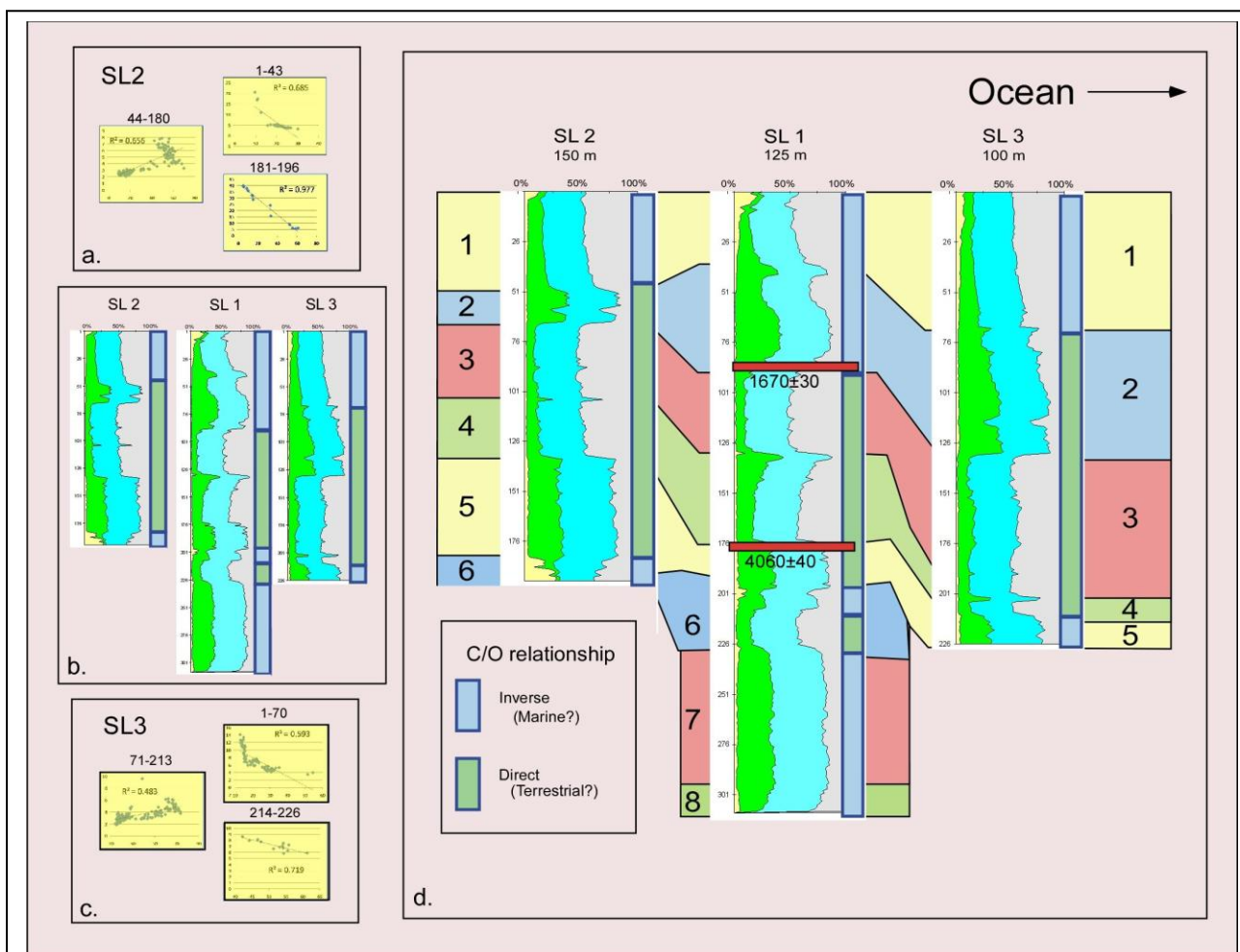
Cores SL2 and 3 display the same pattern of variation between the carbonate and organic percentages as discussed above for core SL, namely an inverse relationship at the top, preceded by first a switch to direct, and then a return to inverse (**Figure 10:10b**). These switches are both abrupt and clear, with high R^2 values (0.656-0.977 for SL2; 0.483-0.719 for SL3) (**Figure 10:10a,c**). An argument has been made above (**Chapter 8**) that, due to differing depositional mechanics, the carbonate-organic relationship can be used to indicate whether marine or terrestrial influences dominated at the time of deposition. According to this hypothesis, a direct (positive) mathematical relationship between carbonate and organic values, as determined by LOI, indicate a terrestrially-dominated depositional environment, while a negative (inverse) relationship indicates a marine-dominated environment. The hypothesized control is that during marine periods carbonates and organics limit each other, with an increase in one resulting in a decrease in the other, while during terrestrial periods they increase/decrease in unison. In the case of these cores, the relationship between carbonates and organics should be inverse (either/or

deposition) for marine periods, and direct (neither/both) for terrestrial periods, perhaps controlled by creation/destruction of the seaward barrier.

The results produced by superimposing these divisions on top of the transect zonation are potentially important (**Figure 10:10d**). One obvious correlation is that the inverse divisions correspond generally to the peaks in carbonate production. This suggests either that the divisions are artifacts of high carbonate production, or that high carbonate content and the inverse relationship are driven by the same external factor; i.e. increased marine influence. A surface sample obtained from an elevated location between the sea and western end of the St. Lawrence Gap contains 9% carbonate, while beach samples from other Barbadian sites contain similar amounts (6-8%).

The correlation between carbonate/organic relationship and LOI zonation is good, but not perfect. The bottom of the upper inverse interval corresponds to the bottom of Zone 1 for SL2 and 3, but the bottom of Zone 2 for SL1. The top of the second inverse interval corresponds to the top of Zone 6 for SL1 and 2, but the top of Zone 5 for SL3(**Figure 10:10**). The lower direct and inverse intervals in SL1 (Zones 6-8) do not appear in SL2 and 3, which terminate at shallower depths. There is also a fairly good correlation between direct intervals and clay deposition, perhaps signifying that clay (derived from inland weathering) accumulates more readily under more terrestrial conditions (**Figure 10:6**).

Such an interpretation implies that the core tops have been deposited under mainly marine conditions, which do not currently exist. This could be accounted for by the closing or heightening of the seaward barrier, perhaps corresponding to the disturbance noted at the top of the cores. Marine conditions could also presumably exist as a result of overwash events and the trapping of saline ocean water in the depression, even without significant geomorphologic



10.10 Carbonate-organic relationship. In regards to the direct/inverse relationship between LOI carbonate and organic percentages both cores SL2 and SL3 display patterns similar to that in core SL1(a, b, c), namely an inverse relationship at the top, which changes to direct, and then back to inverse with depth. The timing of these reversals is fairly consistent across the transect, as correlated with the zonation pattern (d).

change in barrier height or position. The effect of the permeability/plugging of the surrounding limestone is also important as both marine connectivity and the ability of the depression to hold freshwater are potentially highly variable. Perhaps the abrupt sedimentary changes evident across this transect relate to rapidly changing water levels driven by the destruction/formation of clay plugs. Another possibility is an increased ratio between marine water seeping in through the limestone from the sea, and the freshwater derived from precipitation. Such a change would therefore result from climatic conditions and not geomorphologic changes or meteorological events.

At this point it is not possible to determine positively periods (if any) of increased marine influence, or identify the mechanisms responsible for initiation/termination of such periods. A microfossil analysis detailing diatoms/phytoliths and dinoflagellates could help resolve this issue.

10.9.3 Graeme Hall

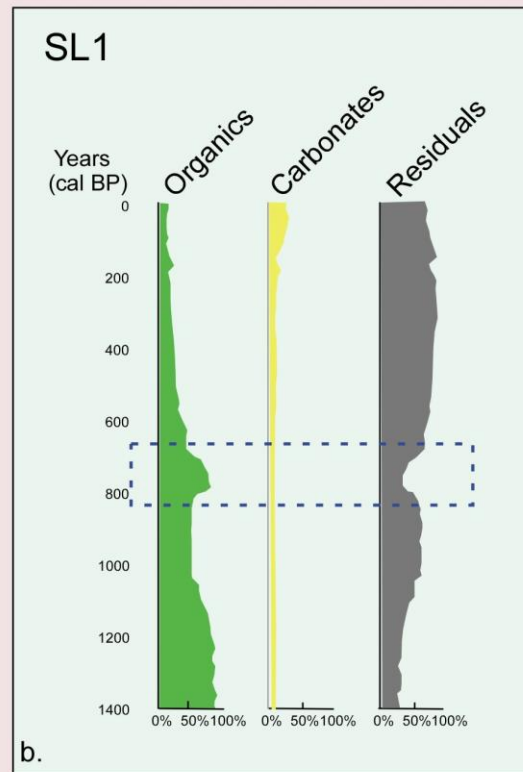
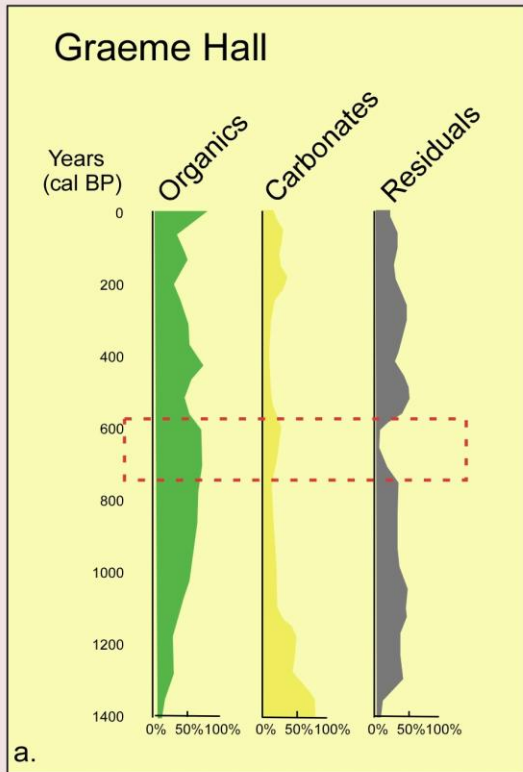
Although an analysis of the carbonate-organic ratio suggests more marine influence for the more recent period, paleoenvironmental reconstruction for Graeme Hall swamp, a few hundred meters to the northwest shows the opposite trend, with an examination of 11 mollusk species indicating that the original marine conditions changed to brackish over time (Ramcharan, 2005). However, the LOI curve for Graeme Hall swamp does not much resemble the SL1 LOI curve presented here, with the bottom sections, in particular, behaving in nearly the reverse fashion for the two cores (**Figure 10:11**). The two areas seem to be subject to a very different depositional regime, with carbonate percentages varying between 20-90% for the Graeme Hall core, while never surpassing 31% and usually <10% for the SL1 interval. Sedimentation rates also are probably very different. The SL curve represents only the top 74 cm

of the core, as, assuming constant sedimentation, that is the calculated depth corresponding to the ^{14}C date of 1409 BP from the base (225 cm) of the Graeme Hall core. Assuming that dates from both cores are correct, this implies a sedimentation rate three times higher for the Graeme Hall core (0.16 cm/yr) than for SL1 (0.05 cm/yr). This is not unreasonable given that the Graeme Hall sinkhole is much larger and drains a larger area than the SL Gap (**Figure 10:2d**). If the state of bottom plugs exerts an important control, there is no reason to expect correspondence between the two sites. The history of ocean connectivity may also be very different.

Ramcharan (2005) suggests that the increases in carbonates ~600 BP (marked by the red dashed box) represents storm overwash, but does not explain why this should correlate with a dip in residuals and an increase in organics. Similar organic and residual changes occur in the SL1 curve at about the same time (blue dashed box), but without the carbonate increase. Ramcharan (2005) argues that a near contemporary increase in weedy pollen (not shown) results from storm-generated biological damage to the tree community, although it seems possible it could also result from agricultural clearing. Storm history, like paleoenvironmental history, may vary for a number of purely local reasons, including differing distance from sea, barrier heights, and storm direction.

10.9.4 Sedimentation Rates

Based on the suggested zonation scheme (**Figure 10:9**), sedimentation rates vary across the transect in a nonlinear spatial temporal pattern. Sedimentation rates for Zones 1-3 decrease landward, while the reverse is true for Zones 4-5. Presumably, sedimentation rates will be highest nearer the source, which could indicate that the relative strength of marine/terrestrial influence changes over time. This pattern is in general agreement with the inverse/direct carbonates/organic relationship, which suggests stronger marine influence during zone 1-2 and



10.11 Comparison of (a) Graeme Hall and (b) SL LOI curves. Despite their close geographical proximity, the two sites have very different depositional records. Chronological correlation is based on calculated calendar dates (shown in black); the dashed boxes represent a loose stratigraphic correlation to what Ramcharan (2005) believes marks a hurricane event at Graeme Hall.

more terrestrial influence during Zones 3-6. However, the overall carbonate percentages, which should be expected to spike during periods of increased marine influences, do not fully support this interpretation. In particular, carbonate values are highest during the top of the proposed marine sections, while one would expect the largest carbonate increase to correspond to the sudden marine intrusions associated with the bottom of the sections. Conversely, the low sedimentation rates for SL3 (the most seaward core) during Zones 4-5 may simply represent limited accommodation space, or any number of local factors.

10.9.5 Hurricane Activity

The local bathymetry is favorable for capturing a hurricane record. Although generally the coast is rather steep (15 m depth is reached 500 m offshore, and 100 m at 2 km), there is a shallow area directly to the west of SL (waves can be seen breaking in Figure **10:2c**) which currently is thickly covered by sand. Combined, these factors favor storm surge overwash deposition in SLL as waves will break close to shore, preserving more energy for the transport of the readily available sand. Unfortunately, the geographical attributes of this site are suboptimal as, facing west along a southeasterly trending coastline, the site is protected from surges driven by the powerful right front quadrant for all storm passing along the usual east to west track. Storms traveling to the north and passing to the west are the most likely to produce powerful surges for the site, but such tracks are rare (**Figure 10:4**). The 1898 storm is one of the few that takes such a path.

10.9.6 Clastic Layers

The SLL cores display very few intervals that fit our standard profile for selecting candidate storm layers. Commonly, such layers are chosen by inspecting intervals corresponding

to dips in the LOI curve and then checking for the presence of such identifying features as chaotic or vertical deposition, carbonate increases, the presence of larger grained material, upward fining, landward thinning, abrupt compositional change, and sharp bottom contact. Although some of the clastic layers in this transect do show abrupt compositional changes and/or sharp bottom contacts, most of the other features are missing. The clastic layers are generally rather thick black or gray clay, showing horizontal sedimentation, and little or no increase in grain size. Silt and sand are rarely present. The rather steady sedimentation rate inferred from the date/depth graph (**Figure 10:7**) argues against attributing the thick clay layers to instantaneous event deposition. Each of the potential layers is reviewed below.

10.9.6.1 Potential Storm-Generated Layers

10.9.6.1.1 Zone 1 Clastic layer A (black rectangle). This layer, at the very top of SL1, 2, and 3 contains some extremely large material (**Figure 10:8-10.12**). As indicated previously these layers probably are the result of human disturbance, not hurricanes.

10.9.6.1.2 Zone 2 Clastic layer B (red circle). There are small distinct dips in the LOI curve at the bottom of Zone 2 for all three cores. The layer thins slightly moving inland, but there is no increase in carbonate percentages. These dips are, at most, barely discernible. The displayed section (**Figure 10:12**) from SL2 is the clearest of the three. There is a slight increase in clay content, but most other storm markers are missing. It is not impossible that this layer is hurricane-generated, but evidence is lacking for definite storm attribution at this time. This interval occurs just above the sample dated to 1670 ^{14}C yr BP. Closer examination of this interval focusing on microfossil identification and detailed grain size analysis would possibly provide useful information.

An alternate possibility is these small dips represent a brief return of the conditions

responsible for the long clay intervals occurring a short distance lower in the cores. In SL1 and 2 the dips are separated from a long clay section by 5 cm of organic material; in SL3 the separation is 14 cm. It is possible that the layers in question merely represent a brief interval of unstable conditions with the depositional environment switching between two states.

10.9.6.1.3 Zone 4 Clastic layer C (blue circle). This is a black/gray clay layer that begins abruptly in all cores. Interval thickness increases from 6 cm (SL3) to 40 cm (SL1), then narrows to 29 cm at SL1. For this interval, organic and water content gradually increase downcore in SL 2, and decrease downcore in SL1. In all three cores the interval appears as a horizontally deposited clay matrix containing a few small fibrous roots. Possible causes of this interval are a sudden increase in water depth, leading to the submergence of the wetland vegetation, and consequent reduction in organic deposition, or, conversely, increased aridity resulting in a much lower organic content. No photos are presented, as, in all cores, the section presents as a featureless dark clay.

10.9.6.1.4 Zone 6 Clastic layer D (black circle). In both SL1 and SL2 at the top of Zone 6 a dramatic carbonate increase and a sharp drop in organics are observed, with organic percentage decreasing to <5% in SL2. The carbonate/organic relationship abruptly reverts to inverse (possibly marine-dominated) for this interval in both cores.

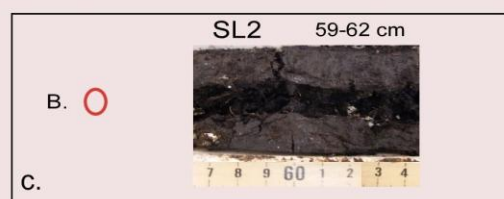
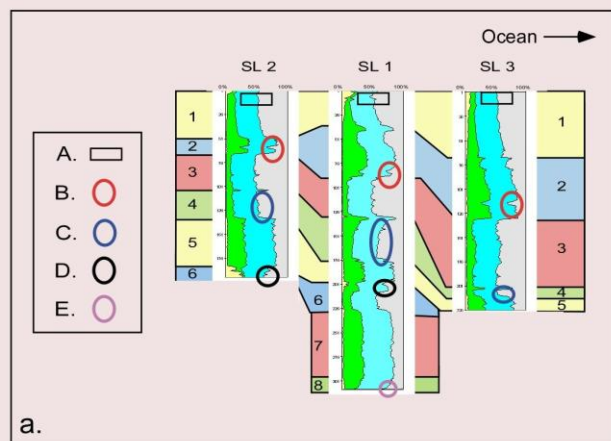
Despite the good stratigraphic correspondence, visual inspection shows the intervals to be unrelated. The section from SL2 is thick (12 cm) and highly distinctive, consisting of a crumbly brown shelly clay mixture. In SL1 the dip is much thinner, consisting of barely visible clastics mixed in with some large organic fragments (**Figure 10:12**). The section from SL2 appears at the very bottom of the core and most likely represents the basal material. The origin of the 3 cm dip for SL1 is unknown, but does not appear to be storm generated.

10.9.6.1.5 Zone 8 Clastic layer E (purple circle). There is a clear reduction in water and organics accompanied by a corresponding increase in residual and carbonates near the very bottom of SL1, the only core that penetrates to Zone 8.

Present, though in reduced abundance, are fragments of the same brownish shelly clay material observed at the base of SL2, which probably represents basal material (**Figure 10:12**). As none of these layers has been positively identified as hurricane-generated, with only a single unrejected candidate, it seems either that at most only one storm of sufficient strength has passed the site during the length of our record, or that we are unable to recognize the sedimentary signal.

10.9.7 Paleoclimatic Record

Although no palynological analysis was done, some general observations concerning paleoenvironmental conditions can be suggested, given the abrupt and drastic changes that occur throughout the cores. The most obvious feature in the cores of this transect is the cyclic oscillation between the deposition of organic-rich peat and the dark clays. Based on the dates recovered from SL1, these changes are multi-centennial to millennial in length, and therefore of the correct scale to be climate-driven. The causes of these changes are not known, and, given the lack of correspondence with the neighboring Graeme Hall swamp record, are possibly due to such purely local factors as the creation/dissolution of sinkhole plugs and the alteration of barrier height. Increasing depth of the SLL can explain the change from peat to clay and could result from a number of causes. Climatic causes should not be dismissed out of hand, particularly given the duration of the changes. With a calculated sedimentation rate of 0.05 cm/yr every 10 cm interval represents 200 years of deposition, thereby reducing the apparent abruptness of change. Possibly the clay intervals result from increased aridity, driven by a southern position of the

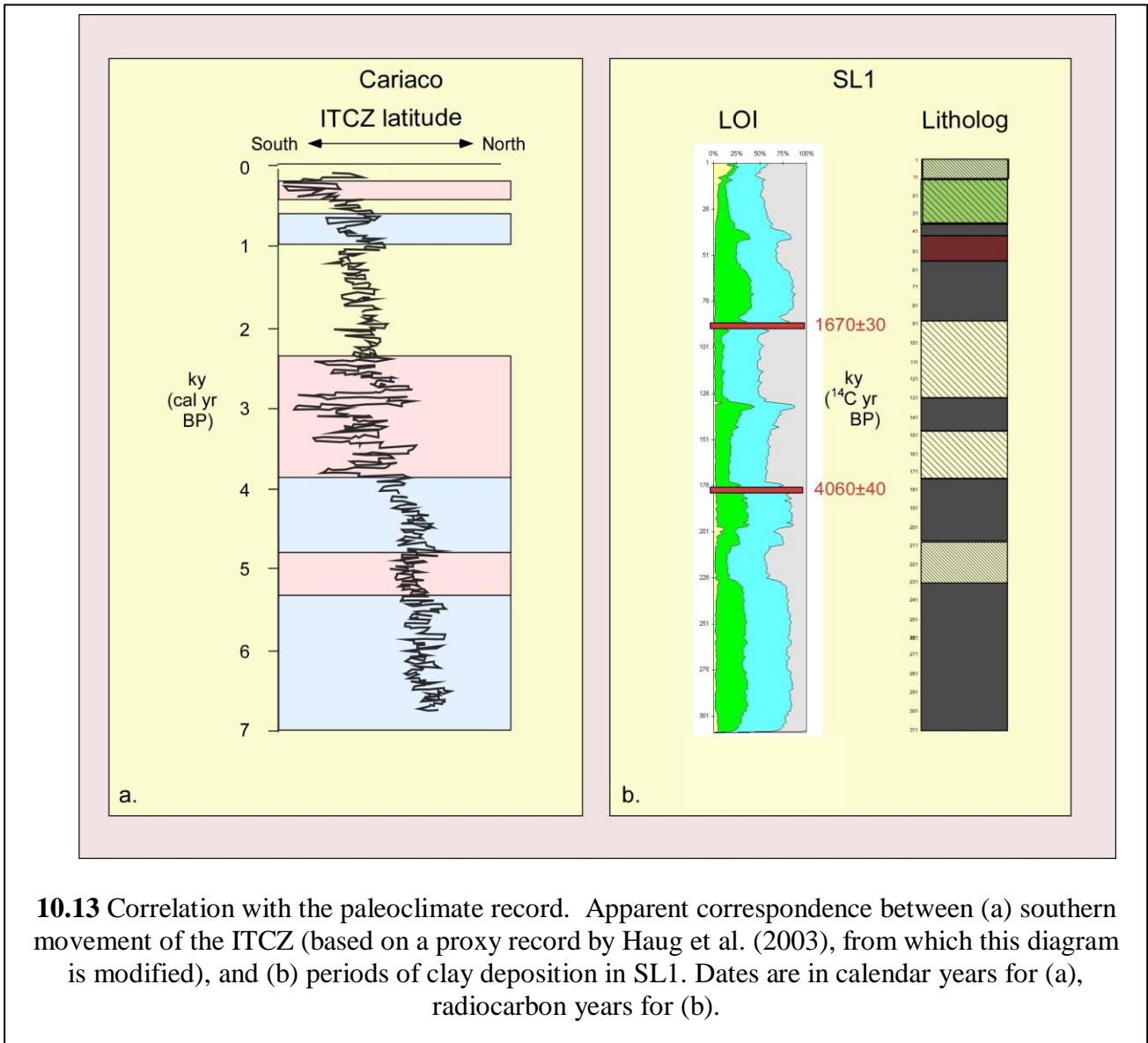


10.12 Potential hurricane generated clastic layers. (a) Five candidate layers identified as occurring across the transect are depicted in (b-f).

Bermuda High (BH). Given the physical setting of our transect in a shallow limestone depression, clay layers could theoretically result from either increased water depth (drowning of marsh vegetation), or difficult growing conditions. Due to the amount of *in situ* roots in the layers the second situation seems more likely. We suspect that these layers result from increased aridity and resultant plant death, probably related to the shrinking/drying up of the marsh. Due to the porous limestone, annual precipitation would not have to decrease drastically, as either a longer or more severe dry season would possibly be sufficient to cause annual desiccation and die offs, thereby accounting for the continued presence of a small amount of roots, but greatly reduced organic content. As the clay intervals are most prevalent from ~4000-1500 ¹⁴C BP, the timing for aridity agrees with that inferred from isotopic analysis of cores from Lake Miragoane, Haiti (Hodell et al., 1991). SL1 organic/clay oscillation also show a fairly good correspondence with latitudinal shifts in mean annual latitude of the Intertropical Convergence Zone (ITCZ), as inferred from an Cariaco proxy record (Haug et al., 2001) (**Figure 10:13**). Clay intervals correlate with southern shifts between 4000-1500 BP and ~5000 BP; and less exactly with the Little Ice Age ~ 300-500 BP (blue boxes, **Figure 10:13**). Peat intervals correlate with northern positions from ~4000-4800 BP, before ~5200 BP, and the Medieval warm Period from ~800-1000 BP (pink boxes **Figure 10:13**). As hypothesized in **Chapter 4**, cold periods in the North Atlantic should result in parallel southern movement of the ITCZ, the BH, and the tropical cyclone zone. Although Barbados' far southern position should presumably shield it from the direct influence of the subsiding dry air issuing from the BH, the correspondence is intriguing.

10.10 Summary

The combination of high population levels and geologic constraints has severely limited the number of appropriate coastal coring sites in Barbados. Our site, though possessing many



promising geological features (a mud-dominated shallow water environment at low elevation in close proximity to the sea, abundant sediment supply, stable bedrock geology, steep bathymetry, and relatively minor anthropogenic disturbance), is severely handicapped by its geographical setting. By facing west, the power of hurricanes passing to the south is blocked by the southeasterly-trending coastline, while hurricanes passing to the north are blocked by the entire mass of the island. Even under the most favorable paths, some reduction of surge height can be expected to result from coastline orientation.

No unequivocal hurricane events were recorded for the transect, although the sedimentary signature of a single event remains under consideration. The date for this possible event is ~1600 BP (^{14}C yr and cal yr BP are very similar for this date). Even if further research positively identifies this as the sedimentary signature of a hurricane strike, the paleostrike record will shed very little light on the long term regional strike patterns.

Nonetheless, clear paleoenvironmental trends can be noted in this record, mainly a cyclic shift from highly organic peat to more inorganic clays, which seem to roughly parallel changes in the proxy record of ITCZ latitudinal position.

The calculated basal date of core SL1 is >7000 ^{14}C yr, making it the longest record in this study. Although the possibility exists that this record is purely local, controlled by barrier height and/or local limestone hydrology, the intriguing match with the Cariaco record, also permits the possibility that important regional climatic data could be contained within this core. A more intense, multi-proxy approach (pollen, diatoms, phytoliths, and isotopes) could perhaps yield impressive results.

10.11 References

- Barbados Statistical Service, 2008. Statistical Service Labor Force Survey. Bridgetown, Barbados.
- Beckles, H., 1990. A history of Barbados: from Amerindian settlement to nation-state. Cambridge University Press, Cambridge.
- Caribbean Tourism Organization. 2007. Individual Country Statistics-Barbados, 2006. <http://www.onecaribbean.org/statistics/countrystats>. Accessed May 10, 2009
- Caribbean Tourism Organization. 2009. Latest Statistics 2008. <http://www.onecaribbean.org/content/files/april16Lattab08.pdf>. Accessed May 10, 2009
- Carpenter, T. A., 1899. The West Indian hurricane, September 1898. *The Quarterly Journal of the Royal Meteorological Society*. 25, 23-32.
- Dunn, G. E., Davis, W. R., and Moore, P. L., 1955. Hurricanes of 1955. *Monthly Weather Review*. 83, 315-326.
- Fairbanks, R. G., 1989. A 17,000-year glacio-eustatic sea level record: influence of glacial melting rates on the Younger Dryas event and deep-ocean circulation. *Nature* 342, 637-642.
- Haug, G. H., Hughen, K. A., Sigman, D. M., Peterson, L. C., and Rohl, U., 2001. Southward migration of the Intertropical Convergence Zone through the Holocene. *Science* 292, 1304-1314.
- Hodell, D. A., Curtis, J. H., Jones, G. A., Higuera-Gundy, A., Brenner, M., Binford, M. W., and Dorsey, K. T., 1991. Reconstruction of Caribbean climate change over the past 10,500. *Nature* 352, 790-793.
- Jones, I. C., and Banner, J. L., 2003. Estimating recharge thresholds in tropical karst island aquifers: Barbados, Puerto Rico and Guam. *Journal of Hydrology*. 278, 131-143.
- Krech, S., McNeill, J. R., and Merchant, C., 2003. *Encyclopedia of World Environmental History*. Routledge, Florence, Kentucky.
- Ministry of Finance, Economic Affairs and Energy, 2008. Barbados Economic and Social Report, 2007. Bridgetown, Barbados.
- Poole, E. G., and Barker, L. H., 1983. *Geology of Barbados*. Geologic Map of Barbados (1983) 1:50000.
- Radtke, U., and Schellmann, G., 2006. Uplift history along the Clermont Nose Traverse on the west coast of Barbados during the last 500,000 Years—implications for paleo-sea level reconstructions. *Journal of Coastal Research* 22,350-356. DOI: 10.2112/05-0439.1.

Ramcharan, E. K., 2005. Late Holocene ecological development of the Graeme Hall swamp, Barbados, West Indies. *Caribbean Journal of Science*. 41, 147-150.

Schomburgk, R. H., 1848. *The History of Barbados*. Longman, Brown, Green and Longmans, London.

Speed, R. C., 1986. Geologic history of Barbados: a preliminary synthesis. *Transactions of the 11th Caribbean Geological Conference*. Barbados. Chapter 29. Government Printing Office. Bridgetown, Barbados.

CHAPTER 11 SUMMARY

11.1 General

The primary purpose of this dissertation is to investigate the relationship between hurricane landfall and climatic conditions in the Caribbean over the late Holocene.

Accomplishing this requires first understanding the temporal correlation of landfall patterns between sites in order to identify any discernable activity patterns, and then the comparison of these patterns with the climatic record in order to determine correlation and possible forcing agents.

11.2 Temporal Correlation

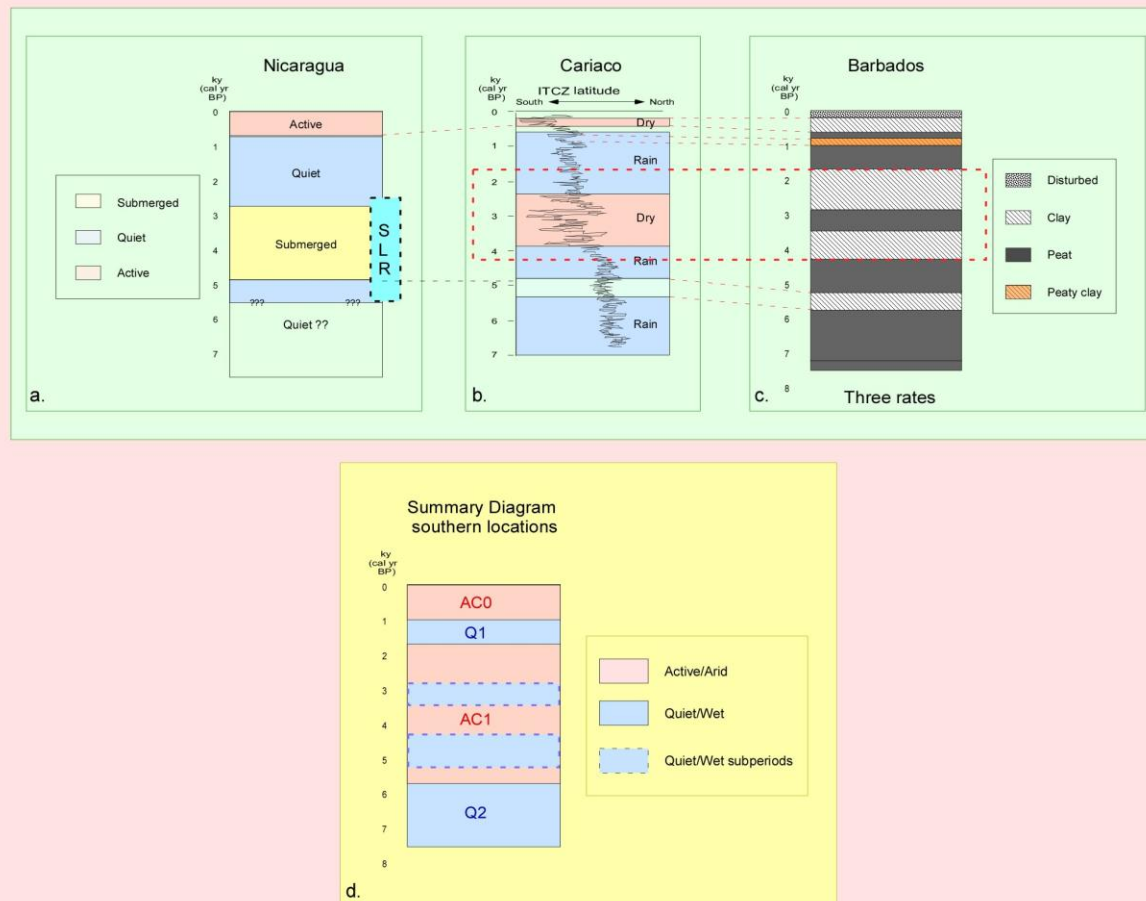
11.2.1 Southern Locations

Multi-millennial records were extracted from three coastal transects in Nicaragua located in a swamp, marsh and mangrove forest, respectively, spanning <90 km (**Chapter 9**), and from a single transect below a floating freshwater marsh in a coastal depression in Barbados (**Chapter 10**). The Nicaraguan sites lie between 11° 52' and 12° 42' N, while the Barbados transect is at 13° 04' N, thus providing sites at similar latitude with >2500 km of longitudinal differences. The sedimentary data from the three Nicaraguan transects have been combined into a single activity regime diagram, with all regime boundaries calibrated into cal yr BP from dated samples taken at the boundaries. Since hurricane activity did not seem to be recorded in the Barbados cores, a simplified litholog is presented, basically identifying the depositional changes from clay to peat. Dating was based on two sedimentation rates, with a higher rate (based on the rate from 1 cm to the dated sample at 88cm) applied to the peat deposition (1-89 cm; 189-309 cm) and a lower rate (determined by dated samples at each end of the interval) for the clay deposition

between 88 and 179 cm. Dates for all sedimentary unit changes were calculated mathematically in ^{14}C yr BP using the appropriate sedimentation rate and then calibrated to cal yr BP, assuming a 40 year error bar. Calibration in both cases was by means of the CALIB 5.0.2 program at (<http://calib.qub.ac.uk/calib/calib.html>) (Stuiver et al., 2005). These diagrams are presented in **Figure 11:1a** and **c**.

The activity diagram for Nicaragua shows an Active period for the last ~750 cal yr BP, preceded by a Quiet period, which begins ~2775 cal yr BP. This is preceded by a “submerged” period beginning ~4900 cal yr BP, during which the location was apparently located under deeper water and probably not recording hurricane landfalls. This was preceded by a short Quiet period extending to the beginning of the record at ~5500 cal yr BP. The submerged period most likely results from sea level rise, not climatic conditions. During the period of initial deposition at 489 cm depth, mean sea level (MSL), according to the Toscano and Macintyre (2003) curve, was ~5 m below present, or slightly below the bottom of the core. By 4900 cal yr BP, however, that same curve estimates sea level as 4 m below present, or slightly higher than the depth of the dated sample at 444 cm. By the beginning of the Quiet period (~2775 cal yr BP), the Toscano and Macintyre (2003) curve shows sea level at ~2 m below present, or slightly below the dated sample at 189 cm. Assuming that the core top is at present MSL and that these dates are correct, sea level rise neatly explains the submerged period, which corresponds to periods when sea level was higher than the contemporary core depths. Above that transition, accretion should have easily remained above the slowing sea level rise. The middle section of this record is therefore unavailable for climatic correlation with other sites.

The Barbados record covers a longer period, with a calculated basal date of ~7500 cal yr BP, in a shorter core, with a total length of 309 cm. Assuming that the core top is near present



11.1 Paleoactivity/climatic/depositional regime correlations for southern sites. Shown are a hurricane activity regime diagram for (a) Nicaragua, a diagram (c) of depositional regimes for Barbados, which is correlated to (b), the proxy record of latitudinal movement of the ITCZ, based on a proxy record by Haug et al.(2003), from which this diagram is modified, and (d) a summary diagram combining the activity and depositional data. The blue box labeled “SLR” in (a) is used to indicate that deposition during this interval was probably controlled by sea level rise and not local environmental factors.

MSL this puts the bottom of the core >5 m above the sea level estimated for the period by Toscano and Macintyre (2003), and therefore beyond the reach of flooding by sea level rise. Hurricane activity regimes cannot be correlated directly, due to the lack of landfall records in the Barbadian cores. However, a rough indirect correlation is possible through their mutual correlation with the regional climatic record. For this reason the Cariaco proxy record for ITCZ movement has been included (**Figure 11:1b**). This record is based on a sediment core extracted at 10°42.73'N latitude, off the coast of Venezuela, slightly south of our sites, and ~ 600 km west of Barbados.

As discussed above (**Chapter 4**), mean annual latitudinal position of the ITCZ is hypothesized to correlate with several climatic and hurricane-related features. Southern movement in the mean annual position of the ITCZ is theorized as resulting in increased aridity for both of our sites, accompanied by an increase in hurricane activity for Nicaragua. Due to its far eastern position, hurricane activity in Barbados should probably be relatively insensitive to activity regime changes (see below). Both our Barbados and Nicaragua sites show a fairly good correspondence with the expected correlation. The ~ 750 year Active Period at the top of the Nicaraguan diagram corresponds reasonably well with the southern position of the ITCZ associated with the Little Ice Age (LIA) cooling, as does the preceding Quiet Period with the northern position from ~750-2200 cal yr BP. The southern ITCZ position from ~4000-2200 cal yr BP does not show up in our Nicaraguan diagram as it occurs during the non-recording submerged period. The short early Quiet Period (~5500-5000) correctly corresponds to a northern position (blue dashed line). The match between Barbados and the ITCZ record is less exact. As discussed above (Chapter 10), the clay layers most likely correspond to periods of increased aridity, presumably associated with southern movement of the ITCZ. The top clay layer

aligns well with the Little Ice Age, as does a clayey peat section slightly lower down with a similar small southern movement ~ 800-1000 cal yr BP. However the two large clay layers achieve only a rough correspondence with the southern position occurring from ~4000-2400 cal yr BP (red dashed box). The lowest clay section, which is much more organic and contains many more roots than the other clay sections, possibly correlates to a small southern movement in the ITCZ position ~ 5000 cal yr BP (lowest dashed red lines).

Combining the Nicaraguan and Barbadian data into a single summary diagram presents difficulties. Not only are different proxies (hurricane activity regimes vs. paleoenvironmental conditions) presented, but the mid-section of the Nicaraguan core is nonrecording. However, by correlating dry conditions in Barbados with Active Periods in Nicaragua, a regional summary can be created (**Figure 11:1d.**) The timing and presence of the top Active/Dry Period (ACO) seems well-defined, as does the presence of the two Quiet/Wet Periods (Q1, Q2), although their timing is somewhat less certain, as is that of the middle, punctuated Active/Dry Period (AC1). The shorter, less distinctive quiet/wet periods within AC1 are classified as “subperiods” to distinguish them from the more distinct Q1 and Q2.

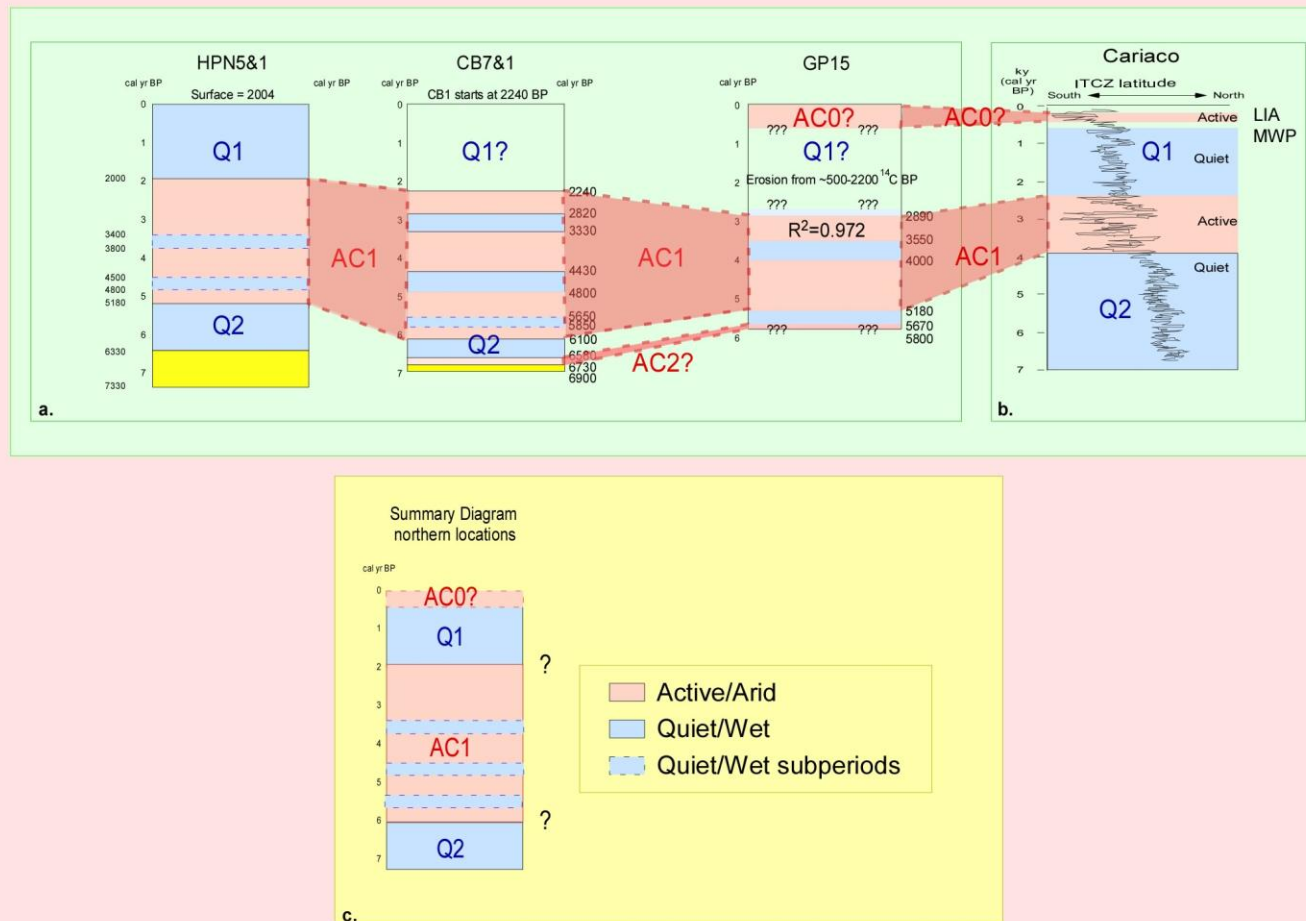
11.2.2 Northern Locations

Sedimentary records were extracted from a variety of locations and environments in Belize including a mainland lake, swamps and marshes, and mangrove islands within an offshore atoll. The atoll sediments appear not to constitute a reliable paleostorm archive, as the requisite proxy is dependent upon the presence of mobile sand sources, which are scarce and transitory within the atoll. Nor do the records contain a reliable climatic record, as deposition appears to be event-driven, with all major sedimentary changes controlled by local seismic activity. Both mainland sites (each consisting of paired transects in differing environments) contain multi-

millennial length records. Although erosion has resulted in an incomplete record for the Mullins River/Gales Point site, composite records from transects obtained from Commerce Bight Lagoon (CB) and Hopkins Marsh (HPN) preserve records extending to ~ 7000 cal yr BP.

The activity regime records inferred from the proxy records for these mainland sites were presented in **Figure 7:47**, and displayed here for ease of reference (**Figure 11: 2a**). Both the GP/MR and the CB/HPN sites display a punctuated Active Period (AC1) lasting for several millennia, although the time frame varies between sites, with initiation varying from ~6100-5200 cal yr BP, and termination from ~2900-2000 cal yr BP. This is preceded by a Quiet Period, and perhaps an earlier Active Period (AC2) before which the sites become non-recording. AC0, an Active Period covering the last 500 years, is indicated for the GP/MR site, but not for CB/HPN. The chronology as presented is not considered definitive, as unresolved dating issues still exist for several of the cores.

Comparing this proxy activity record with the proxy ITCZ climatic record (**Figure 11:2b**) produces some interesting correlations. Theoretically, the latitudinal migration of ITCZ should produce similar results in Belize as in Nicaragua; namely a southern position should result in increased aridity and hurricane activity, with a northern position resulting in the opposite conditions. Due to track patterns (see below), the increased hurricane activity should be more noticeable in the Belize sites. Some general agreement exists between our inferred activity regimes and long-term mean ITCZ latitude, with increased activity correlating to the southern movement from ~2400-4000 cal yr BP (AC1). The early Quiet Period before ~6000 cal yr BP (Q2) also corresponds to a northern position. However, there is no reduction in landfall activity corresponding to the northern position of the ITCZ from ~4000-6000 cal yr BP, and only the



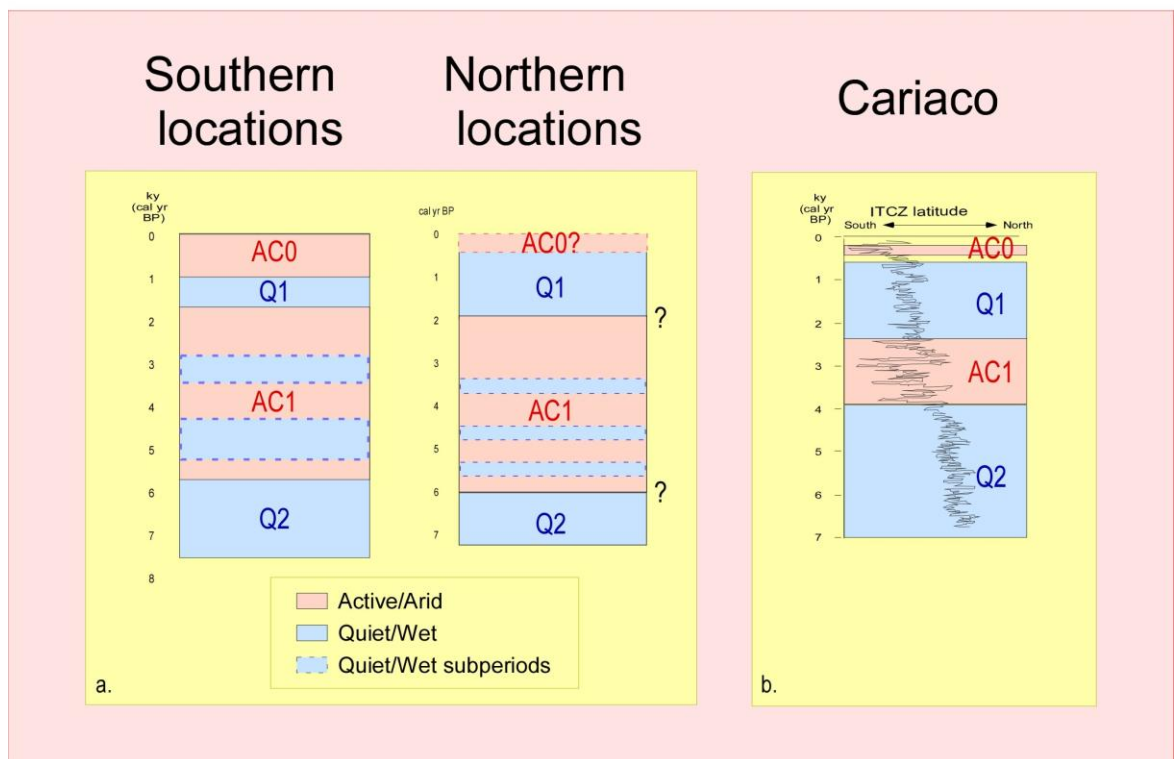
11.2 Paleoactivity regime correlations for the Belizean mainland sites. Shown are the activity regime diagrams for (a) the HPN, CB, and GP transects, correlated to (b) the proxy record of latitudinal movement of the ITCZ, and (c) a summary diagram combining the three activity regime.

GP/MR site shows increased hurricane activity related to the southern movement associated with the recent LIA (ACO). As the record from Turneffe seems to be controlled by local seismic events, it has been excluded from this regional compilation. A summary diagram for the Belize sites, based on the correlation of activity regimes for GP/MR and CB/HPN is presented in **Figure 11:2c**. This diagram is inclusive, meaning that features are included, even if they are not present in all sites.

An example is the most recent Active Period (ACO), which is shown even though it was identified only at GP/MR. Similarly three Quiet subperiods are displayed as occurring in AC1, even though this is the maximum site number, with HPN and GP/MR showing less. The termination/initiation of AC1 is depicted as occurring from the earliest to the latest recorded, even though inter-site discrepancies probably are at least partially the result of dating issues. This chronological uncertainty is indicated by question marks. The exception to this rule is the elimination of AC2, the earliest Active Period, as it rests on extremely limited data at the bottom of two cores.

11.2.3 Combined Locations

Combining the summary activity regime diagrams for the northern and southern sites produces a consistent pattern (**Figure 11:3a**). Both the northern and southern diagrams display a short, recent Active Period (AC0) at the top, preceded by a Quiet Period (Q1), then a punctuated Active Period (AC1), and a basal Quiet Period (Q2). Neither the absolute nor relative ages of the different periods achieve an exact correspondence between diagrams, however. Similarly, both diagrams match the pattern but not the dating of the ITCZ migration diagram, with the biggest difference being the duration of AC1, which is significantly shorter for the ITCZ diagram (**Figure 11:3 b**).



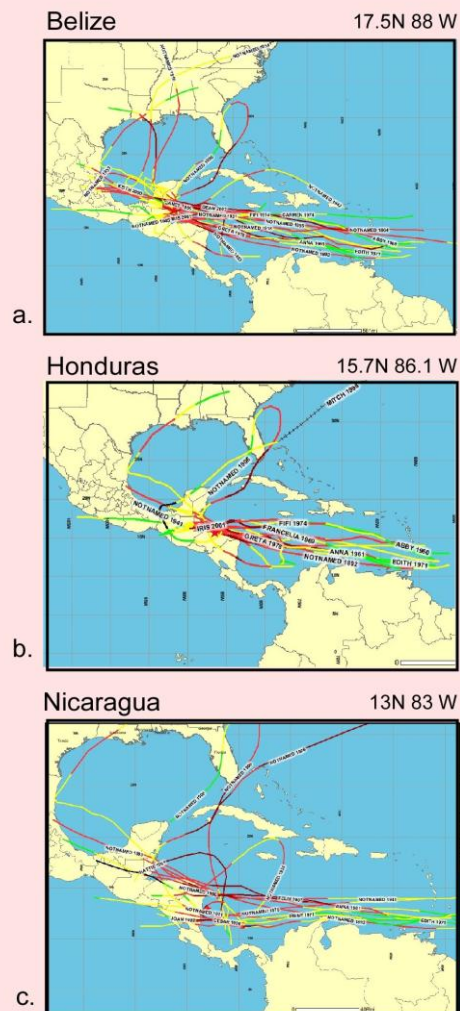
11.3 Combined paleoactivity/climate regimes. Shown are the summary diagrams for (a) the southern and northern locations, and (b) the proxy ITCZ record.

11.3 Landfall vs. Track

This study has demonstrated clear shifts in the frequency of hurricane activity over the late Holocene for our study sites, and has shown at least a rough correlation between the timing of these activity regimes and ITCZ position. We now use the historical record to show both that hurricane activity at these sites is related to specific track patterns, and that these patterns form coherent groupings. Because different atmospheric conditions favor the frequency of different track groups, conditions which favor landfall in Nicaragua or Belize are not the same that favor landfall in Puerto Rico or Long Island. This supports the argument that landfall records are reasonable proxies for atmospheric conditions.

An example is the track pattern related to hurricane activity along the Caribbean coast of Central America. **Figure 11:4** shows all hurricanes that have passed within 150 km of points along the middle of the Belizean (a), Honduran (b), and Nicaraguan (c) coast since 1851. The similarity of the tracks approaching all three locations is striking, consisting almost entirely of horizontal tracks plowing westward across the Atlantic. It can also be noted that the track patterns move progressively southward for the three locations.

Hurricanes within the Gulf of Mexico (GOM) show a different pattern (**Figure 11:5**). The cyclogenesis points are similar for most GOM storms, with early track paths surrounding the Greater Antilles. The point of landfall seems to be controlled by later track events, with increasing recurvature resulting in more eastern landfall. This is clearly demonstrated in the remarkable late divergence between similarly-oriented early tracks for hurricanes striking Matamoros (e) and NW Florida (f). The pattern associated with hurricane activity along the Atlantic coast of North America is markedly different (**Figure 11:6**). Although these storms tend to have both a slightly more northerly cyclogenesis point and early track, they are primarily



11.4 Hurricane histories for the southern Caribbean. Shown are all hurricanes that have passed within 150 km of points along the center of the (a) Belizean, (b) Honduran, and (c) Nicaraguan coasts since 1851. All tracks for Figures 11:4-9, and 11 are based on the NOAA HURDAT (“best track”) data set.

distinguished by their pronounced recurvature.

The general pattern of hurricane tracks in the western NA, Caribbean Sea and the GOM is clear. **Figure 11:7** shows the tracks of all hurricanes since 1851 passing within 150 km of points set up on a 5° grid between $25\text{--}15^\circ\text{N}$ from $80\text{--}60^\circ\text{W}$. The difference between the two end members (bottom left, top right) is obvious; hurricanes that pass through the extreme southwest have nearly horizontal (east to west) tracks, while those passing to the northeast are prominently recurved. For all longitudes recurvature increases with latitude, while for all latitudes the farther west that recurvature begins, the farther south the average landfall. It is important to note that cyclogenesis and early track location are much more uniform than point of landfall for these storms. This suggests that atmospheric conditions in the mid and western Atlantic exert very important control over landfall location. Basically, as most hurricanes begin at similar latitudes and drift west across the Atlantic in somewhat similar tracks, their point of landfall is primarily dependent upon the longitude at which their steering becomes dominated by recurvature. This, of course, primarily results from the position and strength of the BH (Elsner et al., 2000).

Because of this, the location of landfall associated with Caribbean hurricanes is complicated (**11:8**), with small geographical differences in track location resulting in large differences in landfall location. For example, hurricanes passing within 150 km of Jamaica (**Figure 11:8a**), western Cuba (**Figure 11:8b**), southern Dominican Republic (**Figure 11:8c**), and Guadeloupe (**Figure 11:8f**) are likely to make landfall within the GOM, whereas hurricanes passing near Puerto Rico (**Figure 11:8d**) and Barbuda (**Figure 11:8e**) are much more likely to make landfall along the Atlantic coast. The geographical gradient can be surprisingly steep, an example being the differences in track patterns for Barbuda and Puerto Rico (**Figure 11:9**). In all three groupings (tropical storms, hurricanes, and major hurricanes) an increased propensity for

Gulf of Mexico

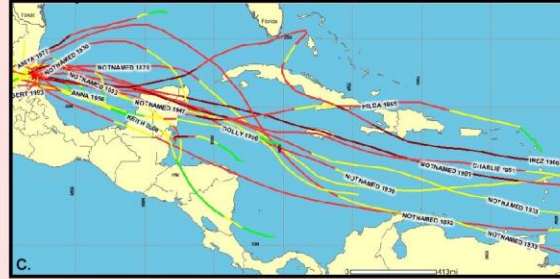
Yucatan



Galveston



Tampico



Lake Shelby



Matamoros



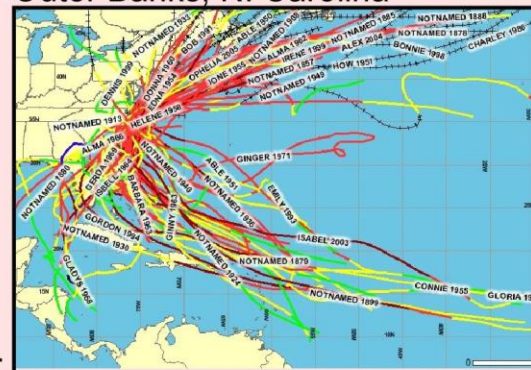
NW Florida



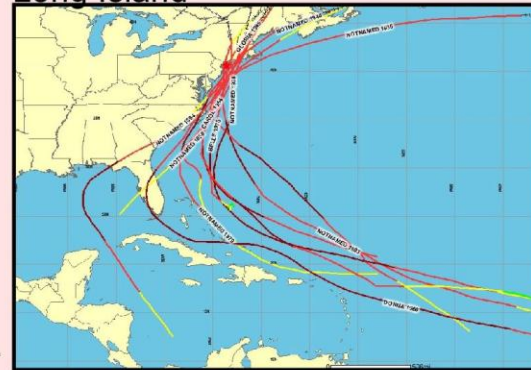
11.5 Hurricane histories for selected locations in the Gulf of Mexico. Shown are the tracks of all hurricanes since 1851 passing within 150 km of the locations named.

[illegible]

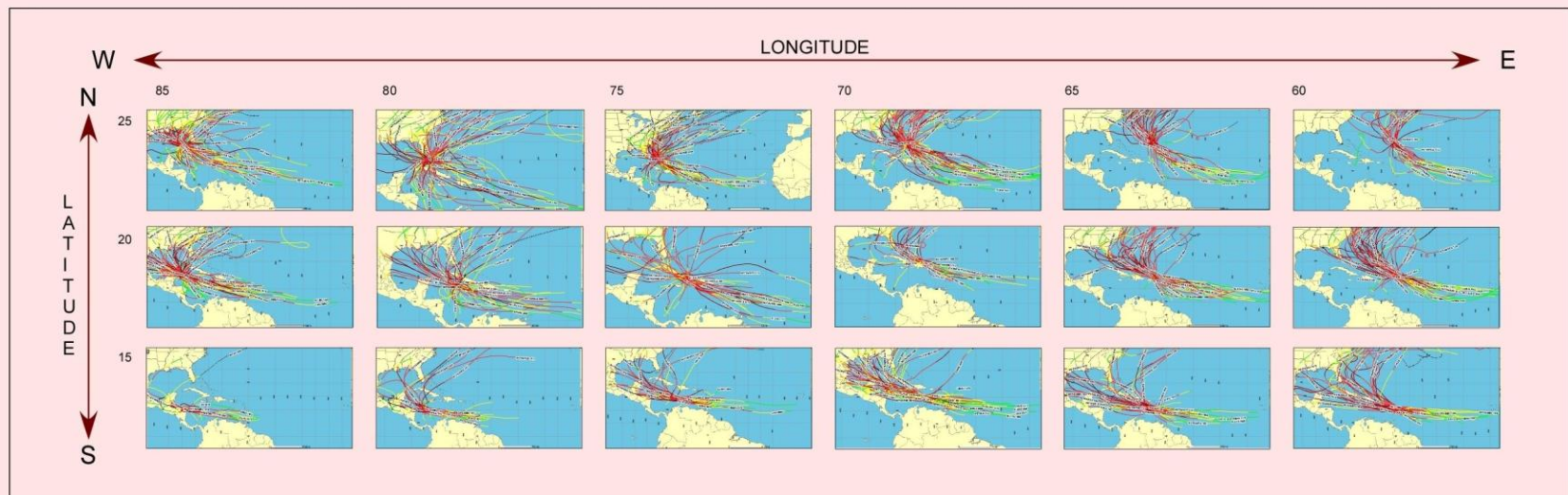
Outer Banks, N. Carolina



Long Island



556



11.7 Hurricane histories for the Caribbean and Gulf of Mexico. Shown are the tracks of all hurricanes since 1851 passing within 150 km of points set up on a 5° grid between 25-15°N from 80-60°W.

for western landfall can be noted for storms passing near Barbuda, even though the two locations are situated <400 km apart with a total latitudinal difference of <75 km.

For the instrumental period the track patterns associated with landfall location can be divided into three groups (**Figure 11:10**). Hurricane activity along the Central American coast from Belize south and the northern coast of South America and the associated islands is associated with a southern track pattern (Zone 3); activity in the Gulf of Mexico is associated with a middle track position (Zone 2), and activity for the northernmost Lesser Antilles, the Bahamas, and the Atlantic coast of North America, are associated with a northern position that features strong recurvature (Zone 1). Naturally there is a fair amount of overlap at zone borders, with much of the Greater Antilles falling into a transition area between Zones 1 and 2.

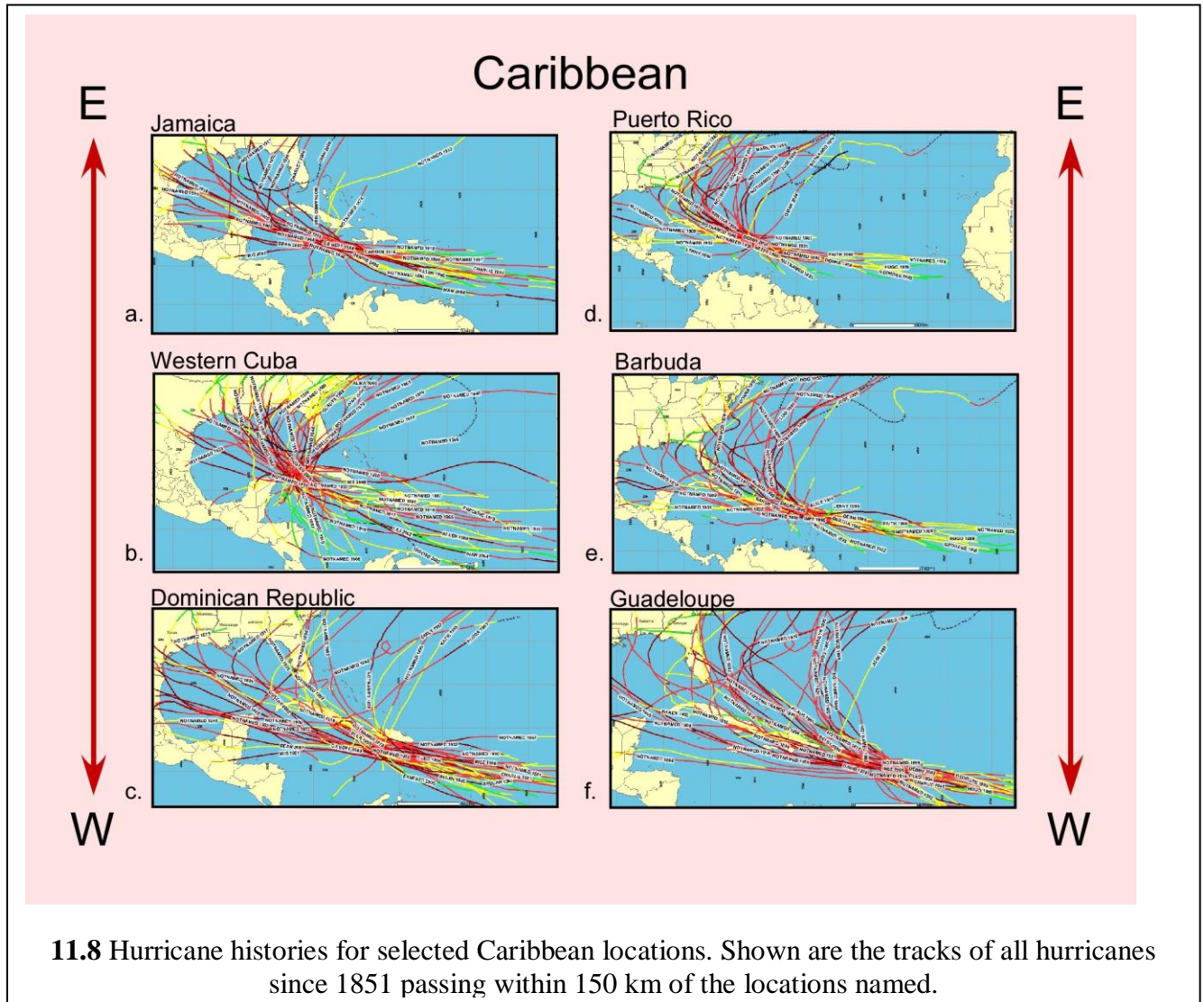
In accordance with the theoretical arguments put forth in **Chapters 3 and 4**, the correspondence between these patterns and circulation, climatic features and timing are the following:

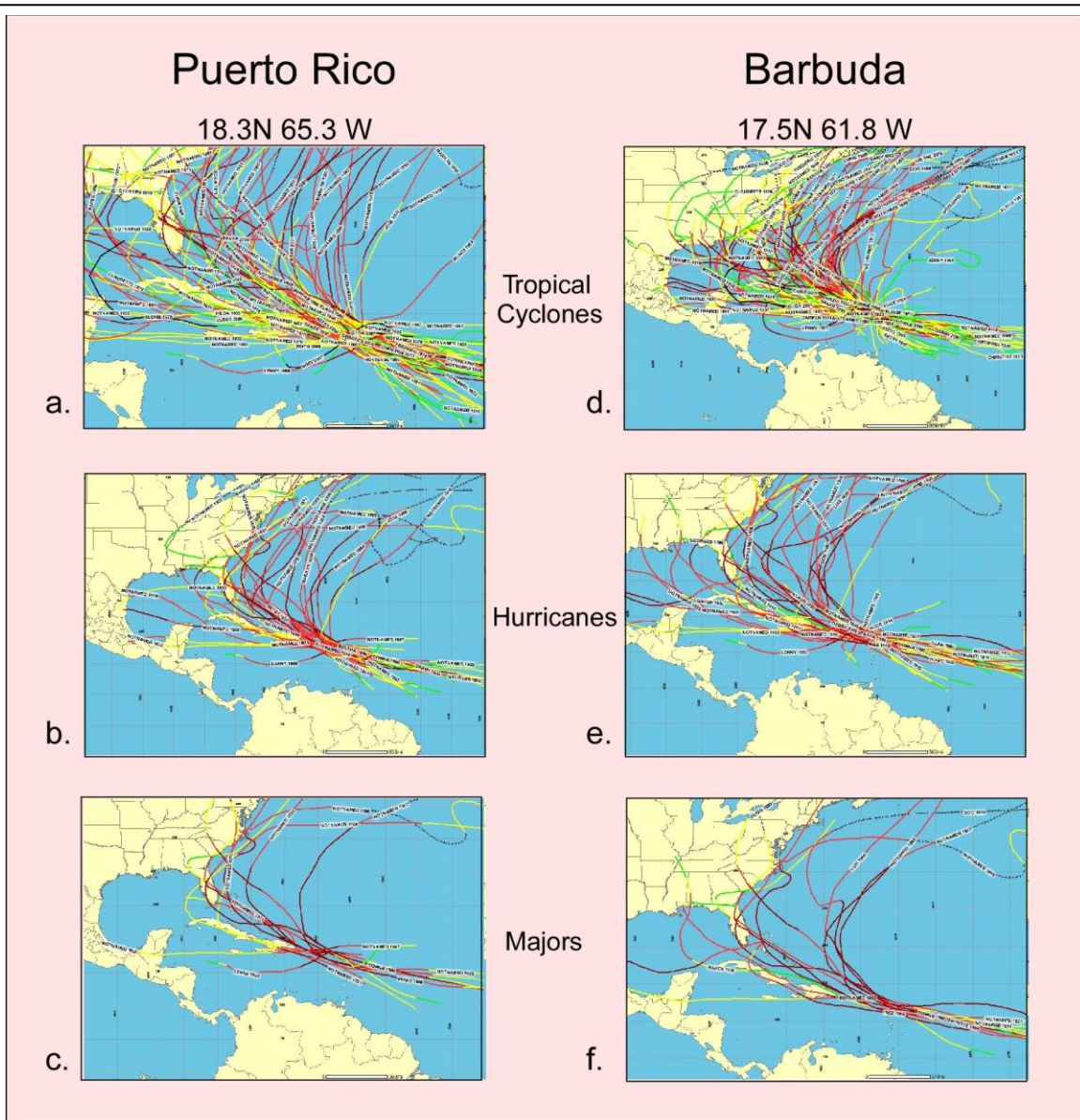
Zone 1-Northern location of ITCZ, strong BH in a northeastern position, weak Pole-Equator gradient (Warm Period), 600-1100 (MWP), >6000 BP.

Zone 2-Intermediate intensity/location of ITCZ and BH, 1100-2400 BP.

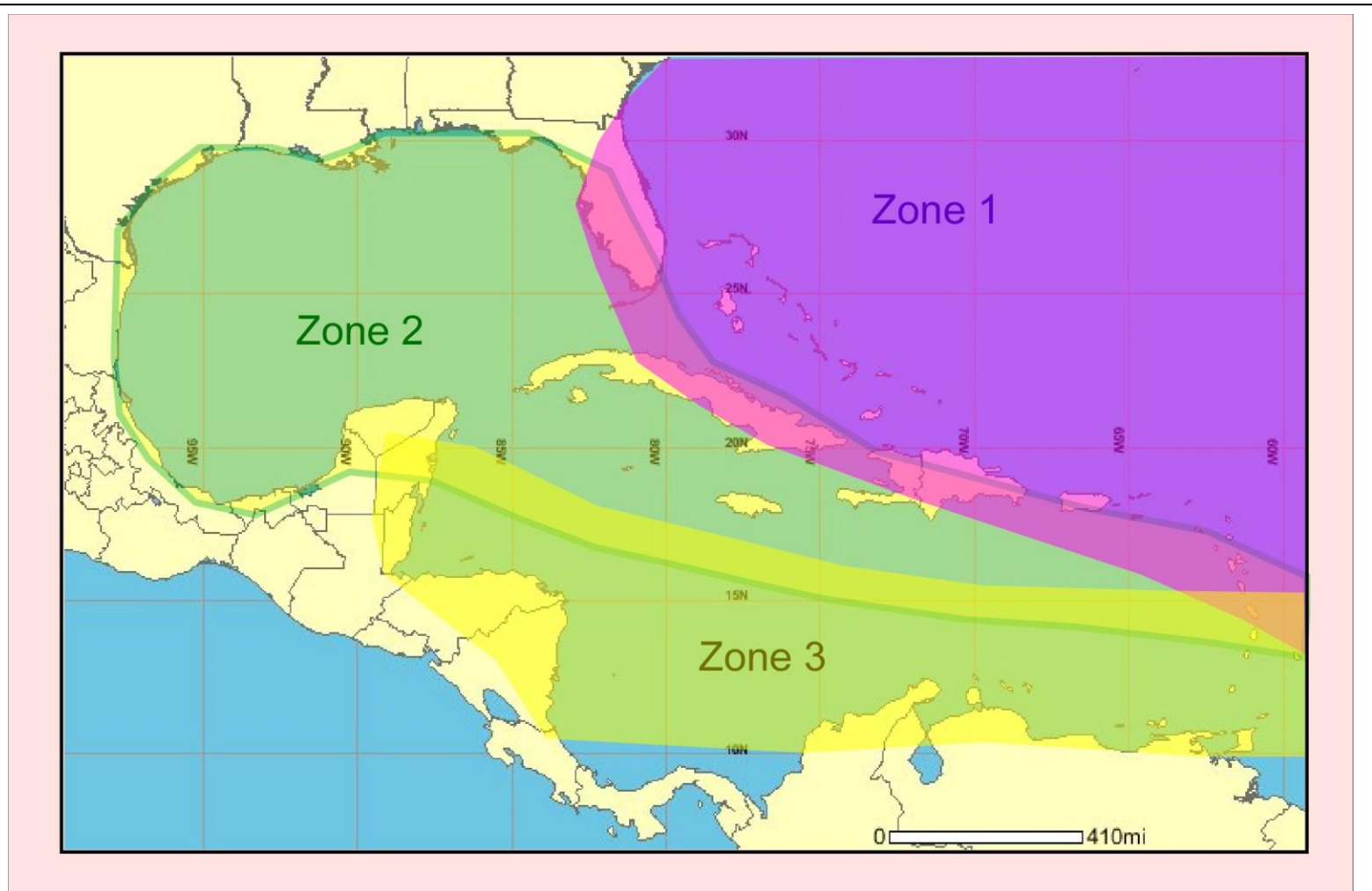
Zone 3-Southern ITCZ, weak BH in a southwestern position, strong Pole-Equator temperature gradient (Cold Period), 0-500 (LIA), 2400-4000 BP.

The far southeastern locations are included in all three zones as they lie east of the point where storms become divided into separate track groups. Barbados serves as an example of this (**Figure 11:11**), as tropical cyclones passing within 150 km of the island have achieved landfall from Nicaragua through Newfoundland (a), although the latitudinal spread is smaller for hurricanes (b), and major hurricanes (c). Therefore, track frequency changes should be minimal in the area, as hurricane passage through the area occurs under all atmospheric conditions.





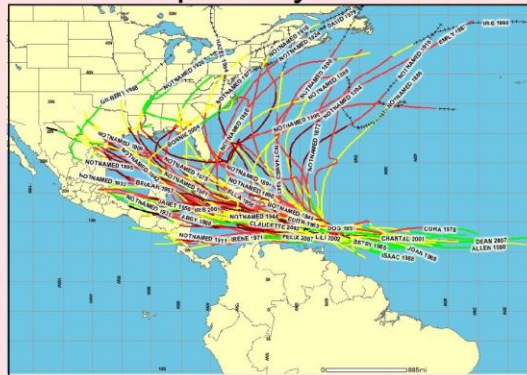
11.9 Tropical cyclone histories for Puerto Rico and Barbuda. Shown are the tracks of (a) all tropical cyclones, (b) hurricanes, and (c) major hurricanes, since 1851 passing within 150 km of the eastern tip of Puerto Rico. Similar records(d, e, and f) are displayed for Barbuda.



11.10 Hurricane track zones. Hurricane landfall locations are generally grouped by regions, with landfall in each of the three zones usually related to specific atmospheric conditions that favor track occurrence within that zone. There is a fair amount of overlap along zone boundaries.

13 N 59.5 W

Tropical Cyclones



a.

Hurricanes



b.

Majors



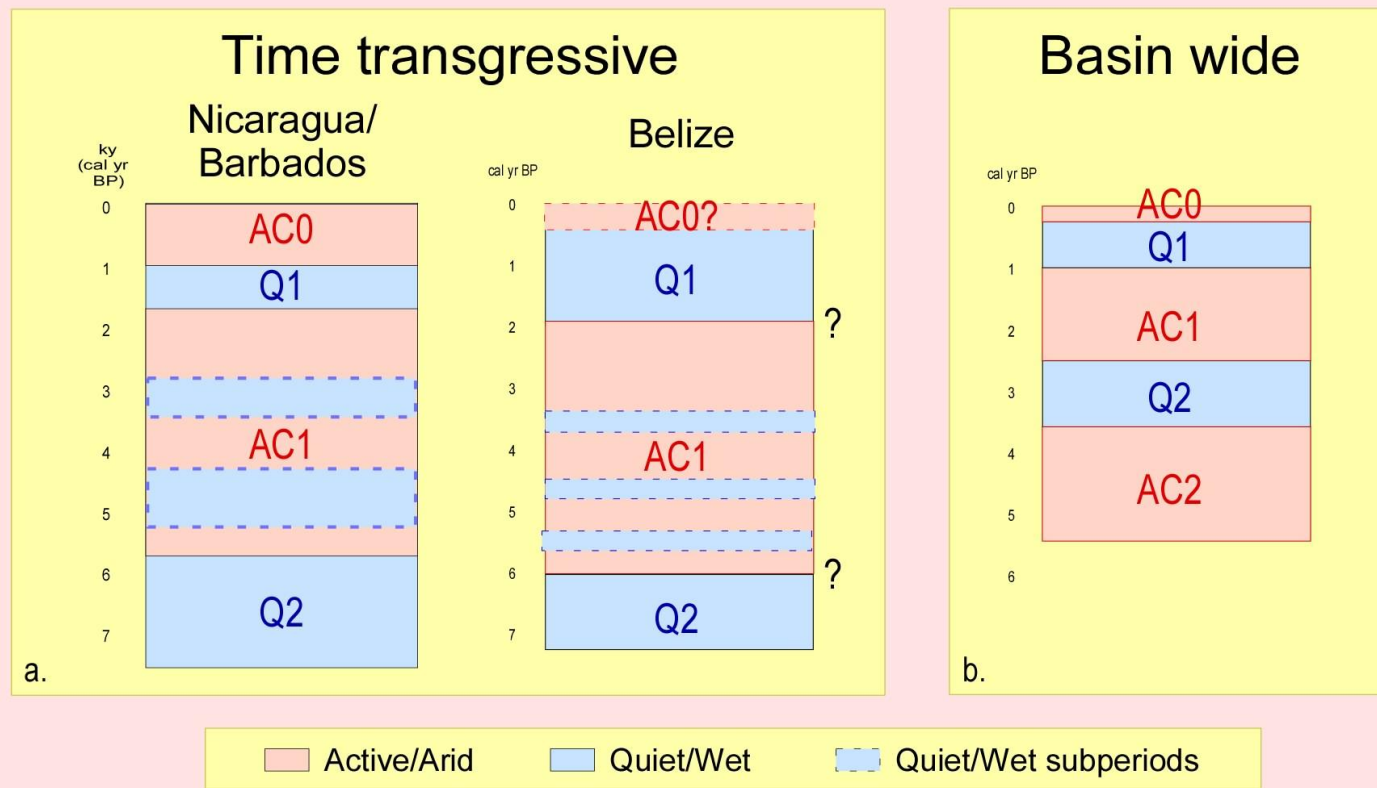
C.

11.11 Tropical cyclone history for Barbados. Shown are the tracks of (a) all tropical cyclones, (b) hurricanes, and (c) major hurricanes, since 1851 passing within 150 km of the island.

11.4 Regional Integration

Nearly all multi-millennial scale sedimentary hurricane strike records so far produced have provided evidence of long-term frequency variability, (Liu and Fearn, 1993, 2000; Collins et al., 1999; Scott et al., 2003; Bertran et al., 2004; Liu 2004; Goman et al., 2005; Donnelly and Woodruff, 2007; Scileppi and Donnelly, 2007; Gischler et al., 2008; Knowles, 2008; Mann et al., 2009; McCloskey and Keller, 2009; Woodruff et al., 2009), leading to universal recognition of abrupt shifts in activity regimes. However, two opposing models currently exist that attempt to explain the nature of these activity changes. Investigators working out of Woods Hole/MIT see these frequency shifts as basin-wide, driven by climatic features, principally the ENSO cycle, the west African monsoon, and NA sea surface temperature (SST) (Donnelly and Woodruff, 2007; Mann et al., 2009). A second group of researchers, principally based at LSU, view the activity regime changes as time transgressive, with Active Periods migrating latitudinally in rough parallel with general movement of the NA circulation system. The basis of the basin-wide view is the synchronicity of regime changes found at a variety of study sites, concentrated along the northeastern coast of the United States, but extending through the mid Atlantic region, to Puerto Rico. For these sites a standard chronology of activity regimes has been established (**Figure 11:12b**).

Some obvious differences exist between that chronology and that developed from this study. Of particular interest is the Q1 Quiet Period, whose chronological reliability is probably quite high, as it occurs so recently. The group advocating basin-wide activity changes has documented this period in several locations, showing an abrupt decrease in activity from either 1000-250 cal yr BP (Donnelly and Woodruff, 2007; Scileppi and Donnelly, 2007), or 800-250 cal yr BP (Mann et al., 2009). However, this is in stark contrast to our well-dated (three



11.12 Comparison of activity regime chronologies. Hurricane activity regime chronology from (a) this dissertation, compared to (b) the activity regime proposed by Mann et al. (2009); and Donnelly and Woodruff (2007).

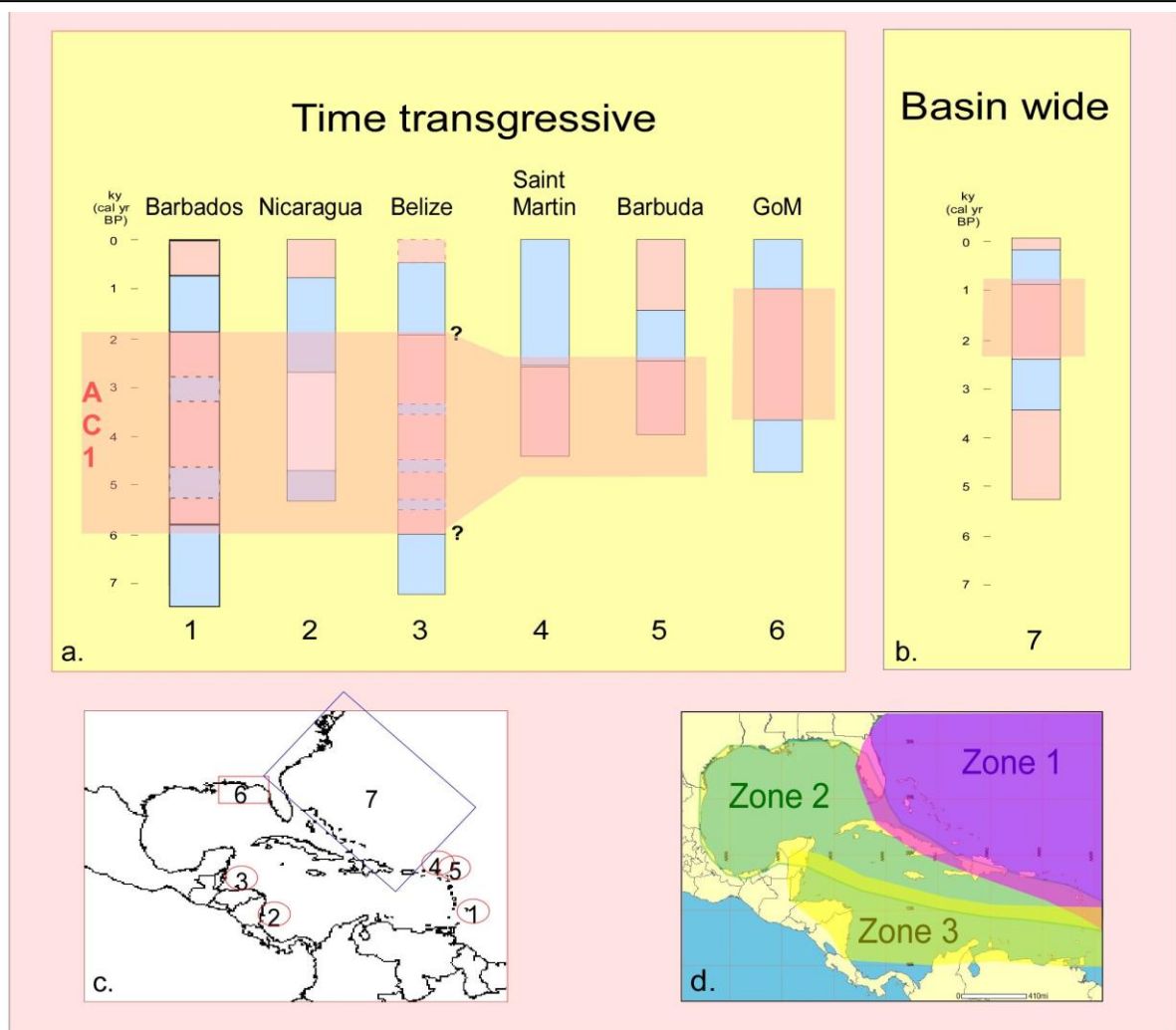
overlapping dates) evidence from Nicaragua of an abrupt increase in activity from ~775 cal yr BP (**Chapter 9**). Similar evidence for an extended AC0 in Belize exists, though less clearly, as it occurs only at GP/MR and not CB/HPN. In fact, there is general disagreement between the basin-wide and time transgressive chronologies, with corresponding regime changes generally posited as occurring more recently under the basin-wide dating scheme.

The findings of this dissertation strongly support the view of NA hurricane hyperactivity as time transgressive. This is especially obvious when correlated with other Caribbean sites, as in **Figure 11:13a**, which highlights the generally younger initiation and termination date of the AC1 Active period in more northern locations. It should be noted that the locations that provide the basis of the “basin wide” activity chronology are located almost entirely within a restricted area (blue box labeled “7”), corresponding to our Zone 1 (Figure 11:13d), whereas locations from all three zones are used in providing the data for the “time transgressive” chronologies.

There is a good chance that the foundation of the “basin wide” vs. “time transgressive” debate result merely from an insufficiency in spatial coverage for the data used in forming the “basin wide” model. According to our analysis, these sites, uniformly located in Zone 1 sites should all show similar temporal trends. However activity trends should differ for sites from the other two zones. This, of course, is precisely what our findings for Zone 2, the northern Gulf of Mexico, and Zone 3, Belize and Nicaragua show, providing clear evidence for the non-synchronous nature of hurricane hyperactivity in the NA over the last 5000-6000 years.

11.5 Climatic Controls

We have been less successful in tying the activity regimes to latitudinal movement of the general NA circulation system, particularly such large features as the ITCZ and BH. As seen in **Figure 11:3**, the match between identified activity regimes and long-term mean latitude of these



11.13 Comparison of regional activity patterns. Two conflicting models of NA hurricane activity exist; one views active periods as occurring across the NA in a time transgressive manner; (a) presents the activity regimes supporting this view are presented. Data for Barbados, Nicaragua, and Belize are from this dissertation; activity regimes for St. Martin is based on Bertran et al. (2004), for Barbuda on Knowles (2008), and for the Gulf of Mexico (GoM) from Liu and Fearn (2000). The opposing viewpoint holds that active periods occur synchronously over the entire basin; (b) displays the basin wide activity regime pattern developed from this model, derived from Donnelly and Woodruff (2007) and Mann et al. (2009). (c) shows the spatial distribution of the sediment cores that form the physical basis of the two models; data forming the basis of the time transgressive model originate at locations 1-6, covering all three track zones (d), data forming the basis of the basin wide model originate within the blue box labeled “7”, mainly restricted to Zone 1 (d).

features is only approximate. The most recent Active Period, AC0, achieves a reasonable match with the hypothesized corresponding ITCZ location, as does part of the preceding Quiet Period, Q1. However, AC1, although generally centered correctly on the large southern shift occurring from ~4000-2400 cal yr BP, extends much too long both into the past and toward the present. Inadequate dating control probably accounts for some portion of this discrepancy but cannot be used to explain all. Our chronology dates the beginning of increased activity in the southern and western Caribbean at some ill- defined point before 5000 cal yr BP, perhaps as early as 6000, during which time the proxy record places the ITCZ far north of its present average annual position. However, at this time, southern migration of the circulation system had begun, which perhaps provided a climatic shove to the hurricane zone. This issue, as well as the outstanding dating issues should be resolvable with more research.

11.6 References

- Bertran, P., Bonnissent, D., Imbert, P., Lozouet, P., Serrand, N., and Stouvenot, C. 2004. Paleoclimat des Petites Antilles depuis 4000 ans BP: l'enregistrement de la lagune de Grand-Case a Saint-Martin. *Comptes Rendus Geoscience* 336, 1501-1510.
- Collins, E.S., Scott, D.B., and Gayes, P. T., 1999. Hurricane records on the South Carolina Coast: Can they be detected in the sediment record? *Quaternary International* 56, 15-26.
- Donnelly, J. P., and Woodruff, J., 2007. Intense hurricane activity over the past 5000 years controlled by El Nino and the West African Monsoon. *Nature* 44, 465-468. DOI:10.1038/nature05834.
- Elsner J.B., Liu, K-b., and Kocher B., 2000. Spatial variations in major U.S. hurricane activity: statistics and a physical mechanism. *Journal of Climate* 13, 2293-2305.
- Gischler, E., Shinn, E. A., Oschmann, W., Fiebig, J, and Buster, N. A., 2008. A 1500-year Holocene Caribbean climate archive from the Blue Hole, Lighthouse Reef, Belize. *Journal of Coastal Research* 24, 1495-1505.

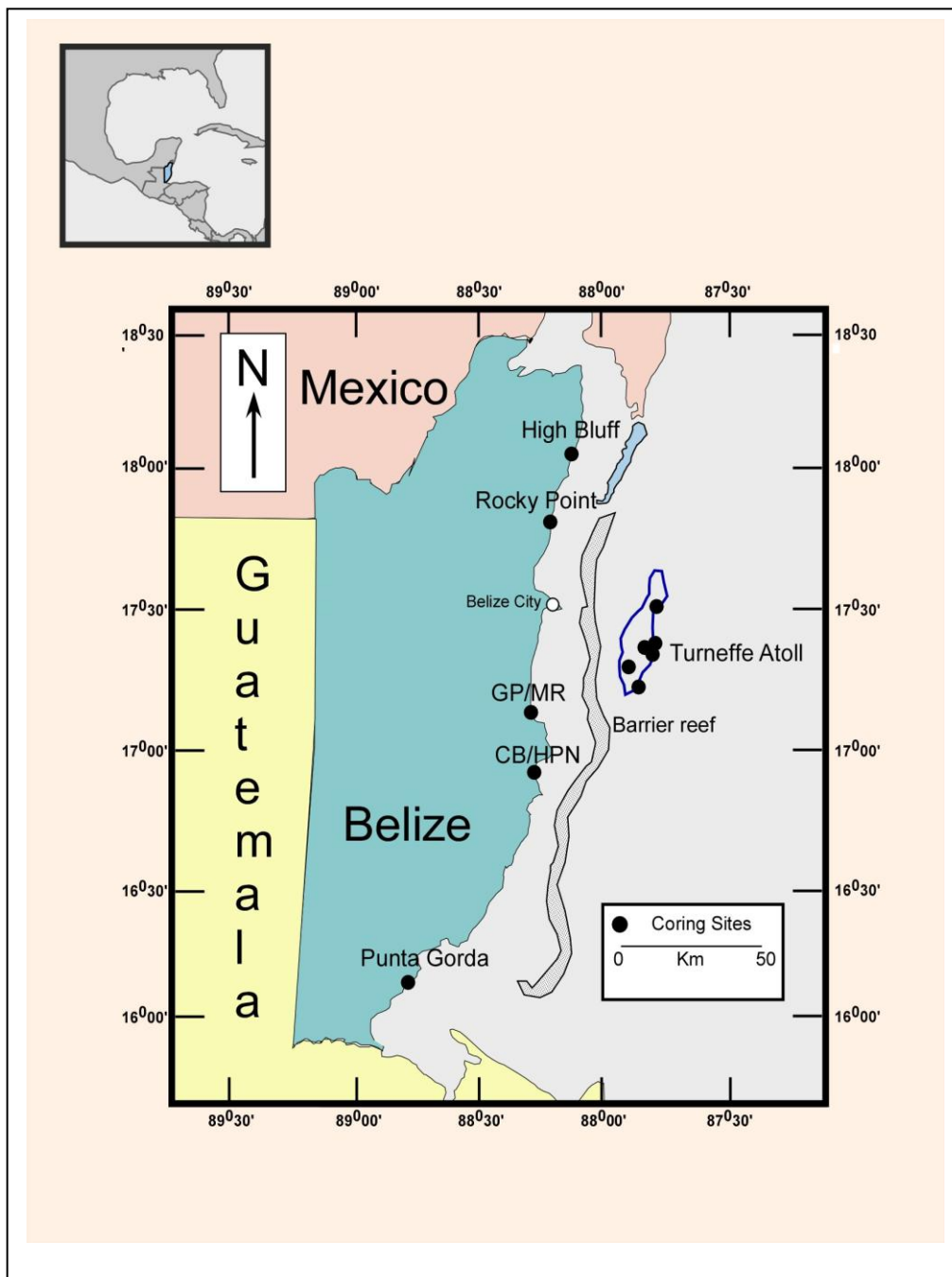
- Goman, M., Joyce, A., and Mueller, R., 2005. Stratigraphic evidence for anthropogenically induced coastal environmental change from Oaxaca, Mexico. *Quaternary Research* 63, 250-260.
- Knowles, J. T., 2008. A 5000-year history of Caribbean environmental change and hurricane activity reconstructed from coastal lake sediments of the West Indies. Unpublished PhD Dissertation, Louisiana State University, Baton Rouge, LA.
- Liu, K-b., 2004. Paleotempestology: principles, methods, and examples from Gulf Coast lake sediments. In: Murnane R.J, Liu K-b., (eds), *Hurricanes and Typhoons: Past, Present and Future*. Columbia University Press, New York.
- Liu, K-b., and Fearn M. L., 1993. Lake-sediment record of late Holocene hurricane activities from coastal Alabama. *Geology* 21, 793-796.
- Liu, K-b., and Fearn M. L., 2000. Reconstruction of prehistoric landfall frequencies of catastrophic hurricanes in northwestern Florida from lake sediment records. *Quaternary Research* 54, 238-245.
- Liu, K-b. and Lu, H.Y., 2005. A paleotempestological record from Nobska pond, Cape Cod: testing the Bermuda High hypothesis. Association of American Geographers Annual Meeting. Denver, CO.
- Mann, M. E., Woodruff, J. D., Donnelly, J. P., and Zhang, Z., 2009. Atlantic hurricanes and climate over the past 1,500 years. *Nature*, 460, 880-883. DOI:10.1038/nature08219
- McCloskey, T. A., and Keller G., 2009. 5000 year sedimentary record of hurricane strikes on the central coast of Belize. *Quaternary International* 195, 53-68.
- Scileppi, E. and Donnelly, J.P., 2007. Sedimentary evidence of hurricane strikes in western Long Island, New York. *Geochemistry Geophysics Geosystems* 8.
- Scott, D. B., Collins, E. S., Gayes, P. T., and Wright, E., 2003. Records of prehistoric hurricanes on the South Carolina coast based on micropaleontological and sedimentological evidence, with comparison to other Atlantic Coast record. *Geological Society of America Bulletin* 115, 1027-1039.
- Stuiver, M., Reimer, P.J., and Reimer, R., 2005. CALIB Radiocarbon Calibration. <http://calib.qub.ac.uk/calib/calib.html>.
- Toscano, M. A., and Macintyre, I. G., 2003. Corrected western Atlantic sea-level curve for the last 11,000 years based on calibrated C-14 dates from *Acropora palmate* framework and intertidal mangrove peat. *Coral Reefs* 22, 257-270.
- Woodruff, J. D., Donnelly, J. P, and Okusu, A., 2009. Exploring typhoon variability over the mid-to-late Holocene: evidence of extreme coastal flooding from Kamikoshiki, Japan. *Quaternary Science Reviews* 28, 1774-1785. DOI:10.1016/j.quascirev.2009.02.005.

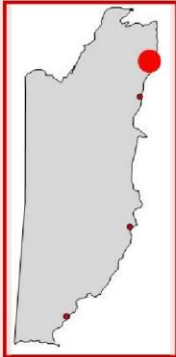
APPENDIX A: LOSS ON IGNITION GRAPHS



Loss on ignition graphs are arranged in order by country; starting with Belize, then proceeding through Nicaragua to Barbados. At the beginning of each country section, maps and/or images provide regional orientation. Transect and core location information is provided for each study site. For the Gales Point Line 1, Mullins River Line 1, and Mullins River Line 2 transects a single graph is presented for each core displaying percentage combusted (wet weight) at 550°C, which combines water and organic percentages. All other core data are presented as four separate graphs, displaying percentages of water (wet weight) as a blue line, organics (dry weight) as a green line, carbonates (dry weight) as a yellow line, and residuals (dry weight) as a gray line.

A.1 BELIZE





High Bluff

Salinity 20.8 ppt

Lake depth ~1 m

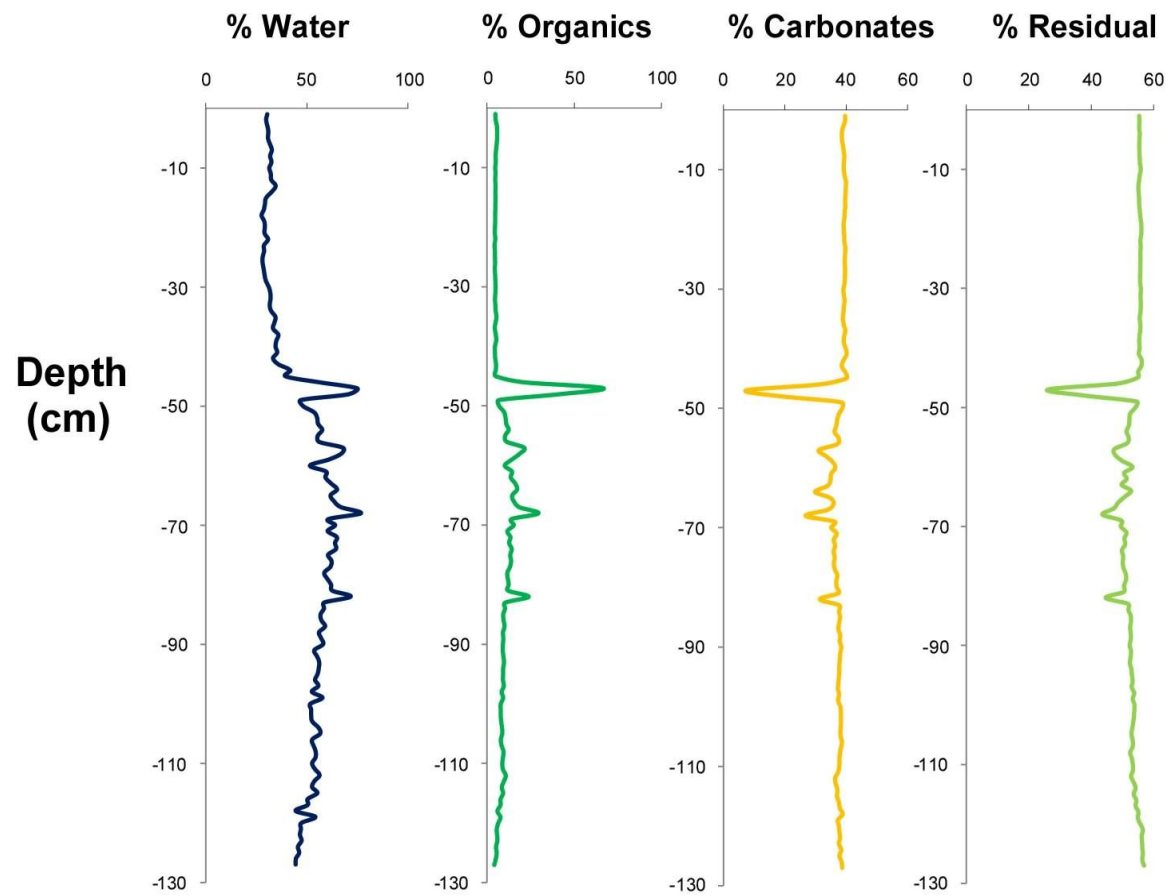
Barrier

Height <1m

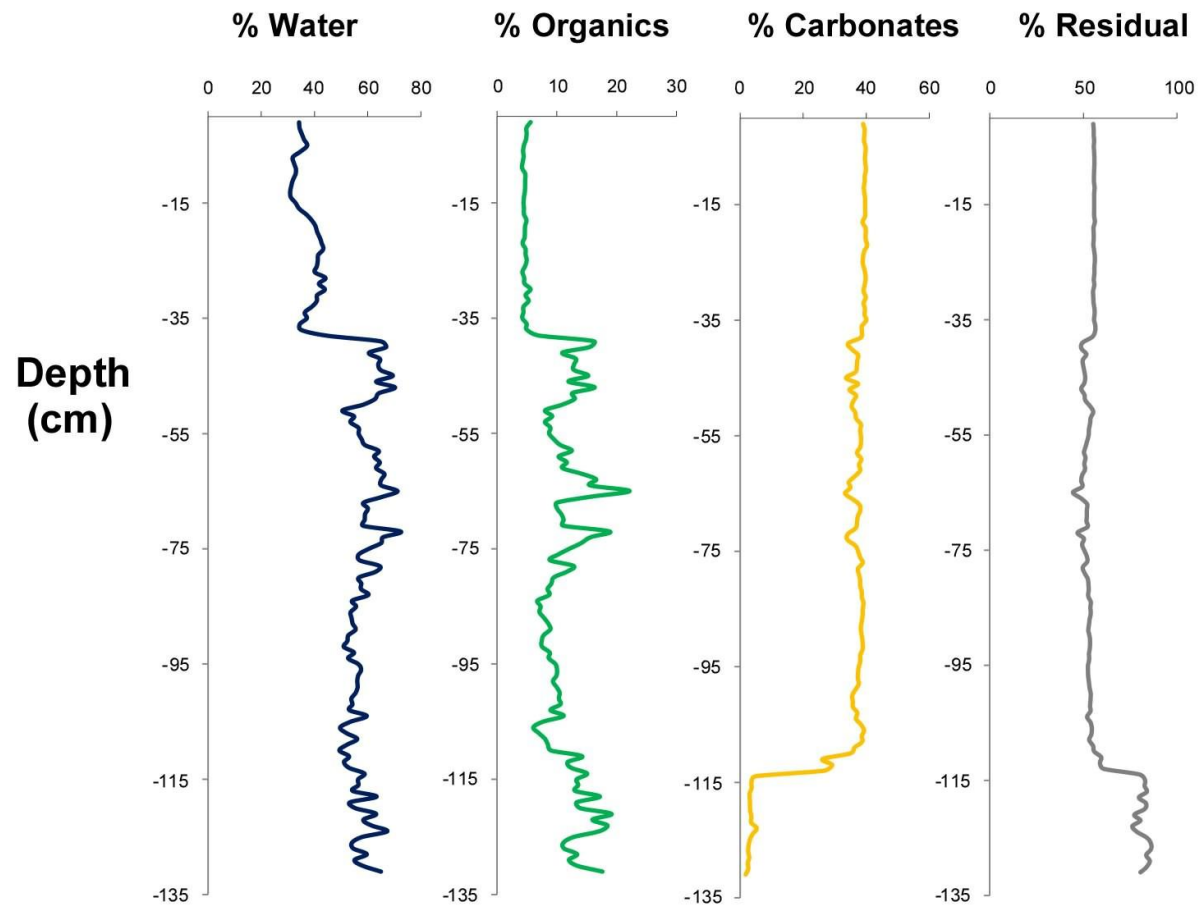
Width 12 m



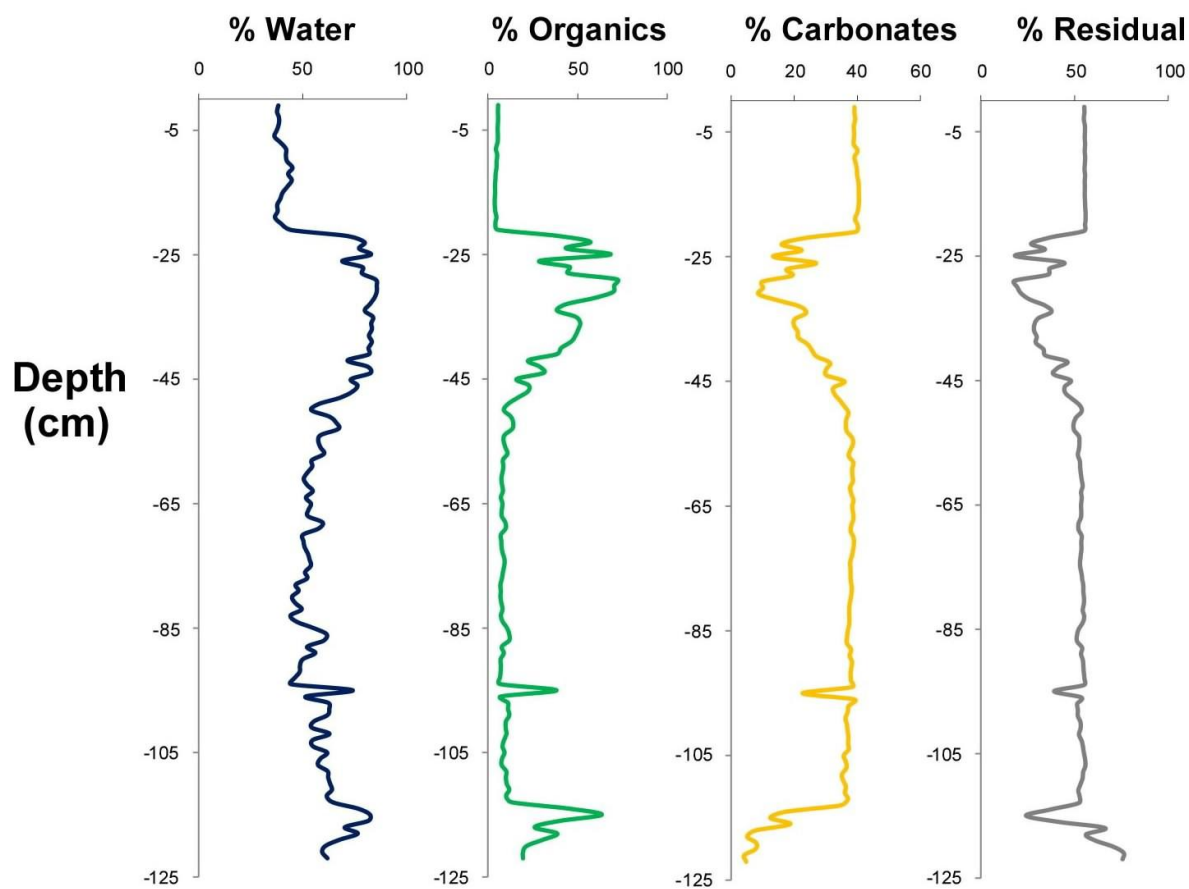
HB 1

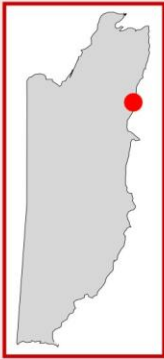


HB 2



HB 3





Rocky Point

Salinity 29.1 ppt

Lake depth ~1 m

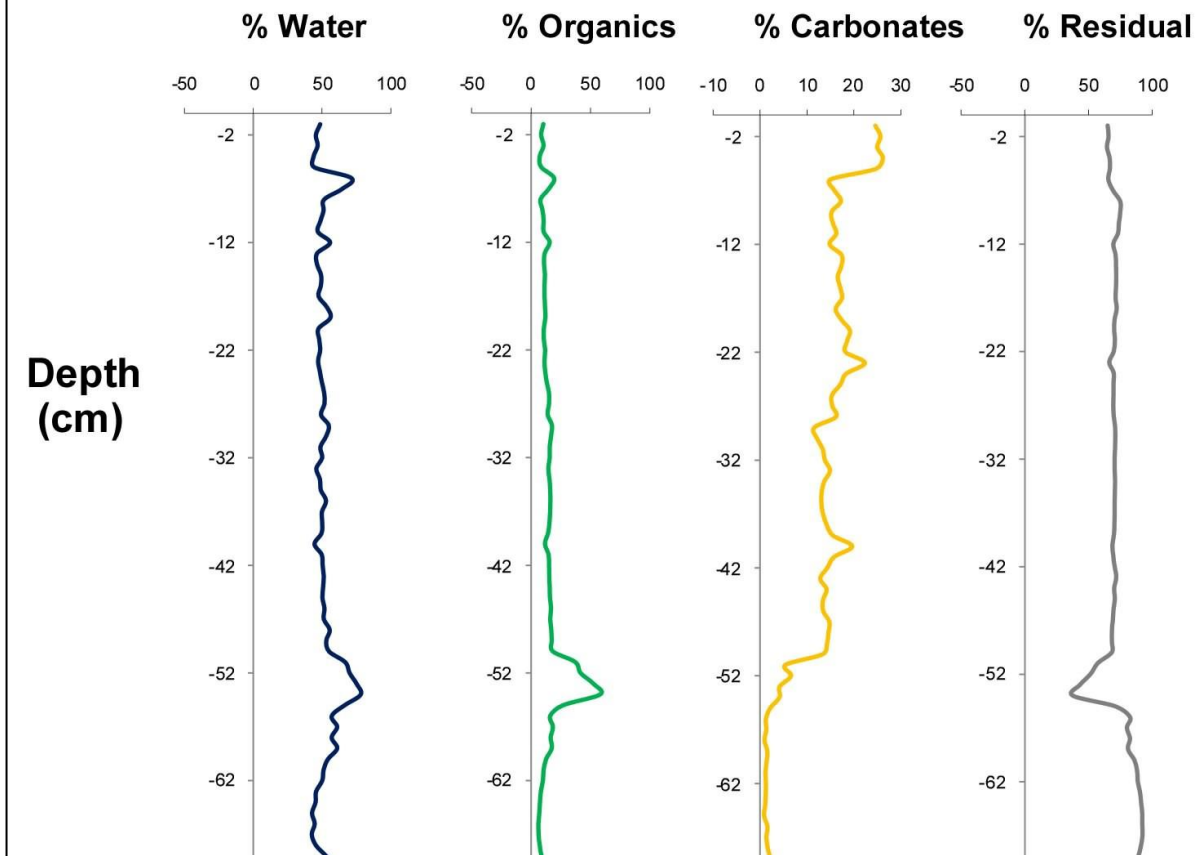
Barrier

Height <1m

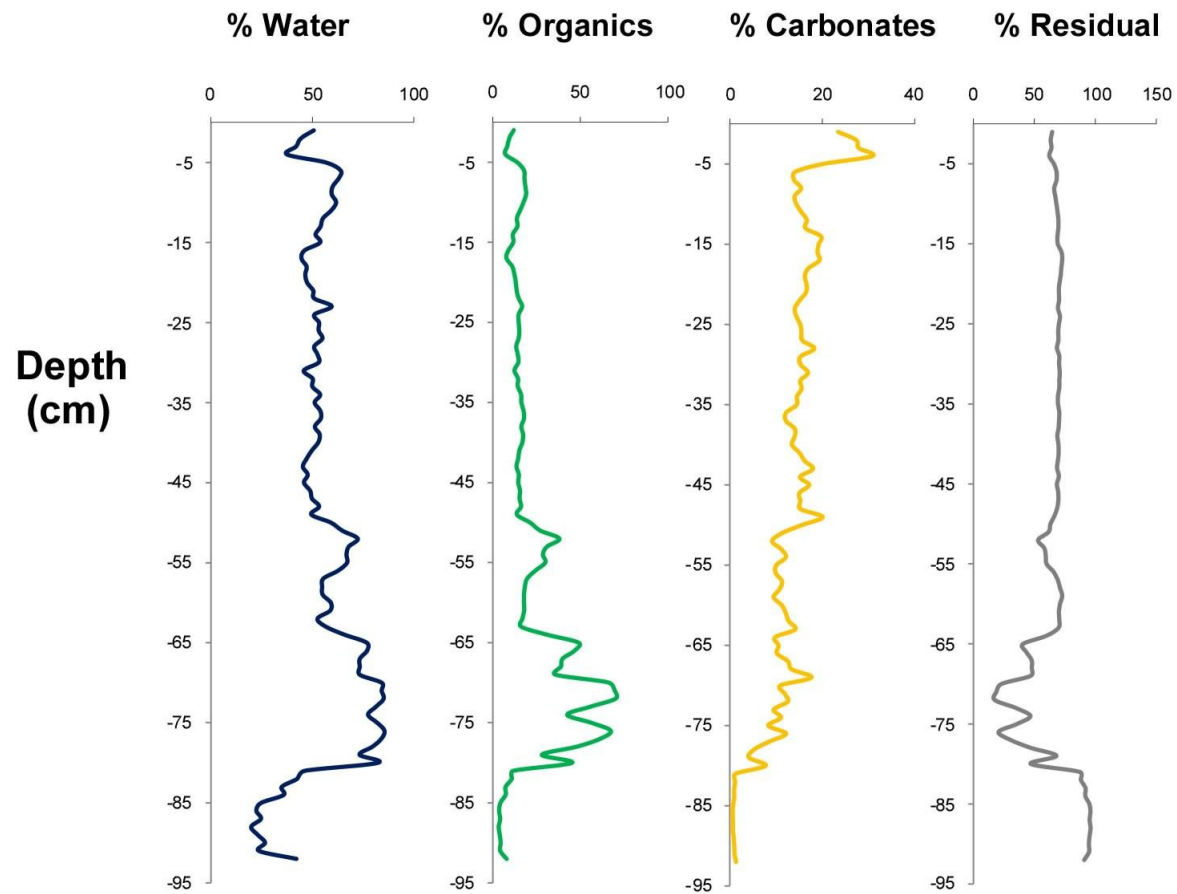
Width 15 m



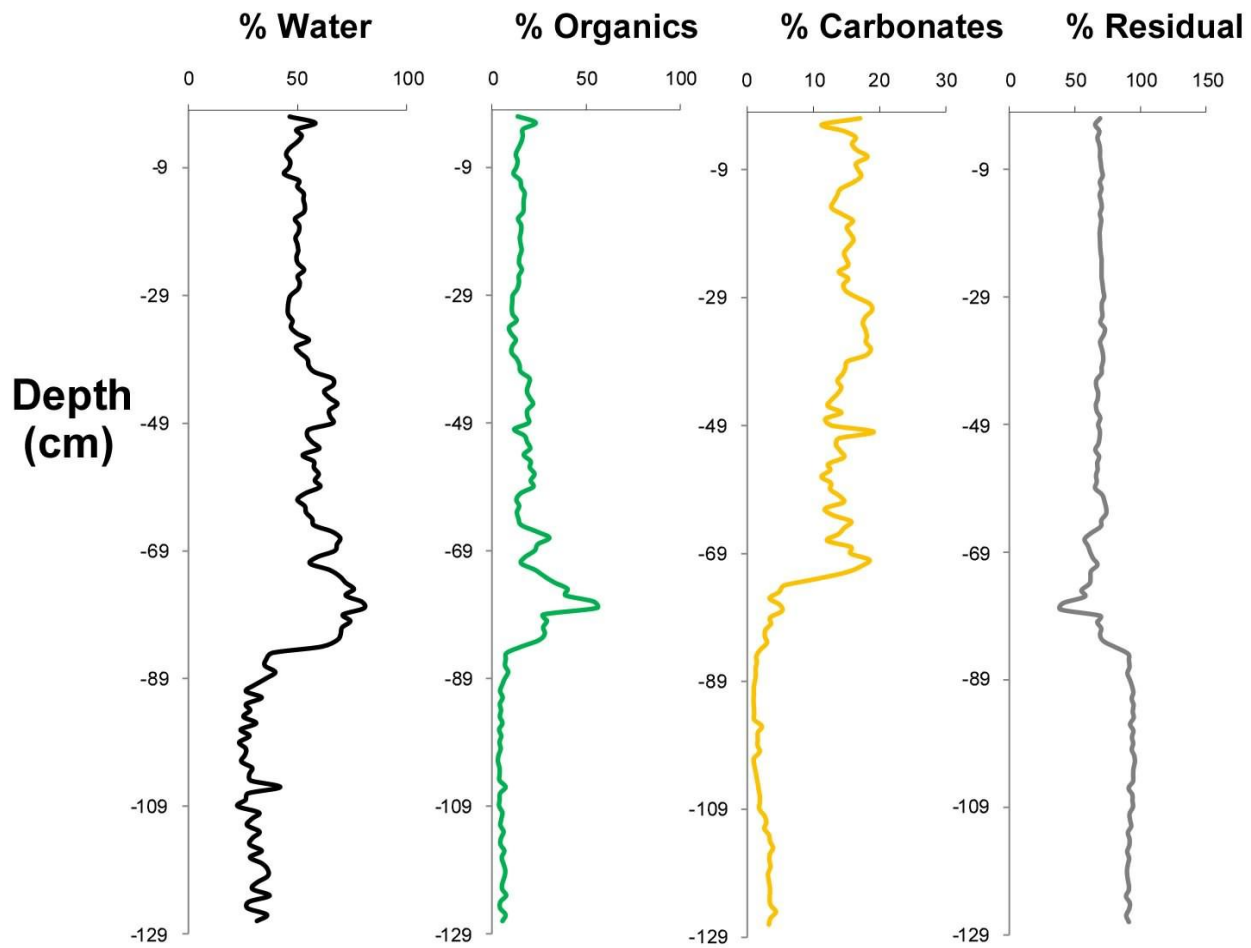
RP 1



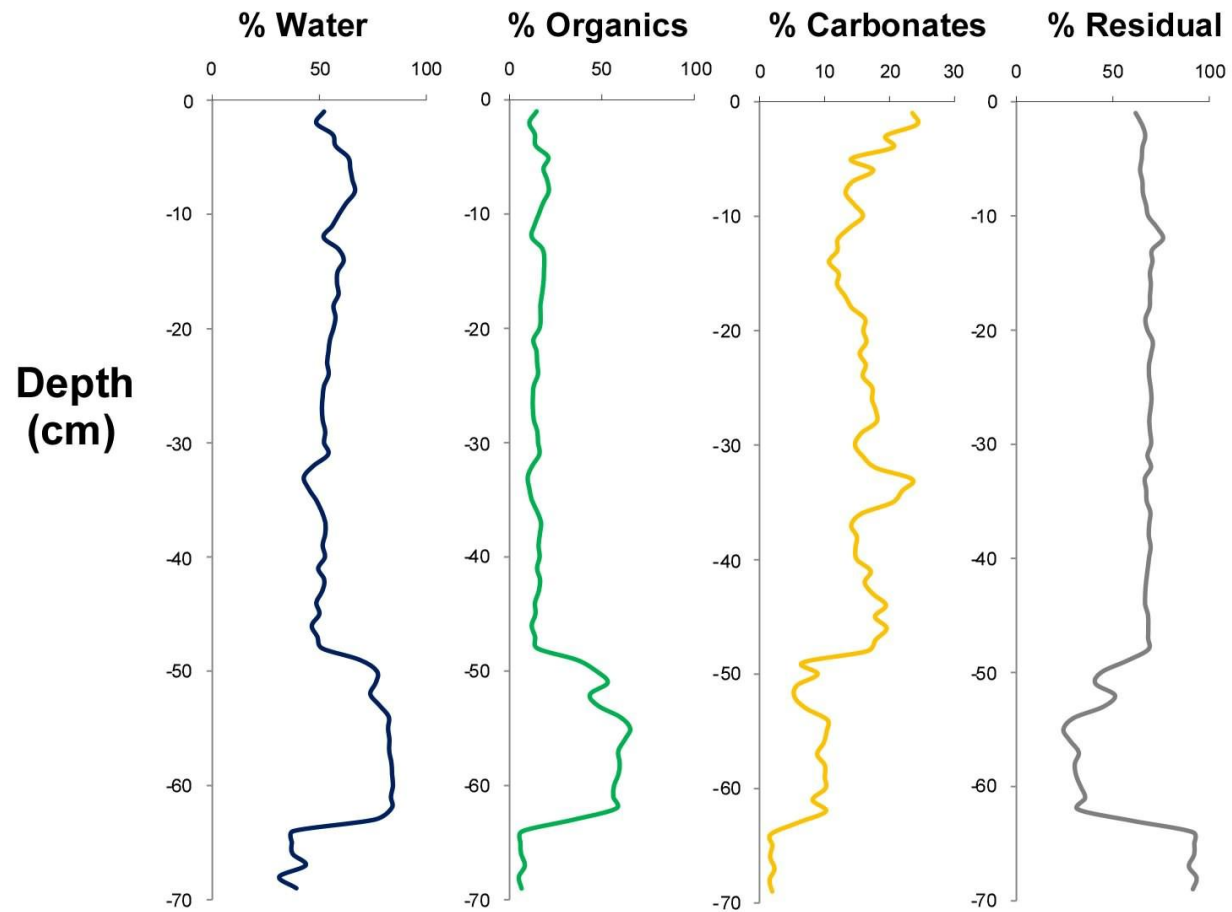
RP 2



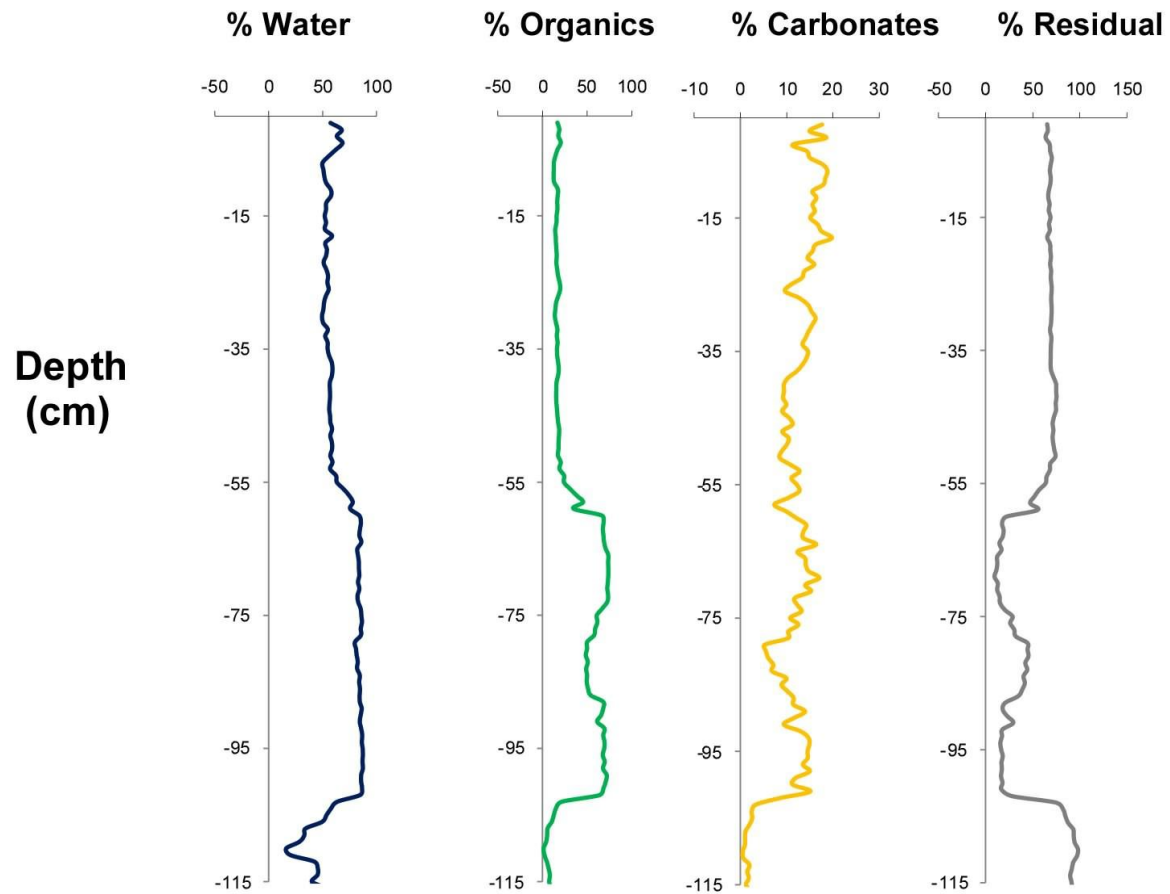
RP 2-RPB



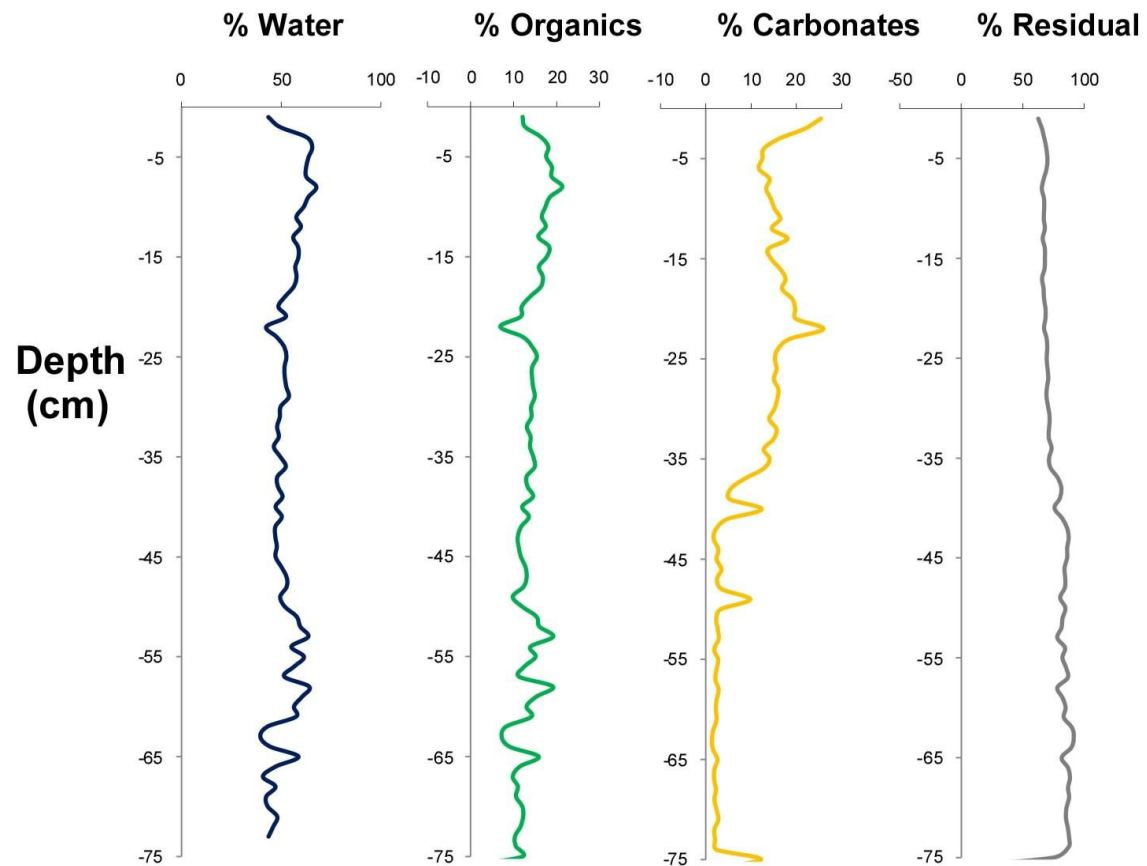
RP 3



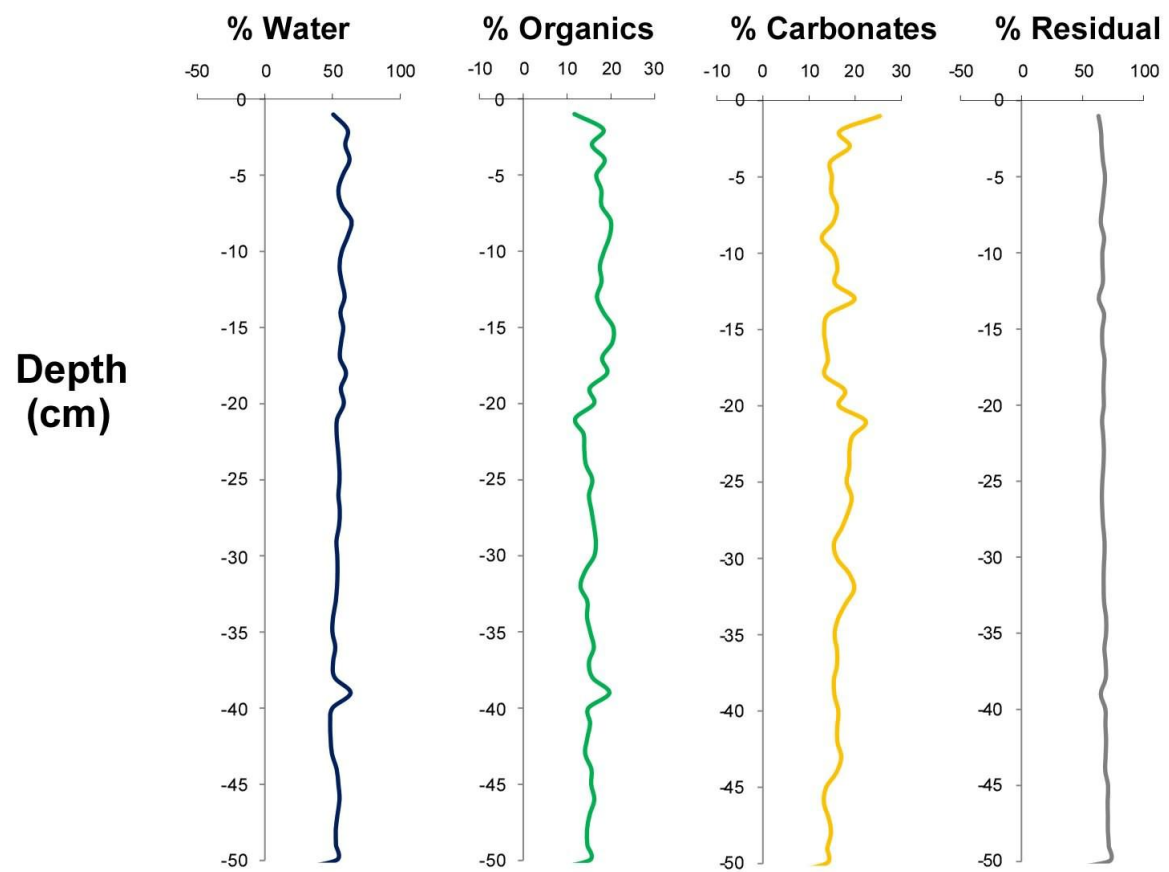
RP 4



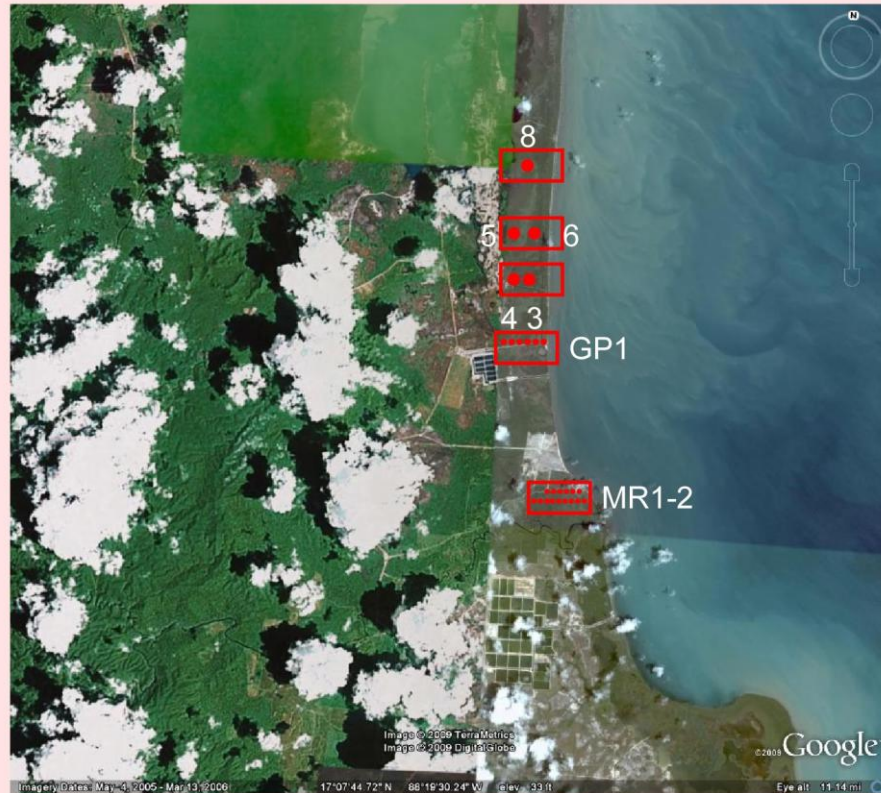
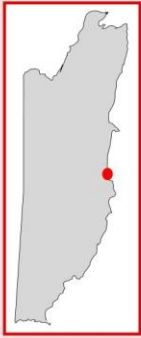
RP 5



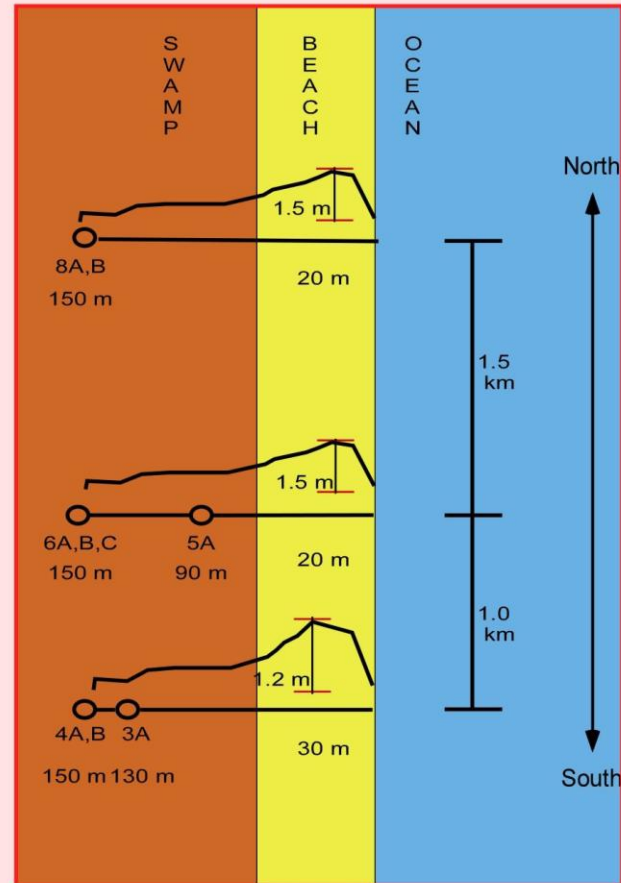
RP 6



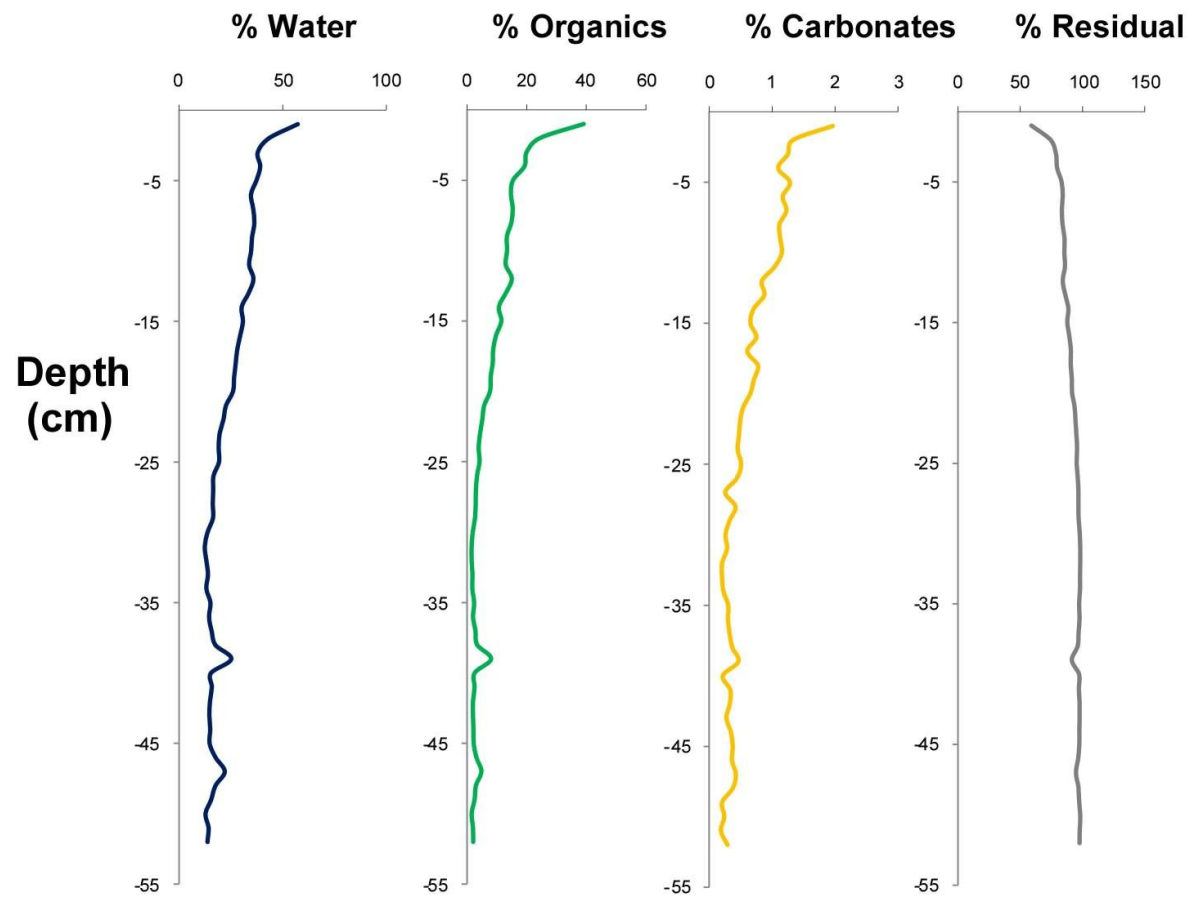
Gales Point Mullins River



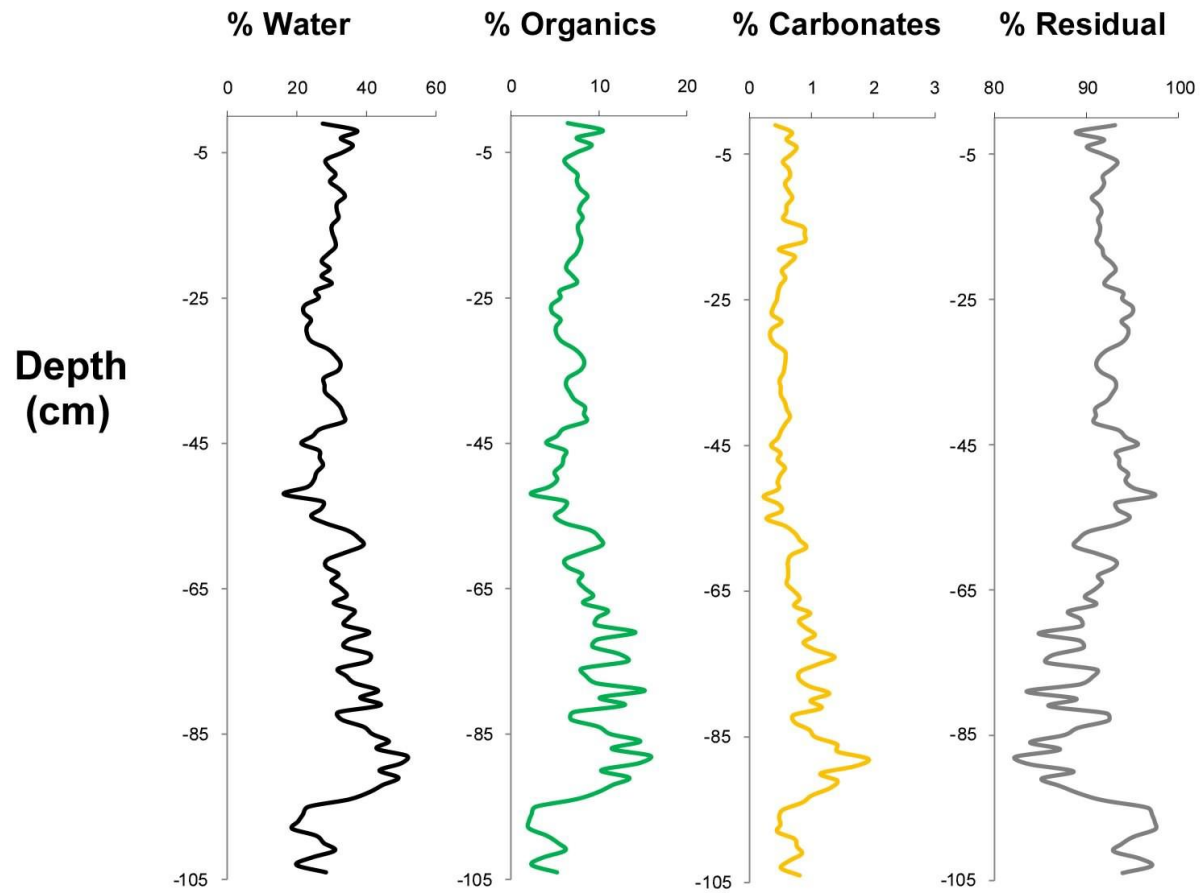
Gales Point North



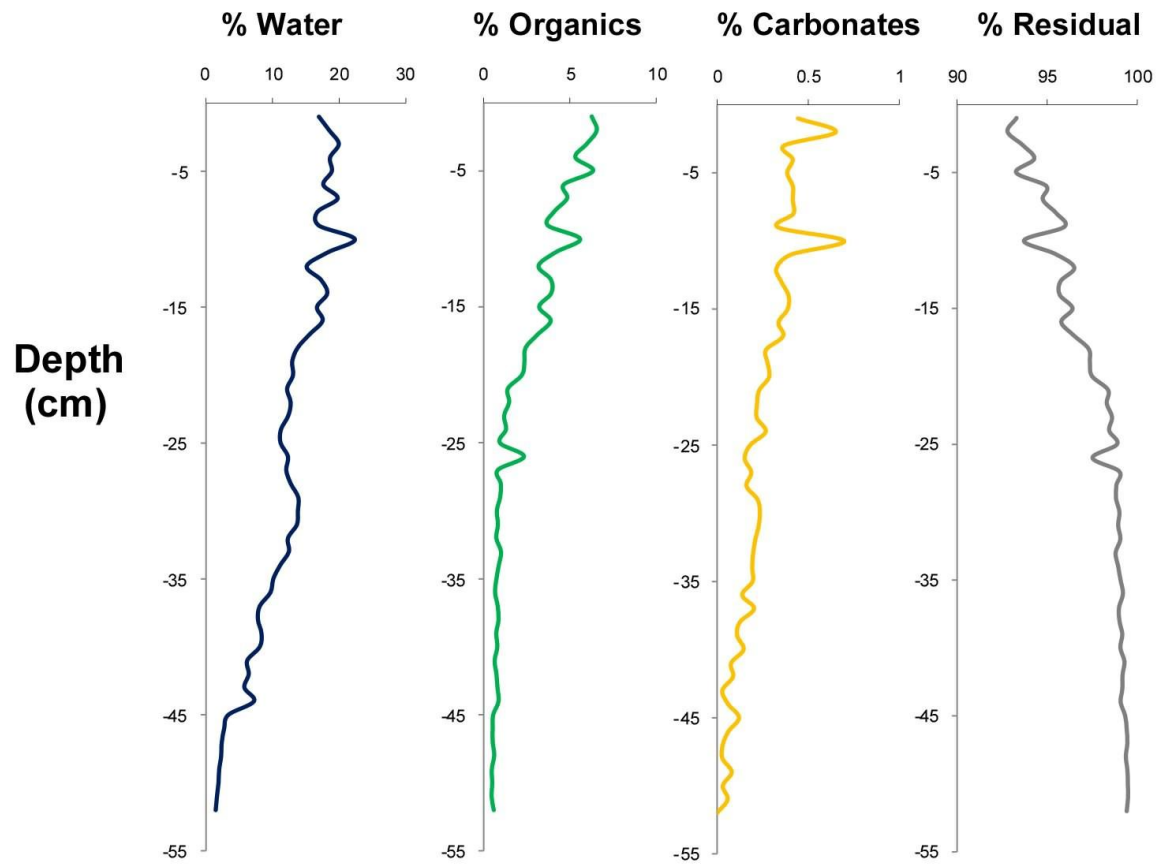
GP 3



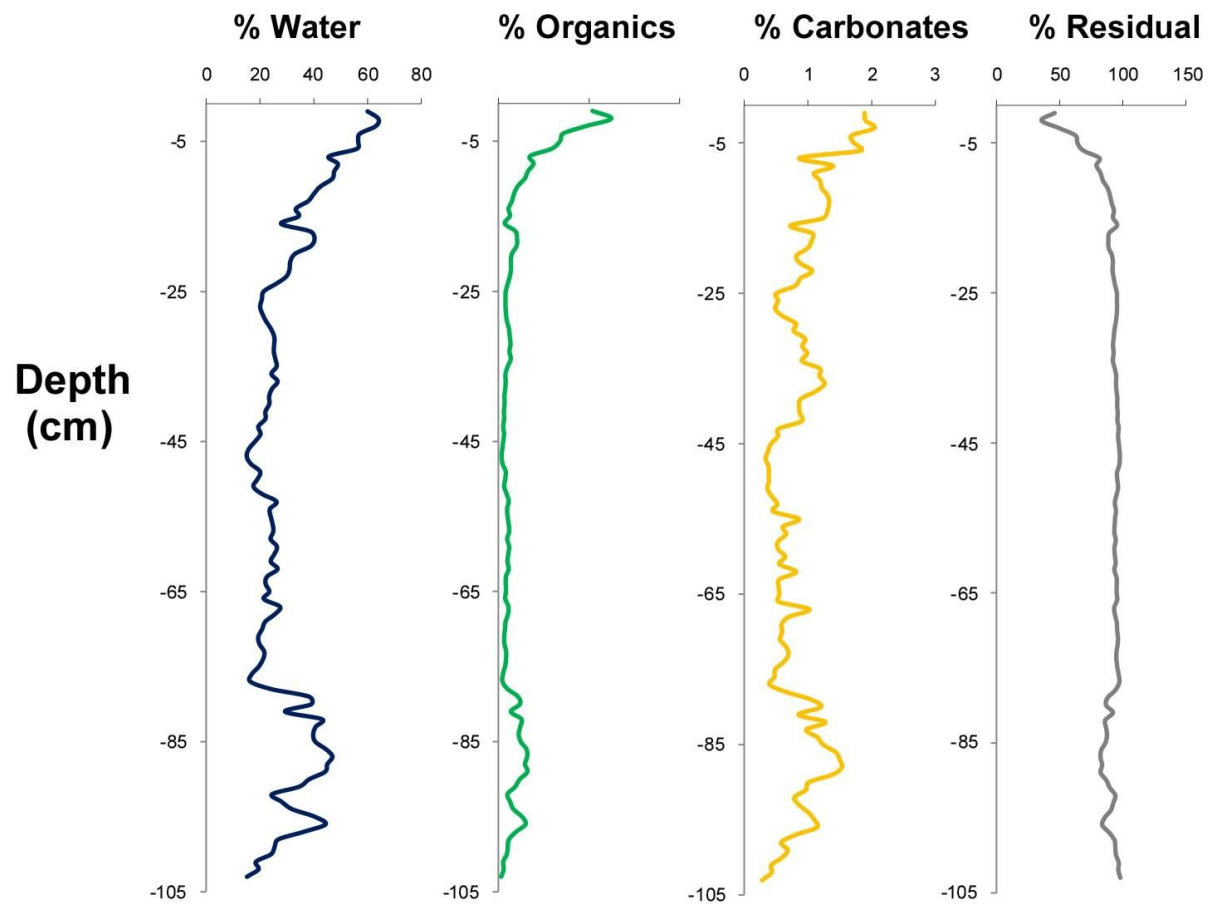
GP 4



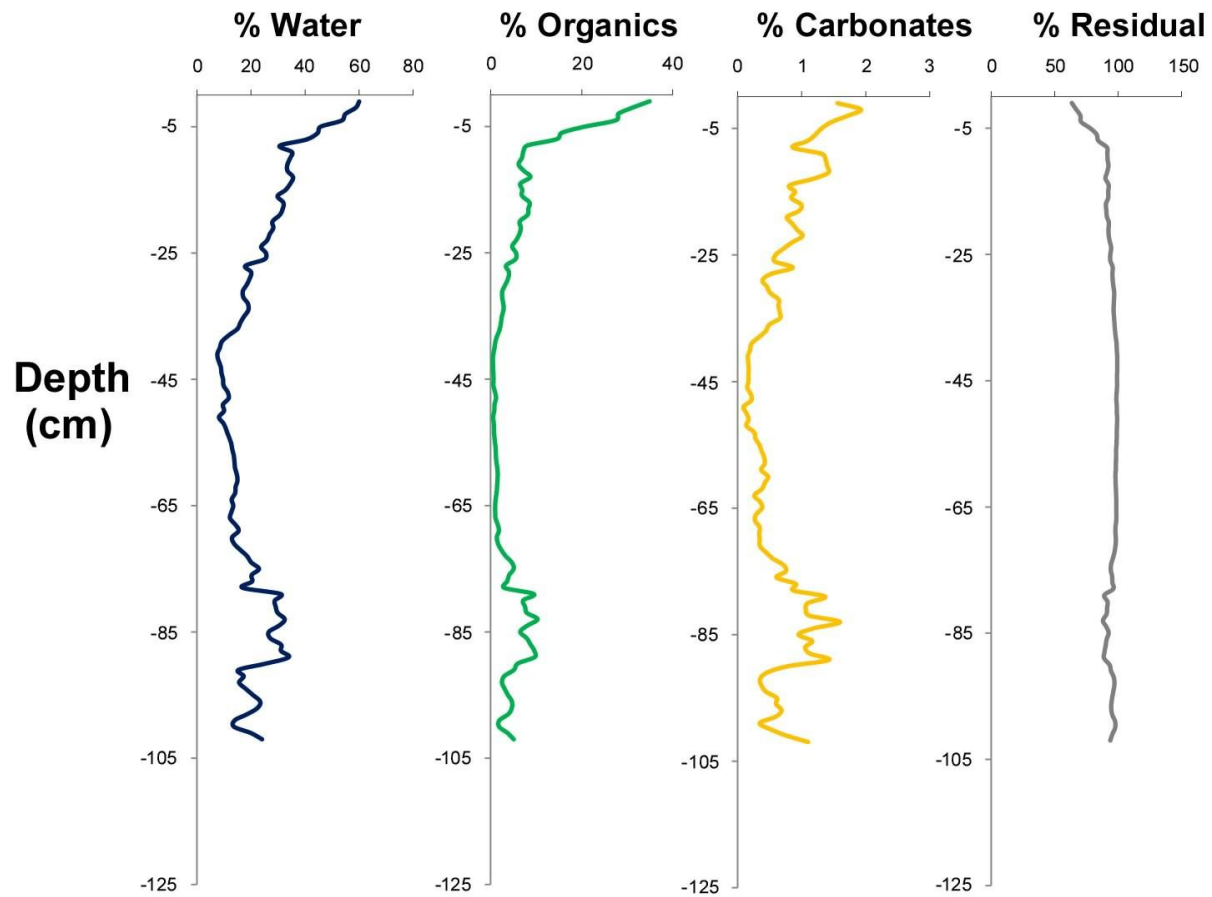
GP 5



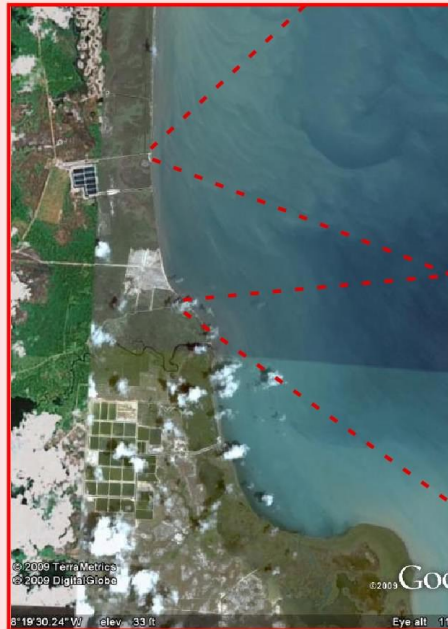
GP 6



GP 8



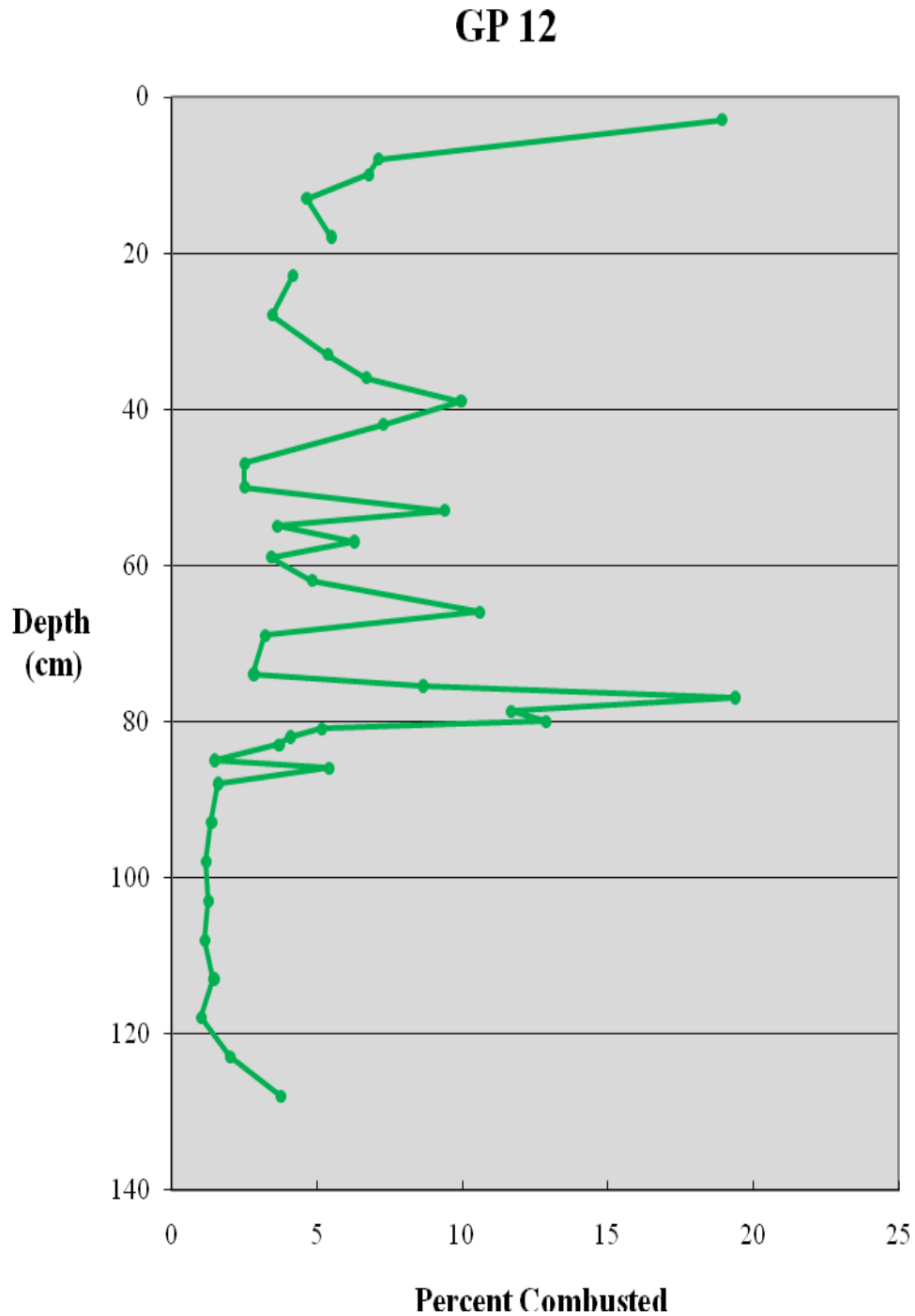
Gales Point



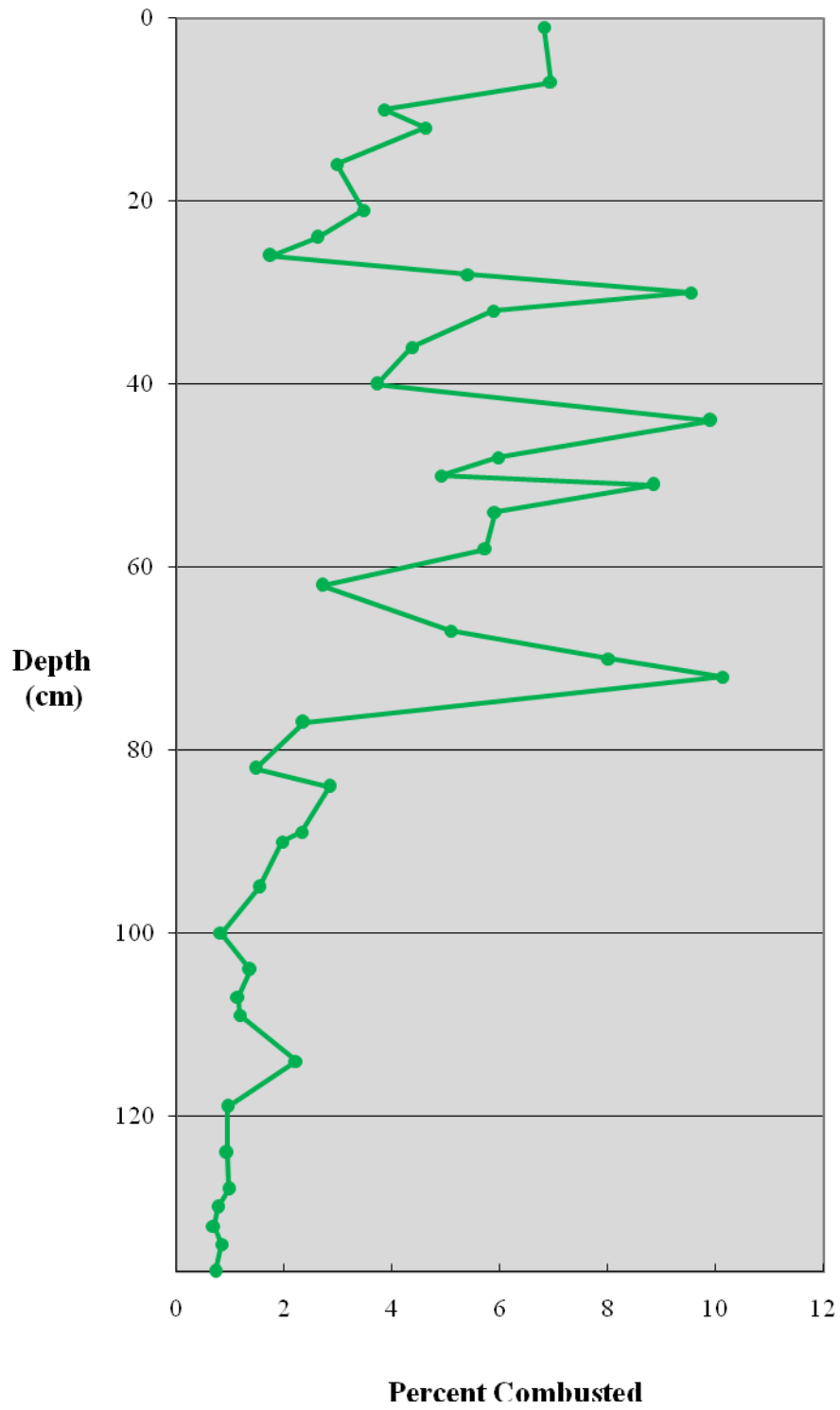
Mullins River

Gales Point Line 1

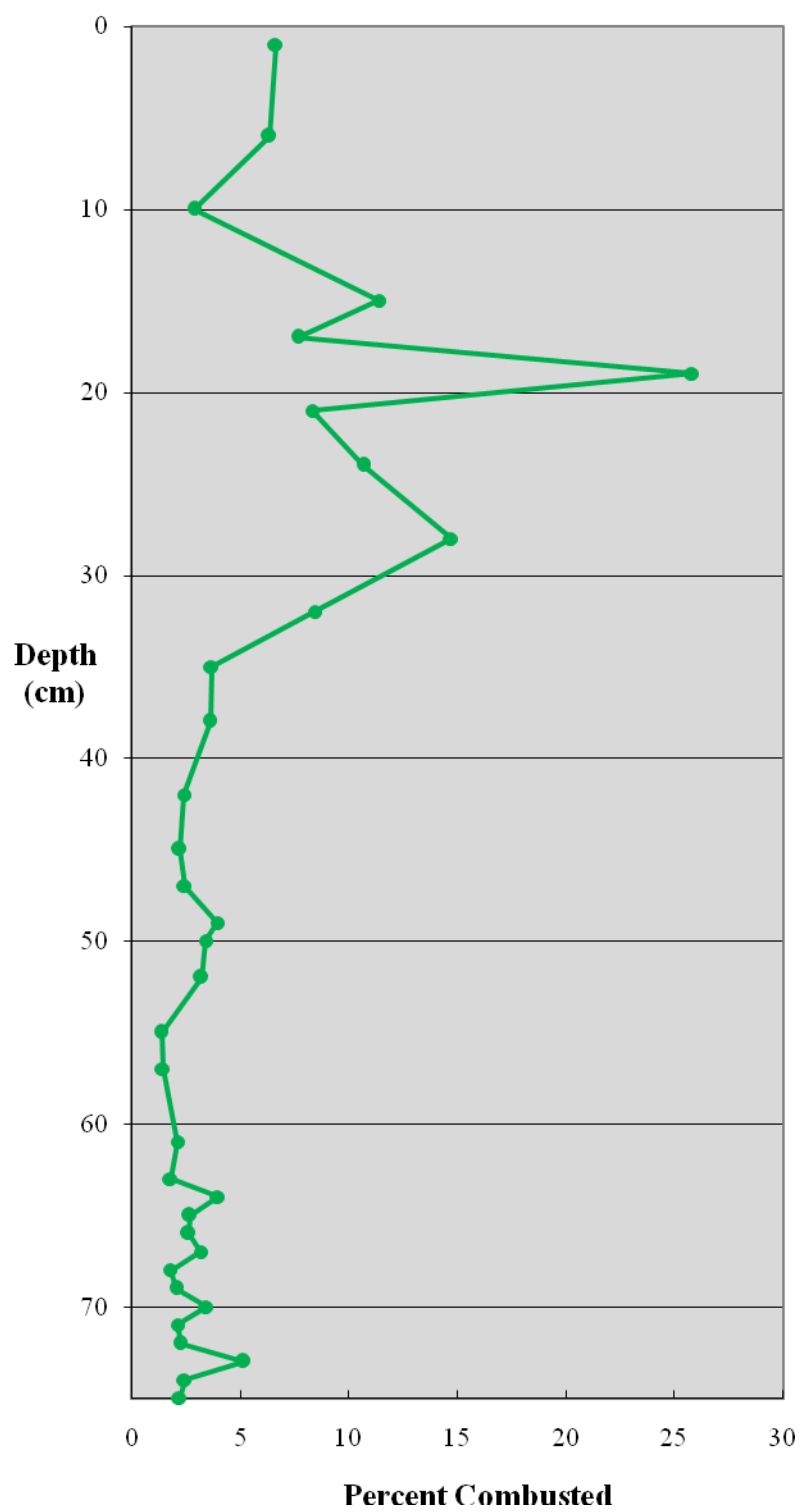
Gales Point Line 1, Mullins River Line 1 and 2 graphs show percentage combusted (wet weight) after a single burning at 550⁰ C, i.e. water and organics percentages combined.



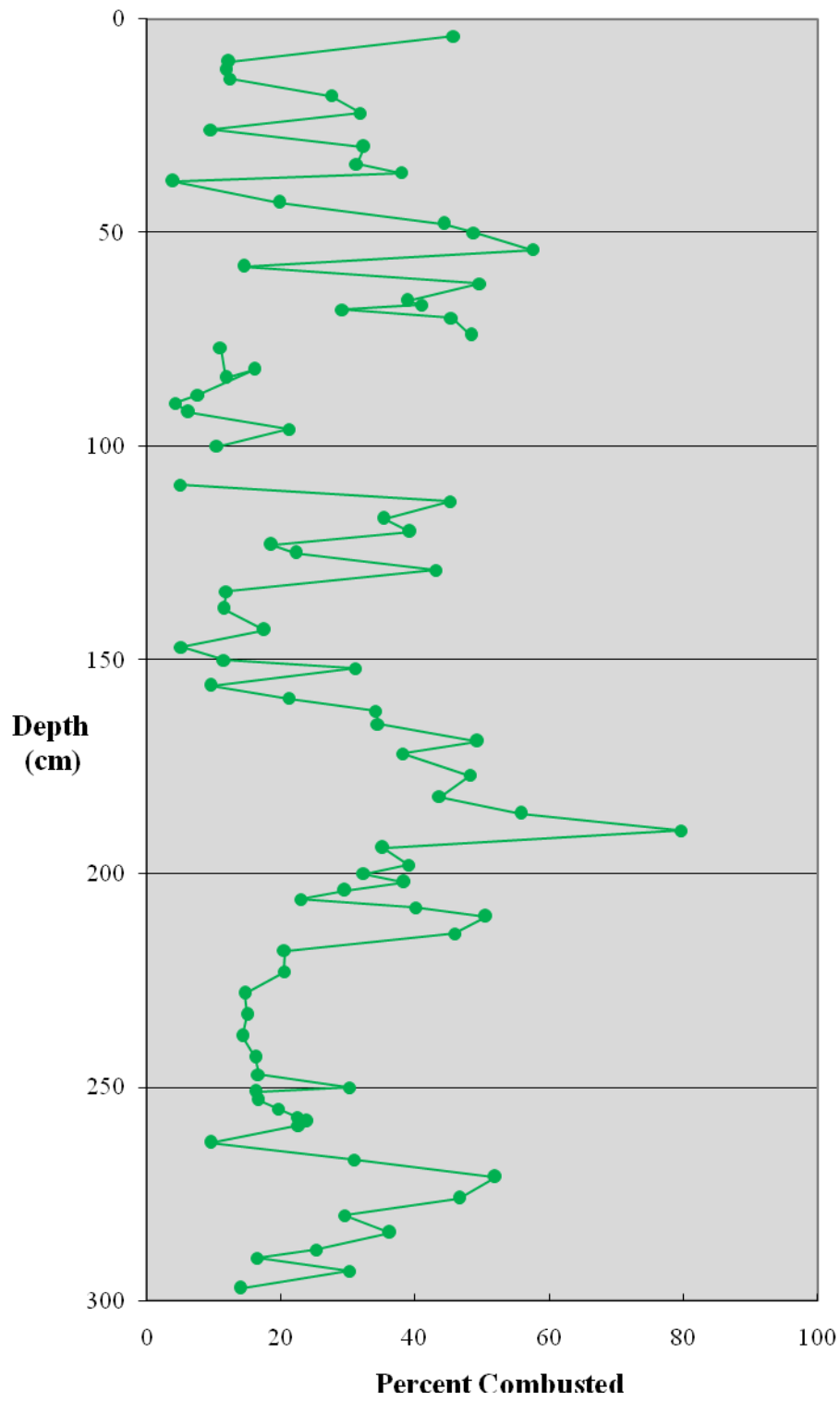
GP 13



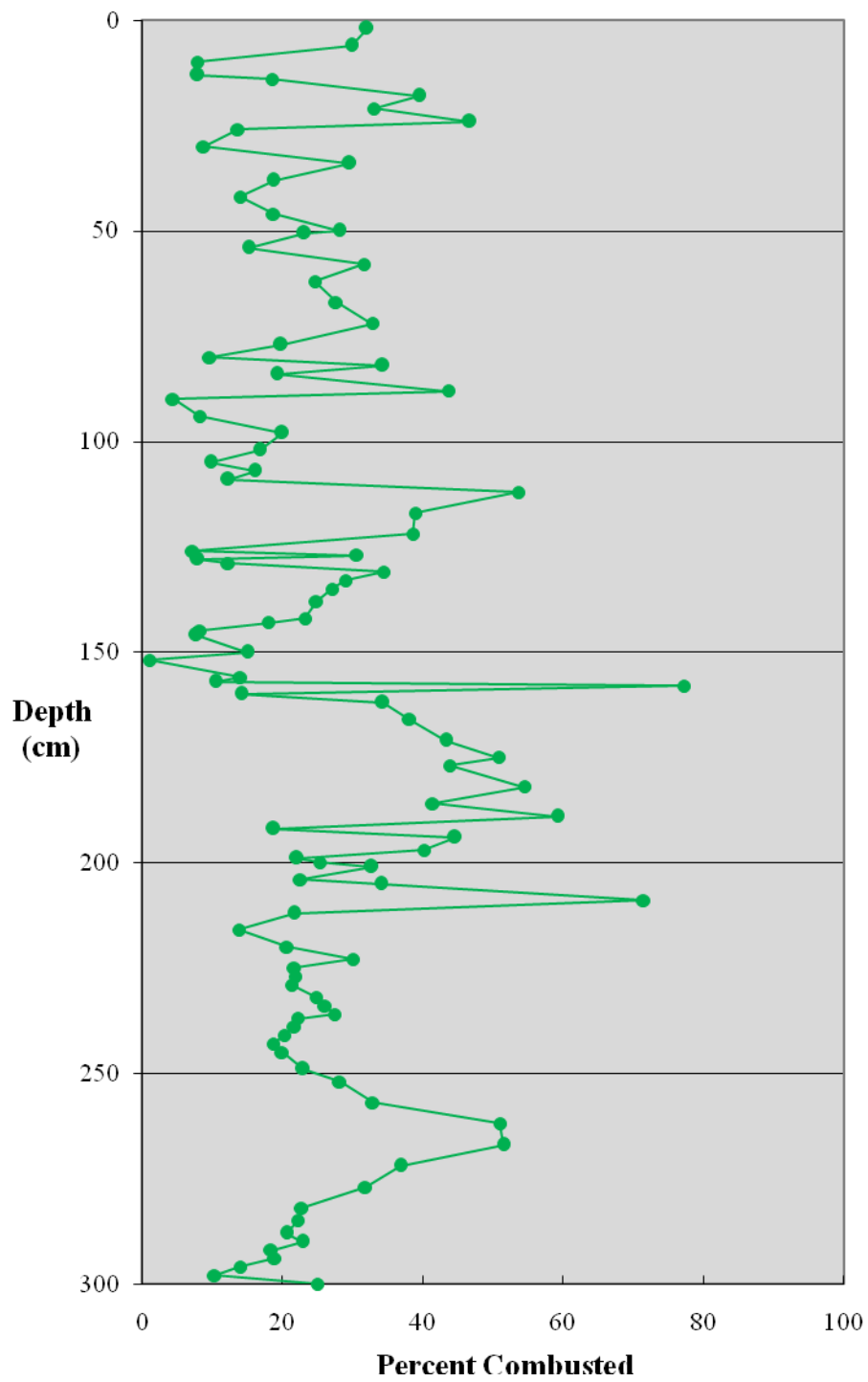
GP 14



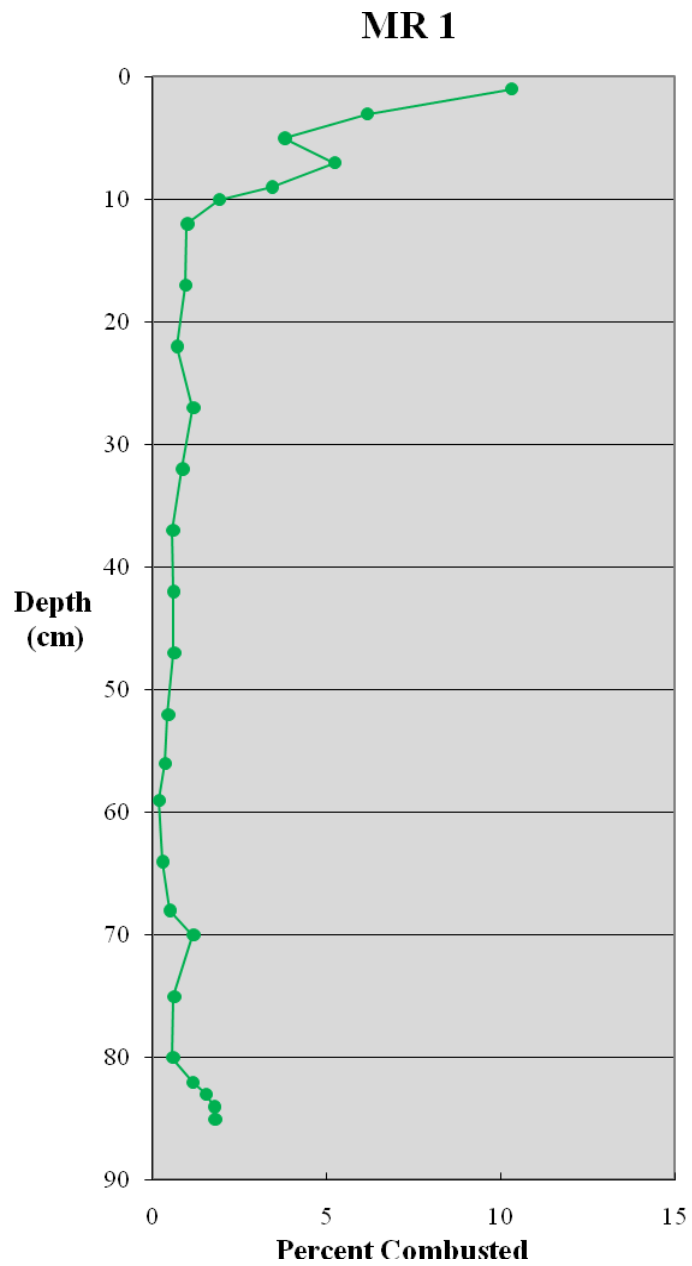
GP 15



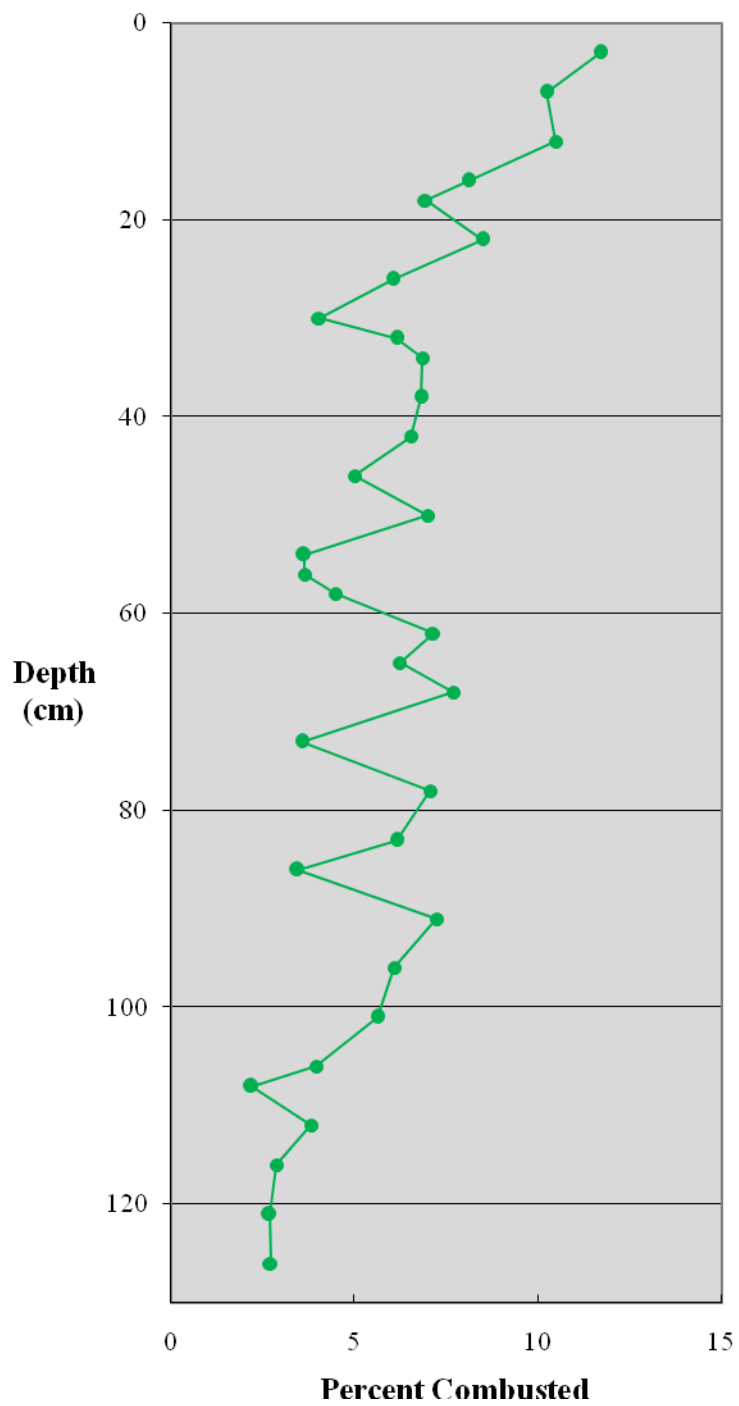
GP 16



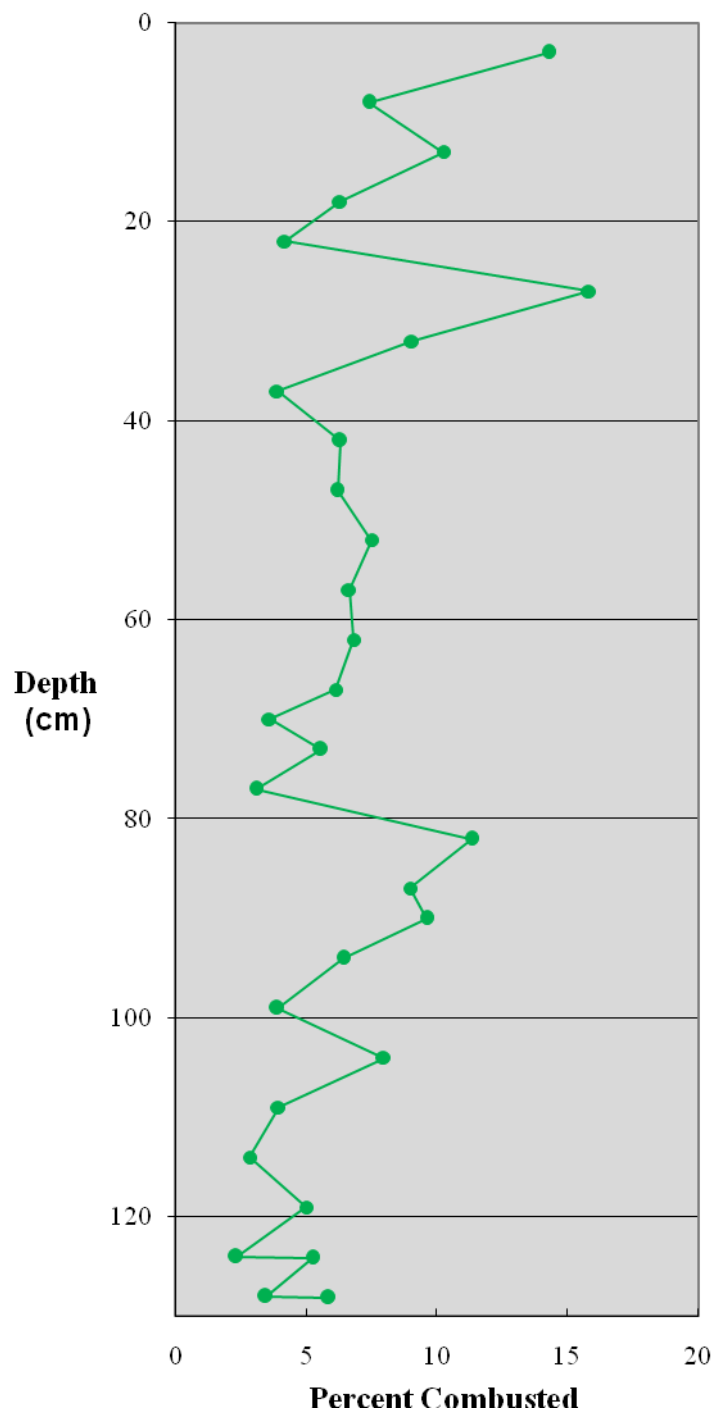
Mullins River Line 1



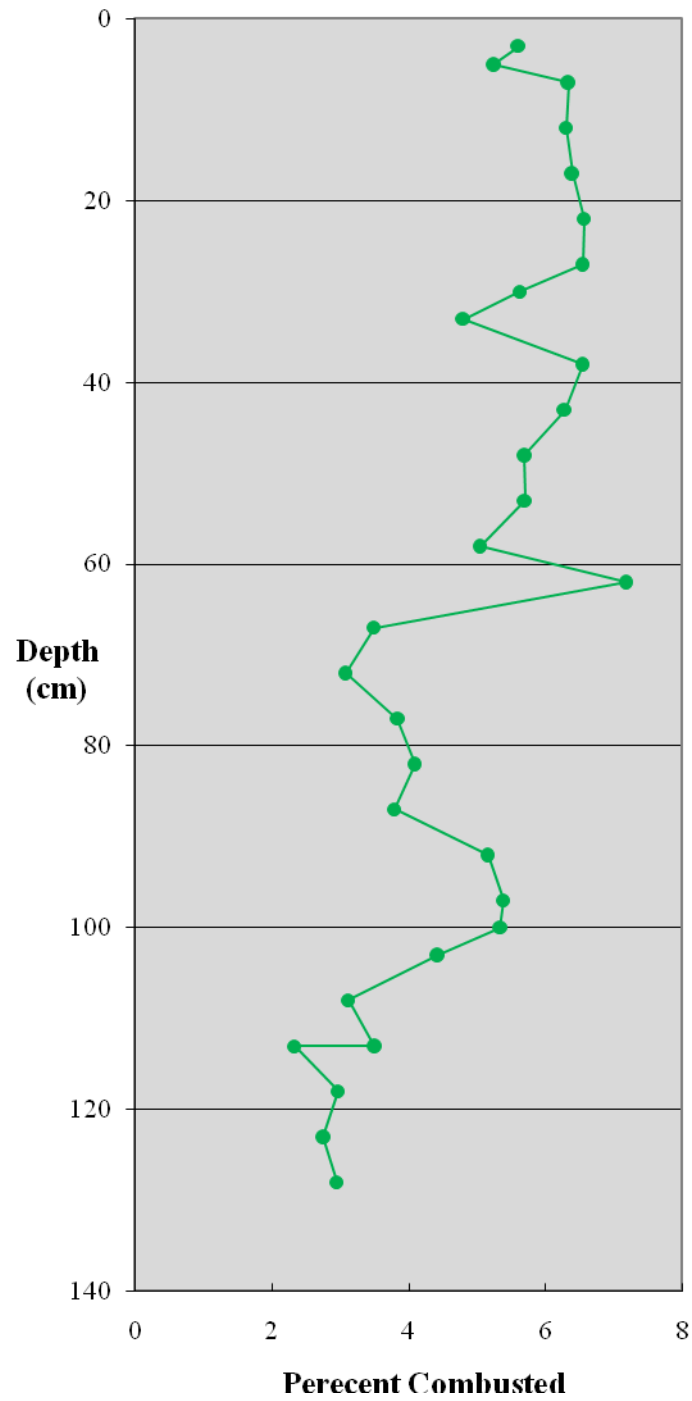
MR 2

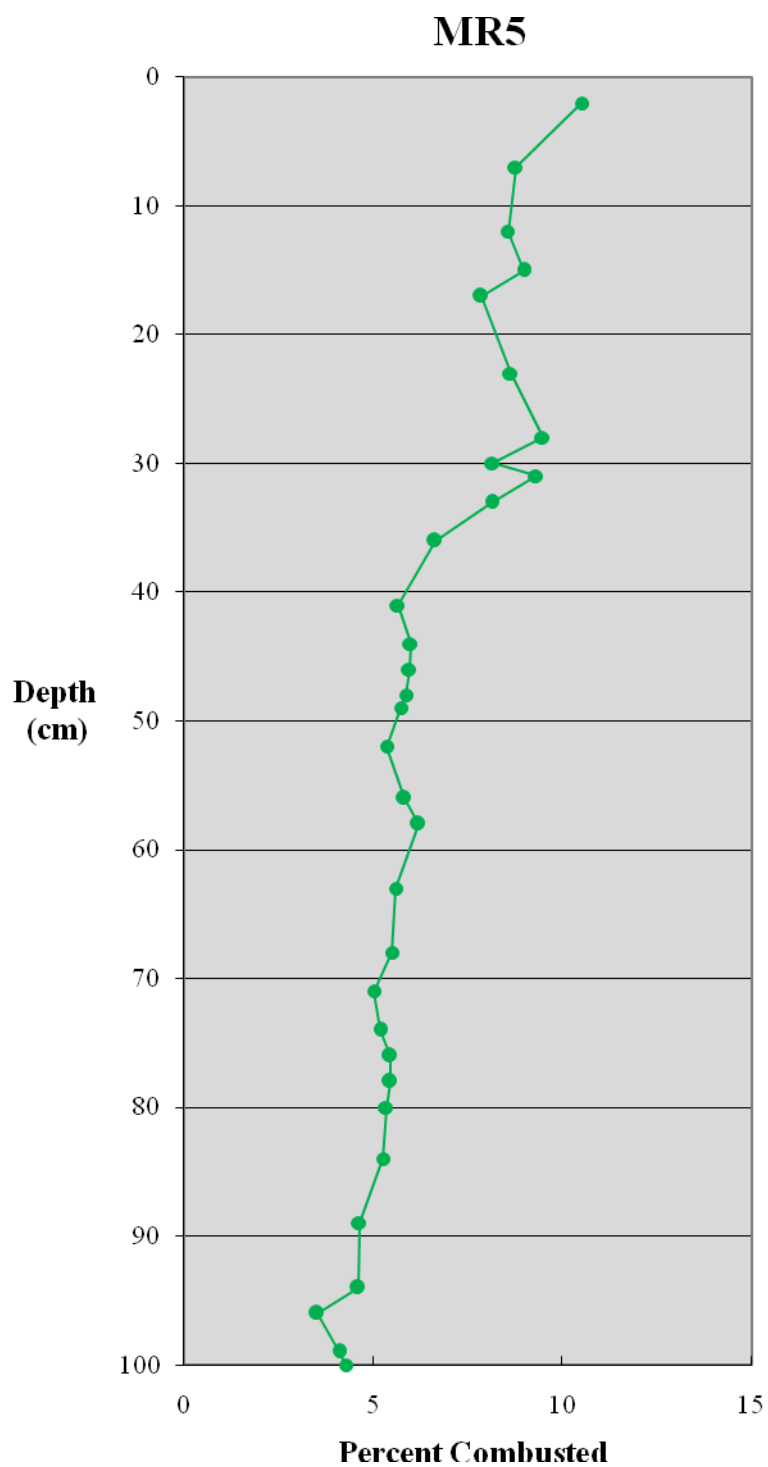


MR 3

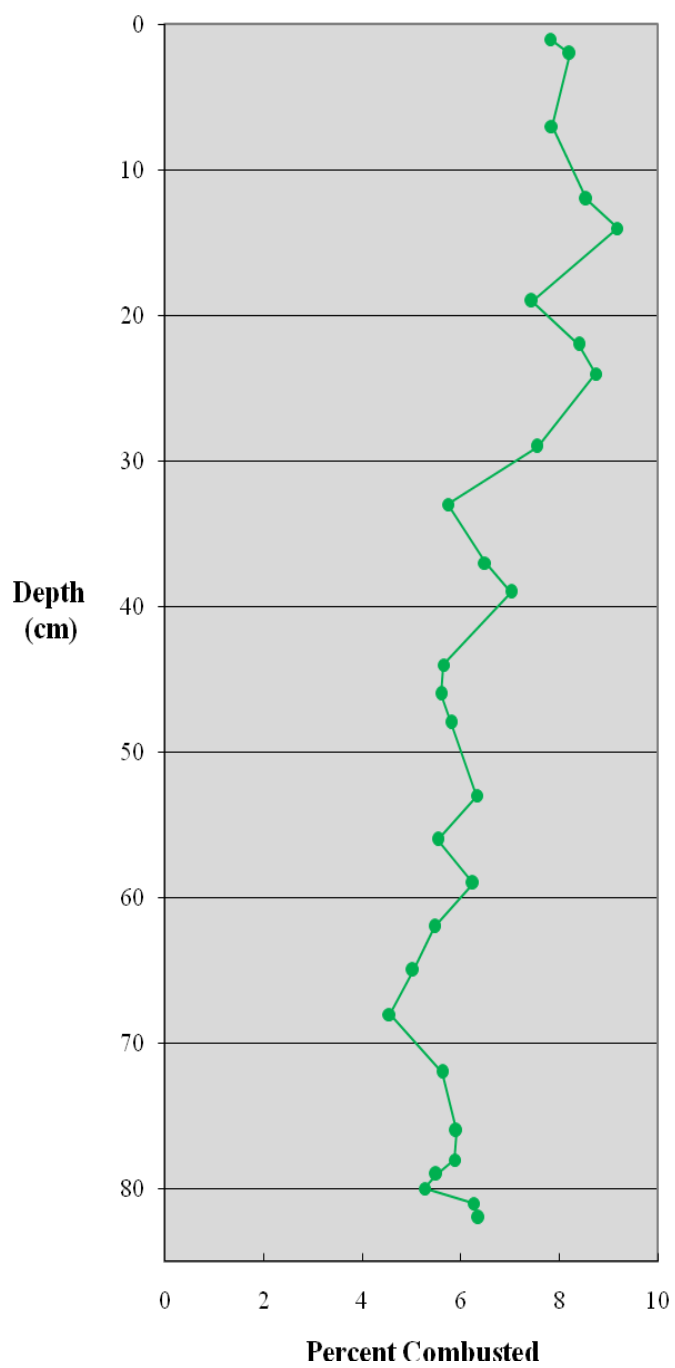


MR 4



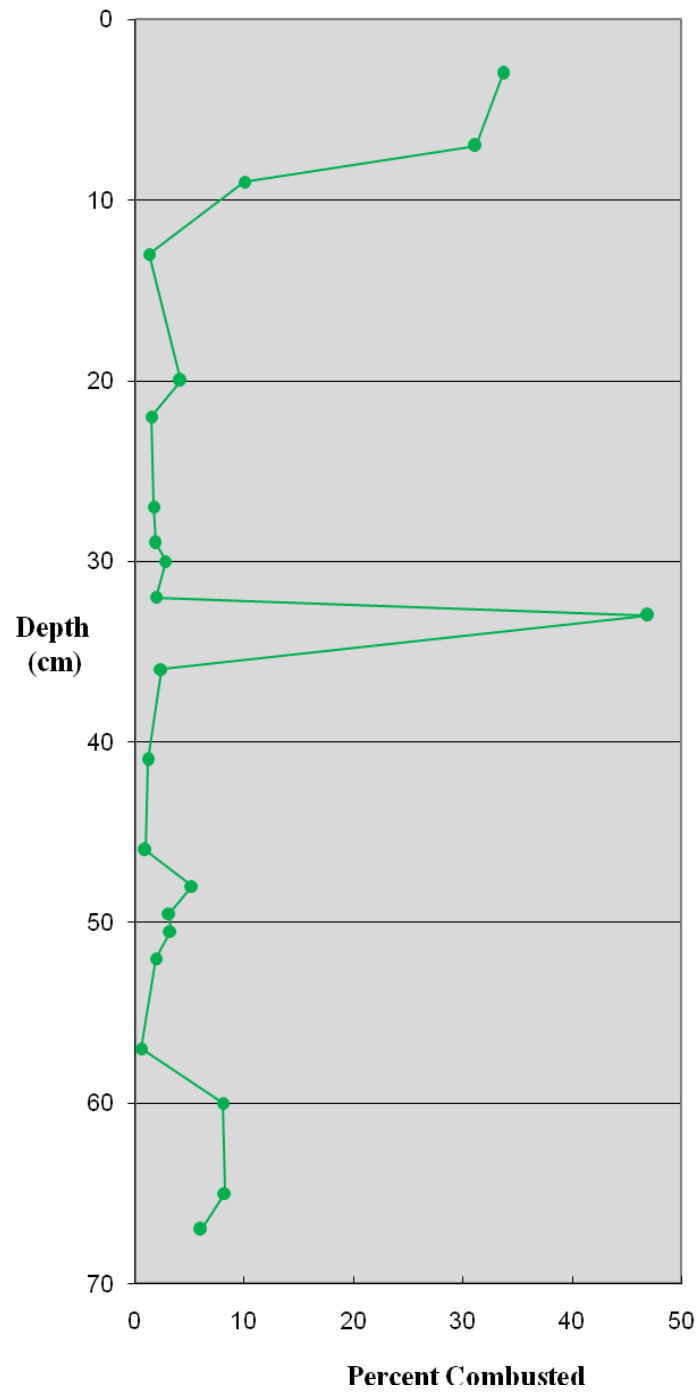


MR 6

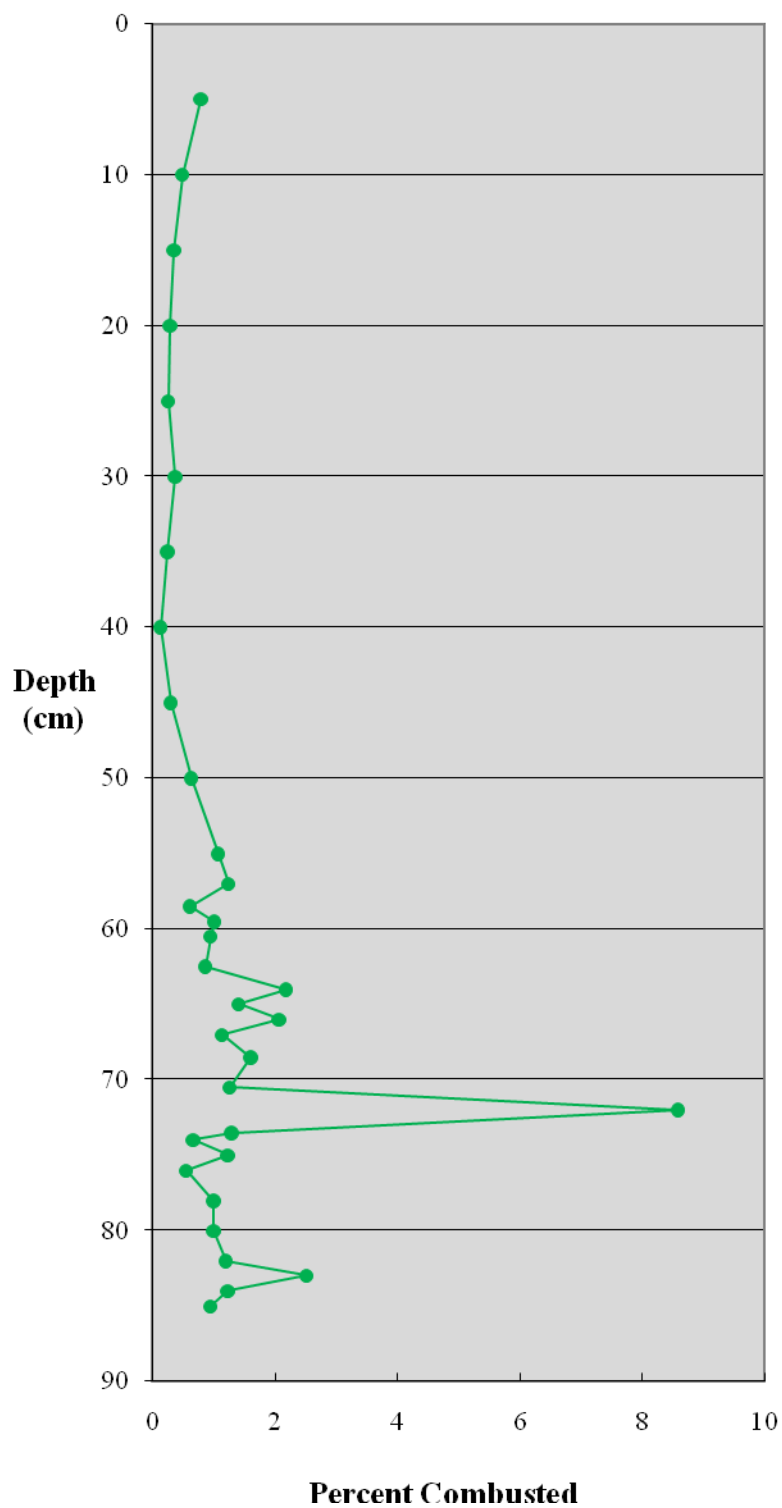


Mullins River Line 2

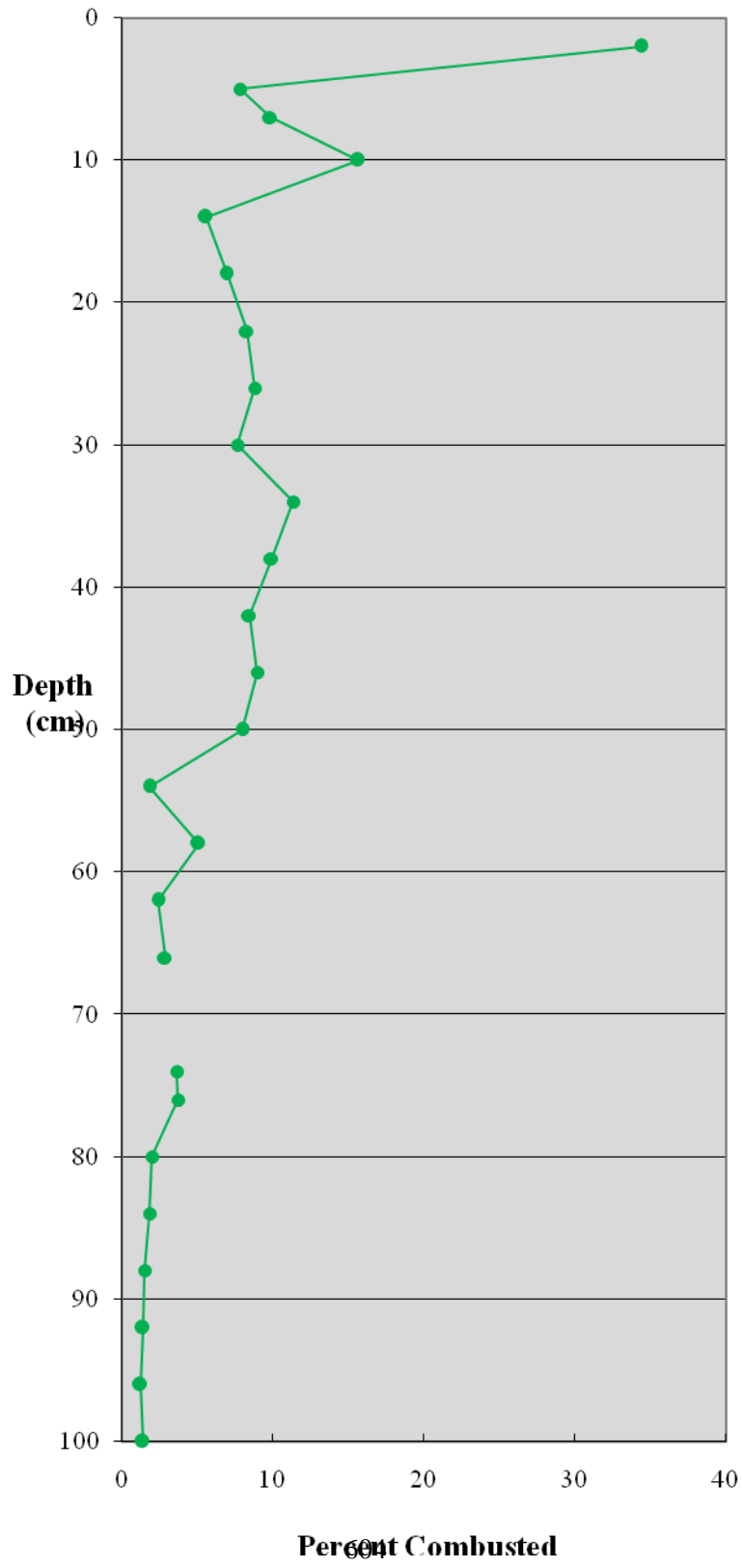
MR S-4



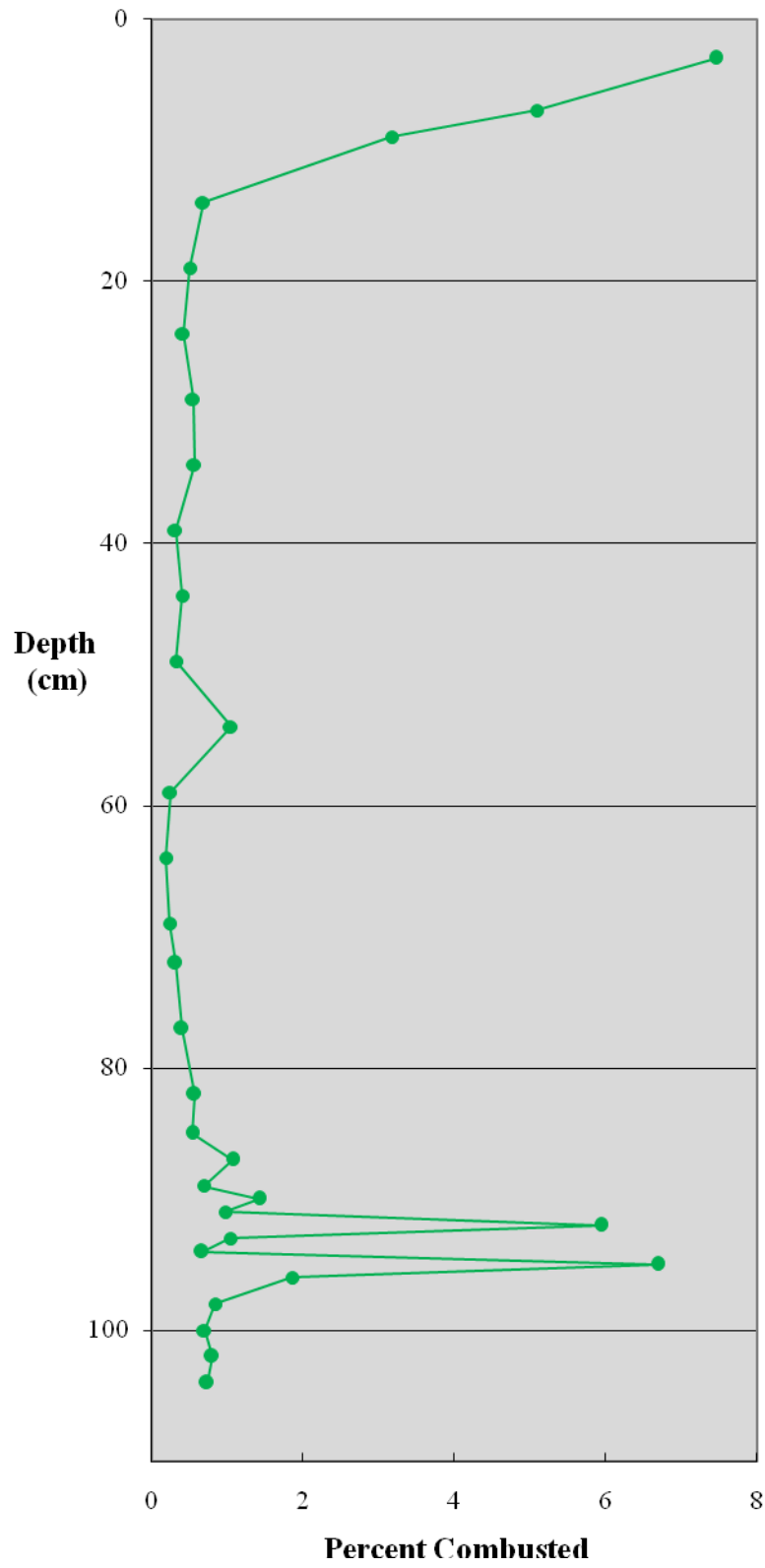
MR S-5

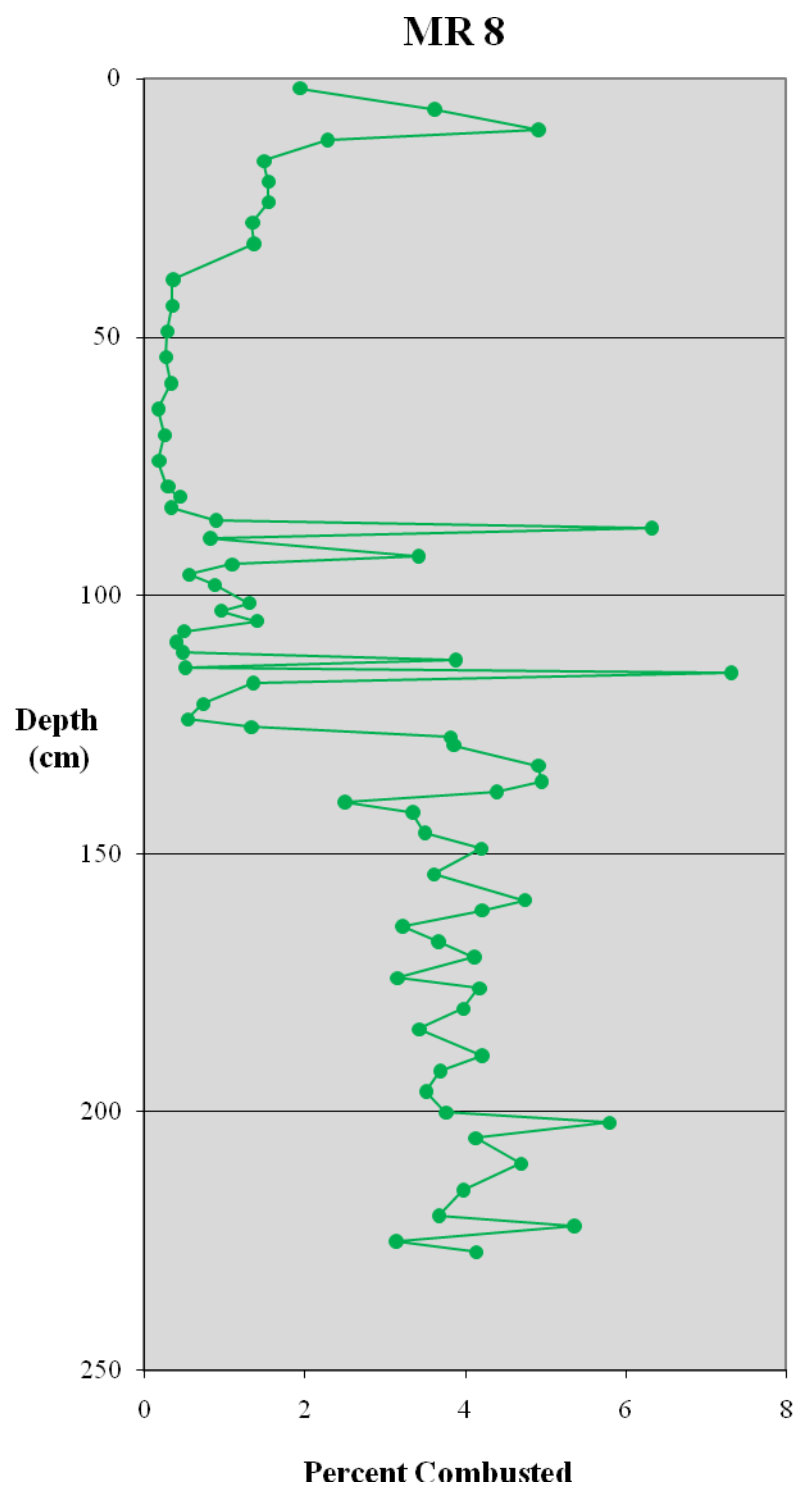


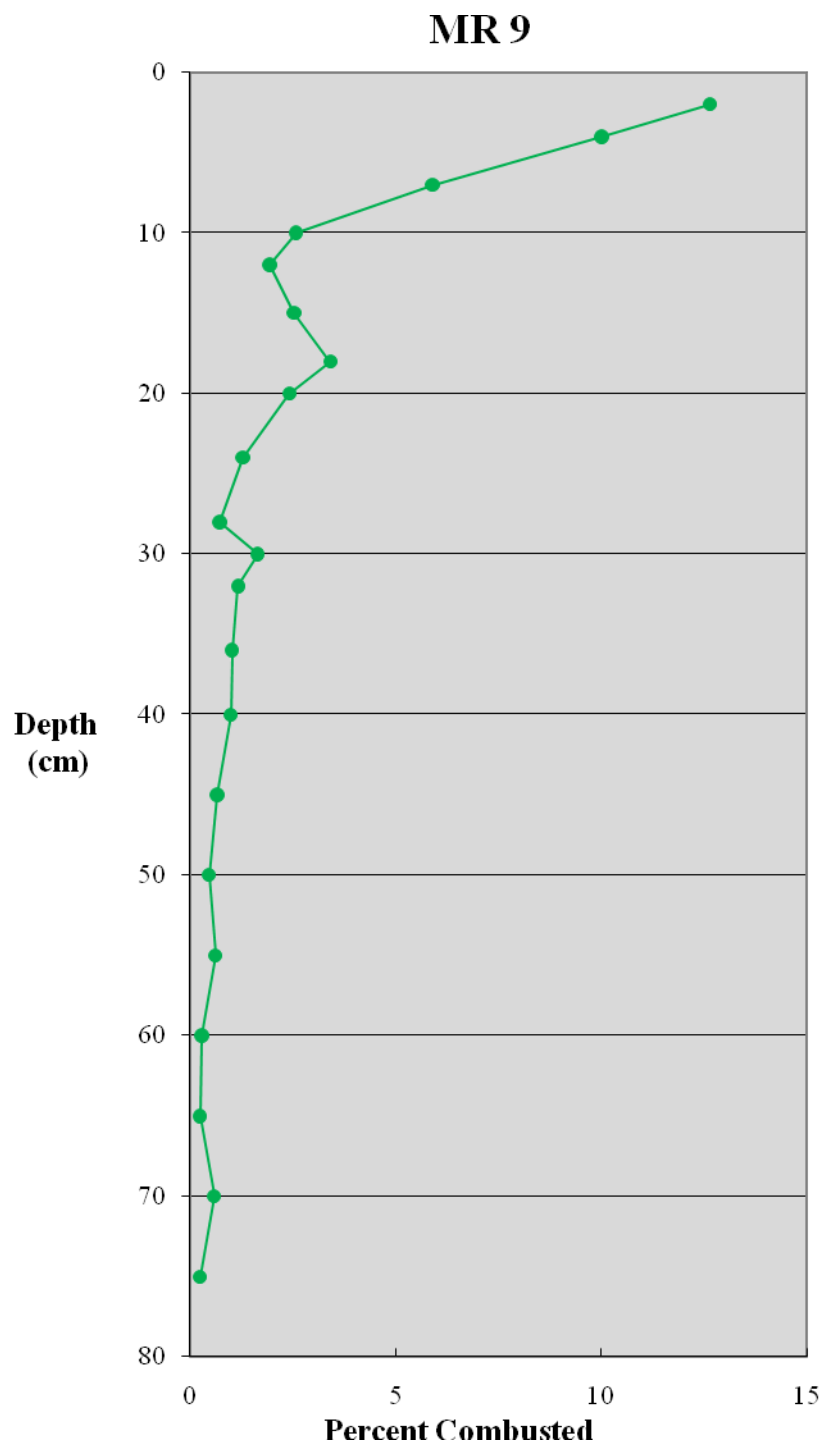
MR P 6



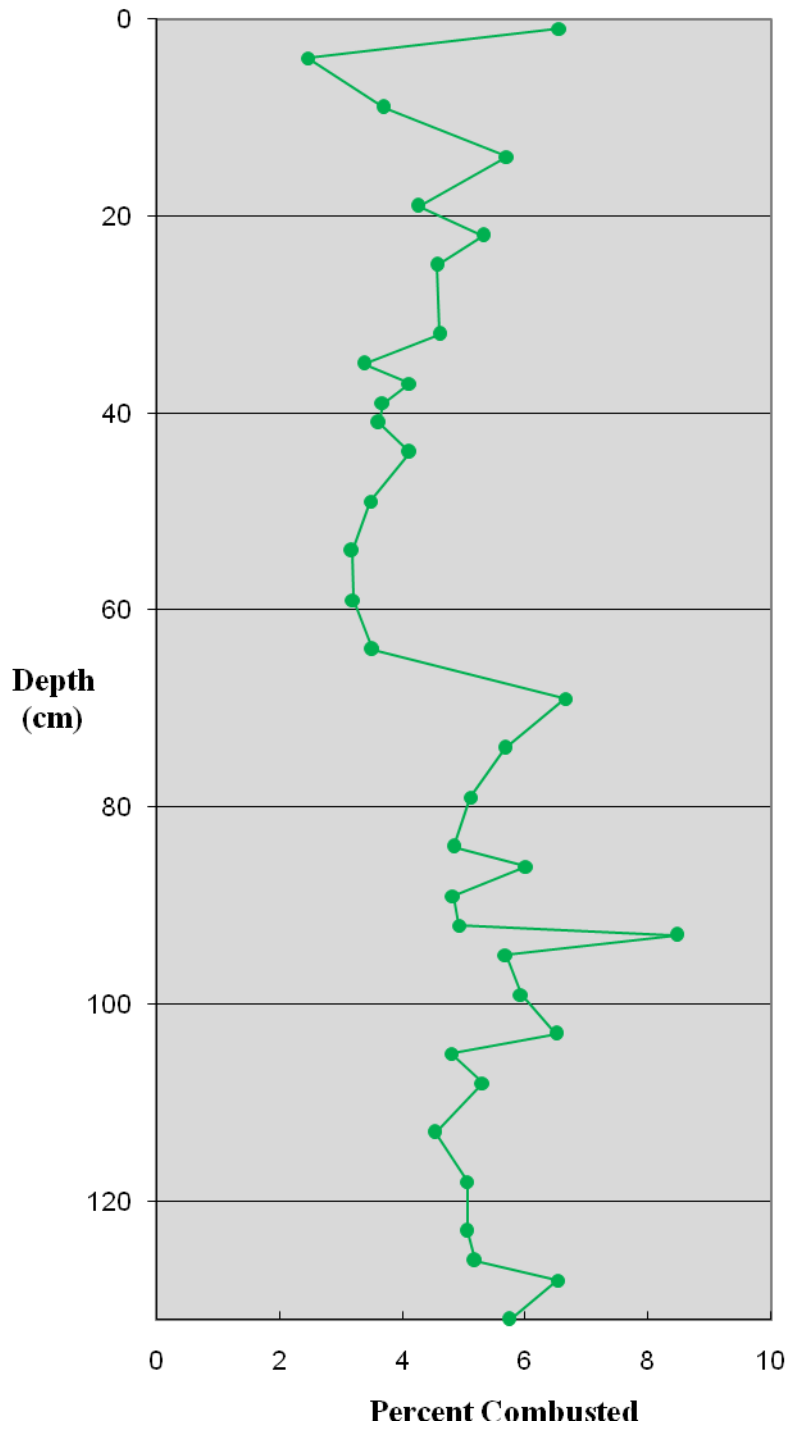
MR 7



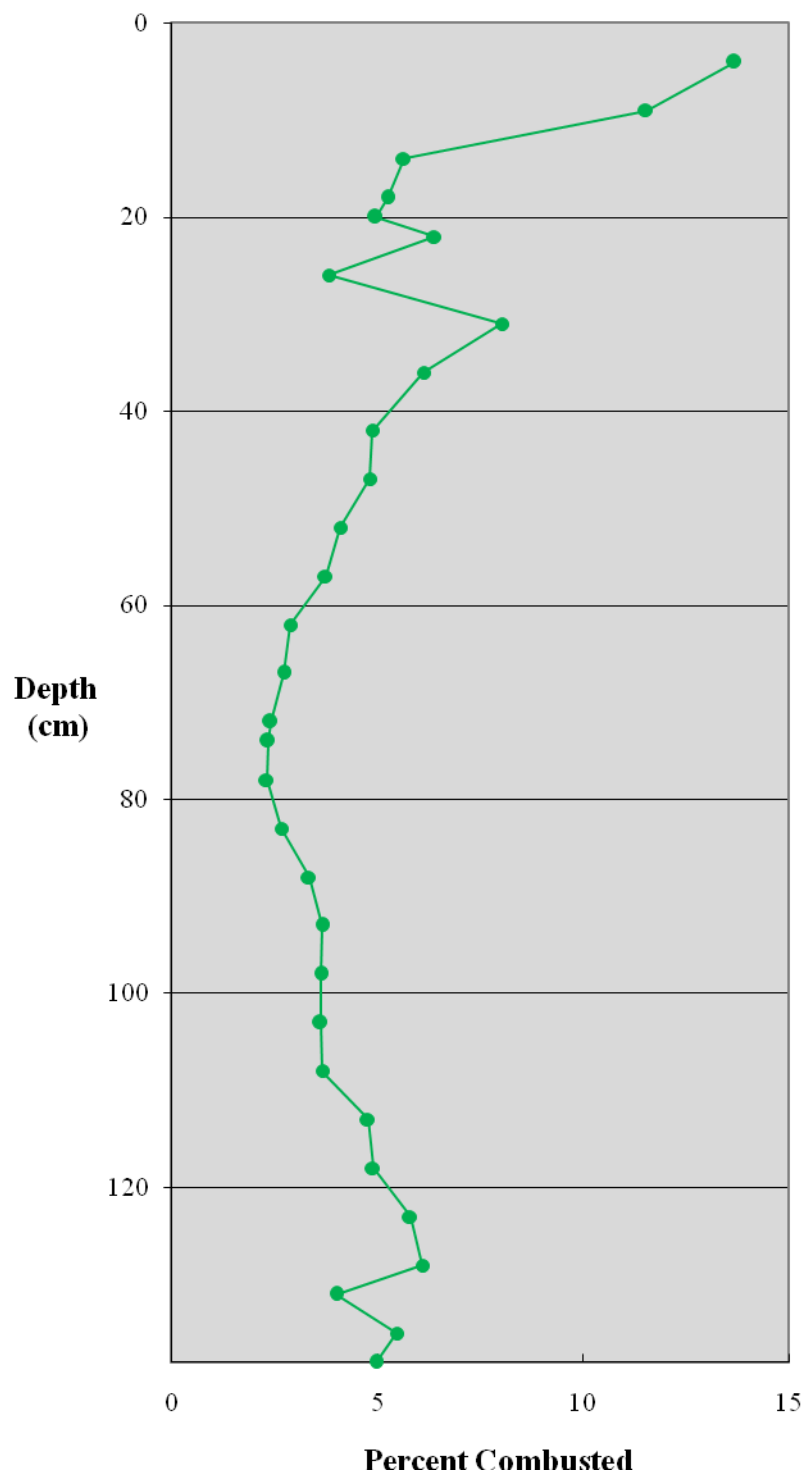


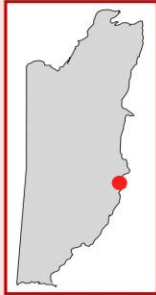


MR 10

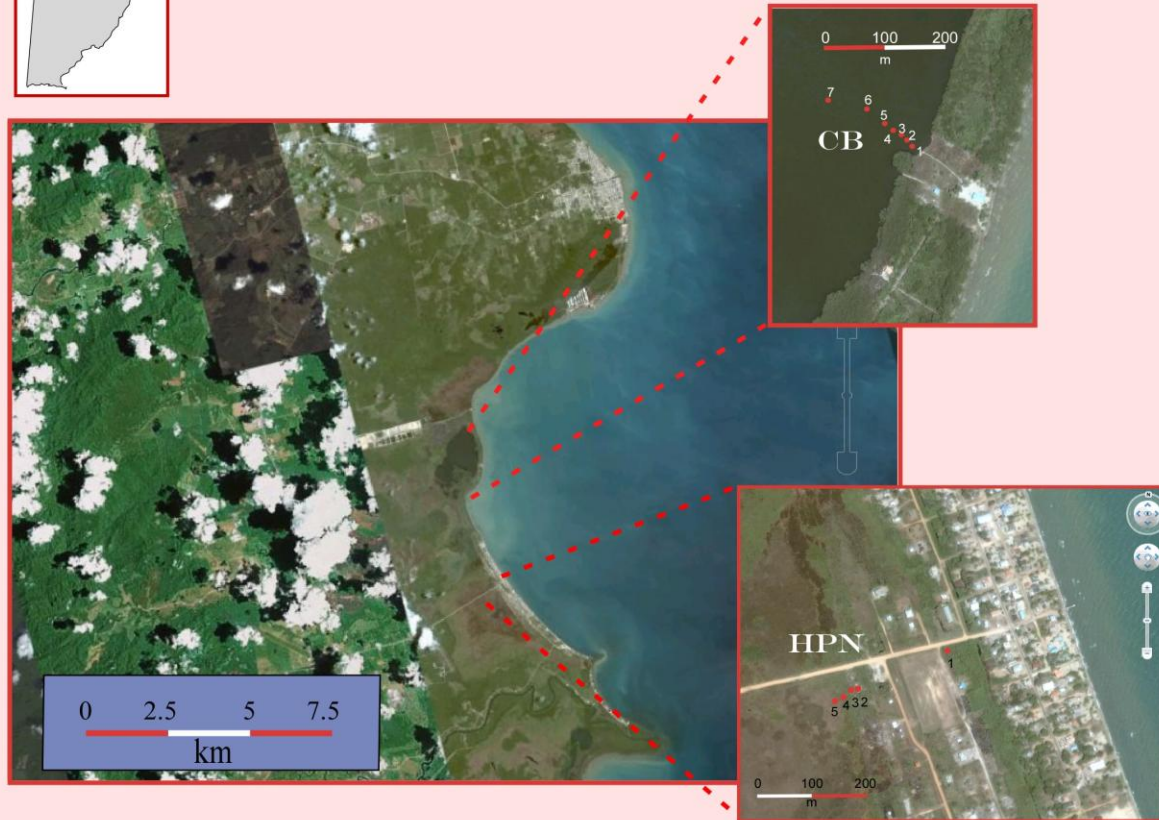


MR 11

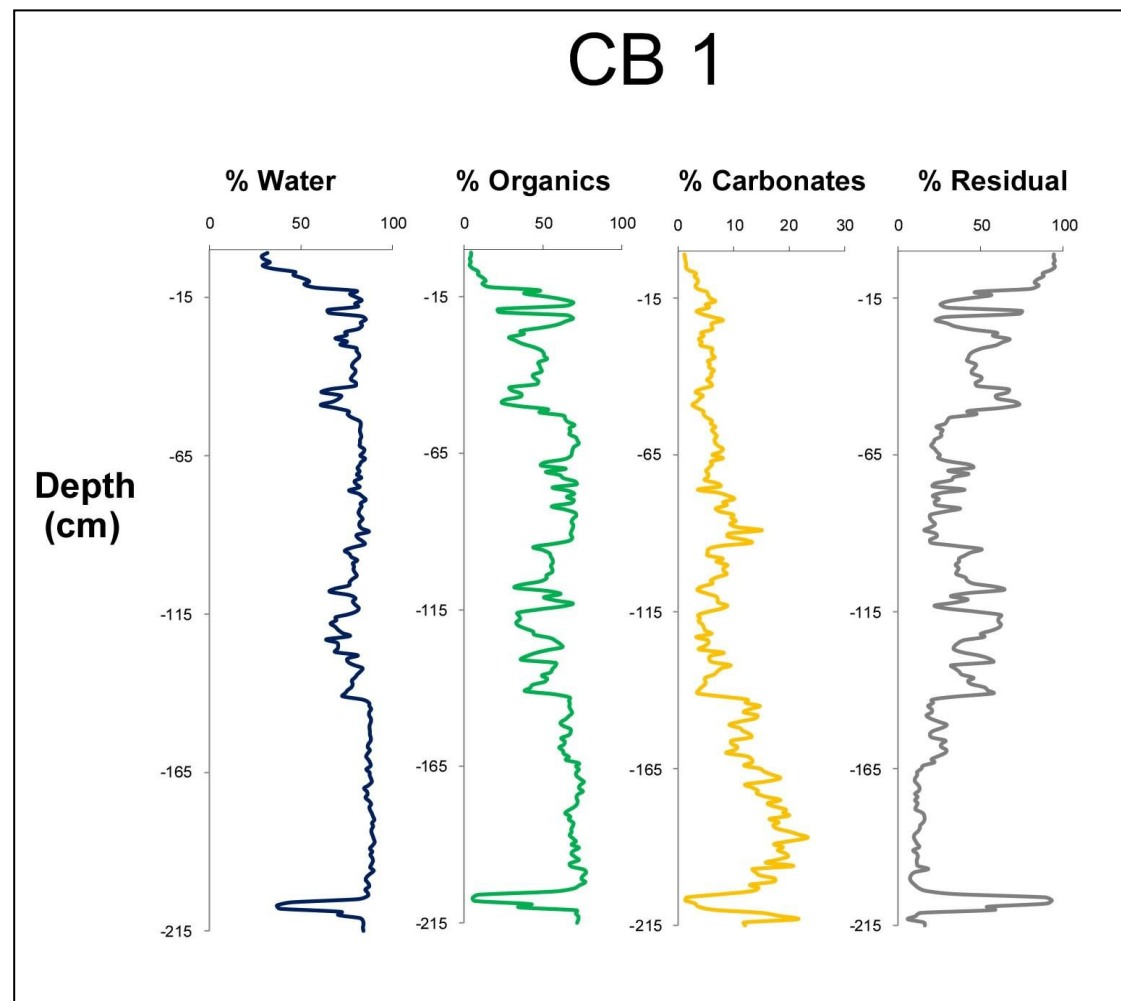




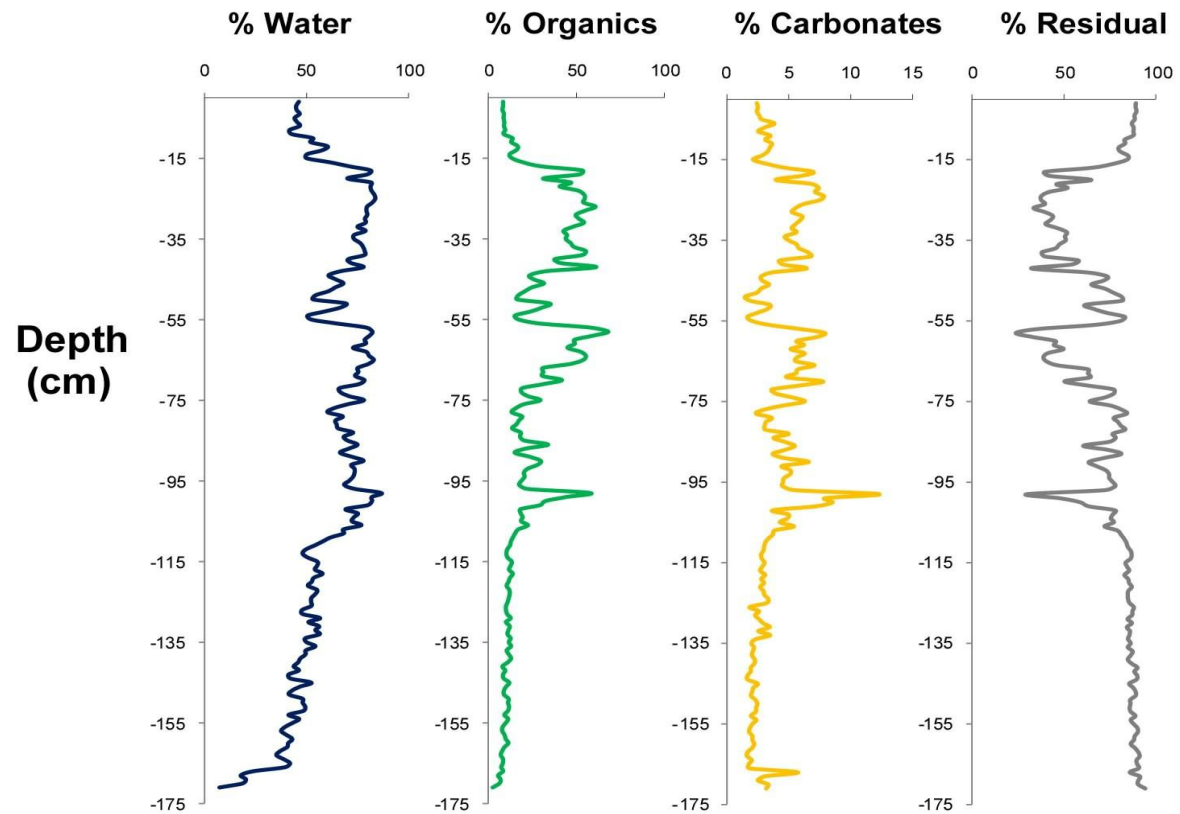
Commerce Bight Lagoon Hopkins Marsh



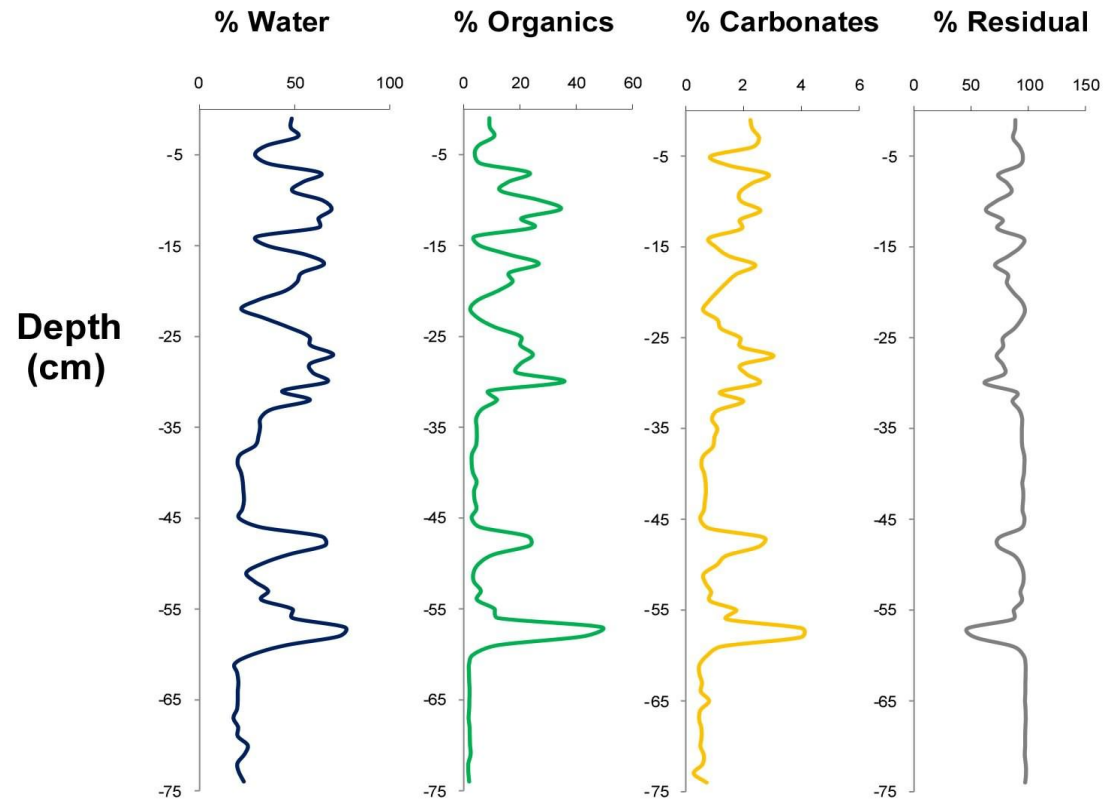
Commerce Bigh Lagoon



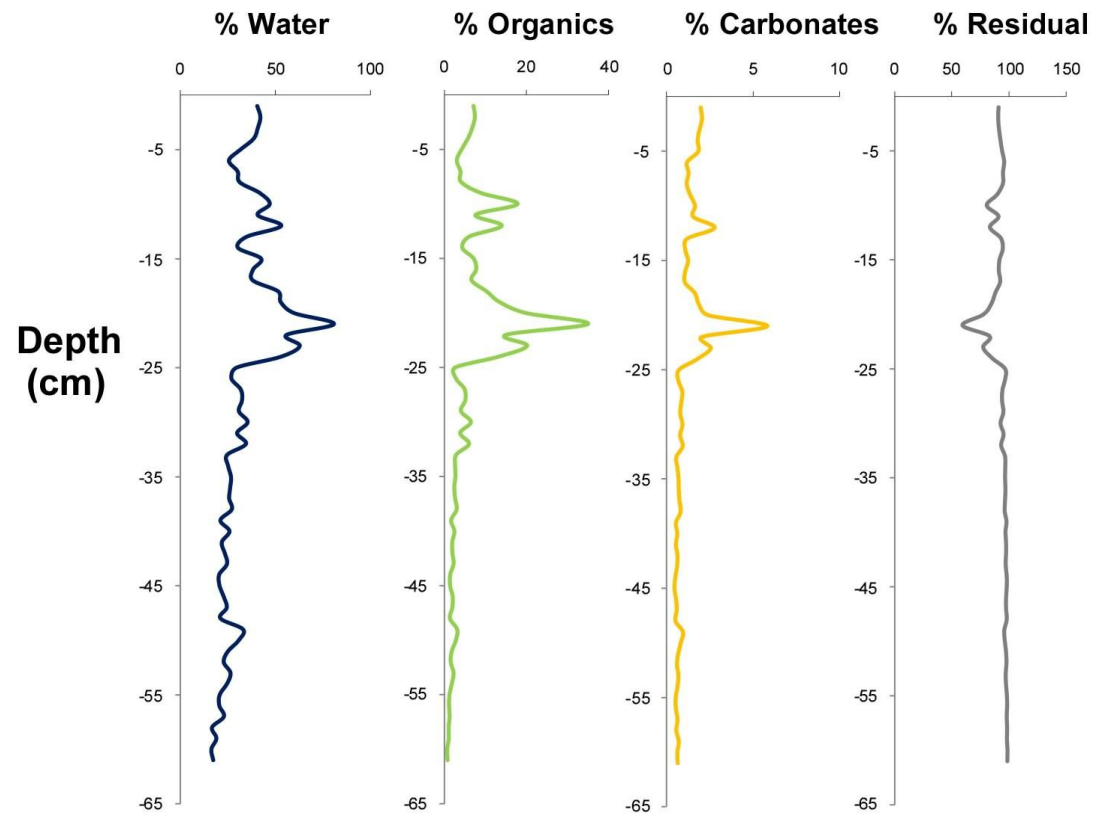
CB 2



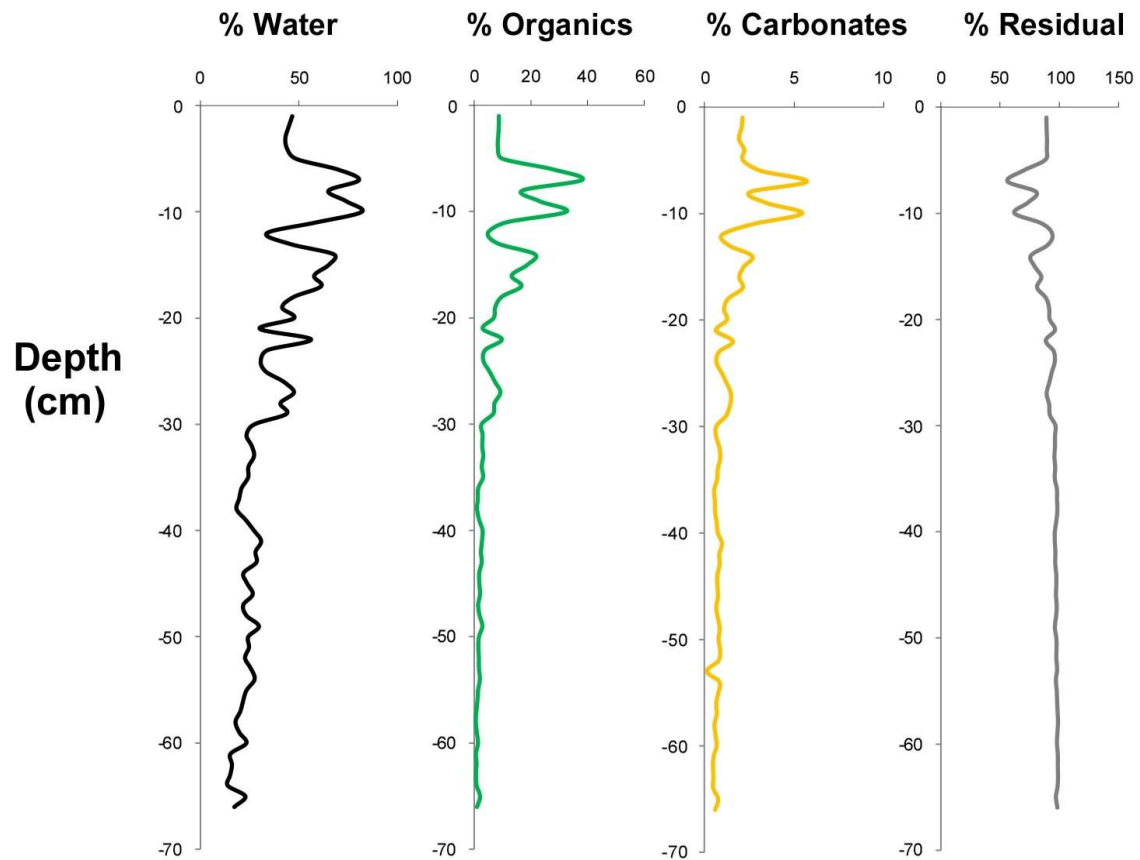
CB 3



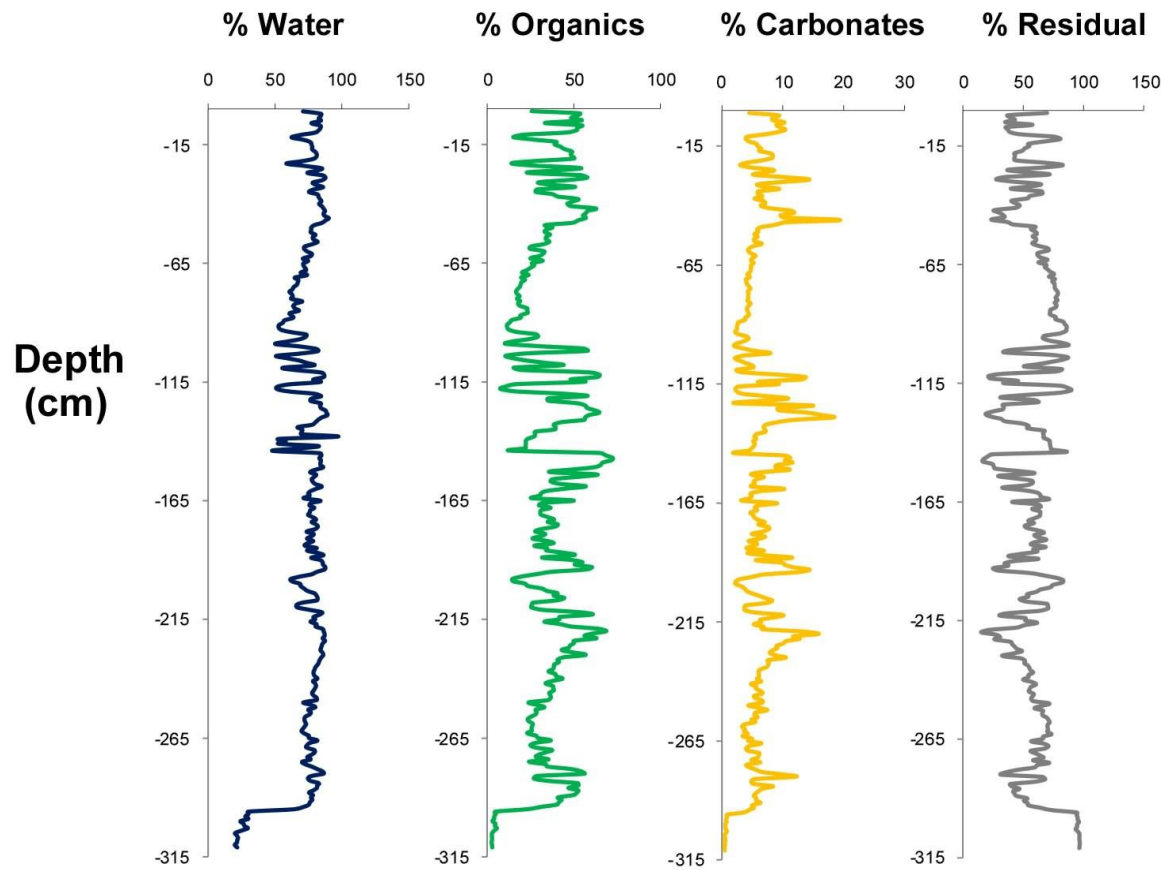
CB 4



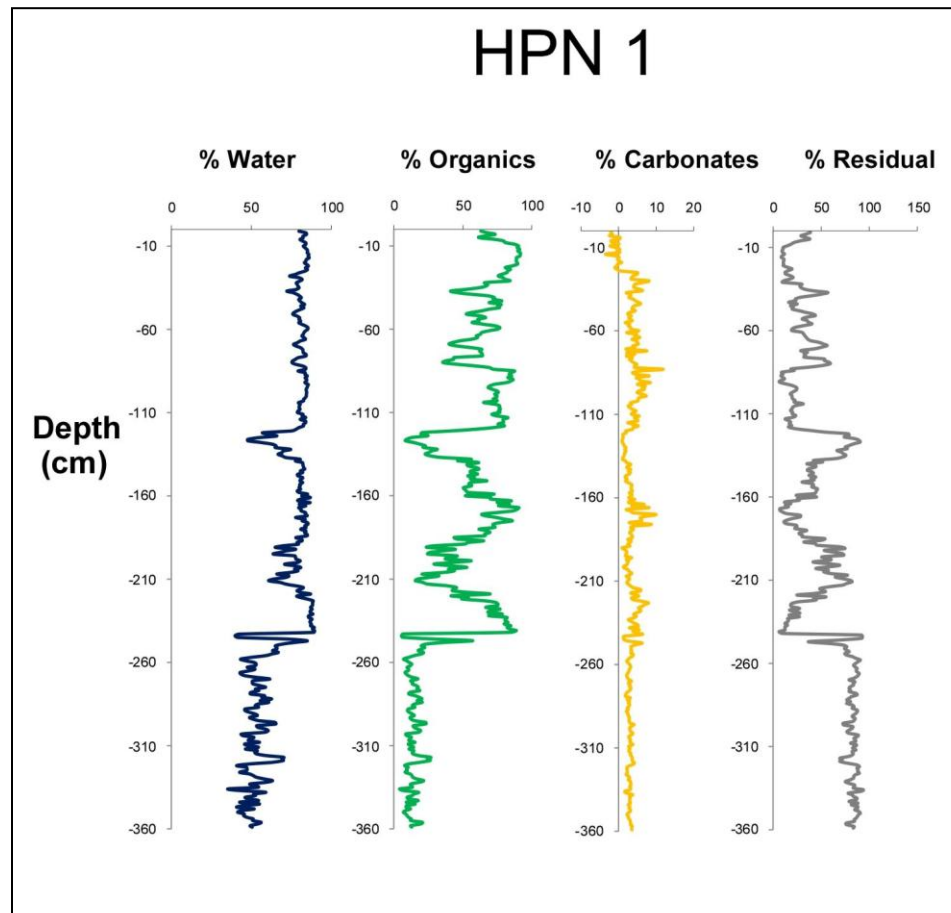
CB 5



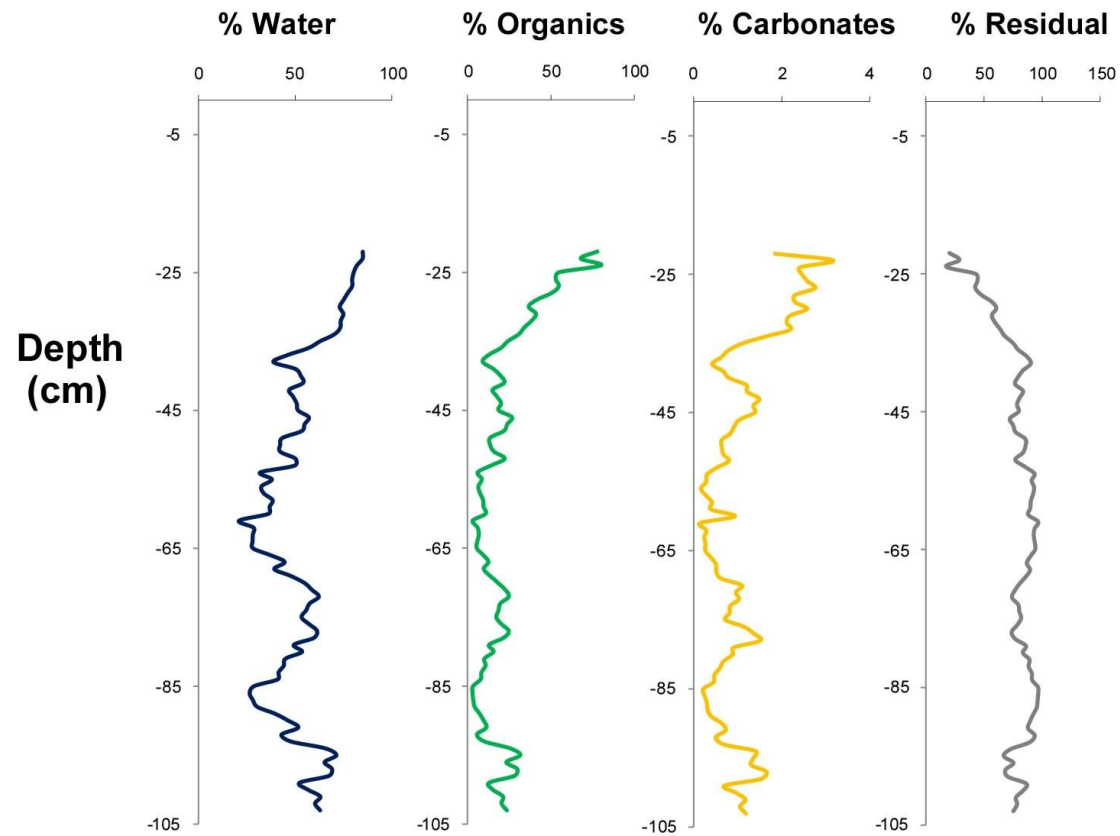
CB 7



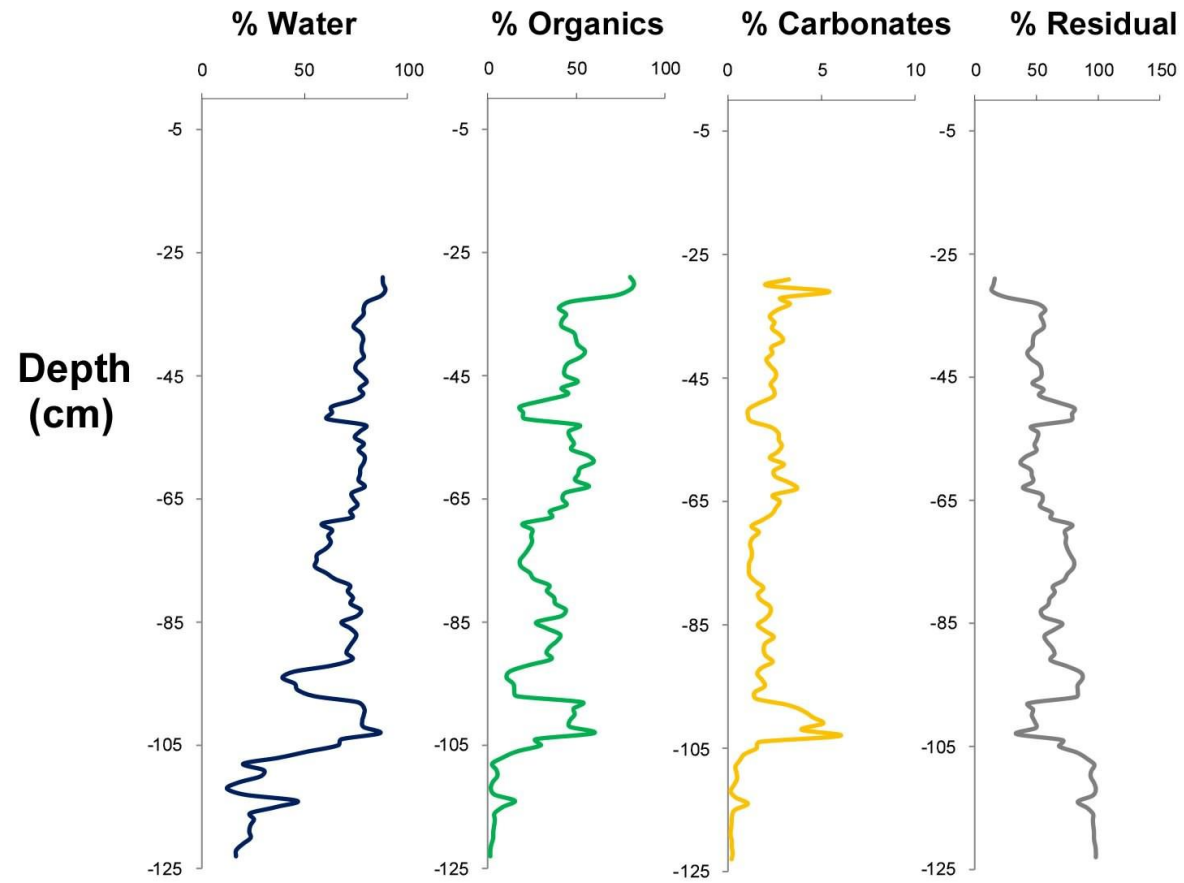
Hopkins Marsh



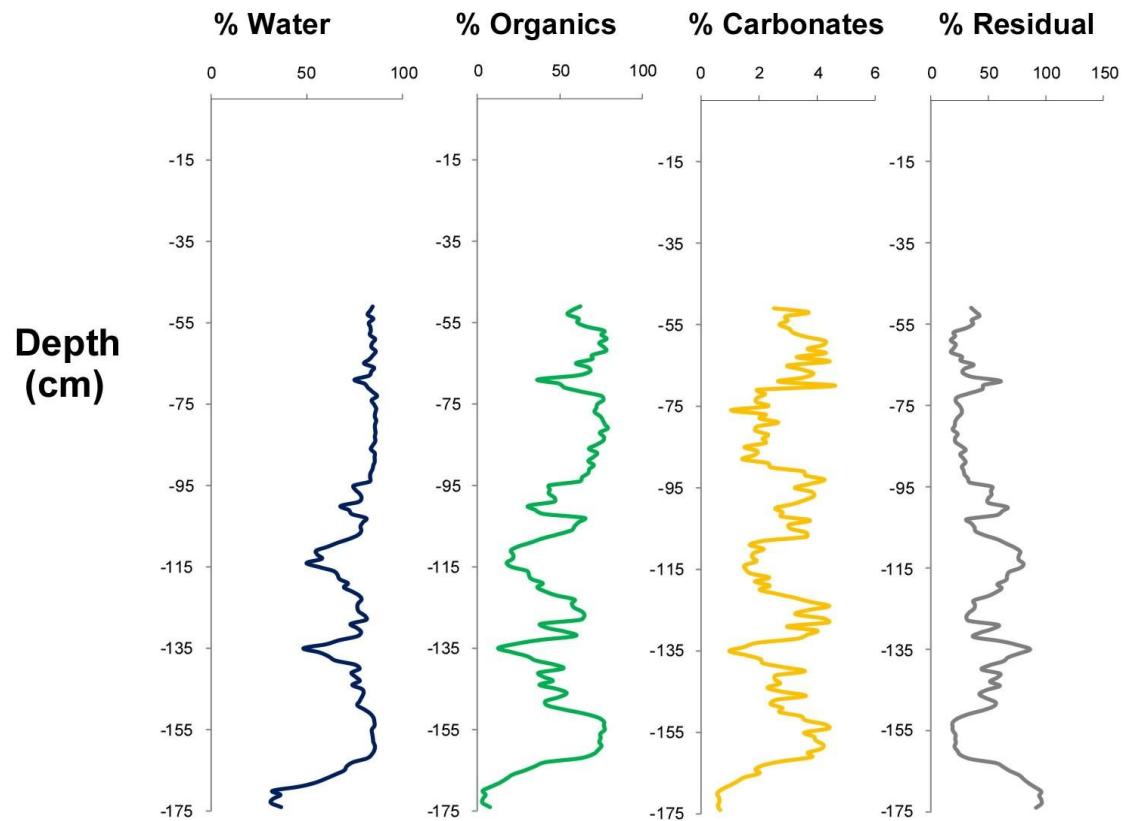
HPN 2



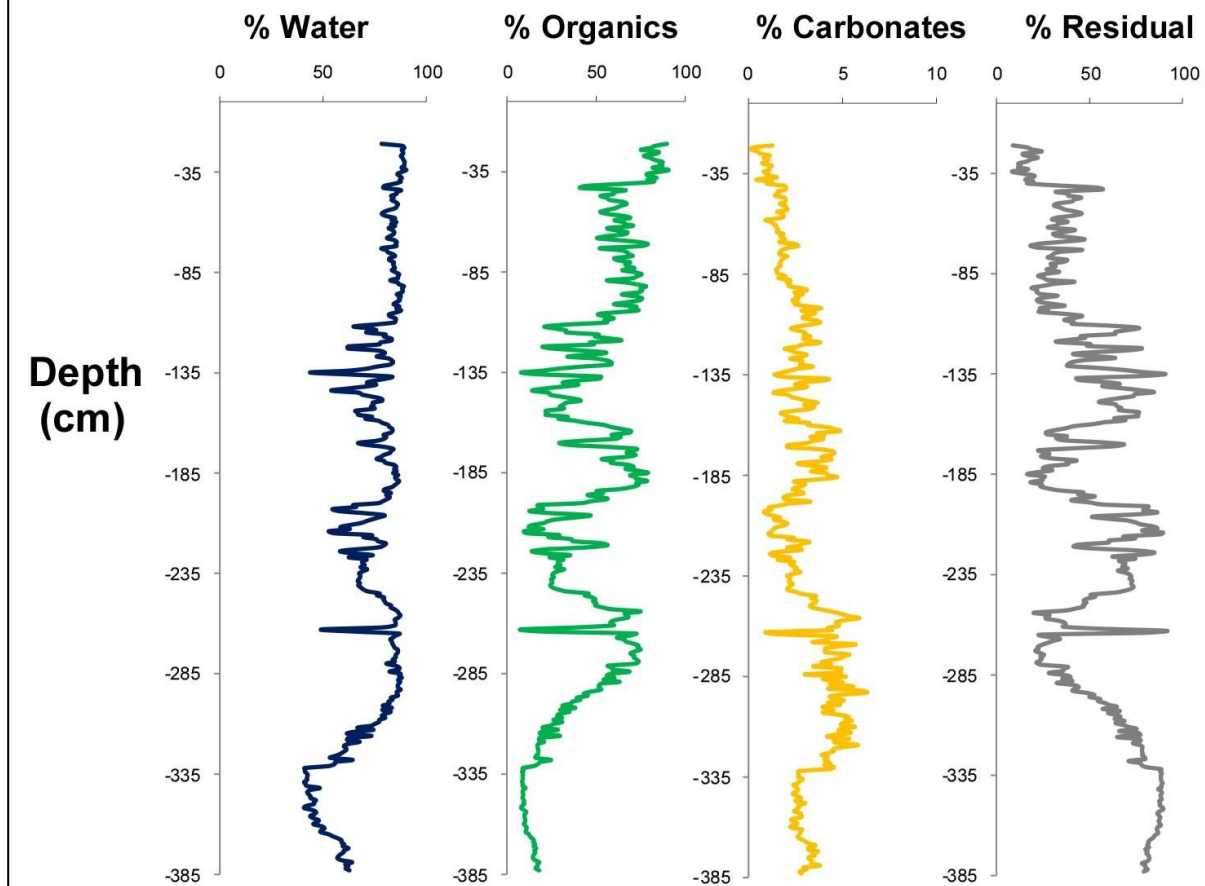
HPN 3



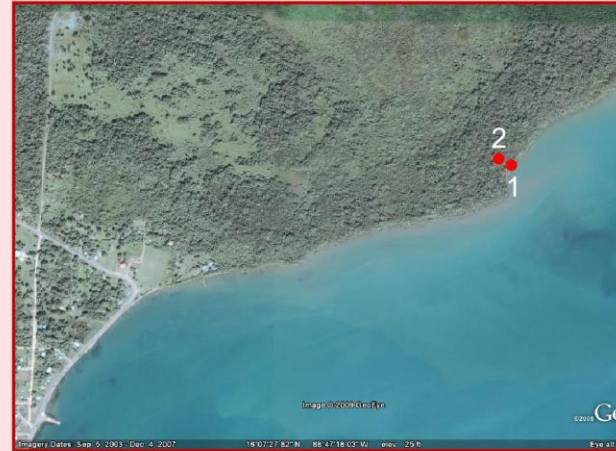
HPN 4



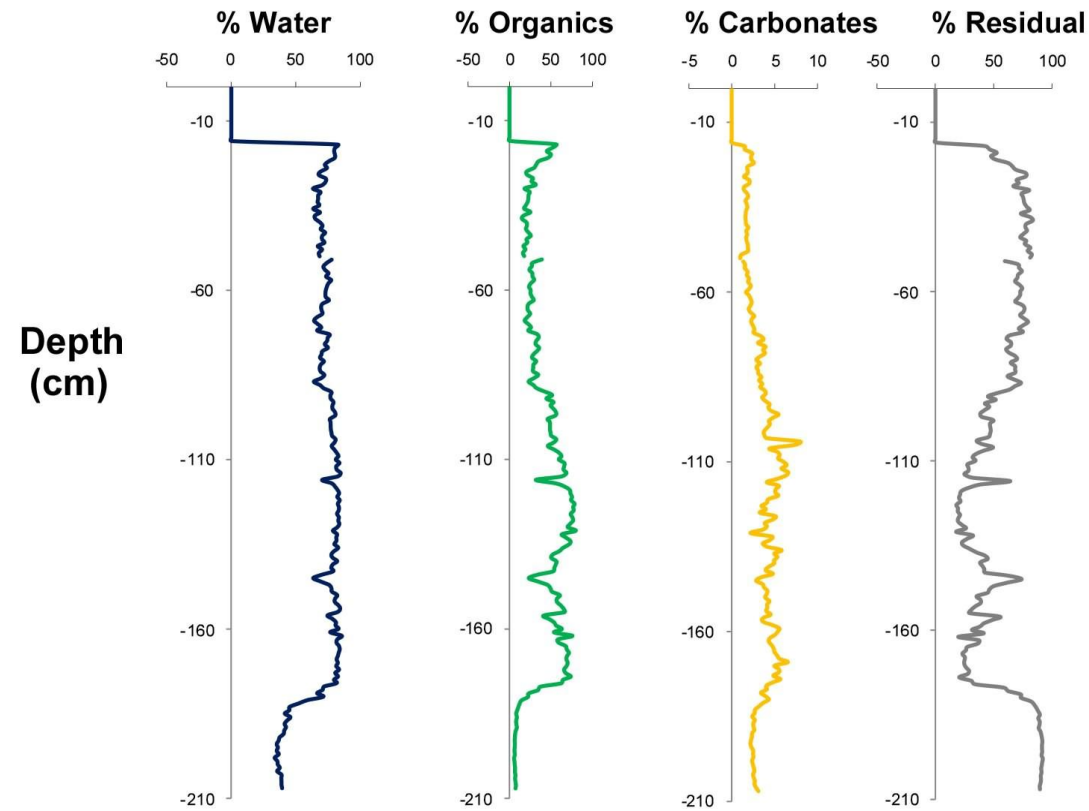
HPN 5



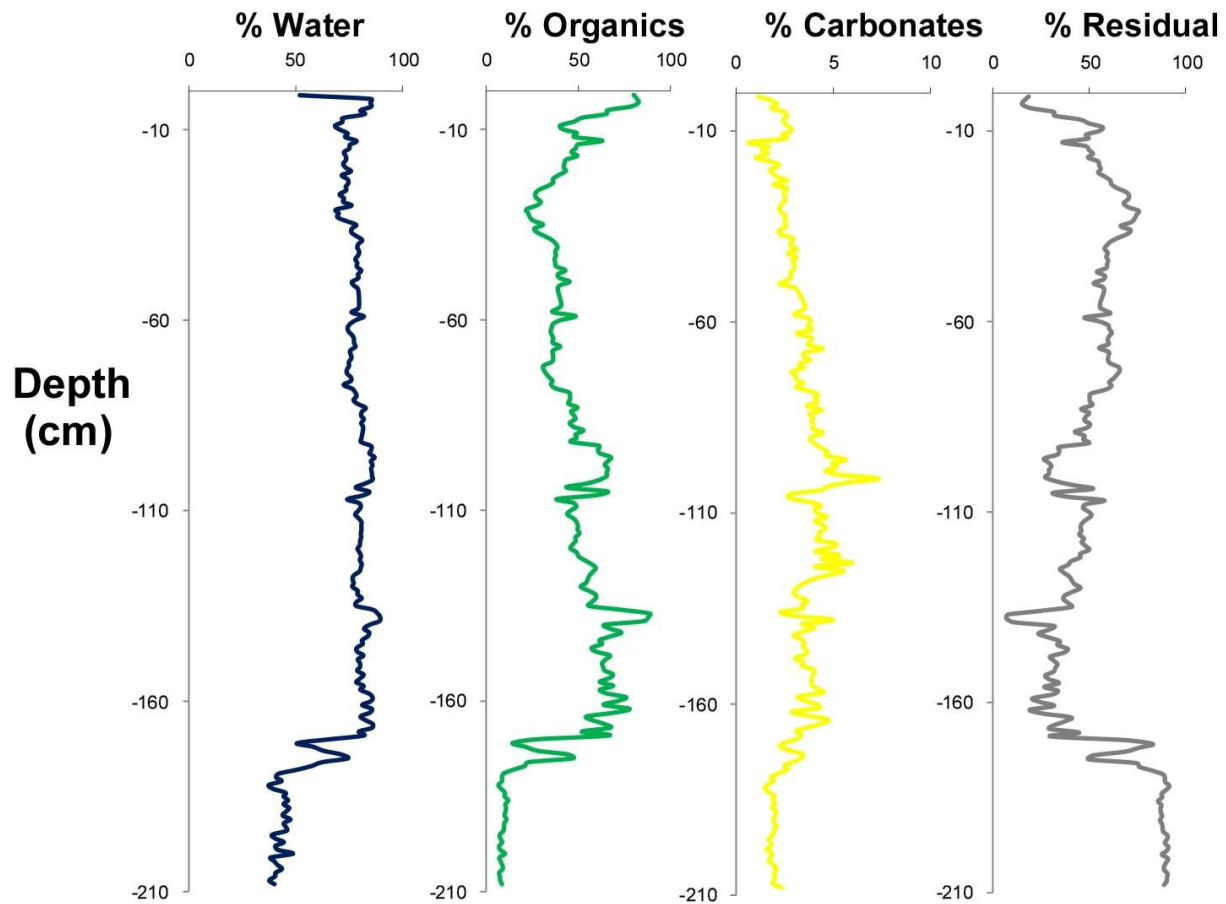
Punta Gorda



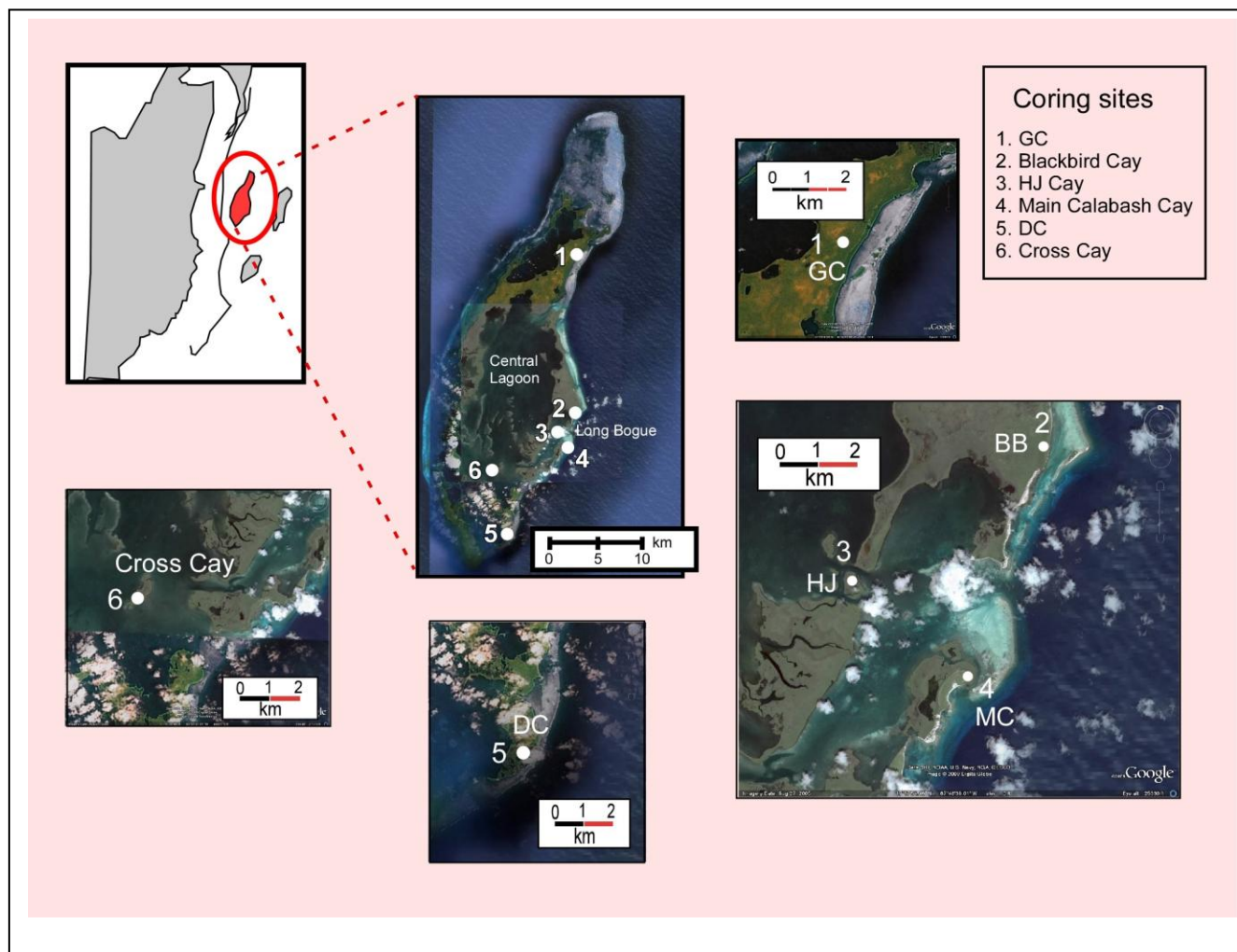
PG 1



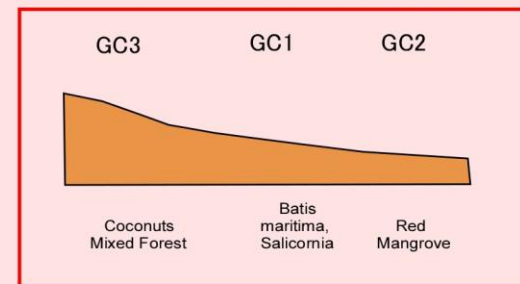
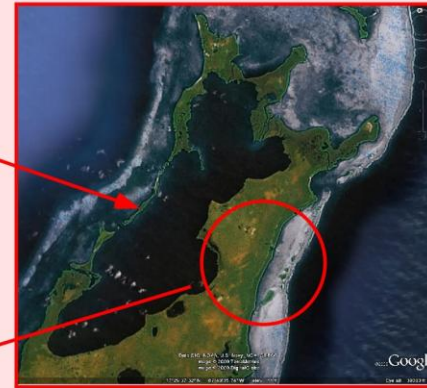
PG 2



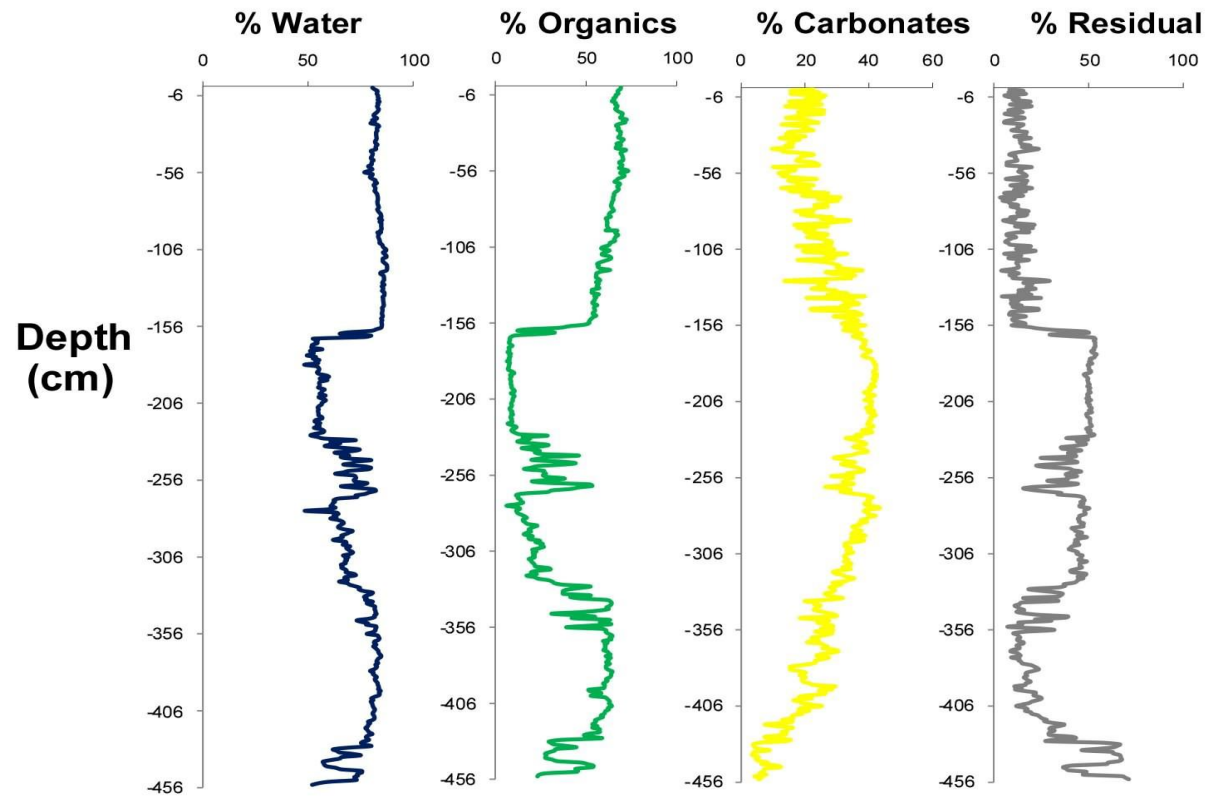
Turneffe Atoll



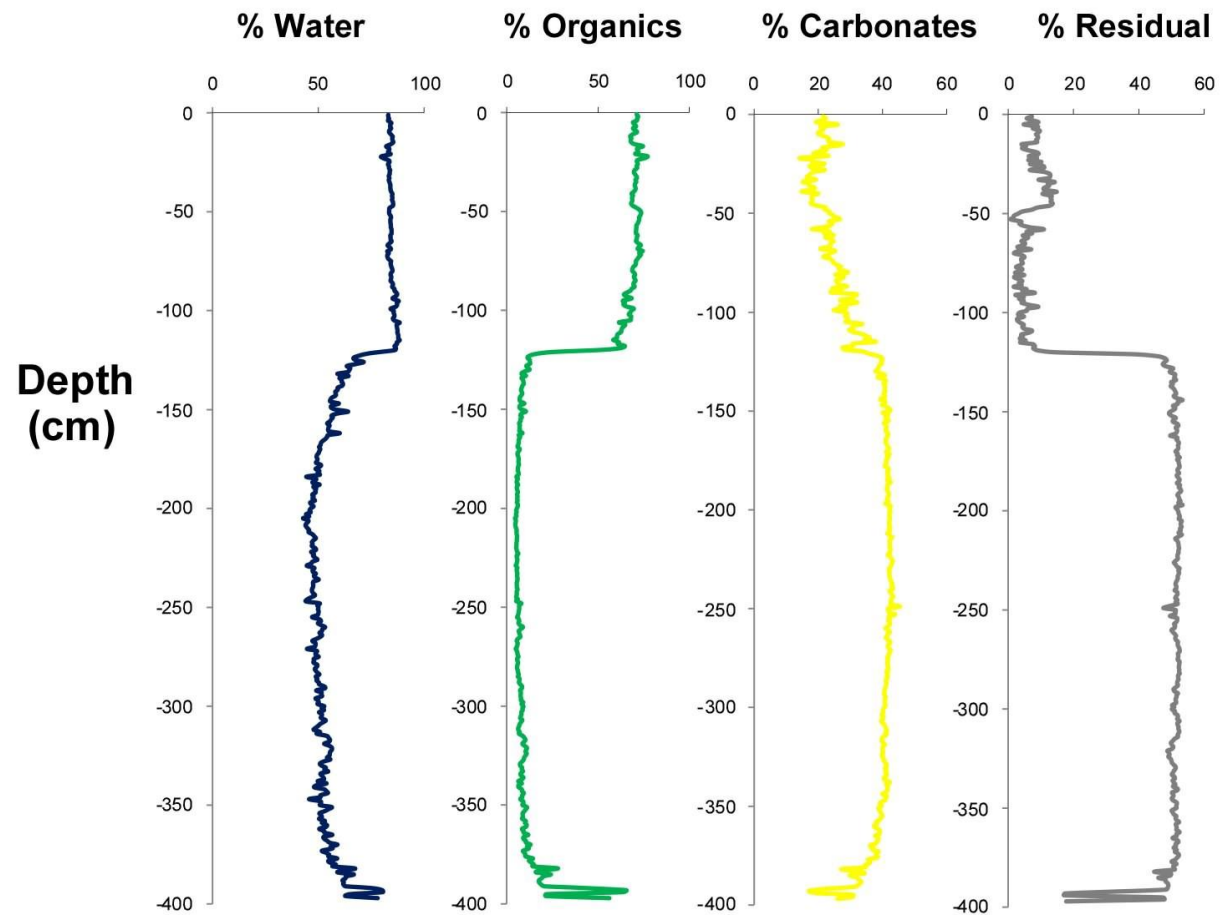
Grassy Cay (GC)



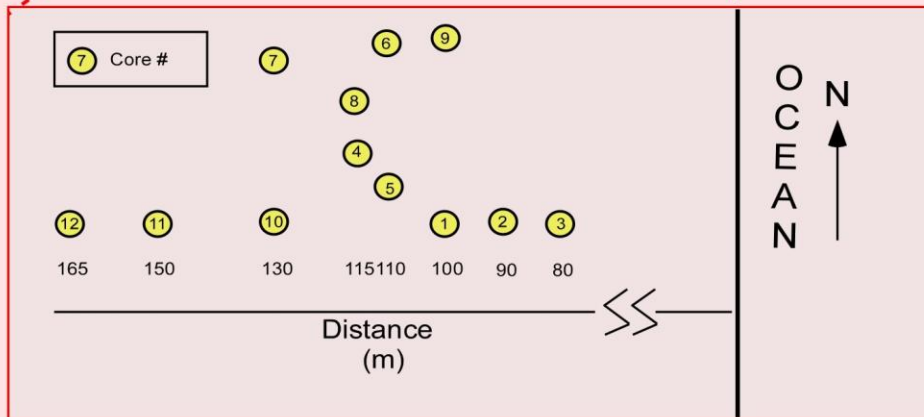
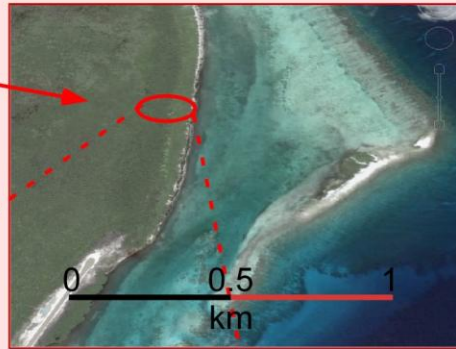
GC 1



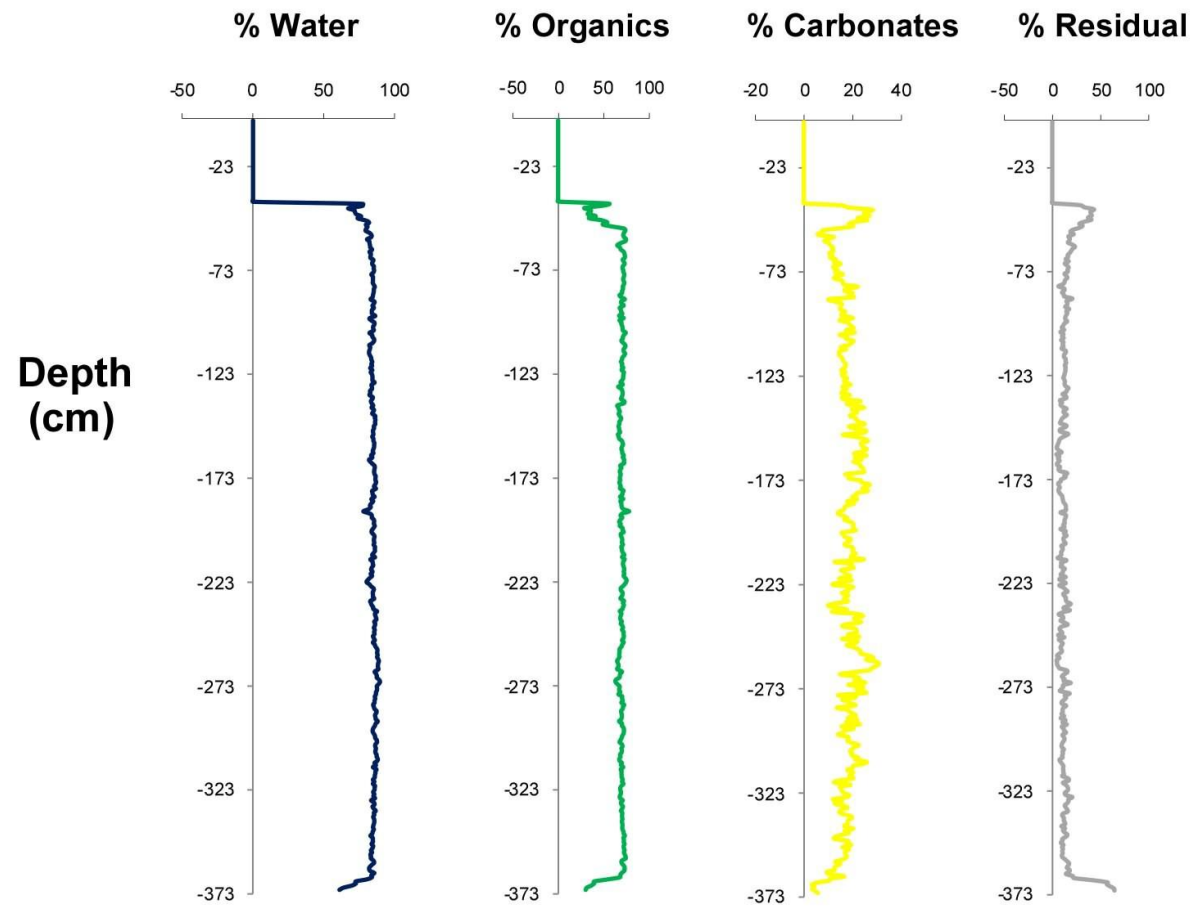
GC 2



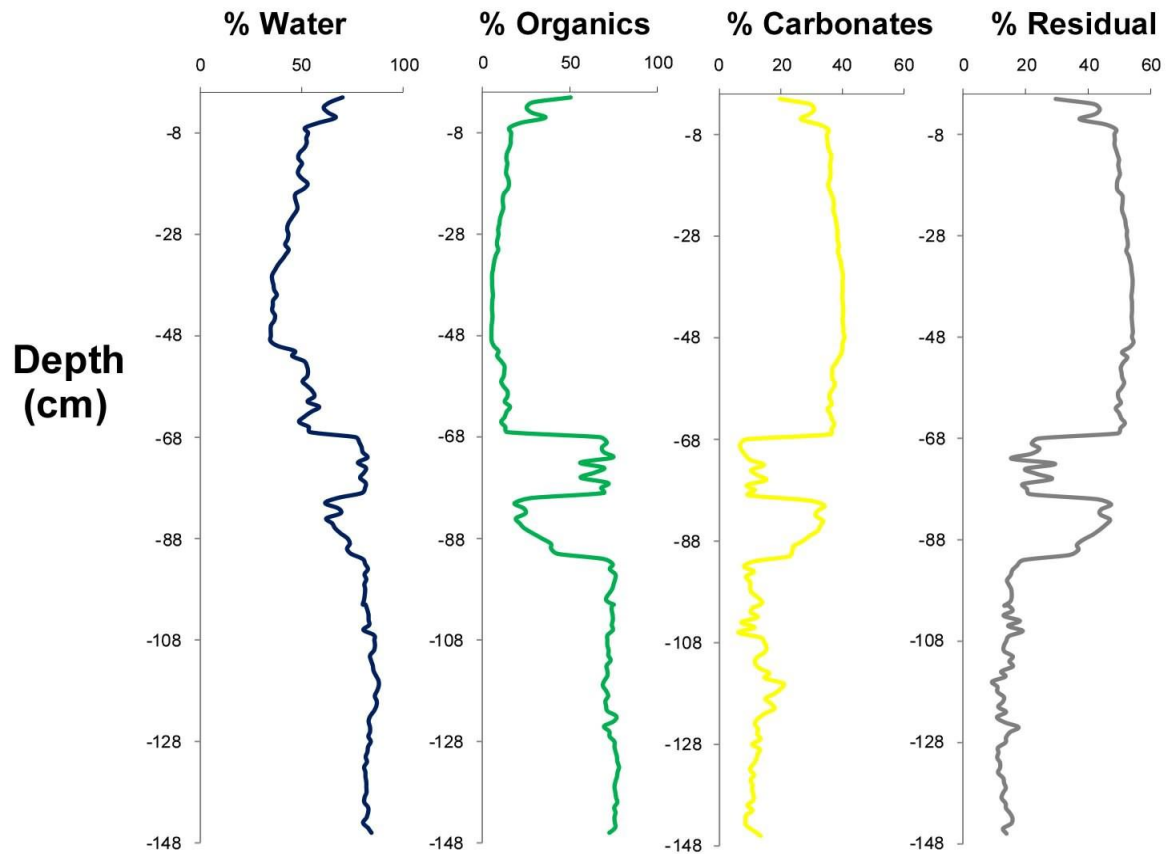
Blackbird Cay (BB)



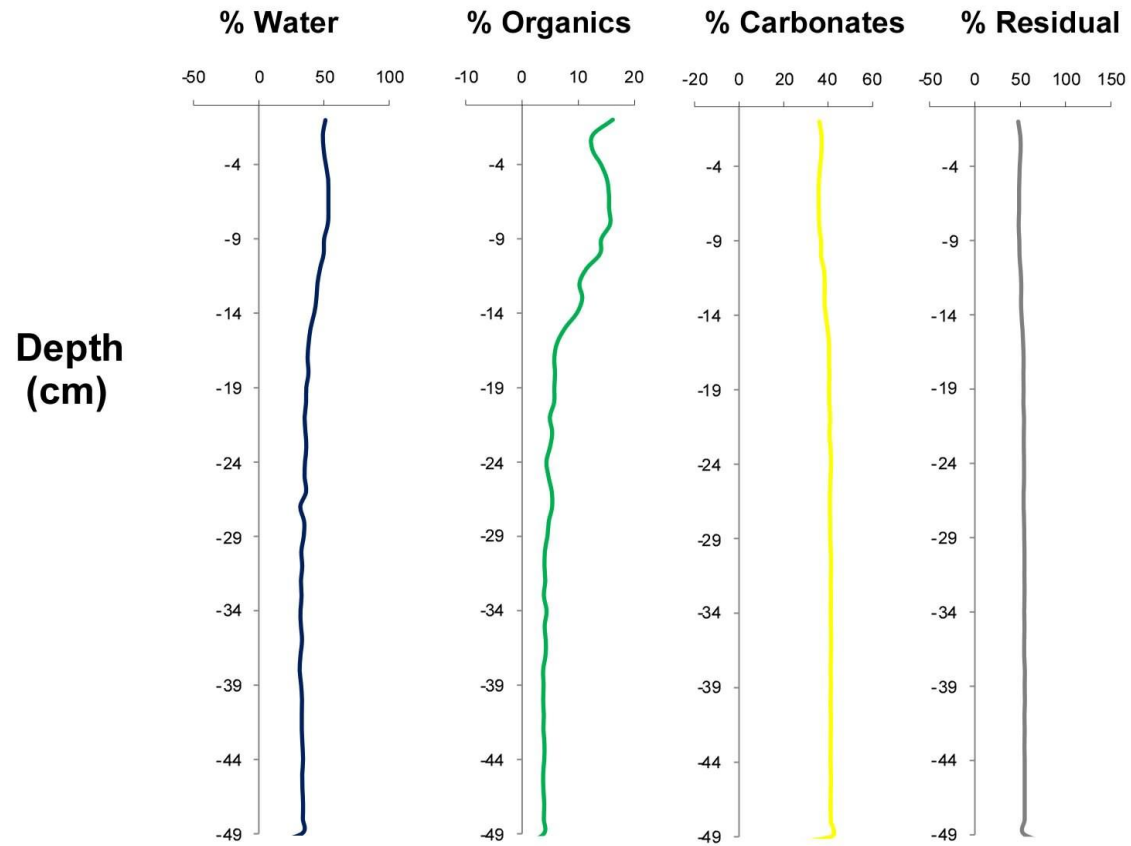
BB1



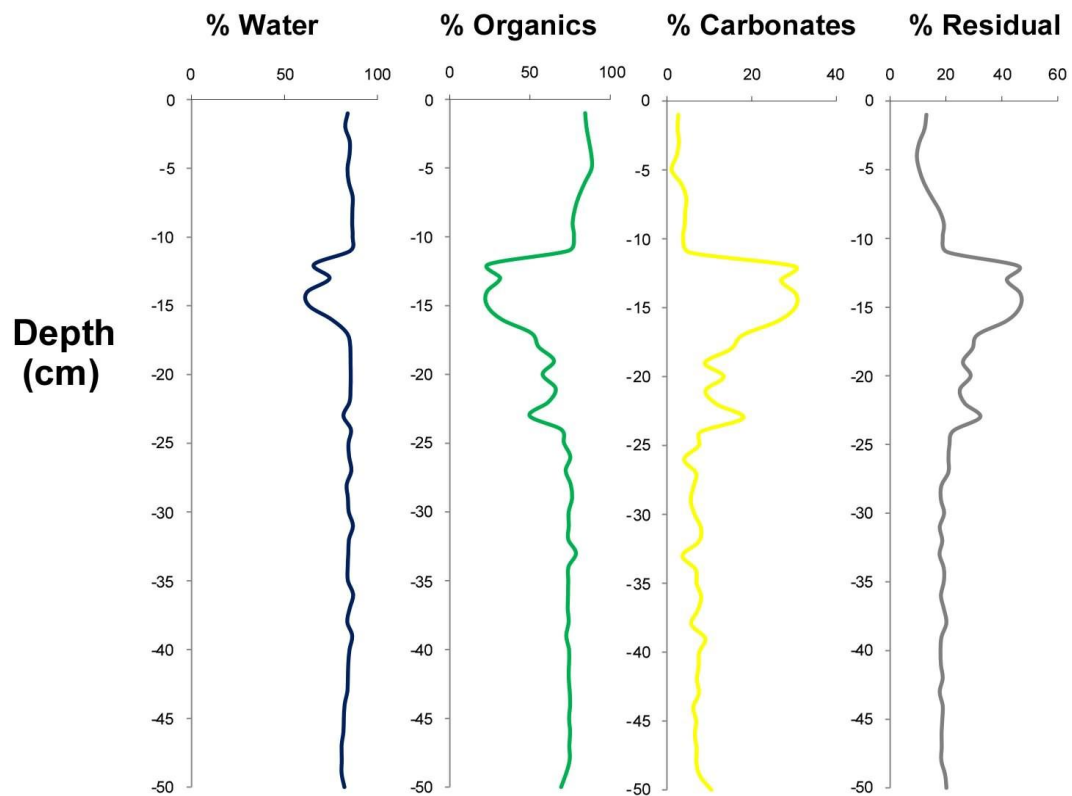
BB 2



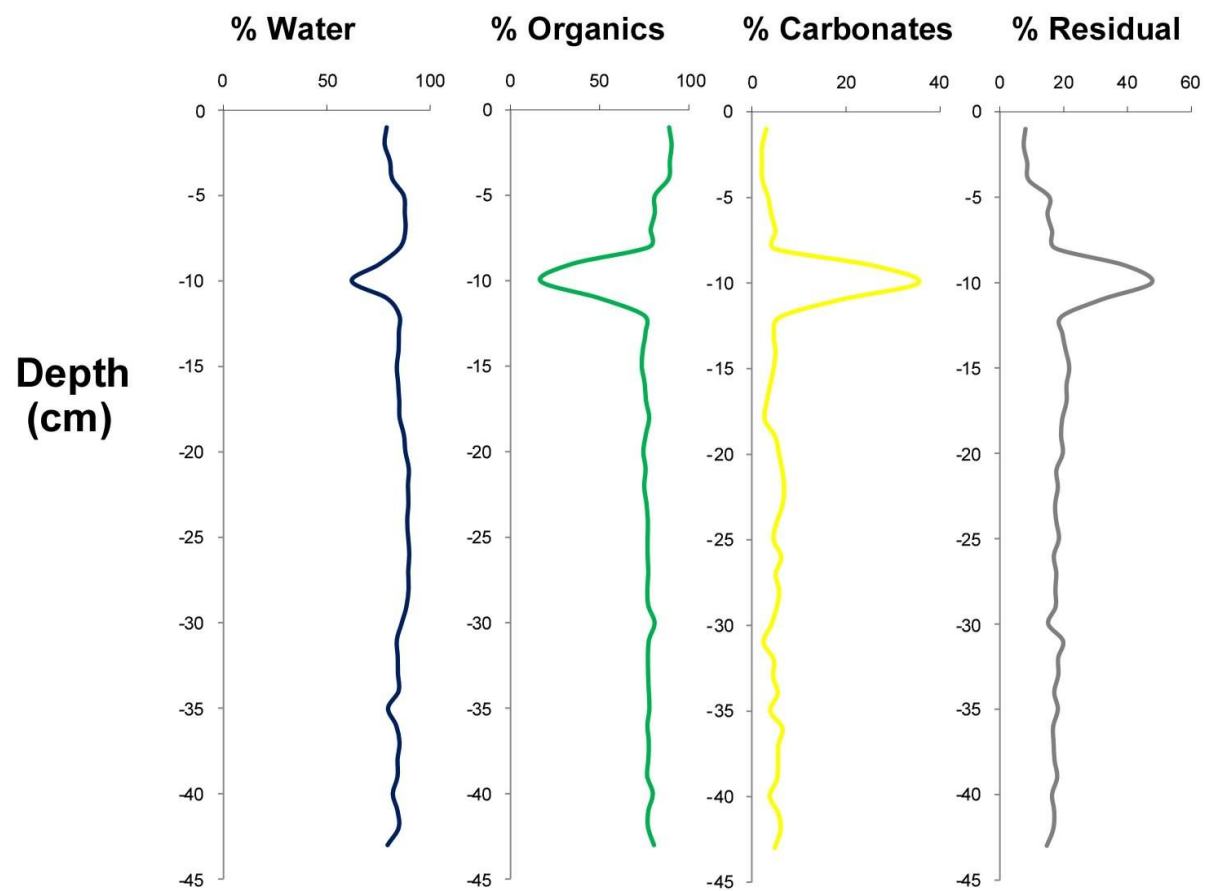
BB 3



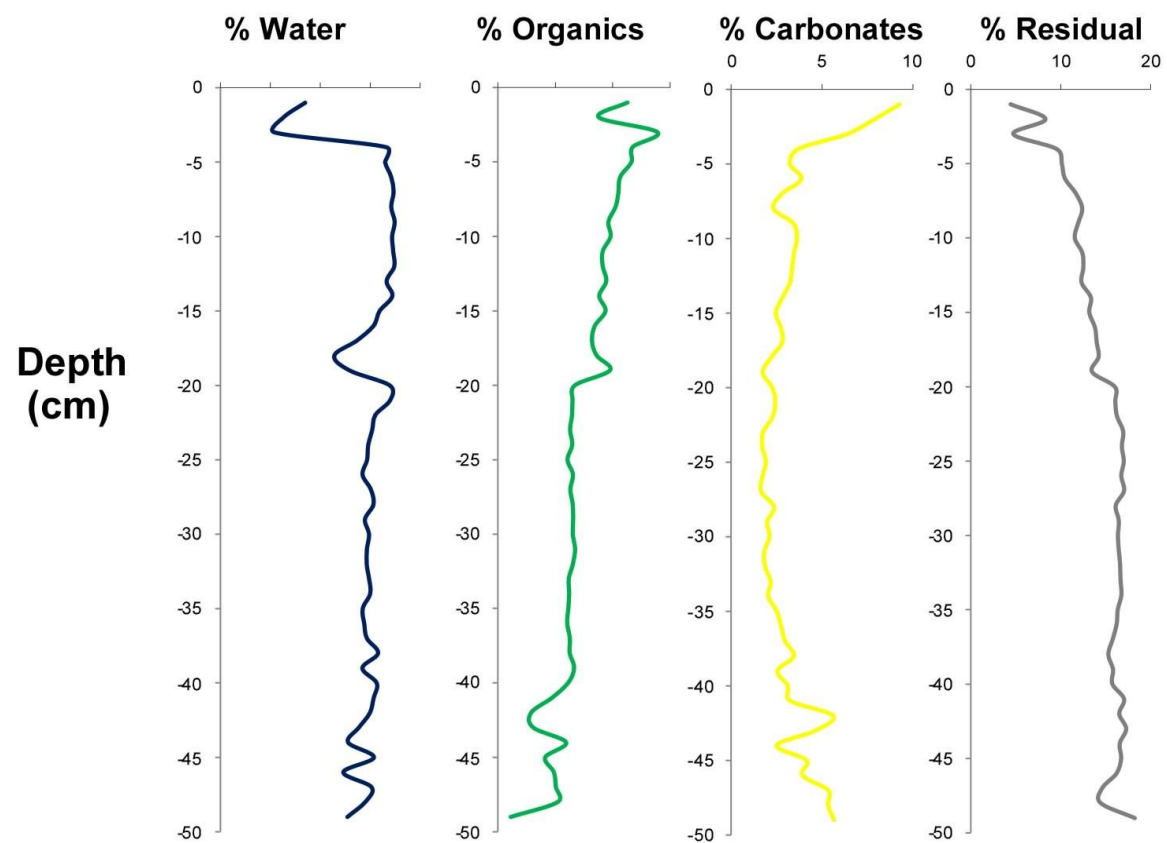
BB 4



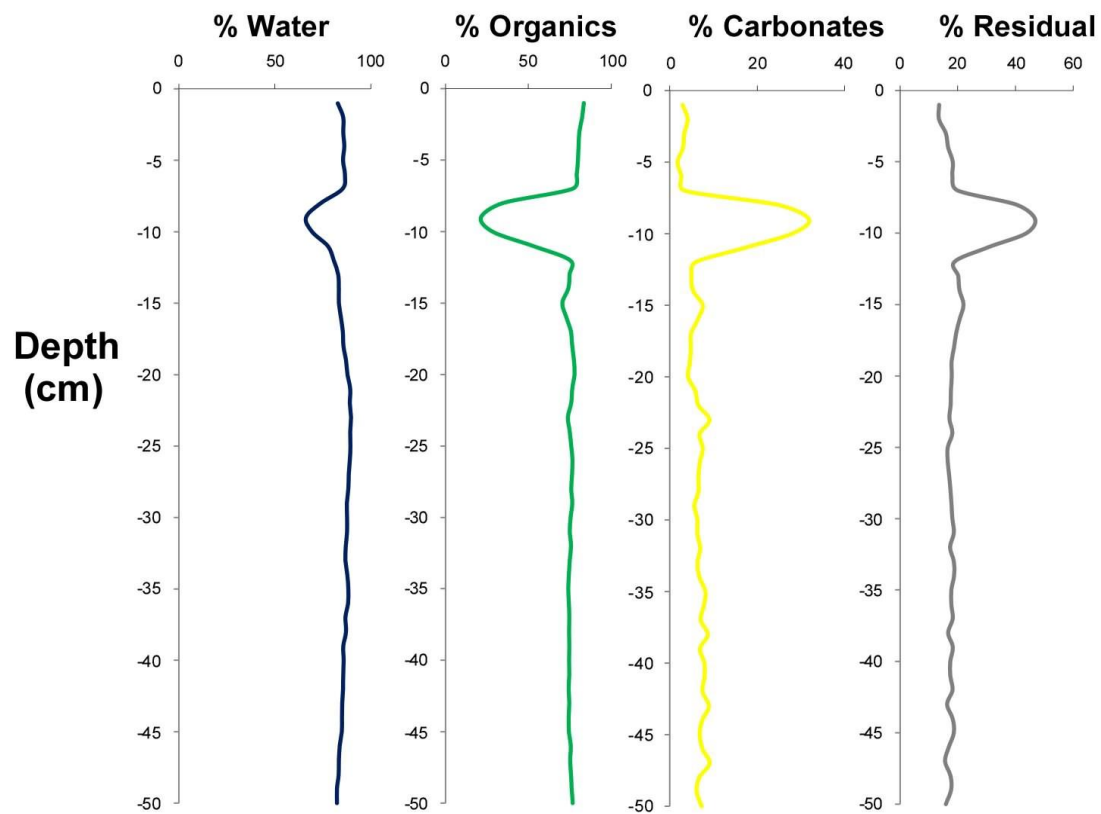
BB 5



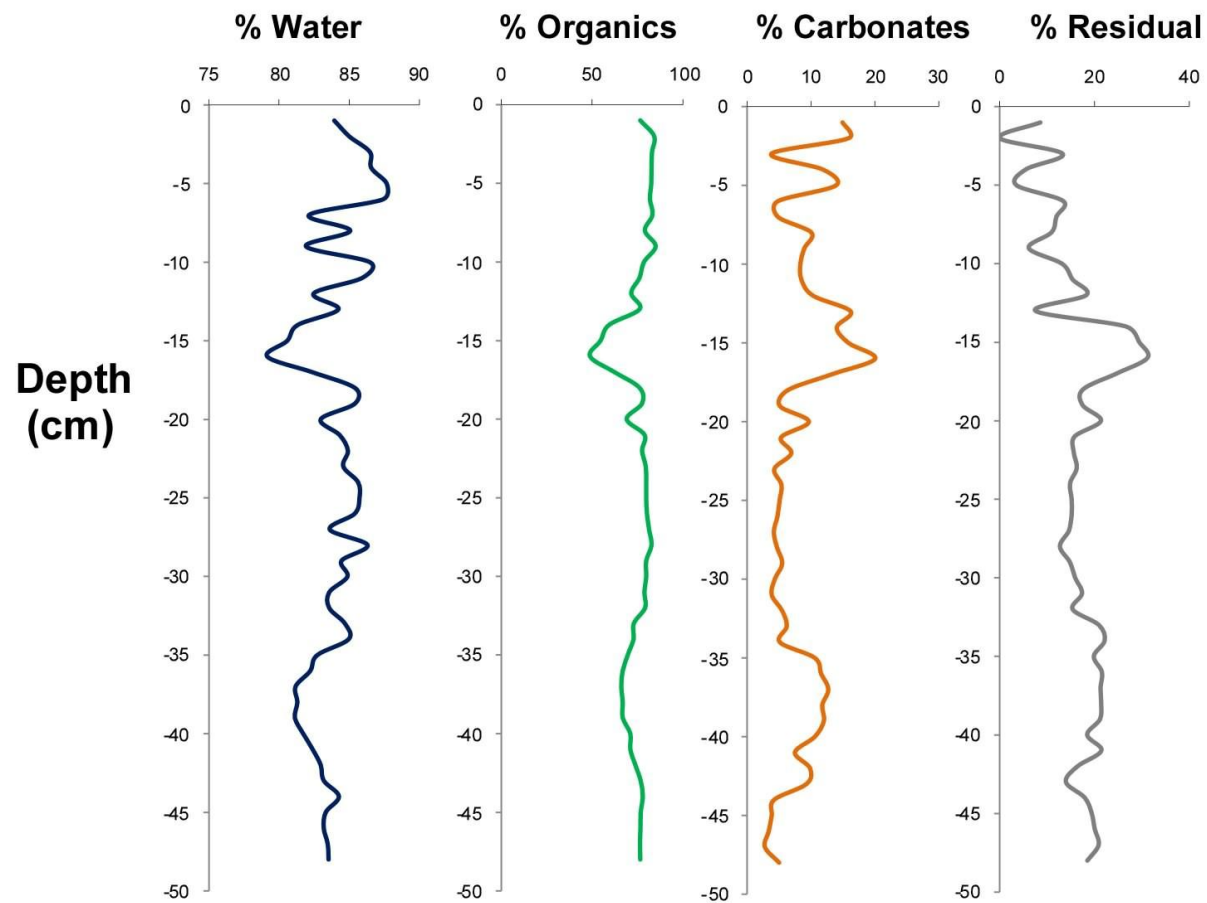
BB 6



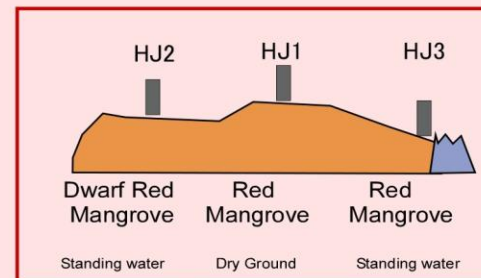
BB 7



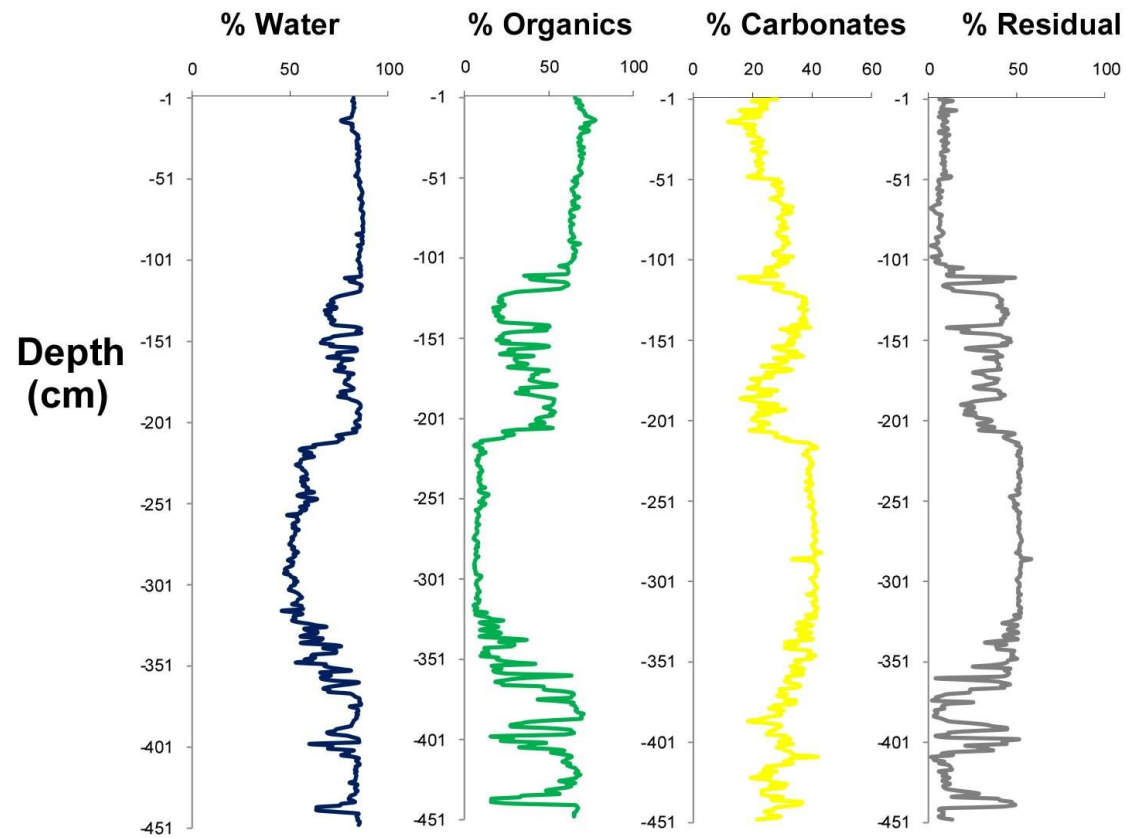
BB 10



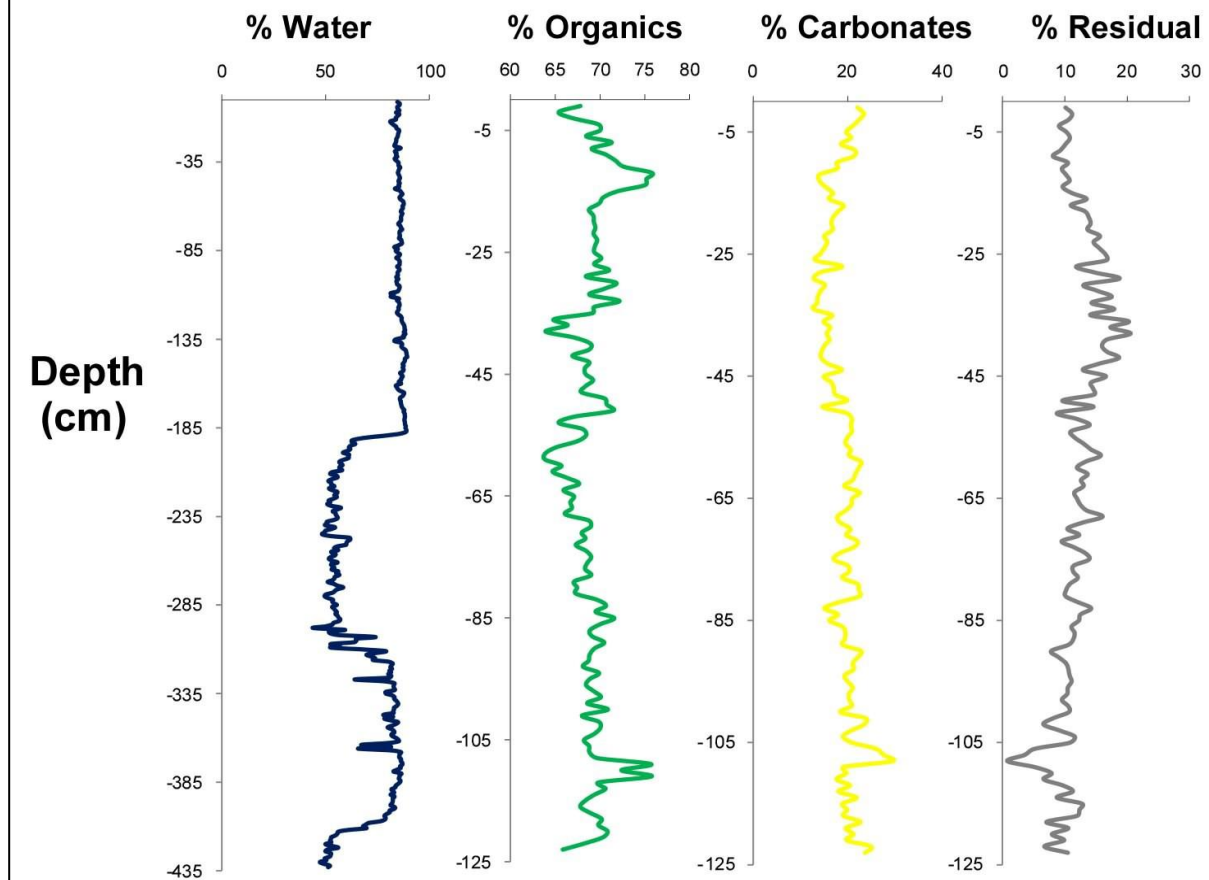
HJ Cay



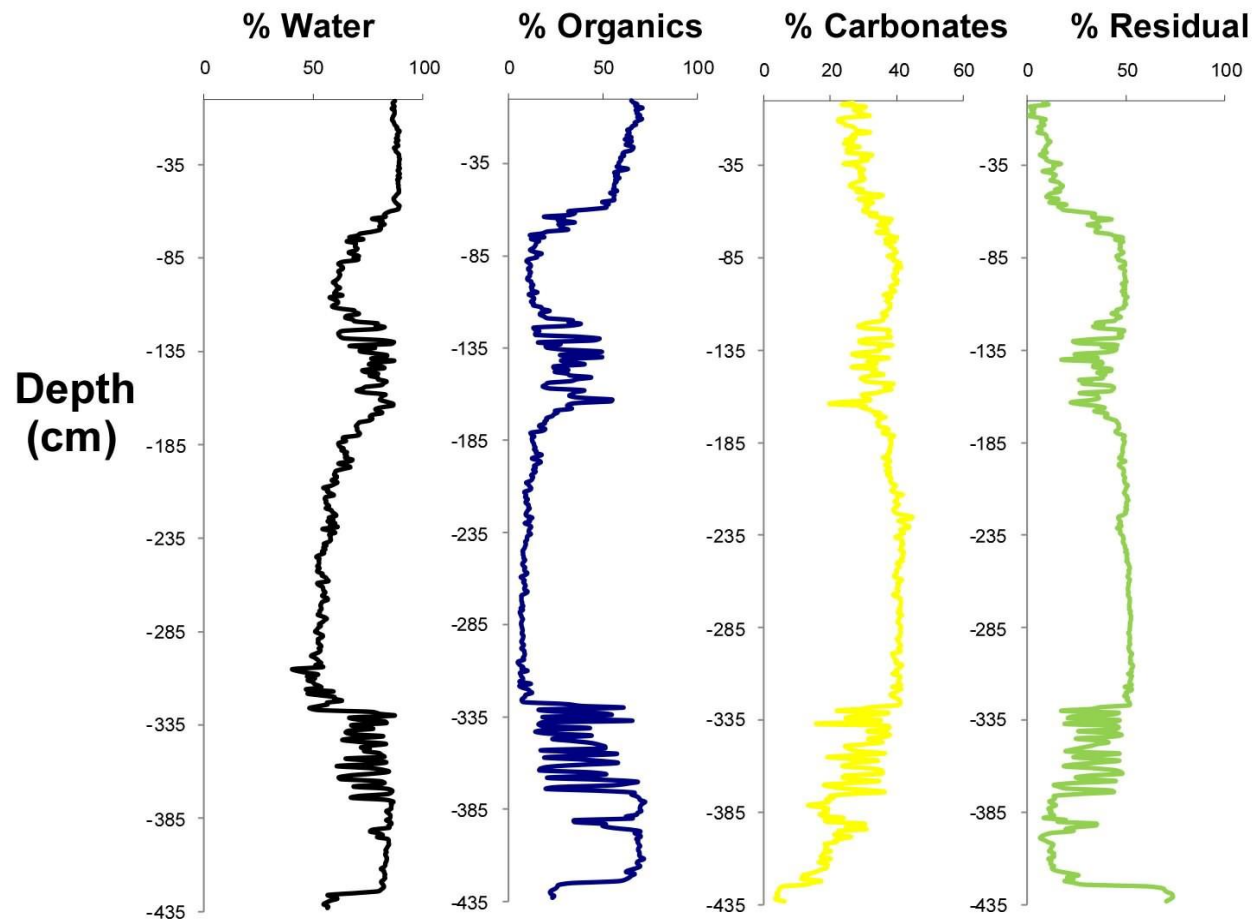
HJ 1



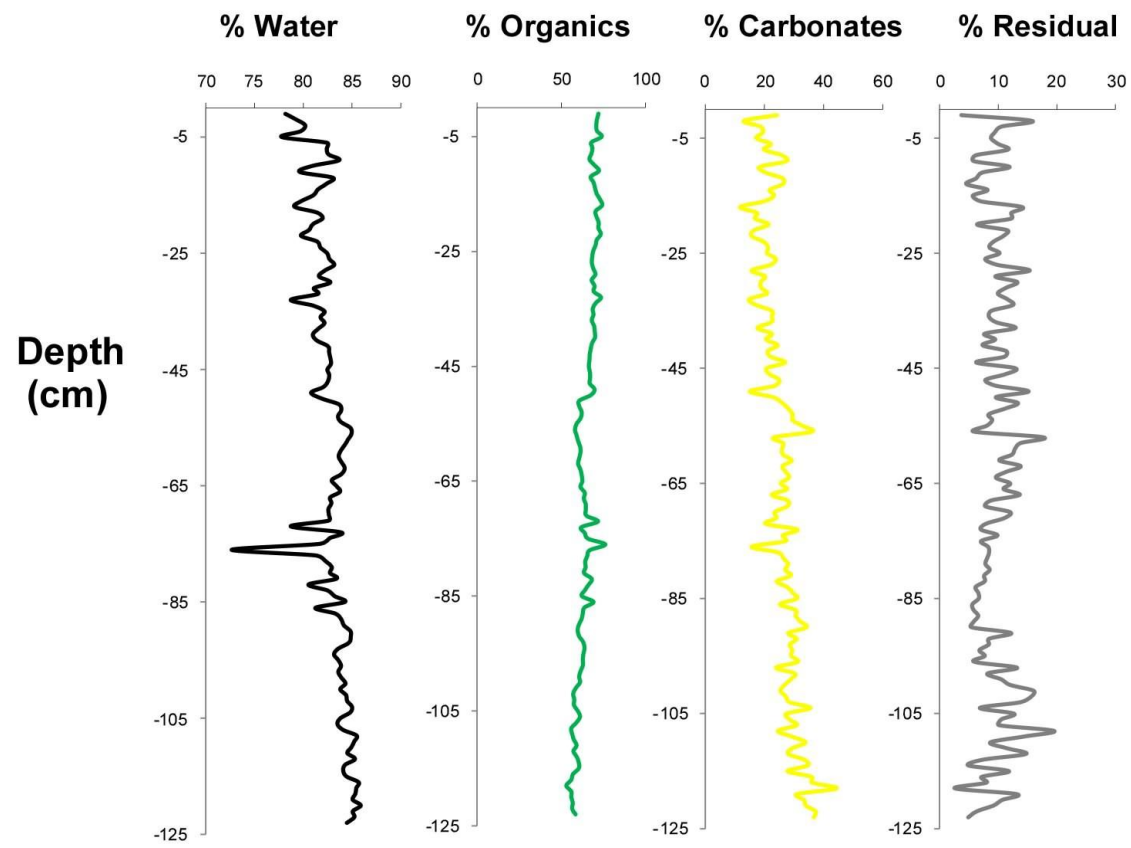
HJ 2



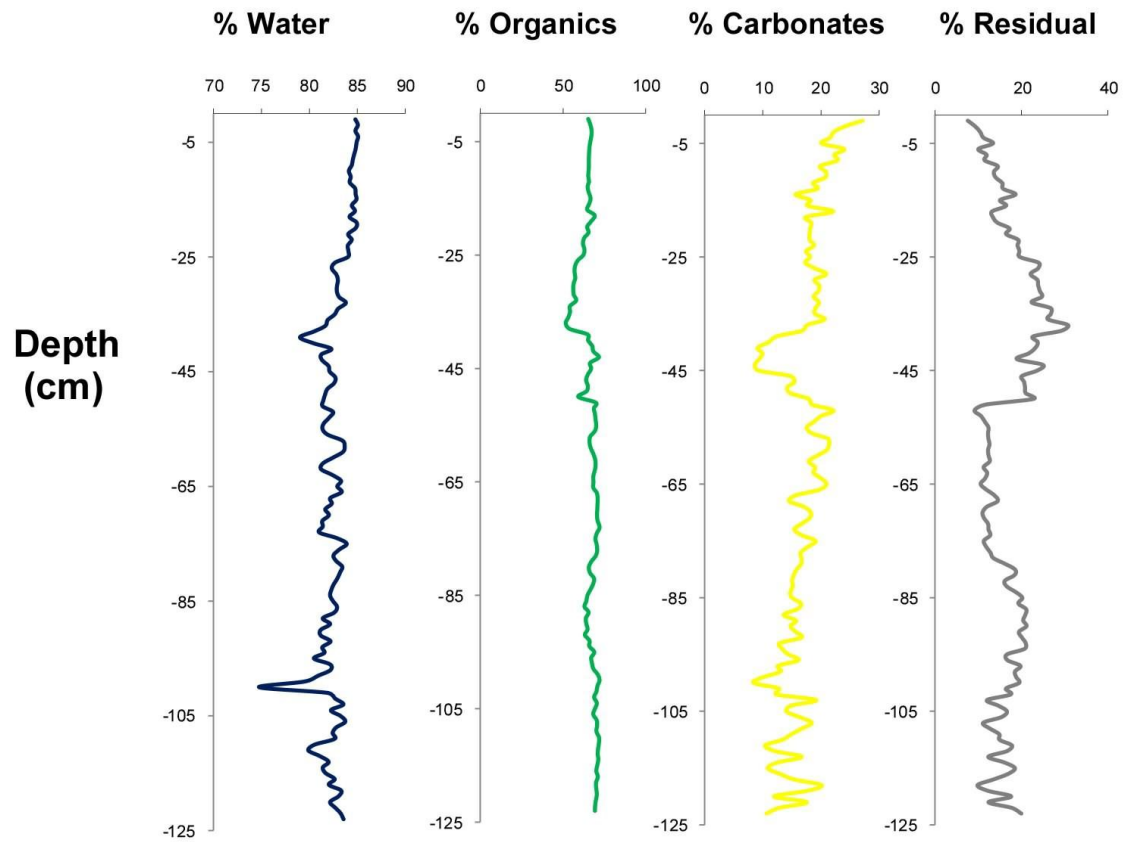
HJ 3



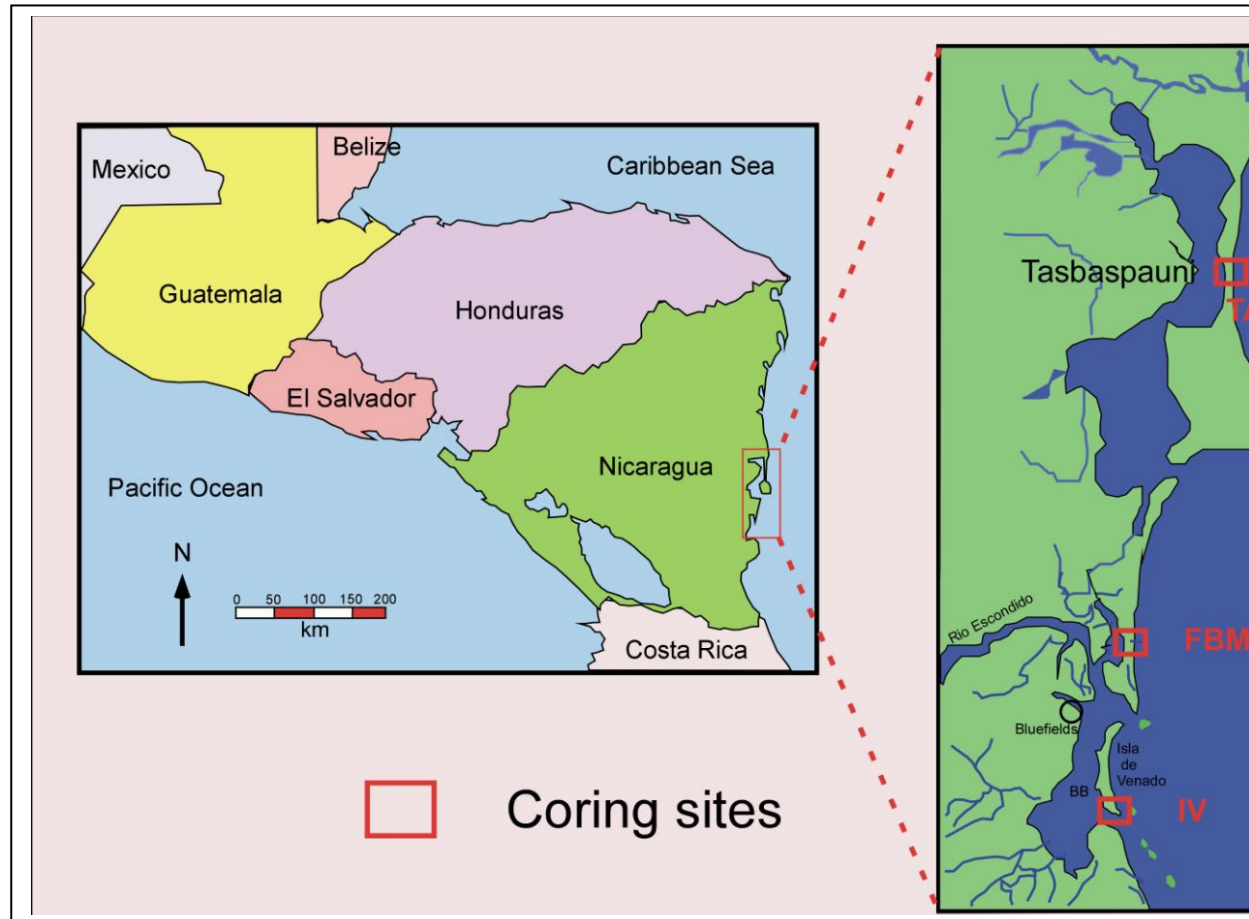
CC 1

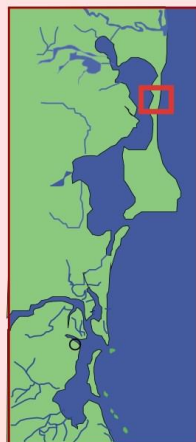


DM 1



A.2 NICARAGUA

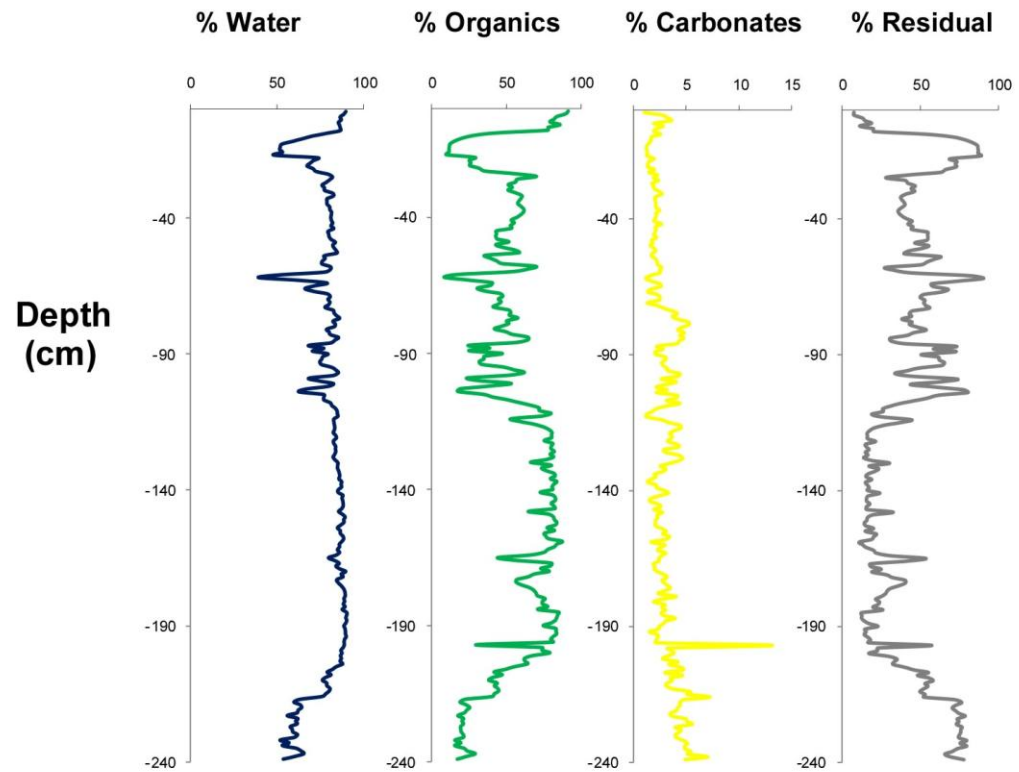




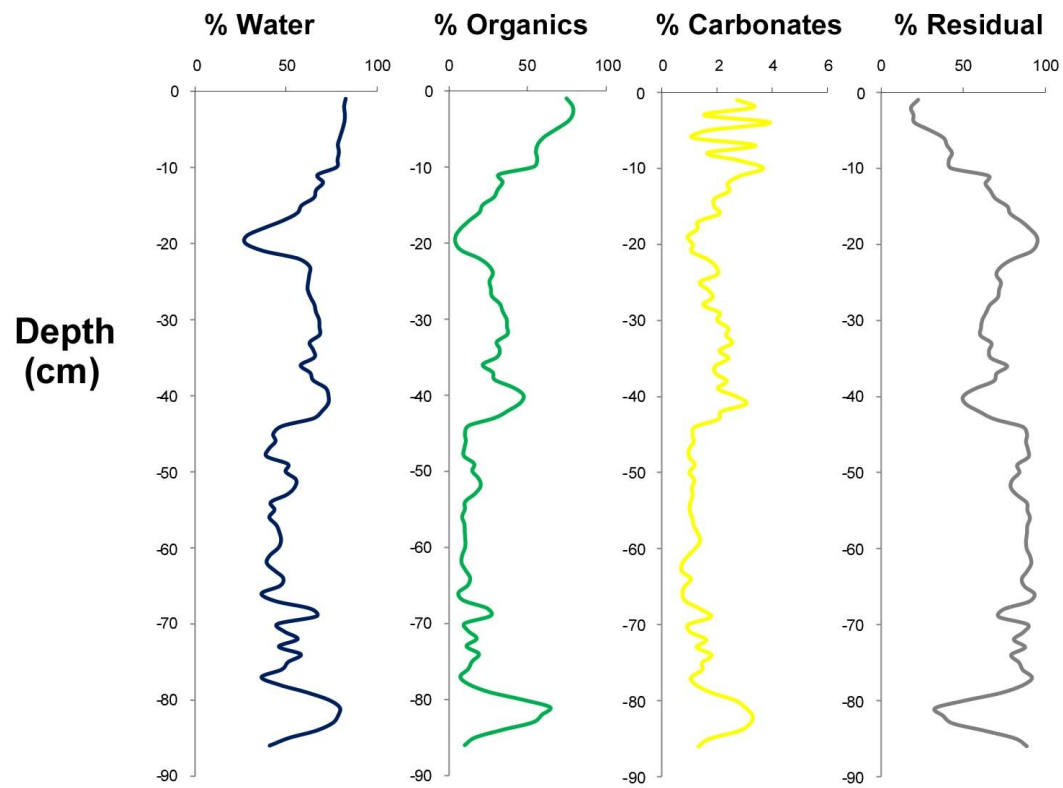
TASBAPAUNI NORTH (TASN)



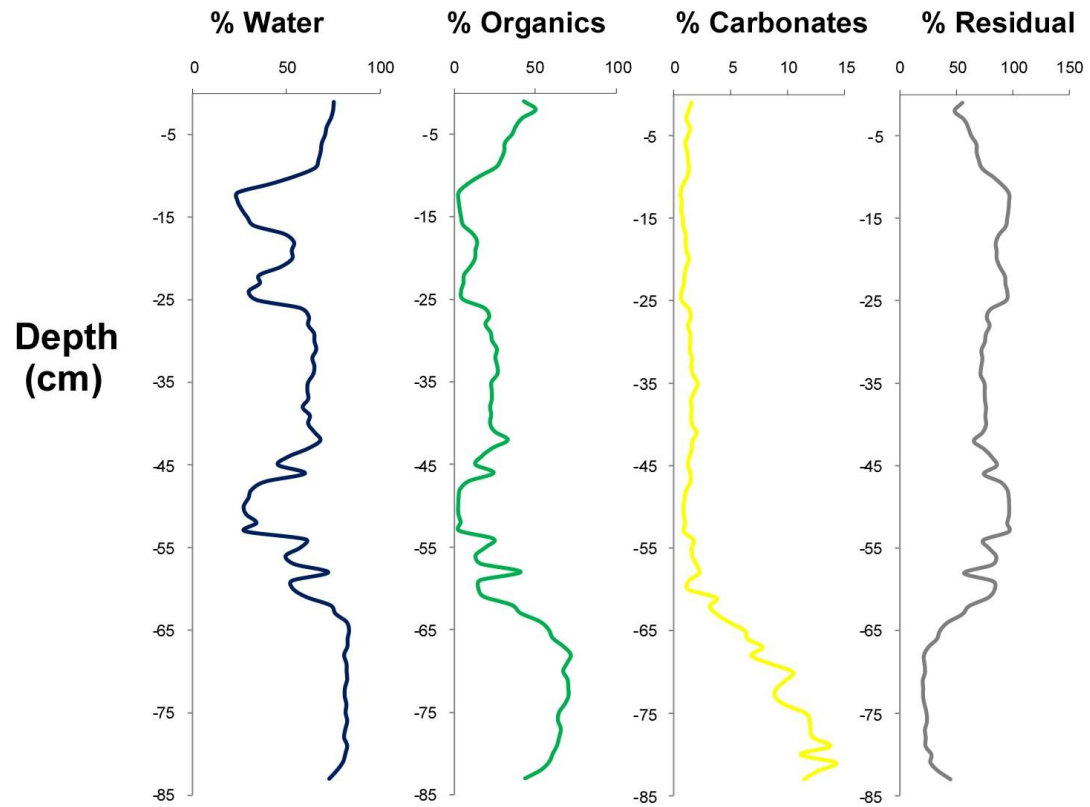
TASN 1



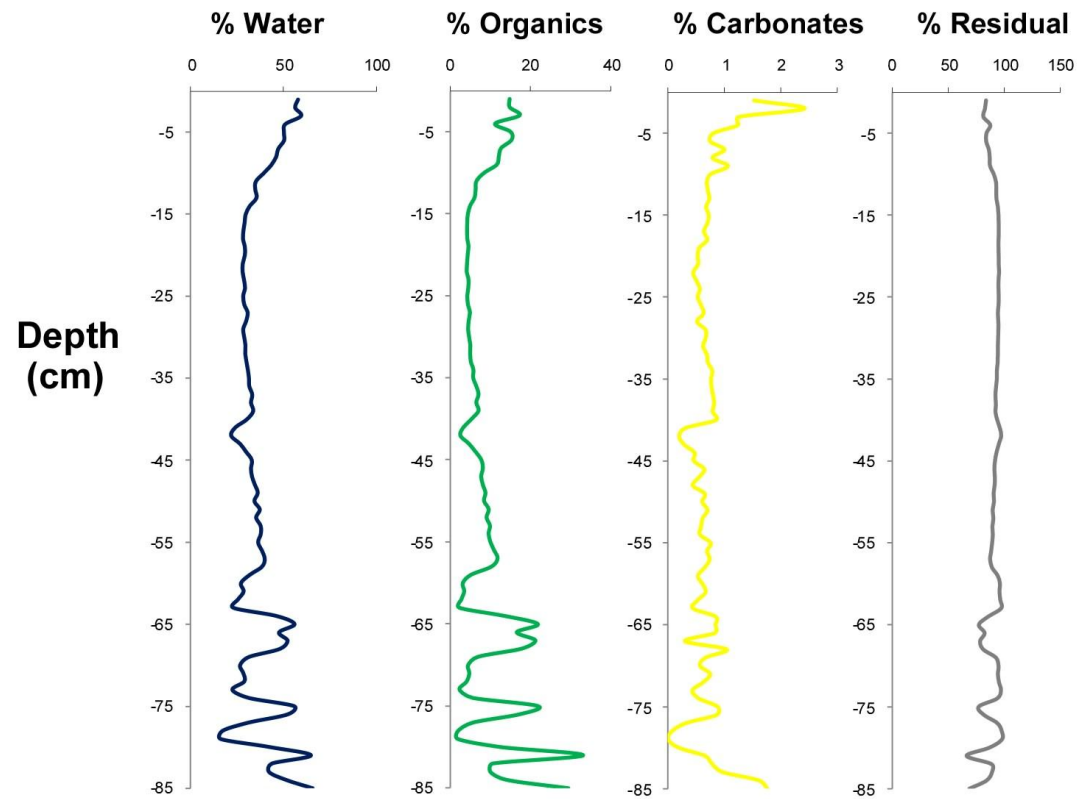
TASN 3



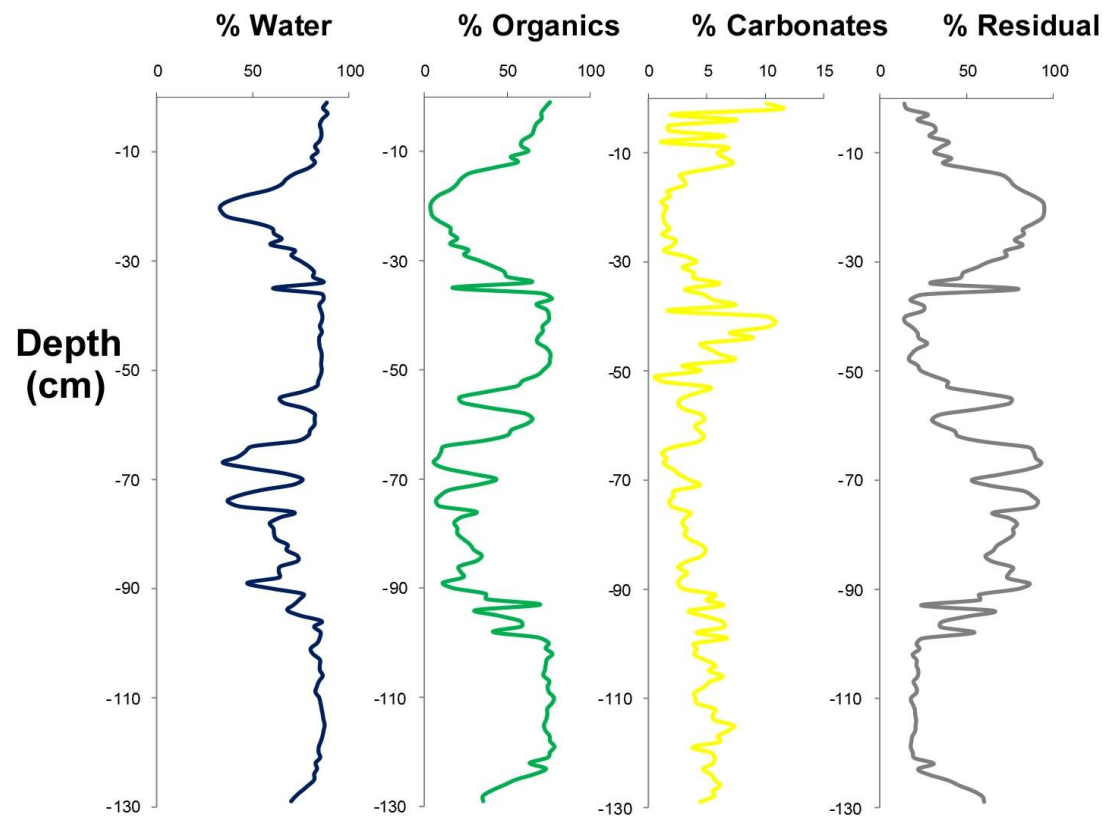
TASN 4



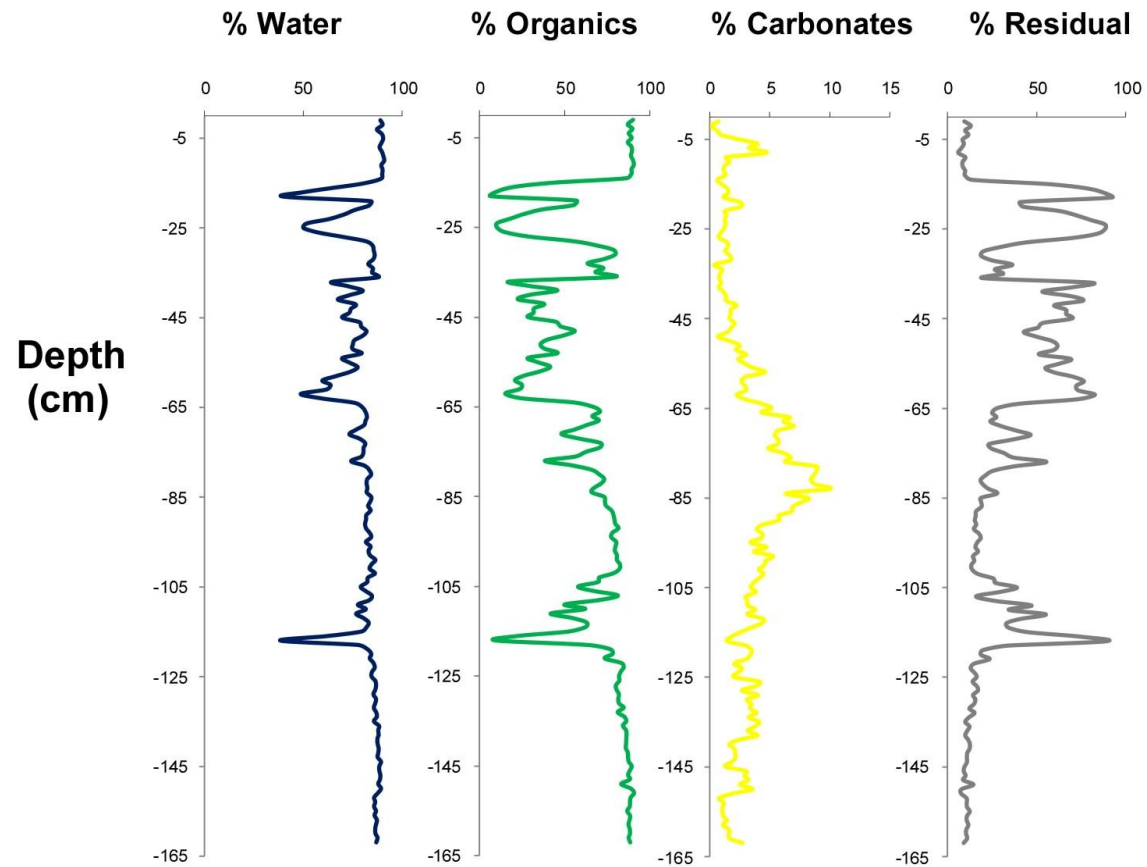
TASN 5



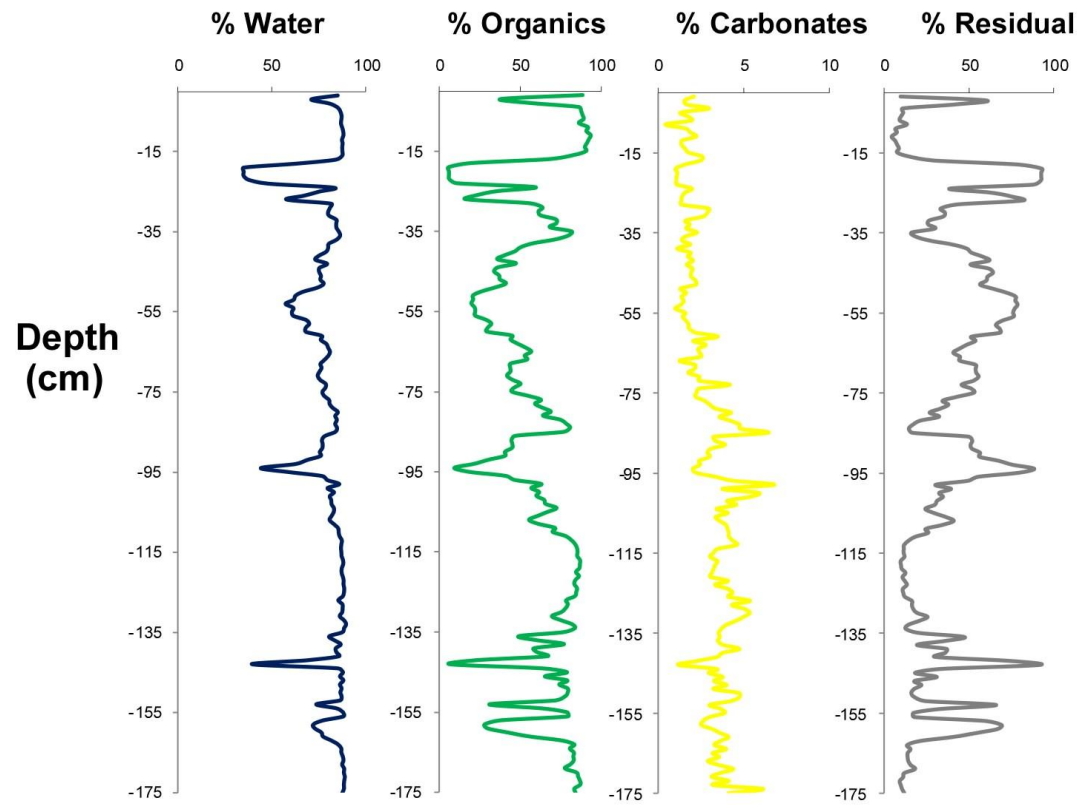
TASN 6



TASN 7



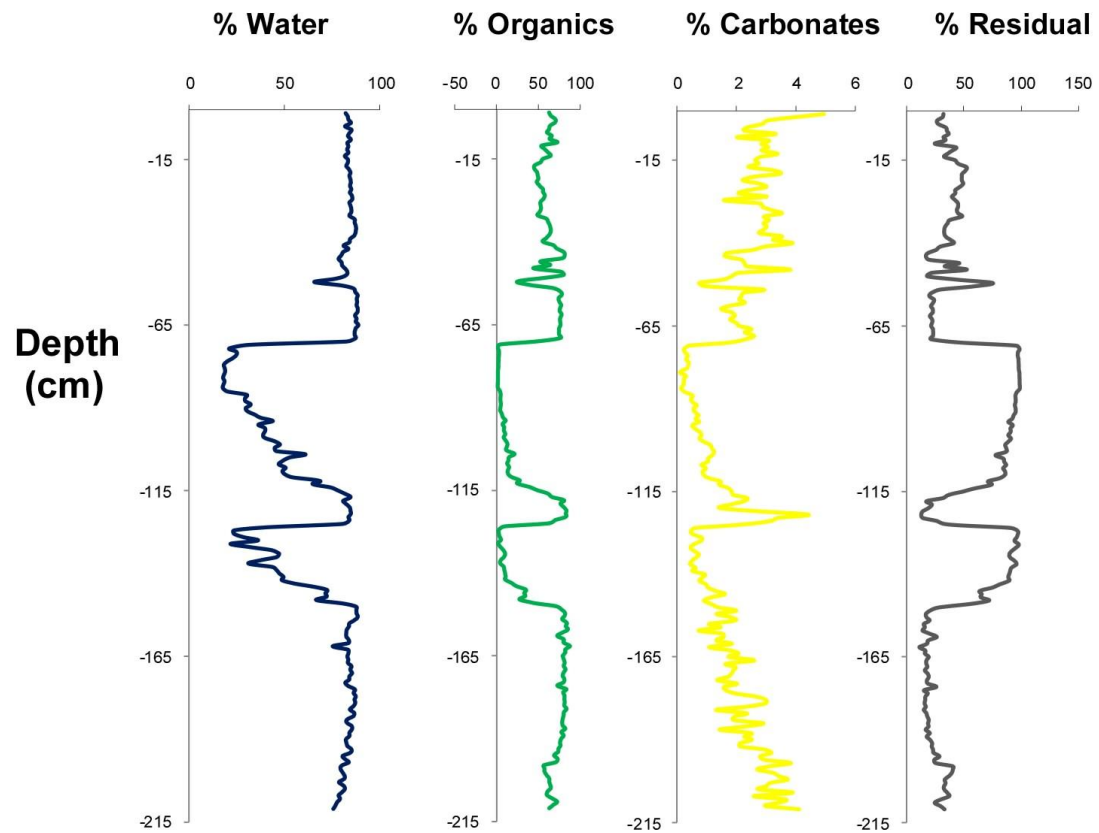
TASN 8



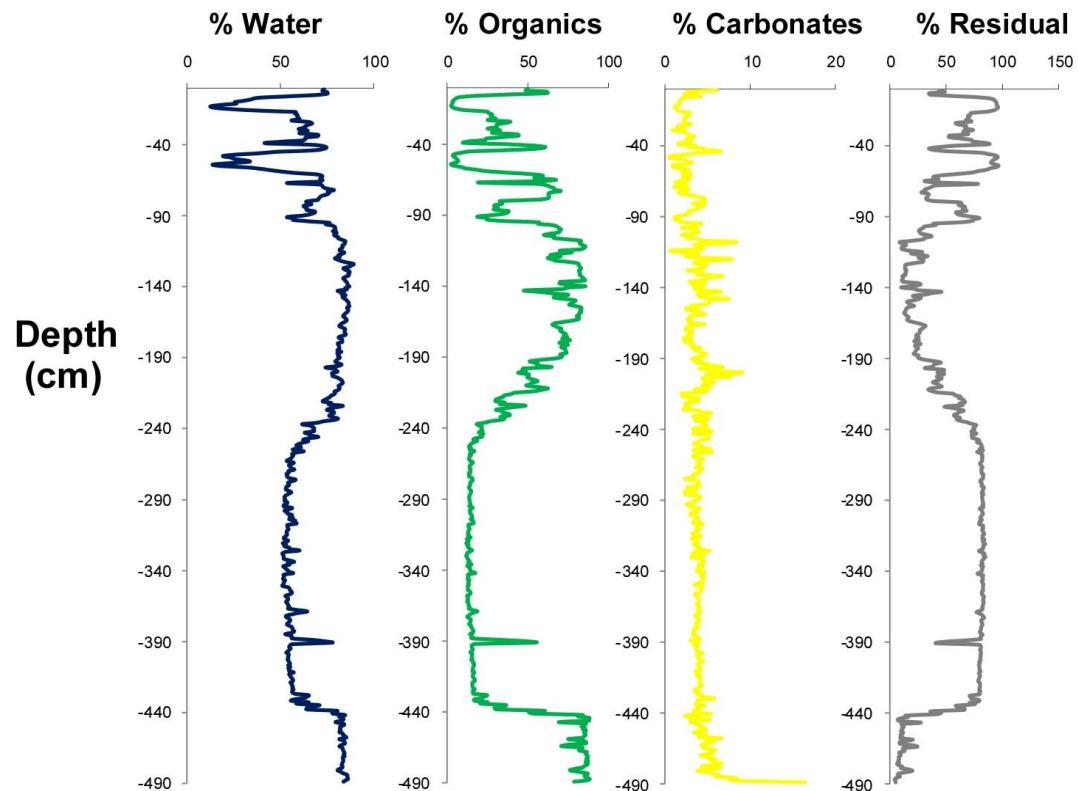
Falso Bluff Marsh (FBM)



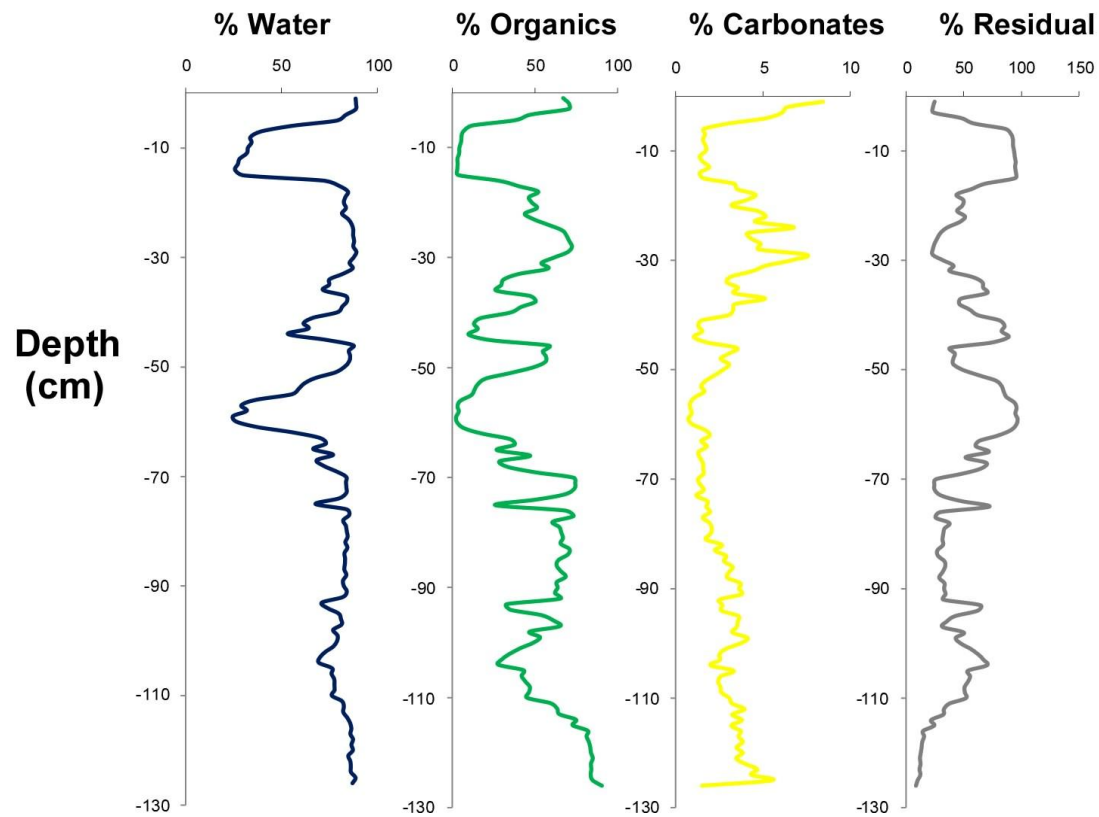
FBB 1



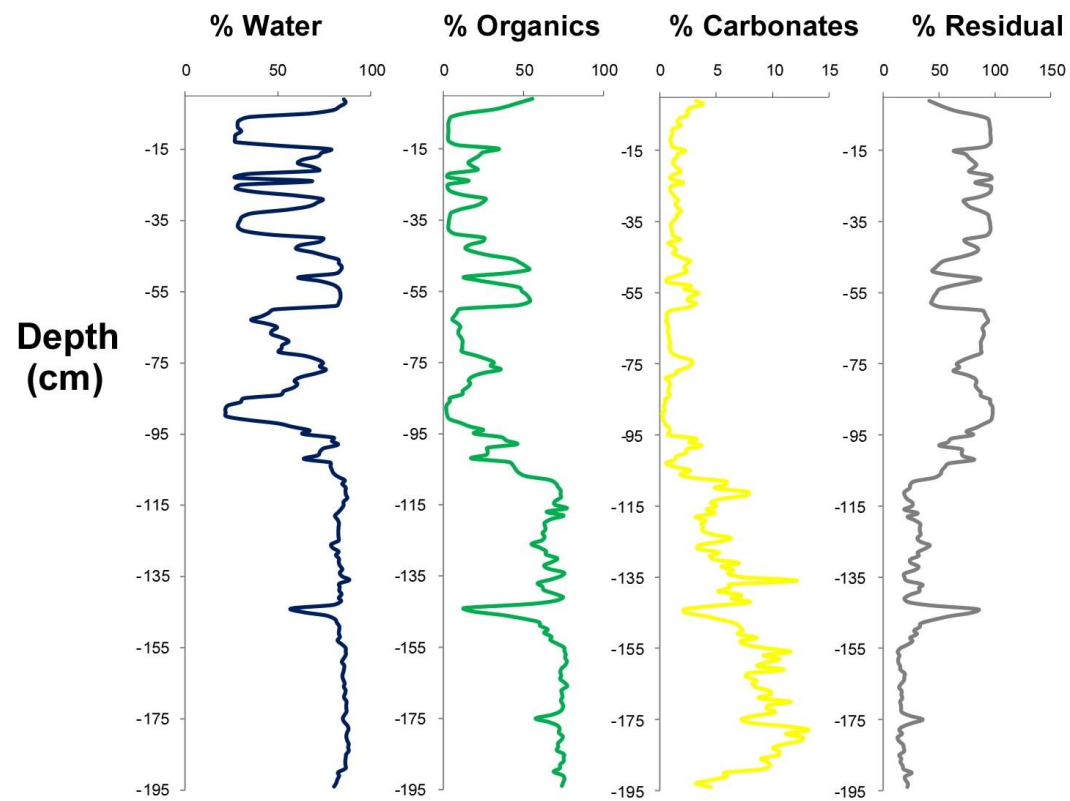
FBM 1



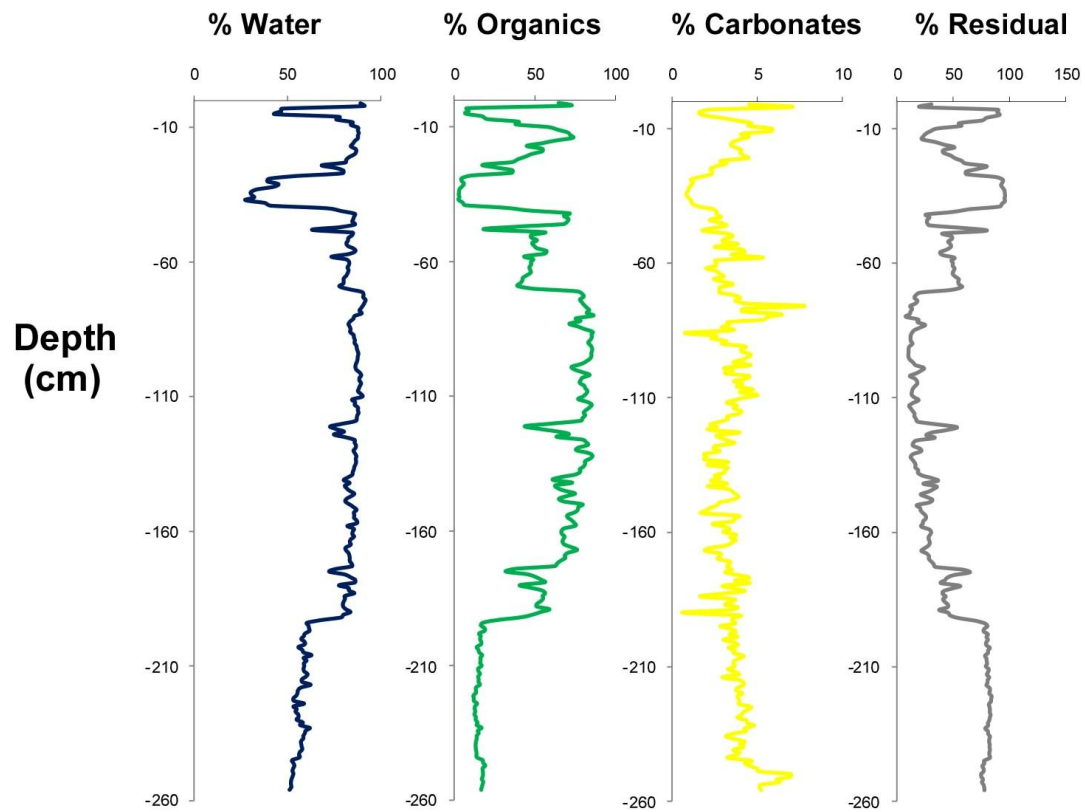
FBM 2



FBM 4



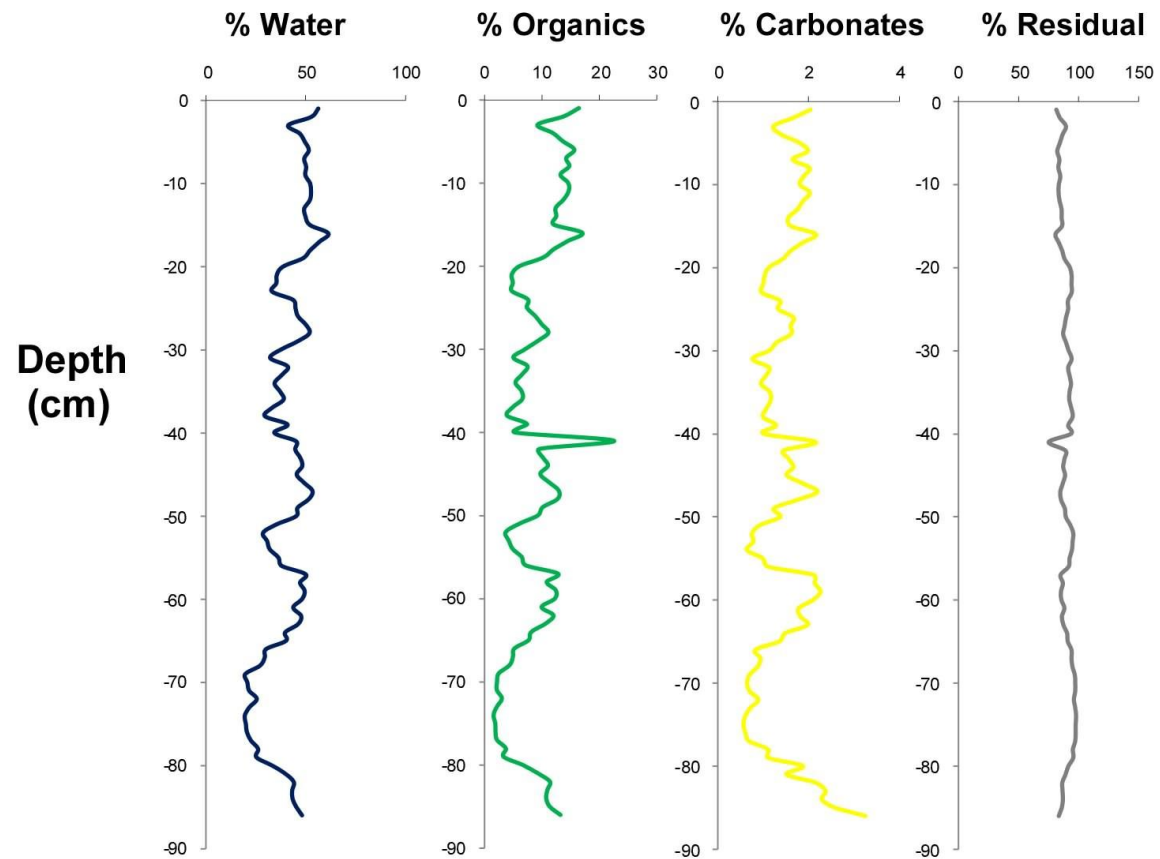
FBM 5



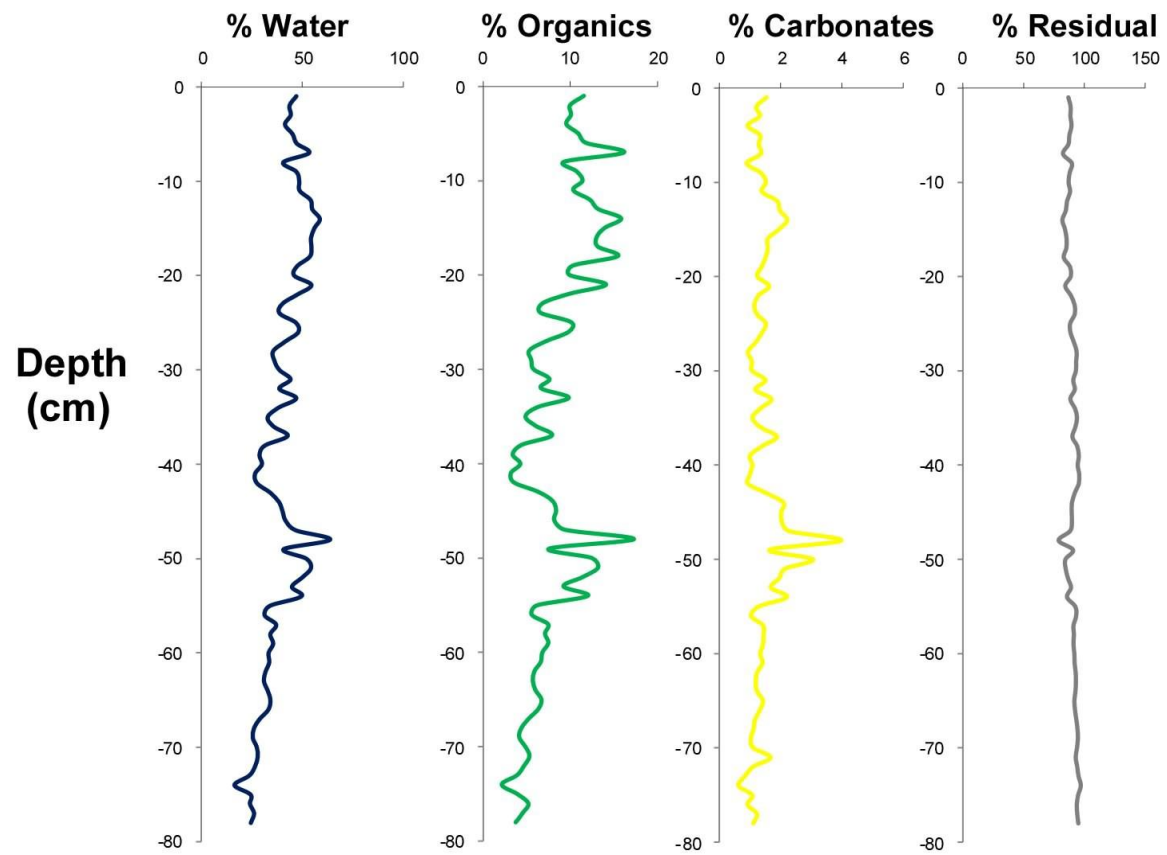
Isla de Venado (IV)



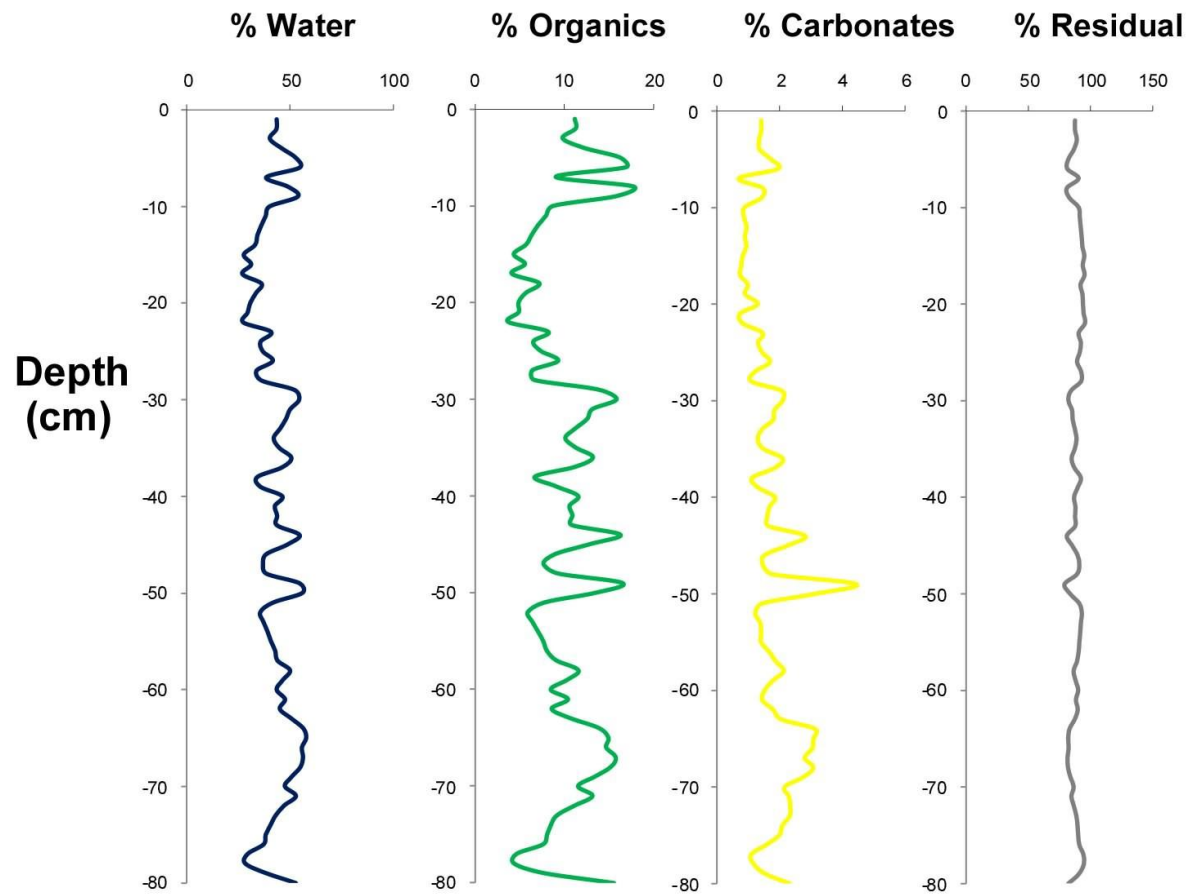
IV 1



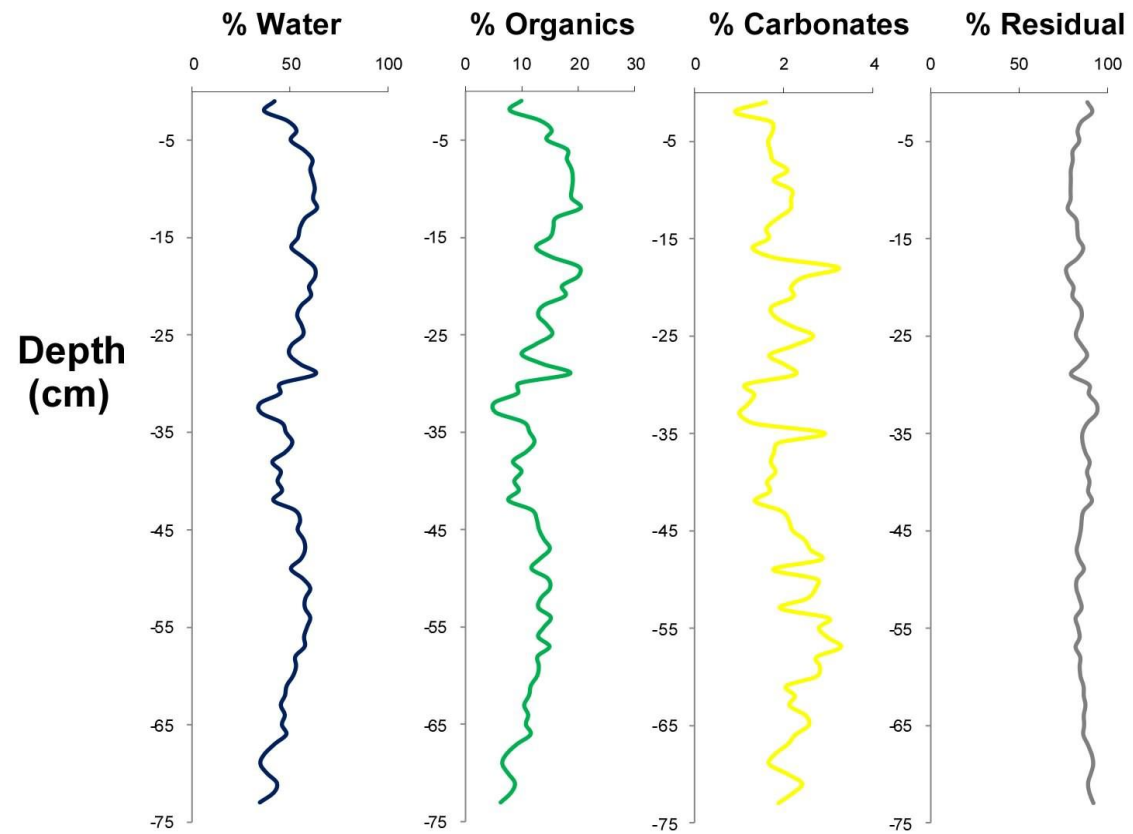
IV 2



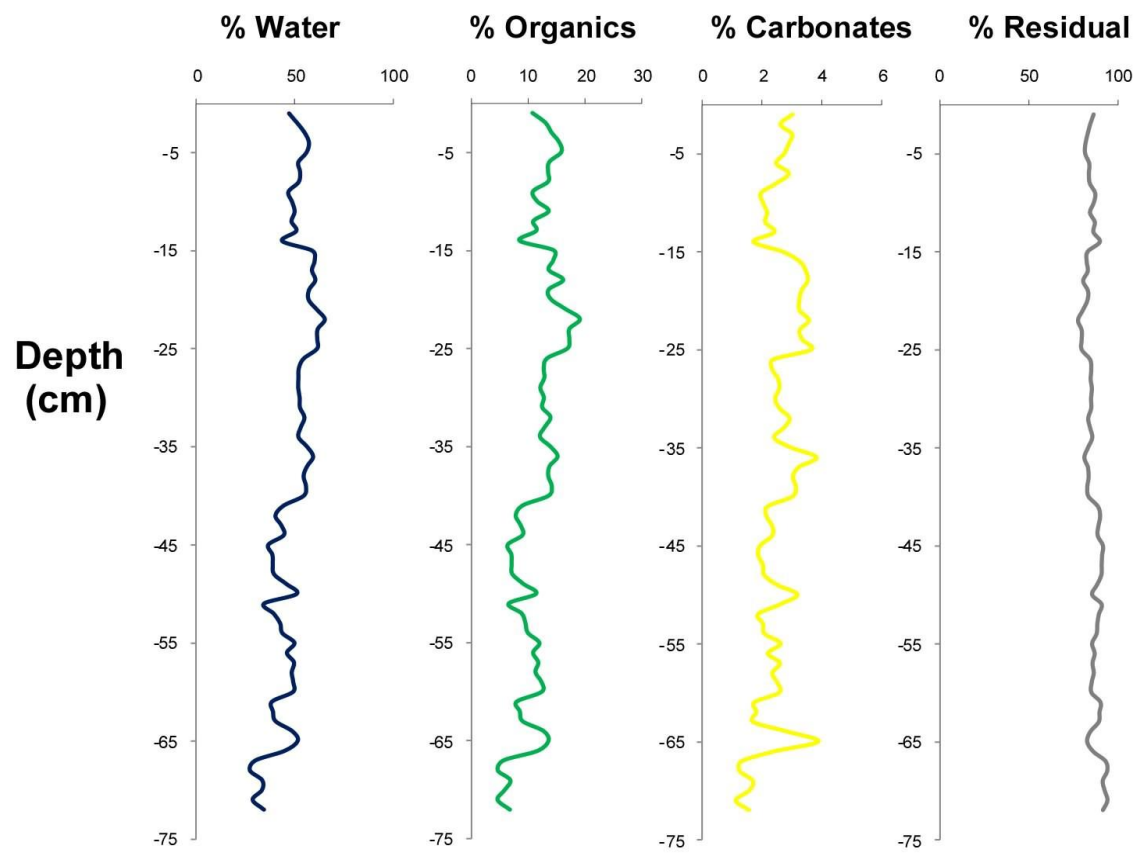
IV 3



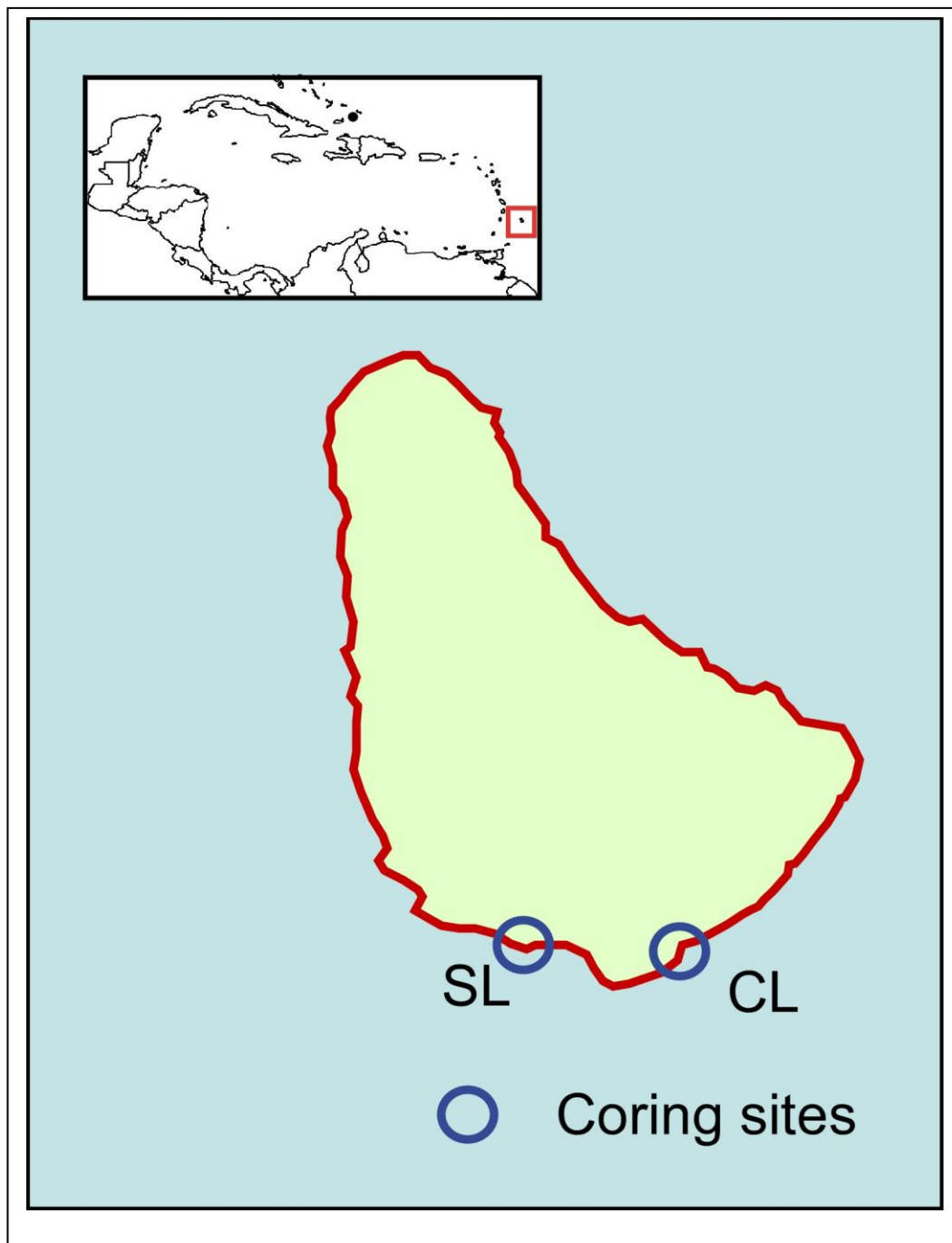
IV 4

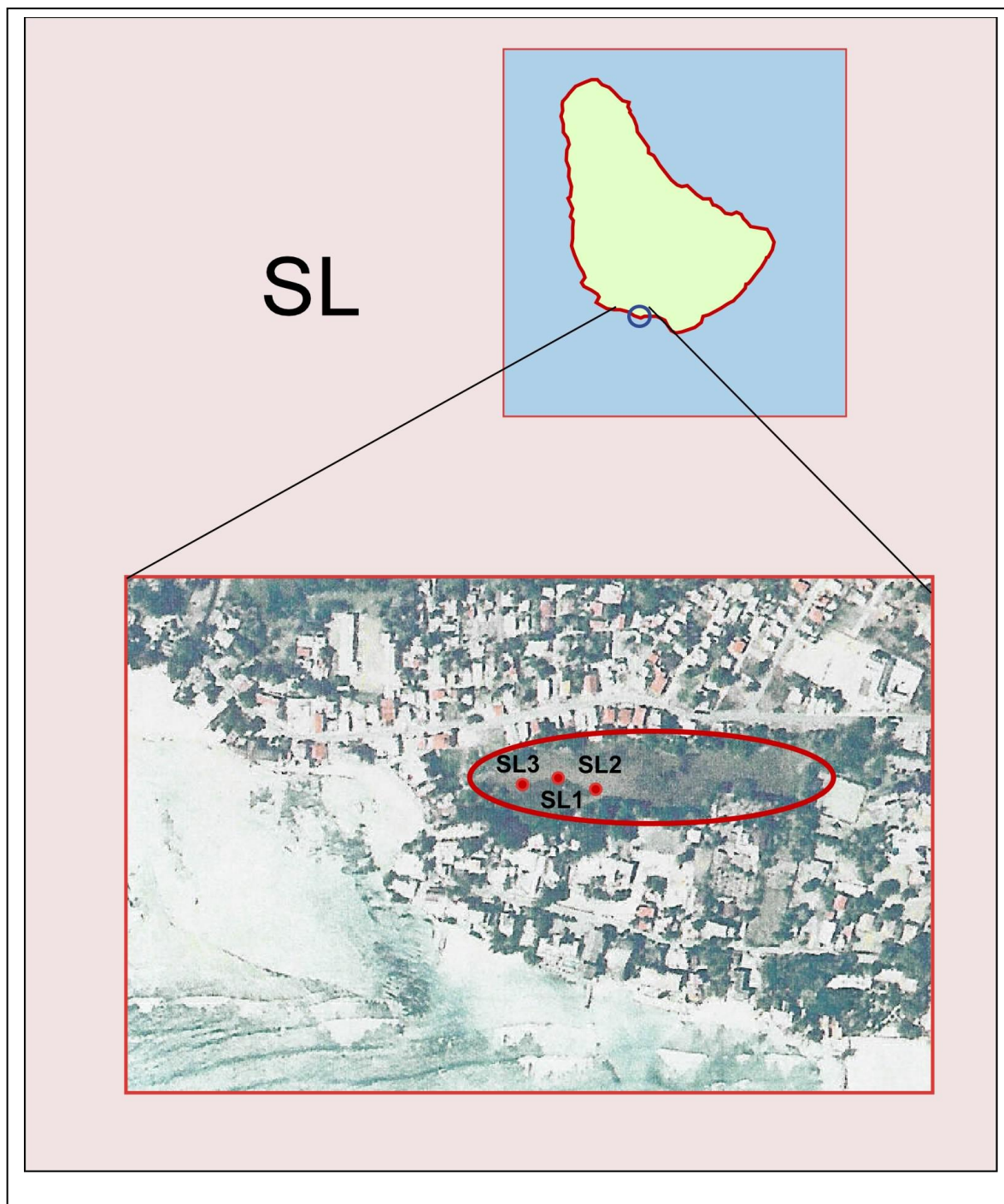


IV 5

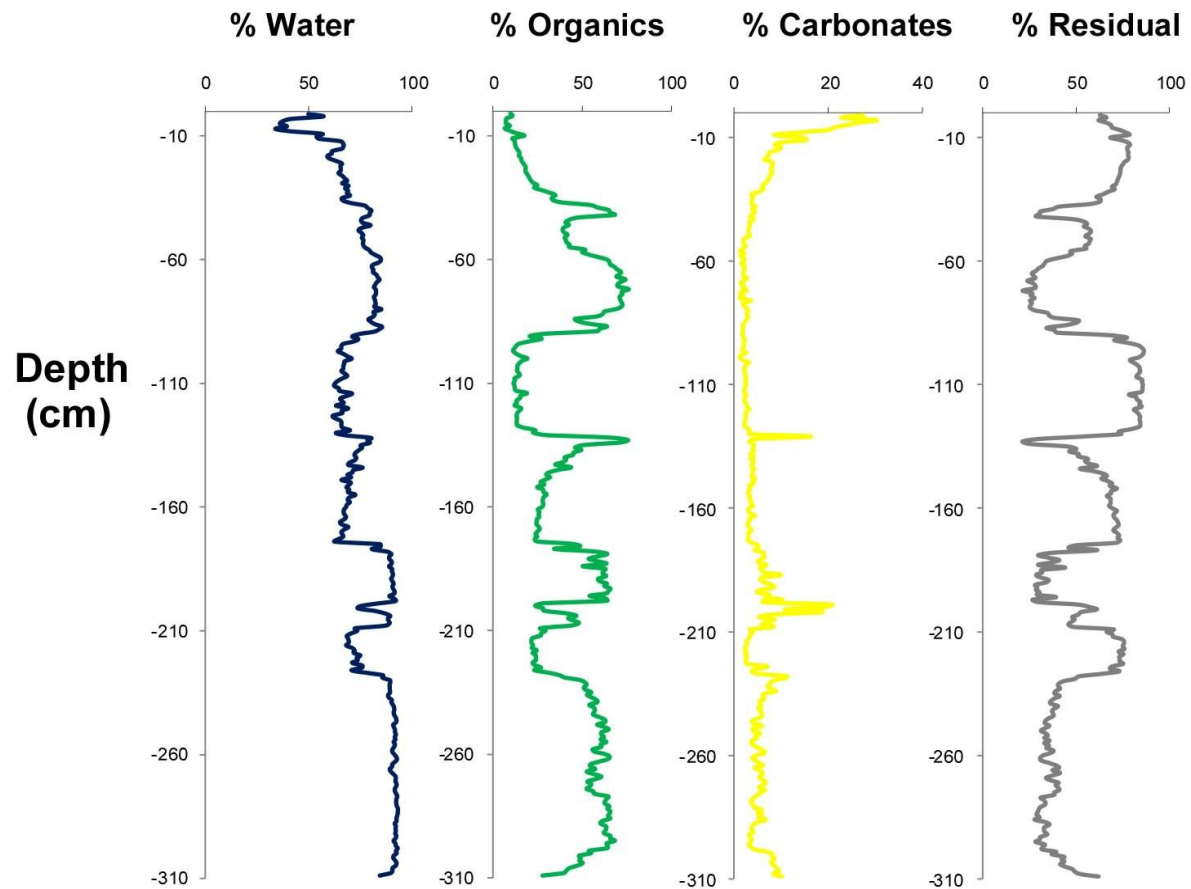


A.3 BARBADOS

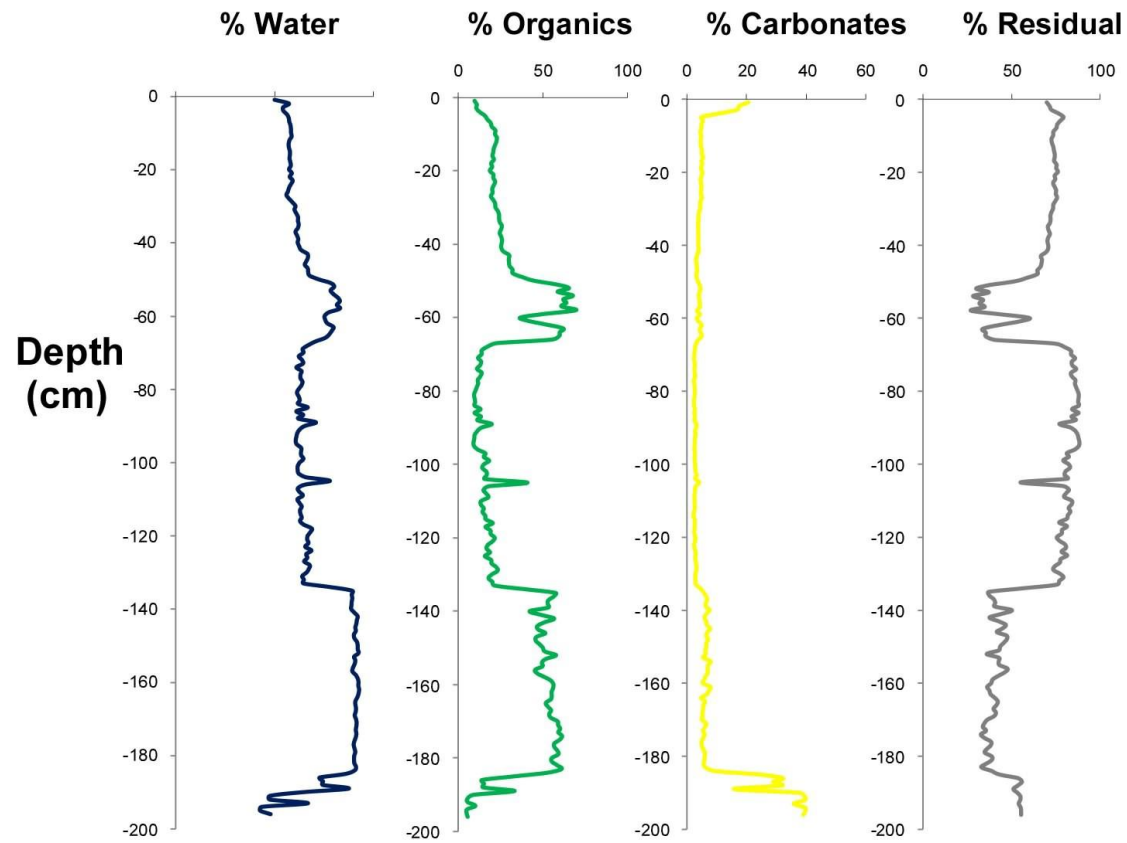




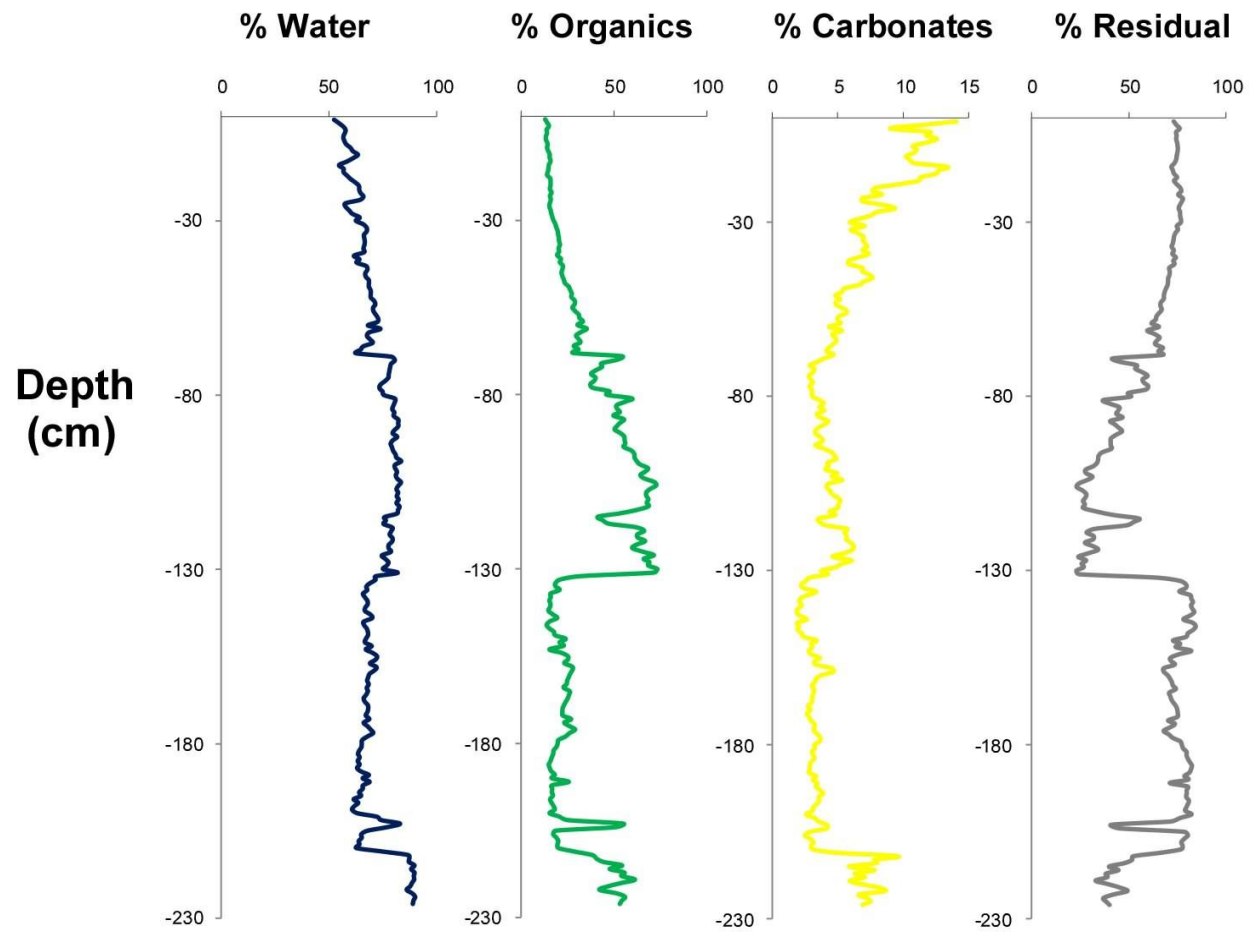
SL 1

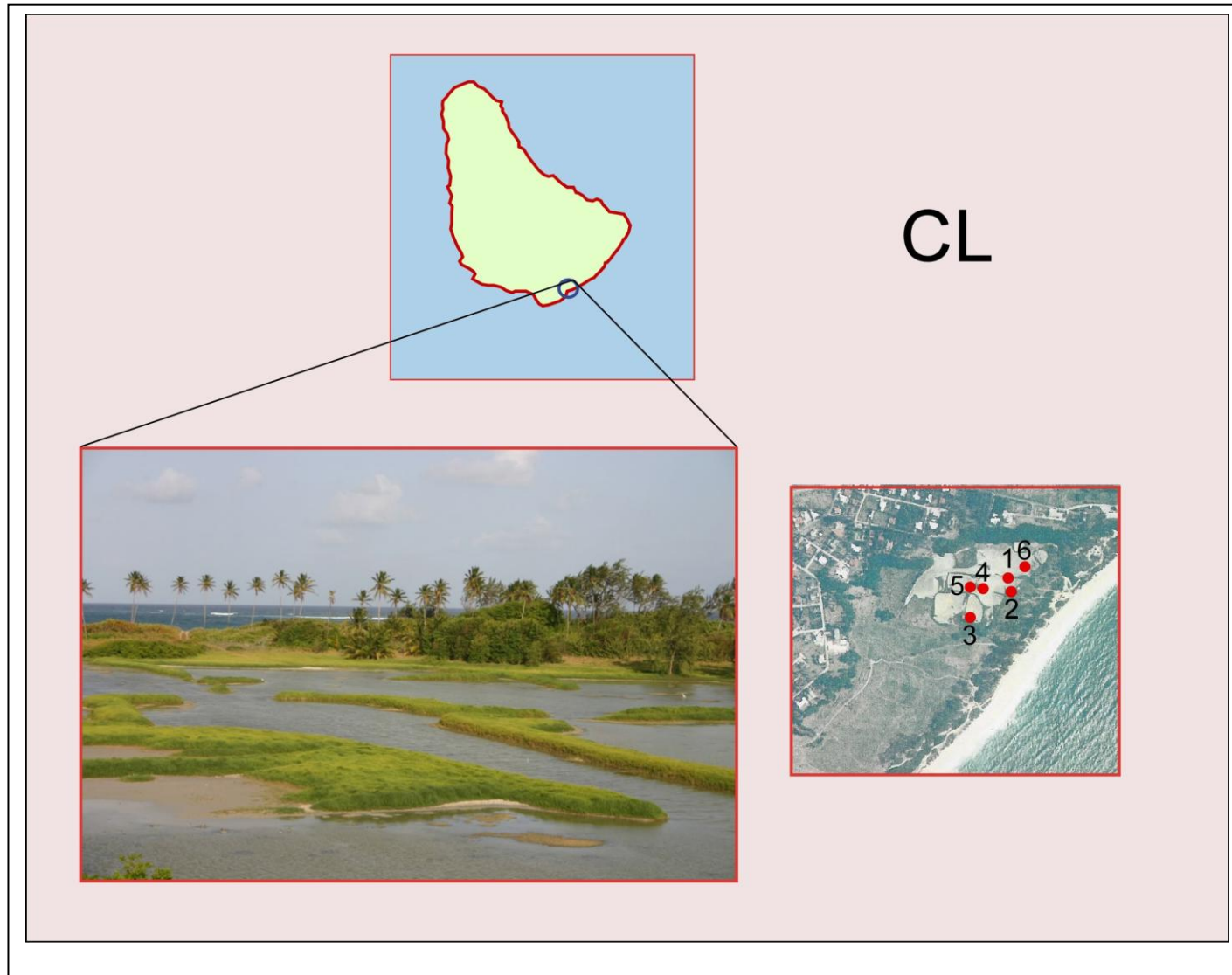


SL 2

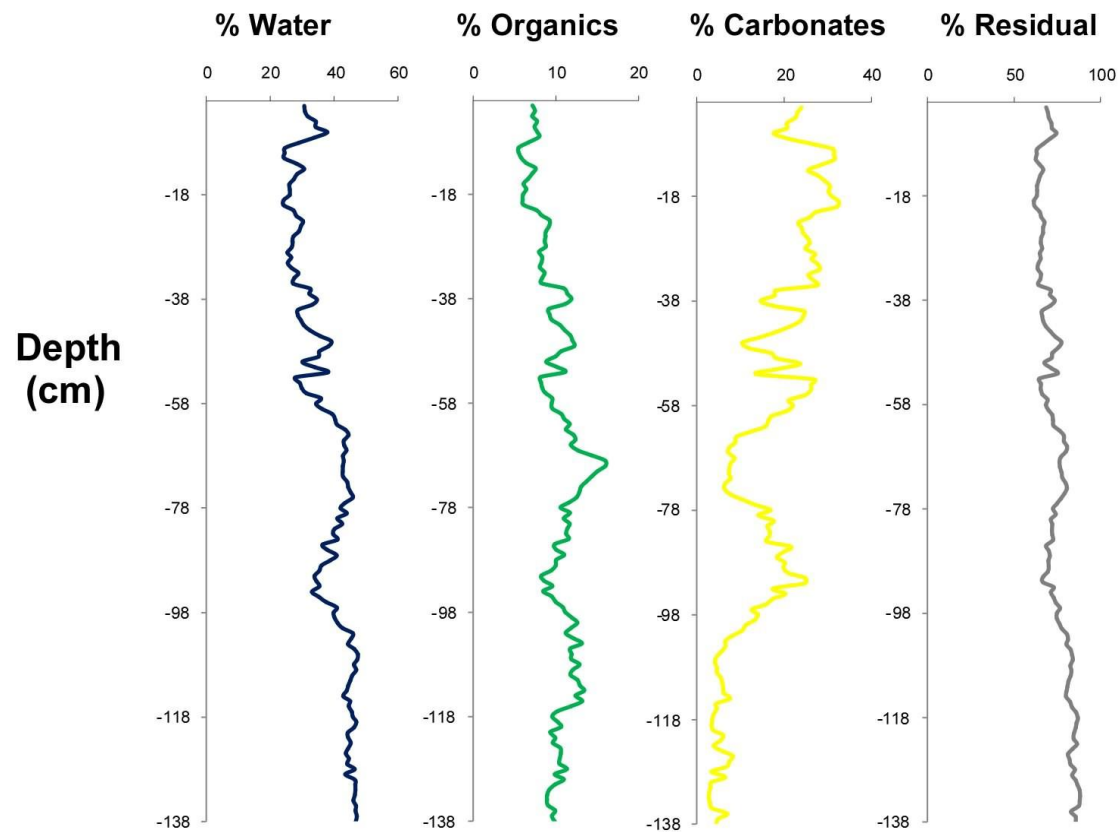


SL 3

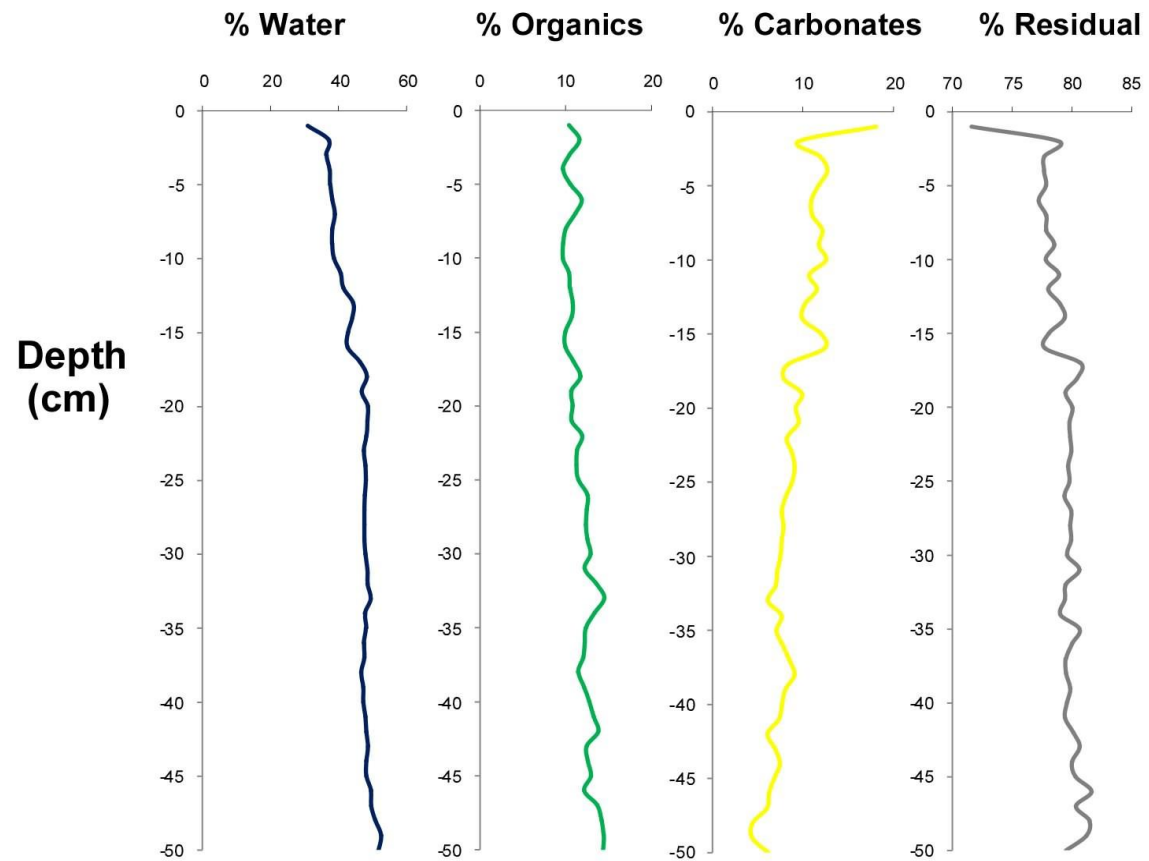




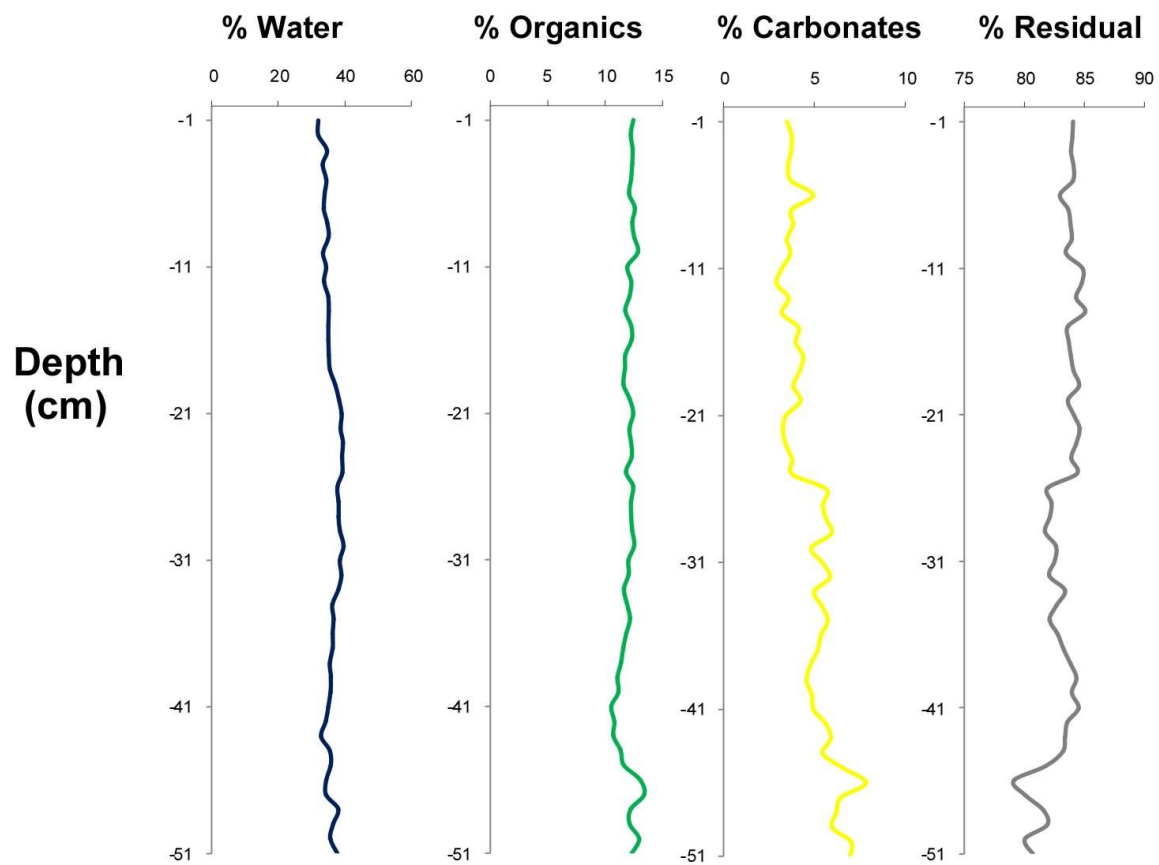
CL 2



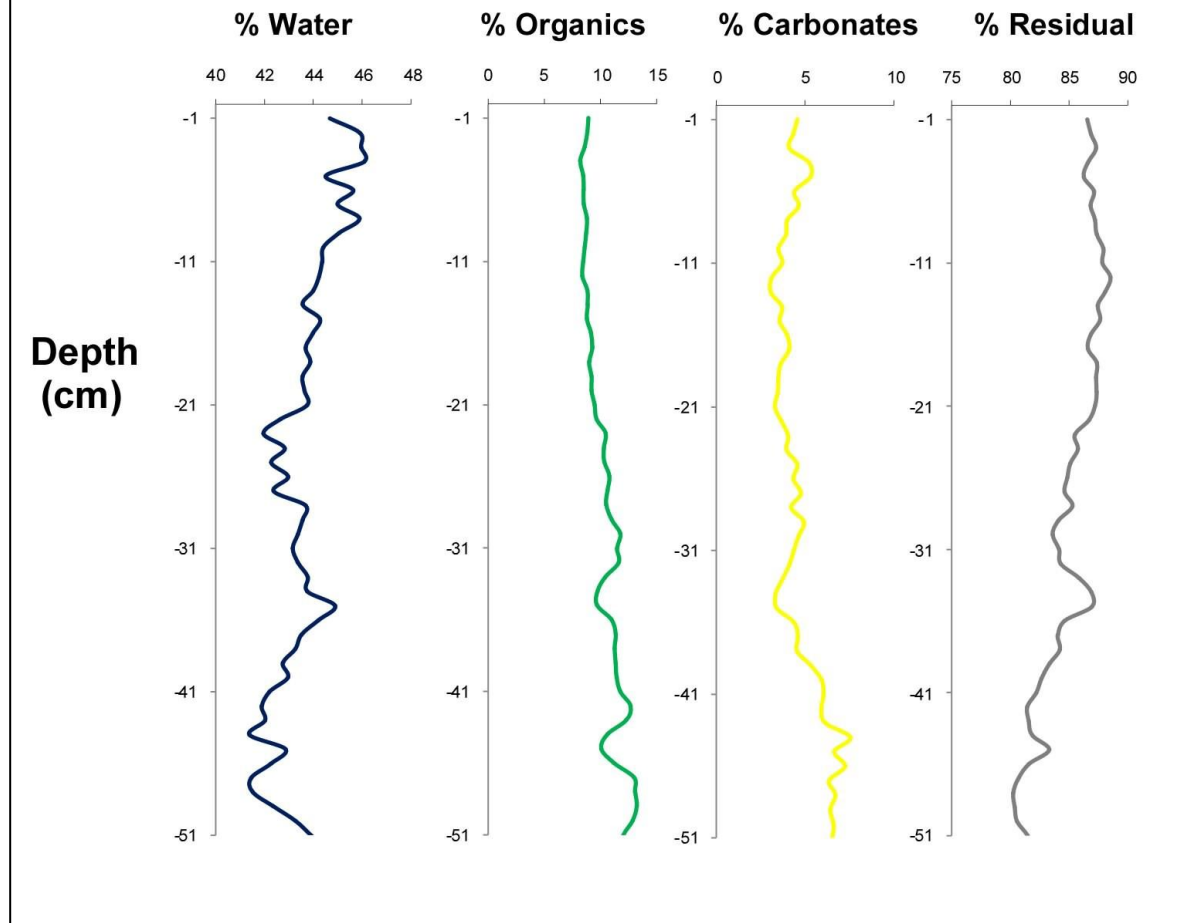
CL 3



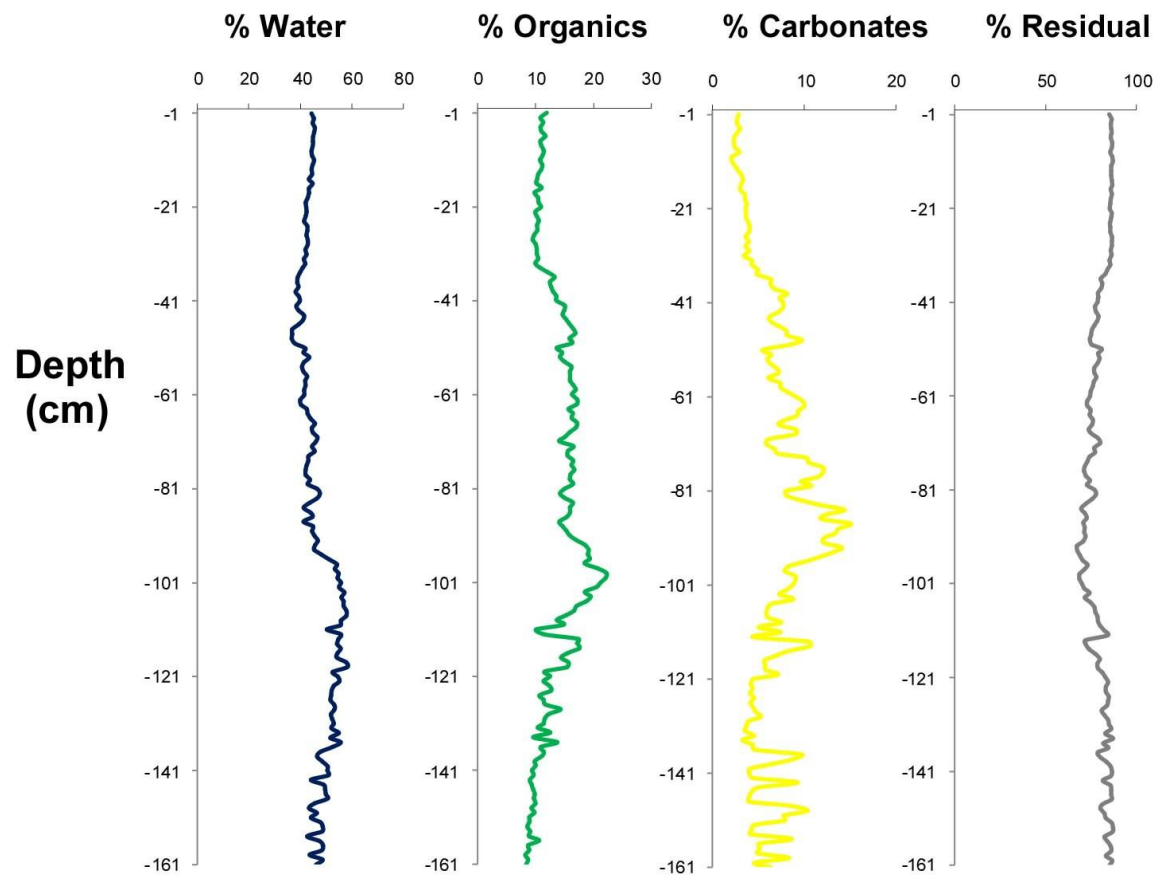
CL 4



CL 5



CL 6



APPENDIX B NOTES ON THE SPATIAL VARIABILITY OF SAND DEPOSITION RESULTING FROM HURRICANE FELIX ON THE CARIBBEAN COAST OF NICARAGUA IN REFERENCE TO PALEOTEMPESTOLOGICAL STUDIES

Introduction

Recent debate concerning the relationship between hurricanes and climate, particularly global warming (Emanuel, 1987, 2005; Knutson et al., 1998; Knutson and Tuleya, 1999, 2004; Walsh and Ryan, 2000; Webster et al., 2005; Elsner et al., 2008; Saunders and Lea, 2008; Wang and Lee, 2008), has highlighted the inadequacies of the historical record as a means of predicting future hurricane behavior. Even in the North Atlantic (NA), the basin with the most complete instrumental record, the accuracy of storm data even during the period of aircraft reconnaissance is sharply debated (Landsea, 2005, 2007; Pielke et al., 2005, Kossin et al., 2007), due to the continuously evolving analytic methodology, with earlier data being considerably less reliable (Landsea, 2005, 2007; Kossin, et al., 2007). Because NA hurricane activity exhibits a multi-decadal oscillation between “active” and “inactive” periods (Enfield et al, 2001; Goldenberg et al., 2001), the most reliable instrumental data barely covers a single cycle under basically static conditions, and can provide no information whatsoever concerning behavior under different boundary conditions. Paleotempestology, the study of ancient hurricanes, is developing as the major vehicle for extending the hurricane record into the past as a means of investigating the hurricane/climate relationship over longer time scales and varying background conditions. Although a wide range of proxy data, including isotopic studies of tree rings, lake sediments, speleothems and coral (Malmquist, 1997; Miller et al., 2006; Frappier et al.; 2007a,b; Nyberg et al., 2007; Nott et al., 2007; Lambert et al., 2008) have been applied to this problem, to date the

most effective approach has been sedimentary, with multi- millennial records produced from several sites along the Gulf and Atlantic coasts of the United States (Collins et al., 1999; Liu and Fearn, 1993, 2000; Donnelly et al., 2001a, 2001b, 2004; Scileppi and Donnelly, 2007; Scott et al., 2003) the Caribbean (Bertran et al., 2004; Donnelly, 2005; Donnelly and Woodruff, 2007; Knowles, 2008, McCloskey and Keller, 2009; Urquhart, 2009) Japan (Woodruff et al., 2009) and Australia (Hayne and Chappell, 2001; Nott and Hayne, 2001). The Australian studies have focused on beach ridge accumulation, producing storm chronologies up to 5000 years in length, based on the identification of the ridges as storm deposits (Hayne and Chappell, 2001; Nott and Hayne, 2001; Nott, 2003). With progressively older dates associated with more inland ridges, this methodology depends upon prograding beaches, which are common in Australia due to abundant sediment supply and the regional late Holocene relative sea level drop resulting from the movement of water to the northern hemisphere associated with isostatic rebound (Masselink and Hughes, 2003). This methodology is generally not applicable in areas subject to landfalling NA hurricanes, where relative sea level has been rising since the last glacial maximum (LGM) around 18000 years ago. For this reason, sedimentary paleotempestology in the NA basin has focused on the identification of hurricane-generated overwash fans preserved in coastal wetlands (Bertran et al., 2004; Donnelly and Webb, 2004; Liu, 2004; Knowles, 2008; McCloskey and Keller, 2009; Urquhart, 2009; Woodruff et al., 2009), and extracted in sediment cores. The theoretical foundation for these studies is that large, hurricane-generated storm surges overtop beach ridges and deposit a layer of inorganic sediments (material removed from the ocean floor and/or beach/dunes) in the low energy, landward environment, be it coastal lakes, marshes, swamps or mangroves (Liu, 2004). Over time, normal deposition (usually organic in nature) resumes, thereby burying and preserving these inorganic layers. This process can be repeated any

number of times, resulting in alternating organic/inorganic layers that can be dated to establish a site specific proxy record of hurricane strikes. Proxy records from several sites can be combined to produce a regional history of hurricane activity, and regional records combined to produce a basin-wide history. Dating (usually based on radiocarbon chronologies) can then be used to correlate regional hurricane activity with the paleoclimatic record, permitting examinations into the climate/hurricane relationship in an effort to determine hurricane response to varying boundary conditions, and, hopefully, identify the climatic drivers responsible for changing hurricane regimes.

Sedimentary paleotempestology endeavors to provide information beyond merely recording the frequency of landfalling events. It has been suggested that close examination of the physical aspects of the overwash layers can be used to infer both the direction of individual storm movement (Liu, 2004) and the relative strength of different storms at a single location (Donnelly et al., 2004; Donnelly and Webb, 2004; Liu, 2004; McCloskey and Keller, 2009). Examination of the sedimentary signatures of historically recorded storms have been used to calibrate the sensitivity of specific site for recording storms and estimate the intensity of prehistoric storms (Liu and Fearn, 1993, 1997, 2000; Liu, 2004; Donnelly and Webb, 2004; Donnelly et al., 2001a,b).

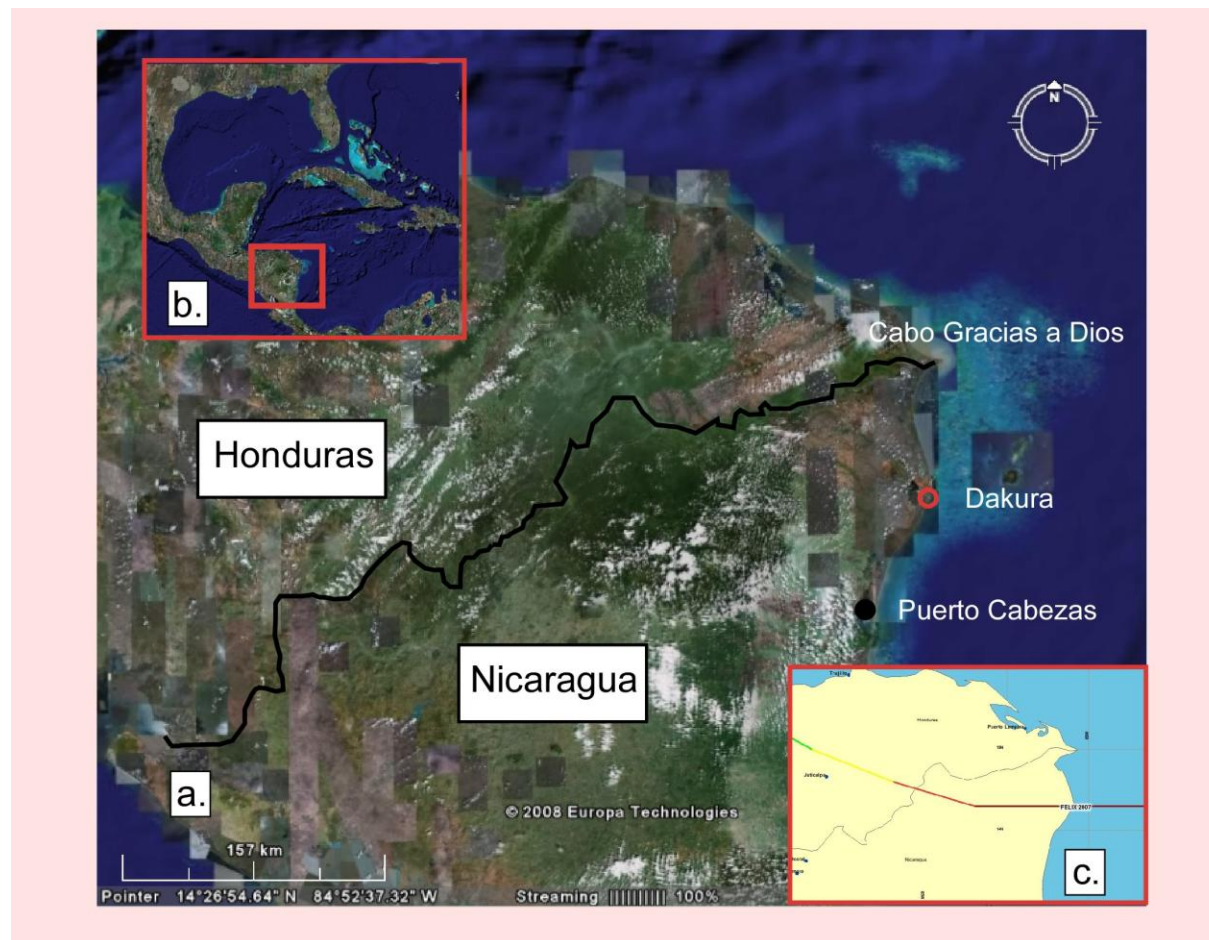
Because such examination of the interbedded clastic layers has become the standard methodology for NA paleotempestology studies, it is important to closely examine the depositional properties of these layers. Typically, hurricane-generated clastic layers occur as overwash fans, consisting of a narrow neck, produced where the storm surge cuts through the beach ridge, and a wider, fan-shaped depositional surface farther inland, where passing beyond the beach ridge the clastic-laden storm surge can spread horizontally (Kraft, 1971; Leatherman,

1979a,b,1981, 1983) (**Figure 2.1**). Generally both the average grain size and thickness of the overwash layer decreases with distance inland (Kraft, 1971). The general assumption is that higher surge/greater storm intensity results in thicker overwash layers, containing larger grain material transported greater distances inland. Although these correlations are generally true, it is important not to overlook the vast spatial variability inherent in storm-generated deposition of the transported material. Large differences in both stratigraphy and layer thickness can occur over very short distances, which needs to be accounted for in sedimentary paleotempestological investigations.

Regional Setting

Environmental

The Caribbean coast of northern Nicaragua is part of the Mosquitia basin (Mills and Barton, 1996) which filled with at least 4500 meters of sedimentary rocks during the Tertiary, topped by alluvium delivered throughout the Quaternary (Donnelly et al., 1990). This fill has resulted in a large coastal plain several tens of kilometers in width extending from eastern Honduras to Costa Rica. Rainfall is heavy throughout the area, with Puerto Cabezas in northern Nicaragua averaging 330 cm/yr, with precipitation increasing to the south (Parsons, 1955; Portig, 1976). Several large rivers drain this plain, transporting vast amounts of sediments from the central interior mountains, with nearly all drainage being to the east. This has resulted in abundant sediment supply to the coast and prograding coasts. As part of the Nicaraguan Rise, offshore bathymetry is shallow, with the 10 m depth contour occurring >12 km offshore. The coast is under populated, with sparse agricultural activity and minimal human geomorphologic disturbance.



B.1 (a) GoogleEarth image of Caribbean coast of northern Nicaragua and northeastern Honduras, study location indicated with red circle.
 (b) Location relative Gulf of Mexico and the Caribbean. Notice the shallow off shore gradient centered on the Cabo de Gracias a Dios.
 Inset (c) shows path of Hurricane Felix (from <http://maps.csc.noaa.gov/hurricanes/viewer.html>).

Study Site

Our study was conducted on the beach slightly to the southeast of the village of Dakura at 14.41 N, 83.22 W, approximately 45 km northeast of Puerto Cabezas, and 65 km south of Cabo Gracias a Dios. Dakura is located on a pronounced coastal protrusion, the seaward edge of which, south of Dakura, is dominated by linear beach ridges, indicating a prograding coast, built by the sediments transported by the Rio Coco (also called Segovia) that discharges at the Cabo Gracias a Dios. (**Figure B:1**). Vegetation along the coast is fairly thick, but low (<3 m), with higher vegetation beginning farther inland.

The beach has a shallow gradient and a very low beach ridge, with the maximum elevation being ~1 m. (**Figure B:2**). Inland there are low bushes and grass, with several low places holding water during our visit at the end of the dry season. During the rainy season this area is generally flooded. Due to this lack of topographical relief and the extended rainy season, Dakura village is located > 1.5 km west of the ocean on a red clay ridge, presumably of Pleistocene age, approximately 8-10 m above MSL.

Hurricane Felix

Our study location is at or near where the eyewall of Hurricane Felix crossed the coast on September 4, 2007 (**Figure B:1b**). Felix made landfall as a category 5 hurricane with sustained winds of over 140 kts/hr, and a central pressure of 934 mb. Though powerful, the storm was rather small, having, at peak intensity, an eye diameter of 15 nautical miles and a maximum diameter of 80 nautical miles for sustained winds of 64 knots. By comparison, Hurricane Katrina (2005) achieved an eyewall diameter of 30 nautical miles, and a maximum diameter of 220 nautical miles for 64 knot winds (<http://www.nhc.noaa.gov/archive>).

NOAA data gives the point of landfall for Felix as 14.3 N, 83.2 W. Although, given the



B.2 Beach at Dakura, showing shallow gradient. Even small sail boats with extremely shallow drafts stay offshore to avoid grounding.

estimated accuracy of position (15 nautical miles), our study site falls within the possible area of eyewall transit, we found no evidence of this. Informants made no mention of a quiet interval or wind reversal during the storm, and direction of tree fall was consistently to the southwest. This suggests that the location of eyewall impact was to the south, thereby placing our study site within the northwest quadrant, subject to the maximum wind speed and storm surge.

Dakura village was devastated by the storm, with at least ten deaths occurring in the village.

Nearly all the large mango trees were uprooted and many houses destroyed. Several concrete block structures, including the large Moravian church, were partially or wholly destroyed

(**Figure B:3**). Villagers informed us that the aeolian sand transport associated with Felix was so intense that they had to protect their eyes at the village situated approximately 1.5 km from the beach. Vast quantities of sand were moved along the beach and the mouth of the tidal inlet leading to the anterior lagoon shifted position, with the old channel (formerly ~ 1 m depth) being filled and achieving an elevation of ~0.5 m. Storm wrack was observed at the base of the ridge upon which Dakura sits, >1 km from the sea.

Methods

We conducted our survey during late March 2008, less than seven months after the passage of Hurricane Felix, concentrating on a sand field along the beach slightly to the south of the village which, according to informants, had been a vegetated area prior to Felix. Our field observations were documented qualitatively by photographs.

Results

Extreme spatial variability in both the occurrence of erosion and the deposition of clastic material (basically quartz sand) by the storm was obvious. Inland of the swash zone, beginning at ~ 45 meters from the shore, a series of abrupt sedimentary transitions occur within a few meters



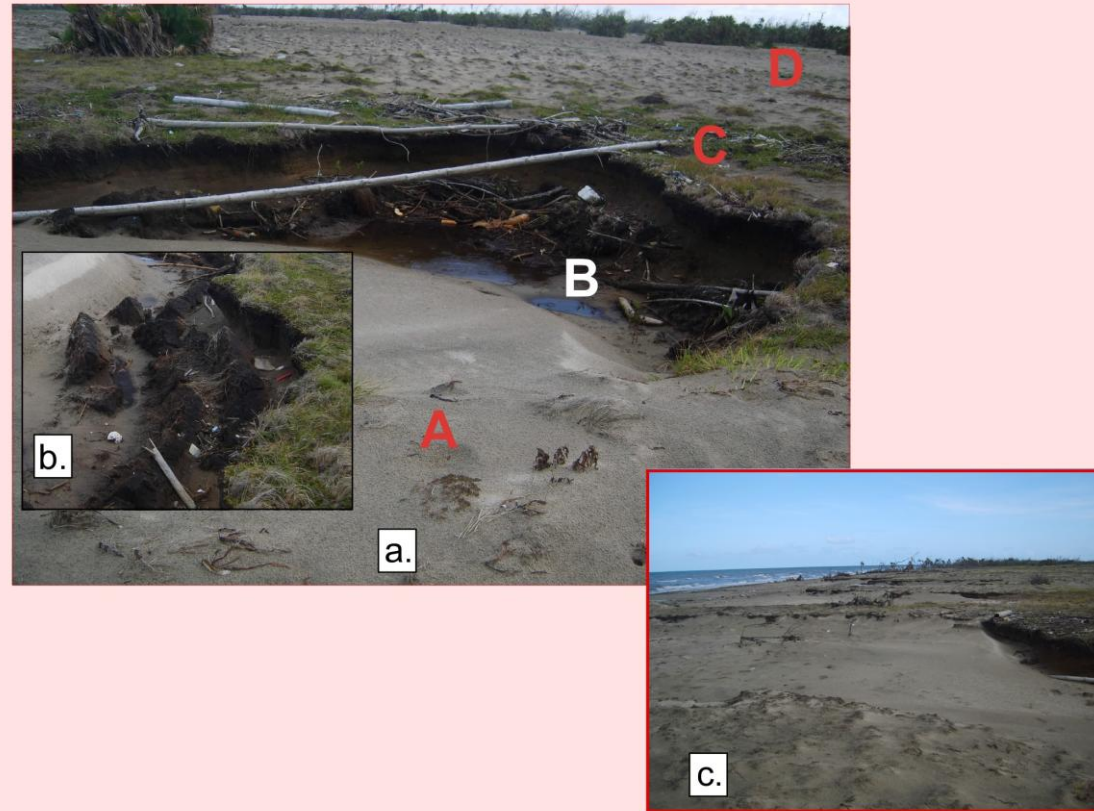
B.3 Wind damage in Dakura village from Hurricane Felix. Most large trees were uprooted and structural damage was sustained by both wooden and concrete structures.

(**Figure B:4**). A thick storm-deposited sand layer (**A**) is immediately followed by a short section consisting of a chaotic mixture of heterogeneously-sized wrack and stratigraphically incoherent soil, eroded from the original surface (**B**). This is immediately followed by a few meters of undisturbed pre-storm surface, covered by grass and free of sand (**C**). Similar cusped hollows filled with similarly diverse mixtures of deposited and eroded material occur at random intervals and varying distances from the ocean (**Figure B:4c**) along the beach in both directions.

A sand field, ~ 300m x 85 m in extent was encountered immediately inland of the uncovered ground (**D**) (**Figure B:5**). In the parts of this field where no substantive vegetation remained, the thickness of the deposited sand, easily distinguishable from the darker pre-storm surface, was fairly uniform, averaging ~15 cm in depth (**Figure B:5b**). However, the presence of vegetation exerted a very significant influence, with difference in depositional depths often varying on the order of 0.5 m within the immediate vicinity of small clusters of shrubs (**Figure B:6a**).

Characteristic swales were also observed (**Figure B:6b**), presumably resulting from a combination of preexisting topography and post-event sand transport. As with the erosional hollows, similar inland sand fields exhibiting similar spatial variability were encountered at random intervals along the beach.

On the extreme landward edge of the sand sheets the variability in layer thickness was often dramatic, especially when occurring in association with preexisting topographic lows. The top of a sediment core extracted from such a location (aluminum pole in **Figure B:7a**) contained only an 8 cm sand layer (**Figure B:7b**), while < 5meters seaward the depth sand layer approached 1 m (where the core is being wrapped). It is unclear how much of this variability occurred during the original storm-generated deposition, and how much resulted from later transport. Following the storm, the depressions would hold water, presumably capable of



B.4 Spatial variability in sand transport (a), showing overwash deposits changing from thick sand sheet (A), through overturned eroded soil and wrack (B) to unaffected ground (C) to patchy sand sheet (D). Beach is to the left. Inset (b) is a closeup of overturned soil from a nearby erosion hollow, while inset (c) shows a series of such hollows extending southward along the beach. Notice that the tree line farther down the beach is seaward of the erosion hollows and sand sheet, indicating that at this location the vegetation was removed/buried by the storm and that this area of erosion is inland of normal tidal range.



B.5 Closeup (a) of the sand sheet showing hummocky nature. Inset (b) displays the easily recognizable interface between the storm deposited sand sheet and the darker preexisting surface.

abruptly halting transport, resulting in the onshore wind forcing accumulation of deeper sand drifts at the front edges. Similar abrupt changes in the thickness of overwash layer when encountering water bodies have been observed in other locations (Liu and Lu, 2005). Surface rippling clearly indicates that post-event aeolian transport is capable of modifying the storm-generated depositional regime (**Figure B:8**).

Discussion

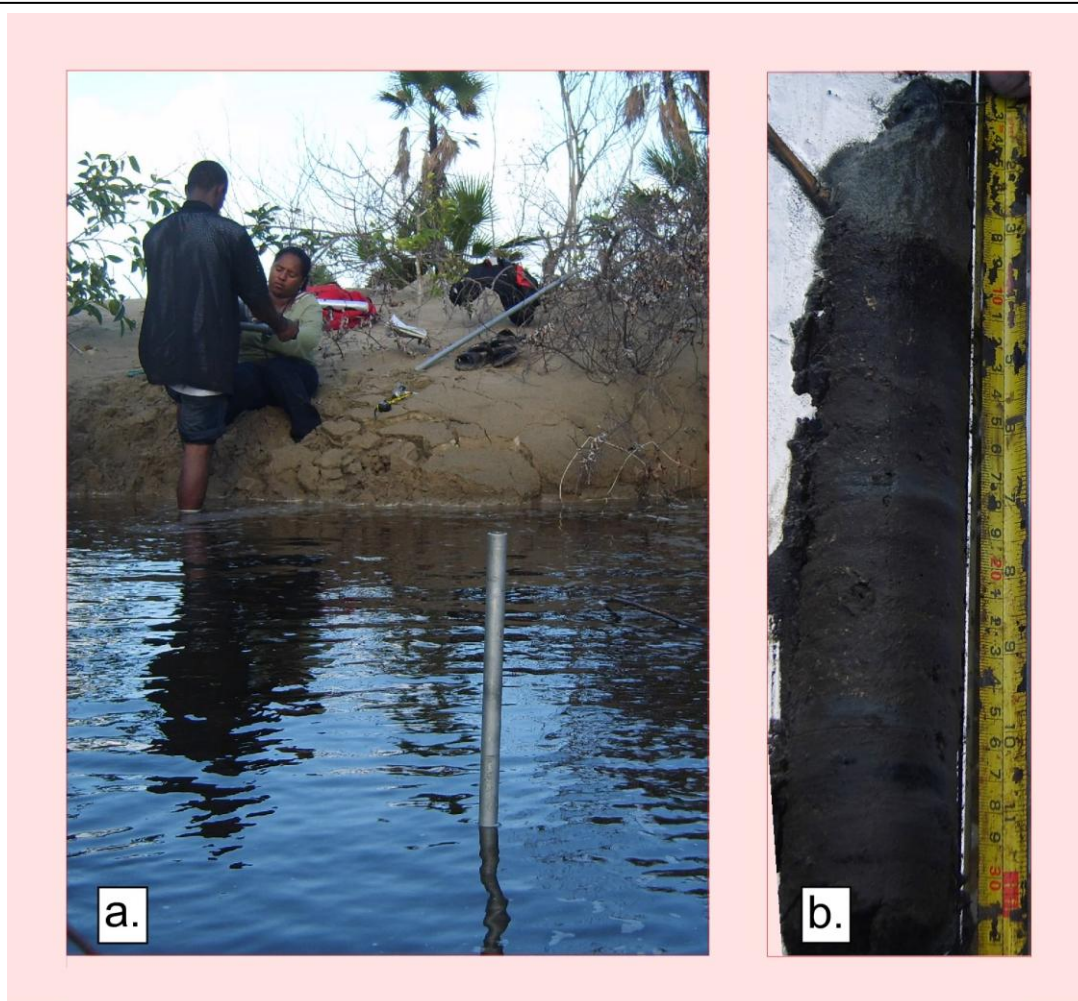
It seems clear, even from this purely qualitative approach, that the thickness and composition of hurricane-generated sand layers can vary dramatically over extremely short distances. In this case, inland from the swash zone a narrow band, characterized by an extremely chaotic mixture of sedimentary and erosional structures, occurs sporadically over long distances, while farther inland sand fields are distributed randomly. Although in these areas the thickness of the sand layer is generally more uniform, they are punctuated by small areas of much larger variability controlled by preexisting topography and the vagaries of vegetational distribution. All of these features are then subject to reworking on a variety of temporal scales.

For paleotempestological reconstructions it is necessary to recognize the spatial variability inherent in the hurricane-generated deposition layers in order to avoid overinterpretation of single cores. If a similar deposition had occurred at some point in the past, and after subsequent burial, cores were extracted along a shore-normal transect over the area shown in **Figure B:4**, each core could exhibit very different stratigraphies, and, consequently, very different hurricane chronologies.

These considerations may be especially important in areas such as Nicaraguan Caribbean coast, where, given the prograding coastline and relative sea level rise, the area discussed in this paper can be expected to develop into a back barrier wetland, the usual environment for



B.6 Effect of vegetation on thickness of sand deposition. Although the transported sand was clearly capable of burying inland vegetation, it did not do so uniformly.



B.7 Effect of topography on thickness of sand deposition. The thick sand layer burying vegetation at the extreme landward edge of the sand sheet (a) reduces to ~ 9 cm 3 m farther inland at the as shown by the sediment core (b) retrieved from the spot marked by the aluminum pole. This abrupt change in layer thickness is probably due to reduction in competence resulting from increased water resistance in the depression both during and after the storm.



B.8 Wind ripples indicating post event sand movement.

paleotempestological coring. Reversing this progression argues that cores currently being extracted from such wetlands may be penetrating former nearshore environments, site of maximum spatial variability. These difficulties can be minimized by the use of transects. Extracting a series of cores, preferably taken both perpendicular and parallel to the shore, permits the identification of a general trend and minimizes the possibility of incorrect generalities being reached from the examination of stratigraphically nonrepresentative cores.

Conclusions

Variability in composition, thickness, and continuity of hurricane-generated overwash deposits can be extreme, particularly along the seaward edge.

This spatial variability must be considered when extrapolating long term paleostrike records from coastal environments.

This potentially confounding factor can be minimized by the use of both shore-normal and shore-parallel transects.

References

- Bertran, P., Bonnissent, D., Imbert, D., Lozouet, P., Serrand, N., and Stouvenot, C., 2004. *Paleoclimat des Petites Antilles depuis 4000 BP: l'enregistrement de la lagune de Grand-Case a Saint-Martin*. *Comptes Rendus Geoscience* 336, 1501–1510.
- Collins, E.S., Scott, D.B., and Gayes, P. T., 1999. Hurricane records on the South Carolina Coast: Can they be detected in the sediment record? *Quaternary International* 56, 15-26.
- Donnelly, J.P. 2005: Evidence of past intense tropical cyclones from backbarrier salt pond sediments: A case study from Isla de Culebrita, Puerto Rico, USA. *Journal of Coastal Research*. SI 41, 201-210.
- Donnelly, J.P. and Webb, T. III, 2004. Back-barrier sedimentary records of intense hurricane landfalls in the northeastern United States. In Murnane, R.J., and Liu, K-b. (eds), *Hurricanes and Typhoons: Past, Present and Future*. Columbia University Press, New York, 58-95.

Donnelly, J.P. and Woodruff, J.D., 2007, Intense hurricane activity over the past 5,000 years controlled by El Nino and the West African monsoon. *Nature* 447, 465-468.

Donnelly, J.P., Bryant, S.S., Butler, J., Dowling, J., Fan, L., Hausmann, N., Newby, P., Shuman, B., Stern, J., Westover, K. and Webb, T. III, 2001a. 700 yr sedimentary record of intense hurricane landfalls in southern New England. *Geological Society of America Bulletin* 113, 714-727.

Donnelly, J.P., Roll, S., Wengren, M., Butler, J., Lederer, R. and Webb, T. III, 2001b. Sedimentary evidence of intense hurricane strikes from New Jersey. *Geology* 29, 615-618.

Donnelly, J.P., Butler, J., Roll, S., Wengren, M. and Webb, T. III, 2004: A backbarrier overwash record of intense storms from Brigantine, New Jersey. *Marine Geology* 210, 107-121.

Donnelly, T. W., Horne, G. S., Finch, R. C, Lopez-Ramos, E., 1990. Northern Central America; the Maya and Chortis blocks. In Dengo, G., and Case, J.E., (eds), *The Geology of North America*, Vol. H, The Caribbean region The Geologic Society of America, Boulder, Colorado. 37-76.

Elsner, J. B., J. P. Kossin, and T. H. Jagger, 2008. The increasing intensity of the strongest tropical cyclones. *Nature* 455, 92-95.

Emanuel, K.A., 1987. The dependency of hurricane intensity on climate. *Nature* 326, 483-485.

Emanuel K. A., 2005. Increasing destructiveness of tropical cyclones over the past 30 years. *Nature* 436, 686-688.

Enfield, D. B., Mestez-Nunez, A., and Trimble, P. J., 2001: The Atlantic multidecadal oscillation and its relation to rainfall and river flows in the continental U.S. *Geophysical Research Letters* 28, 2077-2080.

Frappier, A.B., Sahagian, D., Carpenter, S.J., González, L.A., and Frappier, B.R., 2007a. A stalagmite proxy record of recent tropical cyclone events. *Geology* 7, 111-114. DOI: 10.1130/G23145A.

Frappier, A.B., Knutson, T., Liu, K-b., and Emanuel, K., 2007b. Perspective: coordinating paleoclimate research on tropical cyclones with hurricane-climate theory and modeling. *Tellus* 59A, 529-537.

Goldenberg, S. B., Landsea, C. W., Mestas-Nunez, A. M., and Gray, W. M., 2001. The recent increase in Atlantic hurricane activity: causes and implications. *Science* 293, 474-479.

Hayne, M. and Chappell, J., 2001. Cyclone frequency during the last 5000 years at Curacao Island North Queensland Australia. *Palaeogeography, Palaeoclimatology, Palaeoecology* 168, 207-219.

Knowles, J.T., 2008. A 5000 year history of Caribbean environmental change and hurricane activity reconstructed from coastal lake sediments of the West Indies. Unpublished dissertation, Louisiana State University, Baton Rouge, Louisiana.

Knutson, T. R., and Tuleya, R. E., 1999. Increased hurricane intensities with CO₂-induced warming as simulated using the GFDL hurricane prediction system. *Climate Dynamics* 15, 503–519.

Knutson T. R., and Tuleya R. E., 2004. Impact of CO₂-induced warming on simulated hurricane intensity and precipitation: sensitivity to the choice of climatic model and convective parameterization. *Journal of Climate* 17, 3477-3495.

Knutson T. R., Tuleya R. E., and Kurihara, Y., 1998. Simulated increase of hurricane intensities in a CO₂-warmed climate. *Science* 279, 1018-1021. DOI: 10.1126/science.279.5353.1018.

Kossin, J. P., Knapp, K. R., Vimont, D. J., Murnane, R. J., and Harper, B. A. , 2007. A globally consistent reanalysis of hurricane variability and trends. *Geophysical Research Letters* 34, L04815. DOI:10.1029/2006GL028836.

Kraft, J.C., 1971. Sediment facies patterns and geologic history of a Holocene marine transgression. *Geological Society of America Bulletin* 82, 2131-2158.

Lambert, W.J., Aharon, P., and Rodriguez, A.B., 2008. Catastrophic hurricane history revealed by organic geochemical proxies in coastal lake sediments: a case study of Lake Shelby, Alabama (USA). *Journal of Paleolimnology* 39, 117-131.

Landsea, C.W., 2005. Hurricanes and global warming. *Nature* 438, E11-E13.

Landsea, C. W., 2007. Counting Atlantic tropical cyclones back to 1900. *EOS*, 88, 197-2008.

Leatherman, S.P., 1979a. *Barrier Island Handbook*. National Park Service, Boston, MA.

Leatherman, S.P., 1979b. Migration of Assateague Island, Maryland, by inlet and over-wash processes. *Geology* 7, 104-107.

Leatherman, S.P. 1981. *Benchmark Papers in Geology Vol 58: Overwash processes*. Hutchinson Ross Publishing, Stroudsburg, PA.

Leatherman, S.P. 1983. Barrier dynamics and landward migration with Holocene sea-level rise. *Nature* 301, 415-417

Liu, K-b., 2004. Paleotempestology: principles, methods and examples from Gulf coast lake sediments. In Murnane, R.J., and Liu, K-b. (eds), *Hurricanes and Typhoons: Past, Present and Future*. Columbia University Press, New York, 13-57.

Liu, K-b. and Fearn, M.L., 1993. Lake-sediment record of late Holocene hurricane activities from coastal Alabama. *Geology* 21, 793-796.

- Liu, K-b., and Fearn M.L., 1997. Lake sediment records of Hurricane Opal and prehistoric hurricanes from the Florida Panhandle. In; 22nd Conference on Hurricanes and Tropical Meteorology. Fort Collins, CO. American Meteorological Society.
- Liu, K-b. and Fearn, M.L., 2000. Reconstruction of prehistoric landfall frequencies of catastrophic hurricanes in northwestern Florida from lake sediment records. *Quaternary Research* 54, 238-245. DOI:10.1006/qres.2000.2166.
- Liu, K-b. and Lu, H.Y., 2005. A paleotempestological record from Nobska pond, Cape Cod: testing the Bermuda High hypothesis. Association of American Geographers Annual Meeting. Denver, CO.
- Malmquist, D. L., 1997. Oxygen isotopes in cave stalagmites as a proxy record of past tropical cyclone activity. In Preprints of the 22nd Conference on Hurricanes and Tropical Meteorology, 393-394. Boston. American Meteorological Society.
- Masselink, G., and Hughes, M. G., 2003. Introduction to coastal processes and geomorphology. Arnold Publishing, London.
- McCloskey, T. A., and Keller, G., 2009. 5000 year sedimentary record of hurricane strikes on the central coast of Belize. *Quaternary International* 195, 53-68. DOI:10.1016/j.quaint.2008.03.003.
- Miller, D. L., Mora, C. I., Grissino-Mayer, H. D., Mock, C. J., Uhle, M. E., and Sharp, Z., 2006. Tree-ring isotope records of tropical cyclone activity. *Proceedings of the National Academy of Science*, 10.1073/pnas.0606549103.
- Mills, R. A., and Barton, R., 1996. Geology of the Ahuas area in the Mosquitia Basin of Honduras: preliminary report. *The Association of American Petroleum Geologist Bulletin* 80, 1627-1640.
- Nyberg, J., Malmgren, B.A. Winter, A., Jury, M.R., Kilbourne, K.H. and Quinn. T.M. 2007. Low Atlantic hurricane activity in the 1970s and 1980s compared to the past 270 years. *Nature* 447, 698-702.
- Nott, J. 2003. The Importance of prehistoric data and variability of hazard regimes in natural hazard risk assessment—examples from Australia. *Natural Hazards* 30, 43-58.
- Nott, J, and Hayne, M., 2001. High frequency of “SuperCyclones” along the Great Barrier Reef over the past 5000 years. *Nature* 413, 508-512.
- Nott, J., Haig, J., Neil, H., and Gillieson, D., 2007. Greater frequency variability of landfalling tropical cyclones at centennial compared to seasonal and decadal scales. *Earth and Planetary Science Letters* 255, 367-372.
- Parsons, J. J., 1955. The Miskito pine savanna of Nicaragua and Honduras. *Annals of the Association of American Geographers* 45, 36-63.

- Pielke, R. A., Jr., Landsea, C. W., Mayfield, M., Laver, J., and Pasch, R., 2005. Hurricanes and global warming. *Bulletin of the American Meteorological Society* 86, 1571-1575. DOI: 10.1175/BAMS-86-11-1571.
- Portig, W. H., 1976. The climate of Central America . In Schwerdtfeger W., (ed), *Climates of Central and South America. World Survey of Climatology*, 12. Elsevier, New York, 405-478
- Saunders, M. A. and Lea, A.S., 2008. Large contribution of sea surface warming to recent increase in Atlantic hurricane activity. *Nature* 45, 557-560. DOI:10.1038/nature06422.
- Scileppi, E. and Donnelly, J.P., 2007. Sedimentary evidence of hurricane strikes in western Long Island, New York. *Geochemistry Geophysics Geosystems* 8.
- Scott, D.B. , Collins, E.S., Gayes, P.T. and Wright, E., 2003. Records of prehistoric hurricanes on the South Carolina coast based on micropaleontological and sedimentological evidence, with comparison to other Atlantic Coast records. *Geological Society of America Bulletin* 115, 1027-1039.
- Urquhart, G. R., 2009. Paleoecological record of hurricane disturbance and forest regeneration in Nicaragua. *Quaternary International* 195, 88-97. DOI:10.1016/j.quaint.2008.05.012.
- Walsh, K. J. E., and Ryan, B. F., 2000. Tropical cyclone intensity increase near Australia as a result of climate change. *Journal of Climate* 13, 3029–3036.
- Wang, C., and Lee, S-K., 2008. Global warming and United States landfalling hurricanes, *Geophysical Research Letters* 35, L02708, DOI:10.1029/2007GL032396.
- Webster, P. J., Holland, G. J., Curry, J. A., and Chang, H-R., 2005. Changes in tropical cyclone number, duration and intensity in a warming environment. *Science* 309, 1844-1846.
- Woodruff, J. D., Donnelly, J. P., and Okusus, A., 2009. Exploring typhoon variability over the mid-to-late Holocene: evidence of extreme coastal flooding from Kamikoshiki, Japan. *Quaternary Science Reviews* 28, 1774-1785.

APPENDIX C RELEASE LETTERS

Hello Dr. Paul,

I got your email address from Laurin Becker, who handled the editing on an article I contributed to "Hurricanes and Climate Change" (2009), edited by Dr. J.B. Elsner and T. Jagger. My chapter is titled "Migration of the Tropical Cyclone Zone Throughout the Holocene", pp. 169-188.

I am writing to request a signed release so that I may use this manuscript in my dissertation. I expect to defend this Fall.

The release can be emailed or sent to:

Terry McCloskey
Department of Oceanography and Coastal Sciences
3251 Energy Coast and Environment Building
Louisiana State University
Baton Rouge, LA. 70803
tmcclo1@lsu.edu
Phone: (225) 578-0470
Fax: (225)-578-6423

Thank you for your help.

Terry McCloskey

Dear Terry,

Permission is granted for you to use the chapter in your dissertation provided that full acknowledgement is given to the original source of publication.

Please let me know if you need something more from our office. We do not have a standard release form, and usually an email with permission is sufficient. I will be happy to send a letter if necessary.

Sincerely,

Melinda (Lindy) Paul

Springer

Senior Editor

Environmental Science

233 Spring St | New York, NY 10013-1578

tel (781) 347-1835

melinda.paul@springer.com

Dr. Catto,

Would it be possible to get a signed release from Quaternary International so that I may use the following manuscript in my dissertation?

McCloskey, T. A., and Keller, G.

5000 Year Sedimentary Record of Hurricane Strikes on the central coast of Belize
Quaternary International, 195 (2009) 53-68.

I expect to defend my dissertation this fall.

The release can be emailed or sent to:

Terry McCloskey

Department of Oceanography and Coastal Sciences

3251 Energy Coast and Environment Building

Louisiana State University

Baton Rouge, LA. 70803

tmcclo1@lsu.edu

Phone: (225) 578-0470

Fax: (225)-578-6423

Thank you for your help.

Terry McCloskey

Dear Terry:

Thank you for your letter. Under the standard agreement with Elsevier, you as author retain all the rights to use your material in your thesis without restriction.

As per

<http://www.elsevier.com/wps/find/authorsview.authors/copyright#whatrights>

"As a journal author, you retain rights for large number of author uses, including use by your employing institute or company. These rights are retained and permitted without the need to obtain specific permission from Elsevier. These include:

the right to include the journal article, in full or in part, in a thesis or dissertation;"
as well as ...

"the right to make copies (print or electric) of the journal article for their own personal use, including for their own classroom teaching use;

the right to make copies and distribute copies (including via e-mail) of the journal article to research colleagues, for personal use by such colleagues (but not for Commercial Purposes**, as listed below);

the right to post a pre-print version of the journal article on Internet web sites including electronic pre-print servers, and to retain indefinitely such version on such servers or sites (see also our information on electronic preprints for a more detailed discussion on these points);

the right to post a revised personal version of the text of the final journal article (to reflect changes made in the peer review process) on the author's personal or institutional web site or server, incorporating the complete citation and with a link to the Digital Object Identifier (DOI) of the article;

the right to present the journal article at a meeting or conference and to distribute copies of such paper or article to the delegates attending the meeting;

for the author's employer, if the journal article is a 'work for hire', made within the scope of the author's employment, the right to use all or part of the information in (any version of) the journal article for other intra-company use (e.g. training), including by posting the article on secure, internal corporate intranets;

patent and trademark rights and rights to any process or procedure described in the journal article;

the right to use the journal article or any part thereof in a printed compilation of works of the author, such as collected writings or lecture notes (subsequent to publication of the article in the journal); and

the right to prepare other derivative works, to extend the journal article into book-length form, or to otherwise re-use portions or excerpts in other works, with full acknowledgement of its original publication in the journal. "

Best wishes,
Norm

VITA

Terry McCloskey was born in Missouri in 1953. After attending two years of college in the early 1970s he spent six years as a migrant laborer in Europe, Africa and North and Central America, mainly working on farms, construction sites and doing odd jobs. He wandered into Belize in 1980 and spent the next 20 years there developing a subsistence farm and raising a family near St. Margarets Village, Mile 32 on the Hummingbird Highway. In 2000 he returned to the United States in order to meet the educational and medical needs of his two sons. He enrolled in Princeton University, graduating *magna cum laude* in 2003 with a degree in geosciences and certificates in environmental studies and the Woodrow Wilson School of Public and International Affairs. In the fall of 2003 he began a doctoral program under Dr. Kam-biu Liu in the Department of Geography and Anthropology at Louisiana State University, completing all the necessary coursework and completing his general exams in that department in the spring of 2006. When Dr. Liu switched to the Department of Oceanography and Coastal Sciences the following semester, Terry went with him, completing a second set of coursework and general Exams. He expects to in order to receive his Doctor of Philosophy degree in December 2009.

Terry is married, with two sons, two step-children and four grandchildren.